SOME DIELECTRIC STUDIES OF MOLECULAR AND INTRAMOLECULAR RELAXATION PROCESSES

A Thesis Submitted to

LAKEHEAD UNIVERSITY

Thunder Bay, Ontario, Canada

by

© MD. ENTAZUL HUQUE.

in partial fulfillment of the requirements for

the degree of

MASTER OF SCIENCE

1984

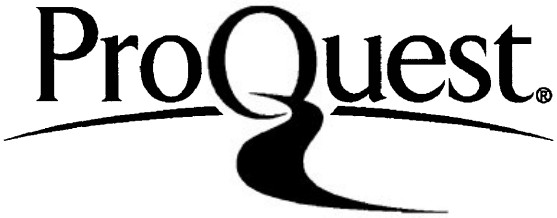

DEDICATION

TO MY CHILDREN: Zahin, Tiba, Tila

ABSTRACT

Dielectric relaxation studies of some potential systems involving molecular interaction particularly intermolecular and/or intramolecular hydrogen bonding as well as of some related molecules have been carried out in which atactic polystyrene and several other glass-forming media, namely, glassy o-terphenyl, bis(m-(m-phenoxy phenoxy)-phenyl) ether (commonly known as Santovac®), cis-decalin and carbontetrachloride were utilized as solvents. Sample preparations and the dielectric measurements by the use of a General Radio 1621 Precision Capacitance Measurement system with appropriate temperature controllable cells have been described. The glass transition temperature (T_g) measurements using the Glass Transition Temperature Measurement Apparatus have also been described. The experimental data as a function of frequency at different temperatures were subject to analysis by a series of computer programmes written in the APL language. The activation energy barriers opposing the dielectric relaxation processes were obtained by the application of the Eyring rate equation.

Different types of polar, fairly spherical, rigid molecules have been studied mainly to provide sources of

relaxation data and activation parameters for comparison with those of flexible molecules of analogous size. The molecular relaxation parameters for these rigid molecules were found to depend on the size, shape and volume of the molecules and the nature of the dispersion medium. The solute concentration has a negligible effect on the molecular relaxaton parameters but it influences the dielectric loss factor, ε'', significantly. At lower concentration, the dielectric loss factor increases linearly with the solute concentration and at higher concentration after a certain point it begins to decrease towards the value observed for the pure molecule. This is accounted for by intermolecular interactions.

Of the flexible molecules, a variety of some simple almost spherical alcohols, and some long-chain aliphatic normal alcohols and thiols have been studied in different glass-forming media. In the usual concentration range of polystyrene matrices ($\sim$5% by wt.) no evidence of intermoleculr hydrogen bonding was found in simple alcohols, long-chain alcohols and thiols. For simple alcohols only molecular relaxation was observed. Long-chain alcohols and thiols exhibited two relaxation processes. The lower temperature processes were attributed to segmental rotation involving CH_2X movement while the higher temperatures were

respective molecular rotation.. Relaxation due to hydroxyl group rotation was not found in any case. At higher concentration molecular relaxation followed by hydrogen bond breaking and in some cases relaxation for hydrogen bonded species was observed in G.O.T.P., carbontetrachloride and polystyrene. As in the case of rigid molecules, similar effects of solute concentration upon the molecular relaxation parameters and dielectric loss factor, ε'', have been observed for simple alcohols in carbontetrachloride.

A wide variety of potentially intramolecular hydrogen bonded substituted phenols has been examined in cis-decalin, G.O.T.P. and Santovac® and in most cases, hydroxyl group relaxation was observed. The relaxation parameters for hydroxyl group rotation were found to be significantly influenced by the strength of the intramolecular hydrogen bond but it was virtually independent of the nature of the dispersion medium as well as the nature of the substituent at the para-position of the ring. No evidence for proton tunneling was detected in these molecules.

ACKNOWLEDGEMENTS

The work described in this thesis was carried out at Lakehead University, Thunder Bay, Ontario, Canada from September 1982 to August, 1984. I would like to express my deepest sense of gratitude to my research supervisor, Professor S. Walker, for his indispensable guidance, invaluable suggestions, constant encouragement and unfailing interest in this work. For his council, I will always be indebted.

I am also grateful to Dr. M. A. Desando and Mr. D. L. Gourlay for their discussions and occasional help in computer work. I also wish to express thanks to my research colleagues, Mr. M.S. Ahmed, Miss Jeanne C.N. Chao and Mr. M.A. Siddiqui for many helpful discussions.

I greatly acknowledge the active co-operation and indispensable technical assistance of Mr. B.K. Morgan. I wish to thank Mrs. J. Parnell for her patience in typing this thesis. Thanks are also due to Lakehead University's Chemistry Department for its financial support and research facilities throughout my years of graduate studies.

Finally, I should like to use this opportunity to express my sincere gratitude to my wife, Khanam Tuhfah Huque for her keen interest and inspiration in my higher studies. I greatly acknowledge the patience and sacrifice of my wife and children (Zahin, Tiba, Tila) without which this work could not have gone forward. Lastly, but by no means least, I owe a life-long debt of gratitude to my father and mother for their keen interest in my studies.

Author

Thunder Bay, Ontario.

August, 1984.

TABLE OF CONTENTS

TABLE OF CONTENTS continued...

LIST OF TABLES

LIST OF TABLES continued...

LIST OF FIGURES

LIST OF FIGURES continued... PAGE

LIST OF FIGURES continued...

LIST OF FIGURES continued...

LIST OF FIGURES continued...

LIST OF FIGURES continued...

LIST OF FIGURES continued...

LIST OF FIGURES continued...

LIST OF FIGURES continued...

LIST OF FIGURES continued...

LIST OF FIGURES continued...

LIST OF FIGURES continued...

LIST OF FIGURES continued...

LIST OF FIGURES continued...

LIST OF FIGURES continued...

LIST OF FIGURES continued....

LIST OF FIGURES continued...

LIST OF FIGURES continued.....

LIST OF FIGURES.continued...

LIST OF FIGURES continued...

CHAPTER I

INTRODUCTION AND BASIC THEORY

I-1: INTRODUCTION

The dielectric absorption approach has been the subject of considerable interest in dealing with a variety of problems: studies of (i) the properties and uses of commercial dielectric materials, and (ii) the structure and molecular forces in different types of systems. A vast majority of dielectric studies (1,2) for gaining information of the molecular structure in dilute solutions of a polar substance in a non-polar liquid or in pure polar liquids has been carried out at microwave frequencies. Aromatic molecules containing rotatable polar groups have been studied extensively by the dielectric absorption technique (3). Information about the dielectric properties of agricultural materials (4,5) as well as systems of biological interest (6,7) have also been the subject of applied studies in this area. Considerable information has also been obtained from dielectric absorption measurements of polymers and their aqueous solutions (8). Dielectric measurements (9) have provided a sensitive means of investigating the properties and uses of commercial dielectric materials in the solid phase.

Dielectric studies of a wide variety of polar solutes dispersed in non-polar solvents of varying viscosities

have indicated that the molecular relaxation times are more sensitive to the viscosity of the medium than the group relaxation times. Consequently, attempts have been made to separate the two processes by increasing the solvent viscosity. In recent years, the dielectric absorption studies of polar solutes dispersed in polystyrene matrices have received considerable attention in the literature. This method has proved successful for determining the accurate intramolecular energy barriers (10,11) which can also be obtained with the other relaxation techniques (12). One of the great advantages of this technique is that for a system with a flexible polar molecule, where there exists a possibility of simultaneous molecular and intramolecular processes, the relaxation time for the former can be increased to such an extent that either it may be slowed down considerably or may even be eliminated owing to the high viscous surrounding medium, so that either or both the processes may be studied separately. Such a technique appeared more straightforward in comparison to the dielectric solution studies, since in the latter situation complications are frequently met owing to the overlap of the different types of absorption processes which for their separation require a Budó analysis. In a number of cases, however, the latter is now known to be unsatisfactory (13). Moreover, the

frequency and temperature ranges accessible to the solution studies are fairly limited, and hence the relaxation parameters cannot be deduced with reasonable accuracy. However, these limitations do not seem to be in the way of the polymer matrix technique, as different instruments can be used to cover a wide frequency range of investigations over a broad range of temperature, (i.e. from liquid nitrogen temperature ($\sim$80 K) to the glass transition temperature of the matrix system). Thus, it seemed that the polystyrene matrix technique can be used more reliably for determining the relaxation parameters comparable to those determined by other direct relaxation methods.

It is now well established that dielectric studies of solutes dispersed in a polystyrene matrix are especially suited to group-relaxation studies and may lead to the accurate determination of intramolecular relaxation parameters (energy barriers). Most recently several other molecular glass-forming solvent systems, namely, cis-decalin, o-terphenyl, and polyphenyl ether (bis m(m-phenoxy-phenoxy)phenyl ether, commonly known as Santovac®) have been used by polymer matrix techniques. Previous works (16) have demonstrated that the intramolecular enthalpies of activation do not change appreciably in any of these solvents.

The phenomenon of hydrogen bonding, because of its special significance in the fields of chemistry, chemical physics and molecular biology, has been of great interest over the last three decades and has stimulated a large and growing volume of study. Infrared absorption and nuclear magnetic resonance spectroscopy have provided very sensitive means of detecting hydrogen bond formation and have been extensively employed in both qualitative and quantitative studies of hydrogen-bonded systems. These are not the only tools available, and many other techniques have provided important results. Each method has its own particular assets and limitations in its application to hydrogen bonding, and these have been well described and discussed elsewhere (14,15). Dielectric absorption techniques are becoming increasingly important as a means for studying the nature and strength of hydrogen bonding. Several texts on hydrogen bonding (14,17,18) and books and reviews on dielectric studies (1,19-21) contain contributions on dielectric phenomenon of hydrogen bonding systems. Of particular interest is the application of relaxation kinetics to these systems which has recently become an important and promising experimental technique.

Relaxation studies by various techniques on hydrogen bonding have been reviewed (22-24) which reveal

the potential of these techniques.

The research work presented in this thesis is concerned primarily with dielectric relaxation studies of some potential systems involving molecular interaction particularly intermolecular and/or intramolecular hydrogen bonding as well as of some related molecules in which polystyrene and several other glass-forming media are utilized as solvents. Relaxation studies for these systems provide Eyring activation parameters for both the molecular and intramolecular motions which, in turn, can reveal molecular size and structure as well as the nature of molecular interactions involved therein.

The basic theory, experimental techniques, sample preparation, and the methods of evaluation of relaxation parameters from dielectric data are described in Chapers I and II.

Chapter III describes a study of some fairly polar, almost spherical, rigid molecules in polystyrene matrices and for some cases in other glass forming media too. The molecular relaxation parameters have been found to vary as the size, shape and volume of the molecules, and the dispersion medium are altered. The molecular

relaxation parameters for these rigid molecules are used for the assignment of a particular process in similarly sized flexible and rigid molecules in different glassy media in the following chapters.

Chapter IV gives a study of some aliphatic long-chain primary alcohols and thiols in the usual concentration range of polystyrene matrices (∿5 % by wt.). No evidence for intermolecular hydrogen bonding is found at the low concentrations employed in this study of alcohols and thiols in polystyrene matrices.

The study of molecular relaxation of 1,1,1-trichloroethane, a fairly polar spherical rigid molecule in another almost similar-sized, spherical non-polar molecule, carbontetrachloride, is described in Chapter V. The influence of solute concentration upon the relaxation parameters, as well as on the dielectric loss factors, has been studied and discussed in this chapter. These are studies of weak molecular interaction and are also useful in conjunction with other studies on virtually spherical molecules in the next chapter.

Chapter VI includes the dielectric relaxation study for some simple, almost spherical alcohols in

different dispersion media at various concentrations. At normal concentration (∿5 % by wt.) no evidence for intermolecular hydrogen bonding, at moderate concentration hydrogen bonding in G.O.T.P. and at higher concentration evidence for polymeric aggregates are found in polystyrene matrices. tert-Butanol has also been studied in the pure solid state and in carbontetrachloride solution at various concentrations. The effect of solute concentration on the dielectric loss factor and on the relaxation parameters has been discussed.

Chapter VII describes a study of some potentially intramolecular hydrogen bonded substituted phenols in cis-decalin, G.O.T.P. and Santovac® and introduces the influence of conjugation on -OH group relaxation. In most of the cases, hydroxyl group relaxation is observed. The influence of (a) the strength of intramolecular hydrogen bond, (b) an electron withdrawing group at the para-position of the ring, (c) bulky tert-butyl group at the ortho-positions of the ring and (d) the nature of the dispersion medium upon the relaxation parameters for hydroxyl group has been discussed. The possibility of proton tunneling in these substituted phenols and in tropolone is considered.

I-2: BASIC THEORY

The fundamental theories and basic equations for dielectric absorption techniques are well established. This is concerned mainly with the polarization and dielectric absorption due to dipole orientation (9).

When one investigates the properties of certain capacitors, it leads to the concept of dielectric constant which is better described by the term dielectric permittivity. When alternating current is switched on, the capacitor will have alternating positive charges and negative charges, and these charges depend on the frequency of the alternating current. The dielectric constant, or permittivity ε', is a characteristic of the medium between two charges. It may be defined as the ratio of the field strength in vacuum to that in the material for the same distribution of charges. It is also given by the ratio of capacitance C, of a condenser filled with the material to the capacitance C_o, of the empty condenser.

At lower frequencies for most simple molecules, the measured dielectric constant does not vary with the measuring frequency and contains contributions from the orientation, atomic and electronic polarization. In this

frequency range the dipole and the field are in phase and the measured dielectric constant has the maximum value and is termed the static dielectric constant, ε_o. As the frequency is increased up to the microwave region, the dipole at some stage lags behind the measuring field and the resulting phase difference, $|\delta|$ between the applied voltage and reorientation of the dipoles causes a dissipation of energy known as Joule heating which is measured by the dielectric loss $|\varepsilon''|$ defined by:

$$\varepsilon'' = \varepsilon' \tan\delta \qquad \text{I-1}$$

where ε' is the real part of the dielectric constant and $\tan\delta$ is the loss tangent or energy dissipation factor. In this high frequency region the dielectric constant becomes a complex quantity (ε^*) where:

$$\varepsilon^* = \varepsilon' - i\varepsilon'' \quad (\text{where } i = (-1)^{\frac{1}{2}}) \qquad \text{I-2}$$

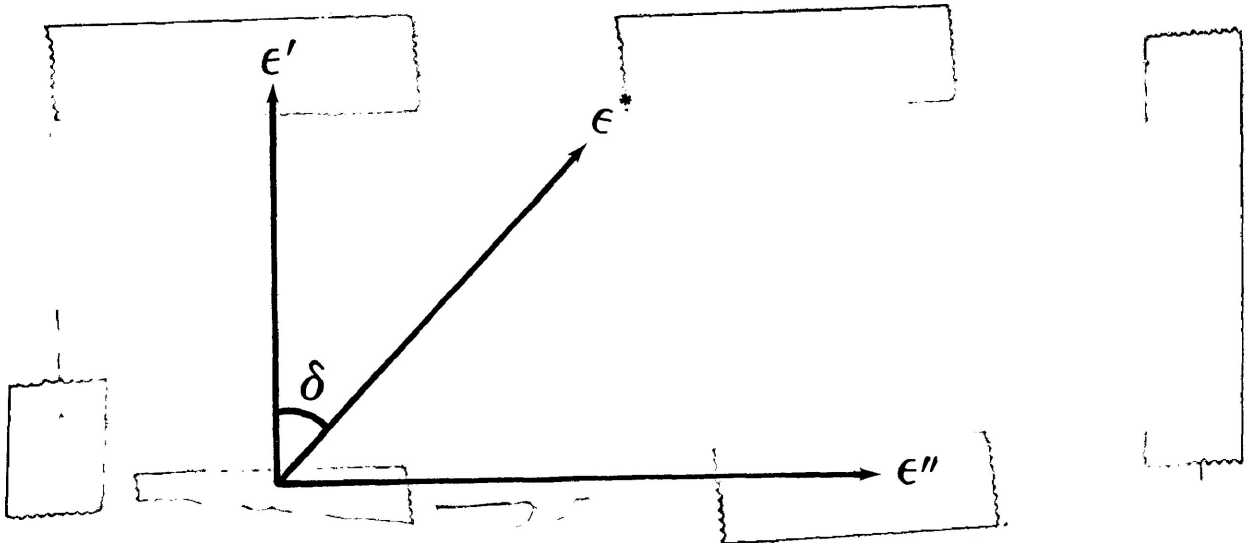

FIGURE I-1: Relationship between ε', ε'' and $\tan\delta$ in the complex quantity of dielectric constant (ε^*).

FIGURE I-2:

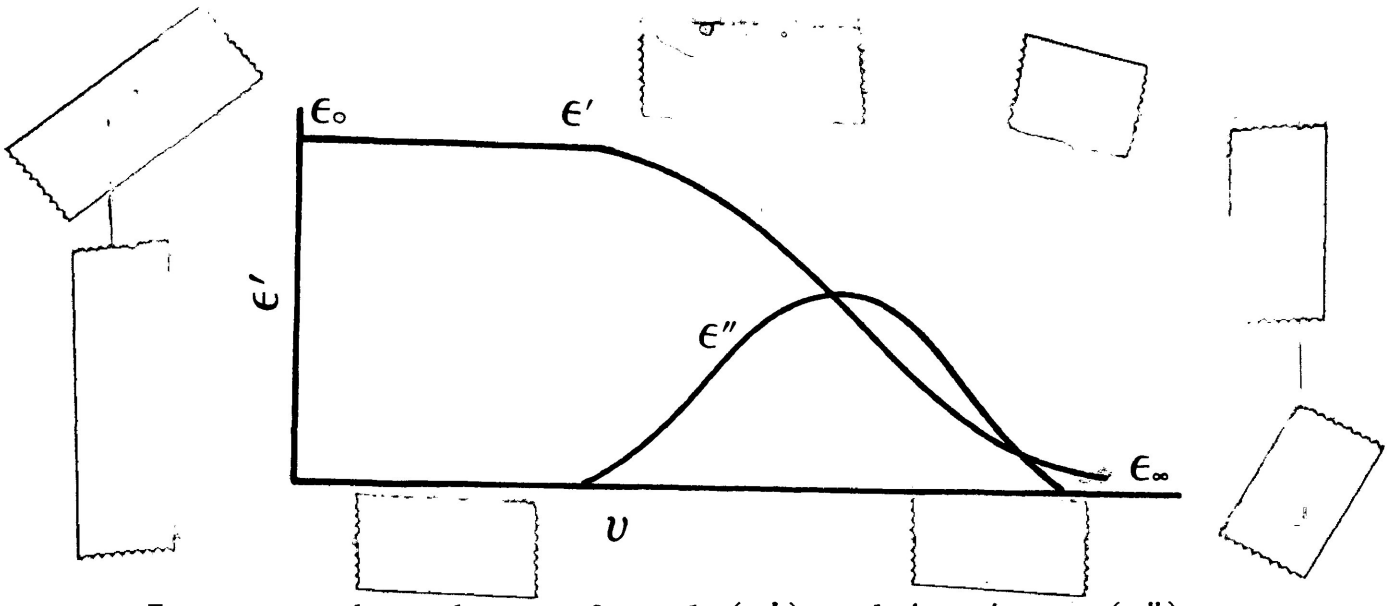

Frequency dependence of real (ε') and imaginary (ε") parts of the permittivity in a relaxation region.

At low frequencies, providing that the molecule is sufficiently small and the retarding force is not great, the dipole responds instantaneously to the field variation with time, but as the frequency is increased, the motion of the molecules is not sufficiently rapid to maintain equilibrium with the field variation. Hence, there is a time lag in the response of the molecules with respect to the field and the polarization P_t at any time t is less than the equilibrium value P_o, as described by the equation:

$$P_t = P_o \, e^{-t/\tau} \qquad \text{I-3}$$

where τ is called the relaxation time of the dielectric. When $\tau = t$:

$$P_t = P_o \cdot \frac{1}{e}$$

So the relaxation time may also be defined as the time in which the polarization is reduced to 1/e times its original value when the field is switched off.

The frequency dependence of the complex permittivity in the region of dielectric absorption for a system characterized by a single discrete relaxation time is given by the Debye equation (25,26):

$$\varepsilon^* = \varepsilon' - i\varepsilon'' = \varepsilon_\infty + \frac{\varepsilon_o - \varepsilon_\infty}{1+i\omega\tau} \qquad \text{I-4}$$

where $\omega = 2\pi\nu$ = the angular frequency in rad s^{-1} and ν is the measuring frequency. Separating the real and imaginary parts:

$$\varepsilon' = \varepsilon_\infty + \frac{\varepsilon_o - \varepsilon_\infty}{1+(\omega\tau)^2} \qquad \text{I-5}$$

and

$$\varepsilon'' = \frac{(\varepsilon_o - \varepsilon_\infty)\omega\tau}{1+(\omega\tau)^2} \qquad \text{I-6}$$

From Equation I-6 it is evident that ε'' is maximum for $\omega\tau = 1$ and:

$$\varepsilon''_{max} = \frac{\varepsilon_o - \varepsilon_\infty}{2} \qquad \text{I-7}$$

Elimination of $\omega\tau$ from equations I-5 and I-6 gives:

$$(\varepsilon' - \frac{\varepsilon_o+\varepsilon_\infty}{2})^2 + (\varepsilon'')^2 = (\frac{\varepsilon_o-\varepsilon_\infty}{2})^2 \qquad \text{I-8}$$

This is the equation of a circle with the centre lying on the abscissa. The locus of ε' and ε'' in an Argand diagram is a semi-circle of radius $(\varepsilon_o-\varepsilon_\infty)/2$ and is known as the Cole-Cole plot (27).

For many systems these equations may be satisfactorily valid, but for the systems, where more than one relaxation process is involved in the dielectric absorption, the analysis of experimental data becomes more complicated. In this case, the centre of the semi-circle is often depressed below the ε'-axis, and the experimental data can normally be represented by an equation developed by Cole and Cole (27):

$$\varepsilon^* = \varepsilon' - i\varepsilon'' = \varepsilon_\infty + \frac{\varepsilon_o - \varepsilon_\infty}{1+(i\omega\tau_o)^{1-\alpha}} \qquad \text{I-9}$$

where τ_o is the mean relaxation time and is obtained from:

$$\tau_o = \frac{1}{2\pi\nu_{max}}$$

where ν_{max} is the frequency at which maximum absorption occurs, α is the distribution parameters, which may have values between 0 and 1, while its deviation from zero measures the distribution of relaxation times. When $\alpha = 0$, the Debye equation is obtained.

A number of other functions has been considered for the non-Debye type of absorption curves. Cole-Davidson (28) have formulated a function which describes right-skewed arcs. The equation is given by:

$$\varepsilon^* = \varepsilon' - i\varepsilon'' = \varepsilon_\infty + \frac{\varepsilon_o - \varepsilon_\infty}{(1+i\omega\tau)^h} \qquad \text{I-10}$$

where h is a constant which may have values $0 \leqslant h \leqslant 1$, with h = 1 corresponding to the Debye equation. This equation seems to be very successful in representing the behaviour of substances at low temperature. It is also often employed to interpret the dielectric absorption for a relaxation mechanism involving cooperative motion (29,30).

The most frequently used empirical expression for non-Debye types of relaxation is the Fuoss-Kirkwood relation (31) given by:

$$\varepsilon'' = \varepsilon''_{max}\ \mathrm{sech}[\beta \ln(\nu_{obs}/\nu_{max})] \qquad \text{I-11}$$

where ν_{obs} is the observed frequency in Hz. and ν_{max} is the frequency at which maximum absorption occurs and β is an empirical constant known as the distribution parameter. This measures the absorption width and may have values between unity for a single relaxation and zero for an infinite range.

For molecules, which contain a rotatable polar group, dielectric absorption may often be characterized by two discrete relaxation times corresponding to molecular and intramolecular rotations. Budó (32) considered that for multiple discrete relaxation processes the complex dielectric constant could be represented by the superimposition of overlapping Debye absorptions. Thus, for systems having two discrete processes with relaxation times τ_1 and τ_2 the following equations can be deduced:

$$\frac{\varepsilon' - \varepsilon_\infty}{\varepsilon_o - \varepsilon_\infty} = \frac{C_1}{1+(\omega\tau_1)^2} + \frac{C_2}{1+(\omega\tau_2)^2} \qquad \text{II-12}$$

$$\frac{\varepsilon''}{\varepsilon_o - \varepsilon_\infty} = \frac{C_1\omega\tau_1}{1+(\omega\tau_1)^2} + \frac{C_2\omega\tau_2}{1+(\omega\tau_2)^2} \qquad \text{II-13}$$

where C_1 and C_2 are the weighting factors of the two contributing absorptions and

$$C_1 + C_2 = 1$$

When C_1/C_2 is small, an almost symmetrical Cole-Cole plot results. The dielectric absorption data for systems with significant τ_1/τ_2 and C_1/C_2 ratio may separate wholly or partially into two distinct absorption regions.

A number of models has been suggested to account for the mechanism of the molecular relaxation processes. Debye (25) has suggested a simple relaxation mechanism and according to his theory each dipole has two equilibrium positions separated by an energy barrier, ΔE. In such a situation the dipoles will oscillate within the potential minima, and sometimes acquire enough energy to jump the barrier, but at any instant there are equal numbers of dipoles occupying each position. If an electric field is applied, a small excess of dipoles will rotate into more favourable positions, thus giving rise to polarization.

The Eyring rate theory (33) is often applied to the reorientation of an electric dipole between two equilibrium positions. According to this treatment if

ΔG_E is the free energy of activation for the dipole to reach the top of the barrier opposing reorientation, then the number of times such a reorientation occurs per second is given by the expression:

$$1/\tau = (KkT/h) \exp(-\Delta G_E/RT) \qquad \text{I-14}$$

where T is the absolute temperature, h is Plank's constant, R is the universal gas constant, k is the Boltzmann's constant and K is the transmission coefficient normally taken to be 1; this corresponds with the case that each time the dipolar molecule is excited to the top of the energy barrier it continues to move in the same direction to the adjacent minimum position. Thus, the process is one of relaxation between two equilibrium positions, but it is commonly referred to as rotation. Using $\Delta G_E = \Delta H_E - T\Delta S_E$ and taking logarithms the equation I-14 can be rearranged to the following form:

$$\ln(\tau T) = (\Delta H_E/RT) + \ln(h/k) - (\Delta S_E/R) \qquad \text{I-15}$$

where ΔH_E is the enthalpy of activation, and ΔS_E the entropy of activation for this dipole relaxation process. From this equation it is evident that a plot of $\log T\tau$ versus $1/T$. should give a straight line of which the slope and the intercept will lead to the values of ΔH_E and ΔS_E respectively.

Through a computer program the relaxation time τ and the free energy of activation ΔG_E at different temperatures can also be obtained.

REFERENCES

1. N. E. Hill, W. E. Vaughan, A. H. Price and M. Davies, "Dielectric Properties and Molecular Behaviour", Van Nostrand Reinhold, London (1969).

2. C. P. Smyth, "Dielectric Behaviour and Structure", McGraw Hill, London (1955).

3. C. P. Smyth, Adv. Mol. Relax. Processes, 1(1967-68)1.

4. T.P. Corcoran, O. S. Nelson, E. L. Stetson and W.C. Schlaphoff, Transactions of the ASAE, 13(No.3) (1970)348.

5. O. S. Nelson, Transactions of the ASAE, 16(2) (1973)384.

6. E. H. Grant, S. E. Keefe and S. Takashima, J. Phys. Chem., 72, 4373(1968).

7. J. L. Selefran, J. L. Salefran, G.Delbos, Cl. Marzat and A. M. Bottreau, Adv. Mol. Relax. Inter. Proc., 10, 35(1977).

8. G. P. South and E. H. Grant, Biopolymers, 13, 1777(1974).

9. R. J. Meakins, "Progress in Dielectrics", 3, 152(1961).

10. M. Davies and J. Swain, Trans. Faraday Soc., 67, 1637(1971).

11. S. P. Tay, S. Walker and E. Wyn-Jones, Adv. Mol. Relax. Inter. Proc., 13, 47(1978).

12. W. J. Orville-Thomas, (ed.), "Internal Rotation in Molecules", John Wiley and Sons, New York, (1979).

13. J. Crossley, S. P. Tay and S. Walker, Adv. Mol. Relax. Proces., 6, 79(1974).

14. G. C. Pimental and A. L. McClellan, "The Hydrogen Bond", W. H. Freeman and Co., London (1960).

15. Symposium on the Hydrogen Bonding, Ljubljana, Pergamon Press, London (1957).

16. M. A. Kashem, M.Sc. Thesis, Lakehead University, (1982).

17. D. Hadzi and H. W. Thompson, Ed., "Hydrogen Bonding", Pergamon Press, Oxford (1959).

18. P. Schuster, G. Zundel and C. Sandorfy, Ed., "The Hydrogen Bond", North Holland Publishing Co., Oxford (1976).

19. (a) M. Remko and J. Polcin, Adv. Mol. Relax. Proc., 11, 249(1977).

(b) B. M. Rode, A. Engelbrecht and W. Jakabetz, Chem. Phys. Lett., 18, 185(1973).

(c) M. Remko, Adv. Mol. Relax. Proc., 11, 291(1977).

(d) P. Schuster and Th. Franck. Chem. Phys. Lett., 2, 587(1968).

(e) M. Remko, Adv. Mol. Relax. Inter. Proc., 15, 193(1979).

(f) P. Bosi, G. Zerbi and E. Clementi, J. Chem. Phys., 66, 3396(1977).

20. M. Davies, Ann. Reports on Progress of Chemistry, 67, 65(1970).

21. V. V. Daniel. "Dielectric Relaxation". Academic Press, New York (1967).

22. E. Jakusek and L. Sobezyk, Dielectric and Related Mol. Processes, 3, 108(1976).

23. J. Crossley, R.I.C. Reviews, 69(1971).

24. (a) R. Zana and J. Lang, Adv. Mol. Relax. Proc., 7, 21(1975).

(b) J. Crossley, Adv. Mol. Relax. Proc., 2, 69(1970).

(c) J. Emery and S. Gasse, Adv. Mol. Relax. Inter. Proc., 12, 47(1978).

25. P. Debye, Polar Molecules, Chemical Catalog, N. Y. (1929).

26. H. Fröhlich, "Theory of Dielectrics", Clarendon, Oxford (1949).

27. K. S. Cole and R. H. Cole, J. Chem. Phys., 9, 341(1941).

28. D. W. Davidson and R. H. Cole, Ibid., 19, 1484(1951).

29. M. Nakamura, H. Takahashi and K. Higasi, Bull. Chem. Soc. Jpn., 47, 1593(1974).

30. T. G. Copeland and D. J. Denney, J. Phys. Chem., 80, 210(1976).

31. R. M. Fuoss and J. G. Kirkwood, J. Amer. Chem. Soc., 63, 385(1941).

32. A. Budó, Phys. Z., 39, 706(1938).

33. S. Glasstone, K. J. Laidler and H. Eyring, "The Theory of Rate Processes", McGraw-Hill, New York (1941).

CHAPTER II

APPARATUS AND EXPERIMENTAL

II-1: INTRODUCTION

When a material of dielectric constant ε completely fills the space between the two plates of an ideal capacitor, the dielectric constant is defined by the simple ratio:

$$\varepsilon = \frac{C}{C_o} \qquad \text{II-1}$$

where C is the capacitance when the space is filled with the material and C_o is the capacitance measured when there is a perfect vacuum between the plates. In fact, ε is not a constant; it is a frequency dependent complex quantity, ε^*, defined as:

$$\varepsilon^* = \varepsilon' - i\varepsilon'' \qquad \text{II-2}$$

where $i = \sqrt{-1}$

If a sinusoidal potential of amplitude E and frequency ω rad s^{-1} is applied to the capacitor, then the current, I flowing through the circuit can be expressed as:

$$I = E\omega C = E\omega C_o\ (\varepsilon' - i\varepsilon'') \qquad \text{II-3}$$

In this equation the real component $E\omega C_o\varepsilon'$, known as the charging current, is 90° out of phase with the applied potential, and therefore, does not involve any electrical work. The imaginary component, $E\omega C_o\varepsilon''$, known as the loss current, is, however, in phase with the applied potential and is related to the energy dissipated as heat since it causes some electrical work to be done given by the dot product $EI = E^2\omega C_o\varepsilon''$. Now, if we define δ as the angle between the total current and the charging current axis, (i.e., the angle by which the charging current fails to become 90° out of phase with the potential) then:

$$\tan \delta = \frac{\text{loss current}}{\text{charging current}} = \frac{\varepsilon''}{\varepsilon'} \qquad \text{II-4}$$

where ε' is the observed dielectric constant according to equation II-1 and ε'' is known as the loss factor, which is directly proportional to the concentration of the polar material in the dielectric. These are the basic principles of all dielectric measurements.

Most of the compounds studied for this thesis were either as pure solid or solutes dissolved in (a) carbon tetrachloride, (b) cis-decalin, (c) polyphenyl ether, (bis m(m-phenoxy phenoxy)phenyl ether), commercially known as Santovac® (1), (d) glassy o-terphenyl, and (e) polystyrene matrices. The solutes were either

solids or liquids. Dielectric measurements were performed by the use of the General Radio 1621 Precision Capacitance Measurement System. Actual measurements were made by bringing the bridge into balance as indicated by the detector for solutions studied in a variety of 3-terminal co-axial and parallel-plate capacitance cells. The glass transition temperature, T_g, of some of the chemical systems, were measured by the use of glass transition measurement apparatus. Both the 3-terminal co-axial cell and the glass transition measurement apparatus were designed by Mr. B. K. Morgan of this laboratory.

II-2: THREE-TERMINAL CO-AXIAL CELL

The 3-terminal co-axial cells which were used for this work are illustrated in the following figures (reproduced by the courtesy of D. L. Gourlay (2)). Figure II-1 and Figure II-2 present the cross-sections of the 3-terminal co-axial and parallel plate capacitance cells. The liquid cell is circular and has concentric stainless steel electrodes, A and B. Their shape permits the rapid transfer of heat to or from the solid aluminium case "C". The undersides of the electrodes are insulated from the case by a 0.25 cm thick Teflon disk. A 0.50 cm thick Teflon sleeve insulated the outer circumference of electrode

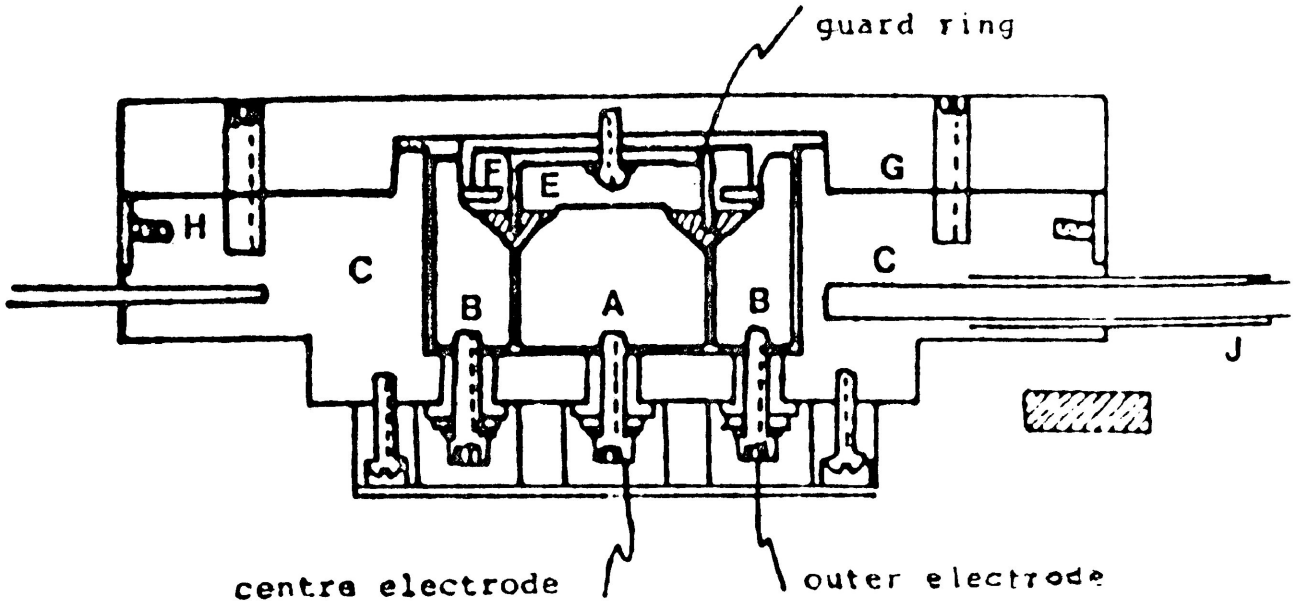

FIGURE II-1: Three-terminal coaxial cell

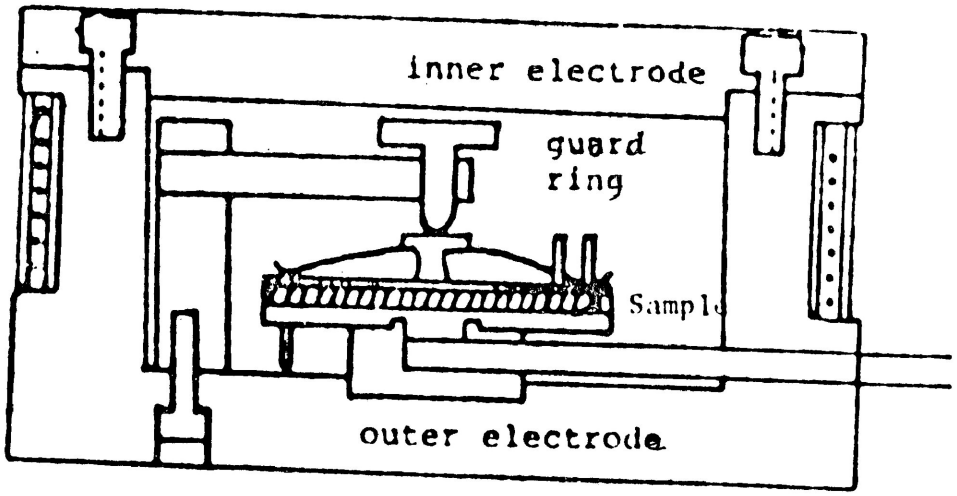

FIGURE II-2: Three-terminal parallel plate capacitance cell

B. The fringe field is practically eliminated by the presence of the grounded case below and a grounded guard ring, E, above. The circular Teflon cap, F, fits closely into the top of electrode B to prevent the escape of liquid vapours.

The sample can be introduced into the 0.5 cm gap between electrodes A and B by a disposable pipette. One and a half ml of sample is sufficient to fill the cell. To clean the cell, the sample is sucked up with a dropper and the electrodes are flushed with solvents (first with acetone and then with cyclohexane) several times. The electrodes are dried by pushing down cotton swabs into the filling hole, wiping around the electrodes by wide strips of cardboard and finally, blowing hot air.

The lid of the cell, G, is secured to the case by four recessed bolts. The surface between G and C is coated with heat conductive grease of the type used with semiconductor heat-sinks. The outer cell wall is insulated by a ring of microcellular polystyrene foam which is flush with the top of G. The insulation has a wall thickness of 5 cm. The cell's underside is also insulated with a 23 cm diameter and 5 cm thick disk of polystyrene. Figure II-2 presents the 3-terminal circular parallel-plate capacitance

cell which was used for dielectric measurements of samples dispersed in polystyrene matrices in the form of a solid disk.

Each cell can be rapidly cooled from the top by conduction through a flat-bottomed, styrofoam insulated, liquid nitrogen container. Heating balance was accomplished through a temperature control circuit consisting of a thermocouple, and a thermoelectric temperature controller model 3814021133 unit (accuracy $\sim\pm 0.1^{\circ}C$) using a nichrome wire heating element surrounding the cell.

II-3: THE GENERAL RADIO BRIDGE

The dielectric measurements for the purpose of this thesis were carried out with the GR1621 Precision Capacitance Measurement System which consists of a GR1616 Precision Capacitance bridge with a GR1316 Oscillator and a GR1238 Detector. This GR1621 system allows measurement of the capacitance and conductivity of a capacitor very precisely at frequencies ranging from 10 Hz to 10^5 Hz.

The GR bridge measures the capacitance and conductivity of the capacitor, which can be related to the components of the complex permittivity by the following equations (3):

$$\varepsilon' = C/C_o \qquad \text{II-5}$$

and

$$\varepsilon'' = G/\omega C_o \qquad \text{II-6}$$

where C_o is the capacitance of the empty condenser; $\omega = 2\pi\nu$ is the angular frequency of the applied field in radian s^{-1} and ν is the frequency in kHz.

Since it is difficult to obtain C_o through measurement in the case of the parallel plate capacitance cell, C_o may be calculated from the relation (4):

$$C_o = \frac{0.08842A}{d} \qquad \text{II-7}$$

where A is the effective area in square centimeters and d is the spacing of the plates in centimeters. Elimination of C_o from these equations gives:

$$\varepsilon' = \frac{Cd}{0.08842A} \qquad \text{II-8}$$

and

$$\varepsilon'' = \frac{\varepsilon' G}{\omega C} \qquad \text{II-9}$$

where C is the capacitance of the cell with the sample in picofarads and G is the conductivity of the system in picomhos. ε'' may be determined either from Equation II-6 or from a combination of Equations II-8 and II-9, if the values of C_o and A are known.

In order to determine the relevant constants (C_o for co-axial and A for parallel plate cells), both systems were calibrated by studying samples of precisely known ε' at a given temperature. The coaxial cell was calibrated with purified cyclohexane at room temperature. A quartz disk, supplied by Rutherford Research Products Co., of 0.1318 cm thickness and a diameter of 3.819 cm was used for calibration of parallel-plate capacitance cell. Calibration studies were also carried out down to liquid nitrogen temperatures to see if there was any variation between values of ε' determined at room temperature and those at lower temperatures. Variation was considered negligible.

II-4: SAMPLE PREPARATION AND DIELECTRIC MEASUREMENTS

Samples placed in the coaxial cells were pure liquid or liquid solutions. The solutions were prepared by adding a given quantity of solute to a required quantity

of solvent such that the resultant solution had a required concentration depending upon the magnitude of the dipole moment of the solute and, in certain cases, on the solubility of the solute in the solvent. The cells were then filled with this solution for dielectric measurement.

In the case of solutions of polar solutes dispersed in atactic polystyrene, the samples were prepared by employing the procedure similar to that described by Davies and Swain (5). The desired amount of solute (0.12-0.20) and polystyrene pellets (2.0 g) was dissolved in ∿10 ml of 1,2-trans-dichloroethylene, in a porcelain crucible. The mixture was stirred thoroughly until it dissolved completely, followed by evaporation in a drying oven and vacuum oven at about 85-100°C. The plastic mass was then placed in a stainless steel die, heated to ∿110°C, pressed by applying a pressure of five tons, cooled, removed, trimmed to size and its average thickness was measured. The weight of the disk was also noted and the molar concentration of the solute in the matrix was calculated according to the formula given by Tay and Walker (6) as:

$$\text{concentration} = \frac{\text{wt. of solute used}}{\text{mol. wt. of solute}} \times \frac{\text{wt. of disk}}{\text{wt. of P.S.+ Solute}} \times \frac{1000}{\text{vol. of disk}}$$

The polystyrene matrix disk was then clamped between the electrodes of the parallel-plate capacitance cell and the

dielectric measurement was carried out.

For a chemical system, the dielectric characteristics of which were unknown, the sample was cooled down to near liquid nitrogen temperature and slowly heated up to the glass transition temperature while capacitance and conductance at recorded temperatures were taken periodically. From the resultant plot of ε'' or tan δ (as calculated from experimental data) versus temperature (K) at fixed frequency (usually 50 Hz and 1 kHz), suspected areas of dielectric absorption were identified. The system was then heated again to room temperature and cooled quickly to some temperature well below the temperature at which the absorption process was expected to begin from the lowest frequency of the measurement. Full frequency dielectric measurements at specific temperatures were then carried out so as to obtain a broad $\log\nu_{max}$ range as possible. The temperature was recorded to an accuracy of ±0.1°C with the help of a Newport 264-3 platinum resistance thermometer.

II-5: ANALYSIS OF EXPERIMENTAL DATA

The experimental data, obtained by dielectric measurements, were analysed by the use of a series of calculator and computer programs. The programs were written

in the APL language. The dielectric loss for the pure solute was obtained by subtracting the loss for the pure solvent at each frequency from that observed for the samples solution, that is:

$$\varepsilon''_{solute} = \varepsilon''_{solution} - \varepsilon''_{solvent}$$

For each temperature, the dielectric loss values at different frequencies were subjected to analysis by the Fuoss-Kirkwood equation, (Equation I-11), the linear form of which is:

$$\cosh^{-1}\left(\frac{\varepsilon''_{max}}{\varepsilon''}\right) = 2.303\,\beta\,(\log\nu_{max} - \log\nu) \qquad \text{II-10}$$

By iteration the program (entitled FUOSSK) finds that value of ε''_{max} which provides the best straight line fit to the plot of $\cosh^{-1}(\varepsilon''_{max}/\varepsilon'')$ versus $\log\nu$. The slope of the straight line gave the value of the distribution parameter (β), and the frequency of maximum absorption (ν_{max}) was obtained from the slope and the intercept of the line on the $\cosh^{-1}$ axis.

The Fuoss-Kirkwood equation does not deal with the real part of the complex permittivity nor does it

deal with the limiting values at low and high frequencies, ε_o and ε_∞ , respectively, except that the total dispersion is given by the expression:

$$\Delta\varepsilon = \varepsilon_o - \varepsilon_\infty = \frac{2\varepsilon''_{max}}{\beta} \qquad \text{II-11}$$

The analysis was therefore, supplemented with the Cole-Cole Equation (I-9) to obtain ε_∞ in conjunction with the following relation (7) for the value of α, the Cole-Cole distribution parameter:

$$\beta = \frac{1-\alpha}{\sqrt{2}\cos(\frac{\pi(1-\alpha)}{4})} \qquad \text{II-12}$$

Using the values of ε' at various frequencies several estimates of ε_∞ were obtained and the average was calculated along with a value for ε' at the frequency of maximum loss.

The results of the foregoing analysis were utilized to obtain the effective dipole moments (μ) involved in the relaxation process from both the Debye (8) Equation (II-13) and the Onsager (9) Equation (II-14):

$$\mu^2 = \frac{2700\ kT(\varepsilon_o - \varepsilon_\infty)}{4\pi NC(\varepsilon'_m + 2)^2} \qquad \text{II-13}$$

$$\mu^2 = \frac{900\ kT(2\varepsilon_o + \varepsilon_\infty)(\varepsilon_o - \varepsilon_\infty)}{4\pi NC\varepsilon_o(\varepsilon_\infty + 2)^2} \qquad \text{II-14}$$

where the value of $\varepsilon_o - \varepsilon_\infty$ is given by the Equation II-11, ε'_m is the value of ε' at $\omega_{max} = 1/\tau_o = 2\pi\nu_{max}$, ε_o is the static dielectric constant derived from the estimated average of ε_∞, and Equation II-11, C is the concentration in mols litre^{-1}, T is the temperature in K, N is the Avogadro's number and k is the Boltzmann constant. These equations yield μ in units of e.s.u.-cm, but commonly this parameter is expressed in Debye units, where:

$$1\ D = 1x10^{-18}\ \text{e.s.u.-cm}$$

From the observed μ-values at different temperatures extrapolated values of the dipole moment at around room temperatures were estimated by a separate computer program, or manually, for comparison with the corresponding literature values.

Dipole reorientation was considered as rate process and the energy barrier opposing the dielectric relaxation process was obtained by use of the Eyring rate Equation I-15 , a procedure commonly adapted in dielectric work (7,10).

$$\ln(T\tau) = \frac{\Delta H_E}{RT} - \left(\frac{\Delta S_E}{R} - \ln\left(\frac{h}{k}\right)\right) \qquad \text{II -15}$$

The plot of $\log T\tau$ versus 1/T yielded good straight lines of which the slope and the intercept yielded the enthalpy of activation and the entropy of activation, respectively, through a computer program. The program also provided the relaxation times (τ) and the free energies of activation (ΔG_E) at different temperatures according to the Equation, $\Delta G_E = \Delta H_E - T\Delta S_E$.

Cooperative processes usually yielded a bent (a non-Arrhenius behaviour) curve at higher temperature. In this case the Eyring activation parameters were calculated by the limiting slope of the plot $\log T\tau$ versus 1/T at the lower temperature limits.

Standard statistical techniques (11) have been employed in fitting the analysis of the experimental data

with various computer programs which provided different confidence interval widths for important parameters viz., $\log\nu_{max}$, β, and enthalpies and entropies of activation. For the present purpose, however, 95% confidence intervals were chosen as a good representation of experimental error.

The Fuoss-Kirkwood parameters, $\log\nu_{max}$, ε''_{max}, τ and β, and the results of Eyring analysis have been given in tables in relevant chapters.

II-6: GLASS TRANSITION TEMPERATURE MEASUREMENT APPARATUS

This apparatus, shown in Figure II- 3 , was constructed by Mr. B. K. Morgan of this laboratory in consultation with Dr. N. Koizumi of Kyoto University, Japan. It detects linear expansion of solid or frozen liquid samples. Heating the sample N causes the inner pyrex tube to move upwards relative to the outer pyrex tube. This movement is transmitted from the cap of the inner tube to the core of the transducer, C. Movement of the core causes a change in the electromagnetic coupling between the input and output coils of the transducer. The output coil is connected to a strip chart recorder which displays a rising trace as the sample is heated

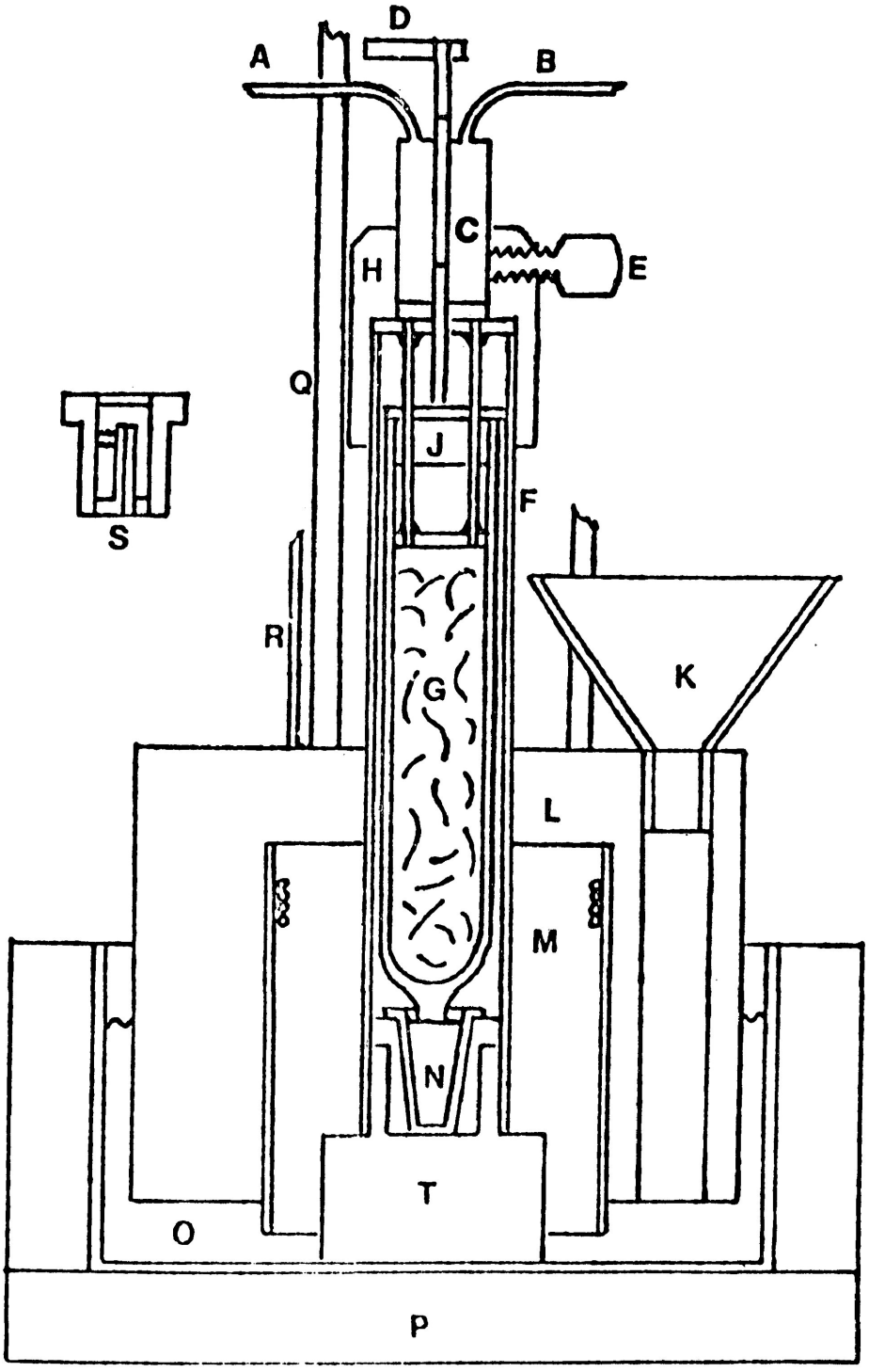

Figure II-3: Glass Transition Temperature Measurement Apparatus.

towards the glass transition temperature. Near the glass transition temperature the trace levels off and then begins to fall as the sample softens. There are two interchangeable sample holders with the apparatus. The sample holder S for the sample solid at room temperature, and N for the samples which are liquid at room temperature.

The solid sample was prepared in the form of a strip roughly 20 mm x 8 mm and 1 or 2 mm thick. The sample was secured at one end by a small screw in a slotted rod which fits freely in sample holders. The liquid sample was poured at room temperature into a disposable polyethylene cup. The cup was placed in its stainless steel holder under the central pyrex tube. The central tube was raised by the cap of the outer tube, to which it was connected by two sliding rods. It was not lowered until the sample had been frozen. The sample holder, sitting within two interlocking circular blocks, M and T, was cooled rapidly by pouring the liquid nitrogen into funnel K. When the sample had been cooled to about 40°C below the expected glass transition temperature, the transducer position was adjusted. The temperature of the sample was then raised manually by raising the digital temperature setting of the controller in increments of 1°C per minute. The temperature was recorded with the help of

a Newport 254-3 platinum resistance thermometer and the temperature was also periodically recorded by hand on the chart until the glass transition temperature passed.

REFERENCES

1. Santovac is the registered trademark of a six-ring meta-linked poly-phenyl ether, bis-m(m-phenoxy phenoxy) phenyl ether, which is a high vacuum medium produced and marketed by Monsanto, Ltd.

2. D. L. Gourlay, M.Sc. Thesis, Lakehead University, Thunder Bay, Ontario, Canada (1982).

3. C. P. Smyth, "Dielectric Behaviour and Structures", McGraw-Hill Book Co., New York, (1955)203.

4. P.E. Terman, "Radio Engineers Handbook". McGraw-Hill Publishing Co. Ltd., London. 1950.

5. M. Davies and J. Swain, Trans. Faraday Soc., 67(1971)1637.

6. S.P. Tay and S. Walker, J. Chem. Phys., 63(1975) 1634.

7. N.E. Hill, W.E. Vaughan, A.H. Price and M. Davies, "Dielectric Properties and Molecular Structure", Van Nostrand-Reinhold, London, England, (1969)292.

8. Ibid., 235.

9. C. J. F. Böttcher. "Theory of Electric Polarization", Elsevier Publishing Co., Amsterdam, Netherlands (1952)323.

10. M. Davies and A. Edwards, Trans. Faraday Soc., 63(1967)3163.

11. B. Ostle, "Statistics in Research", (2nd ed.), Iowa State University Press, Ames, Iowa, U.S.A., 1963.

CHAPTER III

DIELECTRIC RELAXATION PROCESSES OF SOME FAIRLY SPHERICAL, RIGID, POLAR MOLECULES IN SOME ORGANIC GLASSES

III-1: INTRODUCTION

A large number of rigid dipolar molecules has been extensively studied dielectrically in a variety of solvents and in the pure state. Attempts have been made to investigate the dependence of dielectric relaxation time (τ) and enthalpy of activation (ΔH_E) upon such factors as: entropy of activation (ΔS_E), the size and shape of the polar molecules, volume swept out by the molecules in the orientation processes, moments of inertia, the direction of the dipoles within the molecule and also upon the viscosity of the medium.

In an earlier investigation, Higasi (1) showed an almost linear dependence of activation entropy upon the corresponding activation enthalpy for a variety of organic molecules. He tentatively postulated that "the entropy change is zero or has a small negative value if ΔH_E is below 13.4 kJ mol^{-1}". Kalman and Smyth (2) observed the same relationship for the almost spherical molecules, 2,2-dichloropropane, 2,2-dinitropropane, camphor, α-chloronaphthalene, isoquinoline, 2-bromobiphenyl and acridine in Nujol solution. Davies and Edwards (3) have also reported a similar relationship between ΔH_E and ΔS_E for molecular relaxation processes of polar molecules having

various sizes and shapes of the types: camphor, anthrone, cholest-4-ene-3-one, tetracyclone and β-naphthol. This linear dependence between ΔH_E and ΔS_E may be explained qualitatively if the activation energy is assumed to be largely needed to displace adjacent solvent molecules for reorientation of the solute molecule. Thus, the larger the energy required for ΔH_E, the greater will be the local reorganizational entropy. Dicarlo and Smyth (4) studied 4-iodobiphenyl and 2-iodobiphenyl in Nujol and obtained the activation enthalpies of 31.8 and 25.9 kJ mol^{-1}, respectively. The 4-iodobiphenyl molecule, having its dipole moment along the long axis, had a six-times longer molecular relaxation time than that of the 2-iodobiphenyl. This was attributed to a greater volume being swept out by the former molecule in reorienting about its two short axes in comparison with 2-iodobiphenyl, where the principal component of the dipole lies along a short axis of the molecule and relaxation occurs predominantly by rotation around the long axis. Pitt and Smyth (5) demonstrated that for the three rigid dipolar ketones of fairly similar size and shape, viz., anthrone, fluorenone and phenanthrenequinone in benzene solution, the phenanthrenequinone had a longer molecular relaxation time and larger ΔH_E, and this was attributed to a greater volume being swept out by this molecule in orienting about its long axis. Crossley and Walker (6)

examined three non-spherical rigid molecules: quinoline, isoquinoline and phthalazine in cyclohexane solution at 323 K. In these solute molecules of almost identical size and shape, the direction of the dipole moment is varied. It appeared in these molecules that no significant variation of relaxation time was detectable within the limits of the accuracy of measurements. Hassell (7) studied fluoro-, chloro-, bromo- and iodobenzenes in p-xylene at 258 K and found the enthalpies of activation as 5.9, 6.7, 8.4 and 9.2 kJ mol^{-1} respectively. This indicates a slight increase in ΔH_E with an increase in the size of the molecules. Both Hassell (7) and Cooke (8), however, found reasonable correlation between activation enthalpy and volume swept out by the molecule for dilute solutions of mono-halobenzenes, o- and m-dihalobenzenes, nitrobenzene, p-nitrotoluene and p-halotoluenes in p-xylene. Other workers also attempted to explore the dependence of dielectric relaxation time and enthalpy of activation upon direction of the dipole moment within the solute molecule (9), moment of inertia (10) and viscosity of the medium (11,12,13).

In a recent attempt to investigate the effects of solvent on the relaxation parameters of a molecule, a number of solutes has been measured in a variety of

glass forming solvents at temperatures below T_g. These solvents are polystyrene, o-terphenyl, bis(m(m-phenoxy phenoxy) phenyl) ether (Santovac®) and cis-decalin. Extensive studies of carefully selected dipolar rigid molecules in the above solvents, particularly, in a polystyrene matrix, have been reported (10,13,14,15,16). Very broad loss curves were observed for numerous rigid polar solutes, where dipole reorientation necessarily involves whole molecule rotations.

Davies and Edwards (3) studied the spherical rigid dipolar molecule camphor in a polystyrene matrix in the temperature range 243-373 K and in the frequency range 5 Hz to 8.5 GHz. In this temperature and frequency region they found one dielectric dispersion. The Eyring plot, $\log T\tau$ versus $1/T$ for this dispersion was curved, having two slopes above and below the temperature 293 K. The higher temperature slope yielded ΔH_E and ΔS_E values of 3.8 kJ mol^{-1} and 31.4 J K^{-1} mol^{-1}, respectively, whereas the lower temperature slope yielded the corresponding parameters as 21 kJ mol^{-1} and 25 J K^{-1} mol^{-1} respectively. They also observed that the distribution parameter, (β) decreased with the decrease of temperature and this decrease became very pronounced at the temperatures around 293 K. They concluded from this study that the local molecular

environment of camphor undergoes some changes at this temperature from a less rigid to a more rigid form which deserves further study in detail. Clemett and Davies (17) studied spherical rigid dipolar molecules - camphene, camphor and bornyl chloride in the pure solid state and also camphor in camphene solid solution. They obtained very low enthalpies of activation and entropies of activation for the molecular rotation of these molecules as:

	Camphene	Camphor	Bornyl chloride
ΔH_E (kJ mol^{-1})	9.19	7.5	10.5
ΔS_E (J K^{-1} mol^{-1})	-7.9	12.12	7.9

They also found some evidence that the energy barrier increases with the decrease of temperature and suggested that this could be explained by intermolecular interaction. Their Eyring plot was bent which is sometimes an indication of a cooperative process. To obtain a clearcut picture of the molecular rotation of the above molecules we plan to study a number of camphane derivatives in detail in polystyrene matrices and some of the molecules in other media also at very low temperatures (77-300 K) and at low frequency (10 Hz - 10^5 Hz). This study should enable an assessment of Davies' points that ΔH_E for molecular relaxation increases at low temperature. The molecular interaction

may be assessed by varying the dispersion medium whether the dielectric parameters change appreciably with the dispersion medium. Moreover, detailed knowledge of the molecular relaxation parameters and the associated activation energy barriers are essential for the assignment of a particular process in similar-sized flexible and rigid molecules in different dispersion media as will be seen in the following chapters. It is mainly for this second reason that different types of polar rigid molecules have been studied which could also provide, at least, a qualitative interpretation of the activation parameters in terms of size, shape and volume of the dipole units.

III-2: EXPERIMENTAL RESULTS

The dielectric measurements of nine spherical rigid dipolar molecules (listed in Figure III-1) in polystyrene matrices have been made in the frequency range of 10 Hz to 10^5 Hz by the use of a General Radio Precision Capacitance bridge, the procedure being described in Chapter II. In some of the cases other media are also used, viz., GOTP, SV, CCl_4, etc. All the molecules were commercially available with sufficient purity and were dried prior to use.

Figures III-1a to III-9a show the sample plots of dielectric loss, ε'' versus T (K) for the dipolar molecules in the medium mentioned. Sample plots of ε'' versus $\log\nu$ are shown in Figures III-1b to III-9b while Figures III-1c to III-9c, presents the Cole-Cole plots for these molecules in their respective dispersion regions. Sample plots of $\log T\tau$ versus 1/T for different molecules in the mentioned medium are also presented in Figures III-1d to III-9d.

Table III-1 lists the values of Eyring analysis results, ΔH_E, ΔS_E, along with ΔG_E and τ values at 100 K, 150 K and 200 K for each system. Experimental values

of τ, $\log\nu_{max}$, β and ε''_{max} at various temperatures obtained for these molecules from the Fuoss-Kirkwood analysis together with the values of ε_∞ and the experimental dipole moments are listed in Table III-2. The following symbols are employed where appropriate:

P.S. - Polystyrene matrices

G.O.T.P. - Glassy o-Terphenyl

SV - Santovac® (bis(m(m-phenoxy-phenoxy)phenyl)ether

$\Delta T(K)$ - Temperature range in the absolute scale

β-range - Range of variation in the Fuoss-Kirkwood distribution parameters.

ΔG_E - Eyring free energy of activation in kJ mol^{-1}

ΔH_E - Eyring enthalpy of activation in kJ mol^{-1}

ΔS_E - Eyring entropy of activation in J K^{-1} mol^{-1}

ν - frequency in Hz

τ - relaxation time in seconds (s)

FIGURE III-1

1. NORCAMPHOR

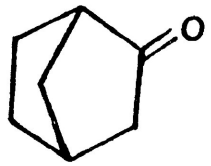

2. CAMPHOR

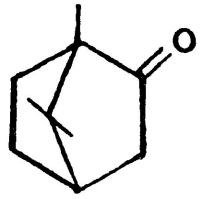

3. CAMPHENE

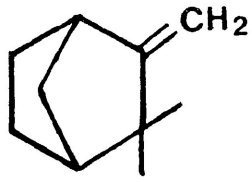

4. 5-NORBORNENE-2-CARBONITRILE

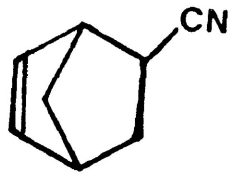

5. 3-CHLORO-2-NORBORNANONE

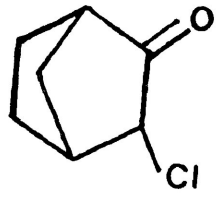

FIGURE III-1 continued...

6. CAMPHOROQUINONE

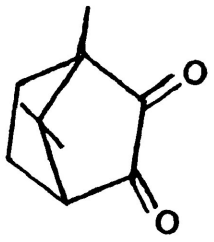

7. exo-2-BROMONORBORNANE

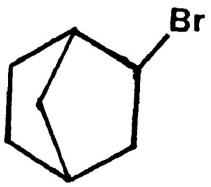

8. 1-FENCHONE

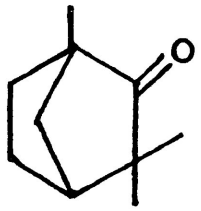

9. 3-METHYLENE-2-NORBORNANONE

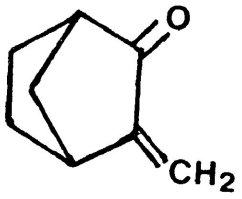

III-3: DISCUSSION

1. Norcamphor

This compound has been studied in four different media, viz., CCl_4, P.S., G.O.T.P. and SV. In all the media except CCl_4, the β value ranges between 0.15-0.21 which is consistent with the values obtained for molecular rotation of different rigid molecules in various media (10,14,13,15). In CCl_4 the β value varies between 0.28-0.37 which seems a little high for molecular rotation. The relaxation time, τ in the four different media at 100 K increases in the order CCl_4 < P.S. < G.O.T.P. < SV (6.6×10^{-6} s, 1.3×10^{-5} s, 5.4×10^{-5} s, 2.7×10^{-4} s). The free energy of activation at 150 K also increases in the same order 12, 14, 15 and 16 kJ mol^{-1}. The enthalpies of activation are 17 (in CCl_4), 15 (in P.S.), 17 (in G.O.T.P.) and 19 kJ mol^{-1} (in SV). The corresponding entropies of activation are 29 , 12, 16 and 25 J K^{-1} mol^{-1}, respectively. Kashem (13) studied a good number of different molecules in P.S., G.O.T.P. and SV and compared the relaxation parameters in these three media. He found that the τ, ΔH_E and ΔG_E for molecular rotation of different rigid molecules in these media increase in the order P.S. < G.O.T.P. < SV. He suggested that this difference may be due to the difference in the

viscosity of the dispersion medium. Our results for norcamphor in the four different media follow the same order suggesting the lowest viscosity in CCl_4. The slightly higher β and ΔS_E values in CCl_4 may be due to the similar size and shape of the dispersion medium, CCl_4. As both the solute and dispersion media are of the same size and spherical, at the time of rotation of norcamphor, a small range of environment is encountered by it at any one temperature. Moreover, any kind of rotation of the solute may easily cause some disorder in the system. The slightly higher value of ΔH_E in CCl_4 in comparison to P.S. is not beyond the error limit.

2. Camphor

This compound was studied previously in a polystyrene matrix by Davies and Edwards (3) and in the pure solid state by Clemett and Davies (17). In polystyrene, the dielectric dispersion was found in the GHz region between the temperature 253-373 K. They found the Eyring plot $\log T\tau$ versus $1/T$ bend having two slopes where the lines intersect at 293 K. The enthalpies of activation calculated from these slopes were 3.8 and 21 kJ mol^{-1}. The corresponding entropies of activation were 31.4 and 25 J K^{-1} mol^{-1}, respectively. The range of their β-value was 0.78 (at 342 K) to 0.44 (at 243 K).

From this change of β-value with the temperature they suggested that there is some change in the local arrangement of the solute molecule at the lower temperatures. In solid state studies the activation enthalpy and entropy were found to be 7.5 kJ mol^{-1} and 12.1 J K^{-1} mol^{-1}, respectively. They found that the ΔH_E value and the distribution of relaxation time increases with the decrease of temperature. These were attributed to the increasing degree of molecular interaction in the solid state as the temperature falls.

Present dielectric studies of this molecule in a polystyrene matrix shows only one relaxation process in the temperature range 89-108 K. The Eyring plot $\log T\tau$ versus 1/T which is a clear straight line (Arrhenius behaviour) yields the activation enthalpy 18 ±1.1 kJ mol^{-1}, activation entropy 18 ±11.3 J K^{-1} mol^{-1}, activation free energy at 100 K, 17 kJ mol^{-1} and the relaxation time, τ at 100 K 2.2×10^{-4} s. The β-value found for this relaxation is in the range 0.19-0.22 which is in good agreement with the literature value for molecular rotation of various molecules in P.S. (10,14,15). Our relaxation parameters are higher than those of Davies et al. This is in agreement with their observations that the ΔH_E value increases with the decrease of temperature. The enthalpy of activation for

camphor is slightly higher than that of norcamphor which is reasonable in terms of size. Moreover, our enthalpy of activation for camphor is in reasonable agreement with the enthalpy of activation of the almost similar-sized molecule, cyclohexanone, 18.7 and 19 kJ mol^{-1} for its molecular rotation in P.S. matrices, obtained independently by Singh (18) and Davies and Swain (19), respectively.

3. Camphene

This molecule was previously studied by Clemett and Davies (17) in the pure solid state in the temperature region 253-373 K, they found molecular relaxation in the GHz range with an enthalpy of activation 9.2 kJ mol^{-1} and entropy of activation -7.19 J K^{-1} mol^{-1}. In this molecule also, as in camphor, they observed the increase of ΔH_E and distribution of relaxation time with the decrease of temperature due to the increasing degree of molecular interaction in the solid state as the temperature falls.

The present dielectric study of camphene in a polstyrene matrix shows one relaxation process in the region 95-109 K. The β-value (0.18-0.22) obtained for this relaxation is reasonable for molecular rotation in the polystyrene matrix. The Eyring activation parameters obtained

for this molecule are ΔH_E = 21 ±2 kJ mol^{-1}, ΔS_E = 40 ±20 J K^{-1} mol^{-1}, $\tau = 5.8 \times 10^{-4}$ s and ΔG_E = 17 kJ mol^{-1} at 100 K, respectively. These parameters are much greater than the Davies (17) parameters which supports their points of increasing molecular interaction at the lower temperatures. Within experimental error, these parameters for camphene are comparable with the corresponding parameters for molecular rotation of camphor in a polystyrene matrix. This is reasonable in consideration of the size of the two molecules.

4. 5-Norbornene-2-carbonitrile

For this molecule the dielectric relaxation in polystyrene matrices was observed in the temperature range 113-138 K. The β-value obtained for this relaxation is 0.13-0.18 which is reasonable for molecular motion in a P.S. matrix. From the Eyring plot log$T\tau$ versus 1/T the activation parameters were found to be ΔH_E = 24 ±1.7 kJ mol^{-1}, ΔS_E = 16 ±14 J K^{-1} mol^{-1}, ΔG_E = 22 kJ mol^{-1} and $\tau = 1.9 \times 10^{-1}$ s at 100 K, respectively. The relatively higher value of ΔH_E and the other parameters for this molecule in comparison to norcamphor (see Table III-1) is in harmony with its size. owing to the presence of bulky -CN group. The ΔH_E value for this molecule is comparable to the activation enthalpy 22 kJ mol^{-1}

obtained for molecular rotation of the almost similar-sized rigid molecule benzonitrile in a polystyrene matrix (15). Kashem (13) studied benzonitrile in a more viscous medium, G.O.T.P. and SV and obtained the enthalpies of activation for molecular rotation as 27 and 29 kJ mol^{-1}, respectively. All of these values are in reasonable agreement with our value for 5-norbornene-2-carbonitrile.

5. 3-Chloro-2-norbornanone

One dielectric dispersion is found for this molecule in a polystyrene matrix in the temperature range 104-122 K. The low β-value 0.16-0.18 for this rotation coincides with the β-values of other molecules for their molecular rotation in polystyrene matrices. The Eyring plot log$T\tau$ versus 1/T yields the activation parameters as ΔH_E = 21 ±1.4 kJ mol^{-1}, ΔS_E = 22 ±12.8 J K^{-1} mol^{-1}, ΔG_E = 19 kJ mol^{-1} at 100 K and $\tau = 3.2 \times 10^{-3}$ s at 100 K. The ΔH_E and other parameters are slightly higher than the corresponding parameters for norcamphor (see Table III-1). This is reasonable on the grounds of its larger size owing to its one chlorine atom at the adjacent carbon of the keto group. The activation enthalpy for this molecule is comparable to the activation enthalpy 16.3 kJ mol^{-1} obtained for molecular rotation of the almost similar-sized molecule, o-dichlorobenzene

in polystyrene by Davies et al (19) within the experimental error.

6. Camphoroquinone

This molecule is very similar in shape and size to camphor except one excess keto group at the 3-position. The dielectric relaxation for this molecule is found in the temperature range 103-121 K in the polystyrene matrix. The Fuoss-Kirkwood analysis yields the β-value for this relaxation as 0.18-0.20 which represents the wide distribution of relaxation time like most other molecular relaxation processes. The Eyring analysis yields enthalpy of activation and entropy of activation as 20 ±1.6 kJ mol^{-1} and 7 ±15 J K^{-1} mol^{-1}. The free energy of activation and relaxation time, τ at 100 K are found to be 19 kJ mol^{-1} and 5.5×10^{-3} s. Within the limit of experimental error, all of these parameters are comparable to our similar sized, rigid camphor molecule parameters (Table III-1). A slightly higher value for camphoroquinone is in harmony with its slightly larger size owing to one oxygen atom more in camphoroquinone than in the camphor.

7. exo-2-Bromonorbornane

Dielectric relaxation for this molecule in a

polystyrene matrix is found in the temperature range 90-109 K with a low β-value 0.14-0.16. The Eyring plot logTτ versus 1/T yields the enthalpy of activation and entropy of activation as 22 ±2.8 kJ mol^{-1} and 47 ±27 J K^{-1} mol^{-1} respectively. The free energy of activation and the relaxation time, τ, at 100 K are 17 kJ mol^{-1} and 4.0×10^{-4} s. Mazid (15) and Kashem (13) studied the almost similar-sized, rigid molecule bromobenzene in polystyrene, G.O.T.P. and SV. For molecular rotation of bromobenzene in these three media they found the free energy of activation and relaxation time at 100 K and the enthalpy of activation as 17.3 kJ mol^{-1}, 5.5×10^{-4} s, 16 kJ mol^{-1} (in P.S.) 20.7 kJ mol^{-1}, 3.3×10^{-2} s, 17.4 kJ mol^{-1} (in G.O.T.P.) 20.1 kJ mol^{-1}, 1.6×10^{-2} s, 18.2 kJ mol^{-1} (in SV), respectively. Within the limits of experimental error, our relaxation parameters for 2-bromo norbornane are comparable to the corresponding parameters for bromobenzene in a polystyrene matrix. Moreover, the higher parameters for 2-bromo norbornane is not unreasonable in comparison to our norcamphor results (see Table III-1) in terms of size as the bromine atom is much larger in size than the oxygen atom.

8. 1-Fenchone

This compound is very similar in size and shape to camphor except that the two methyl groups of the bridging

carbon are linked to the adjacent carbon of the keto group. This molecule has been studied in polystyrene, G.O.T.P. and CCl_4. The dispersion region in the polystyrene matrix is 110-126 K and in G.O.T.P. is 117-135 K. The β-value obtained in both the medium is in the range 0.17-0.19. The enthalpy of activation in polystyrene is 23 and in G.O.T.P. 20 kJ mol^{-1} which are almost the same within the limits of experimental error. The relaxation time and activation free energy at 100 K are 1.4×10^{-2} s and 20 kJ mol^{-1} in polystyrene and 3.3×10^{-2} s and 21 kJ mol^{-1} in G.O.T.P. These values are also comparable within the error limit. The slightly higher values of relaxation parameters for 1-fenchone than those of our camphor parameters (see Table III-1) may be due to some larger volume swept out by this molecule in its rotation than the camphor. Almost similar values in relaxation parameters in different dispersion medium support the Davie's points of molecular interaction in solid state (17).

The dielectric dispersion of this molecule in CCl_4 is found in the temperature range 128-145 K with a β-value Of 0.21-0.40. The dielectric loss, ε" versus log ν gives a very broad asymmetric curve with half width 4-6-decades of frequency (Figure III-8b"). The Cole-Cole plots are semi-circular and the process is not sensitives to the variation of temperature.

The Eyring plot $\log T\tau$ versus $1/T$ gives a straight line (Figure III-8d"). The activation enthalpy and entropy values obtained from this plot are 54 kJ mol^{-1} and 226 J K^{-1} mol^{-1}. The free energy of activation and the relaxation time at 100 K for this dispersion are 31 kJ mol^{-1} and 6.8×10^{3} s. The activation enthalpy and entropy are fairly high for the molecular process, but it is reasonable for the cooperative process. The relaxation time and ΔG_E values are also high which is usual in the case of the cooperative process. Moreover, the higher β-value, 0.21-0.40 is not in favour of the molecular process which is usually within the range of 0.1-0.28 for a molecular process. From all these considerations the relaxation of 1-fenchone in CCl_4 may be assigned as a cooperative process although the half-width of ε'' versus $\log \nu$ curve and $\log T\tau$ versus $1/T$ plots does not clearly indicate the cooperative phenomenon. The cooperative process at such a low temperature may be possible owing to the similar shapes and sizes of both the solute and solvent molecules.

9. 3-Methylene-2-norbornanone

This molecule, similar in size to 1-fenchone, was studied in a polystyrene matrix, and the dielectric dispersion was found in the temperature range 110-124 K.

The β-value for this dispersion is low and ranges between 0.17-0.20 as for other rigid molecules in a polystyrene matrix for molecular rotation. The Eyring plot $\log T\tau$ versus 1/T yields the enthalpy of activation and entropy of activation as 24 kJ mol^{-1} and 36 J K^{-1} mol^{-1}. These values are comparable to our 1-fenchone values in polystyrene matrix (see Table III-1). The relaxation times (τ) and the free energy of activation at 100 K are 9.3×10^{-7} s and 20 kJ mol^{-1}. These values are also in good agreement with our 1-fenchone values. All these relaxation parameters are fairly high in comparison to our norcamphor parameters. This is reasonable in consideration of the swept volume on relaxation of the molecules. As there is a methylene group at the adjacent carbon atom of keto group, its swept volume should be higher than that of norcamphor.

The nine spherical, rigid, polar molecules studied in polystyrene matrices do not have appreciable differences in their size and shape. The only variation is in the polar group. The β-value varies for these nine molecules between 0.13-0.22. The enthalpy of activation varies from 15-24 kJ mol^{-1}. The activation entropy ranges between 7-47 J K^{-1} mol^{-1} while the activation free energy and relaxation time at 100 K varies between 14-22 kJ mol^{-1} and 1.3×10^{-5} - 1.9×10^{-1} s, respectively. The variations in these relaxation parameters

are not appreciable owing to their similar size and shape. It is notable that in systems of similar character, there has been frequently a correlation between the activation enthalpies, ΔH_E and entropies, ΔS_E as has been found by many workers (1,3,6,10,13,15). In our case this correlation does not hold. The linear ΔH_E-ΔS_E relationship is reasonable for any series of molecules when the shape is quite similar and the inclination of the dipole to the principal axis is quite similar. It is also necessary to point out that there is no absolute significance of the activation entropy determined by the Eyring expression since the pre-exponential factor cannot be fully justified. As Davies and Edwards (3) say, "the Eyring entropy terms ΔS^*_E are best regarded as empirical corrections ($\exp(\Delta S_E/R)$) to a predetermined frequency value (kT/h) in the rate equation." Therefore, the breakdown of a single linear ΔH_E-ΔS_E relationship would not be surprising for a wide variety of dipolar molecules. The low values of distribution parameters 'β' for all the rigid dipole molecular motion in polystyrene matrices agree well with the observations by Davies and Edwards (3), Davies and Swain (19), Khwaja (10), Mazid (15) and Kashem (13) for a series of rigid molecules in polystyrene, G.O.T.P. and SV. The enthalpy of activation also increases with the size of the molecule. The results of these nine camphane

derivatives support the Davies' points (17) that the activation enthalpy increases with the decrease of temperature. Our activation enthalpies are much higher than those of Davies et al (3,17) but may be accounted for by the study being at much lower temperatures (and lower frequencies) when the matrix has contracted and the molecular interaction between the solute and the dispersion medium is greater. The similar relaxation parameters in different dispersion medium also support their points of increasing degree of molecular interaction as the temperature falls. In one point we differ from them in that they observed an Eyring plot of non-Arrhenius behaviour having two clearly distinct slopes but in our case only one straight line was obtained (Figure III-2d).

REFERENCES

1. K. Higasi, "Dielectric Relaxation and Molecular Structure Monograph Series of the Research Institute of Applied Electricity", No. 9, (1961).

2. O. F. Kalman & C. P. Smyth, J. Am. Chem. Soc., 82 (1960)783.

3. M. Davies & A. Edwards, Trans. Faraday Soc., 63 (1967)2163.

4. E. N. Dicarlo & C. P. Smyth, J. Phys. Chem., 66 (1962)1105.

5. D. A. Pitt & C. P. Smyth, J. Am. Chem. Soc., 80 (1958)1061.

6. J. Crossley, S. Walker, Can. J. Chem., 46 (1968)2639.

7. W. F. Hassell, Ph.D. Thesis, University of Aston in Birmingham (1966).

8. B. J. Cooke, M.Sc. Thesis, Lakehead University, Thunder Bay, Ontario, Canada (1969).

9. D. A. Pitt & C. P. Smyth, J. Phys. Chem., 63 (1950)582.

10. H.A. Khwaja, M.Sc. Thesis, Lakehead University, Thunder Bay, Ontario, Canada (1978).

11. J. Crossley & S. G. Srivastava, Can. J. Chem., 54 (1976)1418.

12. A. J. Barlow, J. Lamb and N. S. Taskoprülü, J. Acoust. Soc. Am., 46 (1969)569.

13. M.A. Kashem, M.Sc. Thesis, Lakehead University, Thunder Bay, Ontario, Canada (1982).

14. S.P. Tay & S. Walker, J. Chem. Phys., 63 (1975)1639.

15. M.A. Mazid, M.Sc. Thesis, Lakehead University, Thunder Bay, Ontario, Canada (1978).

REFERENCES continued...

16. M.S. Ahmed - Private Communication.

17. C. Clemett & M. Davies, Trans. Faraday Soc., 58 (1962)1705.

18. B. Singh, J. Phys. Soc. Japan, 50 (1981)2306.

19. M. Davies & J. Swain, Trans. Faraday Soc., 67 (1971)1637.

TABLE III-1: Eyring Analysis Results for some Spherical Rigid Molecules in organic glasses

Molecule	Medium	Temperature Range (K)	Relaxation Time τ(s)			ΔG_E (kJ mol^{-1})			ΔH_E	ΔS_E
			100 K	150 K	200 K	100 K	150 K	200 K	kJ mol^{-1}	J K^{-1} mol^{-1}
Norcamphor	Polystyrene	80-95	1.3×10^{-5}	1.8×10^{-8}	6.2×10^{-10}	14	14	13	15±0.5	12±6.7
	G.O.T.P.	84-100	5.4×10^{-5}	4.0×10^{-8}	9.8×10^{-10}	15	15	14	17±0.9	16±9.9
	Santovac	93-108	2.7×10^{-4}	8.0×10^{-8}	1.3×10^{-9}	17	16	14	19±7.8	25± 1.8
	Carbontetra-chloride	82-94	6.6×10^{-6}	5.7×10^{-9}	1.6×10^{-10}	14	12	11	17±1.8	29±20
Camphor	Polystyrene	89-108	2.2×10^{-4}	9.0×10^{-8}	1.7×10^{-9}	17	16	15	18± 1.1	18±11
Camphene	Polystyrene	95-109	5.8×10^{-4}	7.4×10^{-8}	7.7×10^{-10}	17	15	13	21±2	40±20
5-Norbornene-2-carbonitrile	Polystyrene	113-138	1.9×10^{-1}	9.2×10^{-6}	5.9×10^{-8}	22	21	21	24±1.7	16±14
3-Chloro-2-norbornanone	Polystyrene	104-122	3.2×10^{-3}	4.6×10^{-7}	5.1×10^{-9}	19	18	17	21±1.4	22±12.8
Camphoroquinone	Polystyrene	103-121	5.5×10^{-3}	1.2×10^{-6}	1.7×10^{-8}	19	19	19	20±1.6	7±15

TABLE III-1: continued...

Molecule	Medium	Temperature Range (K)	Relaxation Time τ(s)			ΔG_E (kJ mol^{-1})			ΔH_E	ΔS_E
			100 K	150 K	200K	100 K	150 K	200 K	kJ mol^{-1}	J K^{-1} mol^{-1}
exo-2-Bromonorbornane	Polystyrene	90-109	4.0×10^{-4}	4.4×10^{-8}	4.2×10^{-10}	17	15	12	22±2.8	47±27
1-Fenchone	Polystyrene	110-126	1.4×10^{-2}	8.9×10^{-7}	6.5×10^{-9}	20	19	17	23±1.2	31±10.9
	G.O.T.P.	117-135	3.3×10^{-2}	7.0×10^{-6}	9.4×10^{-8}	21	21	21	20±1.3	-7±10
	Carbon tetrachloride	128-145	6.8×10^{3}	2.2×10^{-6}	3.5×10^{-11}	31	20	8	54±2.7	226±20
3-Methylene-2-norbornanone	Polystyrene	110-124	2.0×10^{-2}	9.3×10^{-7}	5.8×10^{-9}	20	19	17	24±1.4	36±12

TABLE III-2: Fuoss-Kirkwood Analysis Parameters, ε_∞, and Effective Dipole Moments (μ) for some Spherical Rigid Molecules in Organic Glasses

T(K)	$10^6\tau$(s)	$\log \nu_{max}$	β	$10^3\varepsilon''_{max}$	ε_∞	μ(D)
0.69 M Norcamphor in a polystyrene matrix						
80.0	1659	1.98	0.17	43.9	2.99	1.05
81.4	1106	2.16	0.17	44.8	2.99	1.07
82.7	772	2.31	0.17	45.5	2.99	1.08
84.3	438	2.56	0.17	46.6	2.98	1.11
86.6	282	2.75	0.18	47.8	2.99	1.11
89.5	131	3.08	0.17	49.0	2.96	1.17
92.4	62.7	3.40	0.18	50.4	2.96	1.18
95.0	36.1	3.64	0.19	51.9	2.97	1.18
4.1 percent (wt/wt) Norcamphor in G.O.T.P.						
84.5	2913	1.74	0.15	16.4	-	-
86.1	1519	2.02	0.18	16.9	-	-
87.7	1062	2.18	0.17	17.3	-	-
89.6	652	2.39	0.17	17.7	-	-
92.0	368	2.64	0.18	18.3	-	-
93.9	239	2.82	0.18	18.7	-	-
96.6	114	3.15	0.18	19.1	-	-
100.0	51.0	3.49	0.19	19.8	-	-
5.3 percent (wt/wt) Norchamphor in Santovac						
93.0	1490	2.03	0.19	30.5	-	-
95.8	810	2.29	0.19	31.5	-	-
97.5	530	2.48	0.19	32.1	-	-
99.2	367	2.64	0.19	32.6	-	-
102.0	194	2.91	0.20	33.4	-	-
104.3	96.9	3.22	0.19	34.0	-	-
107.7	43.5	3.56	0.21	35.3	-	-
3.7 M percent Norcamphor in Carbontetrachloride						
82.4	481	2.52	0.37	10.9	-	-
83.3	386	2.61	0.36	11.2	-	-
84.8	310	2.71	0.36	11.3	-	-
86.4	200	2.90	0.34	11.5	-	-
89.1	95.2	3.22	0.34	12.0	-	-
90.8	57.9	3.44	0.31	12.2	-	-
92.5	33.3	3.68	0.30	12.6	-	-
94.4	19.9	3.90	0.28	12.7	-	-

TABLE III-2: continued...

T(K)	$10^6\tau$(s)	$\log \nu_{max}$	β	$10^3\varepsilon''_{max}$	ε_∞	μ(D)
0.45 M Camphor in a Polystyrene Matrix						
89.8	2596	1.79	0.19	44.8	2.75	1.38
93.4	1132	2.15	0.19	47.1	2.74	1.44
95.7	640	2.40	0.19	48.2	2.74	1.48
97.8	386	2.62	0.20	49.4	2.75	1.47
100.7	210	2.88	0.20	50.7	2.74	1.52
103.9	86.9	3.26	0.20	52.2	2.73	1.57
105.3	64.3	3.39	0.21	52.8	2.73	1.55
108.0	35.8	3.65	0.22	54.5	2.74	1.55
1.31 M Camphene in a Polystyrene Matrix						
94.8	1851	1.93	0.20	3.8	2.92	0.24
97.5	895	2.25	0.20	4.0	2.93	0.25
98.0	950	2.22	0.18	4.0	2.91	0.26
100.8	486	2.52	0.19	4.1	2.91	0.26
102.8	286	2.75	0.19	4.2	2.91	0.27
104.6	200	2.90	0.19	4.2	2.91	0.27
106.6	103	3.19	0.18	4.3	2.91	0.28
108.6	68.8	3.36	0.22	4.5	2.91	0.27
0.91 M 5-Norbornene-2-Carbonitrile in a Polystyrene Matrix						
113.6	6565	1.38	0.13	52.7	3.00	1.33
115.6	2920	1.74	0.15	53.7	3.03	1.26
117.8	1799	1.95	0.15	55.1	3.03	1.29
120.5	1211	2.12	0.15	56.5	3.02	1.32
123.1	759	2.32	0.15	57.6	3.01	1.35
126.6	394	2.61	0.16	59.2	3.02	1.35
130.5	206	2.89	0.17	61.1	3.04	1.34
135.0	83.9	3.28	0.17	62.7	3.02	1.39
138.1	46.7	3.53	0.18	64.4	3.02	1.38

TABLE III-2: continued...

T(K)	$10^6\tau$(s)	$\log\psi_{max}$	β	$10^3\varepsilon''_{max}$	ε_∞	μ(D)
0.49 M 3-Chloro-2-Norbornanone in a Polystyrene Matrix						
104.2	999	2.20	0.16	34.0	3.04	1.28
106.2	644	2.39	0.16	34.7	0.03	1.31
109.1	359	2.65	0.17	35.7	3.04	1.31
111.5	236	2.83	0.17	36.4	3.03	1.33
113.4	167	2.98	0.17	36.8	3.03	1.35
115.4	91.6	3.24	0.16	37.3	3.01	1.42
117.4	60.0	3.42	0.17	38.0	3.02	1.40
119.7	38.7	3.61	0.17	38.7	3.01	1.43
121.5	28.2	3.75	0.18	39.9	3.02	1.41
0.32 M Camphoroquinone in a Polystyrene Matrix						
102.8	2279	1.84	0.18	44.0	2.97	1.71
105.2	1532	2.02	0.18	45.2	2.97	1.75
107.7	975	2.21	0.18	46.3	2.97	1.79
110.0	655	2.39	0.18	47.1	2.96	1.83
111.4	451	2.55	0.18	47.8	2.95	1.85
113.0	333	2.68	0.19	48.5	2.96	1.83
115.8	202	2.90	0.19	49.6	2.96	1.87
117.4	129	3.09	0.19	50.1	2.95	1.90
118.8	94.2	3.23	0.19	50.6	2.95	1.92
121.4	56.6	3.45	0.20	51.7	2.95	1.91
0.40 M exo-2-Bromo-norbornane in a Polystyrene Matrix						
90.9	1551	2.01	0.16	10.0	3.00	0.74
92.7	1224	2.11	0.15	10.2	3.00	0.78
94.9	849	2.27	0.15	10.5	2.99	0.80
97.6	471	2.53	0.15	10.8	2.99	0.82
99.2	363	2.64	0.15	10.9	2.99	0.83
101.2	257	2.79	0.15	11.1	2.99	0.85
102.9	188	2.93	0.15	11.3	2.99	0.87
104.9	113	3.15	0.14	11.4	2.98	0.91
107.0	65.0	3.39	0.14	11.7	2.97	0.93
109.3	40.6	3.59	0.14	11.9	2.97	0.95

TABLE III-2: continued...

T(K)	$10^6\tau$(s)	$\log \nu_{max}$	β	$10^3\varepsilon''_{max}$	ε_∞	μ(D)
0.50 M 1-Fenchone in a Polystyrene Matrix						
110.1	968	2.22	0.17	25.5	2.98	1.12
111.1	758	2.32	0.17	25.7	2.98	1.13
112.8	518	2.49	0.17	26.1	2.98	1.15
114.5	366	2.64	0.17	26.5	2.97	1.16
116.1	275	2.76	0.18	26.9	2.98	1.15
117.9	206	2.89	0.17	27.1	2.97	1.20
120.8	98.1	3.21	0.17	27.7	2.96	1.23
123.4	55.0	3.46	0.18	28.3	2.96	1.22
126.5	31.0	3.70	0.19	29.0	2.97	1.21
2.9 percent (wt/wt) 1-Fenchone in G.O.T.P.						
117.9	707	2.35	0.18	2.3	-	-
119.4	522	2.48	0.17	2.3	-	-
121.4	392	2.61	0.18	2.4	-	-
123.6	277	2.76	0.18	2.4	-	-
125.7	206	2.89	0.18	2.5	-	-
129.0	101	3.20	0.17	2.5	-	-
131.6	75.9	3.32	0.18	2.6	-	-
135.3	45.4	3.54	0.19	2.6	-	-
5.1 M percent 1-Fenchone in Carbontetrachloride						
128.0	4453	1.55	0.21	30.9	-	-
129.8	1856	1.93	0.23	32.4	-	-
132.0	917	2.24	0.23	33.9	-	-
134.5	326	2.69	0.25	35.3	-	-
137.4	111	3.16	0.28	36.3	-	-
140.0	45.3	3.55	0.32	37.3	-	-
141.7	26.0	3.79	0.35	37.9	-	-
144.7	13.0	4.09	0.40	38.8	-	-

TABLE III-2: continued...

T(K)	$10^6\tau$(s)	$\log\nu_{max}$	β	$10^3\varepsilon''_{max}$	ε_∞	μ(D)
1.28M 3-Methylene-2-Norbornanone in a Polystyrene Matrix						
110.4	1156	2.14	0.17	59.6	2.73	1.09
112.8	671	2.38	0.17	60.7	2.73	1.12
113.4	597	2.43	0.18	61.2	2.74	1.09
116.0	343	2.67	0.18	62.6	2.73	1.12
118.4	224	2.85	0.18	63.8	2.73	1.14
120.5	125	3.10	0.19	64.7	2.74	1.13
122.6	81.7	3.29	0.18	65.5	2.71	1.18
125.0	47.8	3.52	0.20	67.3	2.74	1.14

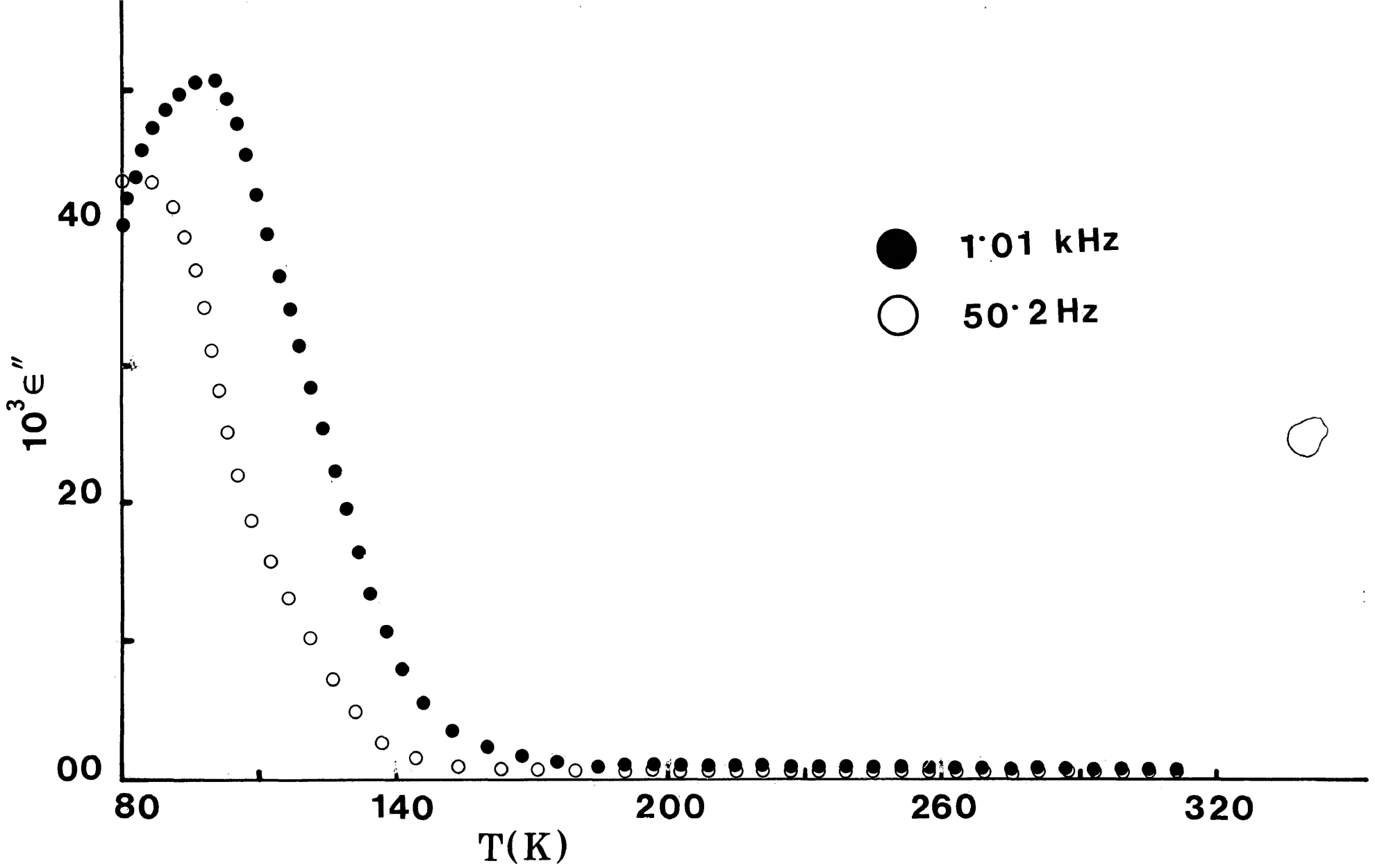

FIGURE III-1a: Plots of dielectric loss factor, ε" versus temperature (K) for norcamphor in a polystyrene matrix

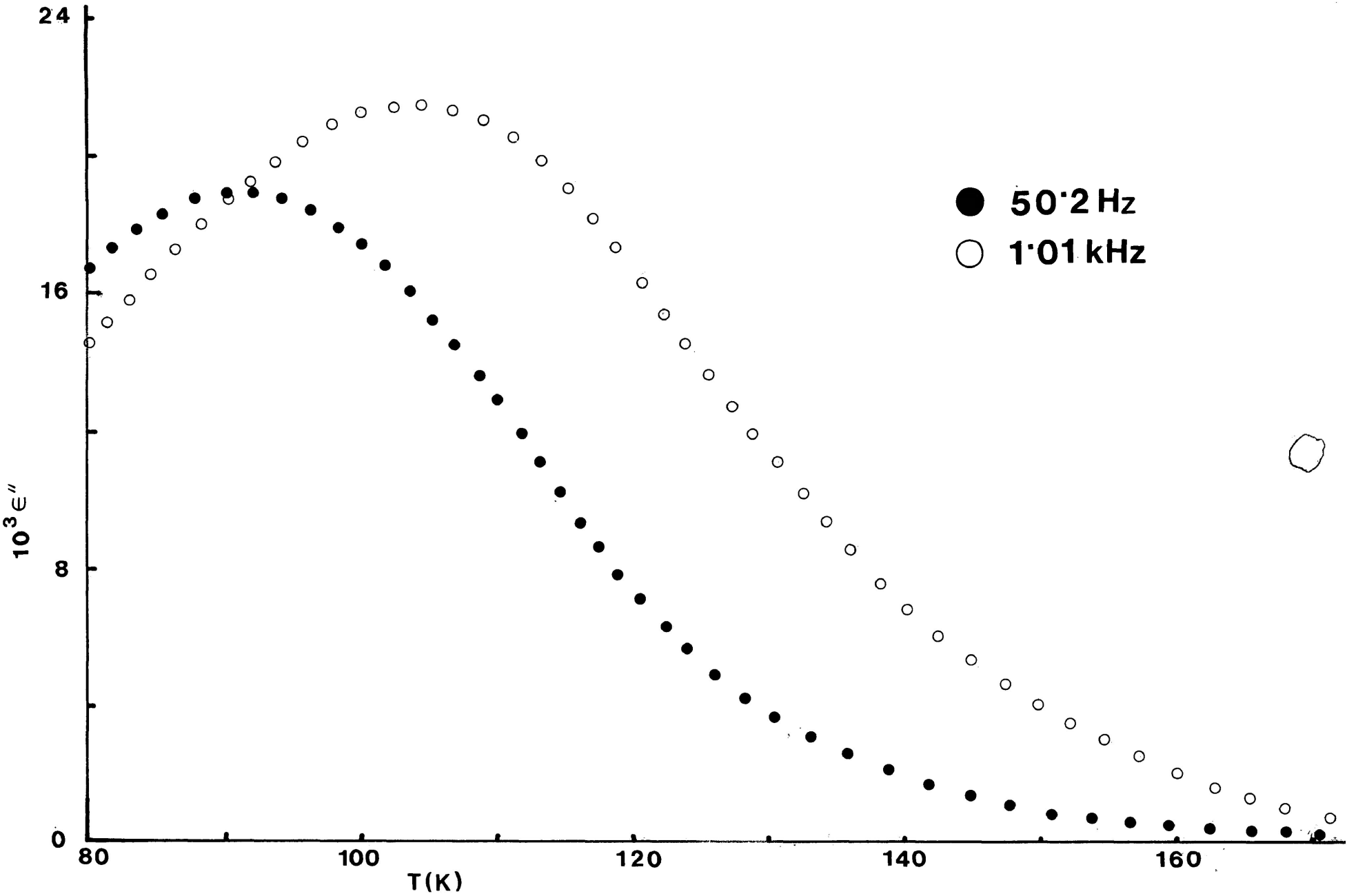

FIGURE III-1a': Plots of dielectric loss factor, ε" versus temperature (K) for norcamphor in G.O.T.P.

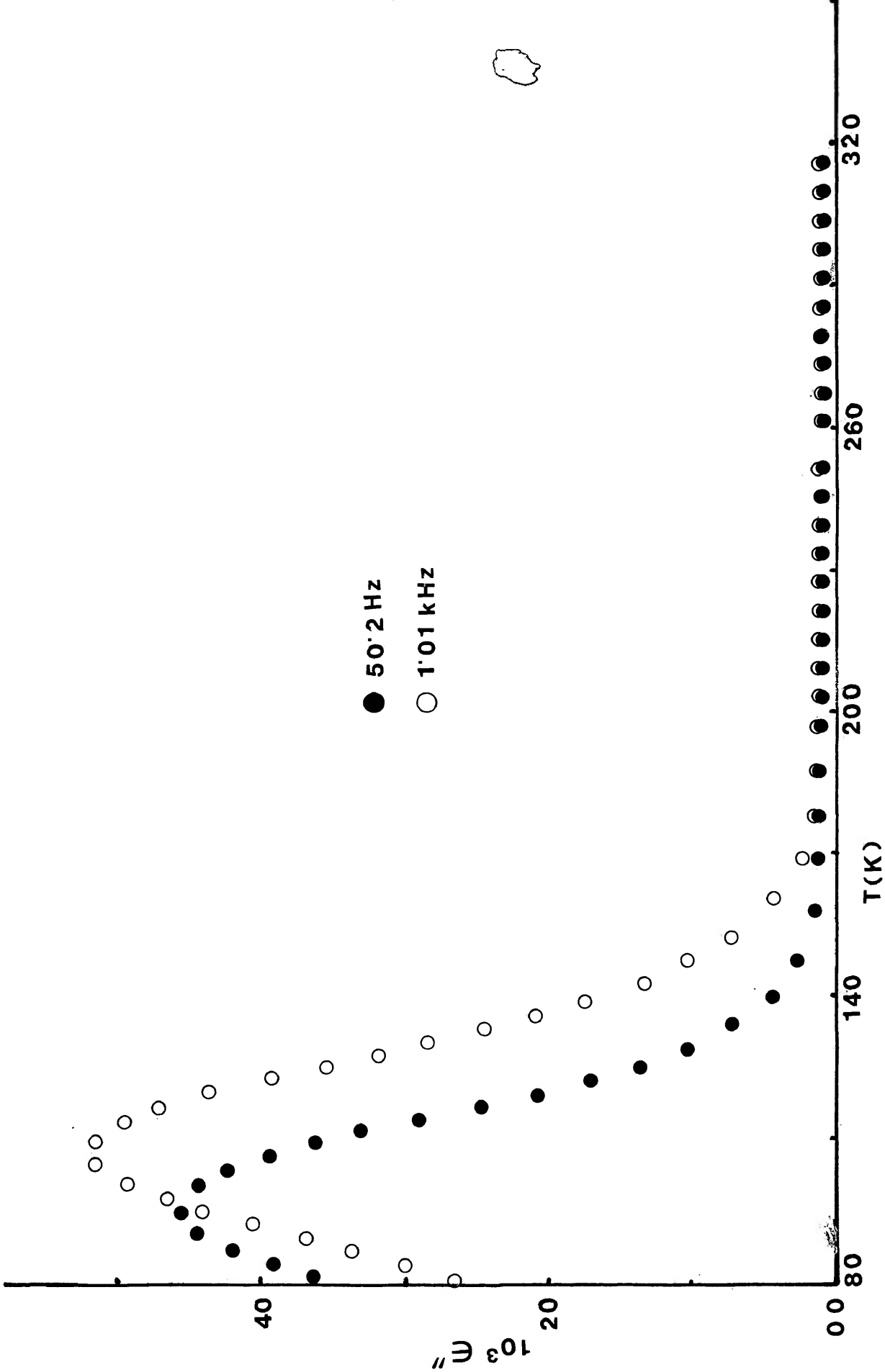

FIGURE III-2a: Plots of dielectric loss factor, ε" versus temperature (K) for camphor in a polystyrene matrix

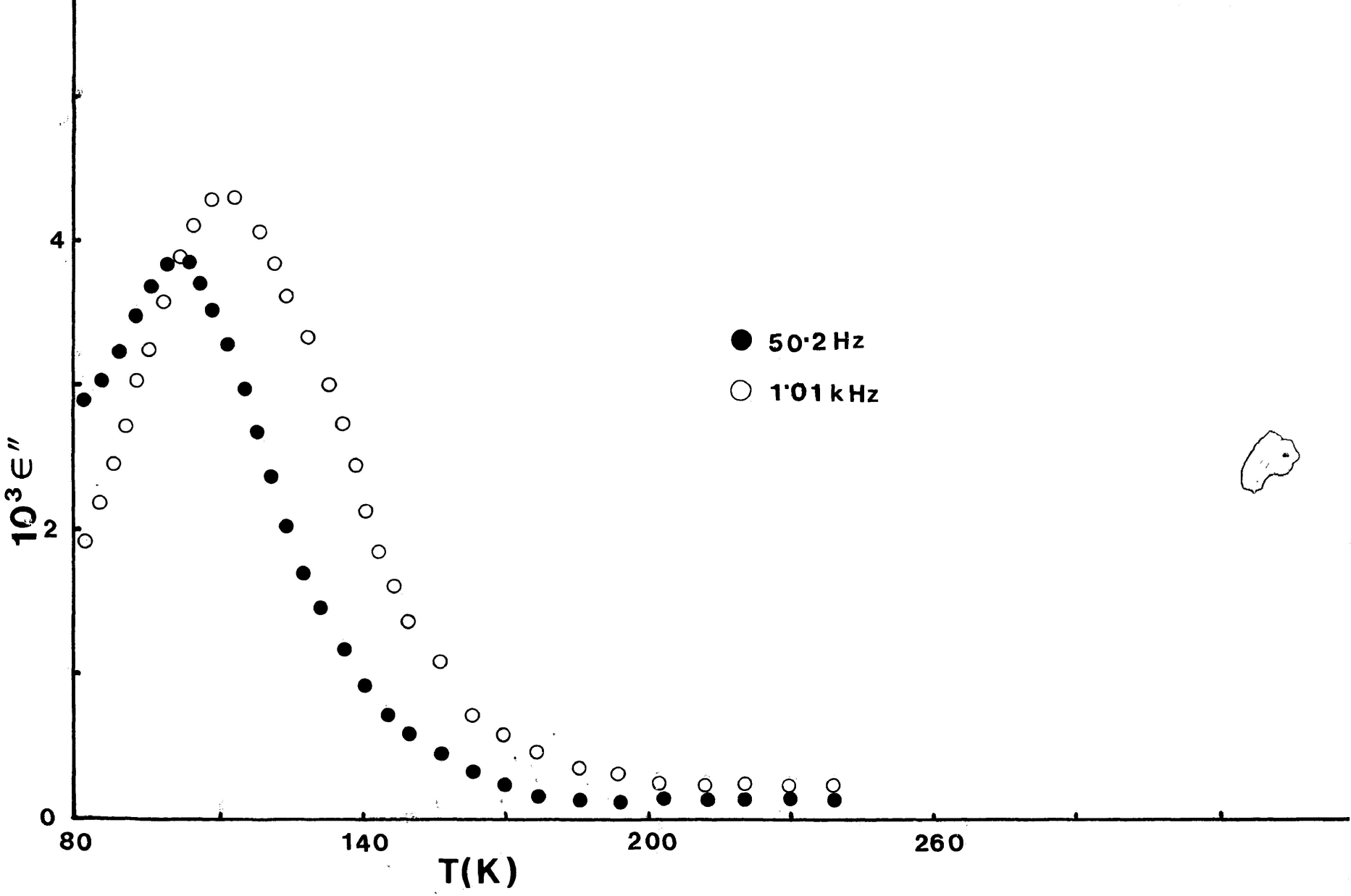

FIGURE III-3a: Plots of dielectric loss factor, ε" versus temperature (K) for camphene in a polystyrene matrix

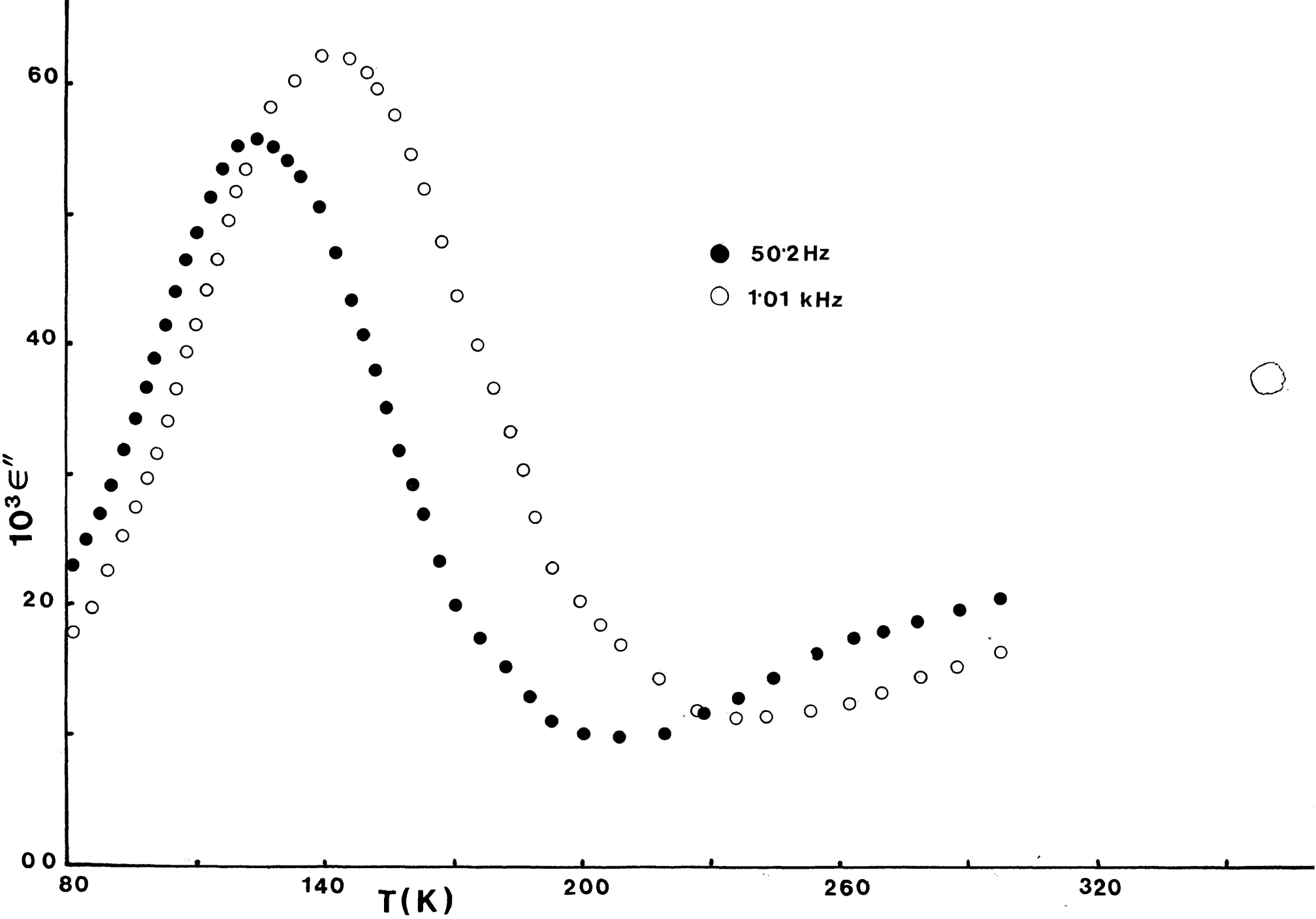

FIGURE III-4a: Plots of dielectric loss factor, ε" versus temperature (K) for 5-norbornene-2-carbonitrile in a polystyrene matrix

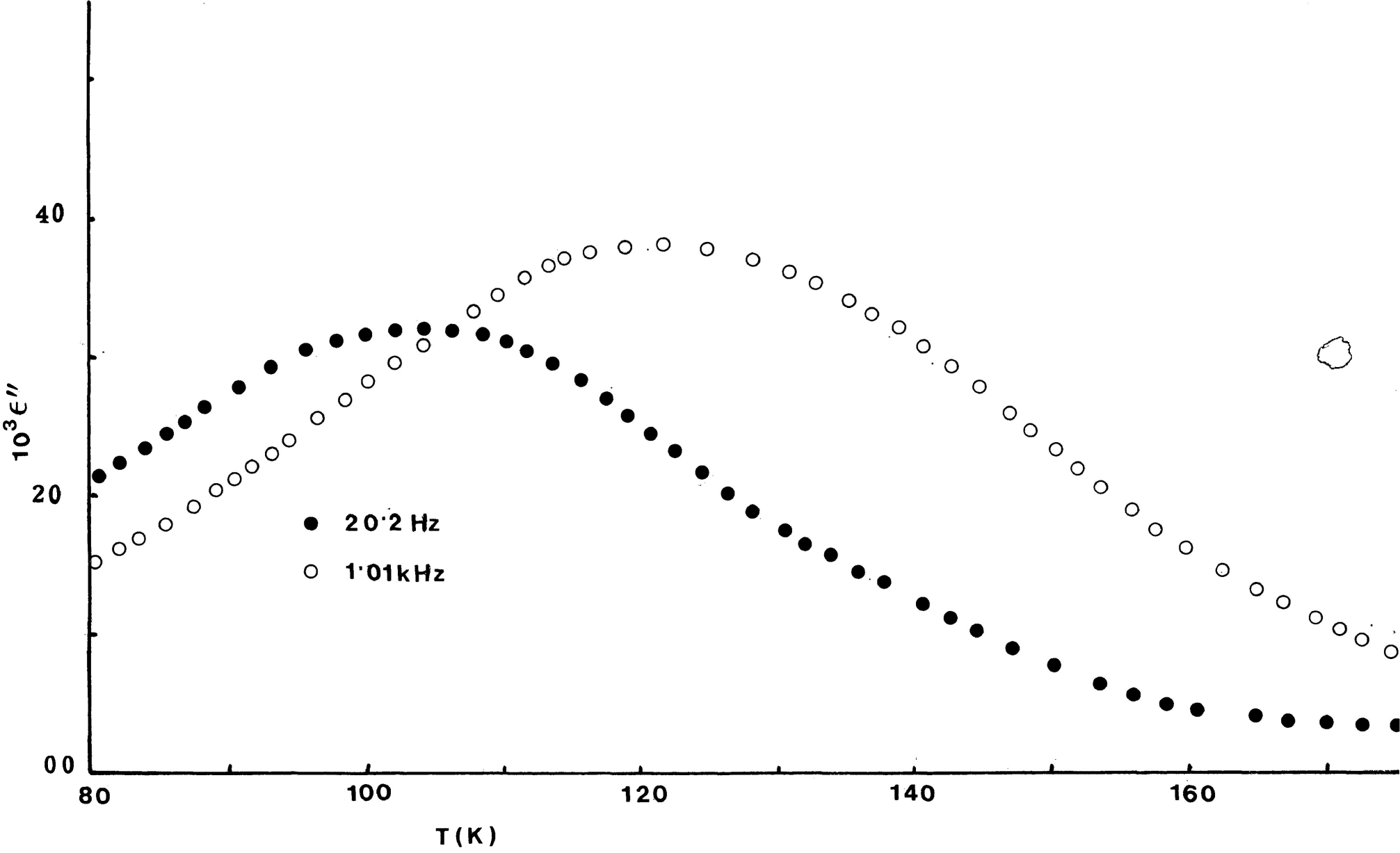

FIGURE III-5a: Plots of dielectric loss factor, ε" versus temperature (K) for 3-chloro-2-norbornanone in a polystyrene matrix

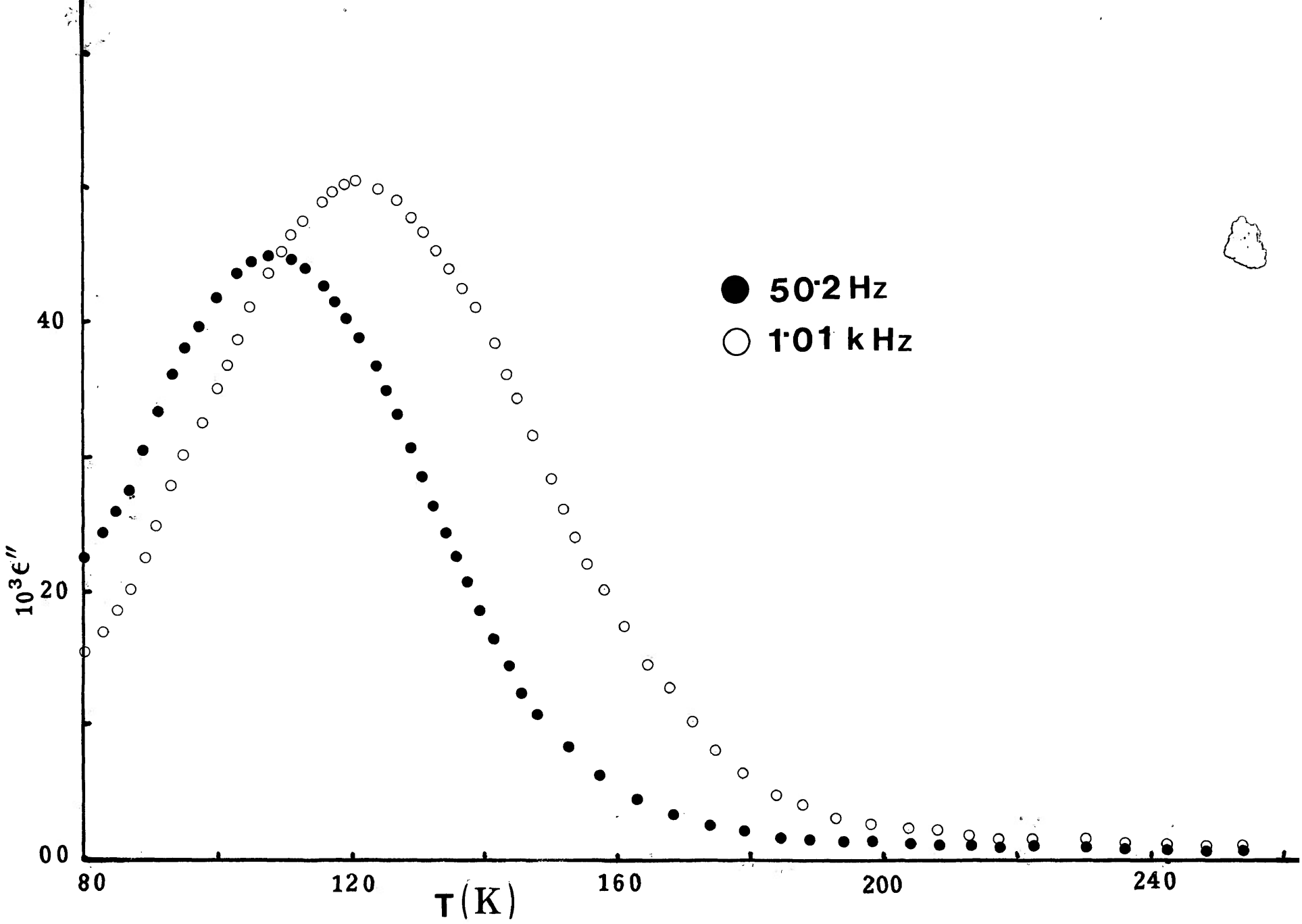

FIGURE III-6a: Plots of dielectric loss factor, ε" versus temperature (K) for camphoroquinone in a polystyrene matrix

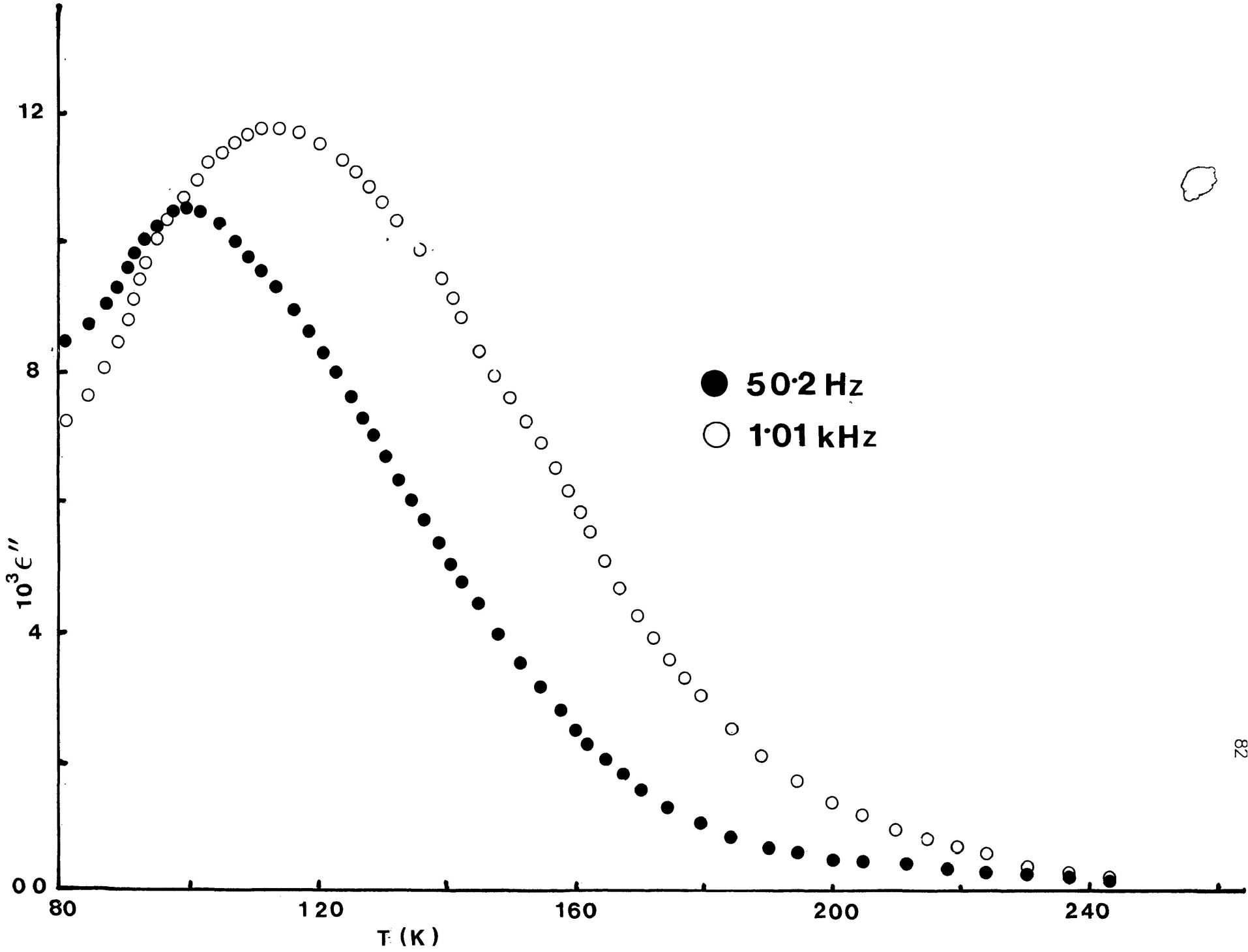

FIGURE III-7a: Plots of dielectric loss factor, ε" versus temperature (K) for exo-2-bromo-norbornane in a polystyrene matrix

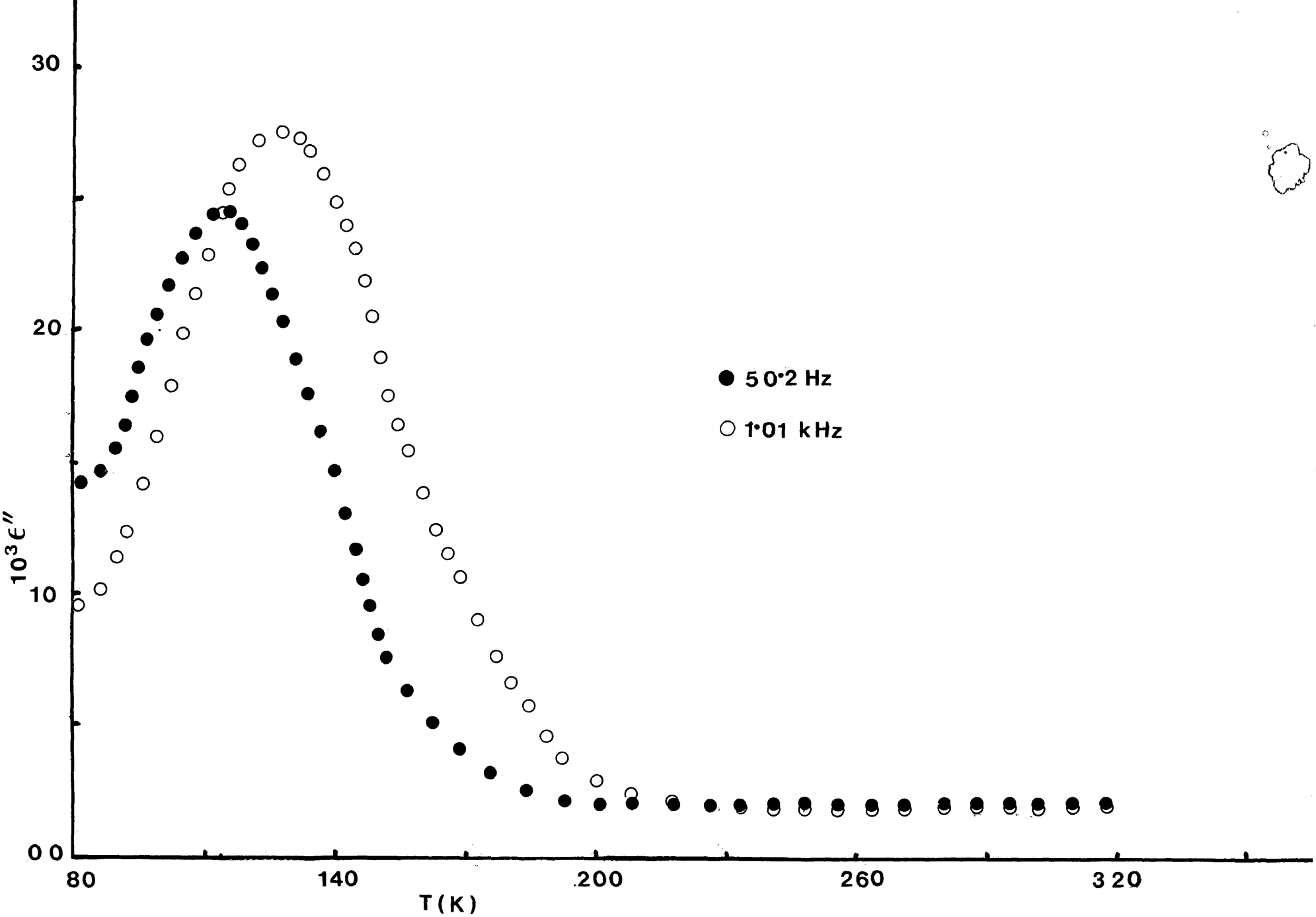

FIGURE III-8a: Plots of dielectric loss factor, ε" versus temperature (K) for 1-fenchone in a polystyrene matrix

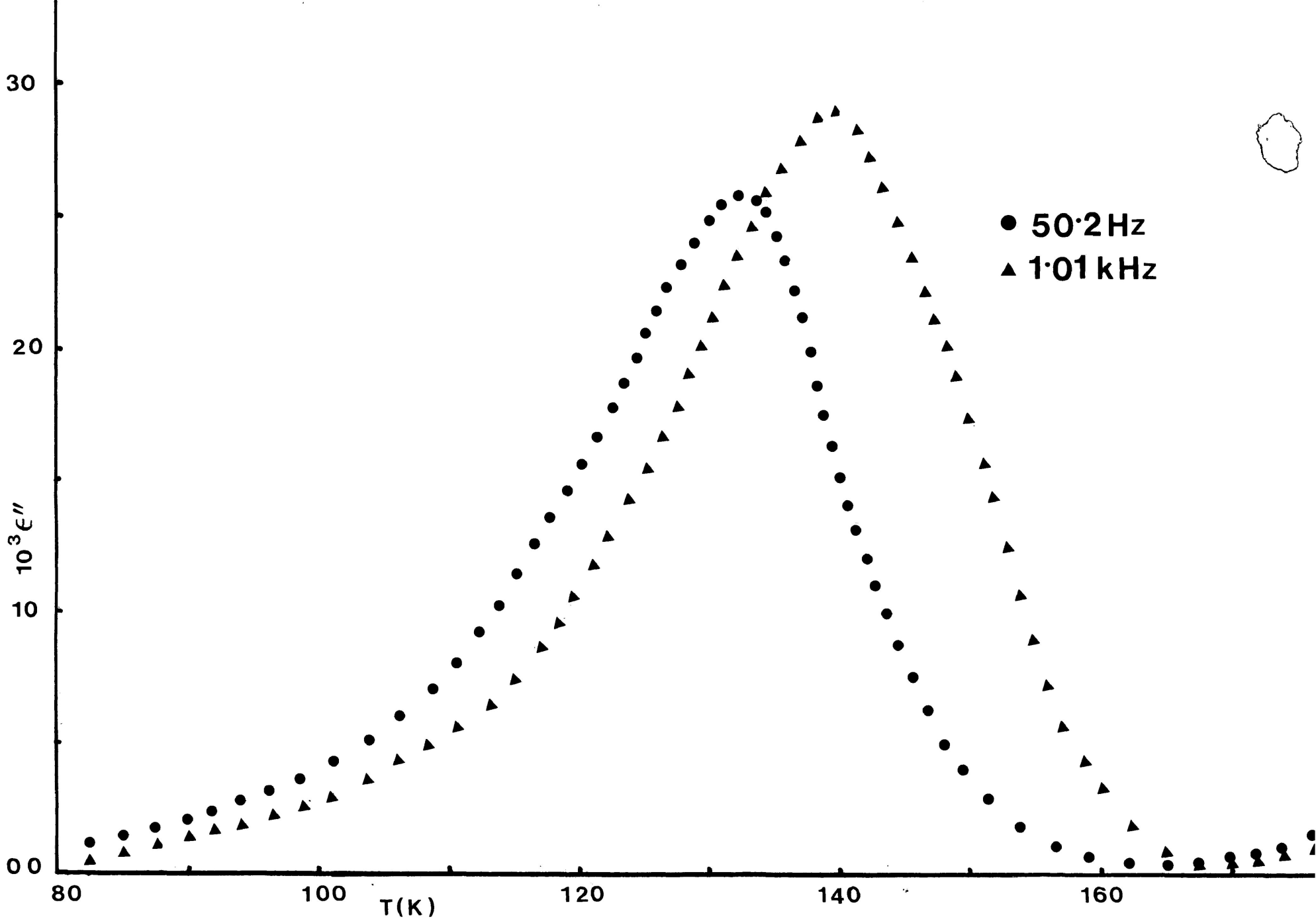

FIGURE III-8a": Plots of dielectric loss factor, ε" versus temperature (K) for 1-fenchone in carbontetrachloride

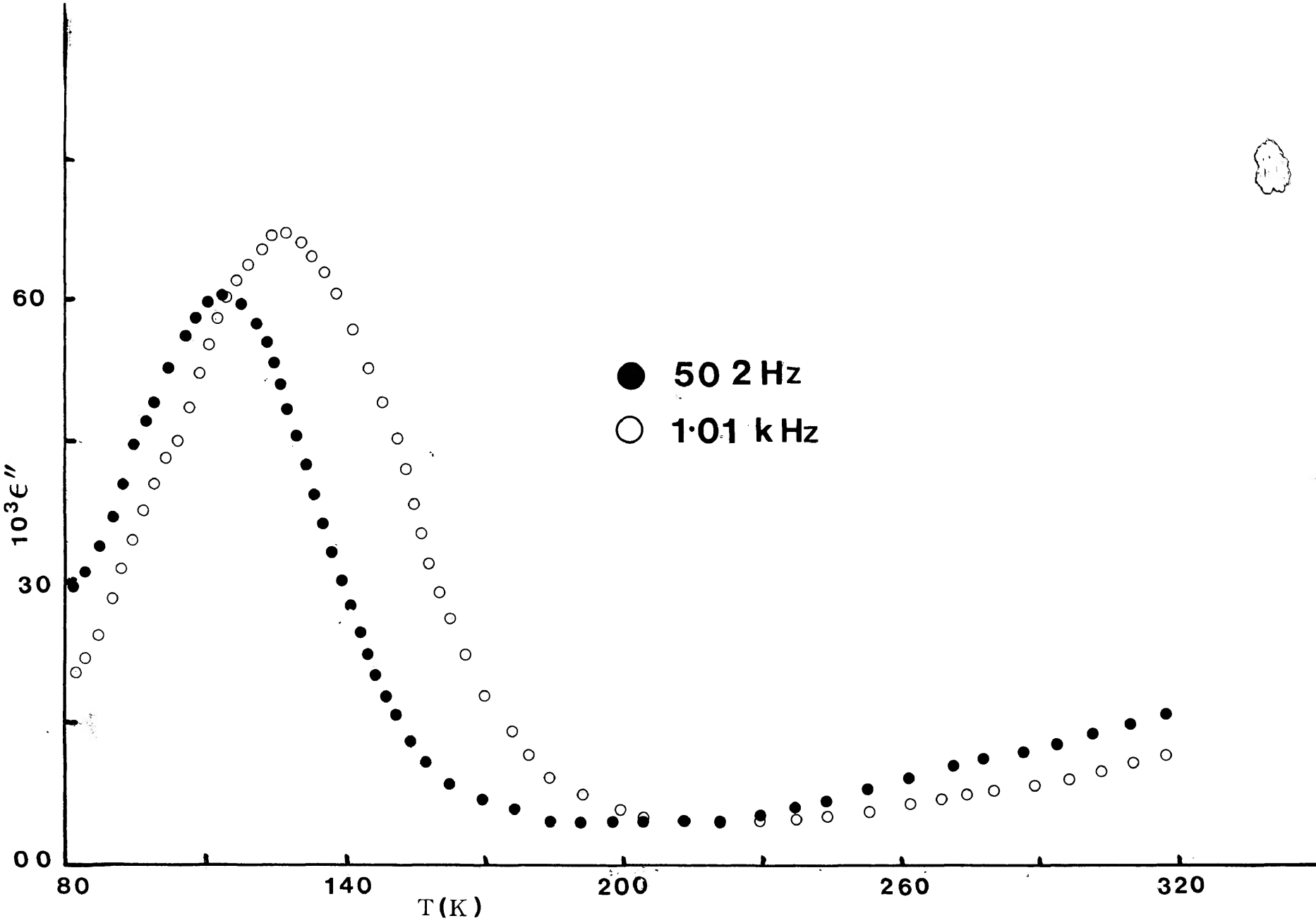

FIGURE III-9a: Plots of dielectric loss factor, ε" versus temperature (K) for 3-methylene-2-norbornanone in a polystyrene matrix

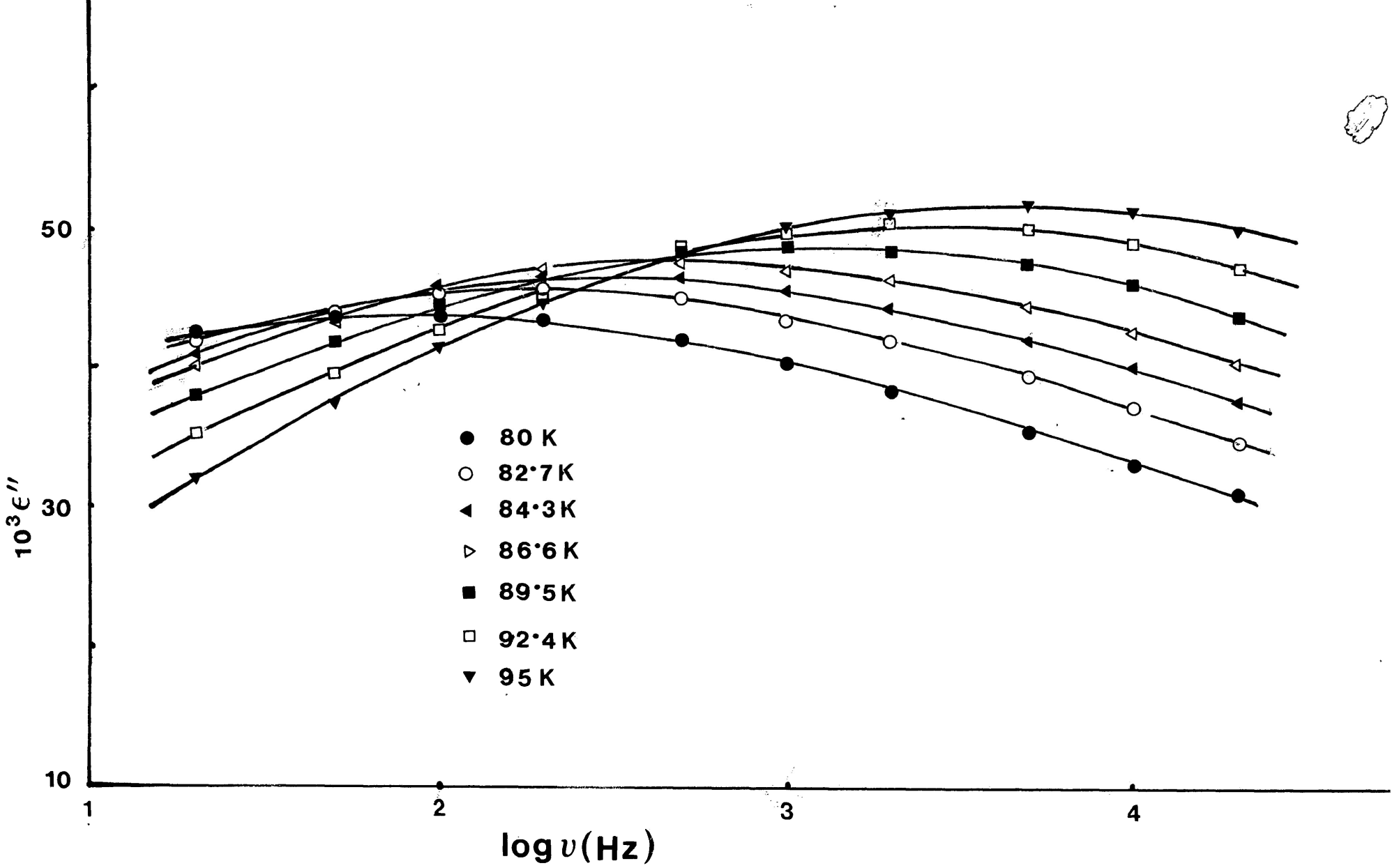

FIGURE III-1b: Plots of dielectric loss factor, ε" versus log frequency (Hz) for norcamphor in a polystyrene matrix.

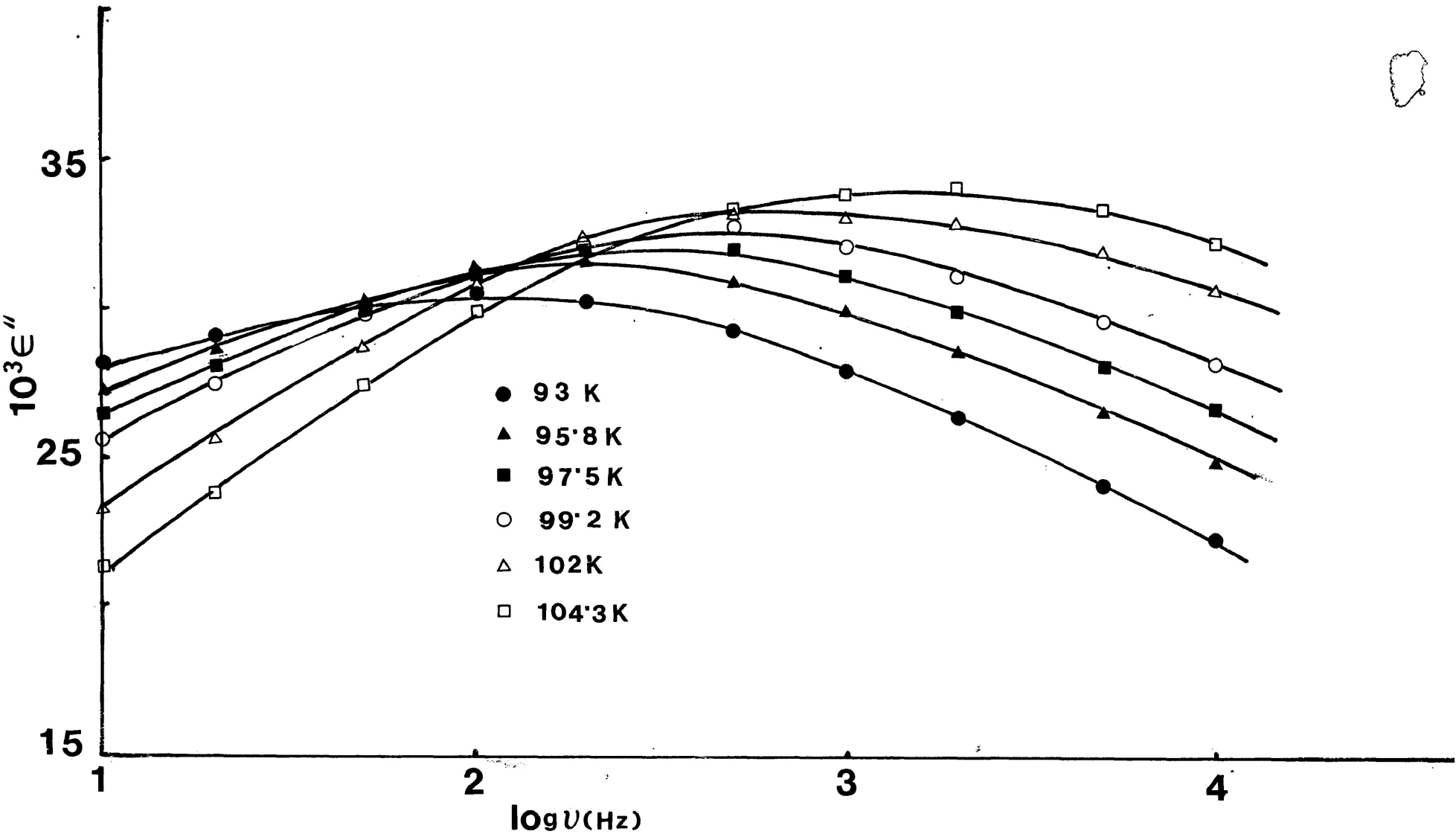

FIGURE III-1b": Plots of dielectric loss factor, ε" versus log frequency (Hz) for norcamphor in Santovac®

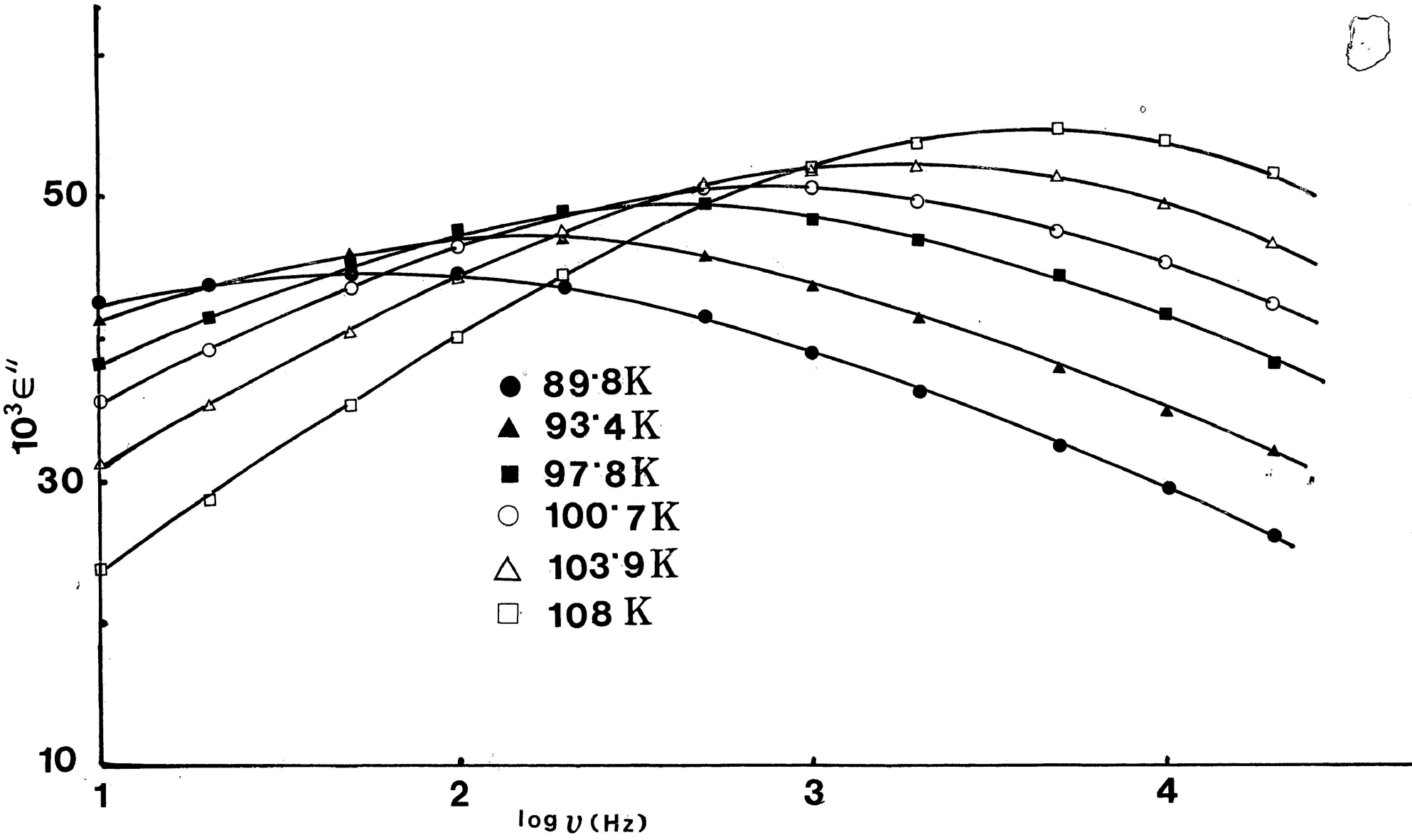

FIGURE III-2b: Plots of dielectric loss factor, ε" versus log frequency (Hz) for camphor in a polystyrene matrix

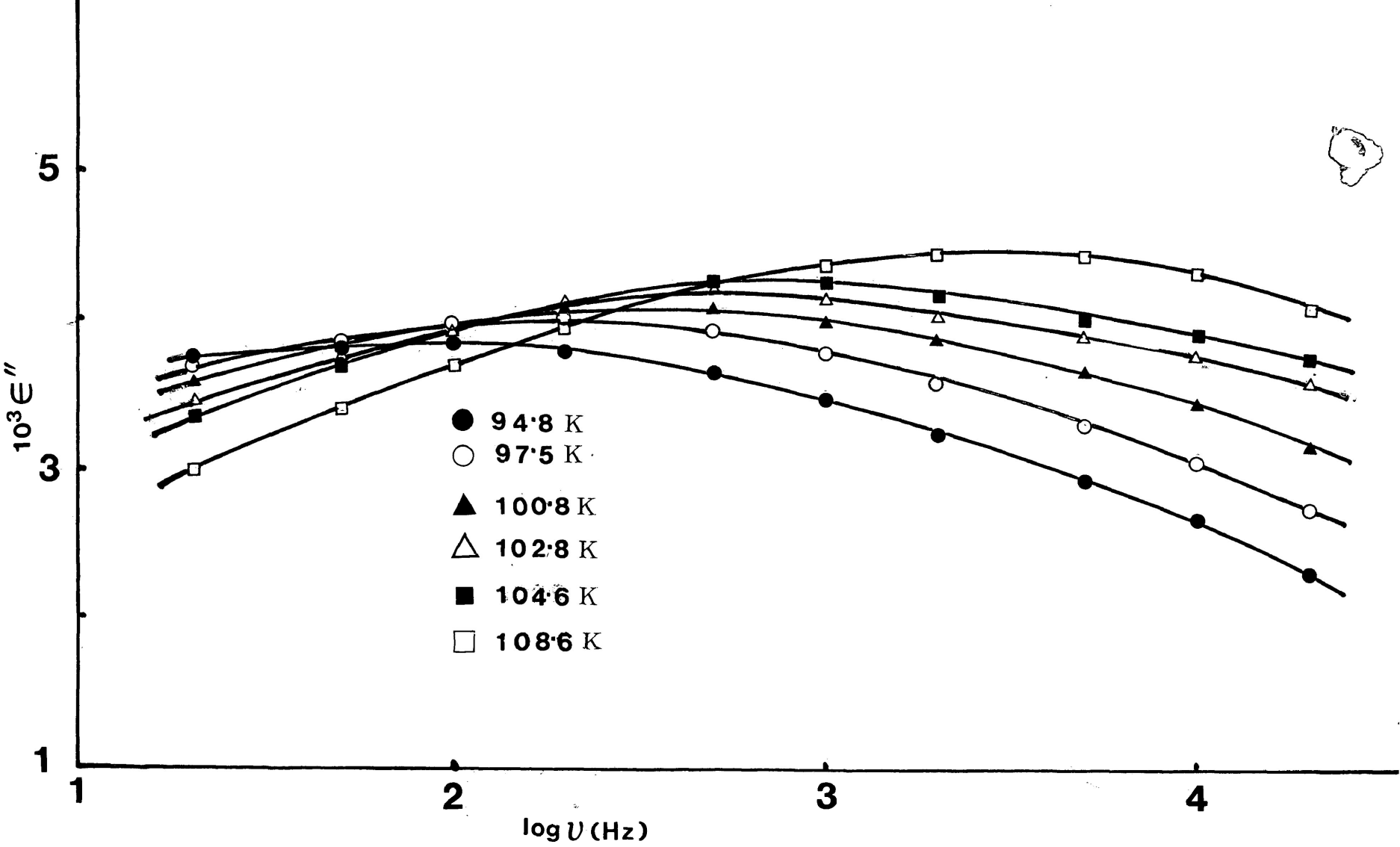

FIGURE III-3b: Plots of dielectric loss factor, ε" versus log frequency (Hz) for camphene in a polystyrene matrix

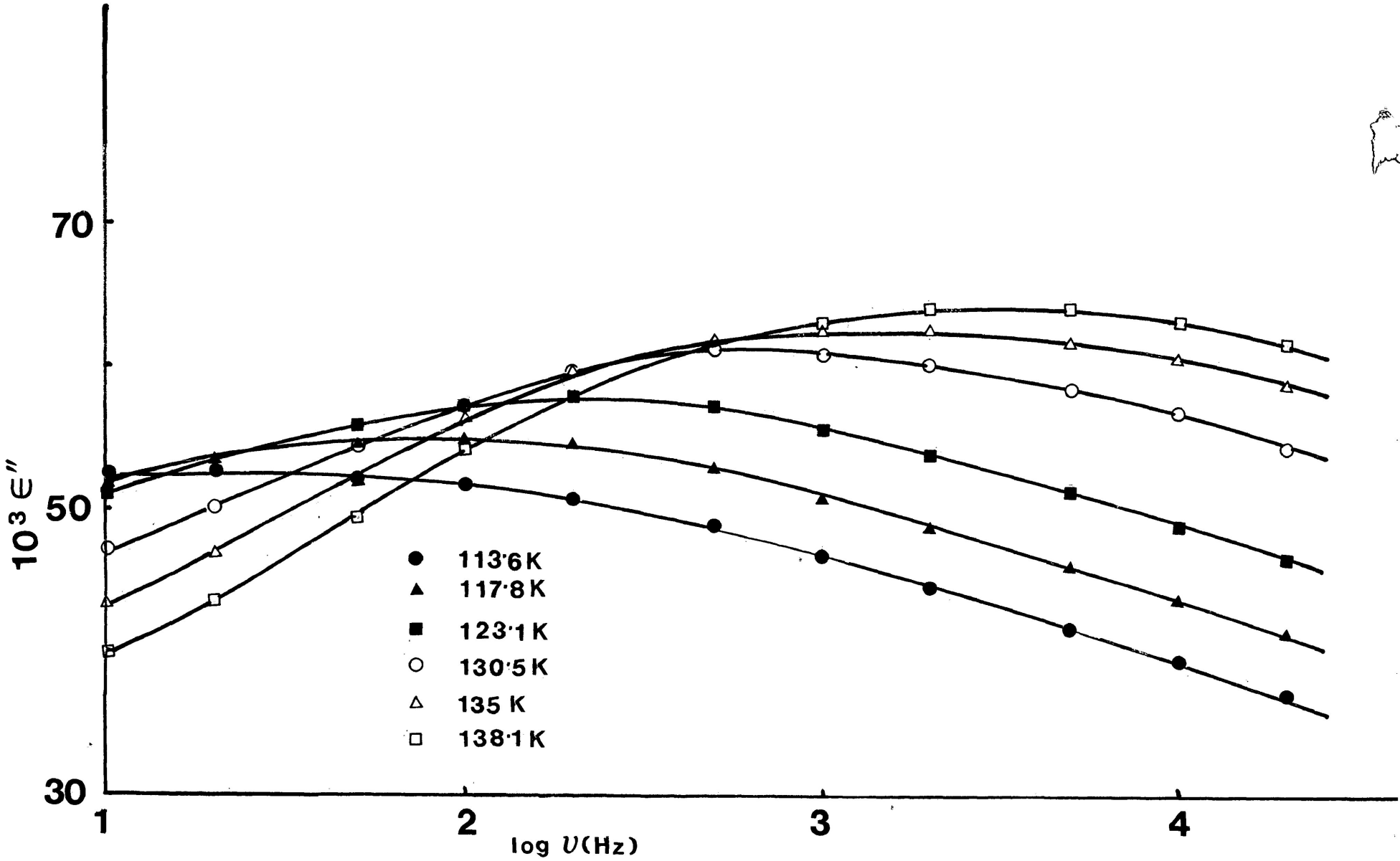

FIGURE III-4b: Plots of dielectric loss factor, ε" versus log frequency (Hz) for 5-norbornene-2-carbonitrile in a polystyrene matrix

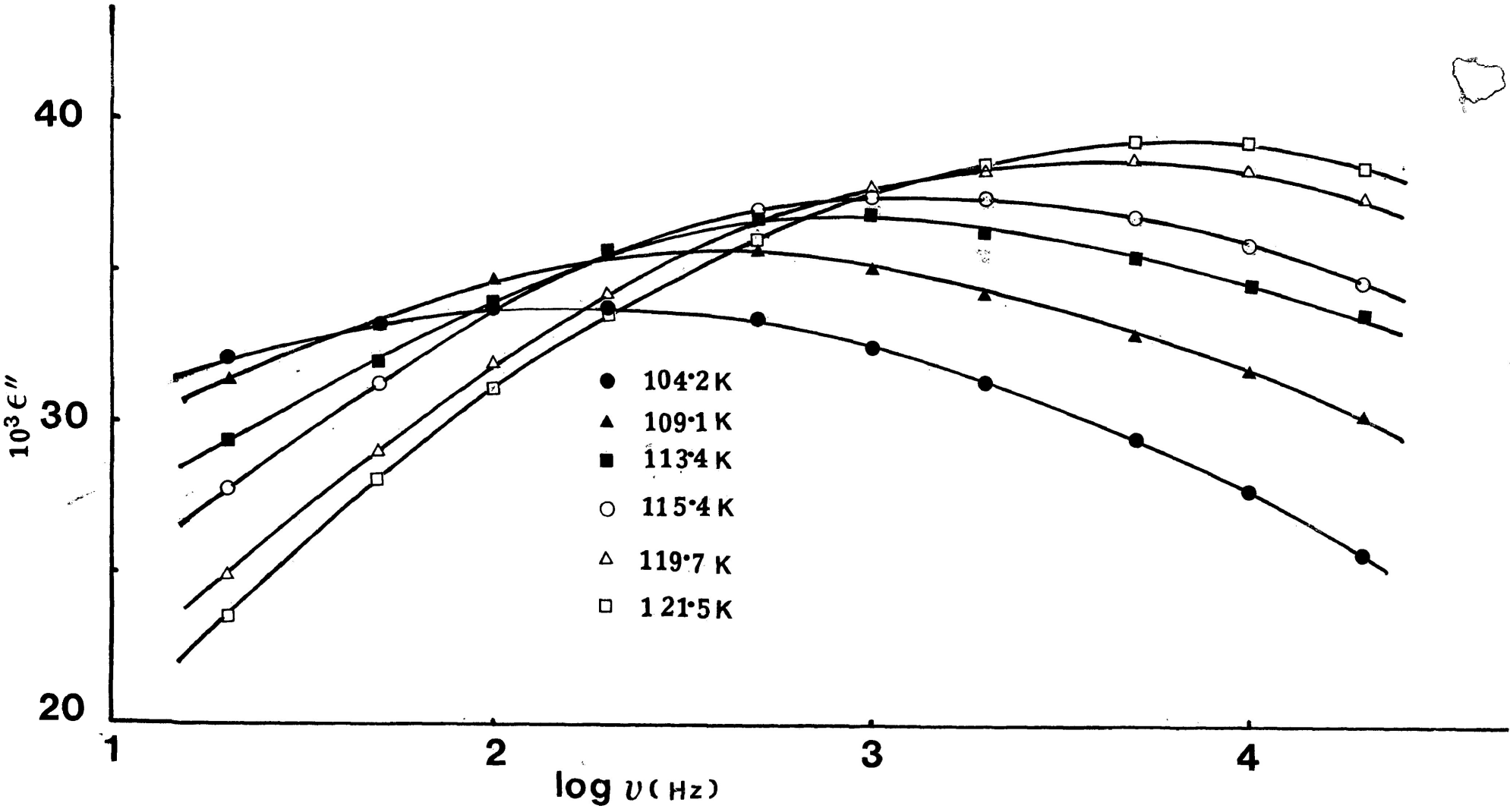

FIGURE III-5b: Plots of dielectric loss factor, ε" versus log frequency (Hz) for 3-chloro-2-norbornanone in a polystyrene matrix

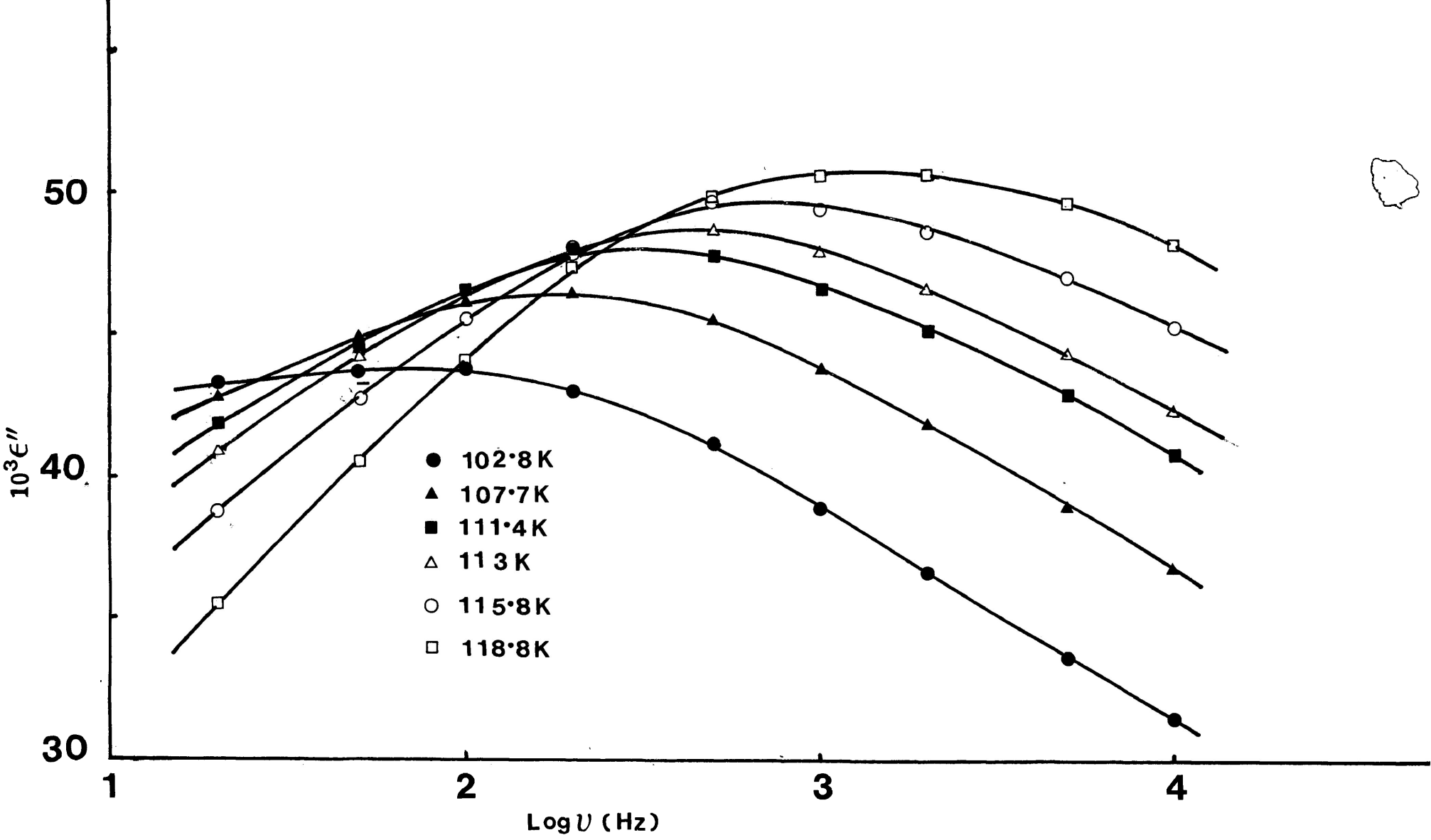

FIGURE III-6b: Plots of dielectric loss factor, ε" versus log frequency (Hz) for camphoroquinone in a polystyrene matrix

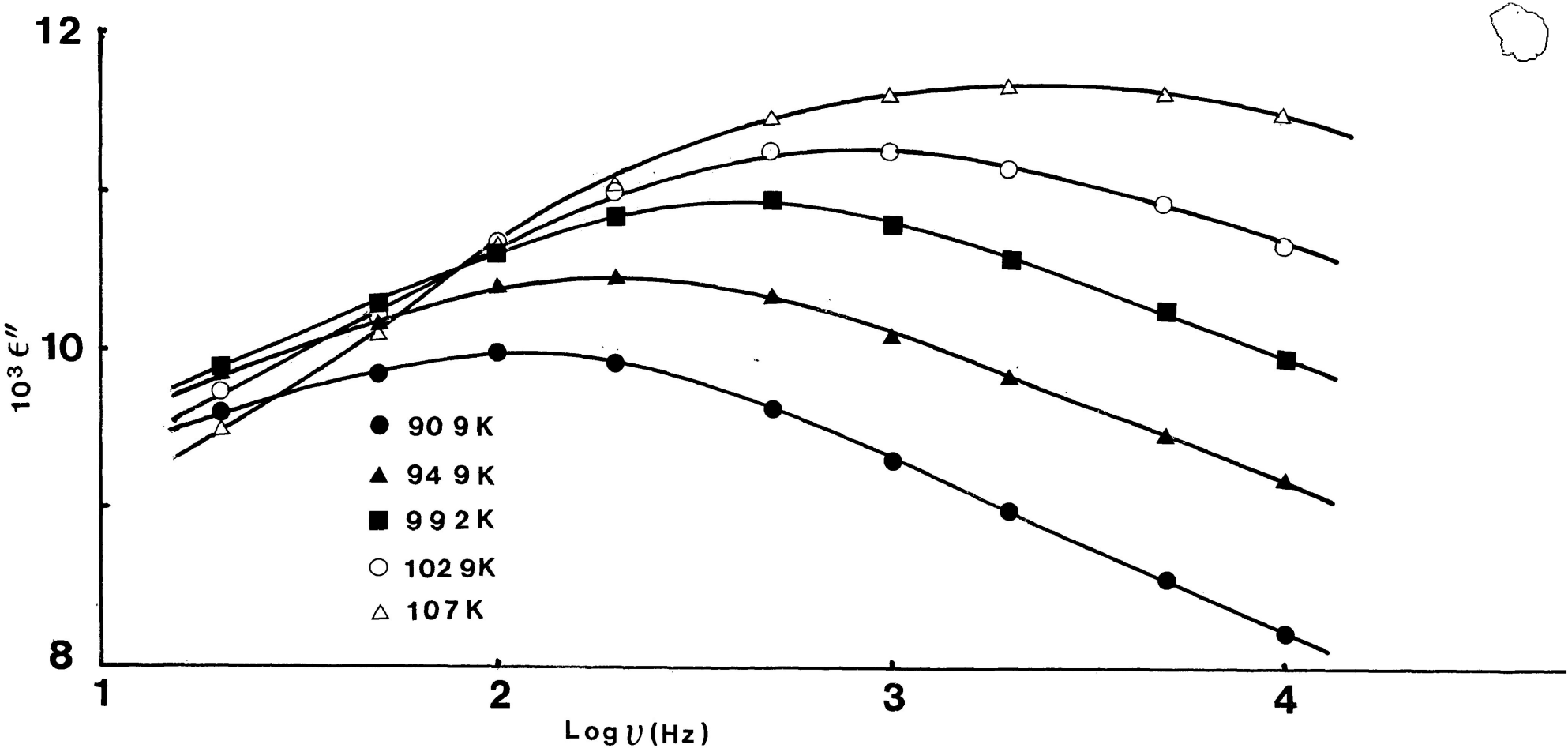

FIGURE III-7b: Plots of dielectric loss factor, ϵ'' versus log frequency (Hz) for exo-2-bromonorbornane in a polystyrene matrix

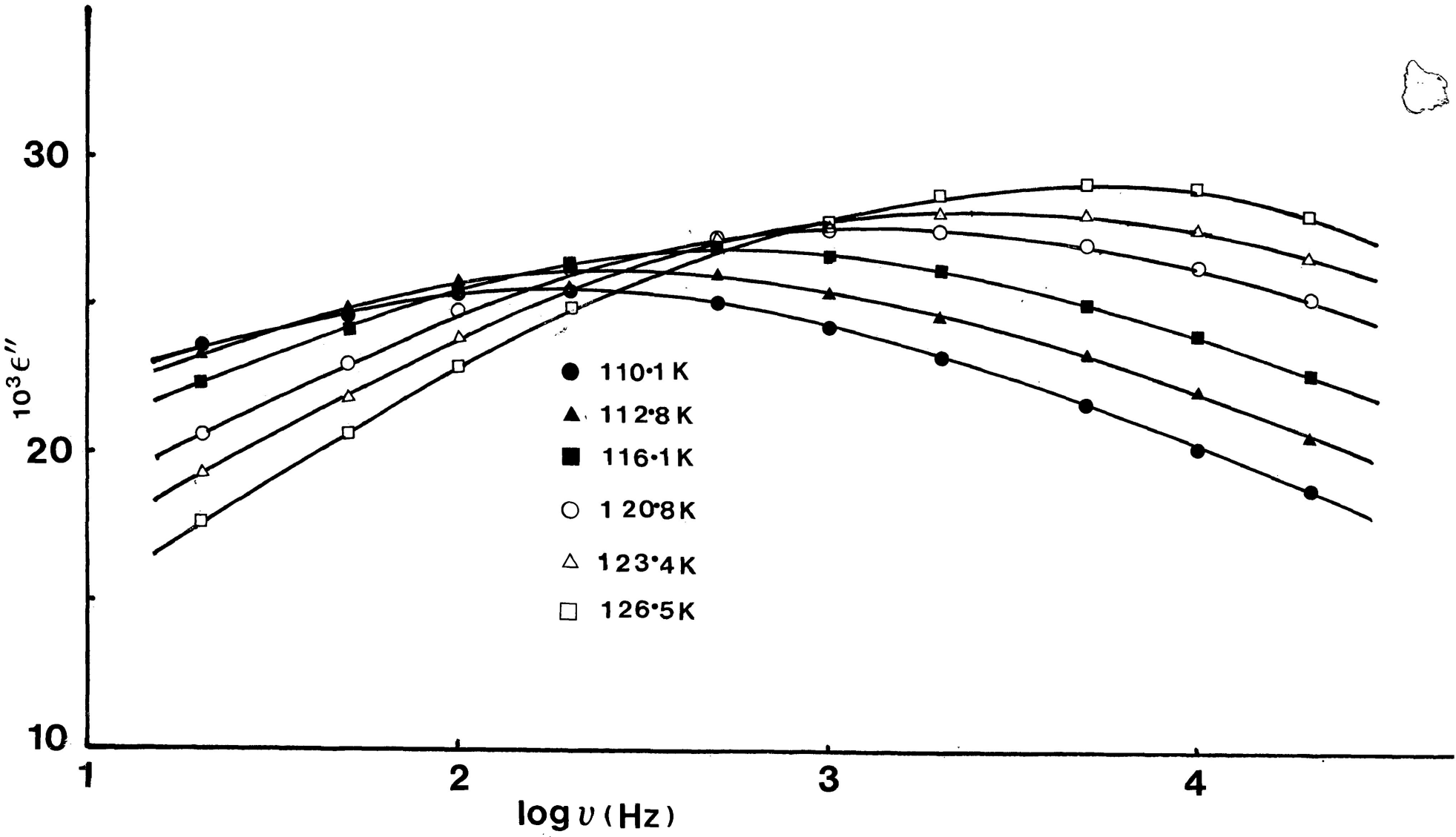

FIGURE III-8b: Plots of dielectric loss factor, ε" versus log frequency (Hz) for 1-fenchone in a polystyrene matrix

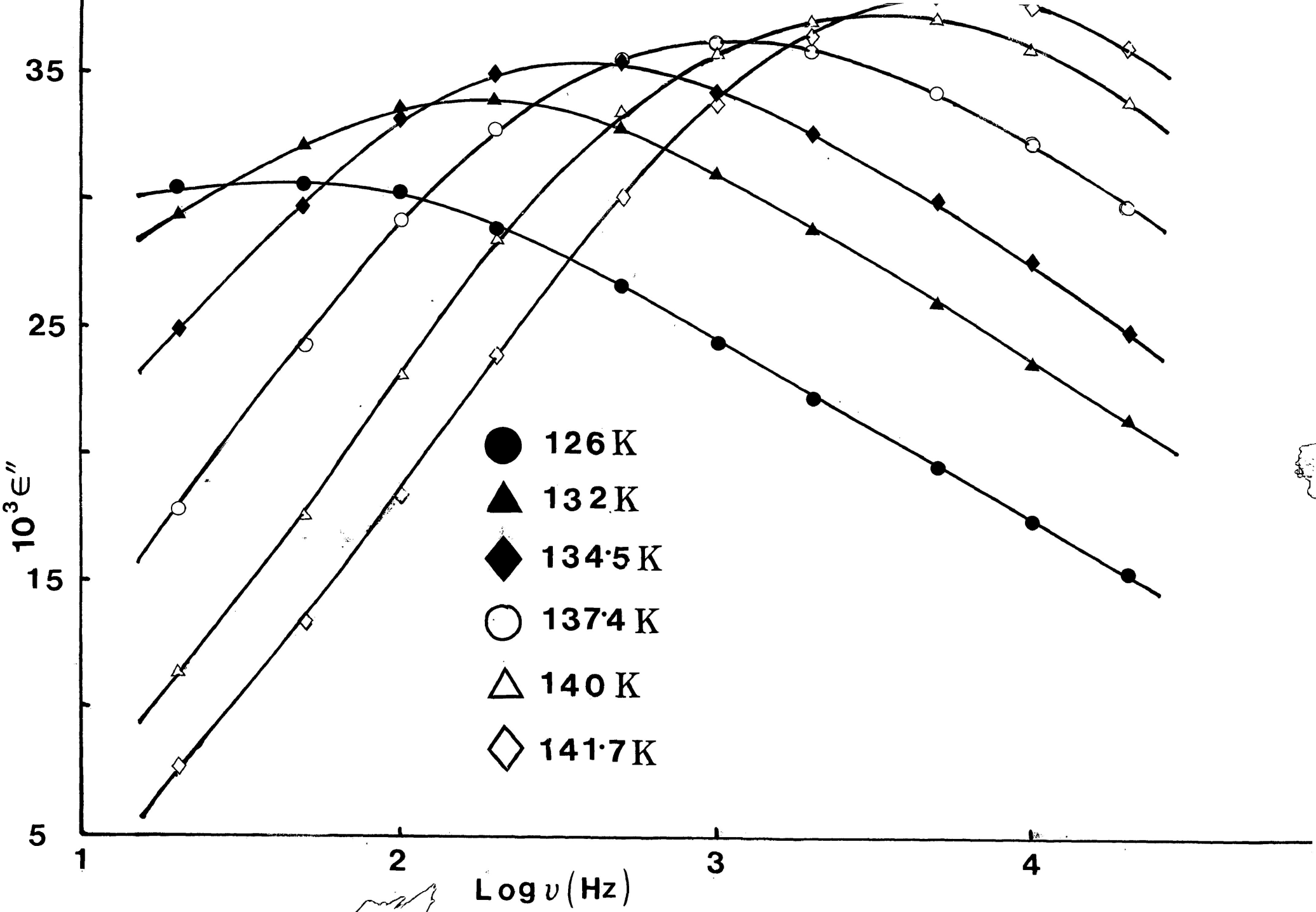

FIGURE III-8b": Plots of dielectric loss factor, ε" versus log frequency (Hz) for 1-fenchone in carbontetrachloride

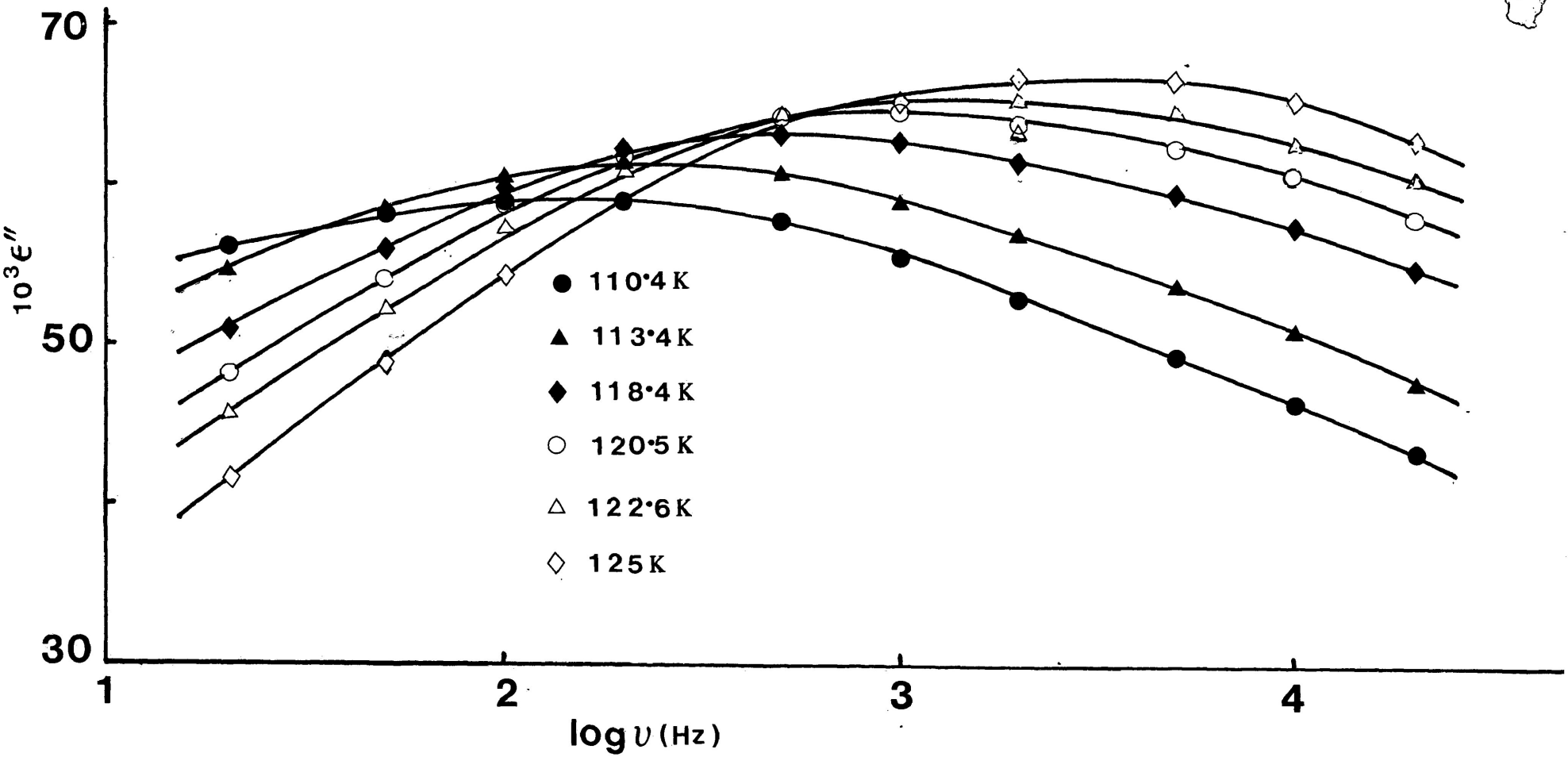

FIGURE III-9b: Plots of dielectric loss factor, ε" versus log frequency (Hz) for 3-methylene-2-norbornanone in a polystyrene matrix

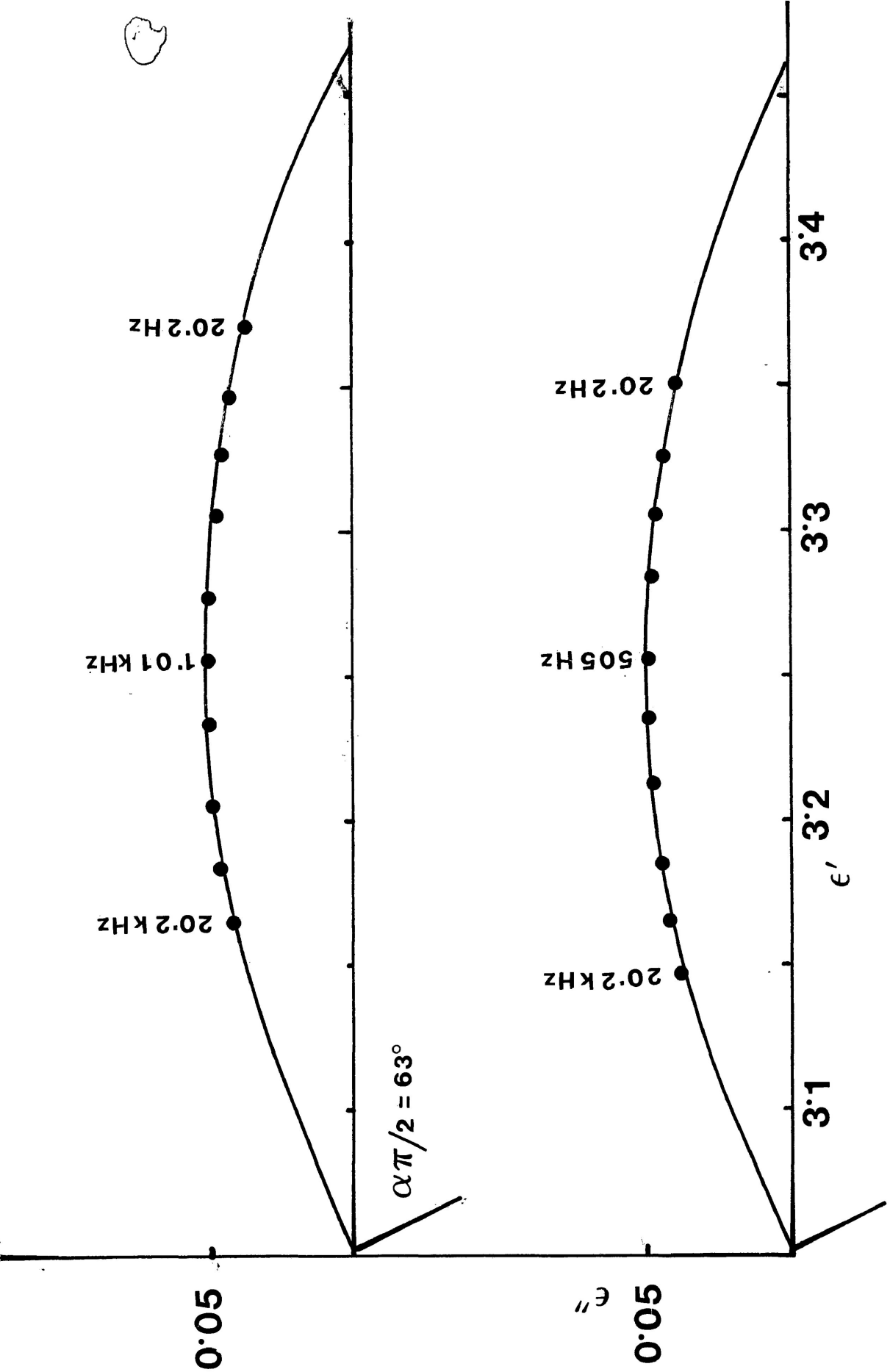

FIGURE III-1c: Cole-Cole plots for norcamphor in a polystyrene matrix at 86.6 K (lower) and 89.5 K (upper).

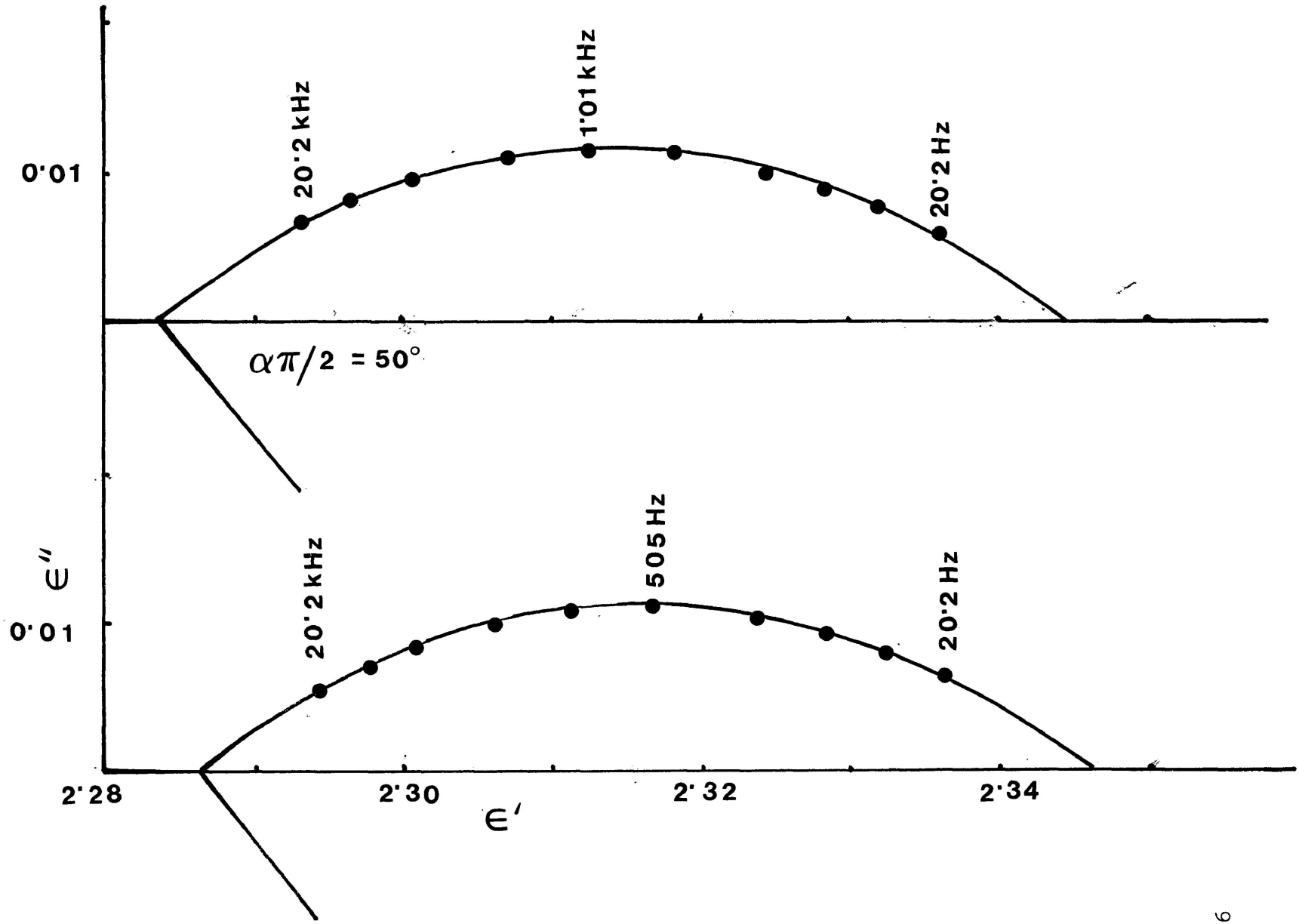

FIGURE III-1c''': Cole-Cole plots for norcamphor in carbontetrachloride at 84.8 K (lower) and 86.4 K (upper)

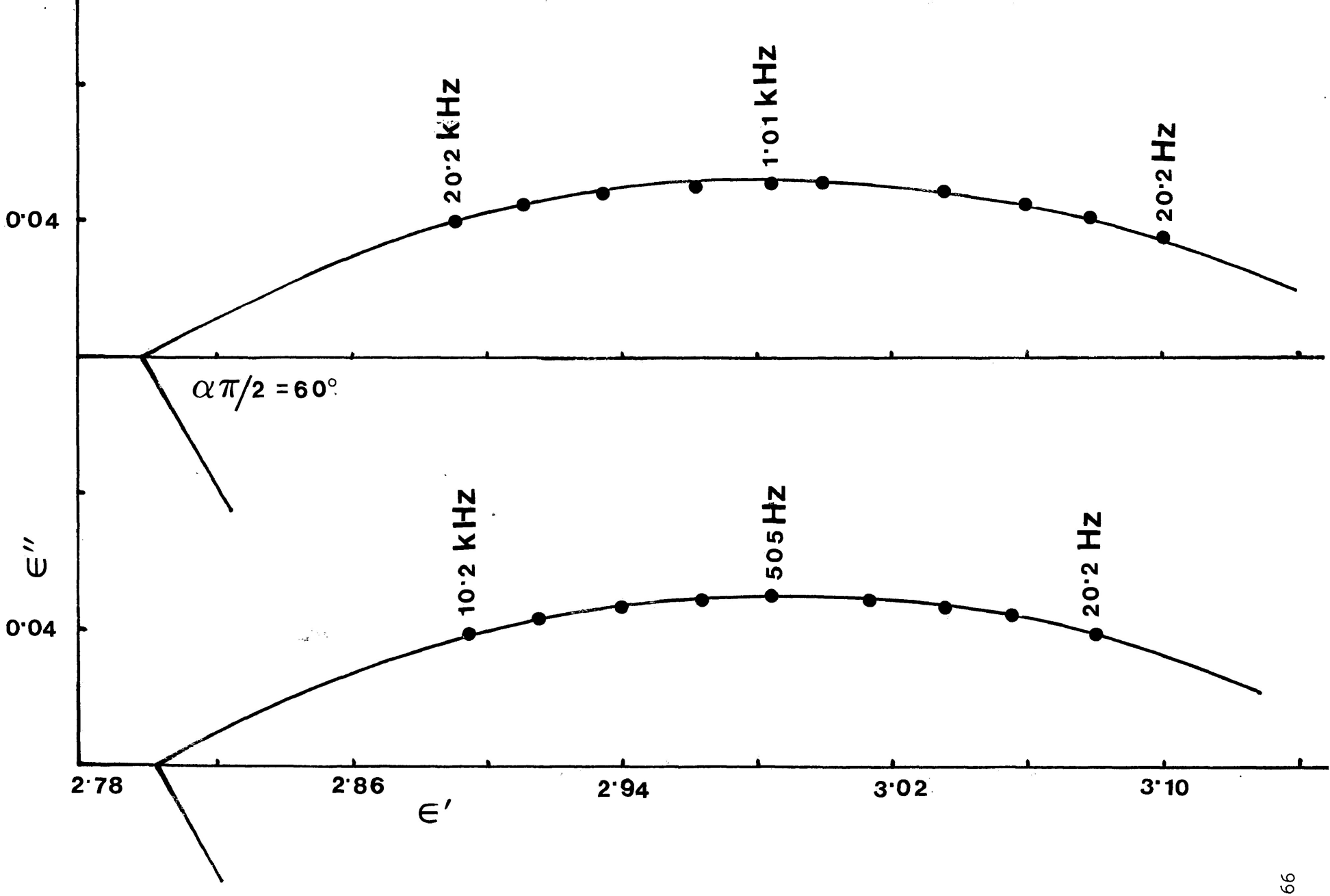

FIGURE III-2c: Cole-Cole plots for camphor in a polystyrene matrix at 95.7 K (lower) and 100.7 K (upper)

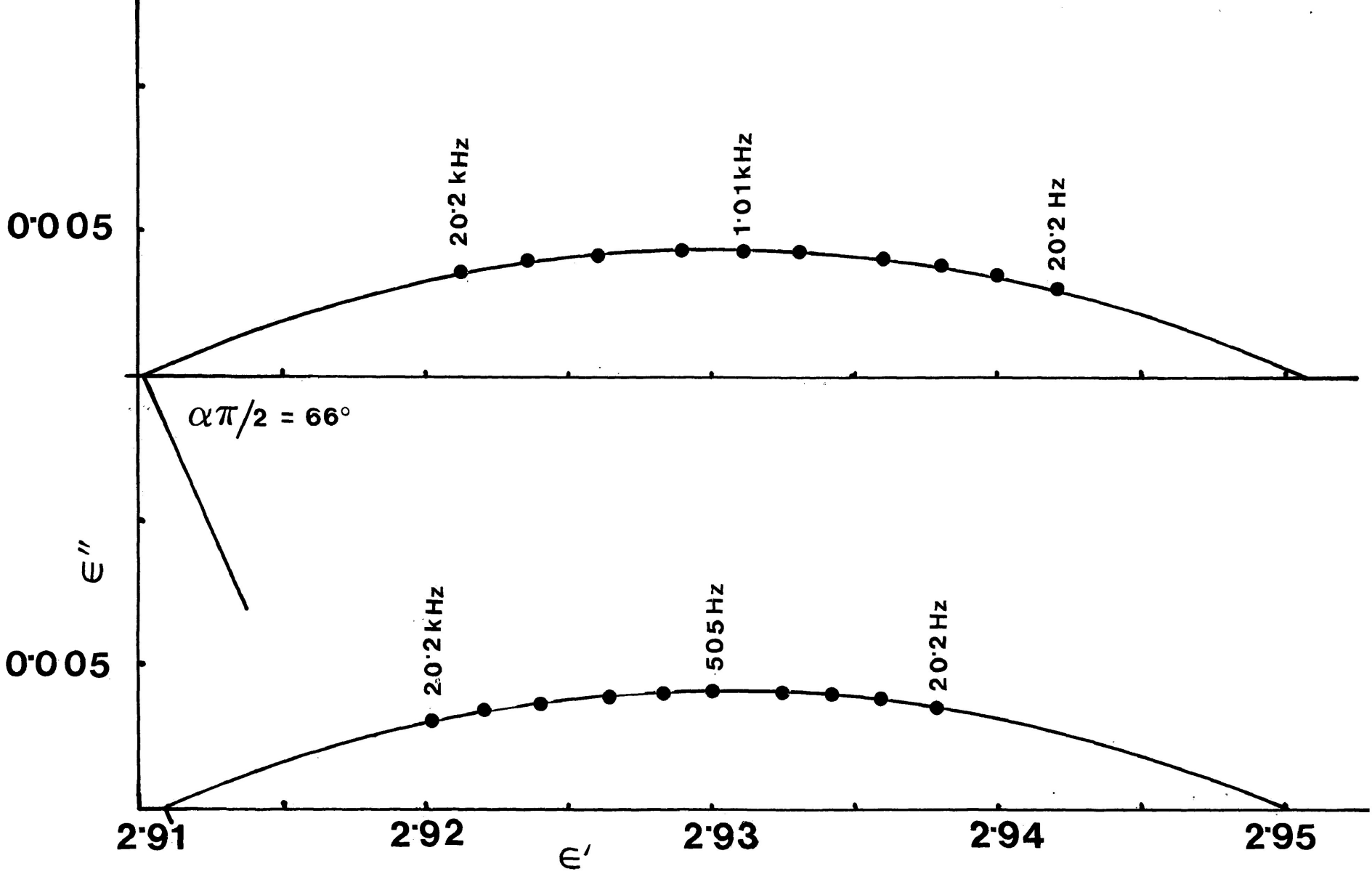

FIGURE III-3c: Cole-Cole plots for camphene in a polystyrene matrix at 100.8 K (lower) and 106.6 K (upper)

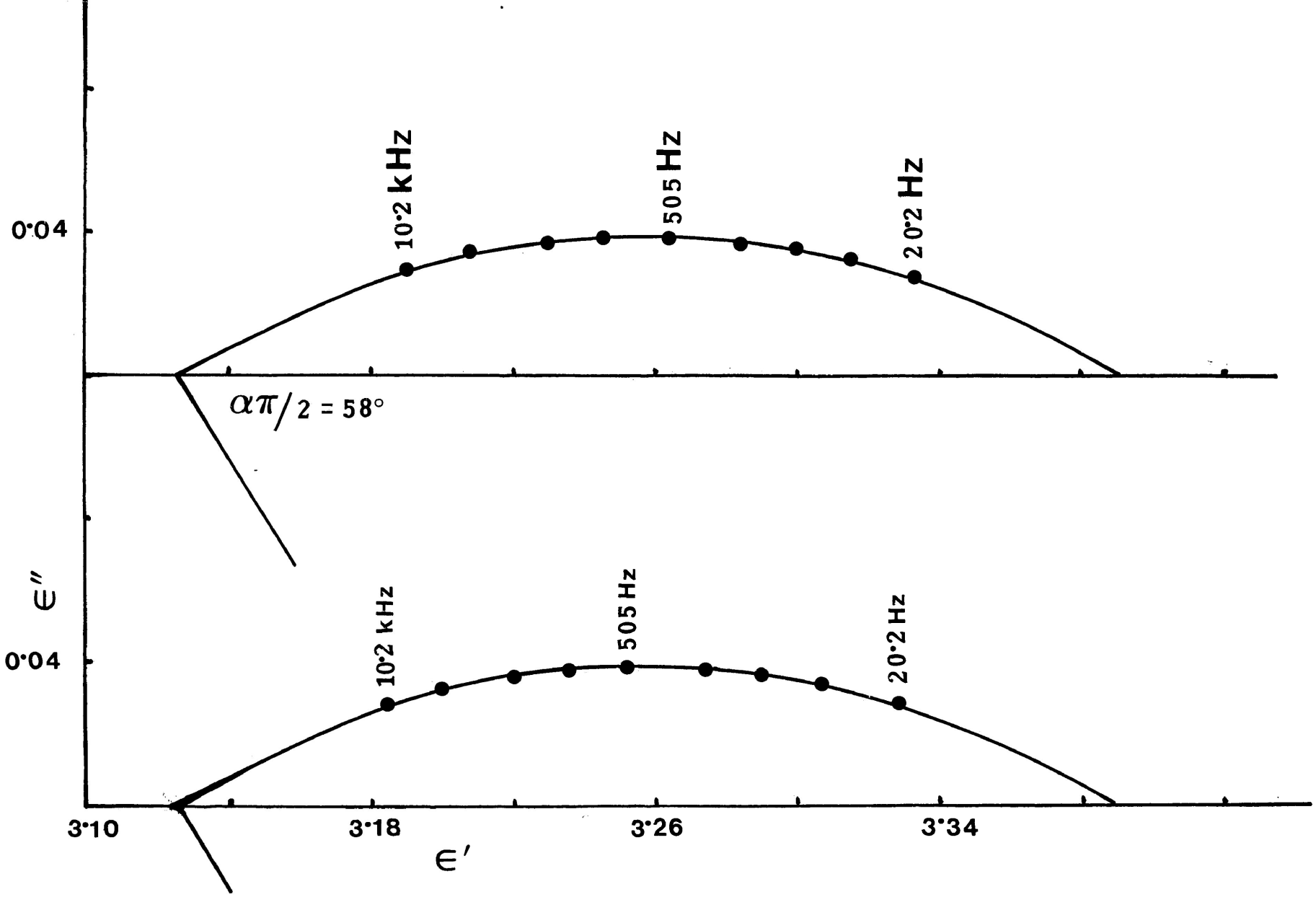

FIGURE III-5c: Cole-Cole plots for 3-chloro-2-norbornanone in a polystyrene matrix at 111.5 K (lower) and 113.4 K (upper)

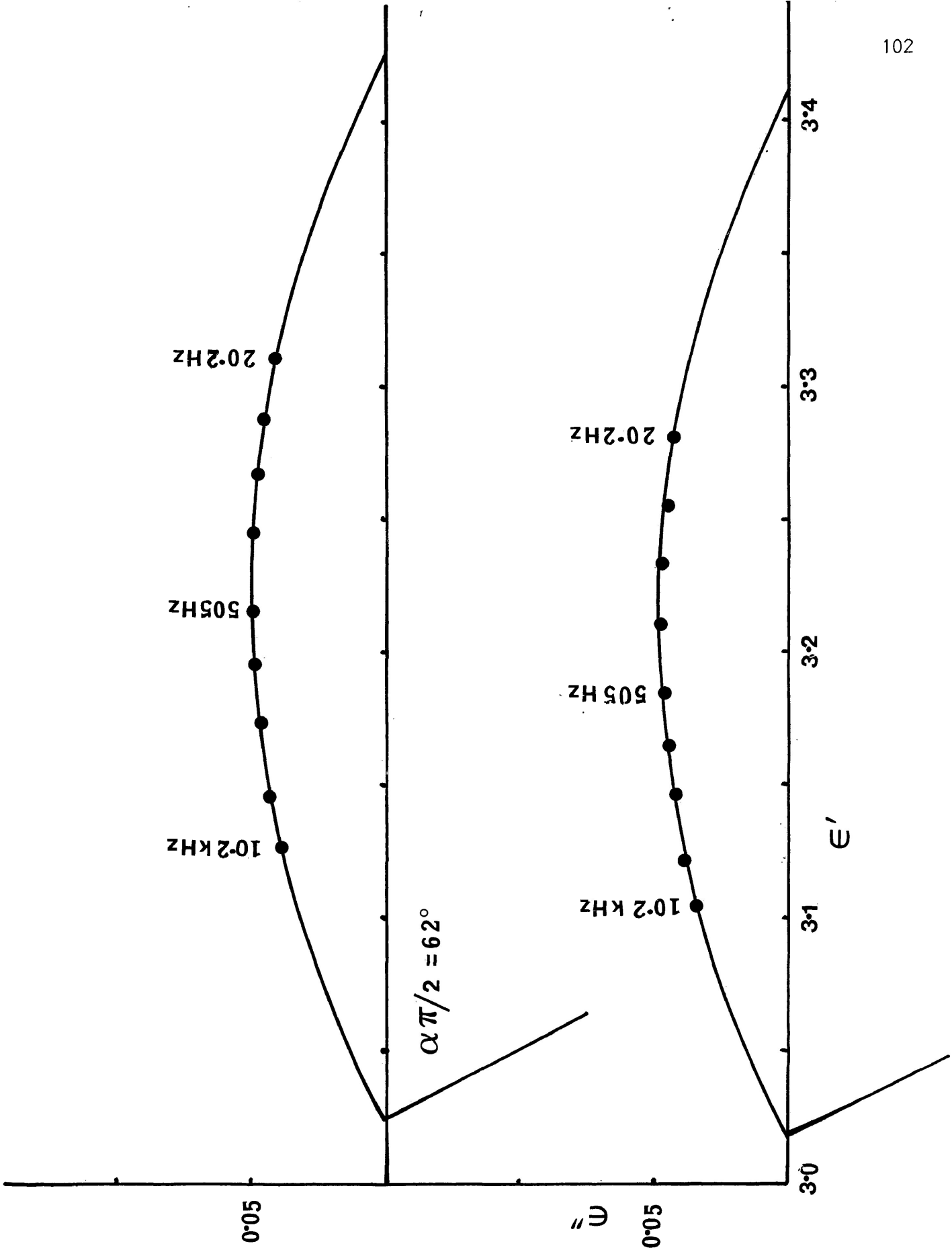

FIGURE III-6c: Cole-Cole plots for camphoroquinone in a polystyrene matrix at 107.7 K (lower) and 113 K (upper)

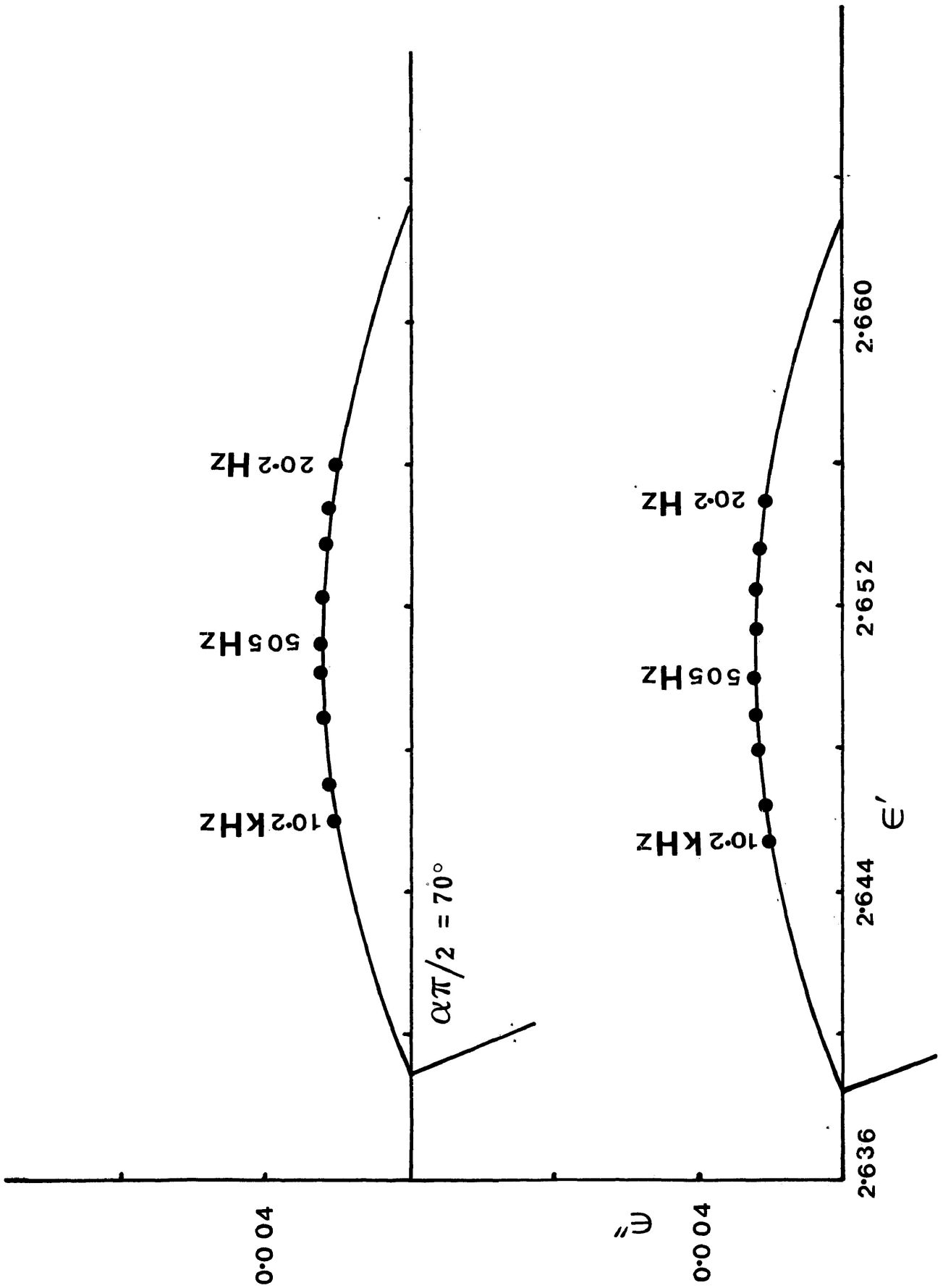

FIGURE III-8c': Cole-Cole plots for 1-fenchone in G.O.T.P. at 121.4 K (lower) and 125.7 K (upper)

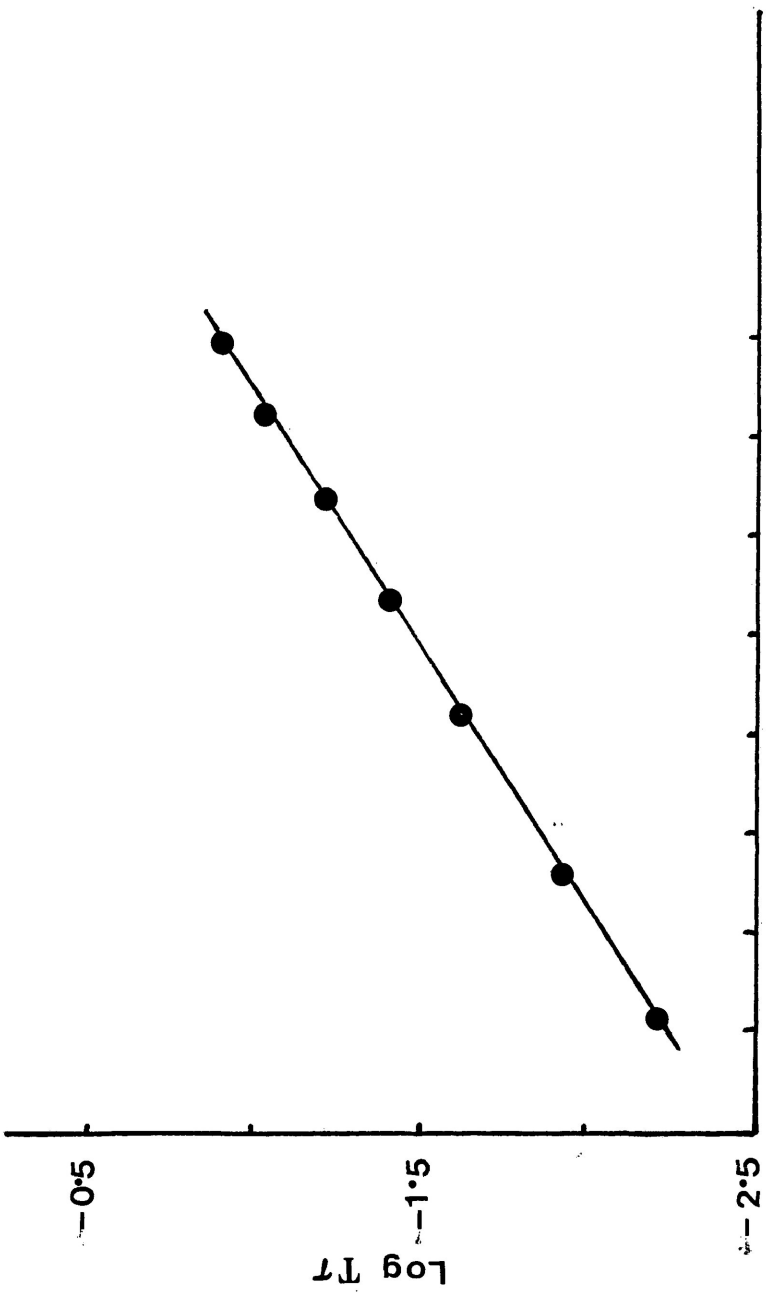

FIGURE III-1d: Eyring plot of $\log T_T$ versus $1/T$ (K^{-1}) for norcamphor in a polystyrene matrix.

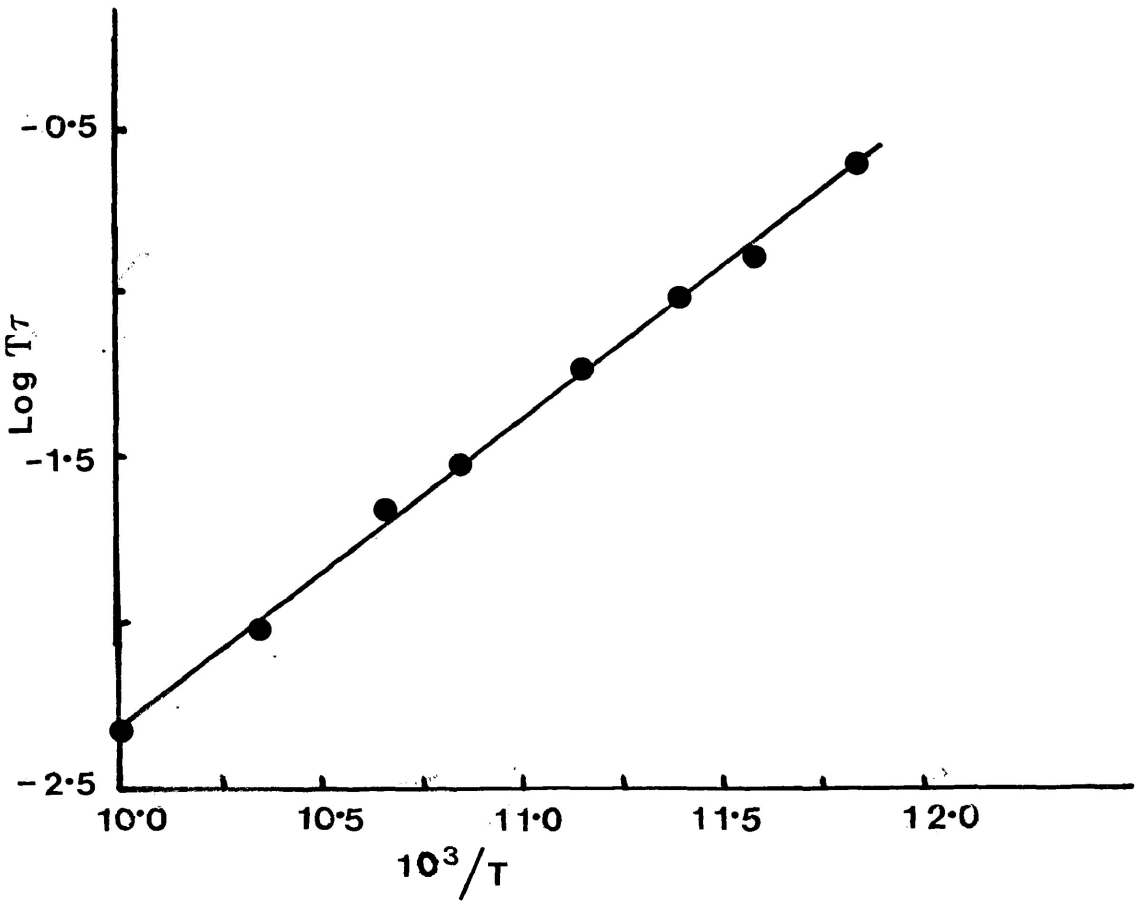

FIGURE III-1d': Eyring plot of logTτ versus 1/T (K^{-1})
for norcamphor in G.O.T.P.

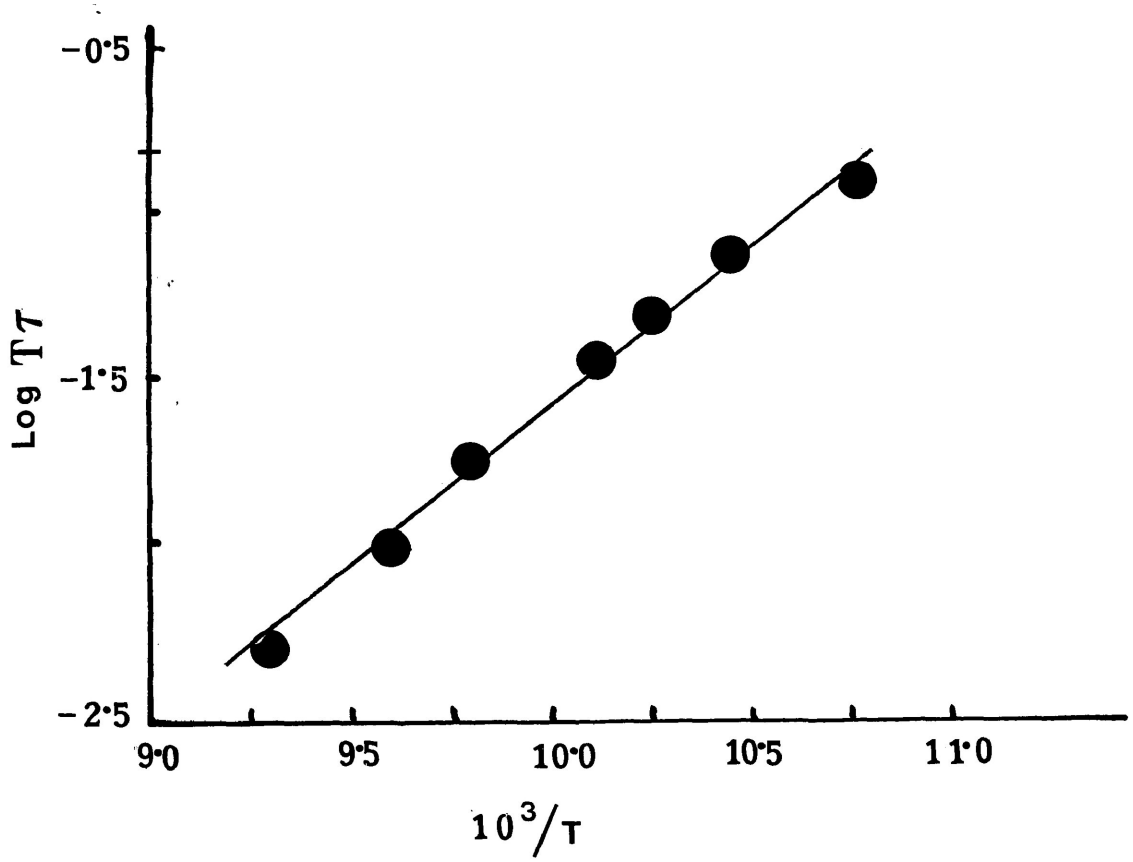

FIGURE III-1d": Eyring plot of logTτ versus 1/T (K^{-1}) for norcamphor in Santovac®

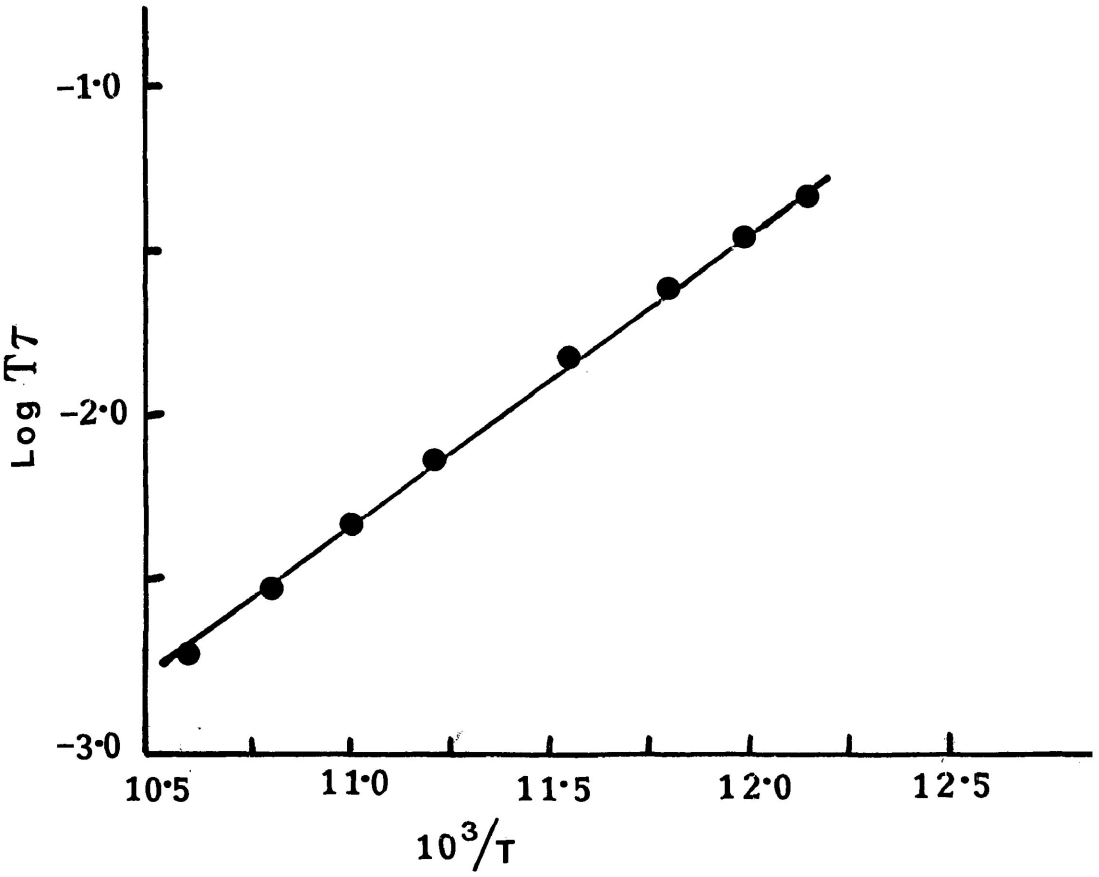

FIGURE III-1d''': Eyring plot of logTτ versus 1/T (K^{-1}) for norcamphor in carbontetrachloride

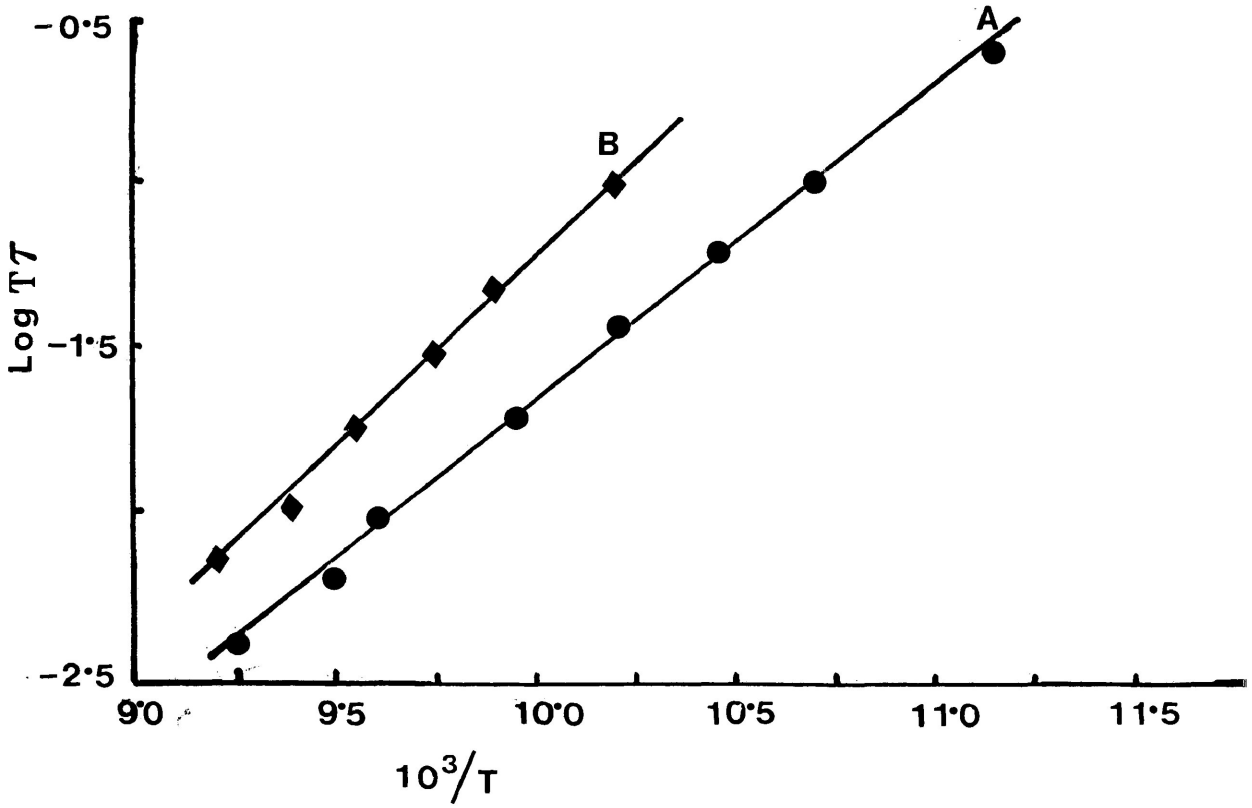

FIGURE III-2d and

FIGURE III-3d: Eyring plots of logTτ versus 1/T (K^{-1}) for (A) camphor and (B) camphene in polystyrene matrices

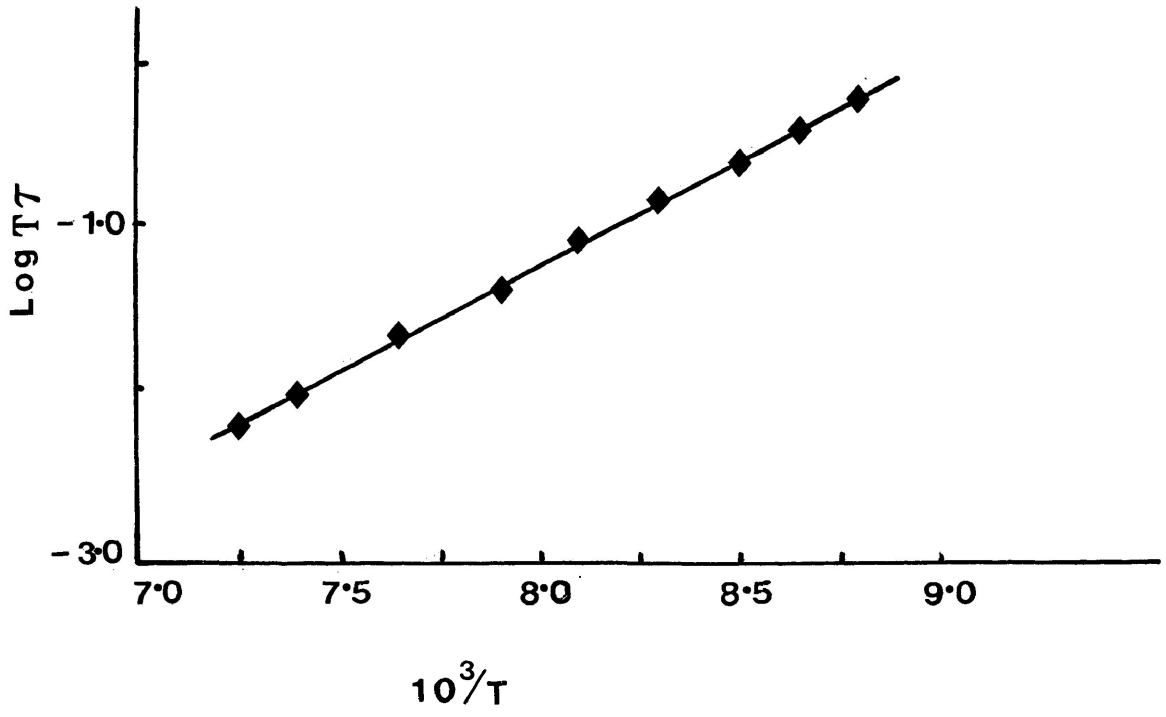

FIGURE III-4d: Eyring plot of logTτ versus 1/T (K^{-1}) for 5-norbornene-2-carbonitrile in a polystyrene matrix

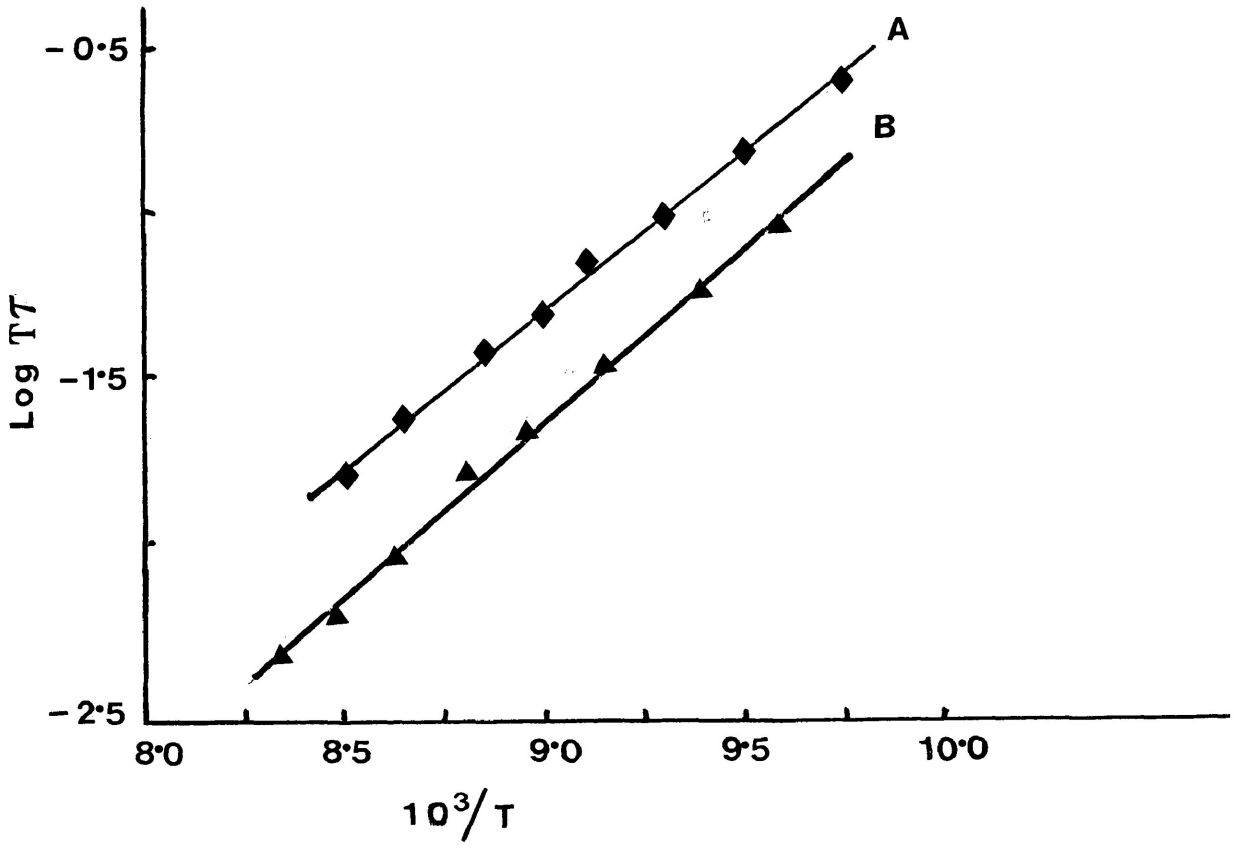

FIGURE III-5d and FIGURE III-6d:

Eyring plots of logTτ versus 1/T (K^{-1}) for (A) camphoroquinone and (B) 3-chloro-2-norbornanone in polystyrene matrices

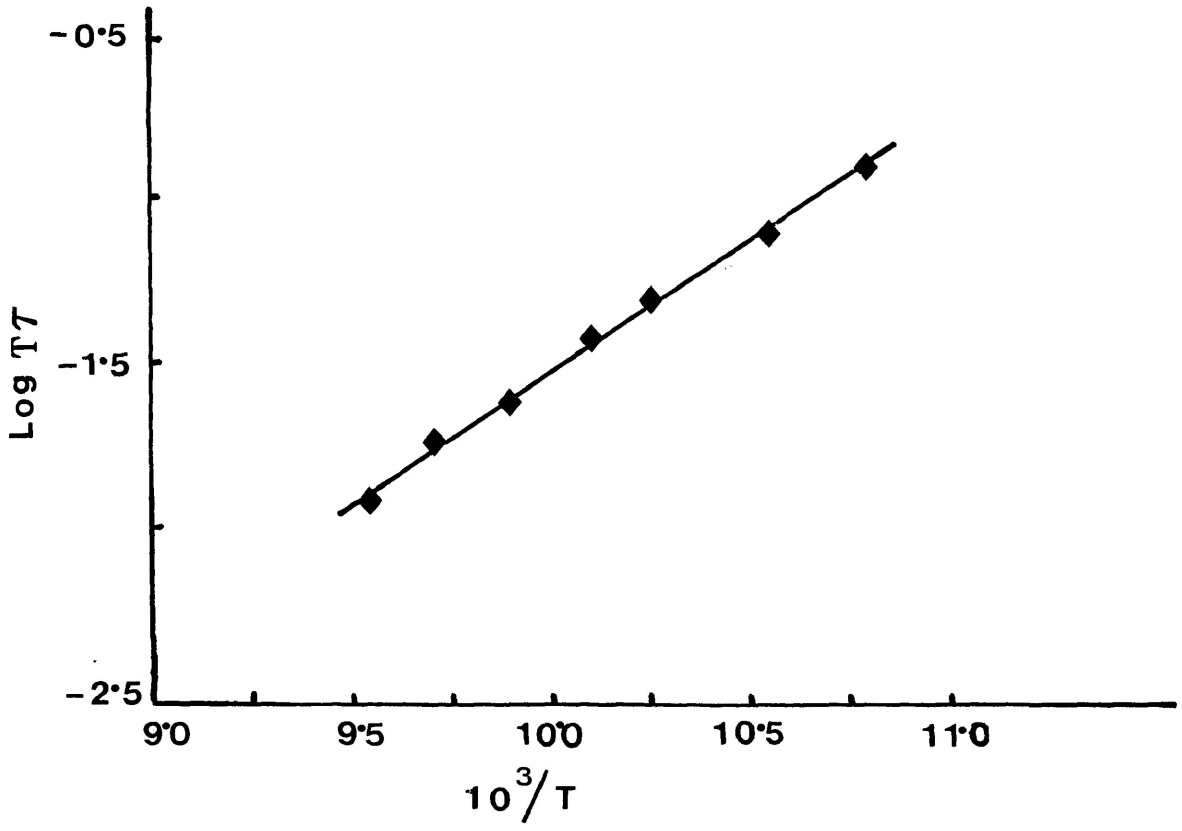

FIGURE III-7d: Eyring plot of logTτ versus 1/T (K^{-1}) for exo-2-bromonorbornane in a polystyrene matrix

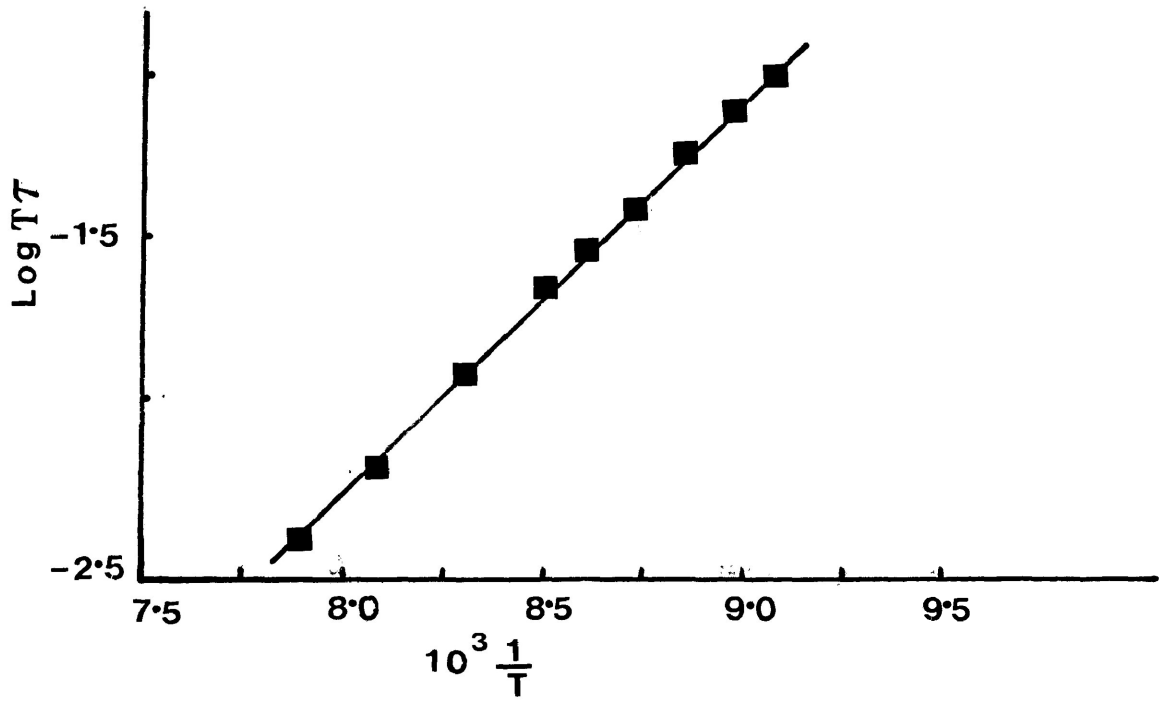

FIGURE III-8d: Eyring plot of logTτ versus 1/T (K^{-1}) for 1-fenchone in a polystyrene matrix

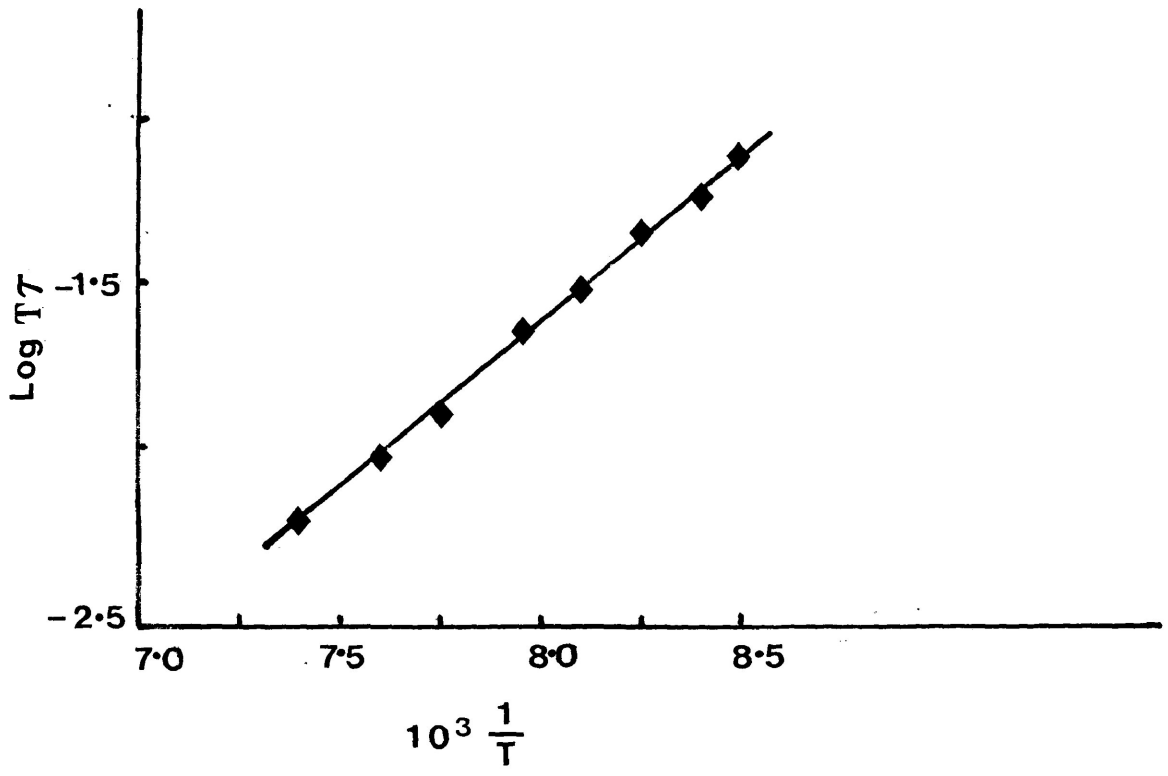

FIGURE III-8d': Eyring plot of logTτ versus 1/T (K^{-1}) for 1-fenchone in G.O.T.P.

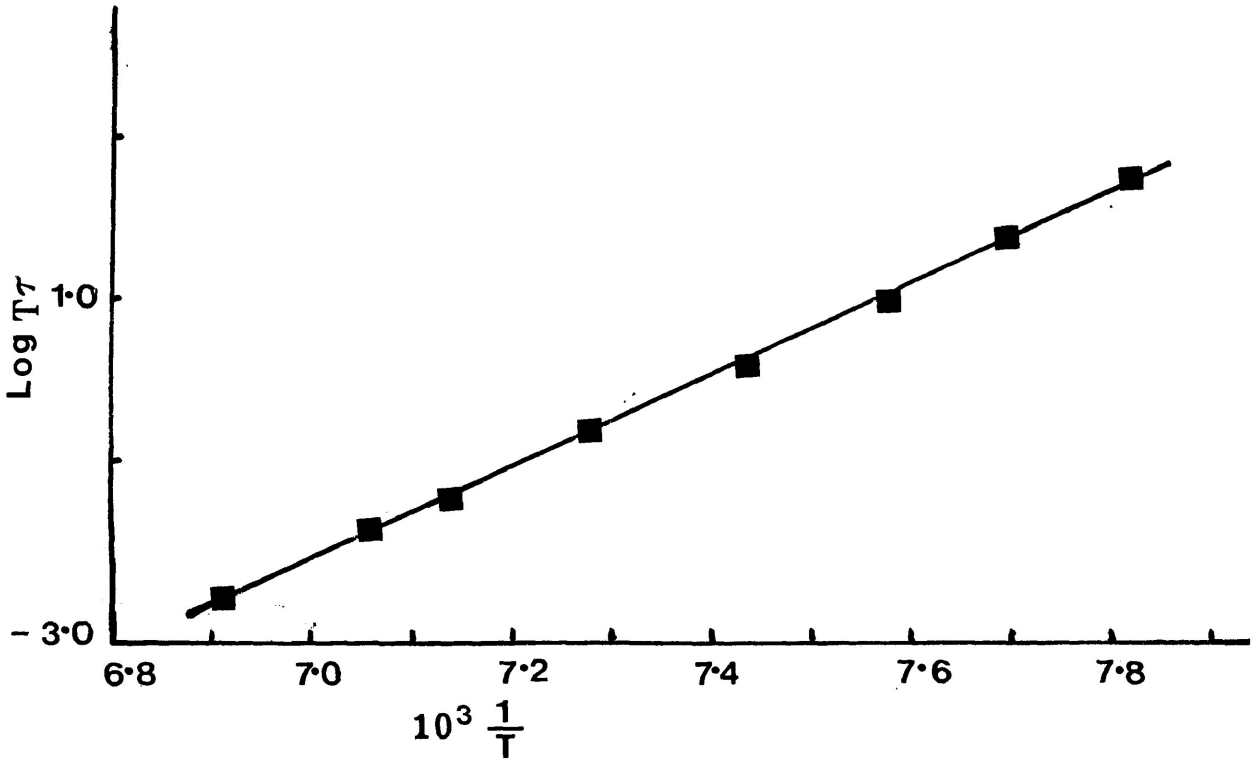

FIGURE III-8d": Eyring plot of logTτ versus 1/T (K^{-1}) for 1-fenchone in carbontetrachloride

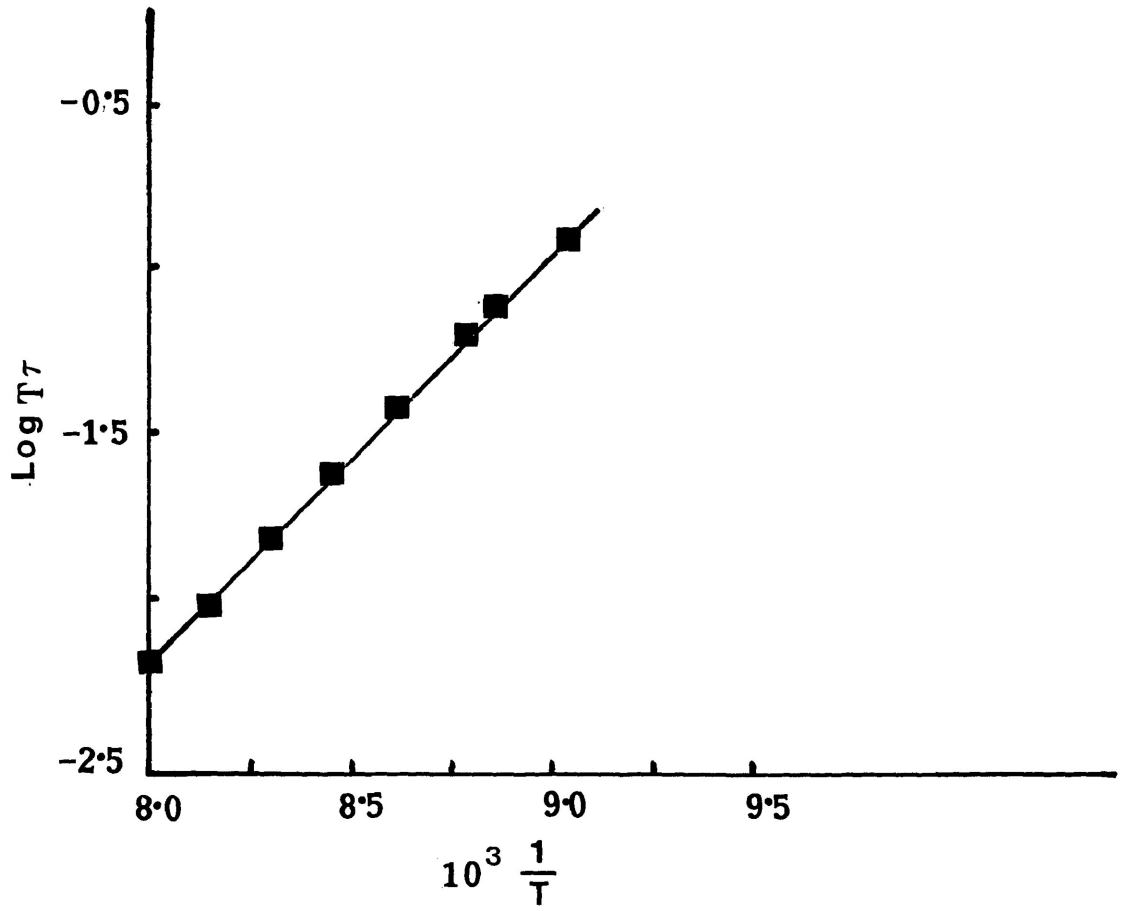

FIGURE III-9d: Eyring plot of logTτ versus 1/T (K^{-1}) for 3-methylene-2-norbornanone in a polystyrene matrix

CHAPTER IV

DIELECTRIC RELAXATION OF SOME LONG-CHAIN ALIPHATIC NORMAL ALCOHOLS AND THIOLS IN POLYSTYRENE MATRICES

IV-1: INTRODUCTION

Because of the possibility of medium strength hydrogen bonding between adjacent molecules, alcohols present a complex and interesting problem in dielectric studies which has been extensively studied by a variety of methods. The first considerable dielectric investigation of alcohols was carried out by Mizushima (1) and discussed by Debye (2). Subsequent high frequency measurements indicated two or more absorption regions (3-7). By using low temperatures, Cole and his co-workers (8-11) were able to bring the dispersion of a few alcohols into the region of audio and radiofrequencies. With the almost continuous coverage of the spectrum they were able to distinguish three separate dispersion regions, all of the Debye-type.

The long chain alcohols, both primary and secondary, show pronounced absorptions in the solid phase, usually below 1 MHz (12-19). The crystalline alcohol shows a larger permittivity than the liquid at the freezing point, which suggests that the chain-association of hydroxyl groups already present in the liquid is further extended by alignment in the solid. Sack (20) proposed that the strong dipolar absorption is the result of a reversal of such a

giant dipole by rotation of the individual hydroxyl groups about the C-O bonds, accompanied by the breaking and re-forming of the hydrogen bonds, and without appreciable movement of the rest of the molecules:

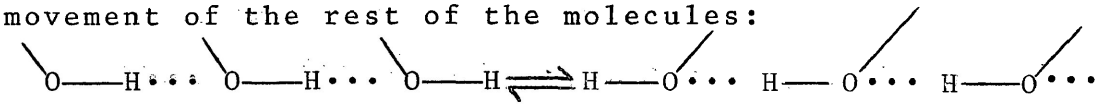

Meakins (21) studied the dependence of the absorption upon the length of the ···O——H··· chain and found that the absorption is in its major aspects independent of the length of the individual alcohol molecules, but there is a marked difference between the primary and secondary alcohols having the activation energies 6.28 and 25 kJ mol^{-1} respectively. This may well result from the head to head layer lattice of the primary alcohols (22), which provides the hydroxyl groups with additional bonding sites (i.e. (a) and (b))

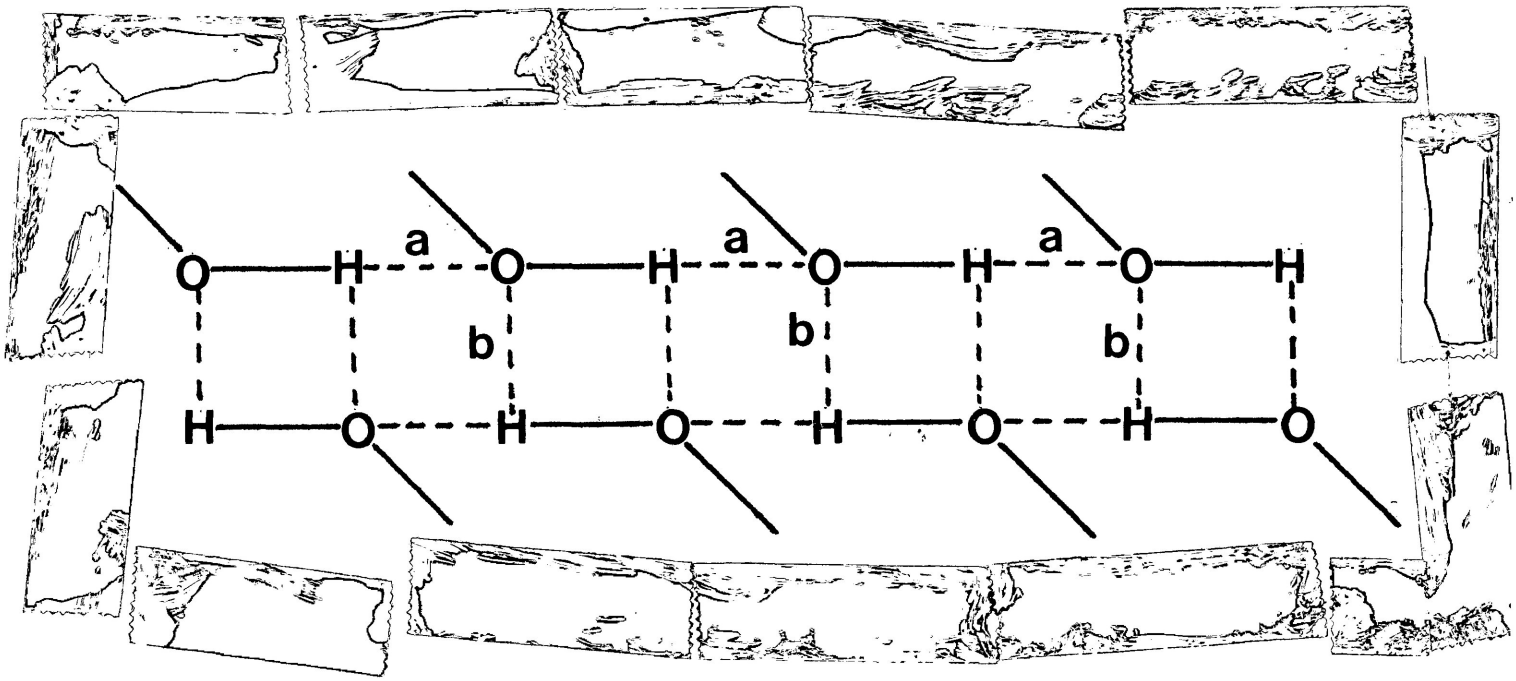

In the secondary alcohols only the one sequence (a) of hydroxyl group interaction is present.

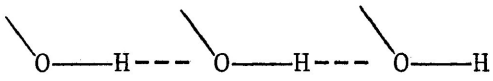

Daniel (23,24) proposed that the dielectric properties of the long-chain secondary alcohols were due to the presence of chains of hydrogen bonds in conjunction with some kind of structural flaws.

Now it is reasonably well established that the dielectric dispersion of primary aliphatic alcohols in the pure liquid form, over a wide temperature range, may be characterized by three relaxation regions with the low-frequency process dominating (8,10,11,25-28). The high frequency processes (τ_2 & τ_3) which provide relatively small contributions in the pure liquids become increasingly important, or alternatively the contribution from the low-frequency process (τ_1) decreases, on dilution with an inert non-polar solvent (29-31). For alcohols with a sterically hindered -OH group the low-frequency process is either very small or completely absent in the pure liquid (32-34), and in an inert solvent the absorption may be represented by the τ_2 and τ_3 processes only (31,35).

The highest frequency process (τ_3) is only slightly dependent on molecular size and alcohol concentration (25,31) and is of the same magnitude as that found for -OH group rotation in phenols (36,37). The fact that this process largely dominates the absorption of alcohols at very low concentrations suggests that the dipole orientation of alcohol monomers occurs primarily by -OH group rotation about the C-O bond in monomers rather than by whole molecule rotation.

The intermediate relaxation time, τ_2, has been accounted for by monomer or OR group rotation (10,25).

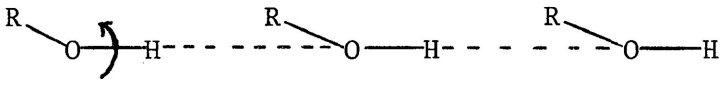

Dannhauser (32) examined eight liquid isomeric octanols in a wide temperature range from -90° to 130°C and proposed a model based on hydrogen-bond associative equilibrium involving both ring dimers

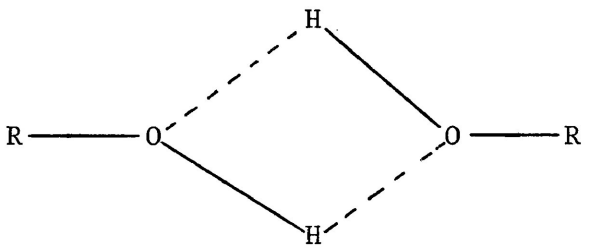

and linear

chain multimers.. Crossley et al (31) considered that for dilute solutions of alcohols with a sterically hindered -OH group, τ_2 is due only to the monomer rotation. In view of the increasing τ_2 and its relative contribution C_2 with increased alcohol concentration they suggested that these quantities are no longer descriptive of monomeric molecules alone but are weighted averages of the values for the monomer and one or more polymers.

The Debye-like (25) long relaxation process (τ_1) is undoubtedly due to a mechanism which is sensitive to the steric environment of the hydroxyl group since it is not evident for the more hindered octanol (31,34). The molecular size dependence of τ_1 and its magnitude (25) suggest that rotation of associated molecular units might be responsible. However, if association is into linear chains the great distribution of sizes for such species would give rise to a distribution of relaxation times conflicting with the Debye-like nature of this dispersion (38). For many years, the dielectric relaxation of alcohols has been interpreted in terms of hydrogen-bond rupture followed by rotation of monomers, where the former is the rate determining step, the required energy being interpreted as the activation enthalpy for dielectric relaxation (27,33,39). An objection

to this theory has been put forward by Sagal (40) who found the relaxation frequency to be influenced by dilution of the alcohol with an apolar solvent. Another difficulty offered by this theory is that it cannot explain that the activation enthalpies of the various monoalcohols differ greatly as has been pointed out by Middelhoek (41,42) who determined activation enthalpies varying between 33 and 65 kJ mol^{-1} for the straight-chain isomeric heptanols.

In a study of 6-, 4- and 2-methyl-1-heptanol, Dannhauser and Flueckinger (43) proposed that in dielectric relaxation hydrogen-bond rupture is a prerequisite rather than a rate determining step. A particular hydrogen-bond will break and reform many times without the reorientation of either the donor or acceptor molecule. Because the local liquid alcohol structure remains, on average, chain associative, the dipolar reorientation is necessarily co-operative and occurs relatively seldom. When it does occur, the rate of reorientation depends upon the size and shape of the entire molecule insofar as this determines the interaction of a specific molecule with its surroundings and also because the structure of the molecule determines the nature of the surroundings. The more highly branched the alkyl group and the more sterically hindered the -OH group, the greater the required degree of co-operation.

A highly polar cyclic tetramer (44) has satisfactorily accounted for the dependence of τ_1 upon molecular size, the absence of any distribution of relaxation times, the larger polarization (32), and if steric effects prevent the association of monomers into multimer other than dimers, the absence of low-frequency process (31,32) and the small polarization for the hindered octanols (32), Maleki (45) proposed another model of association into a mixture of dimers, trimers, tetramers and pentamers and concluded that trimers are cyclic while tetramers and pentamers are open-bonded units.

In contrast to the multiple relaxation processes of primary aliphatic alcohols in dilute benzene (46) and n-heptane (31) solutions, the dielectric absorption of the same alcohols in p-dioxane solution shows a symmetrical distribution of relaxation times with a short mean relaxation time attributable to strong solute-solvent complex formation (46). Crossley (47) examined the dielectric relaxation of some isomeric butanols and 1-decanol in p-xylene, cyclohexane and mesitylene solutions at 25°C over the range 1-35 GHz. The data for the concentrated solutions

separated into two dispersion regions and were analyzed in terms of two relaxation times, both of which are sensitive to the nature of the solvent and solute and their concentration. The author attributed the relaxation times to molecular and -OH group relaxation processes, and found that their magnitudes and weight factors are dependent upon the relative importance of solute-solute and solute-solvent interactions.

Thus it is clear that the alcohols have been most extensively studied, but still there are some conflicts regarding the molecular model capable of satisfactorily explaining the experimental results. In Dannhauser's words, "Unfortunately, after forty years of study, a detailed molecular model for dielectric relaxation in alcohols is still not available".

In recent years, the dielectric absorption studies of polar solutes dispersed in a polystyrene matrix have received considerable attention in the literature. This method has proved its success for the accurate determination of intramolecular energy barriers and separation of molecular and intramolecular processes relate to the different influence the high viscosity dispersion medium has on the two types of processes. The aim of our present investigation

is to gain insight into the types of relaxation processes which can take place in alcohols by using this polystyrene matrix technique. The interpretations of previous investigators have been based largely on arguments from relaxation times and distribution parameter values which sometimes may be quite deceptive as can be Budó analyses. Our present intent was to separate completely the absorption peaks of some or any of the relaxation processes and to characterize the absorption processes with the appropriate relaxation parameters. The use of the polystyrene matrix technique has already proved its success for the separation of molecular and intramolecular processes for a series of long chain aldehydes (48) and 1-bromoalkanes (49).

IV-2: EXPERIMENTAL RESULTS

The dielectric measurements of fourteen long-chain aliphatic normal alcohols of the general formula $CH_3(CH_2)_nCH_2OH$, where n = 3,4,5,6,7,8,10,11,12,13,14,16,17 and 18 have been made in polystyrene matrices in the frequency range of 10 Hz to 10^5 Hz by the use of a General Radio Precision Capacitance bridge, the procedure being described in Chapter II. The operational temperatures were from about 77 to 360 K and were controlled to within ±0.1 K. All the molecules studied were commercially available with sufficient purity and were properly dried prior to use.

Figures IV-1a and IV-2a show the sample plots of dielectric loss, ε'' versus T(K) for the dipolar molecules. Sample plots of ε'' versus $\log\nu$ are shown in Figures IV-3b to IV-17b while Figures IV-18c to IV-23c present the Cole-Cole sample plots for those molecules in their respective dispersion region. Sample plots of $\log T\tau$ versus 1/T for different molecules are also presented in Figures IV-24d to IV-29d. Figure IV-30 represents the plots of relaxation times, τ, versus the number of carbon atoms (n) in the chain for lower temperature absorptions. Plots of ΔH_E versus ΔS_E and ΔH_E versus n are presented in Figures IV-31, IV-32 and IV-33 for both the lower and higher

temperature dispersion. The activation free energy, ΔG_E at 200 K as a function of carbon atoms (n) in the chain for higher temperature absorption is also shown in Figure IV-34.

Table IV-1 lists the values of the Eyring analysis results, ΔH_E, ΔS_E, along with ΔG_E and τ values at 100 K, 150 K and 200 K for each system. Experimental values of τ, $\log\nu_{max}$, β, and ε''_{max} at various temperatures obtained for these molecules from the Fuoss-Kirkwood analysis together with the values of ε_∞ and the experimental dipole moments (μ) are listed in Table IV-2. Table IV-3 presents the extrapolated dipole moments to 330 K for segmental (μ_s) and molecular (μ_m) motion together with the total effective dipole moment (μ_{eff}) and those of the literature value for the molecules listed in Table IV-2. The following symbols are employed where appropriate:

P.S.	Polystyrene
$\Delta T(K)$	Temperature range in the absolute scale
β	Range of variation in the Fuoss-Kirkwood distribution parameters
ΔG_E	Eyring free energy of activation in kJ mol^{-1}
ΔH_E	Eyring enthalpy of activation in kJ mol^{-1}
ΔS_E	Eyring entropy of activation in J K^{-1} mol^{-1}
ν	Frequency in Hz
τ	Relaxation time in seconds (s)

μ	Dipole moment in Debye (D)
$\mu_{(eff)}$	Effective dipole moment in Debye (D)
μ_s	Effective dipole moment for segmental motion
μ_m	Effective dipole moment for molecular motion
$\mu_{(extr)}$	Dipole moment obtained from the extrapolation of the experimental μ_s and μ_m to the temperature 330 K in Debye (D)
$\mu_{(tot)}$	Dipole moment for the molecule obtained from $(\mu_s^2 + \mu_m^2)^{\frac{1}{2}}$ at 330 K
$\mu_{(lit)}$	Literature value of the dipole moment for the molecule in Debye (D)

IV-3: DISCUSSION

When the dielectric loss factor, ε'' was plotted against the temperature at a fixed frequency, all the aliphatic primary alcohols of the general formula $CH_3(CH_2)_n CH_2OH$ where n = 3,4,5,6,7,8,10,11,12,13,14,16,17,18 exhibited two distinct absorption maxima (except n = 3&4) in polystyrene matrices (Figure IV-1a). The lower temperature peak occurs somewhere in the temperature region 84-142 K and the higher temperatures are between 181-283 K. The temperature at which the maximum dielectric absorption occurs at a fixed frequency for each dispersion increases within the range as the number of carbon atoms (n) in the chain increases. In the case of n = 3 and 4 only lower temperature absorption peaks were detected.

Lower Temperature Dielectric Absorption

The half-width, $\Delta T_{\frac{1}{2}}$ (which measures the breadth of the loss-peak at half of the loss maximum in the ε'' versus T plot at a fixed frequency) for lower temperature absorption peaks is approximately the same and lies in the range 56-60 K whereas the $\Delta T_{\frac{1}{2}}$ for the higher temperature absorption peaks increases slightly and lies in the range 98-130 K. The relatively narrow half-width for the lower-

temperature absorption compared with that of higher temperature absorption peaks suggests an intramolecular process for the former. Table IV-2 gives the Fuoss-Kirkwood distribution parameter, β, which does not change significantly when n varies from 3 to 18 and lies between 0.15-0.28, and in most of the cases the values are above 0.2. Such an appreciable value as 0.28 in the lower temperature region suggests the intramolecular nature of the lower temperature absorption. Comparison may be made of the β-values for $CH_3(CH_2)_nCH_2OH$ with those for intramolecular relaxation in molecules containing similar types of bonds for example, the β-values for intramolecular relaxation in long-chain aldehyde ($CH_3(CH_2)_nCHO$) (48) and 1-bromo-alkanes ($CH_3(CH_2)_n CH_2Br$) (49) where β lies in the range 0.22-0.36 at 85-140 K and 0.18-0.35 at 90-150 K, respectively. In these cases the lower temperature absorption was interpreted as segmental rotation involving relaxation of the main polar group. There is considerable similarity between the behaviour of the long-chain normal alcohols and corresponding 1-bromoalkanes and aldehydes. The intramolecular nature of the lower temperature absorption is also borne out by the similar β-values (0.23-0.34) for intramolecular relaxation of some symmetrically substituted diaryl ether compounds in the temperature range 83-141 K (50).

The smallest molecule we studied is n = 3 (n-pentanol). The higher temperature absorption has not been detected for n = 3 and n = 4 compounds (n-pentanol and n-hexanol). Therefore, the lower temperature absorption for these two molecules are either intramolecular or an overlap of the molecular and intramolecular processes. The dielectric parameters obtained for these two molecules are ΔH_E = 16 & 17 kJ mol^{-1}, ΔS_E = ~1 & 3 J K^{-1} mol^{-1}, ΔG_E = 16 kJ mol^{-1} at 100 K and $\tau = 1.3 \times 10^{-4}$ s and 1.8×10^{-4} s at 100 K respectively. These parameters are in excellent agreement with the corresponding values for 1-bromo-hexane in polystyrene matrices (49) for the segmental rotation involving $-CH_2Br$ group, (ΔH_E = 19.5 kJ mol^{-1}, ΔS_E = 24 J K^{-1} mol^{-1}, ΔG_E = 17 kJ mol^{-1} and $\tau = 7 \times 10^{-4}$ s at 100 K).

Figures IV-32 and IV-30 show that the enthalpy of activation, ΔH_E, and relaxation time, τ_{150}, increases as the number of carbon atoms, n, in the chain increasesy exactly in the same way as in 1-bromo-alkanes (49). This clearly indicates that the intramolecular process involves increasing segmental motion as n increases. Since an alkyl segmental relaxation on its own could not account for the substantial absorption, then the segmental motion must be

detected through corresponding movement of the terminal CH_2OH group.

A linear relationship between ΔS_E and ΔH_E appear when ΔS_E plotted against ΔH_E for the lower temperature process in alcohols (Figure IV-31). For the intramolecular process there appears to be no one specific relationship between ΔS_E and ΔH_E. However, for a particular type of intramolecular process, a linear correlation may exist between ΔS_E and ΔH_E. For example, Davies et al (51) established the relationship, ΔS_E (J K^{-1} mol^{-1}) = 4.2 ΔH_E (kJ mol^{-1}) -173 for the butterfly flapping-type of intramolecular motion in thianthrene-type structures, and Desando et al (50) found the relationship $\Delta S_E = 4.1\ \Delta H_E - 110$ for the intramolecular relaxation of symmetrically substituted diaryl ethers and sulfides in a polystyrene matrix. For the intramolecular motion (segmental rotation involving CH_2Br) in 1-bromo alkanes in a P.S. matrix Ahmed (49) obtained the relation:

$$\Delta S_E = 4.1\ \Delta H_E - 70$$

These relationships are strongly contrasted with one found by Khwaja and Walker (52) for rigid molecules in a polystyrene matrix which is:

$$\Delta S_E = 2.2\ \Delta H_E - 72$$

Within experimental error there is a reasonable fit of the $\Delta S_{E(obsd)}$ values for intramolecular rotation of long-chain normal alcohols to the relation obtained for 1-bromo-alkanes (49).

In this way the lower temperature process for alcohols in polystyrene matrices are similar in all respects with the lower temperature process of 1-bromo-alkanes in polystyrene matrices. After a thorough investigation of 1-bromo-alkanes in various dispersion media such as, G.O.T.P., polystyrene, polypropylene, etc., Ahmed (49) concluded that the lower temperature process is the intramolecular one having segmental rotation involving movement of CH_2Br. As the dielectric relaxation parameters for long chain primary alcohols are in good agreement with those for 1-bromo-alkanes, the lower temperature dispersion for alcohols may be attributed to the segmental rotation involving CH_2OH movement in line with the 1-bromo-alkanes (49) where the rotation occurs about C-C bonds in the chain.

As there is no significant difference between the energy barriers of associating molecules, alcohols and the corresponding non-associating molecules, bromoalkanes, in polystyrene matrices, there is no need to invoke intermolecular or intramolecular hydrogen-bonding in the aliphatic long chain primary alcohols in polystyrene matrices. The

enthalpies of activation for lower temperature absorption in $R-CH_2Br$ ($\Delta H_{Br(PS)}$) and $R-CH_2OH$ ($\Delta H_{OH(PS)}$) in polystyrene matrices and that for hydrogen bond breaking followed by some kind of rotation in liquid alcohol R -OH ($\Delta H_{OH(l)}$) (1st dispersion) obtained by Garg and Smyth (25) are listed below (kJ mol^{-1}):

n	$\Delta H_{OH(l)}$	$\Delta H_{OH(PS)}$	$\Delta H_{Br(PS)}$	$\Delta H_{\bar{OH}(l)}$	$\Delta H_{OH(PS)}$	$\Delta H_{\bar{OH}(l)}$	$\Delta H_{Br(PS)}$
3	28.5	16	–	12.5		-	
4	30.0	17	19.5	13.0		10.5	
5	31.0	20	19.5	11.0		11.5	
6	33.5	20	18.7	13.5		14.8	
7	36.0	20		16.0			
8	35.2	22	22.0	13.2		13.2	
10	33.5	23	23.8	10.5		9.7	
				12.5 kJ mol^{-1}		11.9 kJ mol^{-1}	

The average difference in the enthalpies of activation for liquid alcohols and the alcohols in polystyrene matrices is about 13 kJ mol^{-1}. The average difference in ΔH_E for liquid alcohols and the corresponding 1-bromo-alkanes in polystyrene is about 12 kJ mol^{-1}. That is in both the cases the average difference is the same within experimental error. As there is no hydrogen bonding in alchols in polystyrene

matrices, this difference may be taken as a measure of the hydrogen bond strength in liquid alcohols (13 kJ mol^{-1}). This H-bond strength in alcohol is not unreasonable because Davidson (53) found activation energy for hydrogen bond breaking in pure methanol as 12 kJ mol^{-1}. On the basis of this model the lower-frequency relaxation observed in liquid alcohols by Garg and Smyth (25) may be attributed to the breaking of one hydrogen bond followed by segmental rotation of the R-OH molecule as a whole.

Higher Temperature Absorption

All the alcohols except n = 3 and 4 display a second absorption in the temperature range 183-283 K in polystyrene matrices. In n-pentanol and n-hexanol the higher temperature processes are dominated by the lower temperature intramolecular processes. As the ε''_{max} of the latter processes are higher than the former in all cases, this is not unreasonable.

A survey of the Fuoss-Kirkwood distribution parameters shows low values lying in the range 0.13-0.24, and in most of the cases it is below 0.20 which testifies to the wide spectrum of the relaxation times. Rigid molecules, for example, para-halotoluenes and para-halobiphenyls,

absorb with similar β values (0.17-0.24) (52) in the similar temperature range 160-330 K. The β-value ranges between 0.13-0.22 for the molecular rotation in 1-bromo-alkanes (49) in the temperature range 165-300 K. These low β-values for alcohols which are reflected on the broad loss curves having half width 98-128 K would be appropriate for whole molecule rotation.

The ratio of the ε''_{max} of the lower temperature to higher temperature absorption peaks for all the alcohols increases with the number of carbon atoms in the chain. For n = 5 to 14, the ratio increases from 1.5 to 5.1. This means that as the chain length increases, the intensity of the higher temperature absorption peak decreases and the uncertainty in the relaxation parameters obtained for these dispersions increases. Moreover, the loss difference between frequency to frequency is very low for the higher temperature process, especially, in the cases where n is high. This makes an error in the estimation of ν_{max} which in turn makes an error in the relaxation parameters. We tried to increase the loss factor by increasing the solute concentration but failed owing to the low solubility of higher molecular weight alcohols in polystyrene. However, up to n = 12 we could determine the parameters with sufficient reliability and above n = 14, we could not study the higher temperature

process at all.

Within experimental error, the enthalpy of activation, ΔH_E, the free energy of activation, ΔG_E, at 200 K and the relaxation time, τ, at 300 K for a higher temperature process increase linearly with the increase of carbon atoms (n) in the alcohol chain (Figure IV- 34). These indicate that the size of the reorientating unit also increases with the number of carbon atoms in the chain.

The data for the higher temperature absorption processes follow the relationship:

$$\Delta S_E = 2.1\ \Delta H_E - 44$$

within experimental error. This is virtually identical to the one Khwaja and Walker (52) found for molecular relaxation of rigid molecules and Ahmed (49) for various 1-bromo-alkanes in a polystyrene matrix. For molecular rotation there may be considerable disturbances in the surrounding of the dipole, and thus there is greater disorder in the system and this is reflected in the large positive ΔS_E values for the higher temperature process.

Thus, it seems reasonable to assume that the higher

temperature absorption may be attributed to molecular re-orientation. This is borne out by the fact that the relaxation parameters for long-chain aliphatic normal alcohols follow the same order and behaviour of corresponding 1-bromo-alkanes parameters for its molecular rotation (49). The higher temperature absorption cannot be attributed to the co-operative motion of the solute and solvent since the glass transition temperature, for example, of 1-pentadecanol (n = 13) in polystyrene was found to be ∿337 K which is considerably higher than the higher temperature absorption region of the 1-pentadecanol (240-283 K).

Since our results appear to be accounted for by an intramolecular (segmental) process and a molecular one, we adopt the model that the dipole moment is composed of two components μ_m (molecular) and μ_s (segmental) which govern the effective dipole moment, μ_{eff} where:

$$\mu_{eff} = (\mu^2_m + \mu^2_s)^{\frac{1}{2}}$$

Now in line with the procedure adopted by Davies and Swain (51) for flexible molecules, the μ_s may be taken to be the extrapolated value of the dipole moment at 330 K for the lower temperature process and μ_m the extrapolated value of the dipole moment at 330 K for the higher temperature absorption.

Therefore, the estimated value of the total dipole moment for octanol-1 in polystyrene at 330 K is $[(1.71)^2 + (0.65)^2]^{\frac{1}{2}}$ = 1.8_2 D which is in good agreement with the literature value 1.80 at 293 K (54). Estimates of μ_{eff} for the other molecules are given in Table IV-3. On the whole, the agreement is adequate to support the model strongly.

In addition to alcohols, we studied seven other potentially intermolecular hydrogen bonding molecules belonging to the series long-chain aliphatic normal thiols and having the general formula $CH_3(CH_2)_nCH_2SH$ where n = 6,7,8,9.10,11 and 12. All of these thiols exhibited two distinct absorption maxima in polystyrene matrices (Figure IV-2a). The lower temperature peaks occur somewhere in the temperature region 95-136 K and the higher temperatures are between 199-266 K. Like alcohols, and 1-bromoalkanes (49), the temperature at which the maximum dielectric absorption occurs at a fixed frequency for each dispersion increases within the range as the number of carbon atoms (n) in the chain increases.

The half-width $\Delta T_{\frac{1}{2}}$ for the lower temperature absorption peaks are approximately the same and lie in the range 42-48 K (for alcohol 56-60 K) whereas the $\Delta T_{\frac{1}{2}}$ for the higher temperature absorption peaks increases slightly and liesin the range 129-156 K (for alcohol 98-130 K). The

Fuoss-Kirkwood distribution parameter, β for lower-temperature absorption does not change significantly when n varies from 6 to 14 and lies bewteen 0.25-0.35. The corresponding β-values for higher temperature absorption lie in the range 0.13-0.20 (for alcohols, 0.13-0.24).

The enthalpies of activation and the relaxation time for both the lower and higher temperature dispersion increases as the number of carbon atoms (n) in the chain increases. As with the alcohols, the ΔS_E and ΔH_E values for intramolecular rotation of long-chain thiols follow the same linear relation obtained for 1-bromoalkanes (49). Thus, in polystyrene matrices both the long-chain aliphatic normal alcohols and thiols are similar in behaviour and follow the same route as 1-bromo-alkanes.

Now there is a number of articles in the literature suggesting that thiols do not form hydrogen bonds (55). The relative weakness of the -SH as a proton donar accounts for the absence of hydrogen bonds in them. The enthalpies of activation for lower temperature dispersion of thiols are almost similar or slightly higher than those of the corresponding alcohols (Figure IV-32). If there is hydrogen bonding, these values for alcohols should be higher than those of the corresponding thiols where there is no

or very weak, hydrogen bonding. All this evidence clearly indicates that in polystyrene matrices alcohols do not form a hydrogen bond or if one forms, it may not be detectable by our dielectric measurements at the normal concentration range.

Our experimental data settles directly that:

(1) there are at least two relaxation processes in long-chain aliphatic normal alcohols and thiols;

(2) the enthalpy of activation and the relaxation times of each of these processes lengthens with the number of carbon atoms in the chain in line with the 1-bromo-alkanes;

(3) no inter- or intramolecular hydrogen bonding occurs in these alcohols or thiols in the polystyrene matrices.

(4) the strength of hydrogen bond in liquid long-chain alcohols is about 13 kJ mol^{-1};

(5) the low frequency dispersion in liquid alcohols obtained by Garg & Smyth can be attributed to the breaking of one hydrogen bond followed by segmental rotation involving the CH_2OH group.

(6) for the higher temperature process, ΔH_E and ΔS_E are linearly related by the same equation which is obeyed for rigid molecules in a polystyrene matrix.

Our dipole moments, calculated on the basis of the

model of two relaxation processes are in reasonable agreement with the literature values from more direct methods. Thus, μ_m may be identified with molecular rotation while μ_s involves rotation of the segments which lead to movement of the main group moment ($-CH_2OH$, $-CH_2SH$). This is composed of several relaxation motions involving different chain lengths, although it is, of course, always the μ_s component which governs the lower temperature absorption. This refined model then accounts for the lengthening of relaxation times with increased chain length for the lower frequency dispersion in liquid alcohols.

REFERENCES

1. S. Mizushima, Bull. Chem. Soc. Japan, 1, 47, 83, 115, 143, 163(1926).

2. P. Debye, "Polar Molecules", Chemical Catalog Co., New York, N.Y., 1929, p. 95.

3. P. Girard and P. Abadie, Trans. Faraday Soc., 42A, 40(1946).

4. P. Abadie, Ibid., 42A, 143(1946).

5. R. Dalbert, M. Magal and S. Surdut, Bull. Soc. Chim. France. D_3, 45(1959).

6. C. Brot, M. Magat and L. Reiwisch, Kolloid Z., 134, 101(1953).

7. C. Brot, Thesis, University of Paris, 1956; Ann. Phys. (Paris) [13]2, 714(1957).

8. D.W. Davidson and R.H. Cole, J. Chem. Phys., 19, 1484(1951).

9. R.H. Cole and D. W. Davidson, Ibid., 20, 1389(1952).

10. F.L. Hassion and R.H. Cole, Ibid., 23, 1756 (1955).

11. D.J. Denney and R.H. Cole, Ibid., 23, 1767 (1955).

12. J.D. Hoffman and C.P. Smyth, J. Am. Chem. Soc., 71, 431(1949).

13. W.O. Baker and C.P. Smyth, Ibid., 60, 1229 (1938).

14. R.G. Vines and R.J. Meakins, Aust. J. Appl. Sci., 10, 190(1959).

15. R.J. Meakins and J.W. Mulley, Aust. J. Sci. Res., 4, 365(1951).

16. B.V. Hamon and R.J. Meakins, Ibid., 5, 671(1952).

17. R.J. Meakins and R.A. Sack, Nature, 164, 798(1949).

18. Ibid., Aust. J. Sci. Res., A4, 213(1951).

19. R.J. Meakins and H.K. Welsh, Ibid., A4, 359 (1951).

20. R.A. Sack, Aust. J. Sci. Res., A5, 135(1952).

21. R.J. Meakins, Trans. Faraday Soc., 58, 1953 (1962).

22. D.A. Wilson and E. Ott, J. Chem. Phys., 2, 231(1934).

23. V. Daniel, Trans. Faraday Soc., 54, 1834 (1958), 60, 1299(1964).

24. V. Daniel and J. W. H. Oldham, Ibid., 57, 694(1961).

25. S.K. Garg and C.P. Smyth, J. Phys. Chem., 69, 1294(1965).

26. M. Magat, "Hydrogen Bonding". D. Hadzi and H.W. Thompson, eds., (Pergamon N.W., 1959) p. 309.

27. C. Brot and M. Magat, J. Chem. Phys., 39, 841(1963).

28. W. Dannhauser and R.H. Cole, Ibid., 23, 1762 (1955).

29. M. Moriamez and A. Lebran, Arch. Sci., Geneva, 13, 40(1960).

30. D.J. Denney and J.W. Ring, J. Chem. Phys., 39, 1268(1965).

31. J. Crossley, L. Glasser and C.P. Smyth, Ibid., 52, 6203(1970); 55, 2197(1971).

32. W. Dannhauser, Ibid., 48, 1911, 1918(1968).

33. L. Raezy, E. Constant and A. Lebrun, J. Chim. Phys., 64, 1180(1967).

34. W. Dannhauser, L. W. Bahe, R. Y. Lin, and A. F. Flueckinger, J. Chem. Phys., 43, 257(1965).

35. E.F. Hanna and K.N. Abd El Nour, Z. Natur A25, 1685(1970).

36. M. Davies and R.J. Meakins, Ibid., 26, 1584(1957).

37. F.K. Fong and C.P. Smyth, J. Am. Chem. Soc., 85, 1565(1963).

38. J. Crossley, Adv. Mol. Relax. Processes, 2, 69 (1970).

39. S.K. Garg and C.P. Smyth, J. Chem. Phys., 46, 373(1967).

40. M.W. Sagal, J. Chem. Phys., 36, 2437(1962).

41. J. Middelhoek and C.J.F. Böttcher. "Molecular Relaxation Processes". Special Publication No. 20, The Chem. Soc., London, 1966. p. 69.

42. J. Middelhoek, Thesis, Leiden, 1967, p. 61.

43. W. Dannhauser and A.F. Flueckinger, Phys. Chem., Liquids, 2, 37(1970).

44. P. Bordewzjk, F. Granschand and C.J.F. Böttcher, J. Phys. Chem., 73, 3255(1969).

45, J. Malecki, J.Chem. Phys., 43, 1351(1965).

46. G.P. Johari and C.P. Smyth, J. Am. Chem. Soc., 91, 6215(1969).

47. J. Crossley, Can. J. Chem., 49, 712(1971); J. Phys. Chem., 75, 1790(1971).

48. H.A. Khwaja and S. Walker, Adv. Mol. Relax. & Interact. Processes, 22, 27(1982).

49. M.S. Ahmed, Private communication, this laboratory.

50. J. Chao, M.A. Desando, D.L. Gourlay, D. E. Orr and S. Walker, J. Phys. Chem., 88, 711(1984).

51. M. Davies and J. Swain, Trans. Faraday, Soc., 67, 1637(1971).

52. H.A. Khwaja and S. Walker, Adv. Mol. Relax & Interact. Processes, 19, 1(1981).

53. D.A. Davidson, Can . J. Chem., 35, 458(1957).

54. A.L. McClellan, "Tables of Experimental Dipole Moments". W.H. Freeman and Co., 1963.

55. G.C. Pimental and A. L. McClellan. "The Hydrogen Bond", Editor - Linus Pauling. W. H. Freeman and Company, 1960.

TABLE IV-1: Eyring Analysis Results for some Aliphatic Normal Alcohols and Thiols [$CH_3(CH_2)_nCH_2XH$] where X=O or S in polystyrene matrices

Molecule		Temperature Range (K)	Relaxation Time τ(s)			ΔG_E (kJ mol^{-1})			ΔH_E	ΔS_E
			100 K	150 K	200K	100 K	150 K	200 K	kJ mol^{-1}	J K^{-1} mol^{-1}
Pentanol-1	3	84-104	1.3×10^{-4}	1.3×10^{-7}	4.0×10^{-9}	16	16	16	16±1.3	-1±13
Hexanol-1	4	87-106	1.8×10^{-4}	1.5×10^{-7}	3.9×10^{-9}	16	16	16	17±1.2	3±12.7
Heptanol-1	5	95-117	8.0×10^{-7}	2.0×10^{-7}	3.0×10^{-9}	18	17	16	20±1	19±10
		181-206	3.5×10^{11}	1.4×10^{1}	8.2×10^{-5}	46	39	33	59±4	130±22
Octanol-1		99-120	1.6×10^{-3}	3.7×10^{-7}	5.2×10^{-9}	18	17	17	20±1.4	17±12
		196-220	1.4×10^{11}	7.3×10^{1}	1.6×10^{-3}	45	41	38	52±6.3	73±30.7
Nonanol-1		98-120	2.2×10^{-3}	5.5×10^{-7}	7.9×10^{-9}	19	18	17	20±1.1	12±9.8
		198-234	7.7×10^{10}	1.4×10^{2}	5.3×10^{-3}	44	42	40	49±3.3	48±15
Decanol-1	8	102-126	1.0×10^{-2}	1.0×10^{-6}	9.6×10^{-9}	20	19	18	22±0.8	21±7
		219-243	1.5×10^{15}	1.8×10^{4}	5.8×10^{-2}	53	48	44	62±9	91±39
Dodecanol-1	10	104-129	2.0×10^{-2}	1.6×10^{-6}	1.3×10^{-8}	20	19	18	23±1.2	22±10.7
		239-261	1.6×10^{20}	1.3×10^{7}	3.4×10^{0}	62	56	50	74±7	119±28
Tri-decanol-1	11	111-130	5.0×10^{-2}	1.9×10^{-6}	1.0×10^{-8}	21	19	18	24±1	33±8.7
		233-259	1.1×10^{19}	3.6×10^{6}	1.9×10^{0}	60	55	49	71±8	107±33
Tetradecanol-1	12	116-142	1.2×10^{-1}	3.2×10^{-6}	1.5×10^{-8}	22	20	18	25±0.9	35±7.1
		229-256	9.7×10^{16}	5.7×10^{5}	1.3×10^{0}	56	52	49	64±3.3	74±13.8
Pentadecanol-1	13	109-130	1.0×10^{-1}	2.4×10^{-6}	1.1×10^{-8}	22	20	18	26±1.1	39±9.4
		240-283	4.9×10^{15}	5.5×10^{5}	5.4×10^{0}	54	52	51	56±3.4	25±129
Hexadecanol-1	14	115-133	2.2×10^{-1}	3.7×10^{-6}	1.4×10^{-8}	22	20	18	26±1.4	41±11.5
		259-272	4.5×10^{25}	2.3×10^{10}	4.7×10^{2}	73	66	59	87±9.2	141±34.8

TABLE IV-1: continued...

Molecule		Temperature Range (K)	Relaxation Time τ(s)			ΔG_E (kJ mol^{-1})			ΔH_E	ΔS_E
			100 K	150 K	200K	100 K	150 K	200 K	kJ mol^{-1}	J K^{-1} mol^{-1}
Octadecanol-1	16	116-139	1.1×10^{-1}	2.8×10^{-6}	1.3×10^{-8}	22	20	18	25±1.5	36±11.7
Nonadecanol-1	17	115-142	5.6×10^{-1}	5.4×10^{-6}	1.5×10^{-8}	23	22	18	28±2	47±16
Eicosanol-1	18	114-137	3.3×10^{-1}	4.6×10^{-6}	1.6×10^{-8}	23	21	19	27±2	42±16
Octanethiol-1		95-114	9.7×10^{-4}	2.6×10^{-7}	4.0×10^{-9}	18	17	16	20±0.7	17±6.5
		199-234	4.0×10^{5}	1.2×10^{0}	1.9×10^{-3}	34	36	38	31±3.9	-36±18
Nonanethiol-1		101-117	2.8×10^{-3}	4.8×10^{-7}	5.8×10^{-9}	19	18	17	21±1.3	19±11.6
		210-266	2.5×10^{4}	1.2×10^{0}	8.0×10^{-3}	32	36	40	24±4	-83±17.5
Decanethiol-1	8	101-120	7.5×10^{-3}	7.1×10^{-7}	6.4×10^{-9}	20	18	17	22±1.3	26±11.7
		220-256	6.5×10^{9}	1.7×10^{2}	2.5×10^{-2}	42	42	42	43±5	2±21
Undecanethiol-1	9	106-123	1.2×10^{-2}	8.8×10^{-7}	6.9×10^{-9}	20	19	17	23±1.2	28±11
		229-264	3.4×10^{9}	1.9×10^{2}	4.2×10^{-2}	42	42	43	41±5.8	-12±23.6
Dodecanethiol-1	10	111-126	2.2×10^{-2}	1.1×10^{-6}	7.5×10^{-9}	20	19	17	24±0.8	32±6.7
		233-266	2.0×10^{18}	2.9×10^{6}	3.3×10^{0}	59	55	50	67±14	83±57
Tridecanethiol-1	11	109-128	4.4×10^{-2}	1.4×10^{-6}	7.3×10^{-9}	21	19	17	25±2.8	38±23.8
Hexadecanethiol-1	14	114-136	1.8×10^{-1}	4.4×10^{-6}	2.0×10^{-8}	22	21	19	26±0.8	33±6.5

TABLE IV-2: Fuoss-Kirkwood Analysis Parameters, ε_∞ and Effective Dipole Moments (μ) for some Aliphatic Normal Alcohols and Thiols $[CH_3(CH_2)_nCH_2XH$ X=O or S] in Polystyrene Matrices

T(K)	$10^6\tau$(s)	$\log \nu_{max}$	β	$10^3\varepsilon''_{max}$	ε_∞	μ(D)
1.20 M Pentanol-1						
84.9	4630	1.54	0.22	8.9	2.83	0.35
86.4	2525	1.80	0.23	9.2	2.83	0.35
89.6	1353	2.07	0.23	9.6	2.83	0.36
91.4	895	2.25	0.21	9.7	2.82	0.38
94.2	488	2.51	0.22	10.0	2.82	0.39
97.3	258	2.79	0.21	10.3	2.82	0.41
100.2	113	3.15	0.19	10.5	2.81	0.44
104.4	46.6	3.53	0.19	10.9	2.80	0.46
0.76 M Hexanol-1						
86.6	4439	1.55	0.22	7.9	2.97	0.40
89.2	2175	1.86	0.23	8.2	2.96	0.41
91.6	1221	2.11	0.23	8.5	2.96	0.42
94.0	745	2.33	0.23	8.7	2.96	0.43
97.9	336	2.68	0.23	9.0	2.96	0.45
99.4	226	2.85	0.22	9.1	2.96	0.46
102.7	102	3.19	0.21	9.3	2.95	0.49
105.7	48.5	3.52	0.21	9.7	2.95	0.51
0.75 M Heptanol-1	Lower temperature process					
95.5	2398	1.82	0.23	9.6	2.74	0.48
97.2	1555	2.01	0.23	9.8	2.74	0.49
99.7	969	2.22	0.22	10.0	2.73	0.51
102.7	475	2.53	0.22	10.3	2.73	0.53
106.2	232	2.84	0.22	10.7	2.73	0.55
109.0	114	3.14	0.21	10.9	2.73	0.57
111.4	68.5	3.37	0.22	11.1	2.73	0.57
113.9	40.1	3.60	0.22	11.4	2.72	0.58
116.6	21.6	3.87	0.22	11.7	2.72	0.60
0.75 M Heptanol-1	Higher temperature process					
181.1	4260	1.57	0.13	6.7	2.79	0.72
183.4	1856	1.93	0.16	6.8	2.80	0.66
187.2	1075	2.17	0.18	6.9	2.80	0.64
191.6	361	2.64	0.15	7.0	2.79	0.71
196.2	160	3.00	0.17	7.1	2.79	0.68
199.7	76.3	3.32	0.18	7.1	2.79	0.67
203.4	43.9	3.56	0.19	7.1	2.79	0.66
206.5	30.6	3.72	0.20	7.2	2.79	0.65
209.7	24.6	3.81	0.22	7.2	2.80	0.62

TABLE IV-2: continued... (page 2 of Table IV-2)

T(K)	$10^6\tau$(s)	$\log\nu_{max}$	β	$10^3\varepsilon''_{max}$	ε_∞	μ(D)
0.57 M Octanol-1		Lower temperature process				
99.6	1536	2.02	0.23	10.5	2.96	0.56
101.0	1295	2.09	0.22	10.6	2.95	0.58
103.1	811	2.29	0.22	10.8	2.95	0.59
106.2	405	2.59	0.23	11.2	2.95	0.60
109.7	211	2.88	0.23	11.5	2.95	0.62
113.1	96.5	3.22	0.22	11.8	2.94	0.65
116.8	42.2	3.58	0.23	12.1	2.94	0.65
120.4	21.2	3.87	0.23	12.5	2.94	0.68
0.57 M Octanol-1		Higher temperature process				
196.2	2517	1.80	0.18	5.8	3.02	0.66
198.3	1980	1.91	0.19	5.8	3.02	0.63
201.0	1409	2.05	0.20	5.8	3.02	0.63
203.8	913	2.24	0.20	5.8	3.02	0.63
208.9	428	2.57	0.19	5.7	3.01	0.65
214.8	198	2.91	0.20	5.7	3.01	0.65
221.0	57.4	3.44	0.19	5.6	3.00	0.67
0.47 M Nonanol-1		Lower temperature process				
98.0	3439	1.67	0.22	9.1	3.04	0.57
99.7	2119	1.88	0.23	9.3	3.04	0.57
102.3	1359	2.07	0.23	9.5	3.04	0.59
104.4	828	2.28	0.23	9.7	3.03	0.60
108.0	404	2.60	0.23	10.0	3.03	0.62
110.7	228	2.84	0.23	10.2	3.03	0.63
113.8	107	3.17	0.23	10.5	3.02	0.65
116.7	58.8	3.43	0.24	10.7	3.02	0.65
119.4	37.1	3.63	0.25	11.0	3.02	0.66
0.47 M Nonanol-1		Higher temperature process				
197.8	7414	1.33	0.21	3.8	3.06	0.54
201.6	3781	1.62	0.23	3.8	3.06	0.52
205.2	2394	1.82	0.23	3.8	3.06	0.53
210.3	1079	2.17	0.23	3.8	3.05	0.53
215.4	640	2.40	0.22	3.7	3.05	0.54
219.6	385	2.62	0.22	3.7	3.05	0.55
225.0	212	2.88	0.21	3.6	3.05	0.56
230.0	90.7	3.24	0.19	3.5	3.04	0.59
233.9	50.6	3.50	0.19	3.5	3.04	0.59

TABLE IV-2: continued... (page 3 of Table IV-2)

T(K)	$10^6\tau$(s)	$\log\nu_{max}$	β	$10^3\epsilon''_{max}$	ϵ_∞	μ(D)
0.50 M Decanol-1	Lower temperature process					
102.2	5319	1.48	0.21	8.9	2.74	0.61
106.2	1933	1.92	0.22	9.4	2.74	0.63
108.0	1360	2.07	0.22	9.6	2.73	0.64
111.1	689	2.36	0.22	9.8	2.73	0.65
113.6	403	2.60	0.22	10.1	2.73	0.67
117.2	202	2.90	0.22	10.3	2.73	0.69
120.4	98.4	3.21	0.23	10.6	2.73	0.69
124.0	48.0	3.52	0.23	10.9	2.73	0.71
125.8	32.9	3.68	0.23	11.0	2.73	0.72
0.50 M Decanol-1	Higher temperature process					
219.7	1661	1.98	0.20	4.6	2.79	0.66
223.3	1056	2.18	0.20	4.6	2.79	0.66
227.2	615	2.41	0.21	4.5	2.79	0.64
230.0	411	2.59	0.21	4.5	2.79	0.65
233.8	275	2.76	0.20	4.5	2.78	0.67
236.8	187	2.93	0.19	4.4	2.78	0.68
239.5	112	3.15	0.18	4.3	2.78	0.70
243.0	48.8	3.51	0.17	4.3	2.78	0.73
0.35 M Dodecanol-1	Lower temperature process					
104.6	7309	1.34	0.20	7.8	3.01	0.67
106.8	3110	1.71	0.21	7.9	3.01	0.67
108.4	1969	1.91	0.22	8.1	3.01	0.66
110.0	1445	2.04	0.23	8.2	3.01	0.66
113.0	869	2.26	0.22	8.4	3.01	0.69
115.8	480	2.52	0.22	8.6	3.00	0.71
118.6	259	2.79	0.22	8.8	3.00	0.73
121.6	142	3.05	0.22	8.9	3.00	0.74
125.3	63.9	3.40	0.23	9.2	3.00	0.75
129.2	34.5	3.66	0.25	9.5	3.00	0.74
0.35 M Dodecanol-1	Higher temperature process					
239.9	1646	1.99	0.17	3.2	3.00	0.71
242.7	1022	2.19	0.16	3.2	3.00	0.74
246.6	617	2.41	0.17	3.2	3.00	0.72
249.7	390	2.61	0.16	3.2	3.00	0.75
253.5	255	2.80	0.16	3.2	3.00	0.75
257.6	127	3.10	0.16	3.2	3.00	0.76
261.2	65.3	3.39	0.15	3.1	3.00	0.78

TABLE IV-2: continued... (page 4 of Table IV-2)

T(K)	$10^6\tau$(s)	$\log\nu_{max}$	β	$10^3\varepsilon''_{max}$	ε_∞	μ(D)
0.32 M Tridecanol-1		Lower Temperature Process				
111.8	1922	1.92	0.21	7.6	2.77	0.74
113.4	1333	2.08	0.22	7.8	2.77	0.73
115.4	899	2.25	0.22	8.0	2.77	0.75
118.5	446	2.55	0.22	8.2	2.77	0.77
121.4	259	2.79	0.23	8.3	2.77	0.77
124.4	132	3.08	0.22	8.5	2.76	0.80
127.2	69.0	3.36	0.23	8.6	2.76	0.80
130.0	43.2	3.57	0.25	8.9	2.76	0.79
0.32 M Tridecanol-1		Higher Temperature Process				
233.7	3615	1.64	0.18	2.1	3.00	0.58
237.2	1549	2.01	0.21	2.1	3.00	0.54
241.4	1093	2.16	0.21	2.2	2.99	0.56
244.8	656	2.38	0.21	2.1	2.99	0.55
249.7	357	2.65	0.19	2.1	2.99	0.58
254.7	222	2.86	0.20	2.1	2.98	0.57
259.0	75.4	3.32	0.16	2.1	2.98	0.65
0.38 M Tetradecanol-1		Lower Temperature Process				
116.5	1290	2.09	0.21	8.3	2.76	0.72
117.5	1190	2.13	0.20	8.4	2.76	0.75
119.2	764	2.32	0.20	8.5	2.76	0.76
121.8	451	2.55	0.21	8.7	2.76	0.76
124.7	250	2.80	0.22	8.9	2.76	0.76
128.2	113	3.15	0.22	9.1	2.75	0.77
131.8	50.0	3.50	0.23	9.3	2.75	0.78
136.0	29.0	3.74	0.25	9.7	2.75	0.77
139.9	14.9	4.03	0.25	9.8	2.75	0.79
143.0	9.41	4.22	0.26	10.1	2.75	0.79
0.38 M Tetradecanol-1		Higher Temperature Process				
229.1	8573	1.27	0.22	2.5	2.79	0.54
232.8	5198	1.49	0.21	2.4	2.79	0.55
236.3	2800	1.75	0.21	2.4	2.79	0.55
240.0	1886	1.93	0.21	2.4	2.79	0.56
243.5	1123	2.15	0.21	2.4	2.79	0.56
248.0	715	2.35	0.21	2.4	2.78	0.57
252.6	359	2.65	0.19	2.3	2.78	0.59
257.0	192	2.92	0.16	2.3	2.78	0.65

TABLE IV-2: continued... (page 5 of Table IV-2)

T(K)	$10^6\tau$(s)	$\log\nu_{max}$	β	$10^3\varepsilon''_{max}$	ε_∞	μ(D)
0.27 M Pentadecanol-1		Lower Temperature Process				
109.7	6201	1.41	0.18	7.2	2.95	0.80
112.7	2608	1.79	0.19	7.4	2.95	0.80
115.3	1546	2.01	0.20	7.6	2.95	0.80
117.4	927	2.23	0.20	7.8	2.95	0.82
119.6	571.	2.45	0.21	7.9	2.95	0.81
122.5	313	2.71	0.22	8.1	2.95	0.82
125.0	202	2.90	0.22	8.2	2.94	0.83
127.8	97.0	3.22	0.23	8.3	2.97	0.82
131.0	48.7	3.51	0.24	8.5	2.94	0.83
0.27 M Pentadecanol-1		Higher Temperature Process				
240.7	6501	1.39	0.24	1.9	2.94	0.53
244.7	5808	1.44	0.22	1.8	2.94	0.55
248.4	5931	1.43	0.19	1.8	2.94	0.59
262.2	4748	1.53	0.13	1.6	2.93	0.70
269.4	726	2.34	0.15	1.6	2.92	0.66
277.5	296.	2.73	0.14	1.5	2.92	0.67
283.7	243	2.82	0.17	1.4	2.91	0.60
0.29 M Hexadecanol-1		Lower Temperature Process				
115.0	2747	1.76	0.18	7.5	2.94	0.81
117.6	1619	1.99	0.19	7.7	2.94	0.81
120.0	974	2.21	0.20	7.9	2.94	0.81
123.0	526	2.48	0.20	8.0	2.94	0.82
124.5	349	2.66	0.21	8.1	2.94	0.81
126.3	217	2.87	0.21	8.2	2.94	0.82
129.7	115	3.14	0.21	8.3	2.94	0.84
133.5	54.8	3.46	0.22	8.6	2.94	0.84
0.29 M Hexadecanol-1		Higher Temperature Process				
247.0	5066	1.50	0.20	1.8	2.94	0.56
251.5	4579	1.54	0.18	1.8	2.94	0.59
255.5	2598	1.79	0.16	1.7	2.94	0.61
259.7	2296	1.84	0.14	1.7	2.93	0.66
264.0	1159	2.14	0.12	1.6	2.93	0.70
269.2	498	2.51	0.14	1.6	2.92	0.66
273.0	306	2.72	0.13	1.6	2.92	0.69
278.0	268	2.77	0.12	1.5	2.92	0.70

TABLE IV-2: continued... (page 6 of Table IV-2)

T(K)	$10^6\tau$(s)	$\log\nu_{max}$	β	$10^3\varepsilon''_{max}$	ε_∞	μ(D)
0.18 M Octadecanol-1						
115.7	1444	2.04	0.19	5.2	2.89	0.85
119.9	598	2.42	0.19	5.3	2.88	0.87
122.4	356	2.65	0.19	5.4	2.88	0.89
125.0	199	2.90	0.20	5.5	2.88	0.89
127.7	102	3.19	0.21	5.6	2.88	0.88
131.3	45.0	3.55	0.22	5.7	2.88	0.88
133.0	38.6	3.62	0.25	5.8	2.90	0.84
135.8	26.7	3.78	0.26	5.9	2.88	0.84
138.7	17.9	3.95	0.28	6.0	2.88	0.82
0.19 M Nonadecanol-1						
115.4	8558	1.27	0.15	5.4	2.96	0.93
117.6	3106	1.71	0.17	5.5	2.96	0.89
118.5	2019	1.90	0.19	5.6	2.96	0.85
120.5	1411	2.05	0.19	5.7	2.96	0.87
122.6	905	2.25	0.18	5.7	2.96	0.90
126.3	363	2.64	0.19	5.8	2.96	0.90
130.3	174	2.96	0.22	6.0	2.96	0.86
137.1	46.4	3.54	0.24	6.2	2.95	0.86
140.0	29.1	3.74	0.26	6.3	2.96	0.84
0.20 M Eicosanol-1						
114.4	6923	1.36	0.15	3.8	2.87	0.77
116.4	2847	1.75	0.16	3.9	2.87	0.77
118.6	1536	2.02	0.18	4.0	2.87	0.74
120.6	1001	2.20	0.18	4.0	2.87	0.74
122.2	674	2.37	0.19	4.1	2.86	0.74
124.7	404	2.60	0.21	4.1	2.86	0.71
127.6	232	2.84	0.22	4.2	2.86	0.71
130.7	126	3.10	0.24	4.2	2.86	0.69
133.8	72.8	3.34	0.24	4.2	2.86	0.70
137.0	45.3	3.55	0.27	4.3	2.86	0.67

TABLE IV-2: continued... (page 7 of Table IV-2)

T(K)	$10^6\tau$(s)	$\log\nu_{max}$	β	$10^3\varepsilon''_{max}$	ε_∞	μ(D)
0.61 M Octanethiol-1		Lower Temperature Process				
95.3	3102	1.71	0.26	6.6	2.98	0.40
96.6	2132	1.87	0.26	6.7	2.98	0.40
99.4	1140	2.15	0.26	6.9	2.99	0.41
100.8	843	2.28	0.26	6.9	2.98	0.42
102.6	527	2.48	0.26	7.0	2.98	0.42
104.7	329	2.68	0.27	7.2	2.98	0.42
106.7	231	2.84	0.27	7.2	2.98	0.43
109.1	128	3.09	0.27	7.3	2.98	0.44
111.0	80.8	3.29	0.28	7.4	2.98	0.44
113.9	45.4	3.54	0.29	7.6	2.98	0.44
0.61 M Octanethiol-1		Higher Temperature Process				
199.0	1792	1.94	0.20	6.4	2.99	0.64
201.9	1513	2.02	0.20	6.4	2.99	0.64
205.4	1316	2.08	0.18	6.4	2.98	0.69
209.4	931	2.23	0.18	6.4	2.98	0.69
215.4	497	2.51	0.18	6.4	2.97	0.70
218.4	377	2.63	0.18	6.4	2.97	0.71
224.2	220	2.86	0.17	6.4	2.97	0.74
228.9	151	3.02	0.19	6.4	2.97	0.70
233.8	62.6	3.41	0.16	6.4	2.95	0.78
0.46 M Nonanethiol-1		Lower Temperature Process				
101.2	1825	1.94	0.27	6.4	2.78	0.47
104.3	1022	2.19	0.26	6.5	2.78	0.49
105.4	746	2.33	0.27	6.6	2.78	0.49
108.0	413	2.59	0.28	6.7	2.78	0.49
109.7	314	2.71	0.27	6.8	2.77	0.51
112.8	148	3.03	0.27	6.8	2.77	0.52
115.0	94.8	3.23	0.27	6.9	2.77	0.52
117.0	59.7	3.43	0.28	7.0	2.77	0.52
0.46 M Nonanethiol-1		Higher Temperature Process				
210.8	2467	1.81	0.18	5.4	2.78	0.77
213.8	1890	1.93	0.19	5.5	2.78	0.76
217.4	1662	1.98	0.18	5.5	2.77	0.79
221.5	1445	2.04	0.17	5.6	2.77	0.83

TABLE IV-2: continued.... (page 8 of Table IV-2)

T(K)	$10^6\tau$(s)	$\log\nu_{max}$	β	$10^3\varepsilon''_{max}$	ε_∞	μ(D)
0.46 M Nonanethiol-1		Higher Temperature continued...				
225.8	1290	2.09	0.16	5.7	2.77	0.87
230.7	1099	2.16	0.15	5.7	2.76	0.91
237.6	733	2.34	0.14	5.8	2.76	0.96
242.3	561	2.45	0.14	5.9	2.75	0.98
248.0	460	2.54	0.13	5.9	2.75	1.02
256.0	266	2.78	0.13	6.0	2.74	1.05
265.7	172	2.97	0.13	6.1	2.74	1.08
0.47 M Decanethiol-1		Lower temperature Process				
101.9	4694	1.53	0.25	6.5	2.76	0.49
103.9	2287	1.84	0.27	6.6	2.76	0.48
106.1	1523	2.02	0.26	6.8	2.76	0.50
108.6	860	2.27	0.27	6.9	2.76	0.50
110.7	582	2.44	0.27	7.0	2.76	0.51
112.7	329	2.68	0.28	7.1	2.76	0.51
115.0	225	2.85	0.28	7.2	2.76	0.52
116.6	141	3.05	0.28	7.2	2.76	0.53
120.0	67.9	3.37	0.28	7.4	2.75	0.54
0.47 M Decanethiol-1		Higher Temperature Process				
220.2	1790	1.95	0.19	5.3	2.76	0.75
223.9	1386	2.06	0.19	5.4	2.76	0.76
228.7	954	2.22	0.18	5.3	2.75	0.79
233.8	543	2.47	0.18	5.4	2.75	0.80
237.8	386	2.62	0.17	5.4	2.75	0.87
242.4	280	2.75	0.16	5.4	2.74	0.87
245.9	189	2.93	0.15	5.4	2.74	0.90
250.0	118	3.13	0.14	5.4	2.73	0.94
256.1	54.0	3.47	0.14	5.5	2.73	0.97

TABLE IV-2: continued... (page 9 of Table IV-2)

T(K)	$10^6\tau$(s)	$\log\nu_{max}$	β	$10^3\varepsilon''_{max}$	ε_∞	μ(D)
0.21 M Undecanethiol-1		Lower Temperature Process				
106.4	1916	1.92	0.28	5.2	2.76	0.64
108.7	1307	2.09	0.27	5.3	2.76	0.66
111.4	686	2.37	0.28	5.4	2.76	0.66
114.7	346	2.66	0.28	5.5	2.75	0.68
116.5	213	2.87	0.28	5.5	2.75	0.69
119.0	128	3.10	0.29	5.6	2.75	0.69
120.9	86.0	3.27	0.29	5.6	2.75	0.69
123.3	52.3	3.48	0.29	5.8	2.75	0.71
0.21 M Undecanethiol-1		Higher Temperature Process				
229.8	1493	2.03	0.19	2.8	2.74	0.84
234.3	925	2.24	0.19	2.8	2.74	0.85
238.7	653	2.39	0.20	2.9	2.73	0.85
243.6	442	2.56	0.18	2.9	2.73	0.90
248.3	353	2.65	0.16	2.9	2.73	0.97
253.1	243	2.82	0.17	3.0	2.72	0.97
258.3	131	3.08	0.16	3.0	2.72	1.01
263.6	71.2	3.35	0.14	3.0	2.71	1.09
0.36 M Dodecanethiol-1		Lower Temperature Process				
111.4	1021	2.19	0.27	6.7	2.98	0.55
113.6	683	2.37	0.26	6.7	2.98	0.57
115.0	467	2.53	0.27	6.8	2.98	0.56
116.6	342	2.67	0.28	6.9	2.98	0.56
118.4	238	2.82	0.28	7.0	2.98	0.57
121.0	136	3.07	0.28	7.0	2.98	0.58
123.0	88.8	3.25	0.30	7.1	2.98	0.57
123.6	77.1	3.32	0.29	7.1	2.98	0.58
126.3	46.2	3.54	0.31	7.3	2.98	0.57

TABLE IV-2: continued... (page 10 of Table IV-2)

T(K)	$10^6\tau$(s)	$\log\nu_{max}$	β	$10^3\varepsilon''_{max}$	ε_∞	μ(D)
0.36 M Dodecanethiol-1		Higher Temperature Process				
234.0	1971	1.91	0.19	3.4	2.84	0.70
238.6	1182	2.13	0.19	3.4	2.83	0.71
242.2	1137	2.15	0.17	3.5	2.83	0.76
245.7	1012	2.20	0.16	3.5	2.82	0.79
250.7	743	2.33	0.16	3.6	2.82	0.81
255.8	386	2.61	0.17	3.6	2.82	0.80
260.7	230	2.84	0.18	3.7	2.81	0.79
265.8	109	3.16	0.16	3.6	2.80	0.84
0.20 M Tridecanethiol-1		Lower Temperature Process				
109.3	2559	1.79	0.27	4.1	2.79	0.60
112.0	1749	1.96	0.25	4.2	2.79	0.63
113.2	1140	2.14	0.27	4.3	2.79	0.62
115.6	865	2.26	0.26	4.3	2.79	0.64
117.9	378	2.62	0.28	4.4	2.79	0.63
120.6	271	2.77	0.26	4.4	2.79	0.66
122.0	182	2.94	0.27	4.4	2.79	0.65
126.3	52.7	3.48	0.27	4.6	2.78	0.68
128.4	47.3	3.53	0.30	4.6	2.78	0.65
0.29 M Hexadecanethiol-1		Lower Temperature Process				
114.9	2771	1.76	0.26	5.3	2.98	0.57
117.2	1731	1.96	0.26	5.4	2.97	0.58
119.3	1125	2.15	0.27	5.5	2.97	0.58
121.2	711	2.35	0.27	5.6	2.97	0.59
122.9	519	2.49	0.27	5.6	2.97	0.59
124.4	563	2.45	0.35	5.6	2.98	0.52
127.3	202	2.90	0.28	5.8	2.97	0.60
130.5	106	3.18	0.28	5.8	2.97	0.61
133.5	57.1	3.45	0.30	5.9	2.97	0.60
135.9	42.7	3.57	0.31	6.0	2.97	0.60

TABLE IV-3: Extrapolated dipole moments for alcohols to 330 K for segmental rotation (μ_s) and molecular rotation (μ_m); effective dipole moments (μ_{eff}) and the literature value of the dipole moments (μ_{lit}) in Debye (D).

n	$\mu_{(s)}$	$\mu_{(m)}$	$\mu_{(eff)} = (\mu_s^2 + \mu_m^2)^{\frac{1}{2}}$	$\mu_{(lit)}$
3	1.66			1.66
4	1.71			1.73
5	1.75	0.65	1.8_7	1.73
6	1.71	0.65	1.8_2	1.80
7	1.36	0.74	1.5_5	1.61
8	1.15	1.09	1.5_8	1.62
10	1.06	1.00	1.4_6	1.52
11	1.12	0.93	1.4_5	–
12	0.90	0.95	1.3_1	1.60
13	0.97	0.91	1.3_6	
14	0.97	1.05	1.4_5	1.67

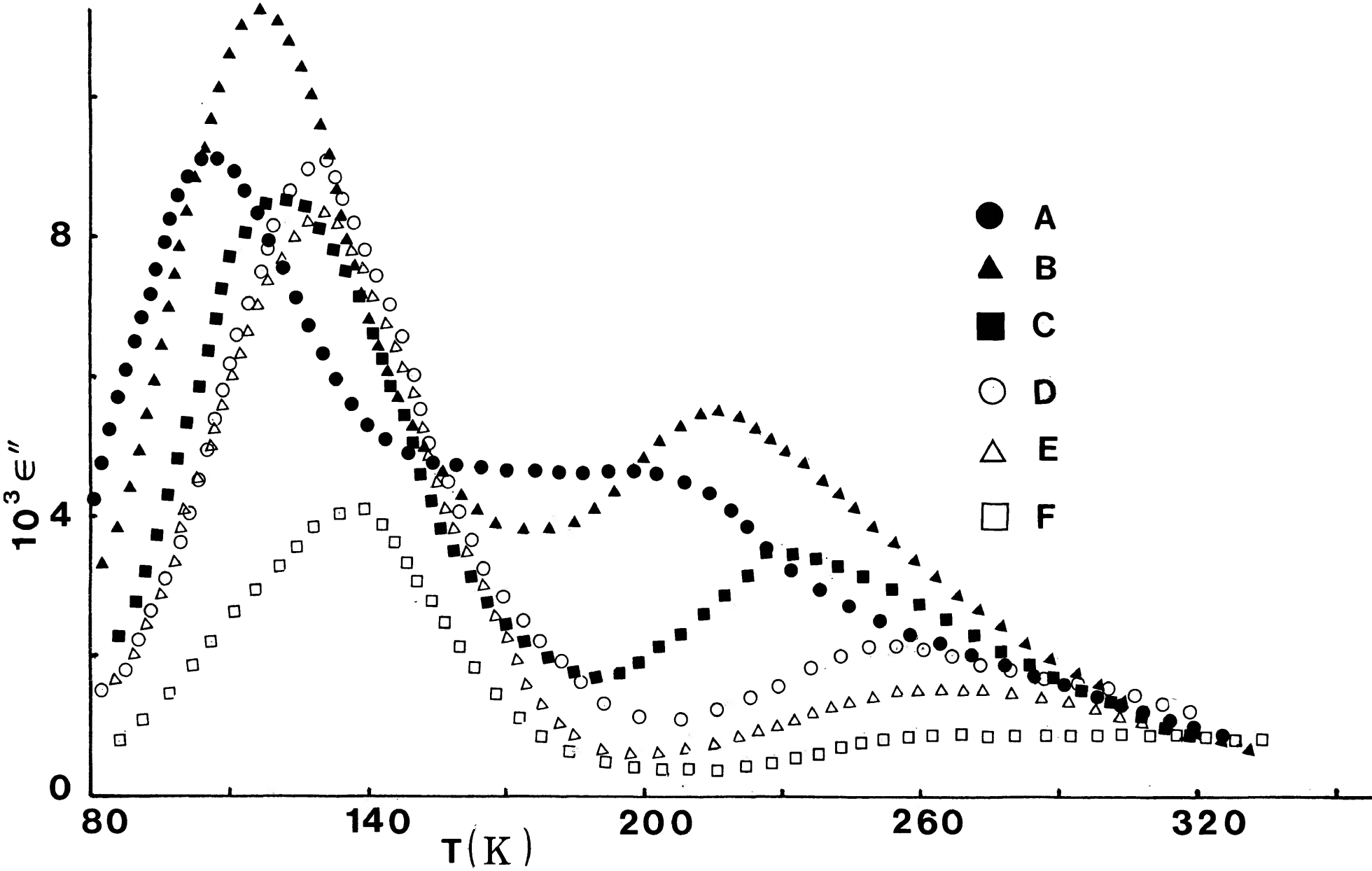

FIGURE IV-1a: Plots of dielectric loss factor, ε" versus temperature (K) for some long-chain normal alcohols in a polystyrene matrix (at 1.01 kHz). A=Hexanol-1; B=Octanol-1; C=Decanol-1; D=Tridecanol-1; E=Pentadecanol-1; F=Eicosanol-1.

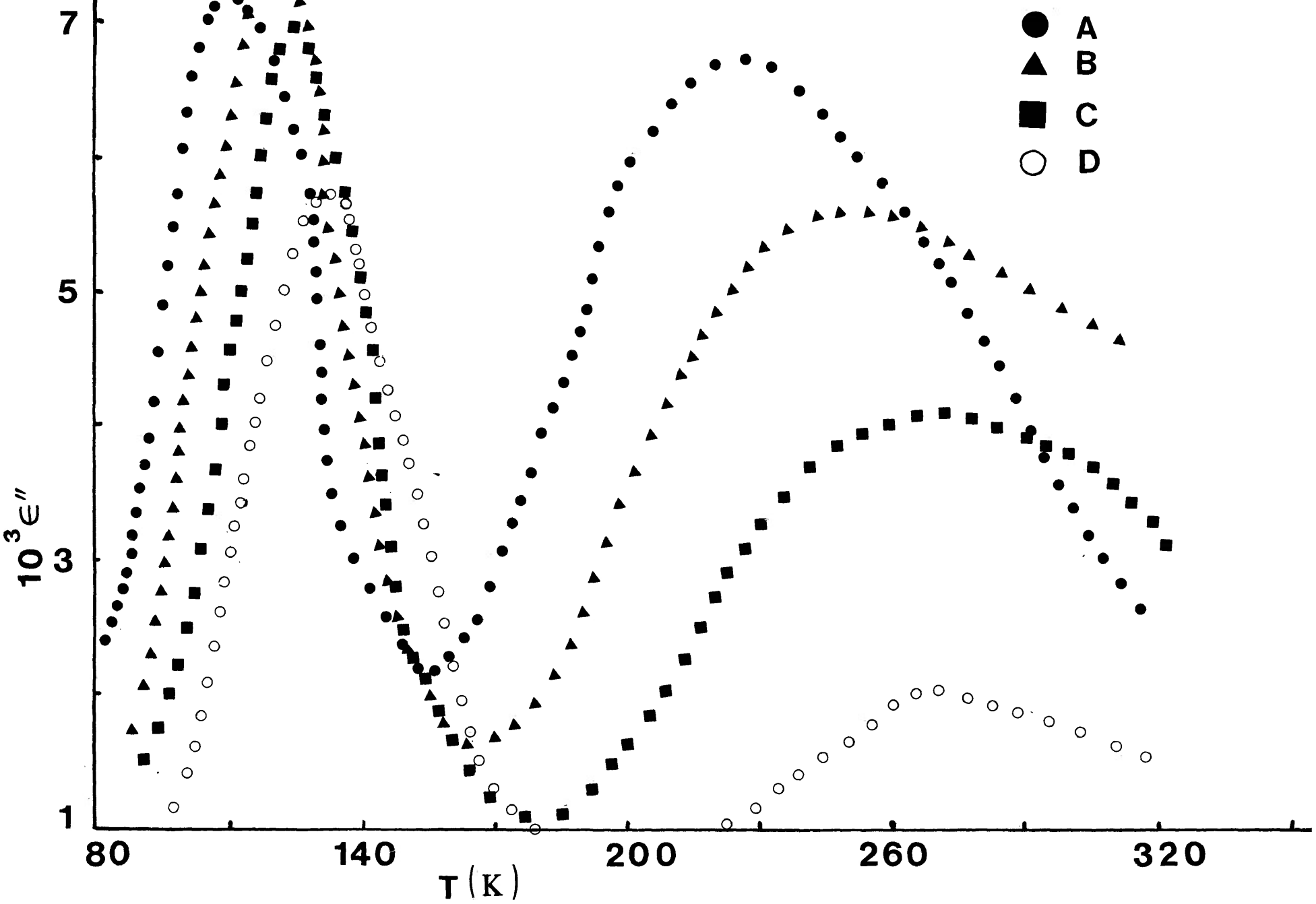

FIGURE IV-2a: Plots of dielectric loss factor, ε" versus temperature (K) for some long-chain normal thiols in a polystyrene matrix (at 1.01 kHz). A=Octanethiol-1; B=Decanethiol-1; C=Dodecanethiol-1; and D=Hexadecanethiol-1.

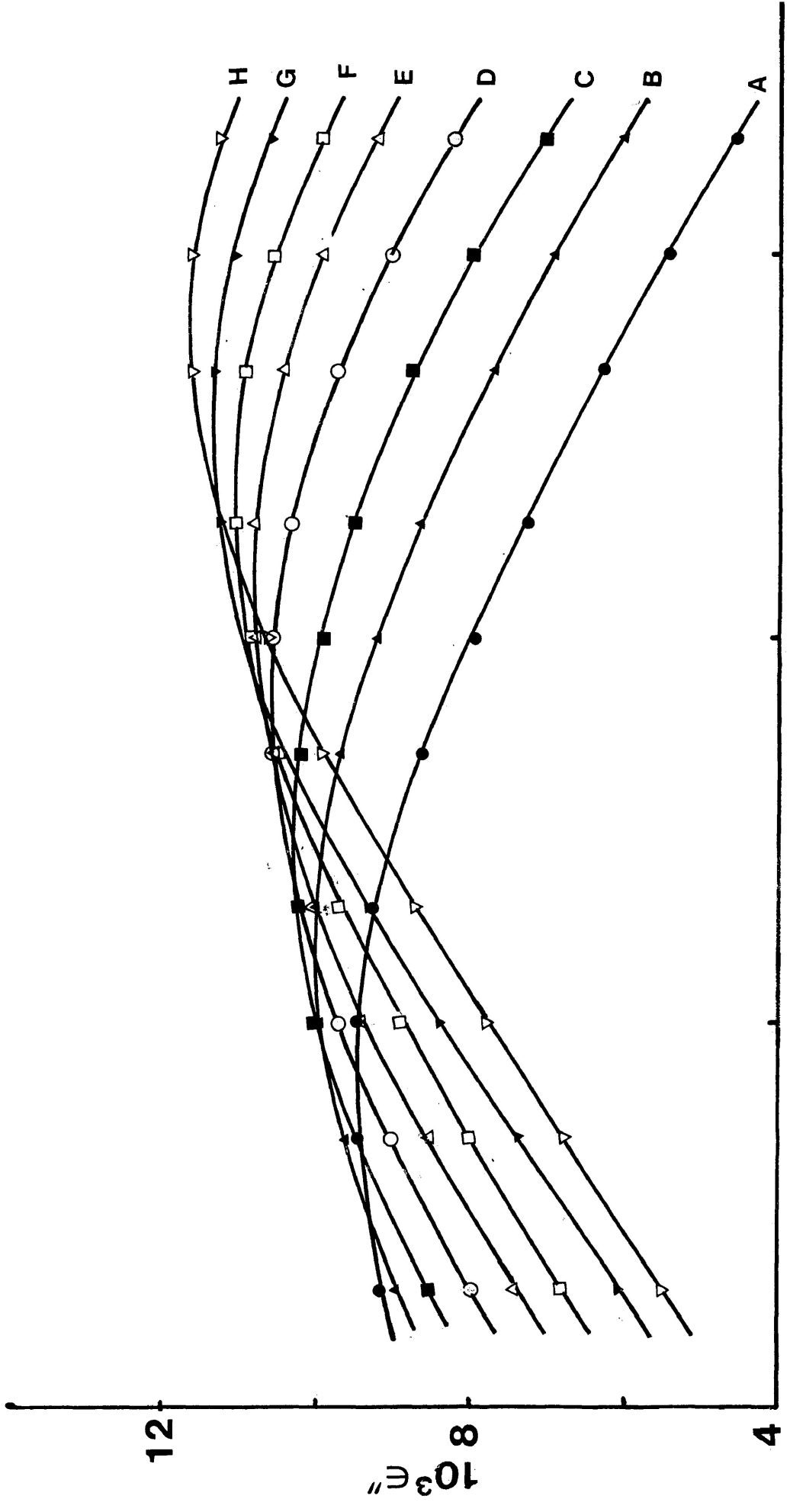

FIGURE IV-3b: Plots of dielectric loss factor, ε'' versus $\log\nu$ (Hz) for heptanol-1 in a polystyrene matrix A=95.5 K; B=99.7 K; C=102.7 K, D=106.2 K; E=109.0 K; F=111.4 K; G=113.9 K; and H=116.6 K.

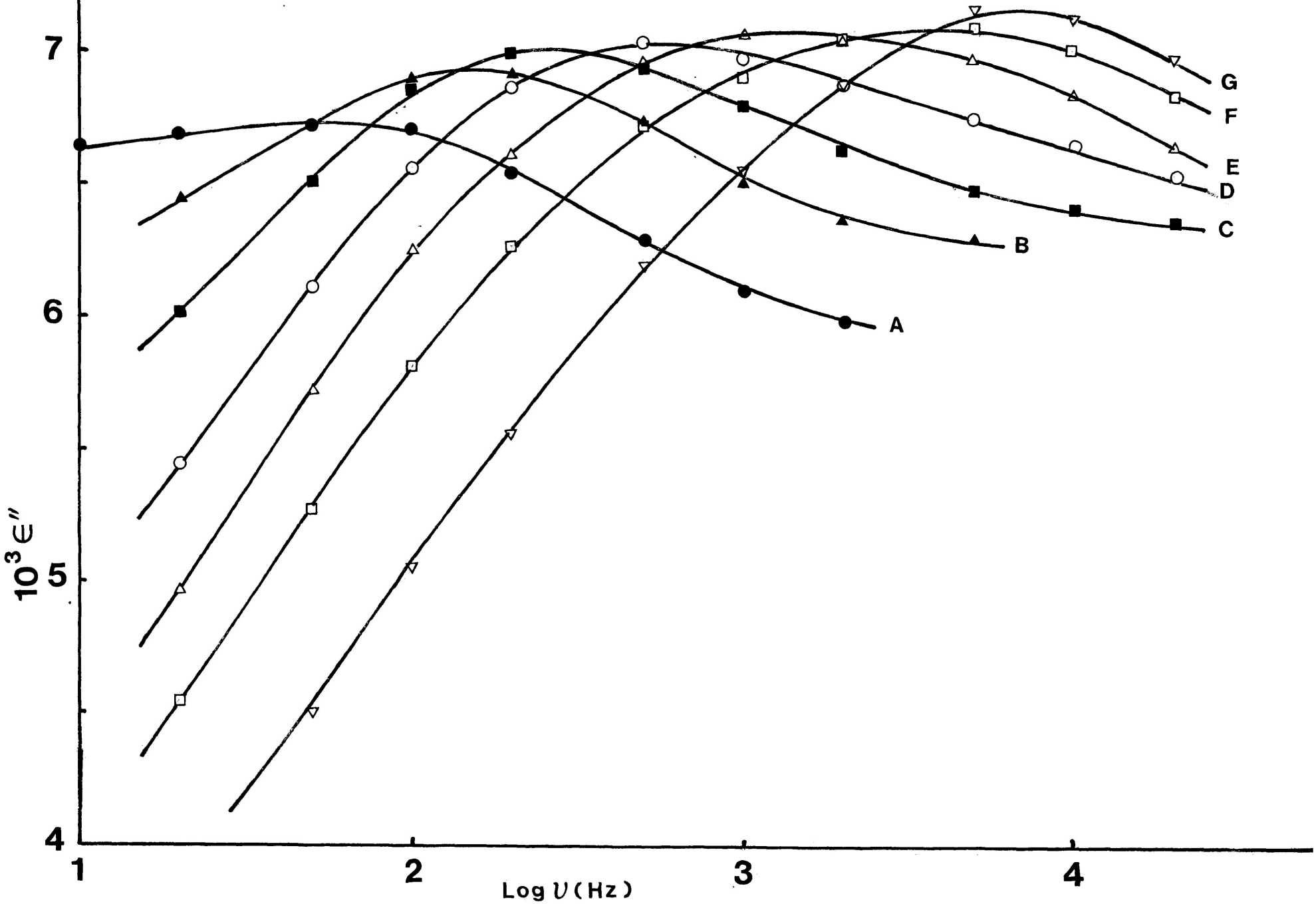

FIGURE IV-4b: Plots of dielectric loss factor, ε" versus logν (Hz) for heptanol-1 in a polystyrene matrix. A=181.1 K; B=187.2 K; C=191.6 K; D=196.2 K; E=199.7 K; F=203.4 K; and G=209.7 K.

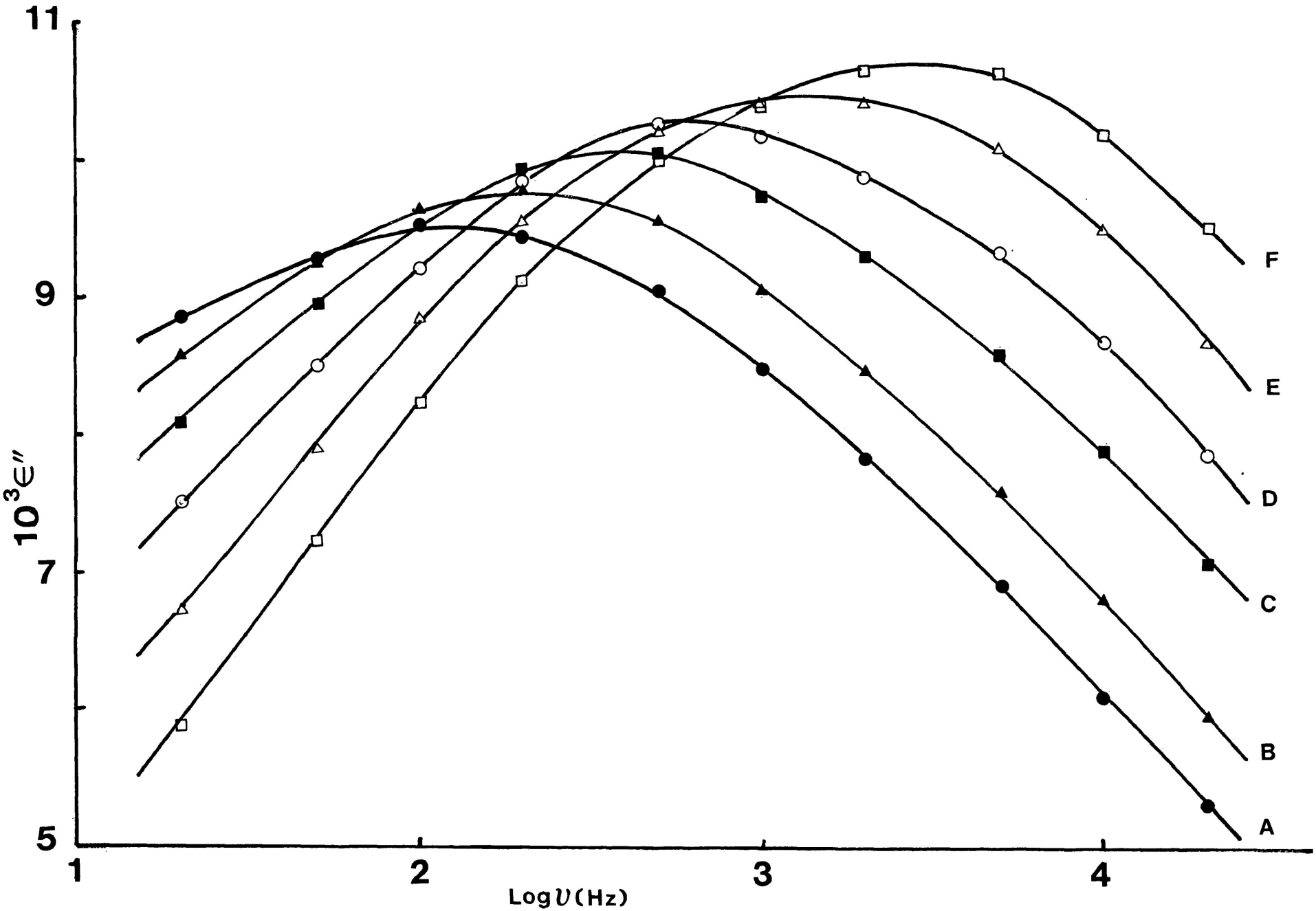

FIGURE IV-5b: Plots of dielectric loss factor, ε'' versus logν (Hz) for nonanol-1 in a polystyrene matrix A=102.3 K; B=104.4 K; C=108.0 K; D=110.7 K; E=113.8 K; and F=116.7 K.

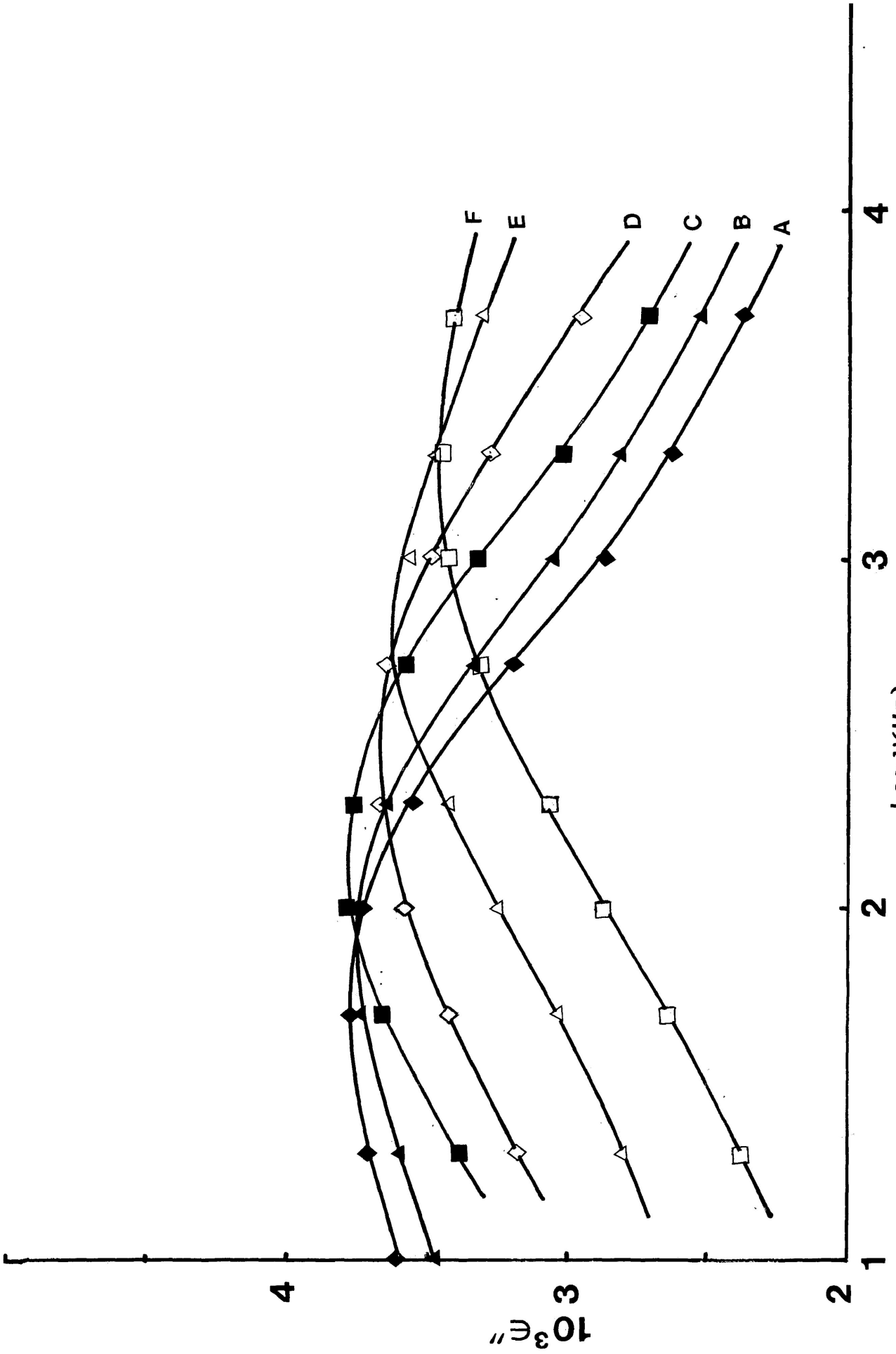

FIGURE IV-6b: Plots of dielectric loss factor, ε'' versus logν (Hz) for nonanol-1 in a polystyrene matrix A=201.6 K; B=205.2 K; C=210.3 K; D=215.4 K E=225.0 K; and F=233.9 K.

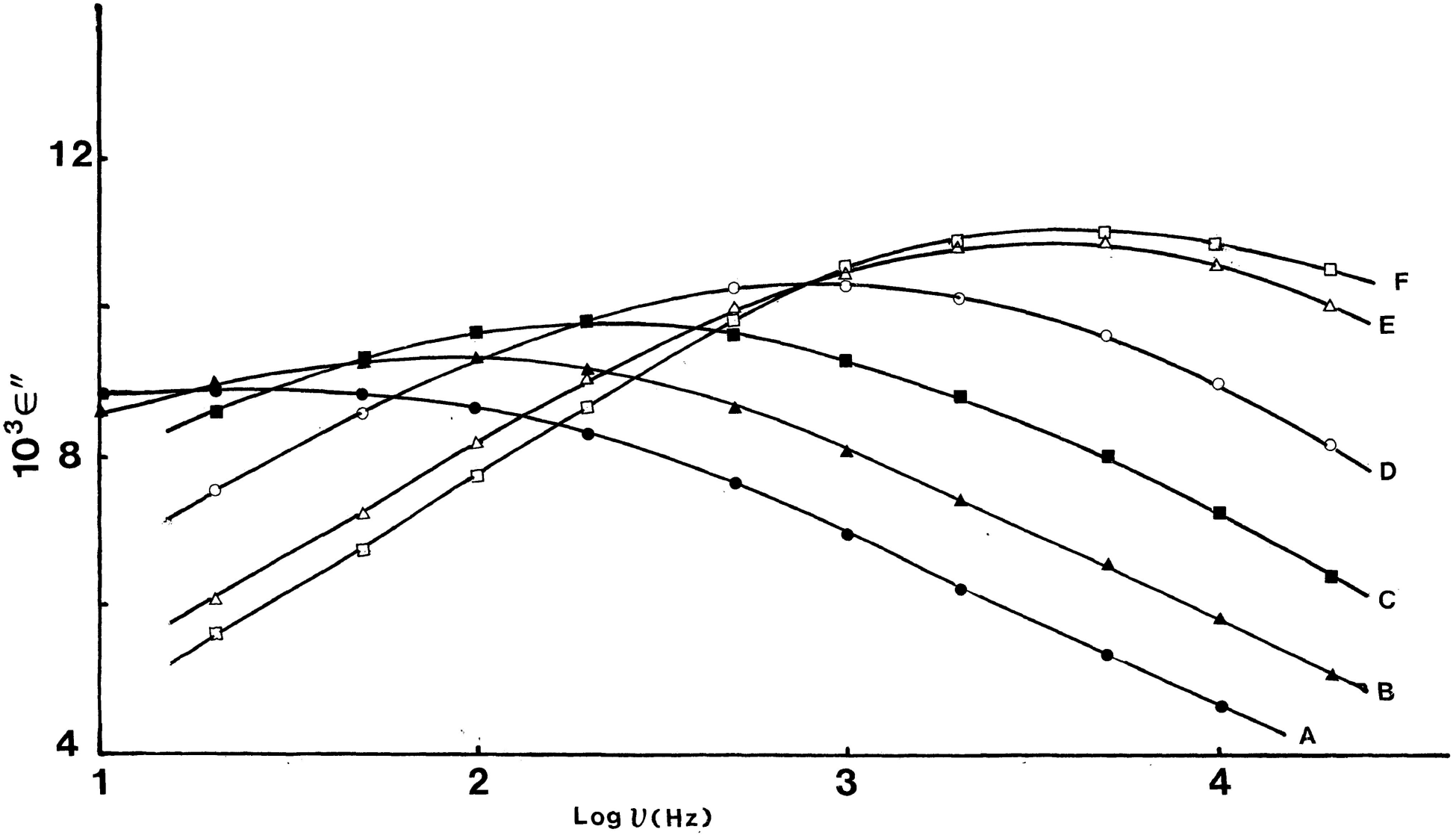

FIGURE IV-7b: Plots of dielectric loss factor, ε" versus logν (Hz) for decanol-1 in a polystyrene matrix. A=102.2 K; B=106.2 K; C=111.1 K; D=117.2 K; E=124.0 K; and F=125.8 K.

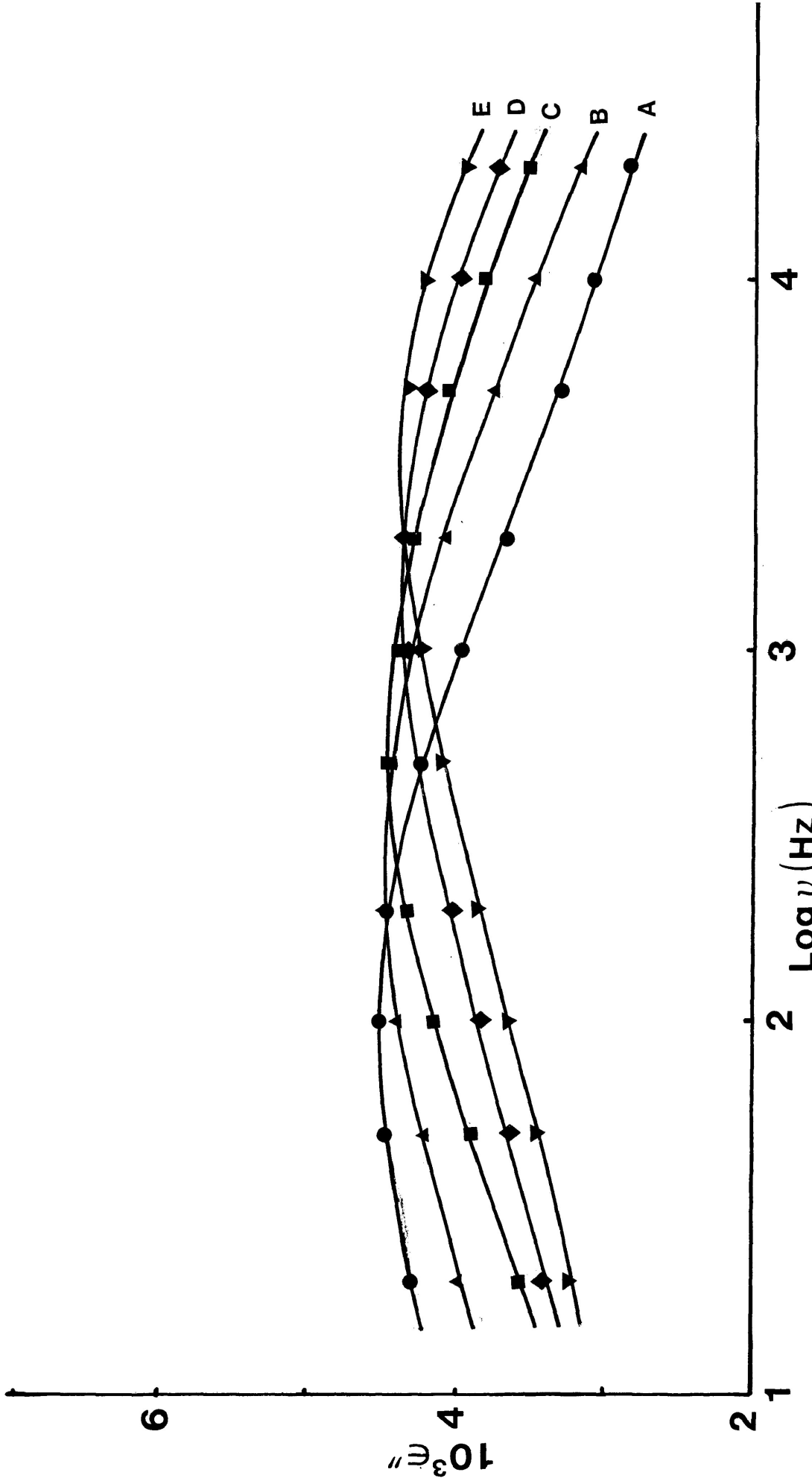

FIGURE IV-8b: Plots of dielectric loss factor, ε'' versus logν (Hz) for decanol-1 in a polystyrene matrix. A=219.7 K; B=227.2 K; C=233.8 K; D=239.5 K; and E=243.0 K.

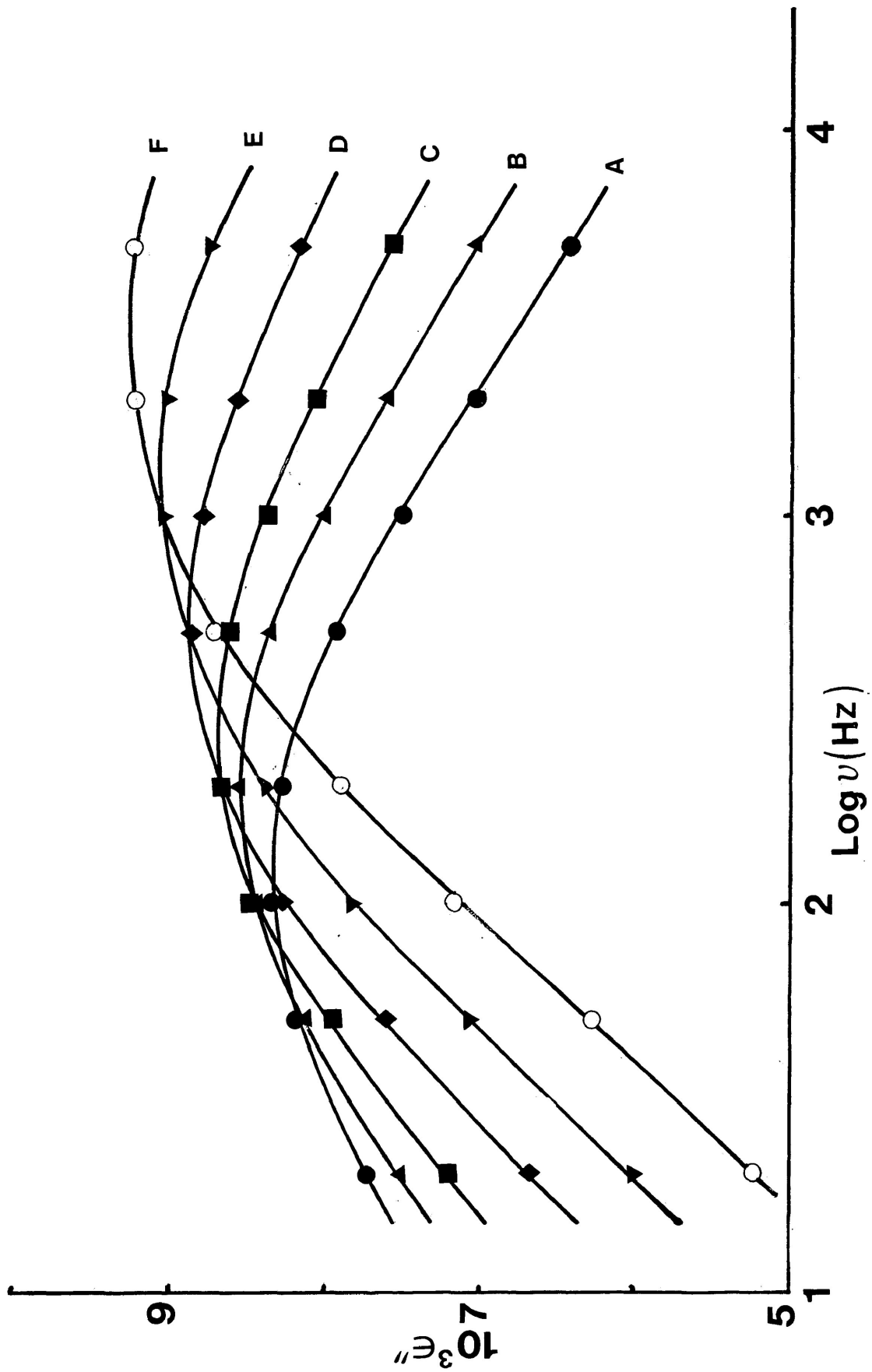

FIGURE IV-9b: Plots of dielectric loss factor, ε'' versus logυ (Hz) for tetradecanol-1 in a polystyrene matrix. A=116.5 K; B=119.2 K; C=121.8 K; D=124.7 K; E=128.2 K; and F=131.8 K.

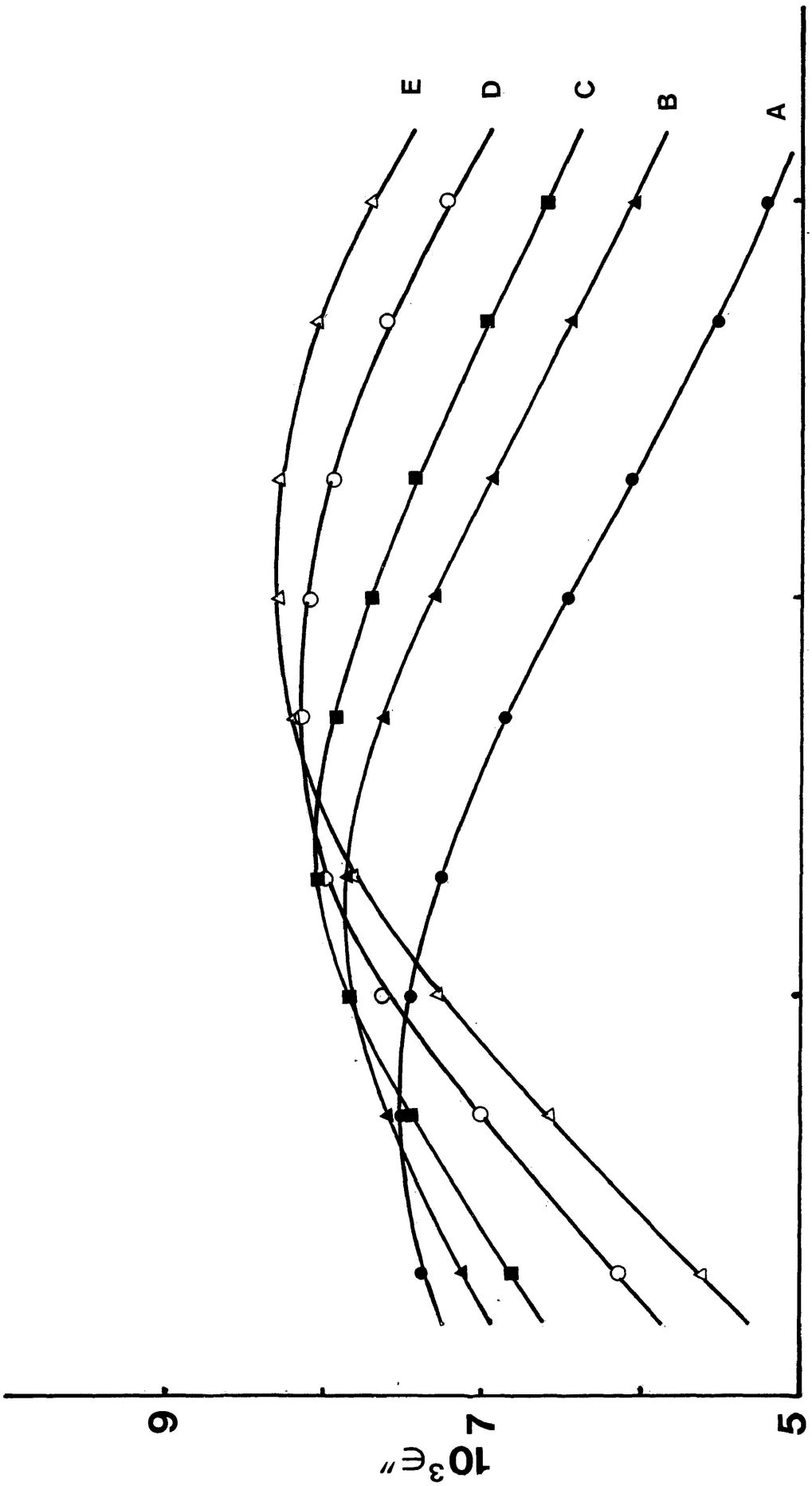

FIGURE IV-10b: Plots of dielectric loss factor, ε'' versus logν (Hz) for hexadecanol-1 in a polystyrene matrix. A=115.0 K; B=120.0 K; C=123.0 K; D=126.3 K; and E=129.7 K.

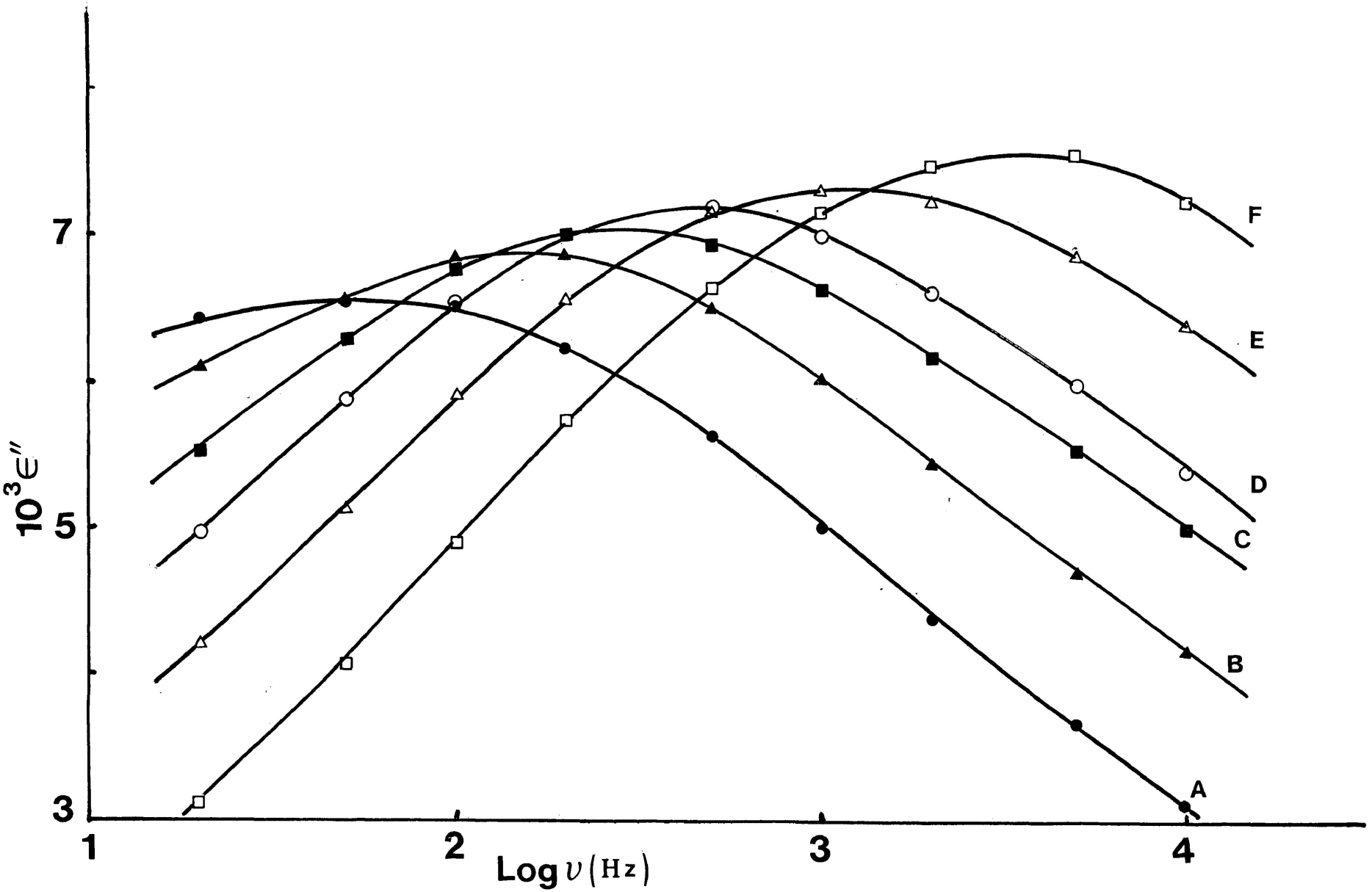

FIGURE IV-11b: Plots of dielectric loss factor, ε'' versus logυ (Hz) for octanethiol-1 in a polystyrene matrix. A=95.3 K; B=99.4 K; C=102.6 K; D=104.7 K; E=109.1 K; and F=113.9 K.

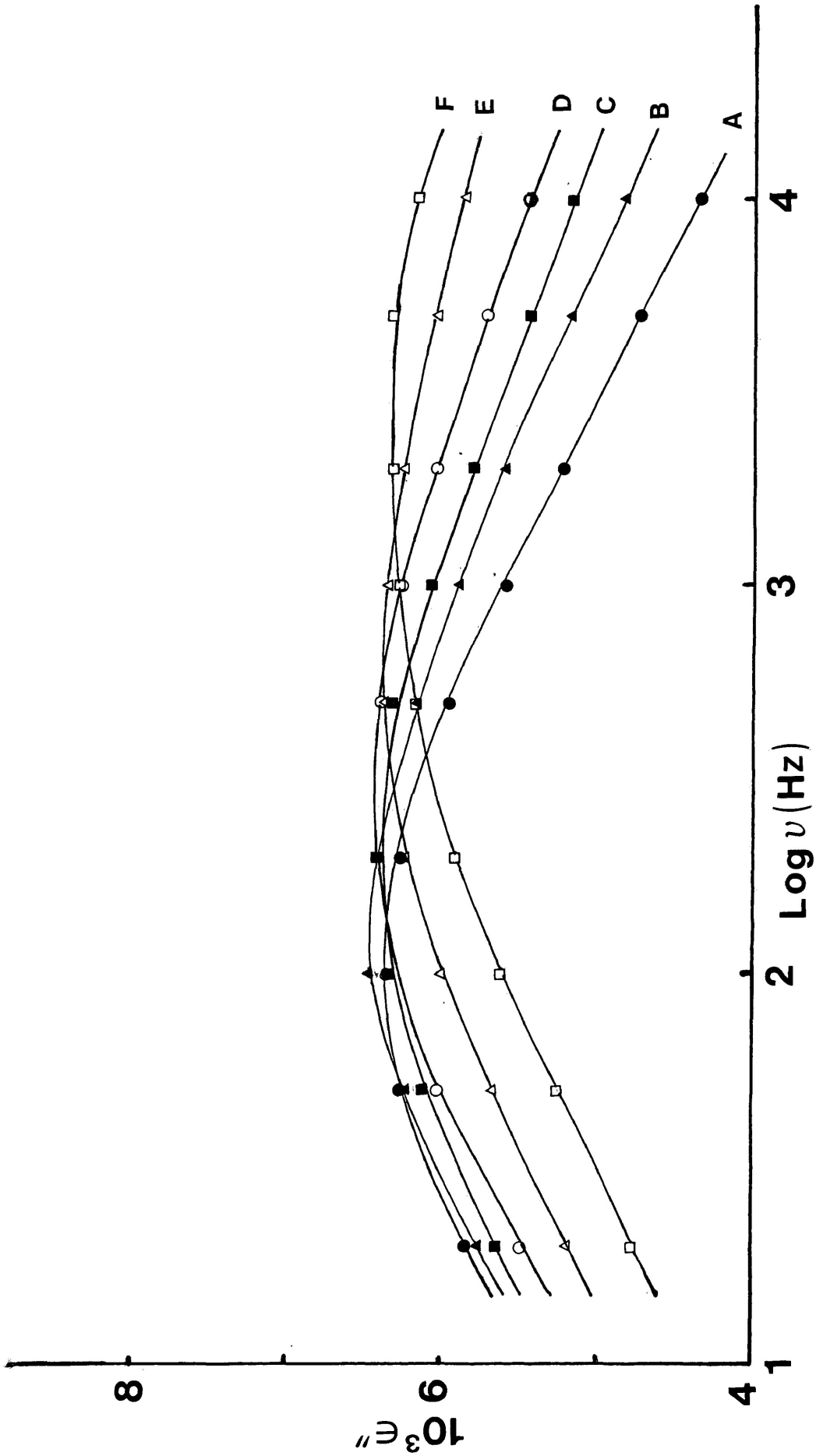

FIGURE IV-12b: Plots of dielectric loss factor, ε'' versus logυ (Hz) for octanethiol-1 in a polystyrene matrix. A=199.0 K; B=205.4 K; C=209.4 K; D=215.4 K; E=224.2 K; and F=233.8 K.

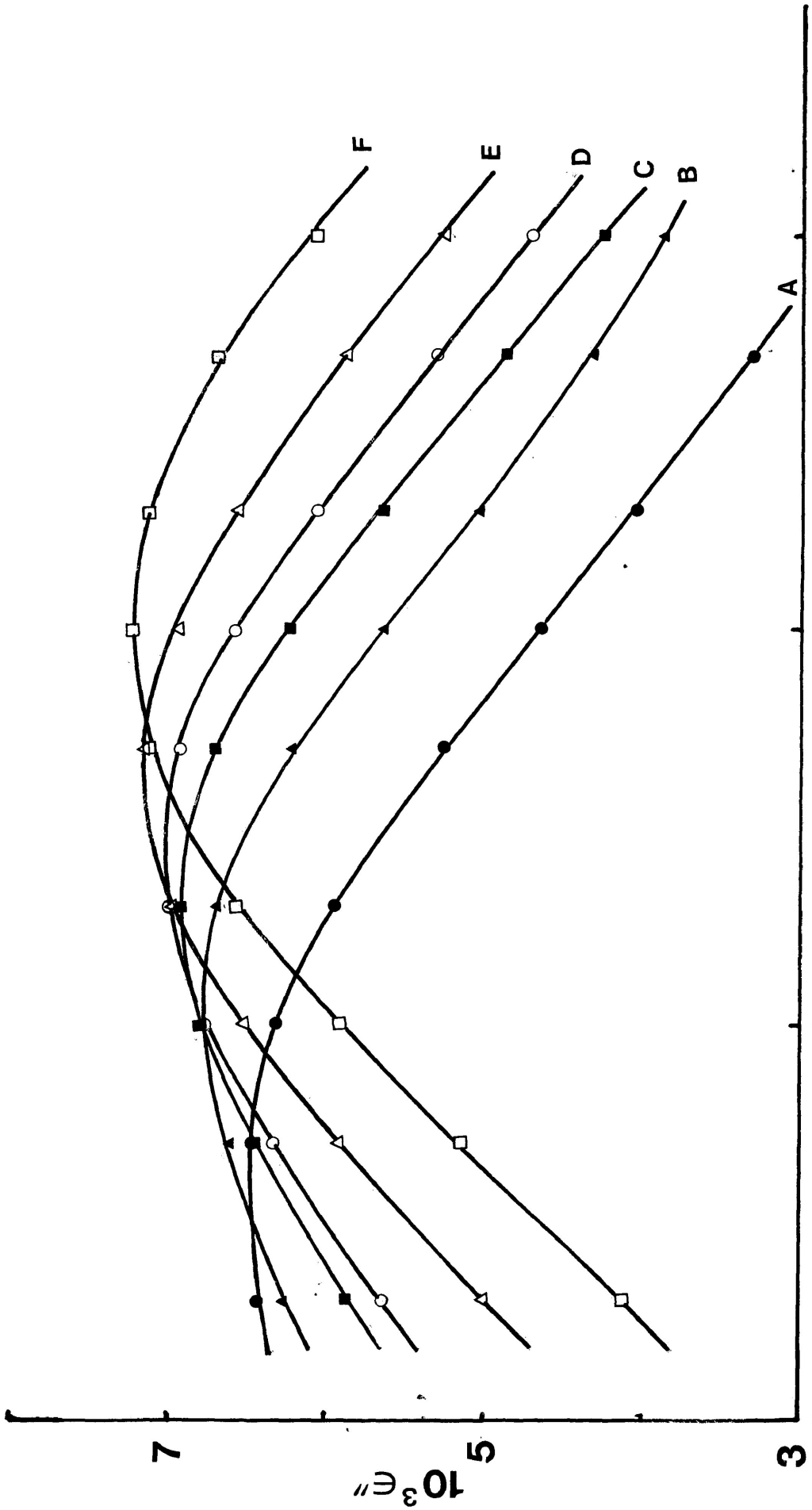

FIGURE IV-13b: Plots of dielectric loss factor, ε'' versus logν (Hz) for decanethiol-1 in a polystyrene matrix. A=101.9 K; B=106.1 K; C=108.6 K; D=110.7 K; E=112.7 K; and F=116.6 K.

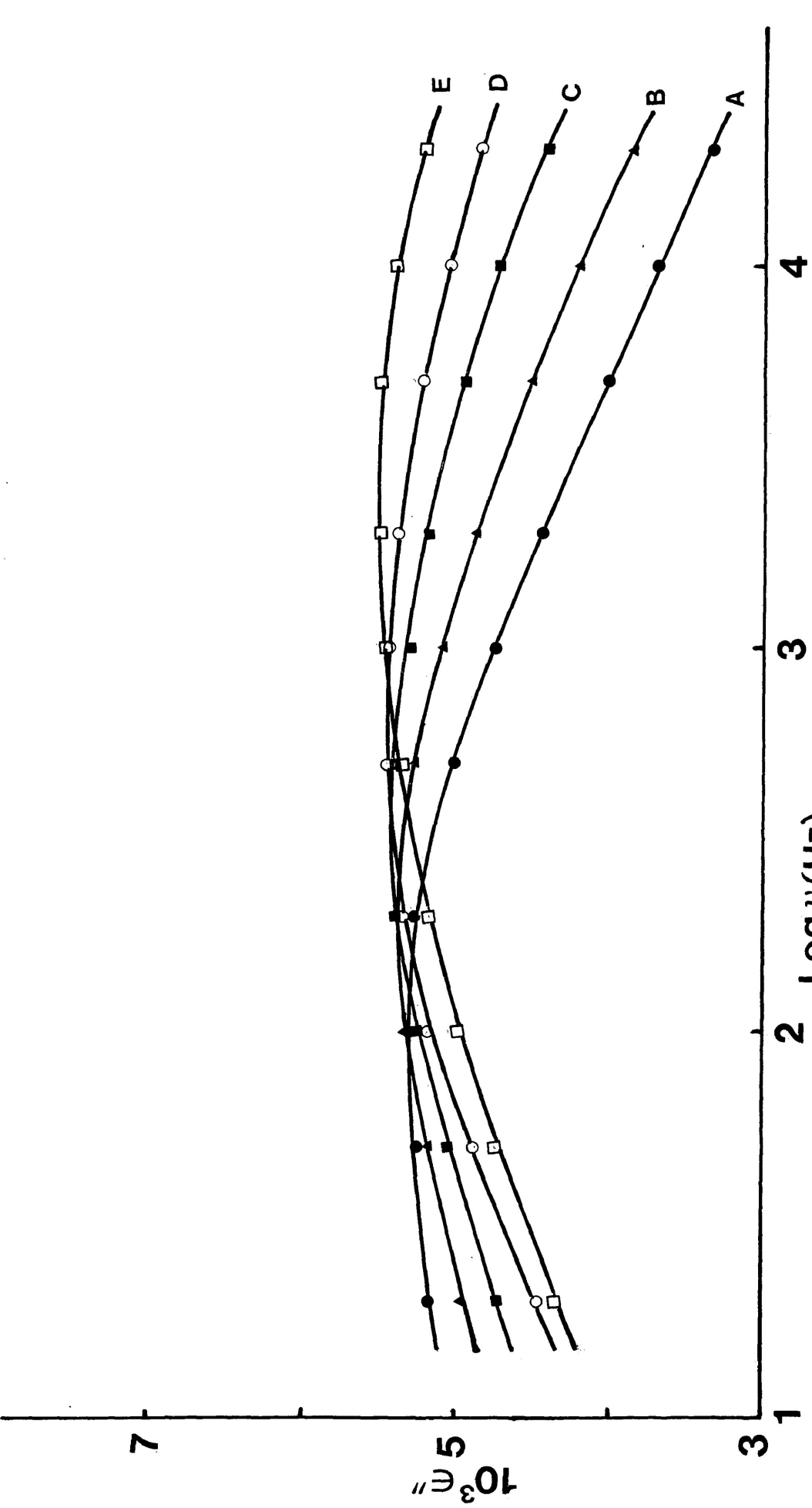

FIGURE IV-14b: Plots of dielectric loss factor, ε'' versus $\log\upsilon$ (Hz) for decanethiol-1 in a polystyrene matrix. A=220.2 K; B=228.7 K; C=237.8 K; D=245.9 K; and E=256.1 K.

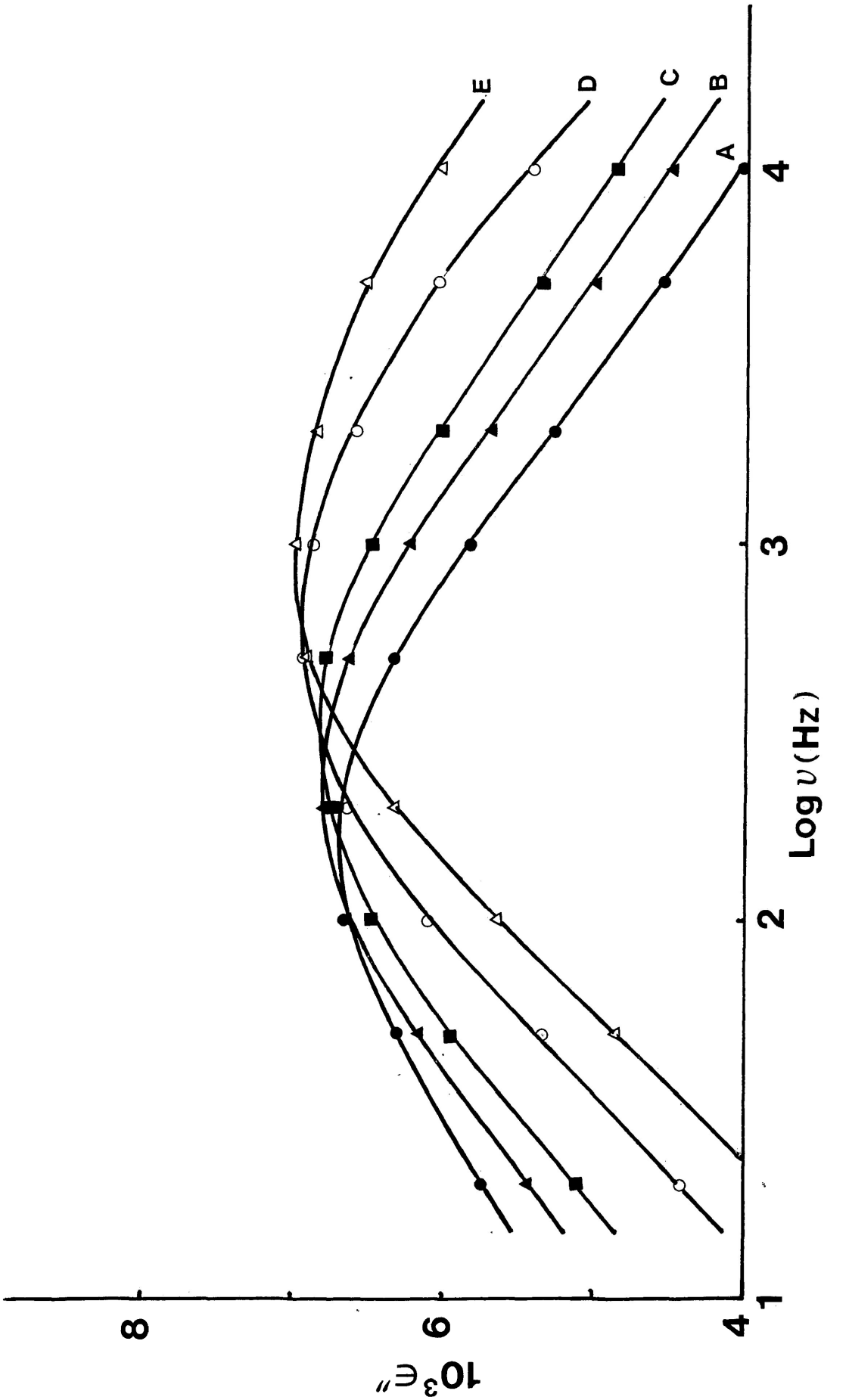

FIGURE IV-15b: Plots of dielectric loss factor, ε'' versus $\log\nu$ (Hz) for dodecanethiol-1 in a polystyrene matrix. A=111.4 K; B=113.6 K; C=115.0 K; D=118.4 K; E=121.0 K; and F=126.3 K.

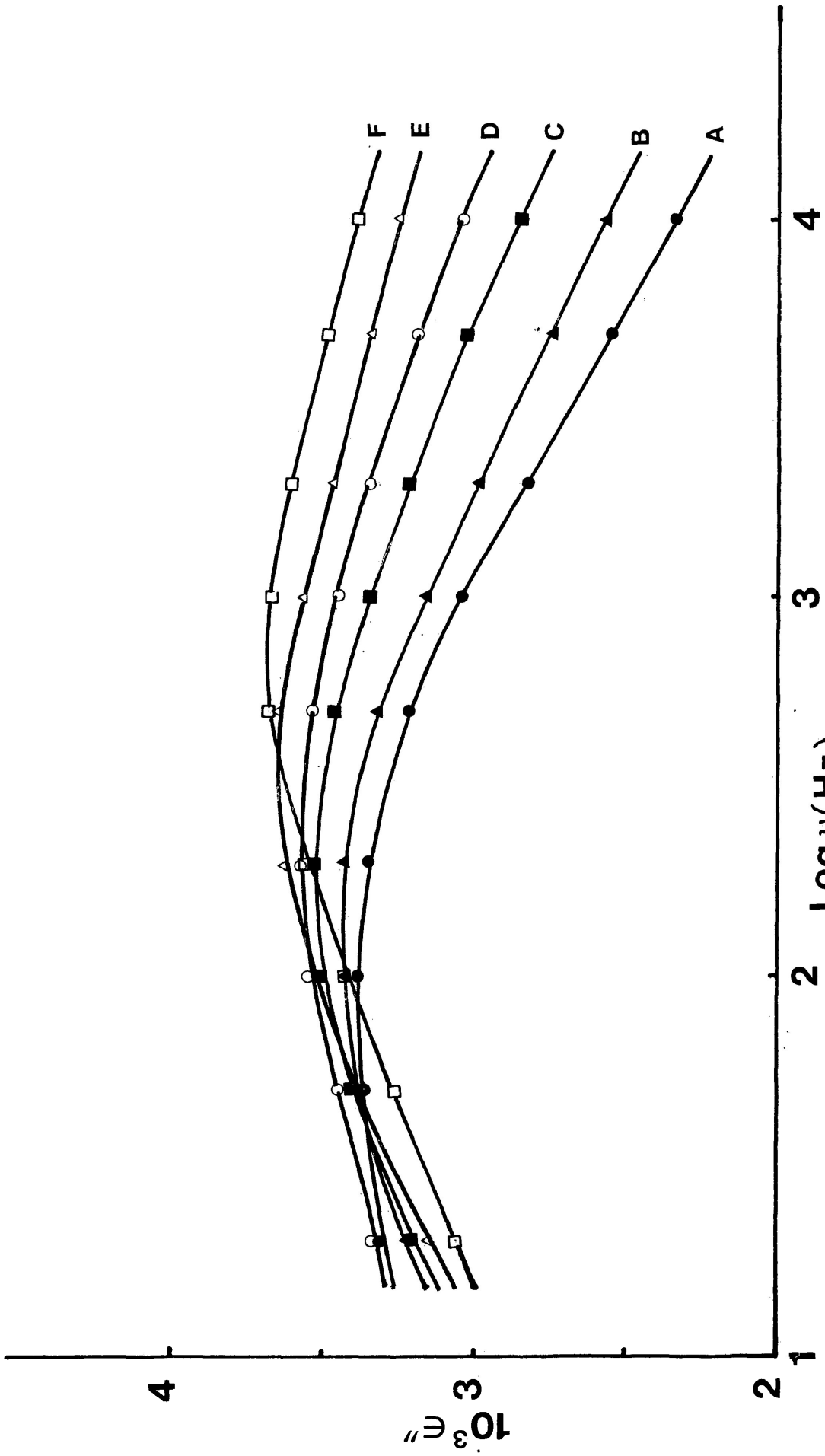

FIGURE IV-16b: Plots of dielectric loss factor, ε'' versus logυ (Hz) for dodecanethiol-1 in a polystyrene matrix. A=234.0 K; B=238.6 K; C=245.7 K; D=250.7 K; E=225.8 K; and F=260.7 K.

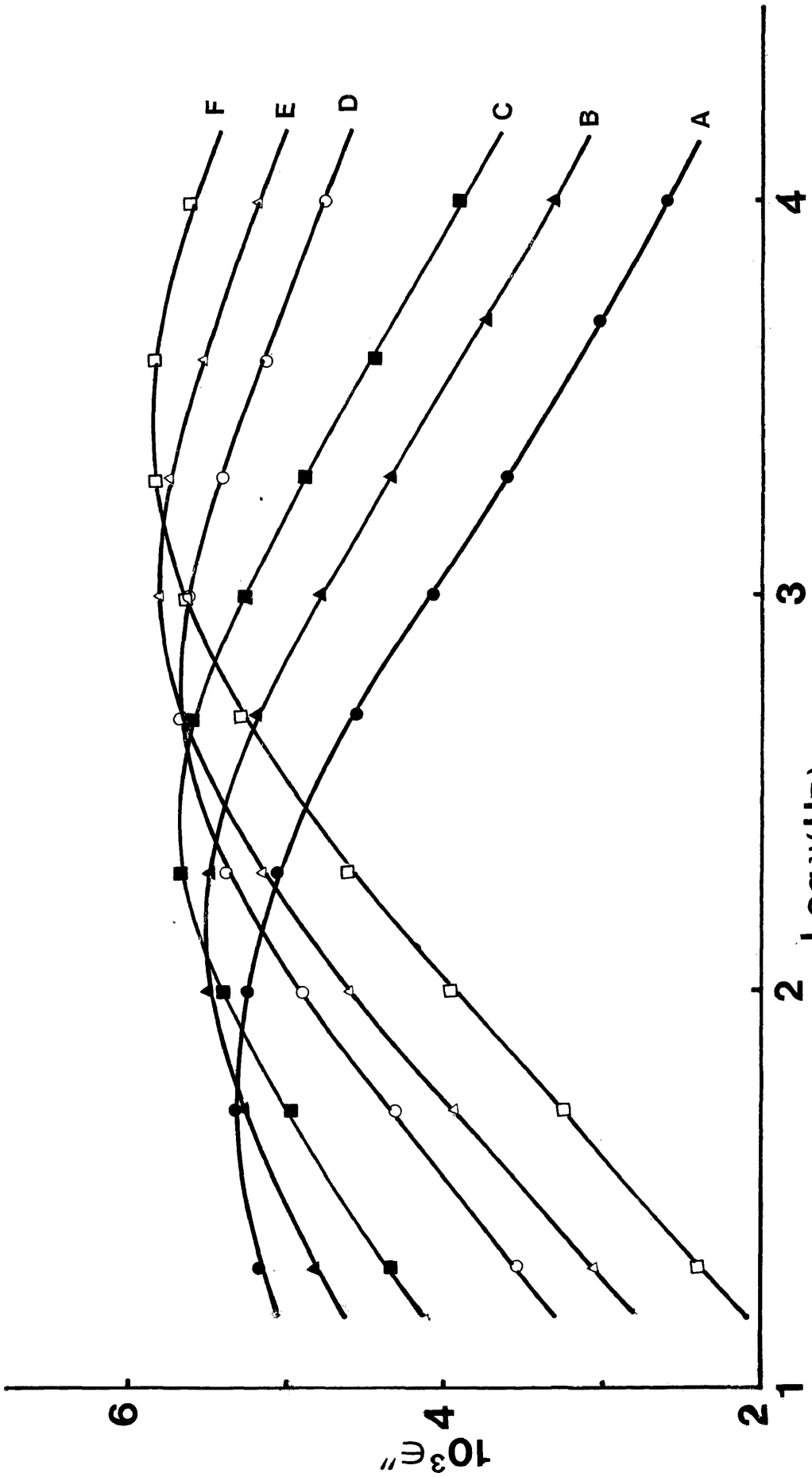

FIGURE IV-17b: Plots of dielectric loss factor, ε'' versus logυ (Hz) for hexadecanethiol-1 in a polystyrene matrix. A=114.9 K; B=119.3 K; C=122.9 K; D=127.3 K; E=130.5 K; and F=133.5 K.

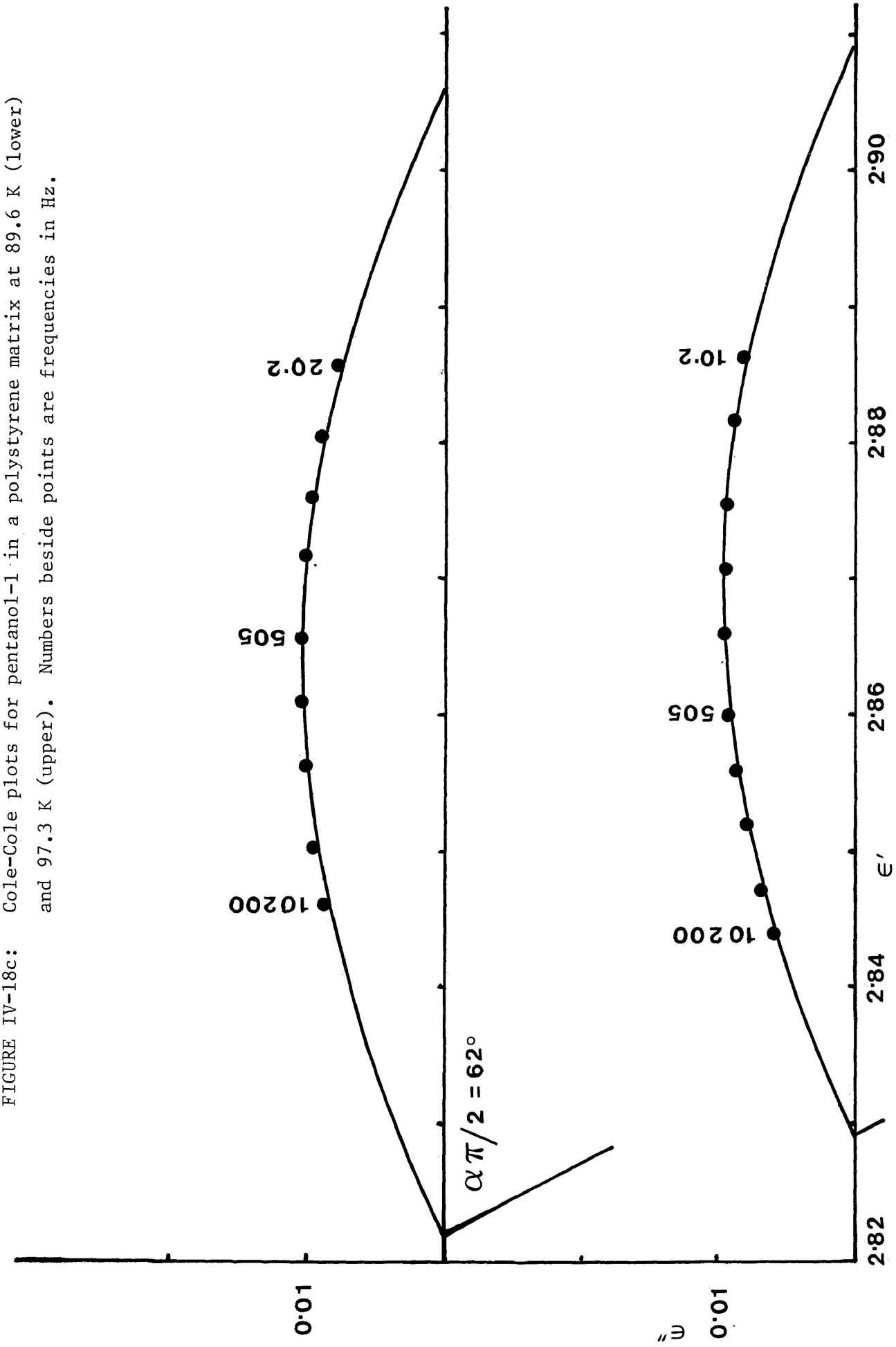

FIGURE IV-18c: Cole-Cole plots for pentanol-1 in a polystyrene matrix at 89.6 K (lower) and 97.3 K (upper). Numbers beside points are frequencies in Hz.

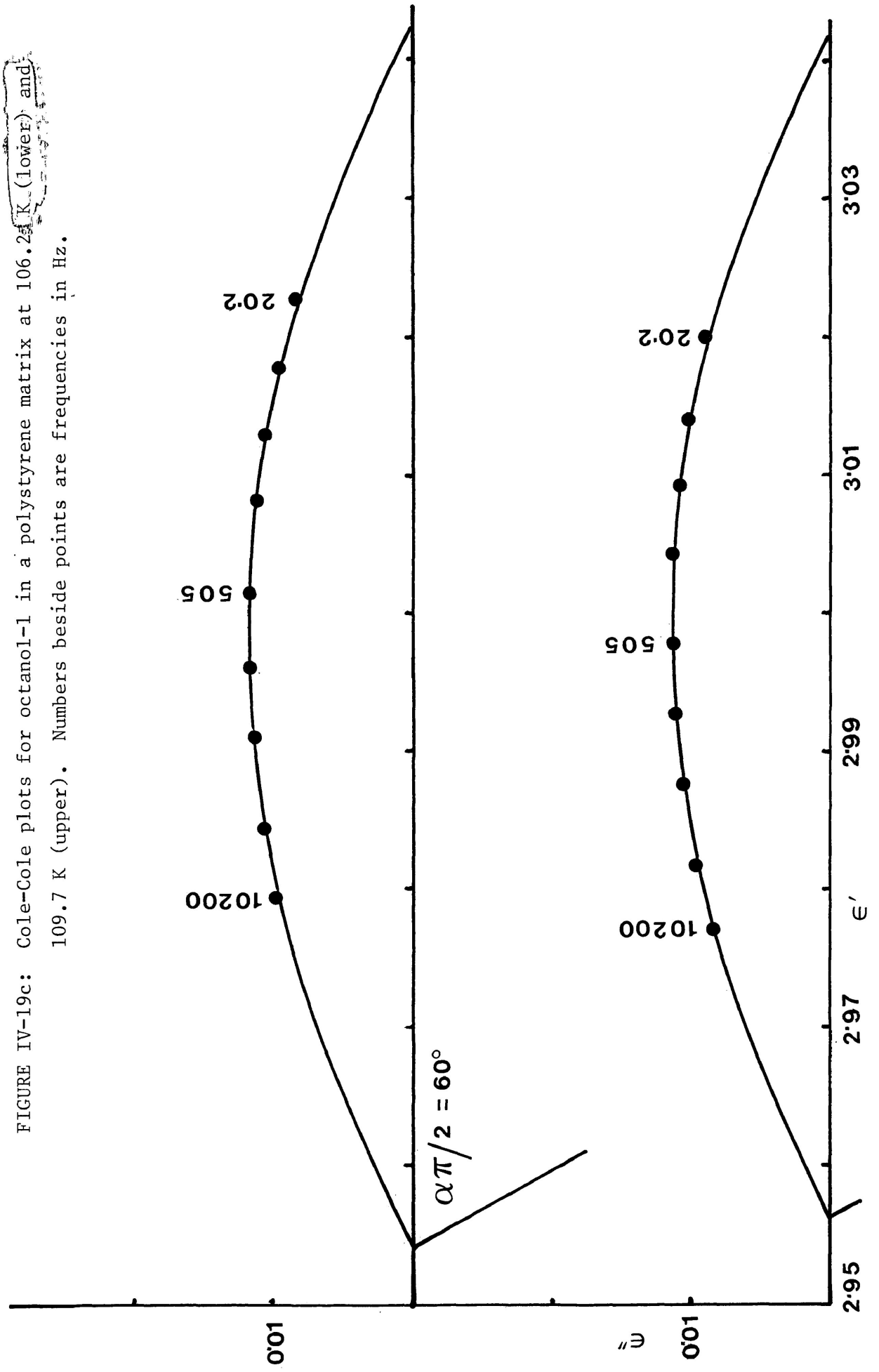

FIGURE IV-19c: Cole-Cole plots for octanol-1 in a polystyrene matrix at 106.2 K (lower) and 109.7 K (upper). Numbers beside points are frequencies in Hz.

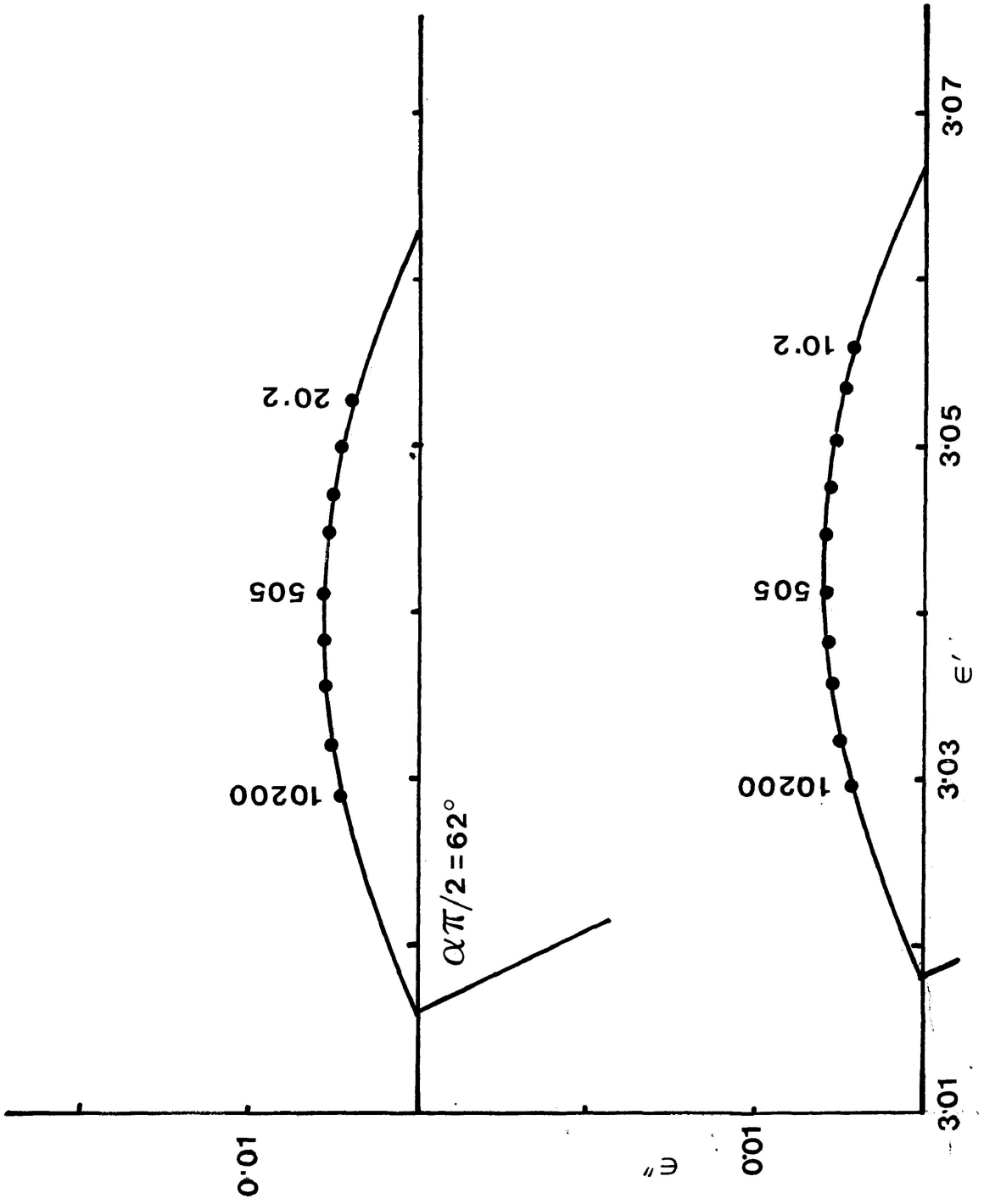

FIGURE IV-20c: Cole-Cole plots for octanol-1 in a polystyrene matrix at 208.9 K (lower) and 214.8 K (upper). Numbers beside points are frequencies in Hz.

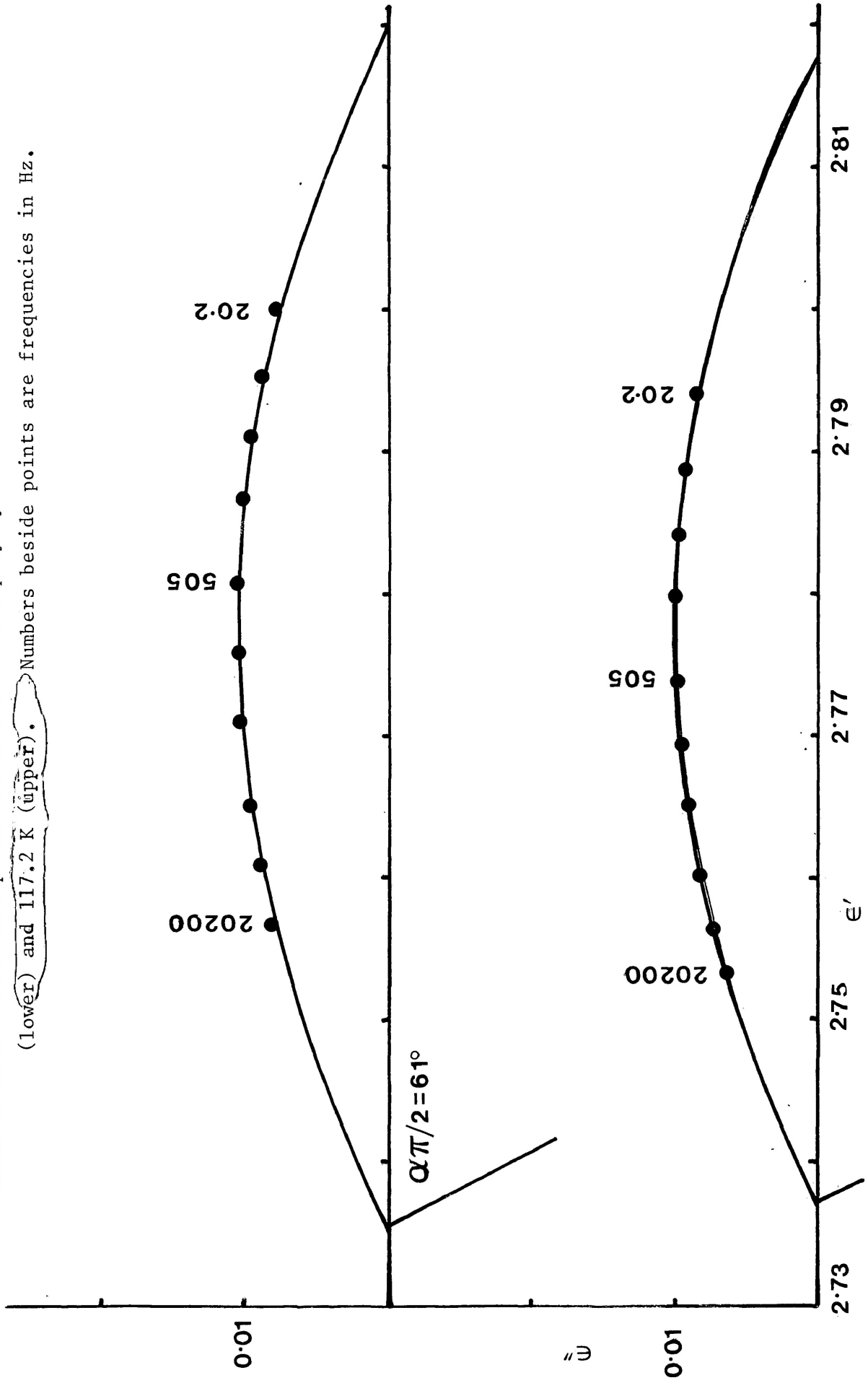

FIGURE IV-21c: Cole-Cole plots for decanol-1 in a polystyrene matrix at 110.1 K (lower) and 117.2 K (upper). Numbers beside points are frequencies in Hz.

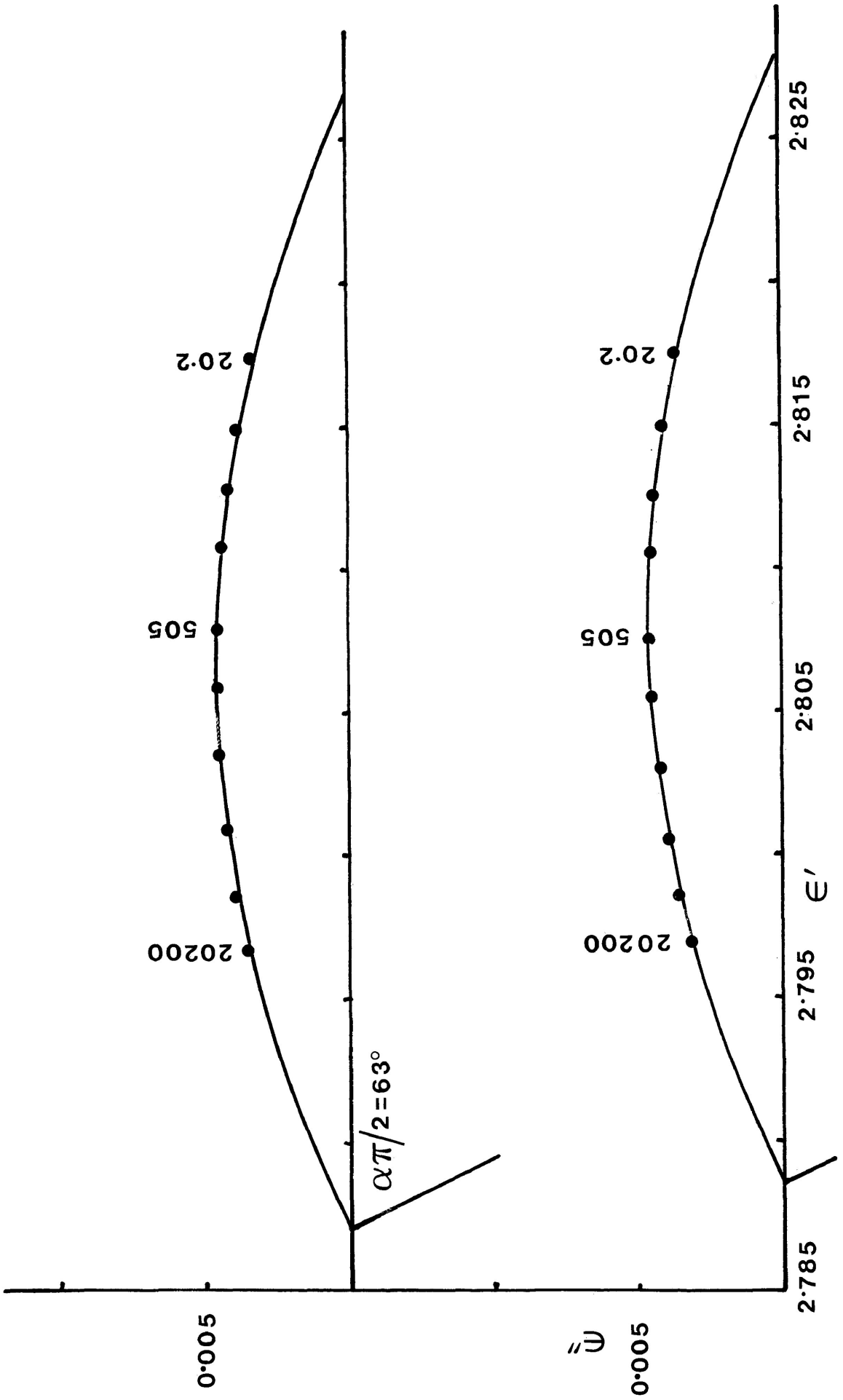

FIGURE IV-22c: Cole-Cole plots for decanol-1 in a polystyrene matrix at 230.0 K (lower) and 236.8 K (upper). Numbers beside points are frequencies in Hz.

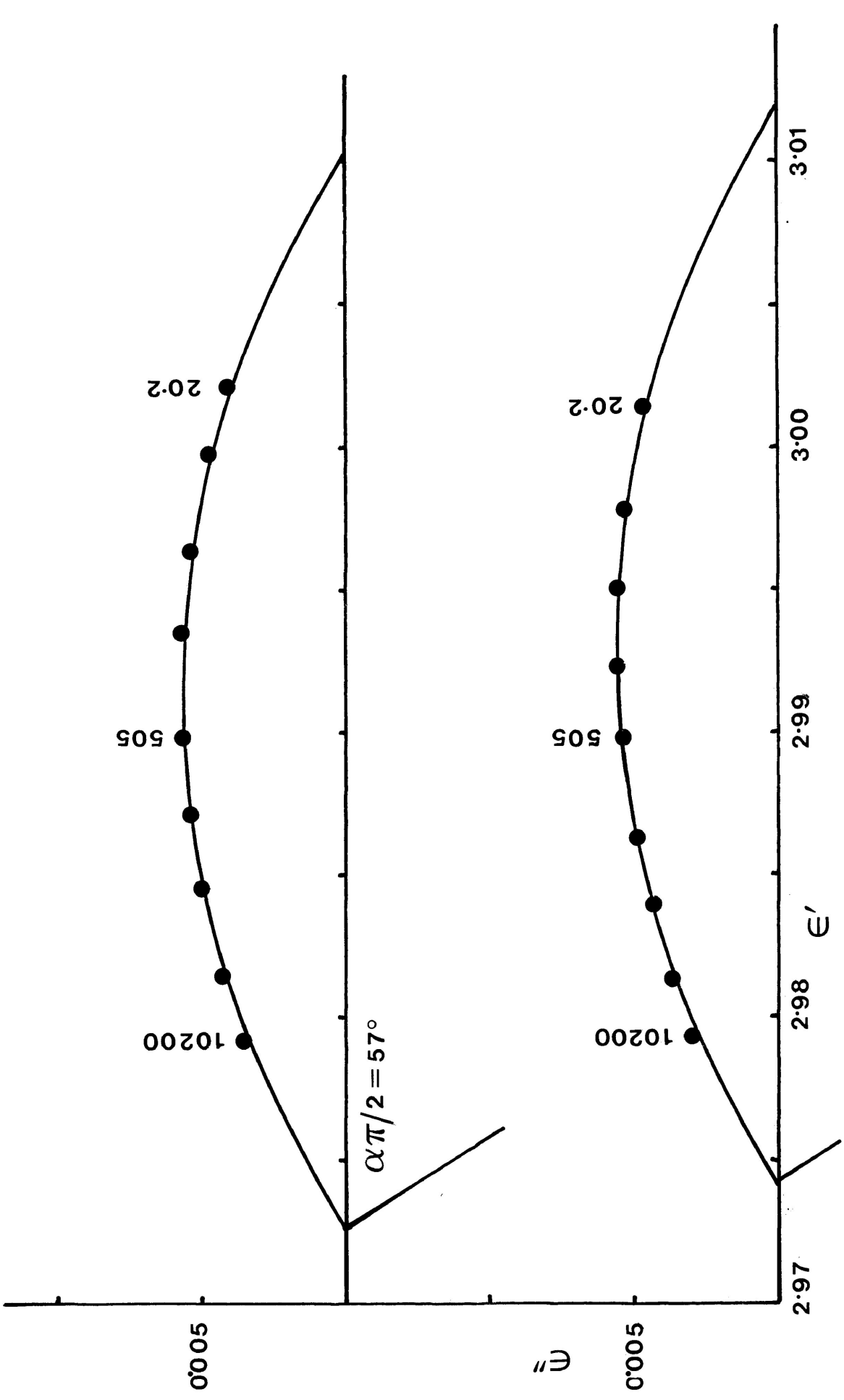

FIGURE IV-23c: Cole-Cole plots for hexadecanethiol-1 in a polystyrene matrix at 119.3 K (lower) and 122.9 K (upper). Numbers beside points are frequencies in Hz.

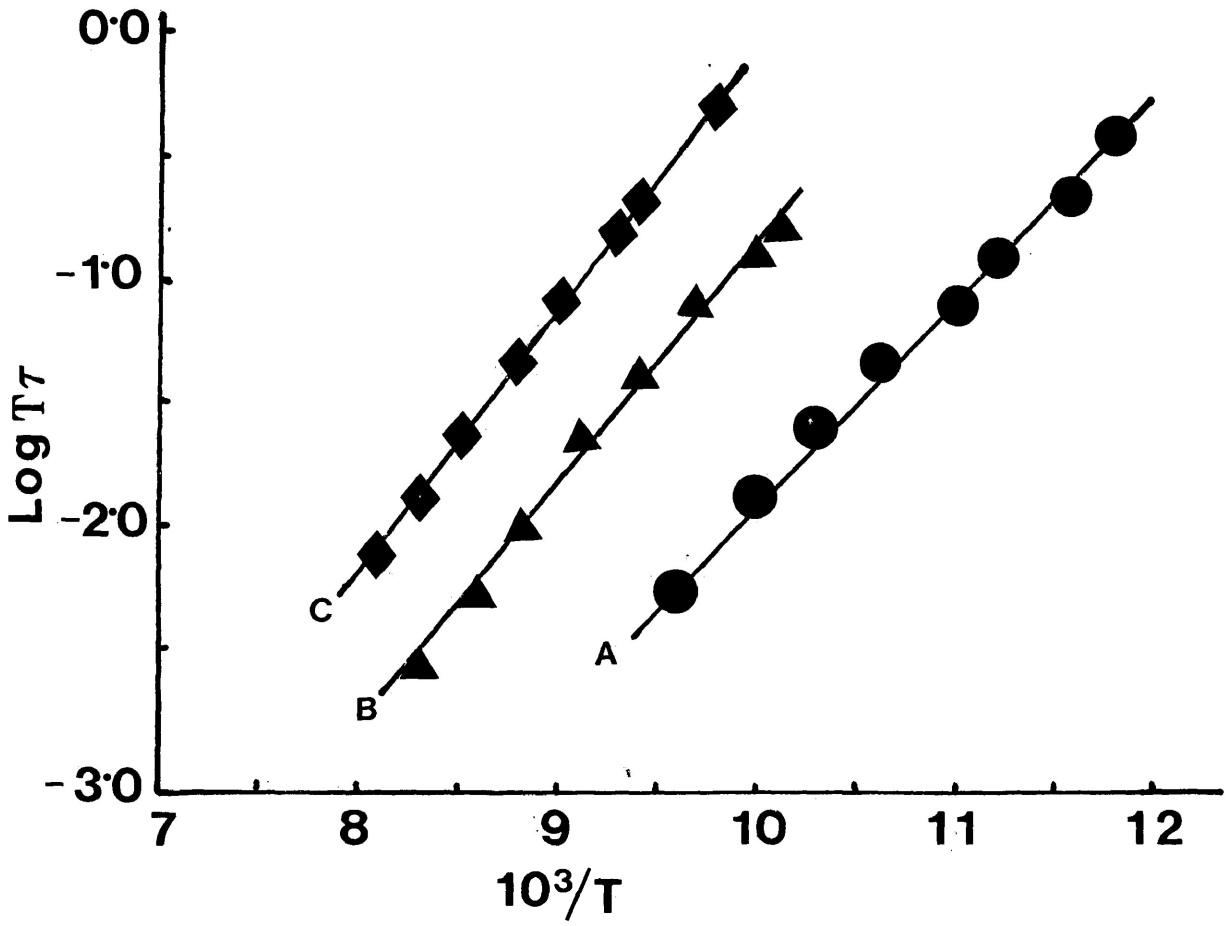

FIGURE IV-24d: Eyring plots of logTτ versus 1/T (K^{-1}) for some long-chain normal alcohols (lower temperature process) in a polystyrene matrix. A=Pentanol-1, B=Octanol-1, and C=Decanol-1

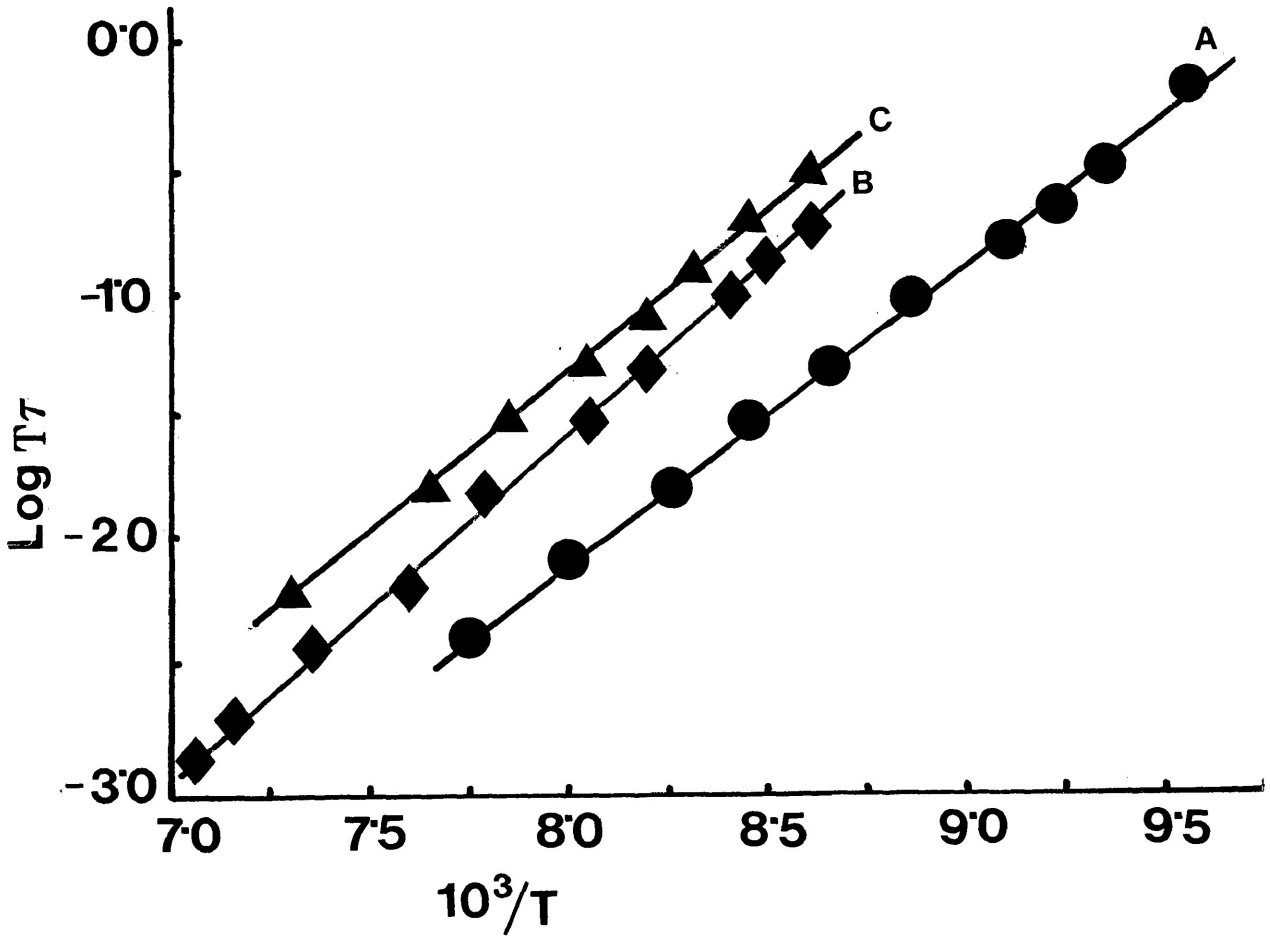

FIGURE IV-25d: Eyring plots of logTτ versus 1/T (K^{-1}) for some long-chain normal alcohols (lower temperature process) in a polystyrene matrix. A=Dodecanol-1; B=tetradecanol-1, C=Eicosanol-1.

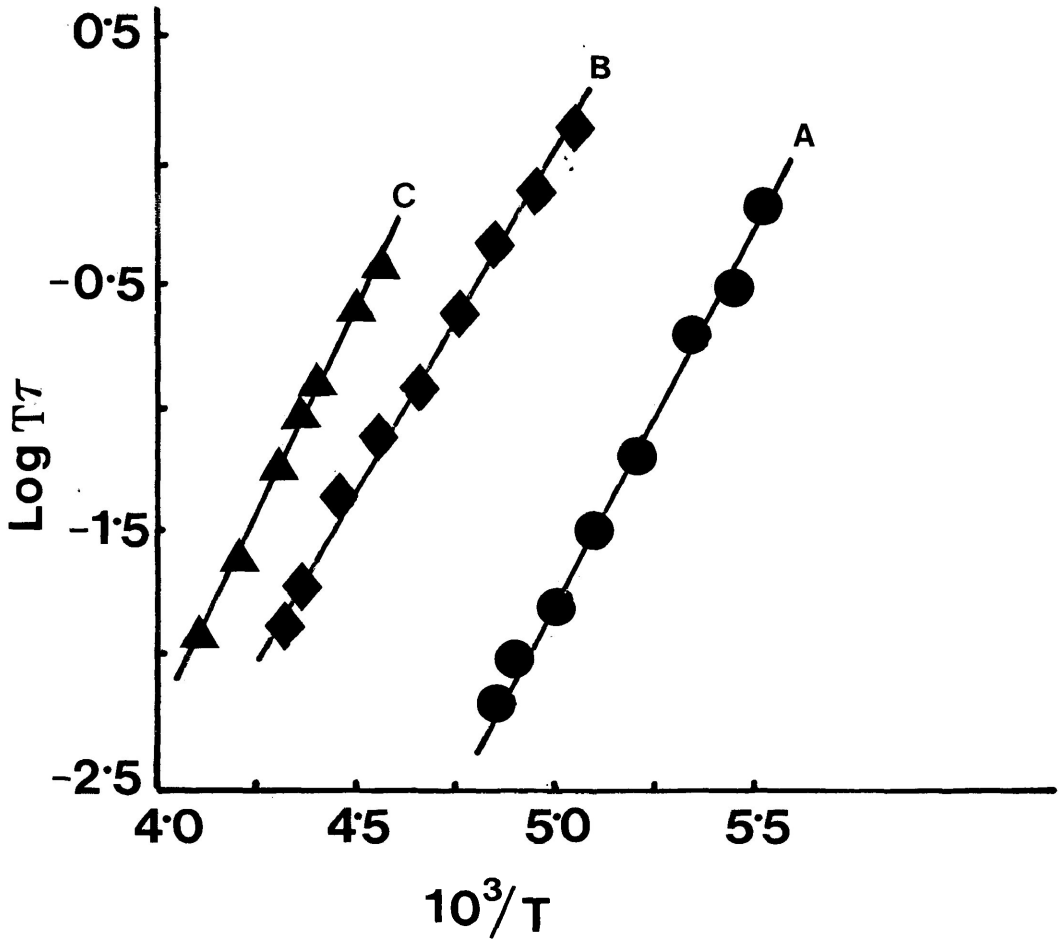

FIGURE IV-26d: Eyring plots of logTτ versus 1/T (K^{-1}) for some long-chain normal alcohols (higher temperature process) in a polystyrene matrix. A=Heptanol-1, B=nonanol-1, and C=Decanol-1.

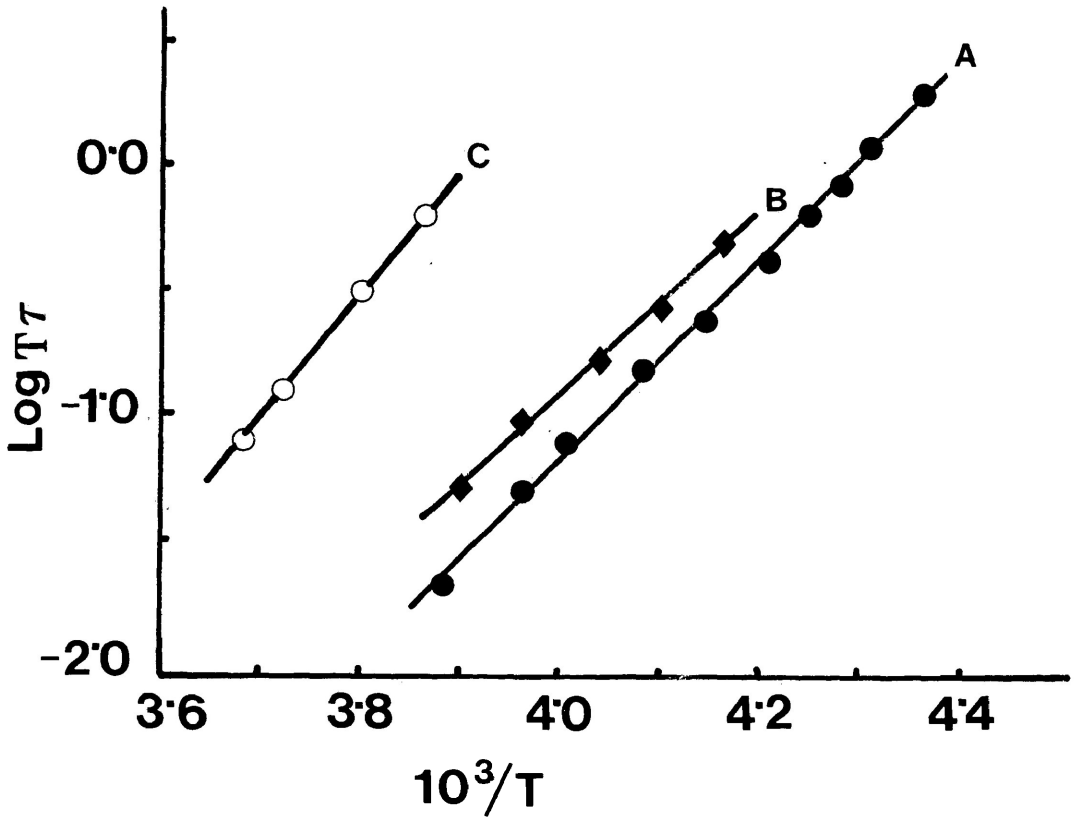

FIGURE IV-27d: Eyring plots of logTτ versus 1/T (K^{-1}) for some long-chain normal alcohols (higher temperature process) in a polystyrene matrix. A=Tridecanol-1, B=Tetradecanol-1 and C=Hexadecanol-1.

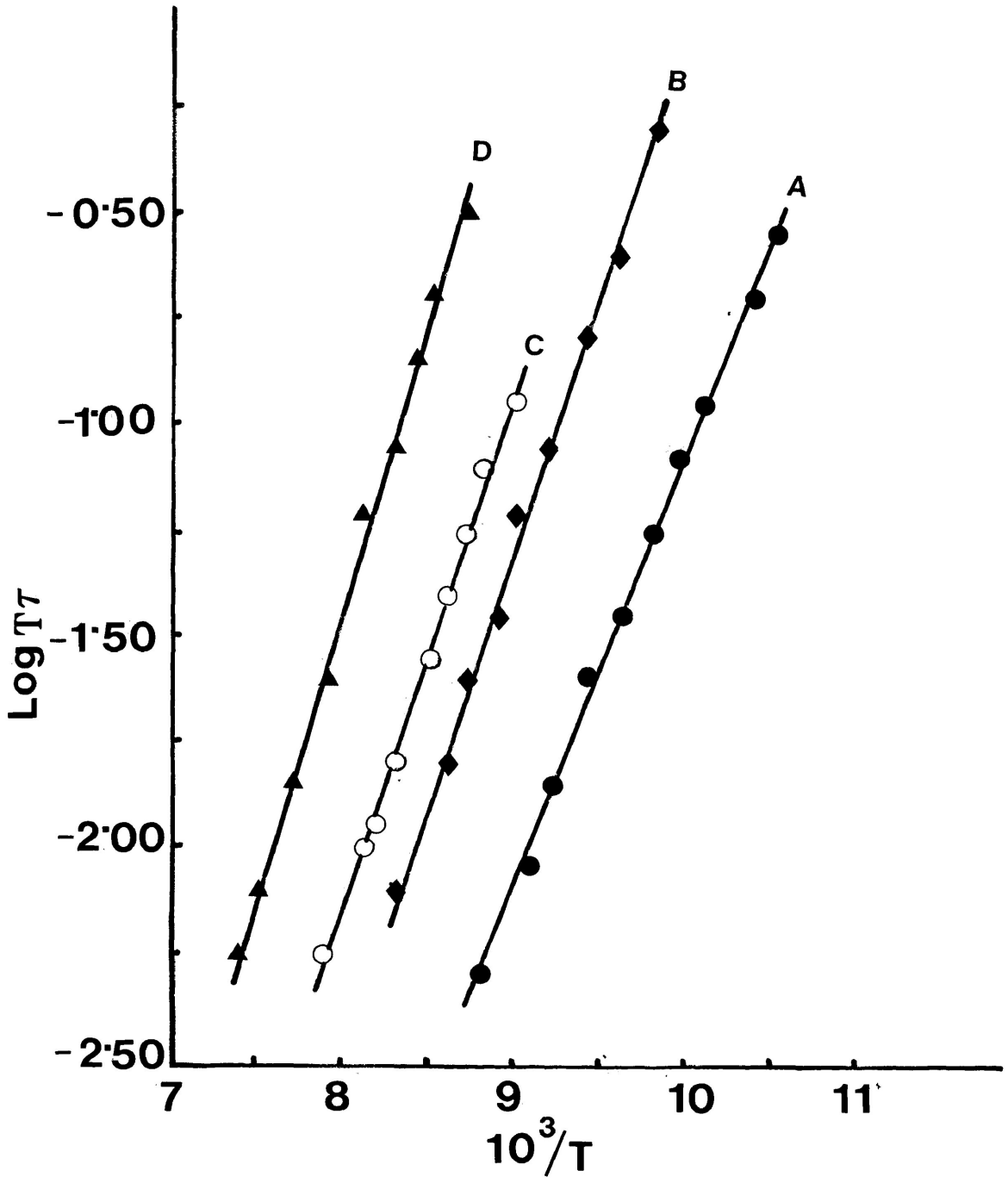

FIGURE IV-28d: Eyring plots of logTτ versus 1/T (K^{-1}) for some long-chain normal thiols (lower temperature process). in a polystyrene matrix. A=Octanethiol-1, B= Decanethiol-1; C=Dodecanethiol-1, and D=Hexadecanethiol-1.

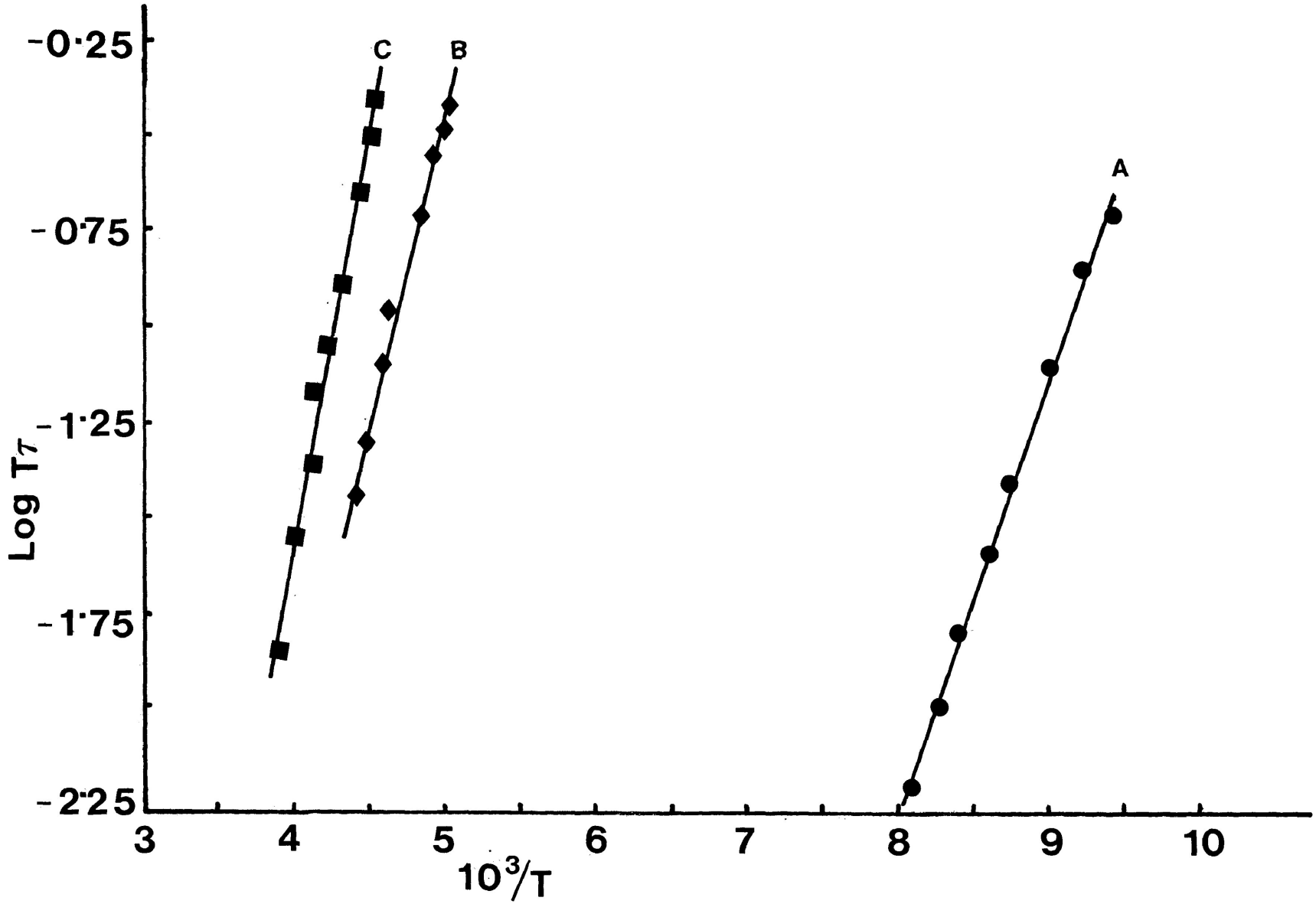

FIGURE IV-29d: Eyring plots of logTτ versus 1/T (K^{-1}) for some long-chain normal thiols in a polystyrene matrix. A=Undecanethiol (lower temperature process); B=Octanethiol; and C=Decanethiol (higher temperature processes).

FIGURE IV-30: Plot of relaxation time, τ (s) at 150 K versus n (number of carbon atoms in the general formulae, $CH_3(CH_2)_nCH_2X$) for the lower temperature absorption processes for some long chain normal alcohols (●) and thiols (○) in a polystyrene matrix.

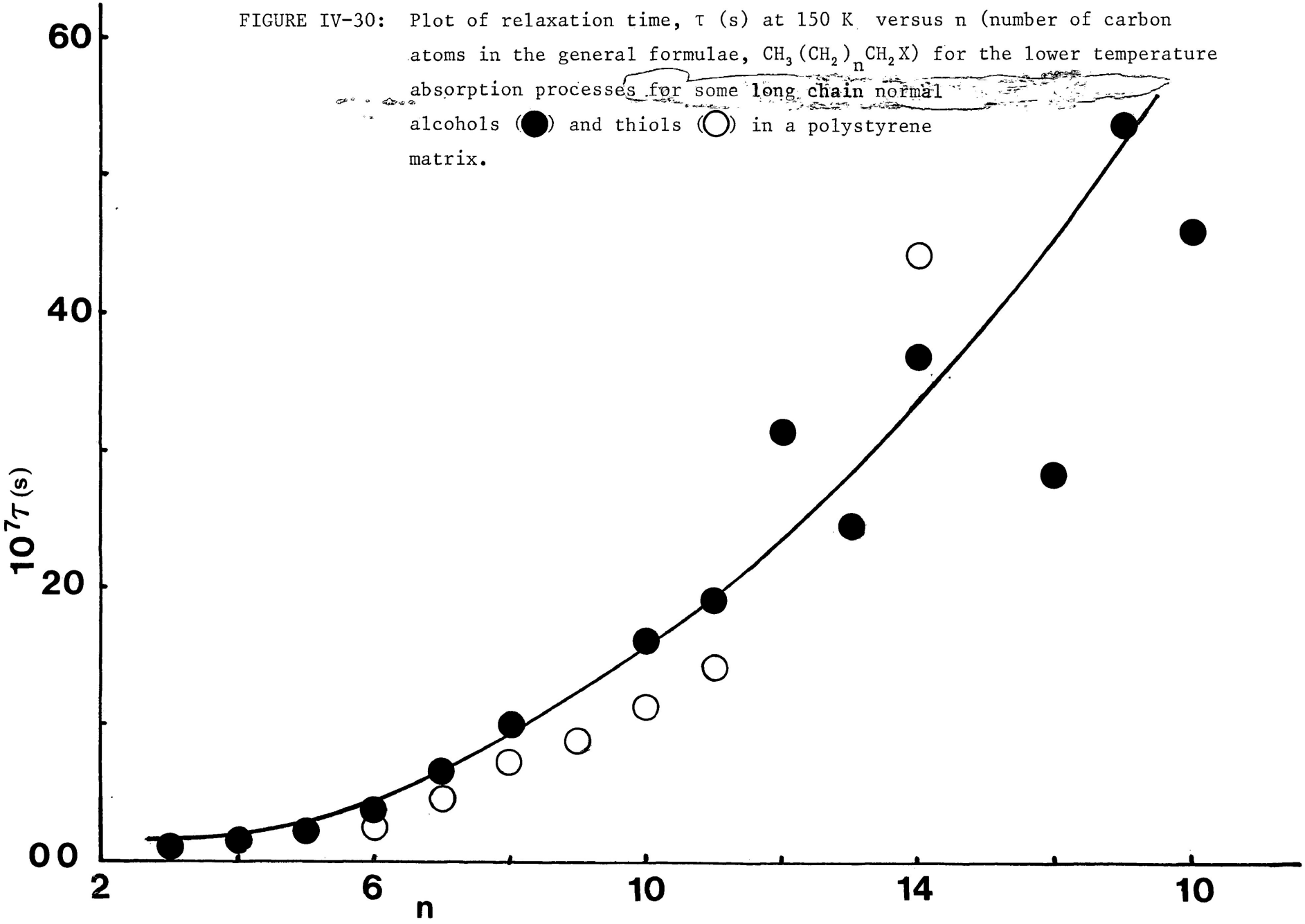

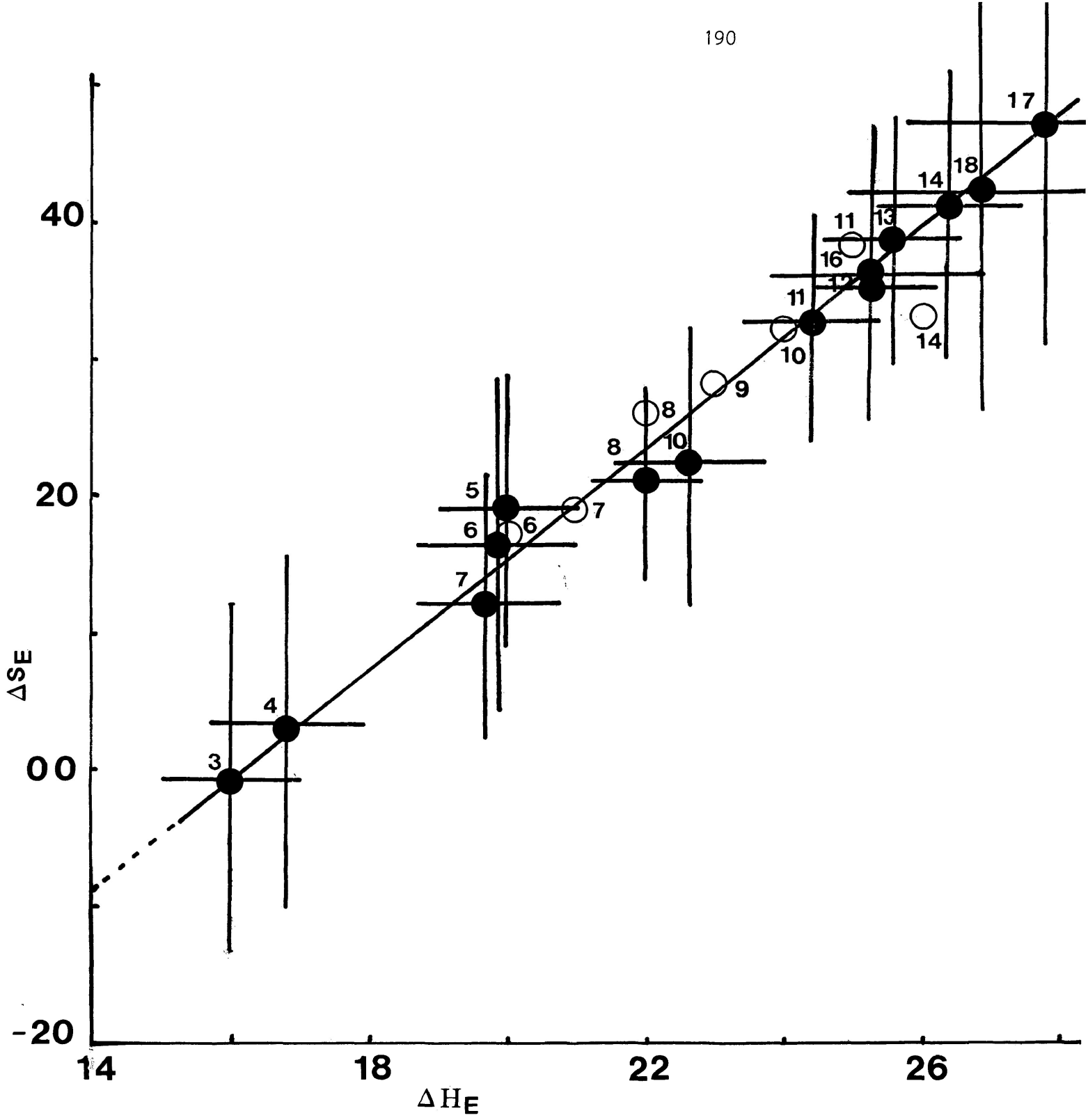

FIGURE IV-31: Plot of entropy of activation, ΔS_E (J K^{-1} mol^{-1}) versus enthalpy of activation, ΔH_E (kJ mol^{-1}) for the lower temperature absorption processes for long-chain normal alcohols (●) and thiols (○) in a polystyrene matrix. The vertical and horizontal bars represent 95 % confidence intervals. Numbers beside points indicate the value of n in the general formulae, $CH_3(CH_2)_nCH_2X$.

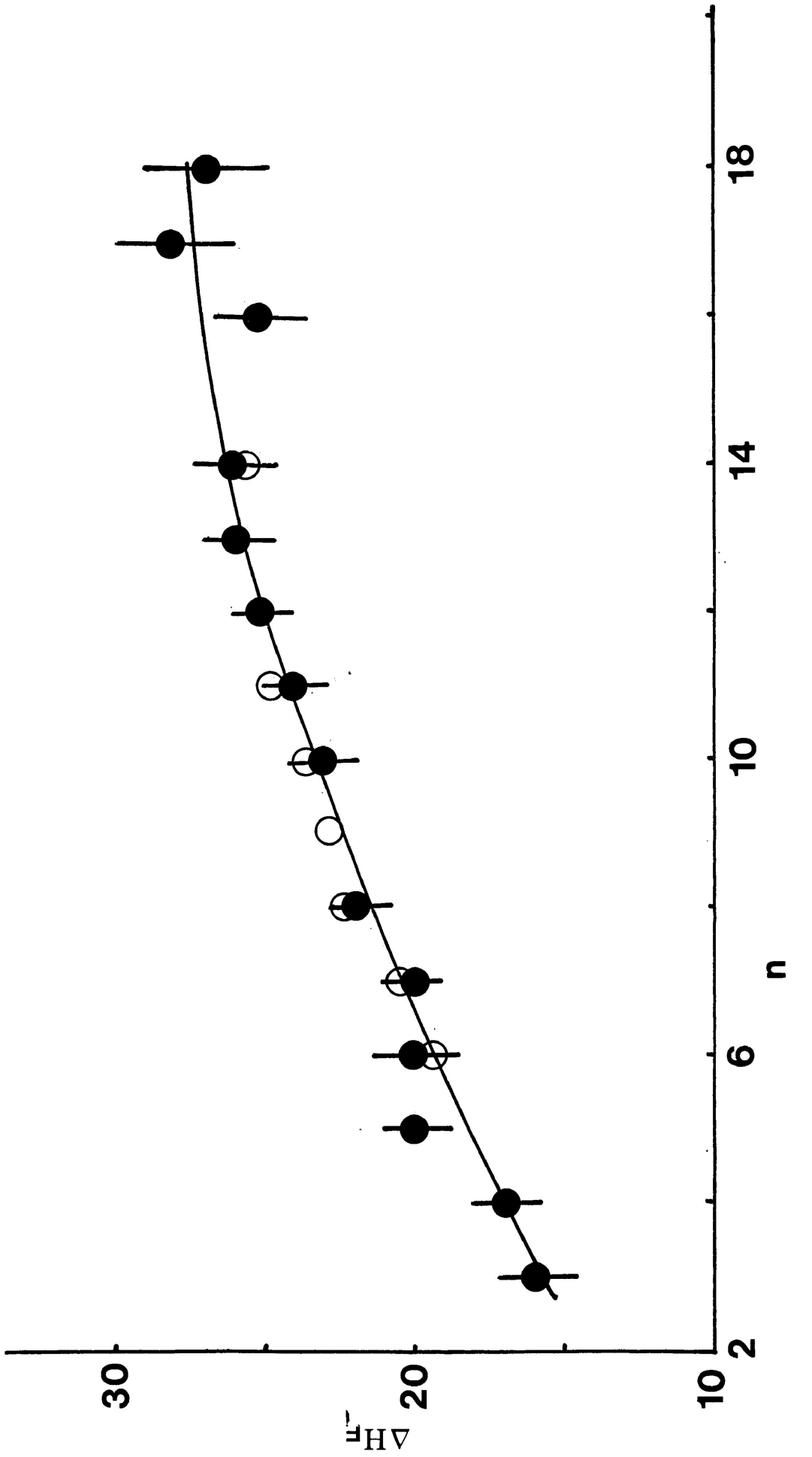

FIGURE IV-32: Plot of enthalpy of activation, ΔH_E (kJ mol^{-1}) versus n (number of carbon atoms in the general formulae, $CH_3(CH_2)_nCH_2X$ for the lower temperature absorption processes for some long-chain normal alcohols (●) and thiols (○) in a polystyrne matrix. The vertical bars represent 95 % confidence intervals on ΔH_E values for alcohols.

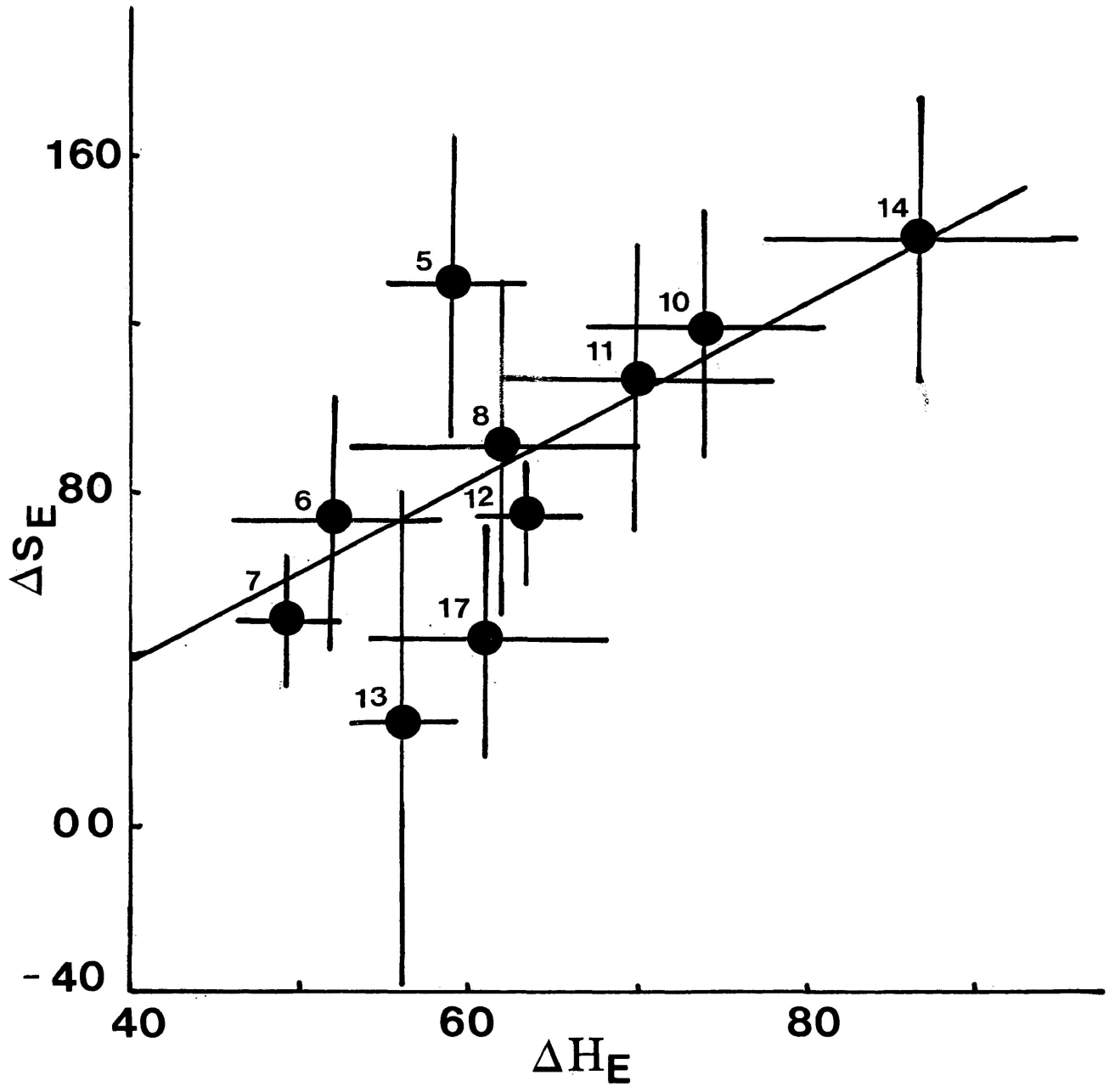

FIGURE IV-33: Plot of ΔS_E (J K^{-1} mol^{-1}) versus ΔH_E (kJ mol^{-1}) for the higher temperature absorption processes for long-chain normal alcohols in a polystyrene matrix. Numbers beside points represent the values of n in the general formulae, $CH_3(CH_2)_nCH_2OH$. The vertical and horizontal bars represent 95 % confidence intervals in the factors.

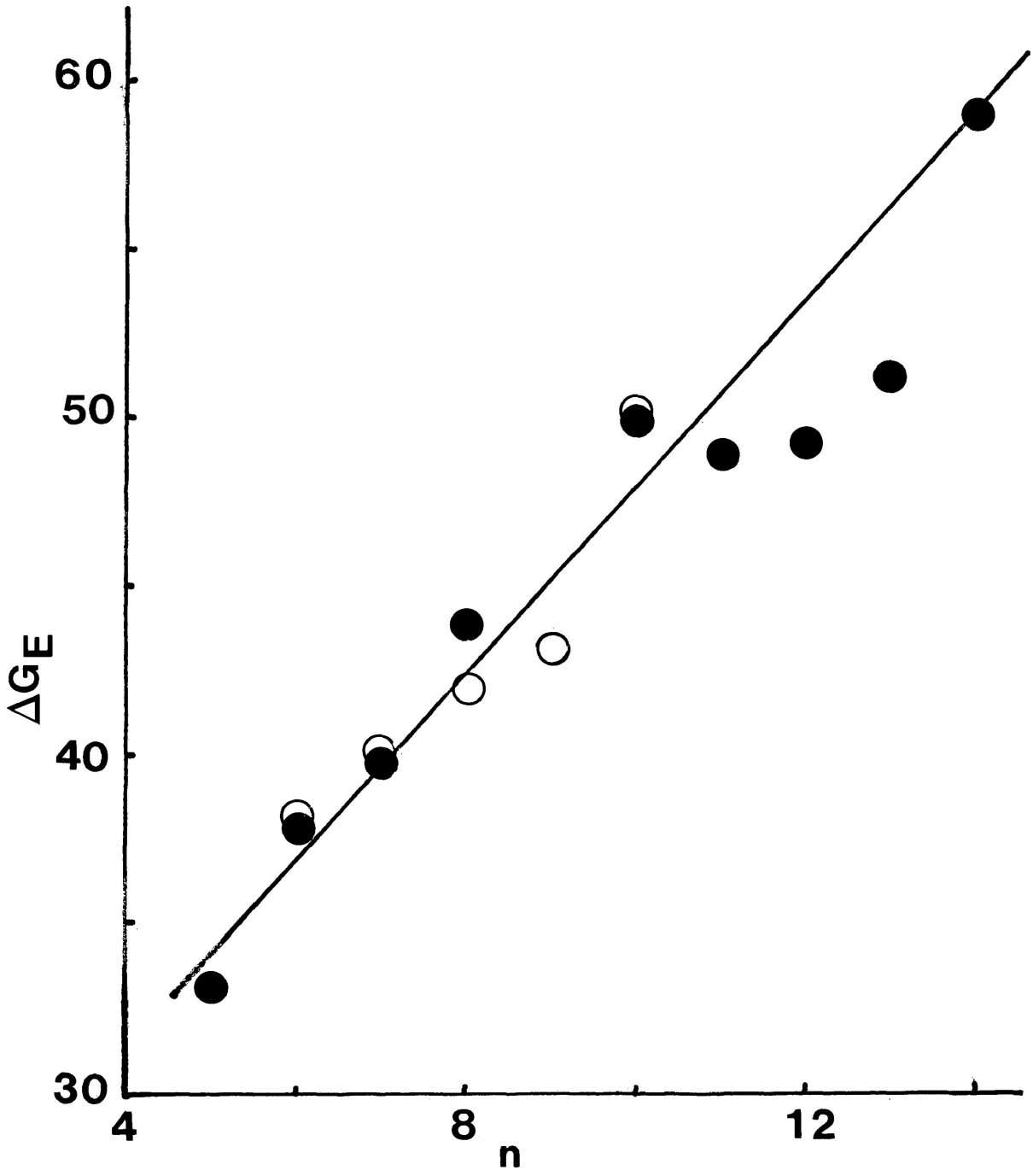

FIGURE IV-34: Plot of free energy of activation, ΔG_E (kJ mol^{-1}) at 200 K versus n (number of carbon atoms in the general formulae, $CH_3(CH_2)_nCH_2X$) for the higher temperature absorption processes for some long-chain normal alcohol (●) and thiols (○) in a polystyrene matrix.

CHAPTER V

DIELECTRIC RELAXATIONS OF A FAIRLY POLAR, SPHERICAL, RIGID MOLECULE, 1,1,1-TRICHLOROETHANE IN CARBONTETRACHLORIDE

V-1: INTRODUCTION

Substances in the glassy state retain some degree of molecular rotational freedom which can be detected by dielectric or mechanical, or n.m.r. studies (1). The presence of such rotational freedom giving rise to the dielectric relaxation has sometimes been associated with the motion of a side group in the case of organic high polymers. Certain rigid, (nearly) spherical, polar molecules show rotational freedom in the solid phase on freezing, and rotational freedom is stopped at a temperature below the freezing point (2-4). However, most of the simple rigid molecules do not have the rotational freedom in the solid phase. Johari and Goldstein (5) have studied the solid phases of a large number of solutions of simple rigid, polar molecules in the rigid, non-polar molecule cis-decalin which is capable of forming a glassy phase. They have observed dielectric relaxation at low temperatures in the solid phase at just above and below the glass transition temperature, T_g, and termed the relaxation above T_g, as α-relaxation and that below T_g as the β-relaxations. Several studies have been made to understand the mechanism of α- and β-relaxations in the cis-decalin and some other glass forming solvents (6-8). It is now well established (8) that:

(i) α-relaxation usually occurs just above T_g but β-relaxation occurs below T_g (e.g. 0.6-0.8 T_g for 1 kHz) and is one to two order(s) of magnitude lower than the α-relaxation.

(ii) the ε" versus logν curve at a fixed temperature for both the processes are asymmetric with a half width of 2-3 decades of frequency for an α-process and 4-6 decades of frequency for β-relaxations.

(iii) for α-relaxation, the frequency of maximum loss ν_{max}, is strongly dependent upon temperature.

(iv) the intensity of the loss peak decreases on annealing but the location of the peak remains the same; as also the broad distribution of relaxation times which increases with the decrease of temperature for β-relaxation.

(v) non-Arrhenius behaviour of Eyring plot with a high apparent activation enthalpy (e.g. 80-400 kJ mol^{-1}) for α-relaxation but for β-relaxation the linear Eyring plot with low apparent activation enthalpy (e.g. 20-40 kJ mol^{-1}) is usually observed.

Detailed studies on supercooled liquids by Williams and co-workers (9-11) suggest that the α-relaxation process is due to cooperative rearrangement of the molecules. This view has also been supported by Johari (12). Goldstein

(13) has suggested that the β-process does not reflect the features of the individual molecules that compose the glass, but arises from common features of amorphous packing. Johari, (12) on the other hand, has proposed that the β-relaxation process arises from the hindered rearrangement of the molecules encaged by a large region which have been made relatively immobile by the stringent requirement of cooperative motion. The features of the β-relaxation process should be independent of the shape of the solute molecules if it is due to amorphous packing, while it should depend upon the molecular shape if it is due to orientation of the encaged molecules. After studying a lot of polar solutes dispersed in an organic glass, such as cis-decalin, glassy o-terphenyl, Santovac® and polystyrene, Walker and co-workers (14) and Agarwal et al (15) support the model proposed by Johari that in the amorphous phase above T_g the dielectric behaviour is governed by the cooperative rearrangement of molecules, while the glassy phase below T_g the β-relaxation process arises from the hindered rotation of polar molecules engaged in the glassy matrix.

To clarify the nature of the relaxation and the variables upon which it depends, Shears and Williams (16) studied di-n-butyl phthalate (DBP) in o-terphenyl from 4.8-100% concentrations to examine the effects of solute con-

centration on relaxation in the supercooled liquid state. It is found that the ε''_{max} values are approximately proportional to solute concentration up to 50% DBP, but at higher concentration the plots curve towards the final pure DBP value. The apparent activation energy is also varied depending upon the concentration of the solute. They rationalized this variation in terms of a distribution of local concentrations in the mixture. Mansingh et al (17) studied chlorobenzene in cis-decalin at five concentrations (12.98, 18.05, 20.80, 21.99 and 25.01 mol%) and reported that the magnitude of the α-relaxation peak increases with increasing concentration, but there is a negligible change in the temperature of the peak with a change in concentration. The activation energy, ∿146 kJ mol^{-1}, also does not show any systematic increase with concentration. The tanδ peaks for the β-relaxation become more pronounced for higher concentration solutions but there is hardly any change in the temperature of the peak with concentration. The fact that α- and β-relaxation peaks in tanδ for different concentrations occur almost at the same temperature at a given frequency suggests that the relaxation frequency is determined mainly by the viscosity of the glassy phase of cis-decalin and that the dipole interactions of the solute molecules have negligible effect

on the relaxation frequency. Saleh (18) studied methyl iodide in cis-decalin at several concentrations and found that the ε''_{max} at a fixed frequency increases with concentration up to a certain limit (23 wt. %) and then decreases with concentration gradually. He could not study this system in detail owing to the limited solubility of methyl iodide in cis-decalin. It seemed worthwhile to carry out systematic dielectric studies on the effect of the concentration of the solute molecules on the α- and β-relaxations in greater depth than any available in the literature. We have chosen 1,1,1-trichloroethane and carbontetrachloride for the purpose for the following reasons:

(a) both the 1,1,1-trichloroethane and carbontetrachloride are almost perfectly spherical and should pack in a sphere-like manner;

(b) dielectrically 1,1,1-trichloroethane may be regarded as a rigid molecule;

(c) it would be simpler than any other detailed study of two-component mixtures in the literature, and

(d) both are miscible in any proportion.

V-2: EXPERIMENTAL RESULTS

Both 1,1,1-trichloroethane and carbontetrachloride were procured from the Aldrich Chemical Company. Although these chemicals were of high grade purity (above 99%) they were further dried and purified through fractional distillation before use. The measured boiling points and refractive indices showed good agreement with the literature values. Thirteen concentrations (from 0.9 to 83.4 mol%) of 1,1,1-trichloroethane in carbontetrachloride and one 50 mol% solution of 1,1,1-trichloroethane in silicon tetrachloride were studied. Pure 1,1,1-trichloroethane and carbontetrachloride were also measured.

Measurements were done on the GR1621 Precision Capacitance Measurement System with the use of a three-terminal coaxial cell between 10 Hz to 10^5 Hz in the temperature range 77-220 K. The empty cell was tested from room temperature to liquid nitrogen temperature, and it showed no observable dielectric loss at any frequencies though there was a little variation of capacitance. This shows that the cell has no contribution to the dielectric loss factor. Some of the systems were measured twice (both by a heating and cooling technique) and each time the dielectric relaxation

was observed almost at the same temperature region, suggesting that the absorptions were not the consequence of cracks in the sample. The apparatus and the procedures employed in the measurements, and the preparation of samples have been described in a previous chapter (Chapter II). The methods employed for the evaluation of relaxation and activation parameters have also been described previously (Chapter II).

Table V-1 collects the values of ΔH_E, ΔS_E along with the ΔG_E and τ values at 100 K, 150 K and 200 K for each system where appropriate. Tables V-2 and V-3 present the results obtained by Hossain (19) and Saleh (18).

Experimental values of τ, $\log\nu_{max}$, β and ε''_{max}, at various temperatures obtained for these systems are listed in Table V-4.

The plots of dielectric loss factor ε'' versus temperature (K) at a fixed frequency for some of the systems are given as sample plots in Figures V-1a to V-4a Figures V-5b to V-12b show the sample plots of ε'' versus $\log\nu$ for the systems mentioned. The Eyring plot, $\log T\tau$ versus $1/T$ is presented as sample plot for the mentioned systems in Figures V-13d to V-20d while Figures V-21 and V-22 represent

the variation of maximum dielectric loss factor, ε''_{max}, with the concentration of the solute (in mol %) in carbon-tetrachloride and in cis-decalin at a fixed frequency, 1.01 kHz.

V-3 DISCUSSION

Two absorption processes were found for 1,1,1-trichloroethane in the pure solid state; one in 96-105 K and the other in the 117-123 K region. The lower temperature absorption gives broad asymmetric loss curves with a half-width of ∿5 decades of frequency. The linear Eyring plot, $\log T\tau$ versus 1/T, yields the activation parameters as, ΔH_E = 16 kJ mol^{-1}, ΔS_E = -16 J K^{-1} mol^{-1} and ΔG_E = 18 kJ mol^{-1} and $\tau = 1.2 \times 10^{-3}$ s at 100K. The β value for this relaxation ranges between 0.21-0.26. These parameters are in agreement with those obtained by Hossain (19). N.m.r. studies on 2,2-dichloropropane and 1,1,1-trichloroethane in the pure solid state yielded values of 13 and 19 kJ mol^{-1} for the molecular tumbling of these molecules (20). The ΔH_E obtained for molecular rotation of the almost similar sized molecule, 2-bromo-2-methyl propane, is 13 kJ mol^{-1} (19) Within experimental error, these values are close to our value which suggests that the lower temperature process of 1,1,1-trichloroethane in the pure solid state may be attributed as the molecular process. This is also supported by the lower β-values (0.21-0.26).

The higher temperature dispersion yields asymmetric loss curves with half-width ∿2.2 decades of

frequency. The loss curves are highly temperature sensitive. The β-value for this dispersion ranges between 0.51-0.71. The Eyring plot, $\log T\tau$ versus 1/T, though not appreciably curved, yields higher dielectric parameters, such as, ΔH_E = 71 kJ mol^{-1}, ΔS_E = 440 J K^{-1} mol^{-1} and ΔG_E = 27 kJ mol^{-1} and $\tau = 7.2 \times 10^{1}$ s at 100 K. These values are very close to the values obtained for other almost similar-sized spherical molecules (19): 2,2-dichloropropane, 2-chloro-2-methyl-propane, 2-bromo-2-methyl propane and methyl trichlorosilane for their α-relaxation. Baker and Smyth (21) found similar values for 1-bromo-2-methyl propane and 1-bromo-2-methyl butane in the glassy state. They interpreted their results in terms of a co-operative process similar to those obtained for associated liquids such as glucose. In this mechanism it is envisaged that a dipole may only reorientate with the cooperation of a large region of surrounding molecules. The ΔH_E for cooperative relaxation of supercooled n-propyl benzene which is very similar to 1,1,1-trichloroethane is about 80 kJ mol^{-1} (22). Thus the higher temperature dispersion of 1,1,1-trichloroethane having fairly high ΔH_E, ΔS_E and β values may be attributed to a cooperative relaxation process involving the motion of large regions of the glassy solid.

In our frequency range dried and purified carbontetrachloride gives a relaxation process in the temperature range 183-199 K with a dielectric loss of the order 1.5×10^{-4}. This process is reproducible both by heating and cooling techniques. The dielectric loss factor and the peak position does not change appreciably after saturating carbontetrachloride with water for several days. The relaxation process of carbontetrachloride follows all the characteristics of a cooperative process, such as asymmetric loss curves with a half width of $\sim$1.5 decades of frequency, non-Arrhenius behaviour of Eyring plot, $\log T\tau$ versus $1/T$, temperature sensitivity of the process with high β values (0.6-0.99) and the fairly high activation parameters: ΔH_E = 47 kJ mol^{-1}, ΔS_E = 67 J K^{-1} mol^{-1}, and ΔG_E = 40 kJ mol^{-1} and $\tau = 5.9 \times 10^{8}$ s at 100 K.

Carbontetrachloride has no permanent dipole, although it has a small induced moment in the liquid phase which is considered to arise from collisions of the neighbouring molecules having quadrupole and higher multiple moments (23). The results of carbontetrachloride are not in harmony with what is to be expected from theory in that a dipole moment is essential to detect an α-(or a β-) process. Very recently Walker and his coworkers (24)

reported that cis-decalin exhibits an α-process whereas trans-decalin, which by viture of its symmetry has no permanent dipole moment, exhibited no absorption in the range 80-208 K. The results are in harmony with those

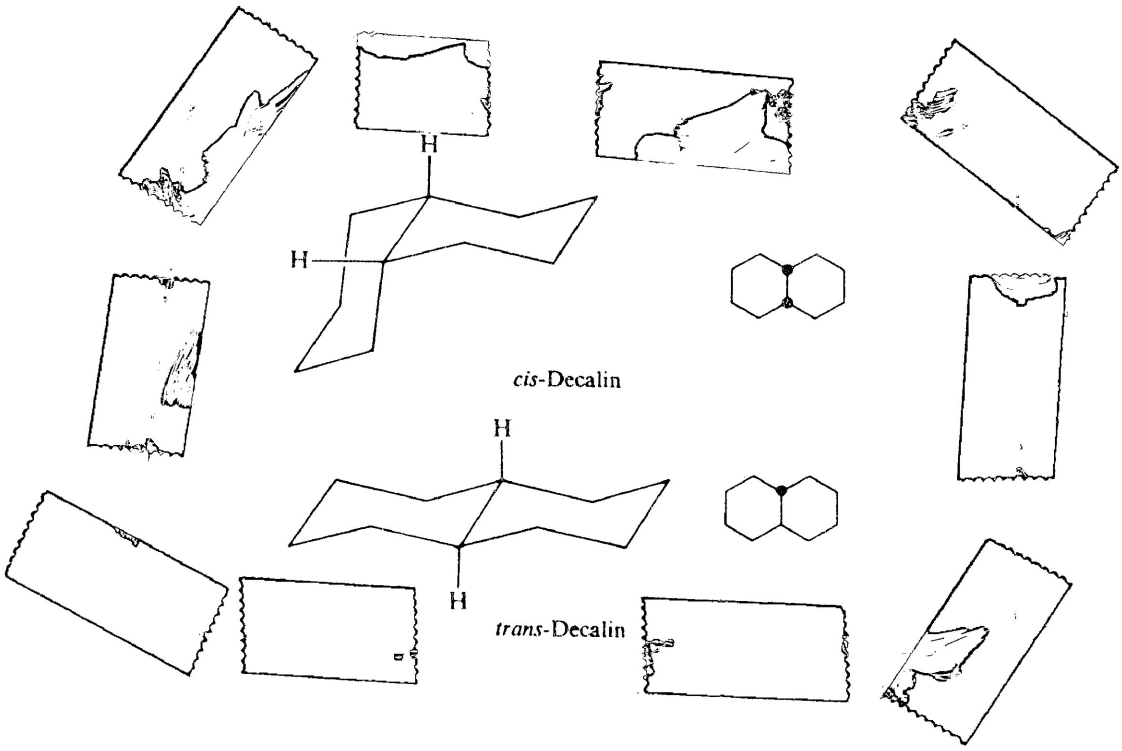

expected from theory. They found that the presence of 17.2, 1.0 or even 0.2 mol % chlorobenzene (μ=1.58 D) in trans-decalin leads to the detection of an α-process. This behaviour is also found in another non-polar molecule cyclohexane. From these they concluded that an α-process may occur in these non-polar molecule but is detected only when a polar-molecular

probe is inserted. The implication from these results is that 0.2 mol% impurity of even a moderately polar molecule can lead to the detection of an α-process in a non-polar molecular system. Very few liquids have a better purity than 99.8%. Even the spectroscopic-grade chemicals are only 99% pure or better. Thus when extremely low loss (e.g. $\varepsilon''_m \leq 10^{-4}$) are detected for an α-process, the purity of the sample needs to be questioned, but normally it is extremely difficult to establish that a compound is completely pure. From all these it can be concluded that the cooperative process in carbontetrachloride may be attributed either (a) to the presence of trace amounts of polar impurities which are acting as a probe or (b) to the induced dipole moment for the highly polarizable chlorine atoms in carbontetrachloride.

Mixtures of 1,1,1-trichloroethane and carbontetrachloride in various proportions (from ∿0.9-83 mol %) in the solid state give signs of only one type of relaxation process for each system within the temperature range 98-138 K. The magnitude of the relaxation peaks depend upon the concentration, but there is a negligible change in the temperature of the peak with change in concentration. The relaxation parameters for this dispersion over these wide concentration ranges are: ΔH_E = 22-26 kJ

mol^{-1}, ΔS_E = 31-64 J K^{-1} mol^{-1} and ΔG_E = 19-21 kJ mol^{-1} and $\tau = 2.9 \times 10^{-3}$ s at 100 K respectively. It is remarkable that ΔH_E and ΔG_E stay virtually constant over this wide concentration range. This bears out that we are dealing with the same process over this concentration range. This type of behaviour is also reported by Mansingh (17) for chlorobenzene in a limited study of chlorobenzene/cis-decalin mixtures. These dispersions exhibited by 1,1,1-trichloroethane in carbontetrachloride have different characteristics from those of an α-process. In fact, they satisfy the criteria which characterize a β-process in glassy media, namely broad asymmetric loss curves, linear Eyring plots, and relatively small ΔH_E values. These observation cannot be accounted for by internal rotation in this molecule as there is no perpendicular component of the dipole moment to the C—C axis.

Comparison of the ΔH_E values for the β-process of the three most spherical molecules, 2,2-dichloropropane, 2-methyl-2-bromopropane (19) and 1,1,1-trichloroethane in the pure solid state and cis-decalin media (18) (Tables 1, 2 and 3) indicates that both the ΔG_E at 100 K and ΔH_E values are significantly higher in the former state. This would seem reasonable in that more interaction may be expected between the polarizable halogen atoms than with the

halogen and methylene groups (in cis-decalin). When the dispersion medium is changed from cis-decalin to carbontetrachloride for the solute 1,1,1-trichloroethane, almost similar ΔH_E results (Table V-1) to that for the pure solid. If the β-process for 1,1,1-trichloroethane in the pure solid and in carbontetrachloride were a molecular process, then these results would be understandable since in each case the 1,1,1-trichloroethane would be reorienting in similar environments of chlorine atoms. It is worth noting that n.m.r. studies on 2,2-dichloropropane and 1,1,1-trichloroethane in the solid state yielded values of 13 and 19 kJ mol^{-1} for the molecular tumbling of these molecules (20). Thus, our ΔH_E values for 1,1,1-trichloroethane in both the pure solid state and in the dispersion medium carbontetrachloride are closely similar to the n.m.r. values for molecular tumbling. It would seem that in this case at least molecular relaxation may well be the mechanism which accounts for the β-process. The same order of ΔH_E values for 1,1,1-trichloroethane in the pure solid state and in carbontetrachloride may be appreciated in that both the 1,1,1-trichloroethane and carbontetrachloride are spherical and may pack together in a similar manner with no shape or size factors differently influencing the packing of the pure 1,1,1-trichloroethane and of a mixture of this and carbontetrachloride. At the time of rotation

of the solute molecules the disorder in the system will be higher for the similar spherical shape and size of the solute and solvent molecules but a very narrow range of environments will be encountered by the solute molecules at any one temperature. This accounts for the relatively higher entropy of activation and the Fuoss-Kirkwood distribution parameters, β, for these systems.

An exactly similar type of relaxation process, as for 1,1,1-trichloroethane and carbontetrachloride mixture, is obtained for 50 mol % (1:1 mixt.) 1,1,1-trichloroethane in silicontetrachloride in the solid state with slightly different relaxation parameters, which are $\Delta H_E = 29$ kJ mol^{-1}, $\Delta S_E = 61$ J K^{-1} mol^{-1} and $\Delta G_E = 23$ kJ mol^{-1} and $\tau = 4.7 \times 10^{-1}$ s at 100 K respectively. This also bears out that the relaxation frequency is determined mainly by the viscosity of the glassy phase and that the dipole dipole interactions of the solute molecules have negligible effect on the relaxation frequency. As silicontetrachloride and 1,1,1-trichloroethane mixture is corrosive to our cell we could not make a detailed study of this system.

One feature which remained when a comparison was made of the dielectric data of the pure solid (19) and

the solute in cis-decalin (18) was the enormous difference in the ε''_{max} values. In the pure solid it ranged between 1.5 to 3×10^{-3} whereas for the solute in cis-decalin the values for methyl iodide, 1,1,1-trichloroethane, tert-butyl bromide and tert-butyl chloride were 12, 58, 69 and 90×10^{-3}. The dielectric loss depends upon (a) the square of the dipole moment for the relaxation process involved, (b) the number of the dipoles in a given volume and (c) the ease with which the dipole can rotate. Off-hand the loss in the pure solid might have been anticipated to be the greater since the number of highly polar molecules in a given volume would be much greater. As a consequence, we made a detailed study of the influence of concentration on ε''_{max} for:

(a) methyl iodide in cis-decalin (18), and

(b) 1,1,1-trichloroethane in carbontetrachloride.

The results are presented in Figure V-21 and Figure V-22 respectively. From these figures it may be observed that only at low concentrations, the maximum dielectric loss ε''_{max} for a particular frequency (1.01 kHz) is proportional to the concentration of the solute and that at higher concentrations it begins to decrease and may (as in Figure V-21 drop off very rapidly from 347×10^{-3} (for 43 mol %) to 47×10^{-3} (for 50 mol %) and then linearly decrease towards the final pure solute value. Thus, as the case of the pure solid is approached, the loss factor may be appreciably lower than

the value for a 7 mol % concentration - a typical measurement concentration.

It would seem feasible that at the high concentrations where molecular interaction would be the greatest either:

(i) relatively few molecules have sufficient free volume for rotation to be permitted,

or

(ii) the molecules are permitted to turn through a very limited angle,

or

(iii) a combination of (i) and (ii).

REFERENCES

1. N.G. McCrum, B.E. Read and G. Williams. Anelastic and dielectric effects in polymeric solids". (John Wiley, New York), 1967.

2. Krishnaji and A. Mansingh, J. Chem. Phys., 44, 1590(1966).

3. C. Clemett and M. Davies, J. Physique (Geneva), (1960) 77.

4. N.E. Hill, E. Vaughan, A.H. Price and M. Davies, "Dielectric properties and molecular behaviour". (Van Nostrand Reinhold, London) 1969.

5. G.P. Johari and M. Goldstein. J. Chem. Phys., 53, 2372(1970).

6. M. Goldstein, J. Chem. Phys., 51, 3728(1969).

7. G.P. Johari and C.P. Smyth, J. Chem. Phys., 56, 4411(1972).

8. G.P. Johari, Ann. New York Acad. Sci., 279, 117(1976).

9. G. Williams and P.J. Hains, Chem. Phys. Lett., 10, 585(1971).

10. Ibid., Faraday Symp. Chem. Soc., 6, 14(1972).

11. M. F. Shears and G. Williams, J. Chem. Soc. Faraday Trans. II, 69, 609(1972).

12. G.P. Johari, J. Chem. Phys. 58, 1766(1973).

13. M. Goldstein, Ann. N.Y. Acad. Sci., 279, 68(1976).

14. J. Crossley, A. Haravi & S. Walker, J. Chem. Phys. 75, 418(1981).

15. C.B. Agarwal and A. Mansing J. Chem. Phys. 76, 4606(1982).

16. M.F. Shears and G. Williams, J. Chem. Soc. Faraday Trans. II, 69, 608(1973).

17. A. Mansingh, C. B. Agarwal and R. Singh, Indn. J. Pure and Appld. Phys., 18, 583(1980).

18. M.A. Saleh, Private Communication, this laboratory.

19. M.S. Hossain, M.Sc. Thesis, Lakehead University, 1982.

20. E. O. Stejskal, D.E. Woessner, T.C. Farrar and H.S. Gutowsky, J. Chem. Phys., 31, 55(1959).

21. W.O. Baker and C.P. Smyth, J. Am. Chem. Soc., 61, 2798(1939).

22. T.G. Copeland and D.J. Denney, J. Phys. Chem., 80, 2106(1976).

23. J. K. Vij, Nuano Cimento, 1983, 2D, N3, 751.

24. M. S. Ahmed, J. Chao, J. Crossley, M.S. Hossain and S. Walker, J. Chem. Soc. Faraday Trans. II, 80(1984).

TABLE V-1: Eyring Analysis results for 1,1,1-trichloroethane in carbontetrachloride

Concentration in Mol %	T(K)	τ(s)			ΔG_E (kJ mol^{-1})			ΔH_E	ΔS_E
		100 K	150 K	200 K	100 K	150 K	200 K	(kJ mol^{-1})	(J K^{-1} mol^{-1})
0.91	111-137	8.7×10^{-2}	2.1×10^{-6}	9.8×10^{-9}	22	20	18	25±1.6	39±12
2.78	109-139	6.3×10^{-2}	2.4×10^{-6}	1.4×10^{-8}	21	20	18	24±1.3	31±11
5.86	114-137	5.4×10^{-2}	2.1×10^{-6}	1.2×10^{-8}	21	20	18	24±0.8	32±6
6.43	110-137	6.3×10^{-2}	1.7×10^{-6}	7.9×10^{-9}	21	19	17	25±1.5	40±12
10.35	111-136	5.2×10^{-2}	1.7×10^{-6}	8.7×10^{-9}	21	19	17	25±1.1	37±9
12.93	110-134	4.3×10^{-2}	1.3×10^{-6}	6.6×10^{-9}	21	19	17	25±1.6	40±13
16.62	107-132	5.4×10^{-2}	8.5×10^{-7}	3.1×10^{-9}	21	19	16	26±2.2	50±19
19.93	109-131	2.4×10^{-2}	8.1×10^{-7}	4.3×10^{-9}	21	18	16	25±1	42±9
33.33	105-127	1.7×10^{-2}	4.9×10^{-7}	2.4×10^{-9}	20	18	15	25±1.5	49±13
42.80	197-126	1.2×10^{-2}	3.0×10^{-7}	1.4×10^{-9}	20	17	14	26.±0.9	55±8
50.00	101-120	6.8×10^{-3}	1.4×10^{-7}	6.0×10^{-10}	19	16	13	26±1.4	64±13
66.67	101-121	5.4×10^{-3}	1.5×10^{-7}	7.4×10^{-10}	19	16	13	25±1.3	59±12
83.35	98-122	2.9×10^{-3}	2.4×10^{-7}	2.0×10^{-9}	19	17	15	22±1.7	37±16
1,1,1-trichloroethane (Pure)	96-105	1.2×10^{-3}	1.1×10^{-6}	3.1×10^{-8}	18	19	20	16±3.5	-16±34
	117-122	7.2×10^{1}	2.0×10^{-11}	9.3×10^{-18}	27	5.1	-16	71±3.7	440±31
Carbontetrachloride (Pure)	183-199	5.9×10^{8}	2.5×10^{0}	1.5×10^{-4}	40	37	33	47±4	67±22
1,1,1-trichloroethane in silicontetrachloride (50 mol %)	114-138	4.7×10^{-1}	2.8×10^{-6}	6.1×10^{-9}	23	20	17	29±1.4	61±11

TABLE V-2: Relaxation parameters for some organic compounds in the pure solid state

Molecule	T(K)	$\varepsilon''_{max} \times 10^3$	β-Range	Relaxation times τ(s) at 100 K	ΔG_E in kJ mol^{-1} at 100K	ΔH_E in kJ mol^{-1}
Bromomethane	82-104	2.5	0.31-0.47	2.0×10^{-5}	15	5 ±0.2
Iodomethane	103-109	2.6	0.28-0.36	1.0×10^{-2}	20	71 ±5
2,2,-dichloro-propane	95-100	2.5	0.14-0.20	2.0×10^{-5}	15	65 ±2
1,1,1-tri-chloroethane	95-110	2.0	0.30-0.40	1.5×10^{-3}	18	17 ±1
	115-123	24.0	0.38-0.62	7.0×10^{-2}	29	81 ±6
2-chloro-2-methylpropane	144-159	12.5	0.22-0.42	3.0×10^{-9}	42	75 ±8
2-bromo-2-methylpropane	79-95	3.0	0.34-0.86	4.0×10^{-6}	13	13 ±1
	129-142	12.0	0.20-0.28	6.5×10^{-7}	39	85 ±3
Methyltri-chlorosilane	120-131	16.0	0.23-0.33	4.0×10^{-4}	32	81 ±9

NOTE: Data provided through the courtesy of M. S. Hossain (Ref. 19)

TABLE V-3: Relaxation Parameters for some Organic Compounds in cis-decalin

Molecule	T(K)	$\varepsilon''_{max} \times 10^3$	β-Range	ΔG_E in kJ mol^{-1} at 100K	ΔH_E in kJ mol^{-1}
Iodomethane	80-94	12.0	0.16-0.20	12.6	7.6
2,2,-dichloro-propane	81-85	90.0	0.19-0.21	11.1	9.3
1,1,1-tri-chloroethane	90-86	58.0	0.18-0.20	11.6	8.7
2-bromo-2-methylpropane	81-89	69.0	0.18-0.20	11.3	10.6

NOTE: Data provided through the courtesy of M.A. Saleh (Ref. 18)

TABLE V-4: Fuoss-Kirkwood Analysis parameters for 1,1,1-trichloroethane, carbontetrachloride and solutions of 1,1,1-trichloroethane in carbontetrachloride and silicontetrachloride.

T(K)	$10^6\tau$(s)	$\log\nu_{max}$	β	$10^3\varepsilon''_{max}$
10.03 M 1,1,1-trichloroethane (Pure) Lower Temperature Process				
96.1	2832	1.75	0.21	1.1
98.6	1470	2.03	0.25	1.2
101.9	770	2.32	0.26	1.4
104.9	458	2.54	0.26	1.6
10.03 M 1,1,1-trichloroethane (Pure) Higher Temperature Process				
117.0	254	2.80	0.51	16.4
117.7	164	2.99	0.53	16.3
118.5	91.0	3.24	0.59	16.5
119.3	55.0	3.46	0.65	16.9
120.0	36.9	3.63	0.68	16.8
120.9	23.0	3.84	0.71	17.0
121.7	14.5	4.04	0.71	17.1
10.36 M Carbontetrachloride (Pure)				
183.1	2143	1.87	0.62	0.14
186.1	1412	2.05	0.60	0.14
190.9	570	2.45	0.71	0.16
196.3	268	2.77	0.87	0.16
199.0	169	2.97	0.99	0.14
202.1	165	2.98	1.00	0.14
204.7	191	2.92	1.00	0.13
208.4	2210	1.86	0.81	0.31
8.40 M 1,1,1-Trichloroethane (5:1 mixt., 83.35 mol %)				
98.0	7729	1.31	0.26	6.8
99.6	3495	1.66	0.29	7.1
102.2	1369	2.07	0.35	7.8
104.1	749	2.32	0.38	8.3
106.5	483	2.52	0.40	9.0
108.2	309	2.71	0.42	9.5
110.7	187	2.93	0.43	10.6
113.7	92.6	3.24	0.44	12.0
116.7	52.2	3.48	0.41	13.7
119.4	34.2	3.67	0.40	15.7
122.0	22.5	3.85	0.38	18.2

TABLE V-4: continued... (page 2 of Table V-4)

T(K)	$10^6\tau$(s)	$\log\nu_{max}$	β	$10^3\epsilon''_{max}$
6.78 M 1,1,1-Trichloroethane (2:1 mixt., 66.67 mol %)				
101.0	4307	1.57	0.33	19.4
102.0	3472	1.66	0.36	19.8
103.5	1638	1.99	0.40	21.0
106.0	865	2.26	0.42	22.6
109.4	343	2.67	0.44	24.9
112.1	173	2.96	0.47	26.7
116.0	65.8	3.38	0.55	30.1
119.1	37.5	3.63	0.55	32.5
121.6	23.2	3.84	0.53	35.4
5.1 M 1,1,1-Trichloroethane (1:1 mixt., 50 mol %)				
101.4	5303	1.48	0.37	30.4
102.5	3270	1.69	0.39	31.6
103.6	2221	1.86	0.41	32.4
104.3	1738	1.96	0.42	32.9
106.3	897	2.25	0.45	34.9
107.8	627	2.40	0.46	36.2
110.6	275	2.76	0.50	38.6
113.4	134	3.07	0.55	40.9
118.6	47.3	3.53	0.62	45.5
120.2	34.8	3.66	0.65	47.6
4.37 M 1,1,1-Trichloroethane (1:1.33 mixt., 42.80 mol %)				
107.8	1332	2.08	0.37	283
110.0	714	2.35	0.36	290
112.1	404	2.60	0.39	294
113.5	267	2.77	0.43	302
116.2	142	3.05	0.42	308
119.3	70.2	3.36	0.49	321
122.0	43.1	3.57	0.55	326
123.7	26.8	3.77	0.57	337
126.6	16.9	3.97	0.63	346

TABLE V-4: continued... (page 3 of Table V-4)

T(K)	$10^6\tau$(s)	$\log\nu_{max}$	β	$10^3\epsilon''_{max}$
3.42 M 1,1,1-Trichloroethane (1:2 mixt., 33.33 mol %)				
105.5	3801	1.62	0.31	231
108.5	1425	2.05	0.36	240
111.5	652	2.39	0.39	249
114.3	337	2.67	0.37	254
117.6	141	3.05	0.44	264
120.5	75.2	3.33	0.50	271
123.3	45.2	3.55	0.57	277
127.5	23.6	3.83	0.70	290
2.05 M 1,1,1-Trichloroethane (1:4 mixt., 19.93 mol %)				
109.0	2207	1.86	0.35	177
110.9	1193	2.13	0.39	182
113.6	544	2.47	0.45	186
116.6	270	2.77	0.51	190
119.6	162	2.99	0.46	193
122.2	87.4	3.26	0.52	196
126.3	41.2	3.59	0.62	200
128.9	23.8	3.83	0.65	209
131.5	15.7	4.01	0.67	211
1.71 M 1,1,1-Trichloroethane (1:5 mixt., 16.62 mol %)				
107.7	6987	1.36	0.29	139
108.6	4200	1.58	0.32	140
111.6	1393	2.06	0.38	145
115.8	502	2.50	0.44	151
118.4	258	2.79	0.49	154
121.0	160	3.00	0.50	155
124.8	66.2	3.38	0.57	160
128.7	35.1	3.66	0.66	164
131.5	24.9	3.81	0.74	167

TABLE V-4: continued... (page 4 of Table V-5)

T(K)	$10^6\tau$(s)	$\log\nu_{max}$	β	$10^3\varepsilon''_{max}$
1.33 M 1,1,1-Trichloroethane (1:6.7 mix., 12.93 mol%				
109.7	3417	1.67	0.33	110
111.7	1773	1.95	0.36	112
113.4	1052	2.18	0.40	115
116.4	485	2.52	0.47	117
119.4	238	2.83	0.55	120
122.3	139	3.06	0.57	121
125.5	67.1	3.38	0.62	124
128.4	42.5	3.57	0.65	124
131.1	28.5	3.75	0.72	129
134.5	18.0	3.95	0.80	131
1.07 M 1,1,1-Trichloroethane (1:8.7 mixt., 10.35 mol %)				
111.5	2459	1.81	0.46	90.3
113.4	1373	2.06	0.47	91.9
116.1	710	2.35	0.53	93.4
118.5	400	2.60	0.55	93.9
120.3	271	2.77	0.60	96.1
122.9	143	3.05	0.58	96.4
127.5	68.3	3.37	0.72	100
130.1	36.3	3.64	0.64	99.6
132.7	26.4	3.78	0.72	103
135.7	17.1	3.97	0.80	105
0.66 M 1,1,1-Trichloroethane (1:14.6 mixt., 6.43 mol %)				
109.7	8374	1.28	0.28	62.9
112.8	2085	1.88	0.35	64.3
115.7	825	2.29	0.42	65.9
120.0	284	2.75	0.51	65.5
122.9	191	2.92	0.51	68.1
125.9	103	3.19	0.60	68.6
128.6	64.7	3.39	0.67	69.8
131.0	37.9	3.62	0.67	68.3
134.3	20.0	3.90	0.72	71.1
136.7	14.3	4.05	0.78	72.1

TABLE V-4: continued... (page 5 of Table V-4)

T(K)	$10^6\tau$(s)	$\log\nu_{max}$	β	$10^3\varepsilon''_{max}$
0.61 M 1,1,1-Trichloroethane (1:16 mixt., 5.86 mol %)				
114.3	1141	2.14	0.40	61.6
117.0	694	2.36	0.41	61.7
118.9	450	2.55	0.46	62.8
120.6	314	2.71	0.44	62.0
123.7	165	2.98	0.53	63.4
126.6	92.4	3.24	0.62	64.0
129.2	52.4	3.48	0.63	65.3
131.8	33.8	3.67	0.70	65.1
134.9	22.9	3.84	0.78	66.0
137.5	13.1	4.08	0.79	67.4
0.29 M 1,1,1-Trichloroethane (1:35 mixt., 2.78 mol %)				
109.4	14515	1.04	0.27	31.2
112.2	3868	1.61	0.31	30.9
115.5	1150	2.14	0.40	32.1
118.0	587	2.43	0.45	32.1
120.9	279	2.76	0.52	32.3
124.1	187	2.93	0.52	33.1
126.9	108	3.17	0.59	33.1
129.5	55.2	3.46	0.64	33.4
132.7	36.0	3.65	0.69	32.7
135.8	19.5	3.91	0.75	33.7
138.5	13.5	4.07	0.80	34.1
0.09 M 1,1,1-Trichloroethane (1:108.7 mixt., 0.91 mol %)				
111.9	6276	1.40	0.29	10.9
114.6	2008	1.90	0.35	11.2
117.4	881	2.26	0.45	11.3
120.3	382	2.62	0.50	11.5
124.1	178	2.95	0.61	11.6
126.8	112	3.15	0.68	11.5
129.4	59.8	3.43	0.60	11.5
132.0	36.4	3.64	0.64	11.5
134.7	23.9	3.82	0.70	11.7
137.4	17.1	3.97	0.77	11.5

TABLE V-4: continued... (page 6 of Table V-4)

T(K)	$10^6\tau$(s)	$\log\nu_{max}$	β	$10^3\varepsilon''_{max}$
5.0 M 1,1,1-Trichloroethane in Silicontetrachloride (1:1 mixt., 50 mol %)				
114.2	7674	1.32	0.38	156
116.4	3289	1.68	0.41	156
118.3	1847	1.94	0.43	155
120.9	1008	2.20	0.44	158
123.8	447	2.55	0.48	158
127.7	170	2.97	0.55	161
130.2	106	3.18	0.55	162
132.6	63.6	3.40	0.59	164
135.0	40.2	3.60	0.60	160
137.7	27.1	3.77	0.59	166

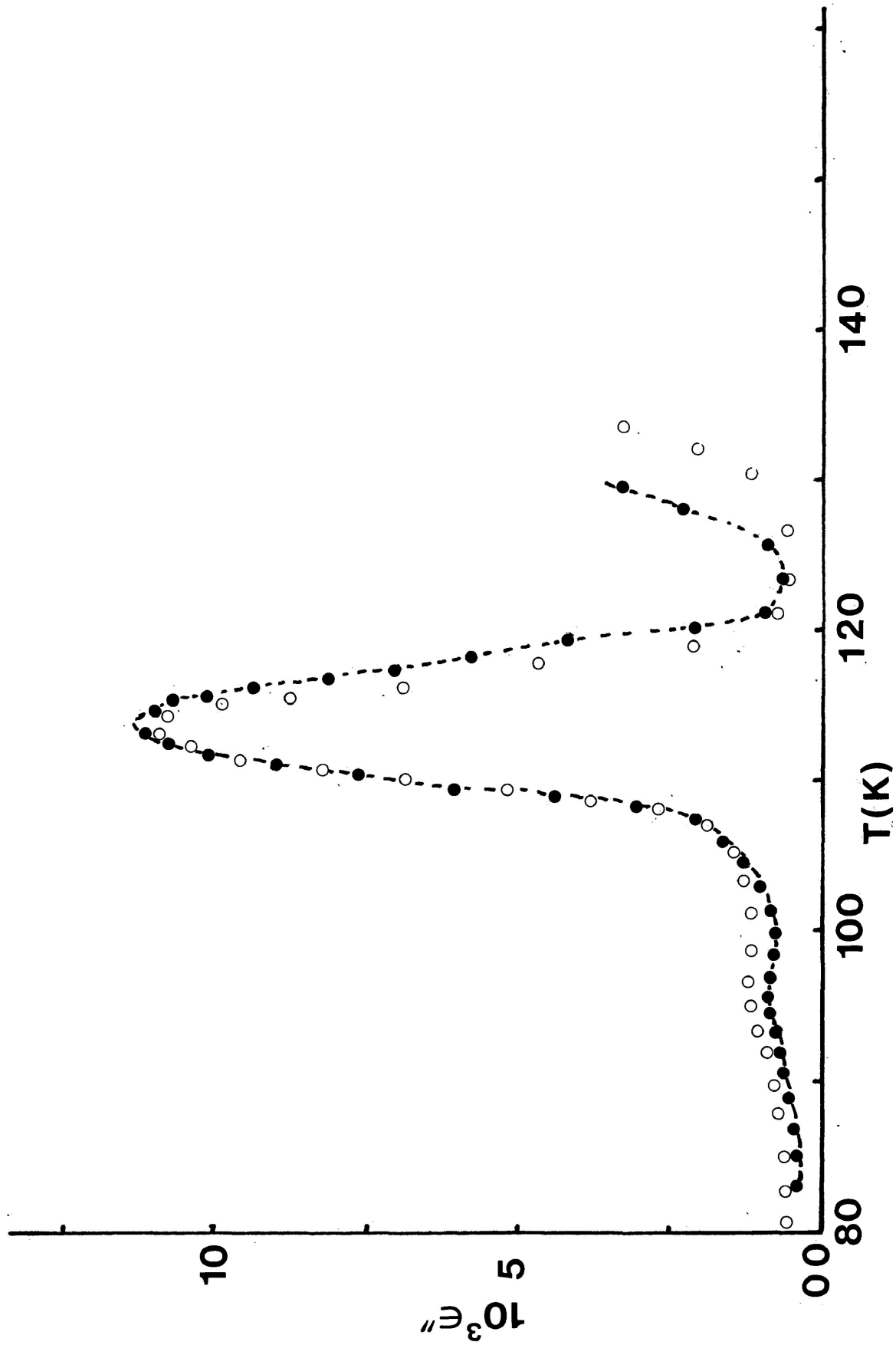

FIGURE V-1a: Plots of dielectric loss factor, ε'' versus temperature (K) for 1,1,1-trichloroethane in the pure solid state at 50.2 Hz both by heating (●) and cooling (○) technique.

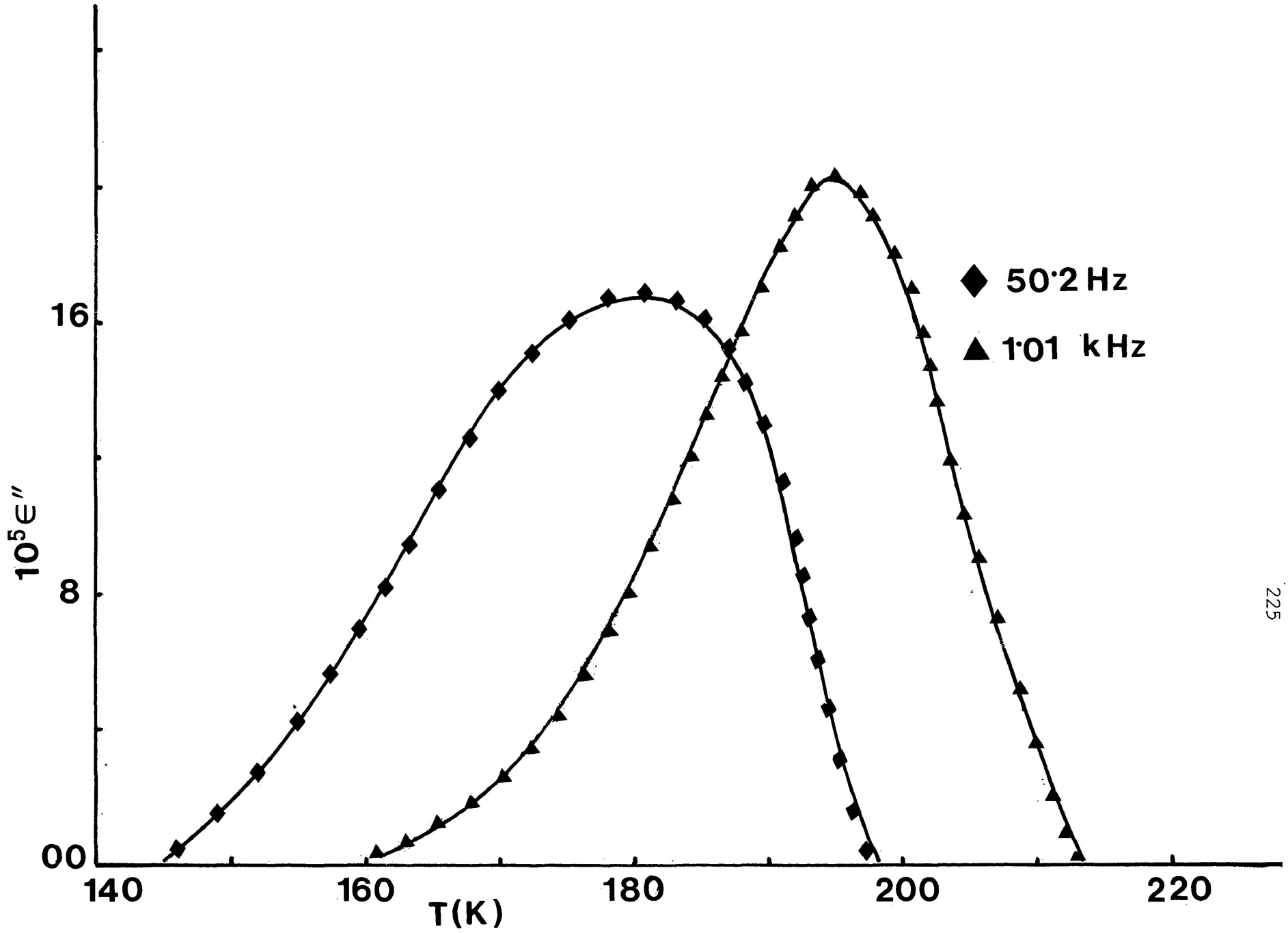

FIGURE V-2a: Plots of dielectric loss factor, ε" versus temperature (K) for carbontetrachloride in the pure solid state

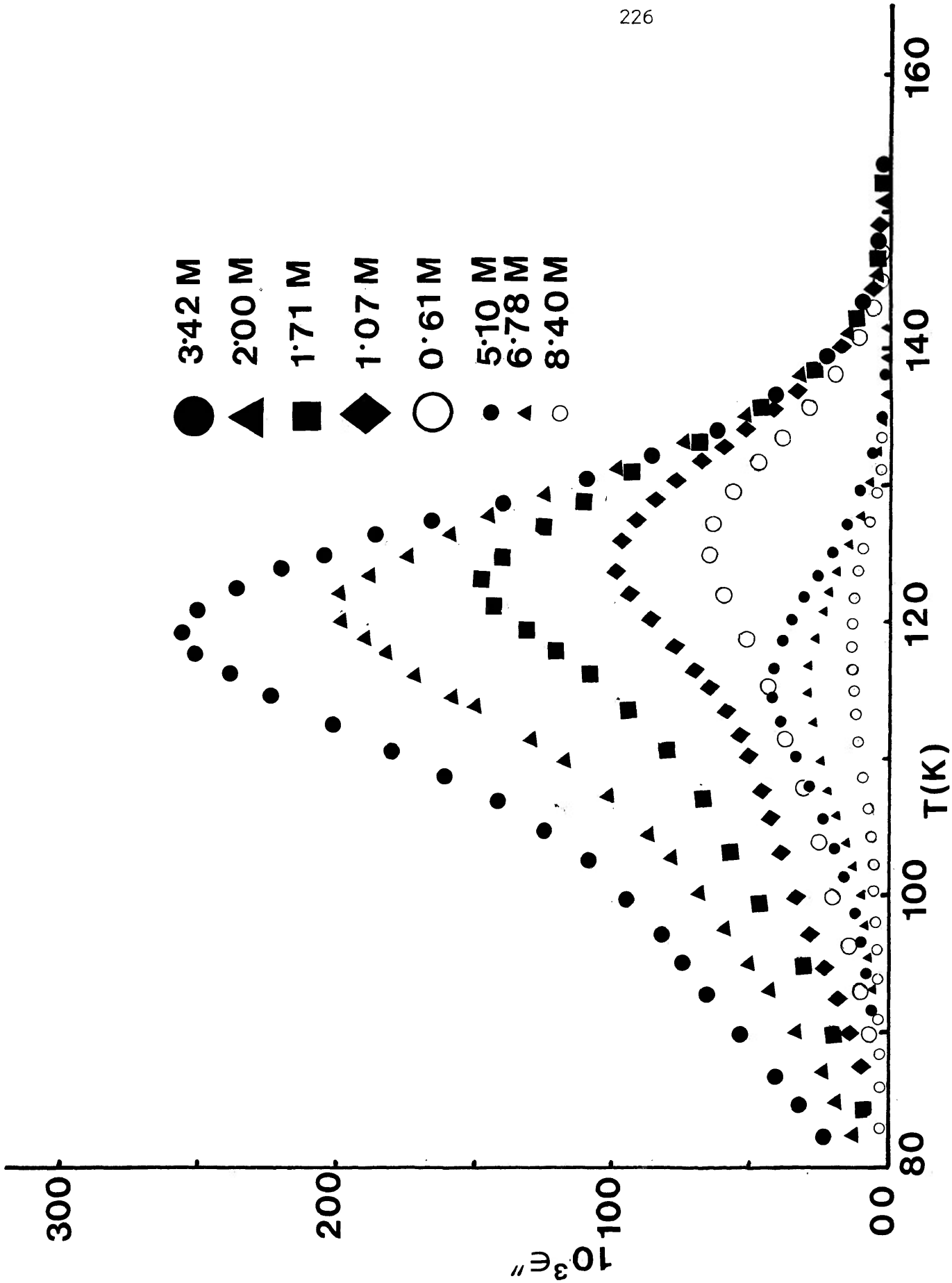

FIGURE V-3a: Plots of dielectric loss factor, ε'' versus temperature (K) for 1,1,1-trichloroethane (at 1.01 kHz) in carbontetrachloride at several concentrations (molarity)

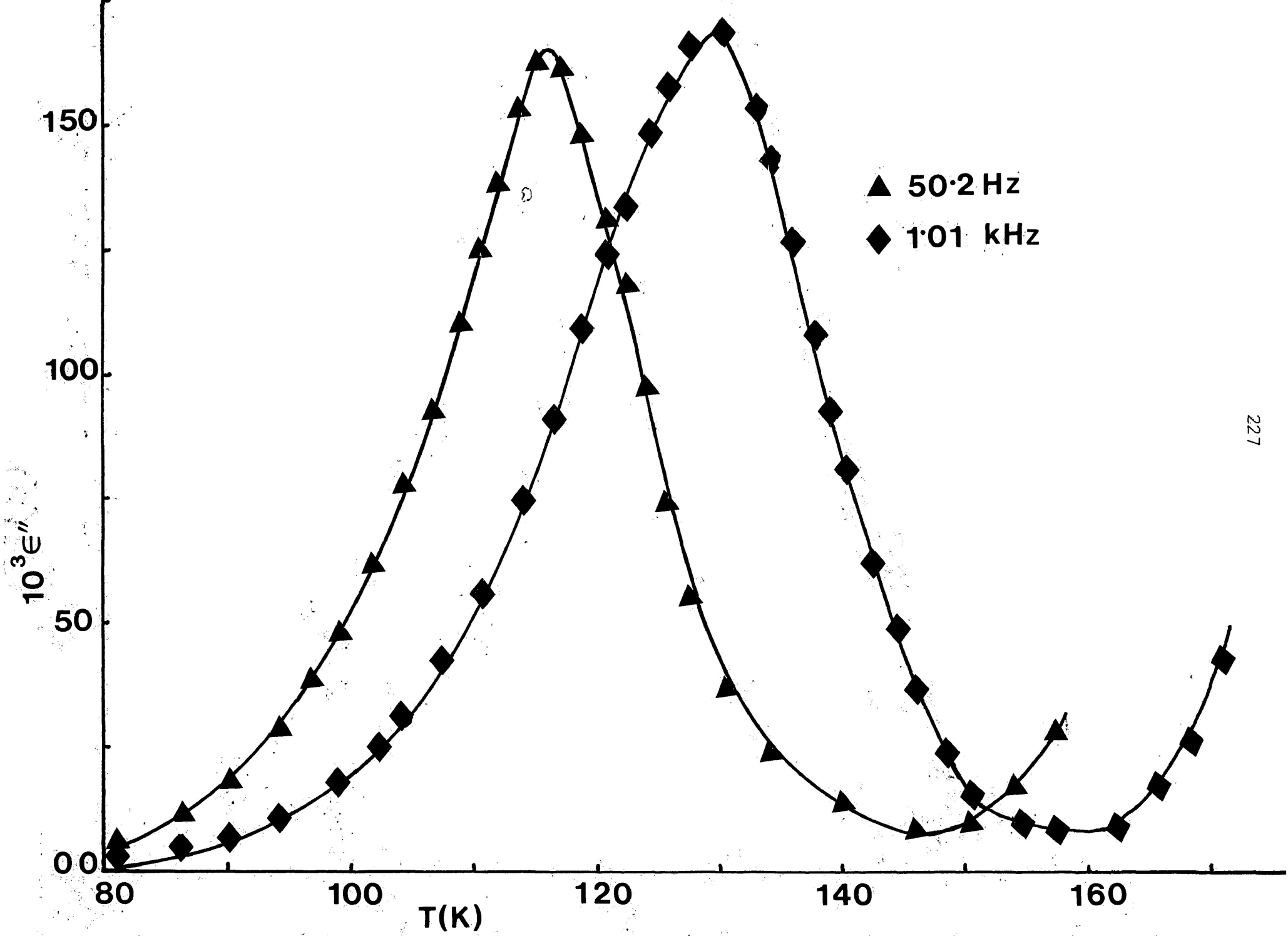

FIGURE V-4a: Plots of dielectric loss factor, ε" versus temperature (K) for 1,1,1-trichloroethane in silicontetrachloride (5.0 M)

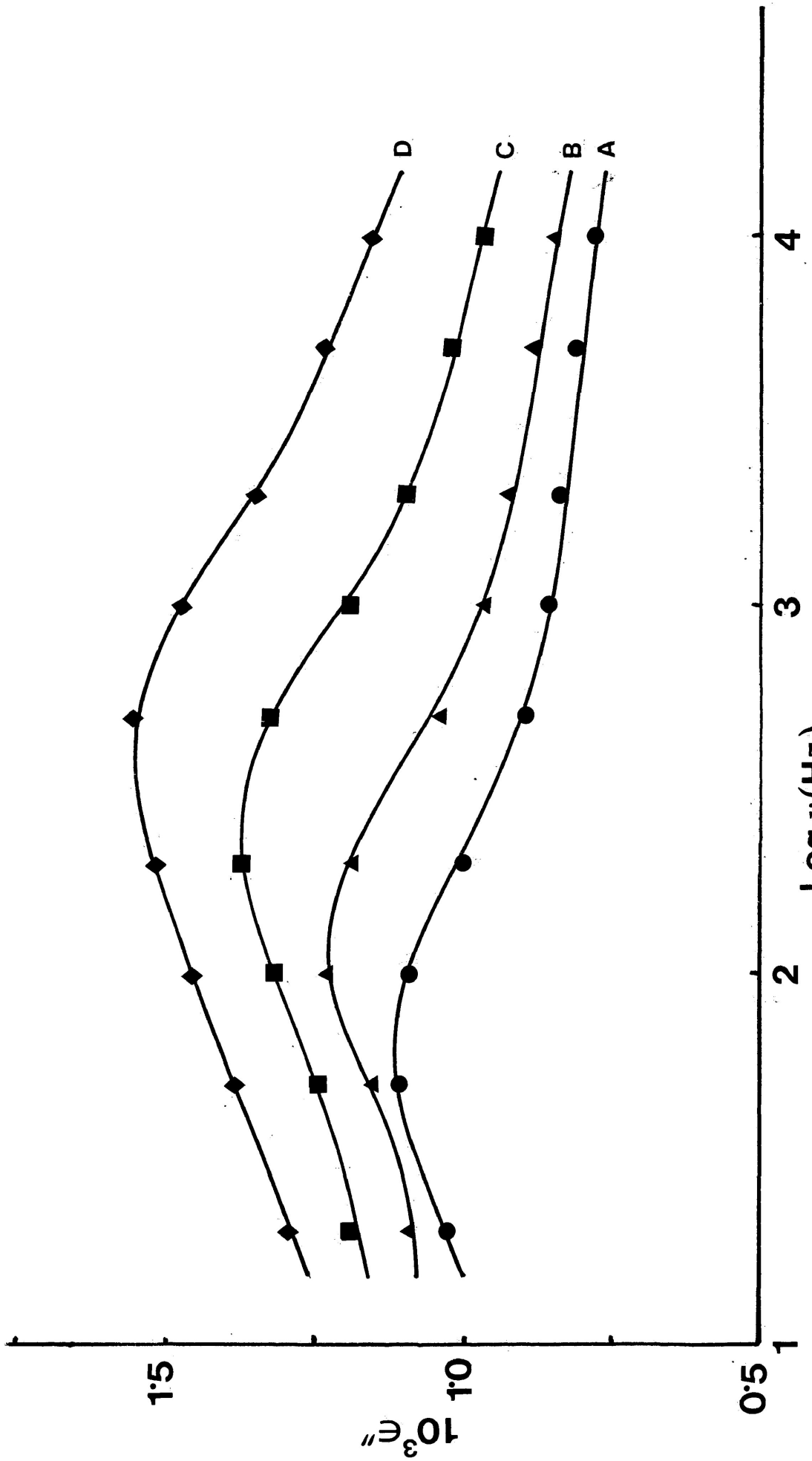

FIGURE V-5b: Plots of dielectric loss factor, ε'' versus logν (Hz) for 1,1,1-trichloroethane in the pure solid state. A = 96.1 K, B = 98.6 K, C= 101.9 K, and D = 104.9 K.

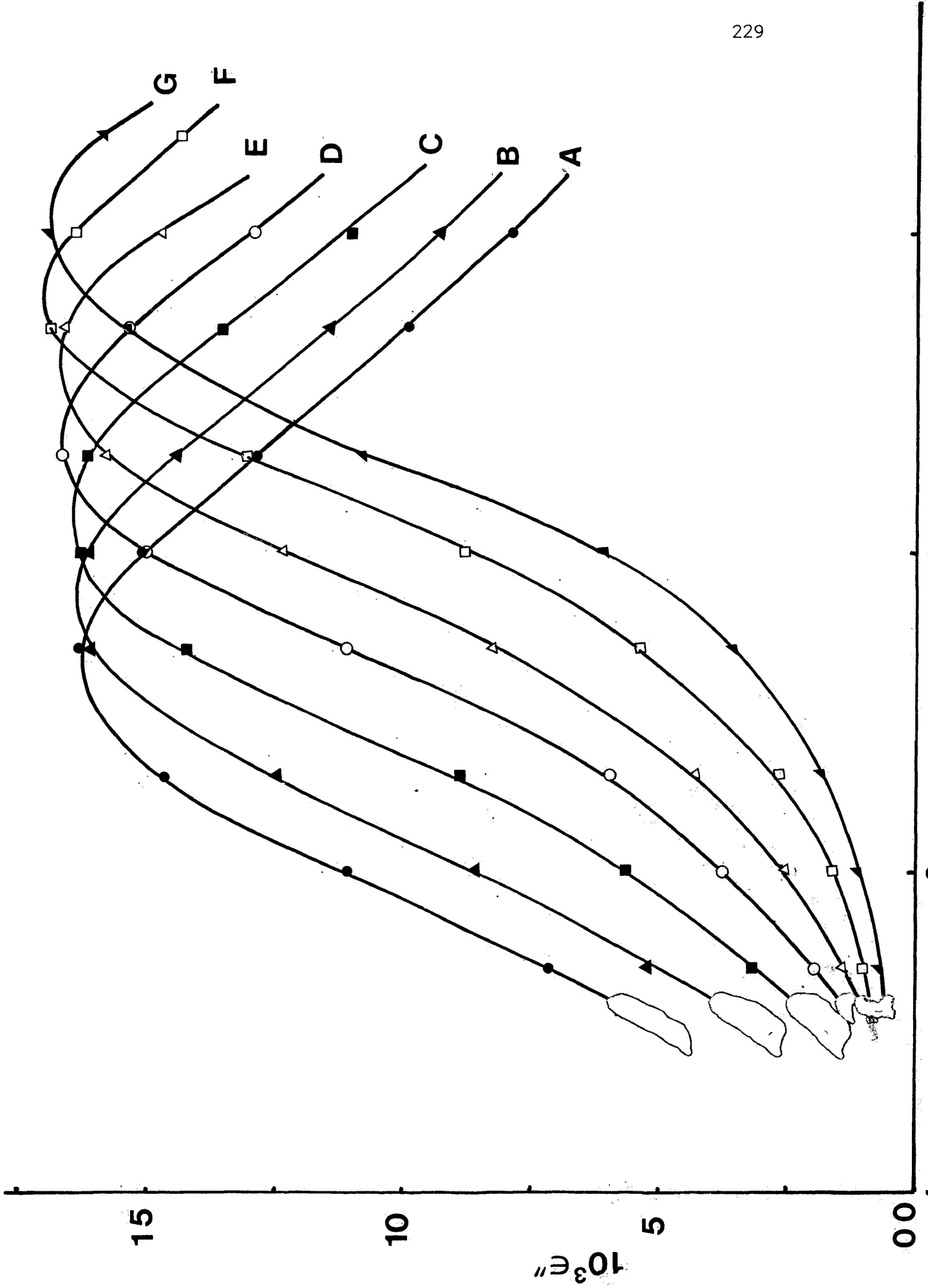

FIGURE V-6b: Plots of dielectric loss factor, ε'' versus $\log_{10}\nu$ (Hz) for 1,1,1-trichloroethane in the pure solid state: A=117.0 K; B=117.7 K; C=118.5 K; D=119.3 K; E=120.0 K; F=120.9 K and G=121.7 K.

FIGURE V-7b: Plots of dielectric loss factor, ε" versus logν (Hz) for carbontetrachloride in the pure solid state. A=183.1 K; B=186.1 K; C=190.0 K; D=196.3 K; and E=199.0 K.

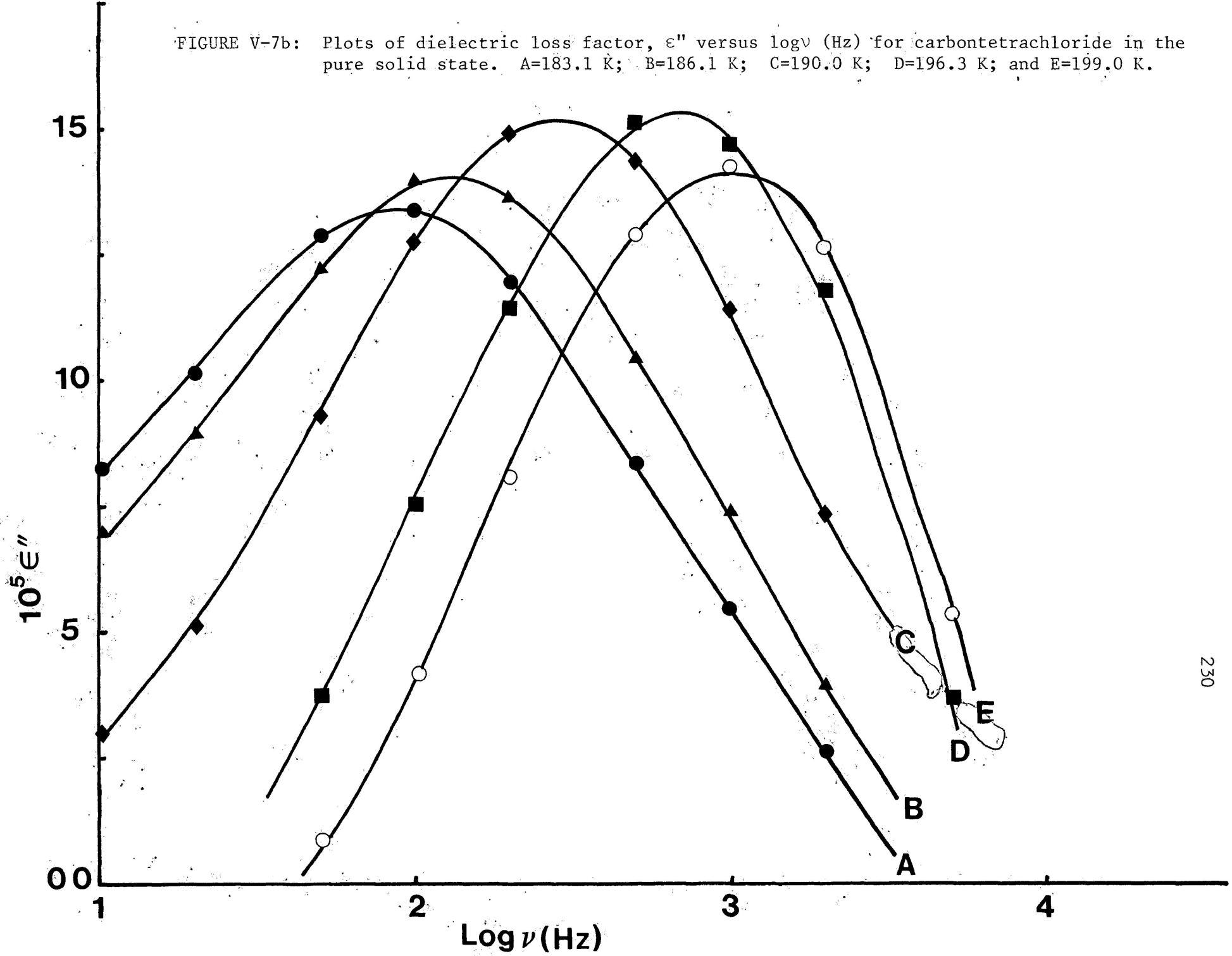

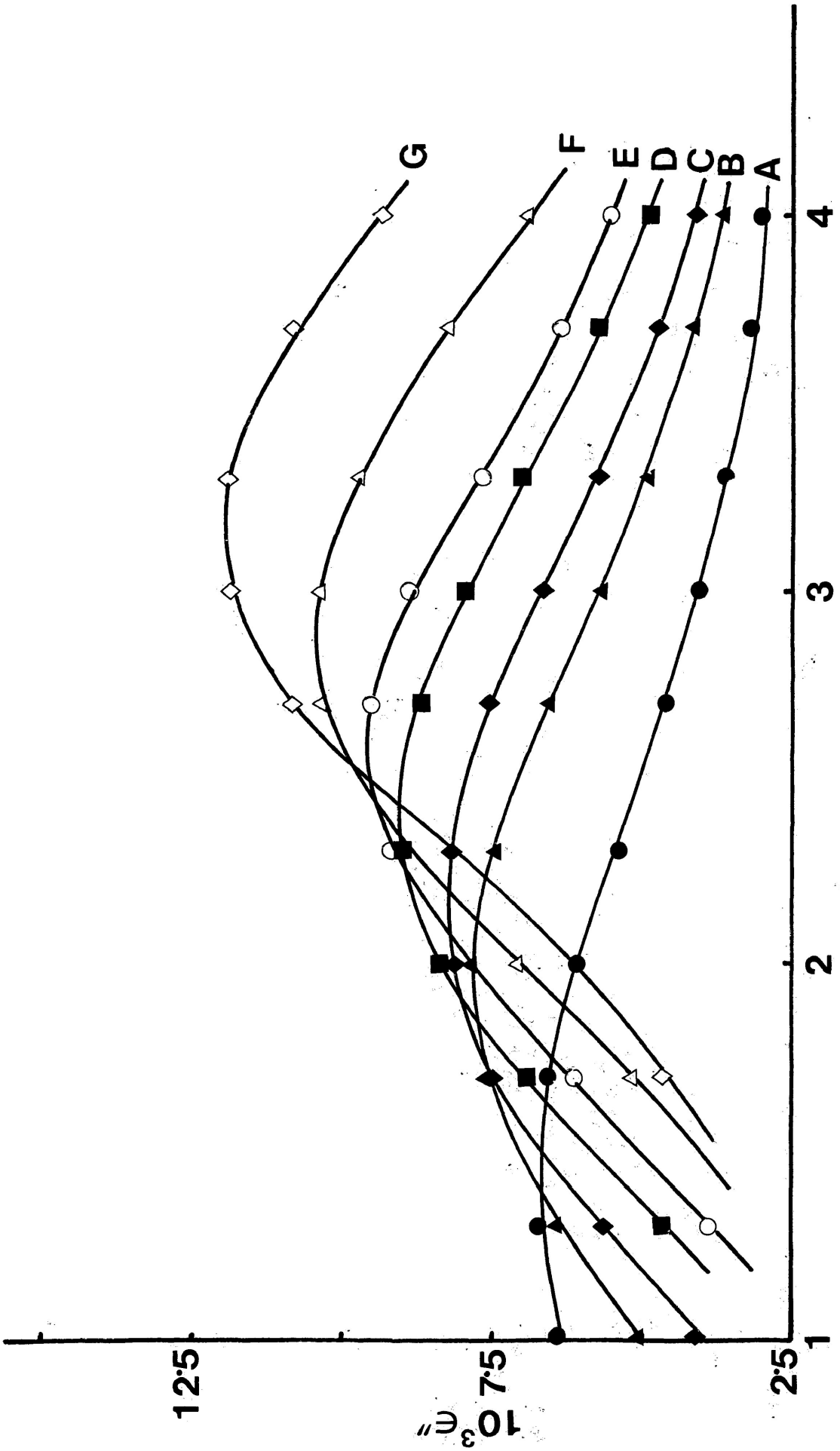

FIGURE V-8b: Plots of dielectric loss factor, ε'' versus $\log\nu$ (Hz) for 1,1,1-trichloroethane in carbontetrachloride (8.4 M). A=98.0 K; B=102.2 K; C=104.1 K; D=106.5 K; E=108.2 K; F=110.7 K; and G=113.7 K.

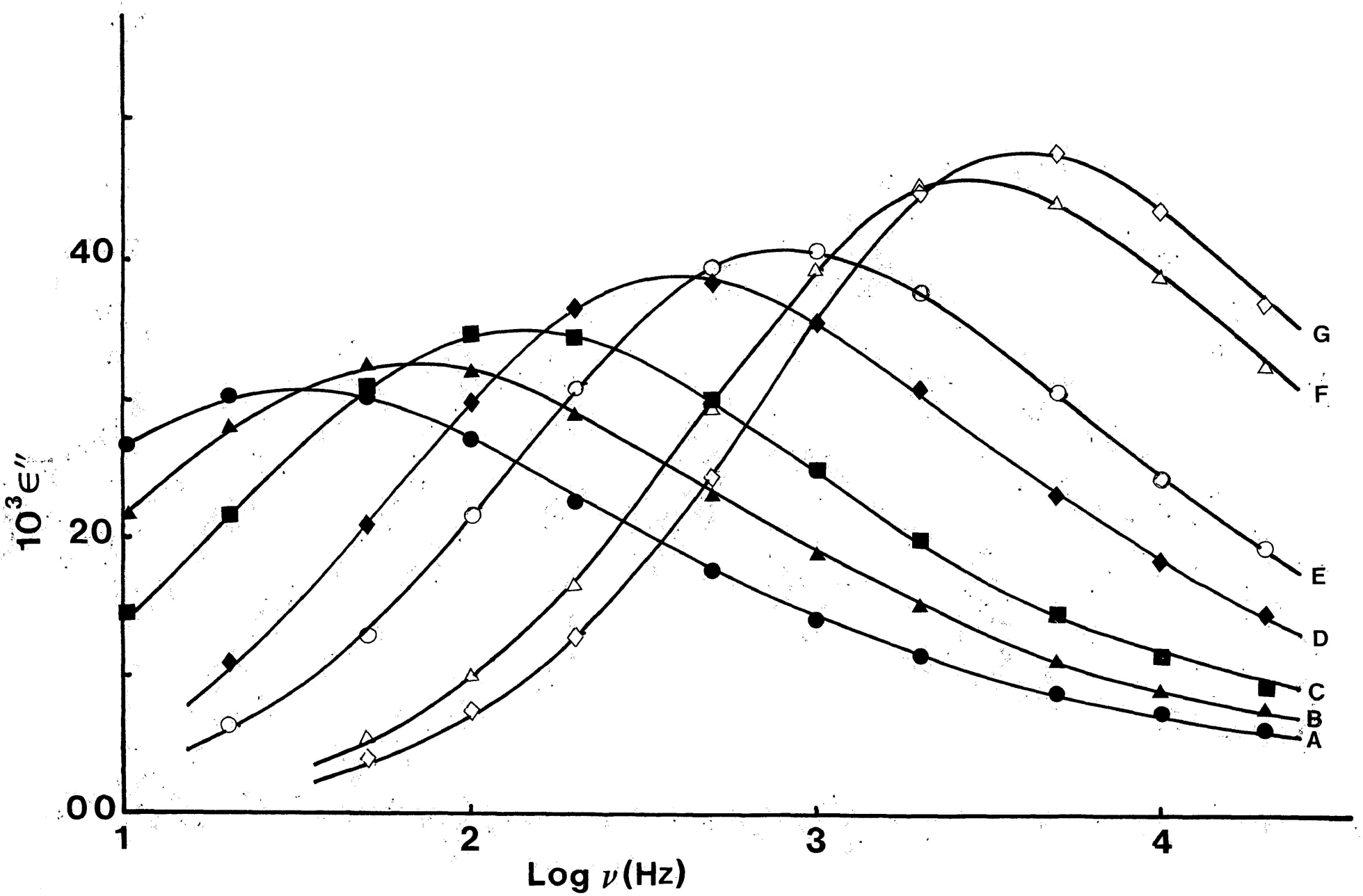

FIGURE V-9b: Plots of dielectric loss factor, ε'' versus logν (Hz) for 1,1,1-trichloroethane in carbontetrachloride (5.1 M). A=101.4 K; B=103.6 K; C=106.3 K; D=110.6 K; E=113.4 K; F=118.6 K; and G=120.2 K.

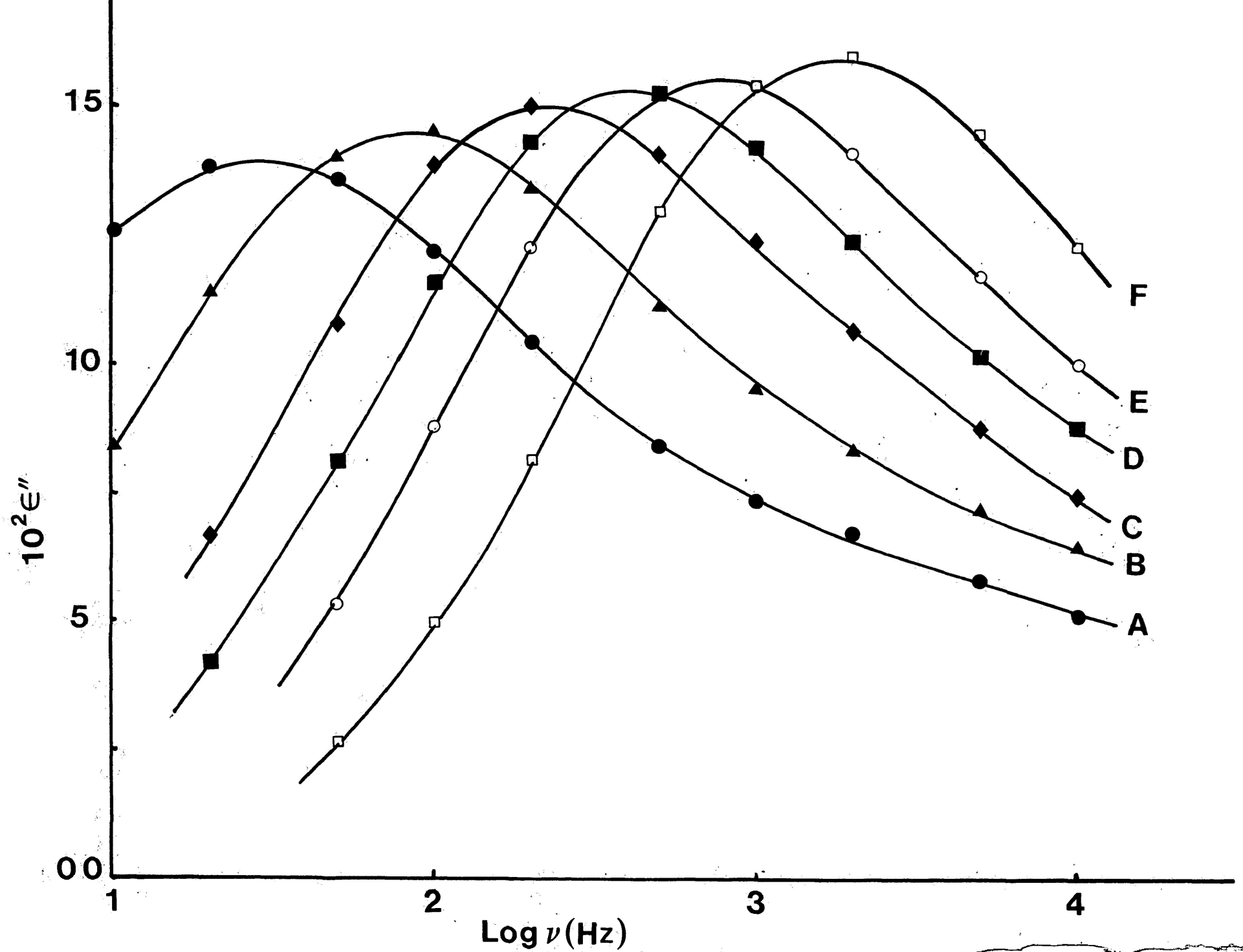

FIGURE V-10b: Plots of dielectric loss factor, ε" versus logν (Hz) for 1,1,1-trichloroethane in carbontetrachloride (1.71 M). A=107.7 K; B=111.6 K; C=115.8 K; D=118.4 K; E=121.0 K; and F=124.8 K.

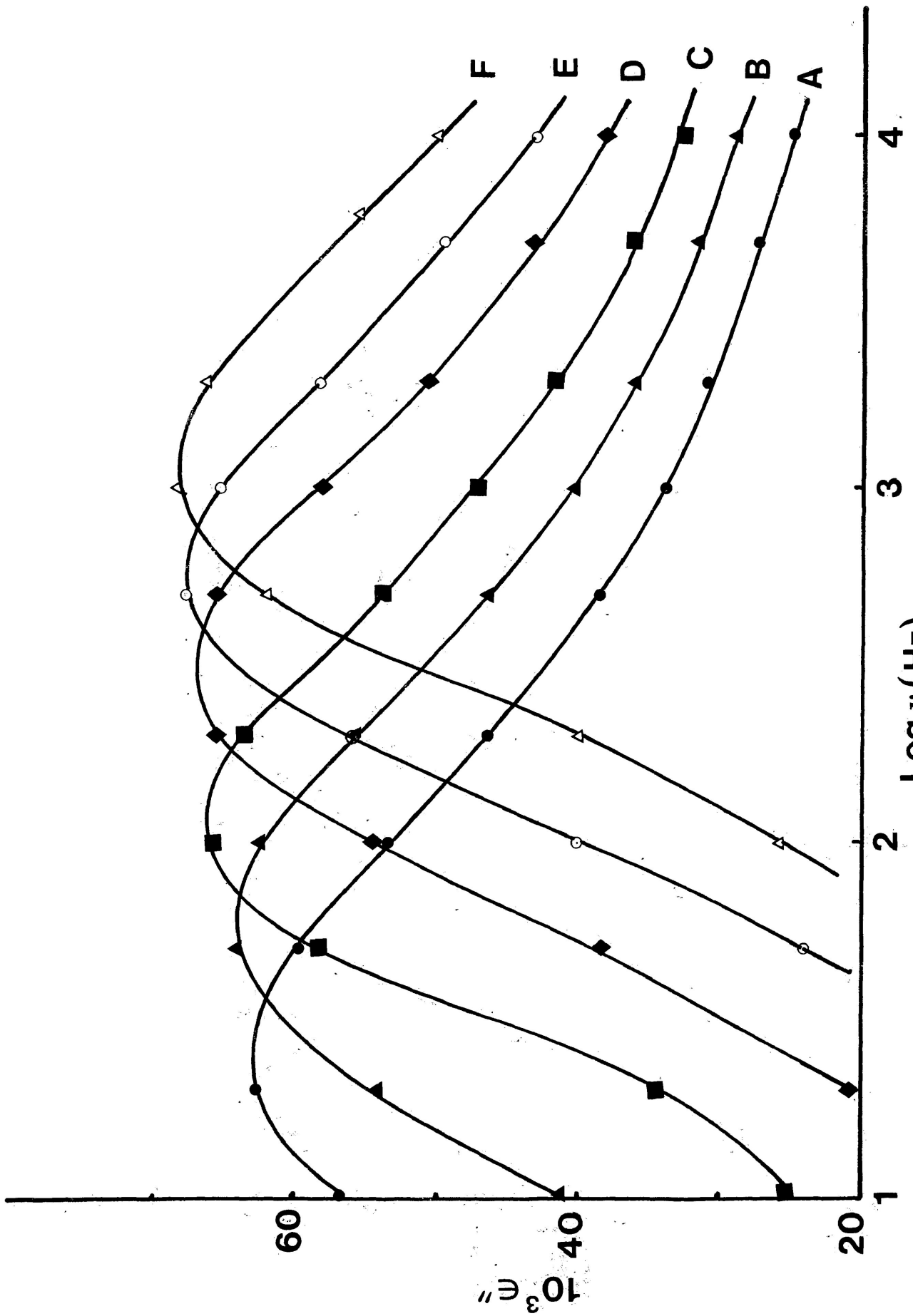

FIGURE V-11b: Plots of dielectric loss factor, ε'' versus logν (Hz) for 1,1,1-trichloroethane in carbontetrachloride (0.66 M). A=109.7 K; B=112.8 K; C=115.7 K; D=120.0 K; E=122.9 K; and F=125.9 K.

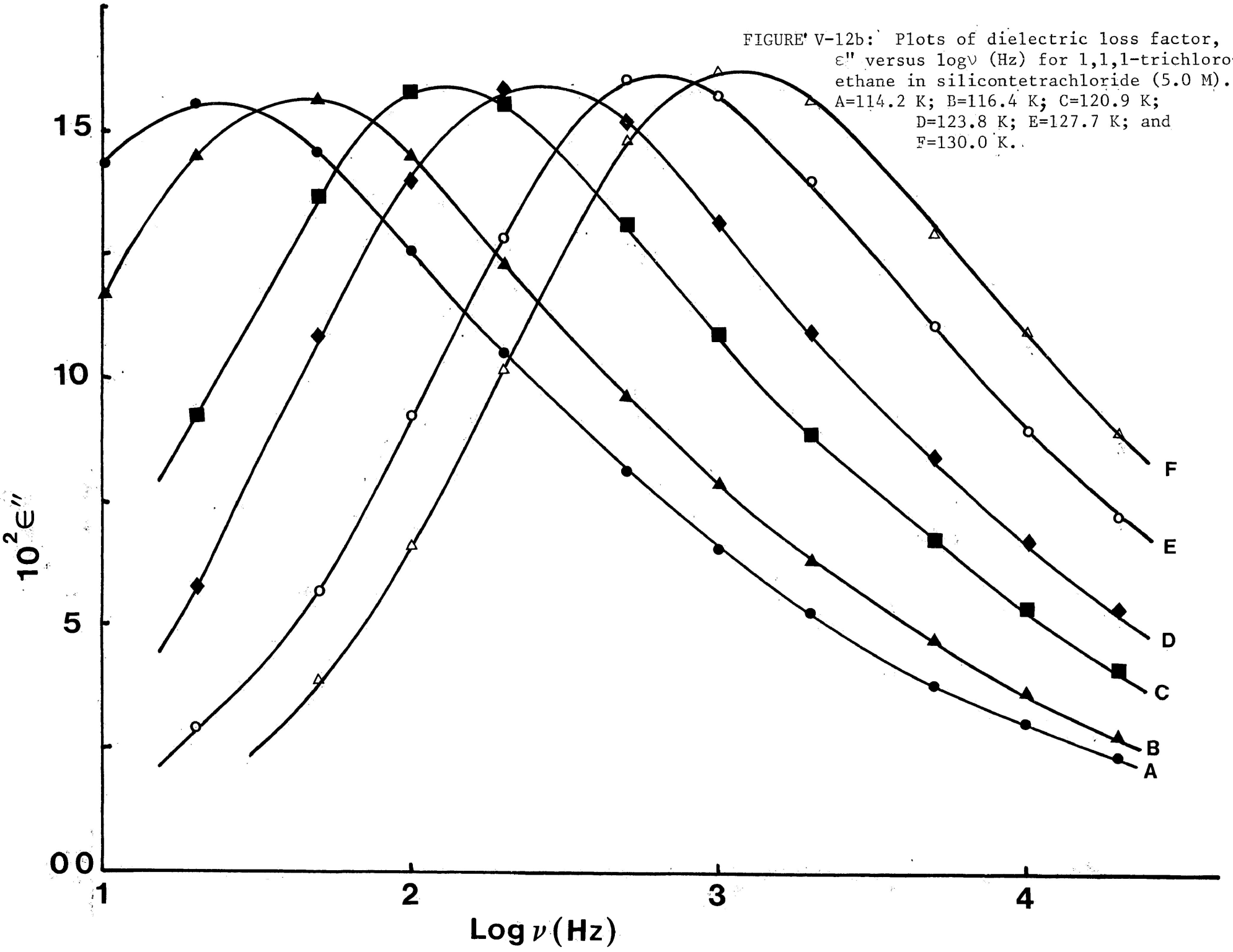

FIGURE V-12b: Plots of dielectric loss factor, ϵ'' versus logν (Hz) for 1,1,1-trichloroethane in silicontetrachloride (5.0 M). A=114.2 K; B=116.4 K; C=120.9 K; D=123.8 K; E=127.7 K; and F=130.0 K.

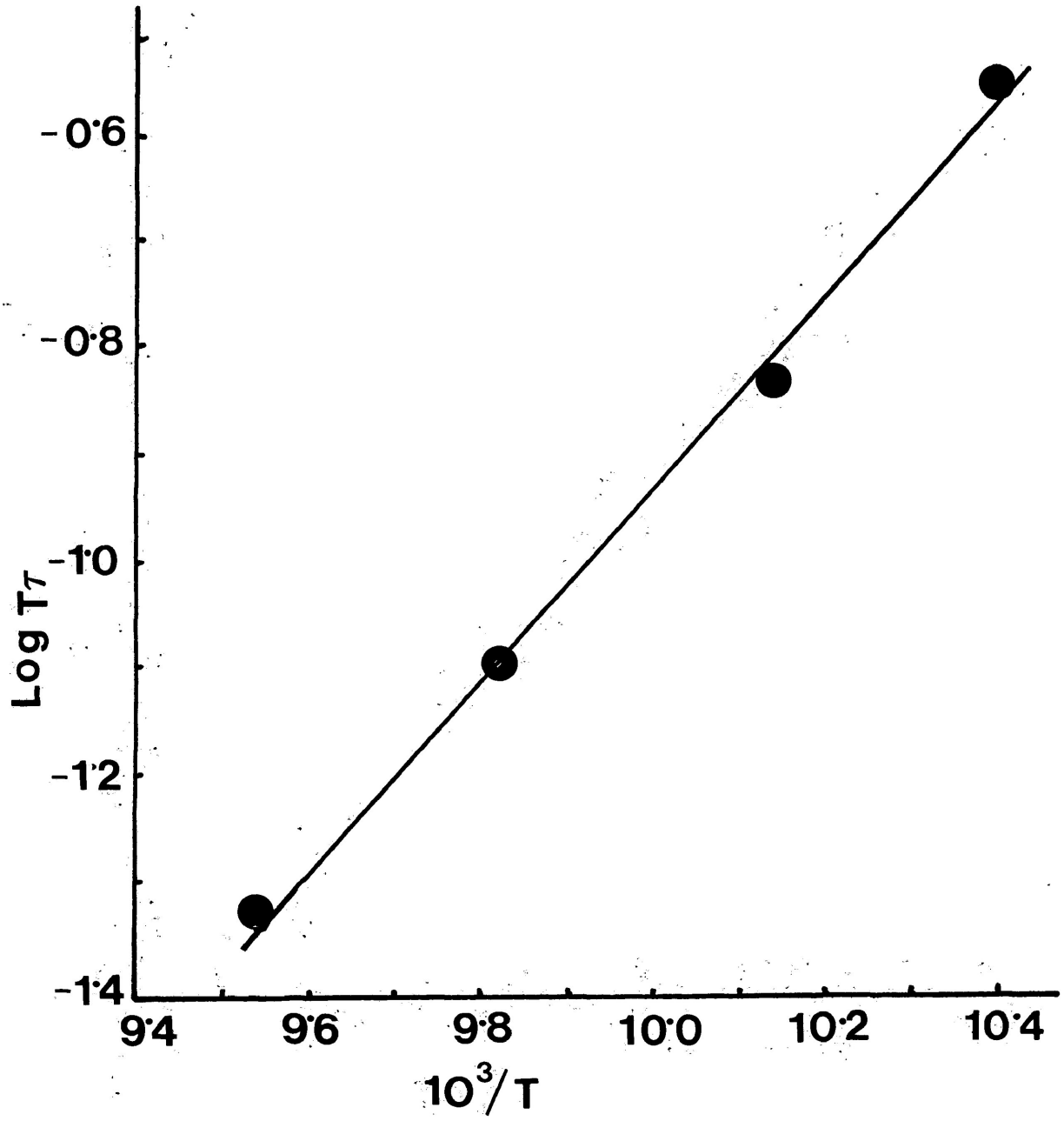

FIGURE V-13d: Eyring plot of logTτ versus 1/T (K^{-1}) for 1,1,1-trichloroethane in the pure solid state.

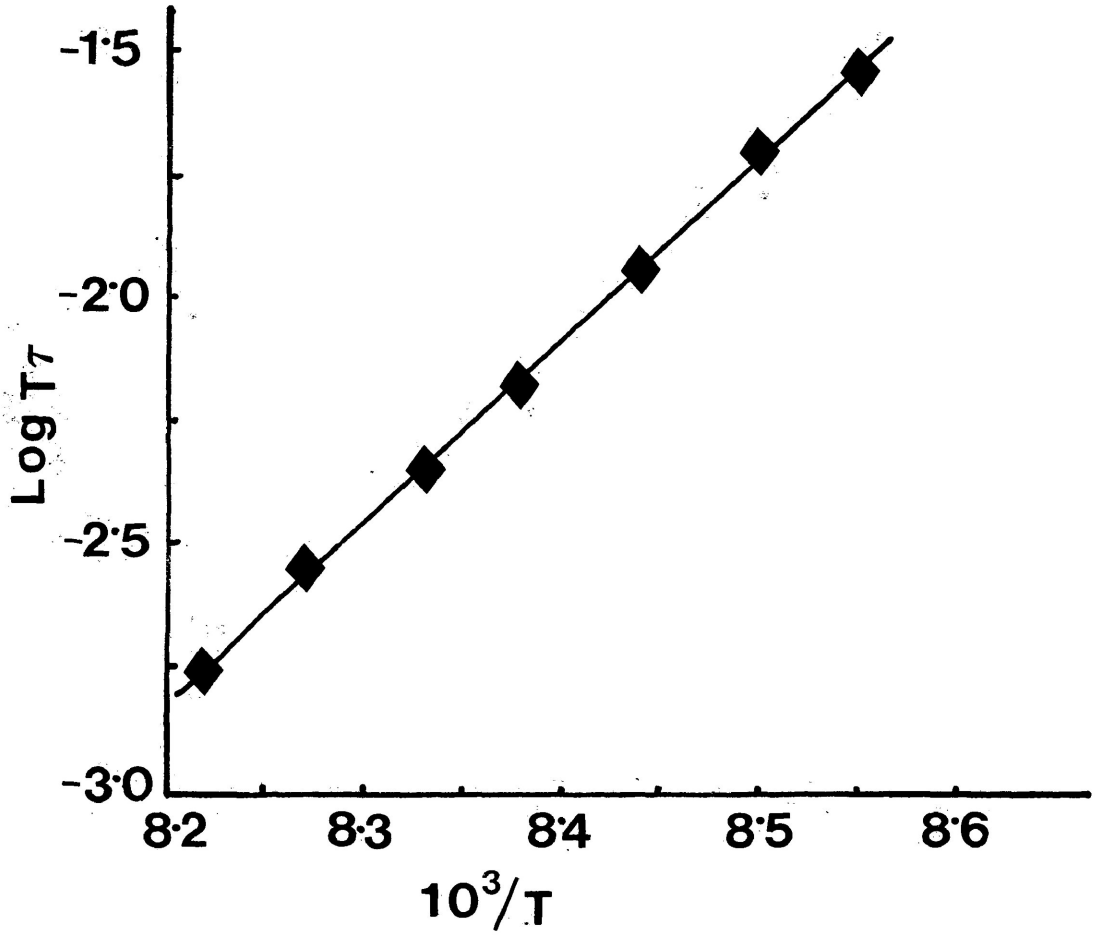

FIGURE V-14d: Eyring plot of logTτ versus 1/T (K^{-1}) for 1,1,1-trichloroethane in the pure solid state

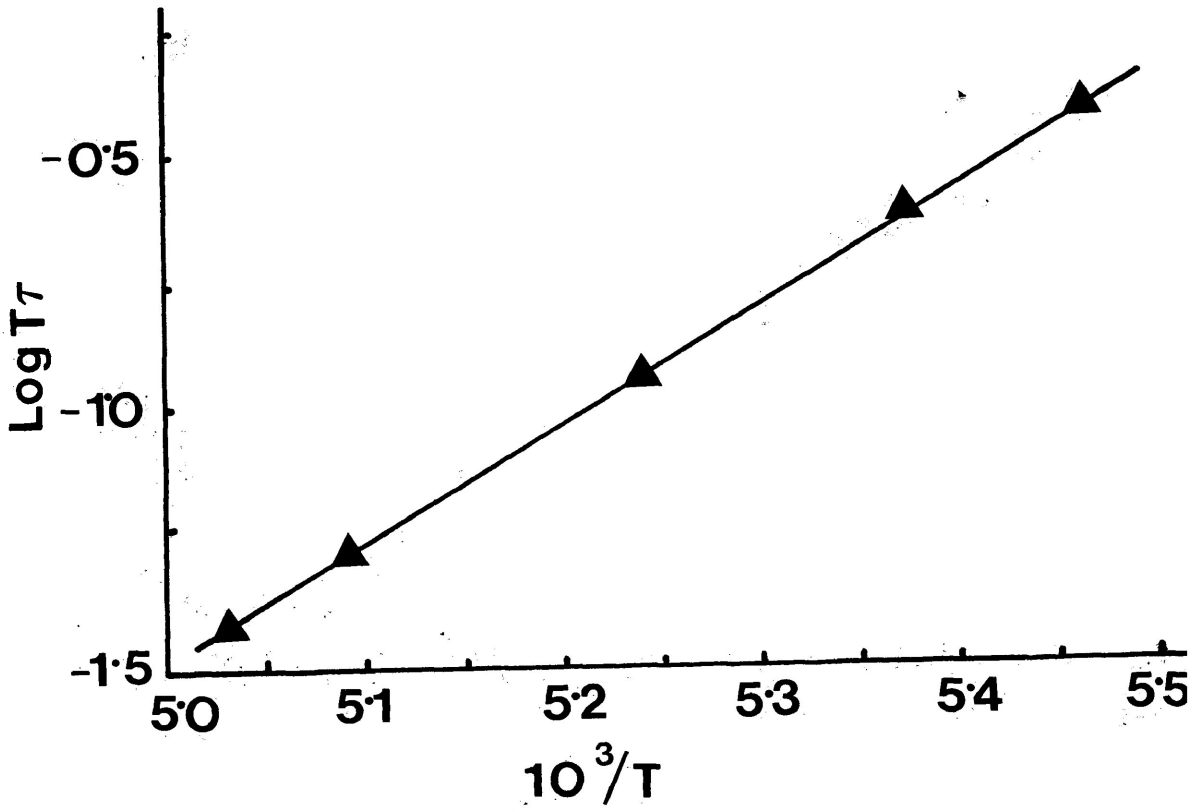

FIGURE V-15 d: Eyring plot of logTτ versus 1/T (K^{-1}) for carbontetrachloride in the pure solid state.

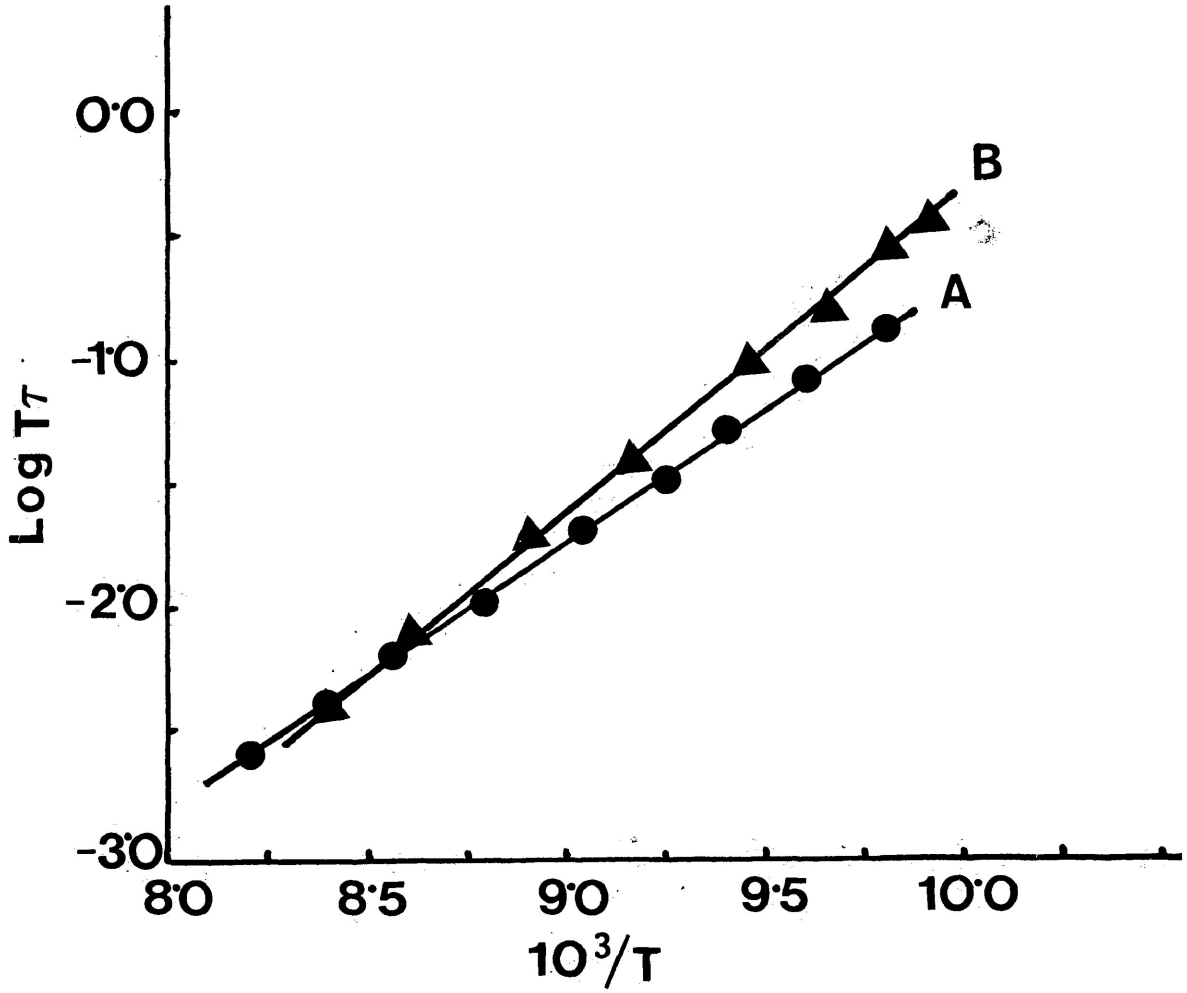

FIGURE V-16d: Eyring plots of logTτ versus 1/T (K^{-1}) for 1,1,1-trichloroethane in carbontetrachloride. A=8.4 M and B=6.78 M

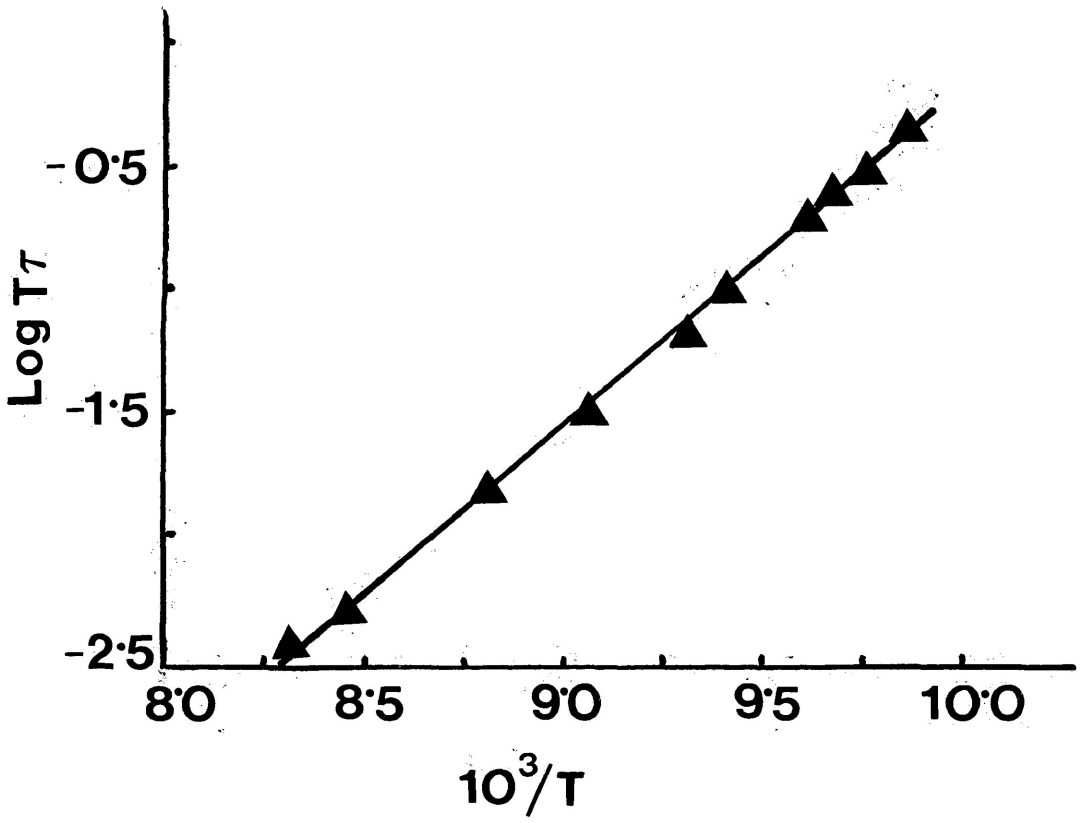

FIGURE V-17d: Eyring plot of logTτ versus 1/T (K^{-1}) for 1,1,1-trichloroethane in carbontetrachloride (5.1 M)

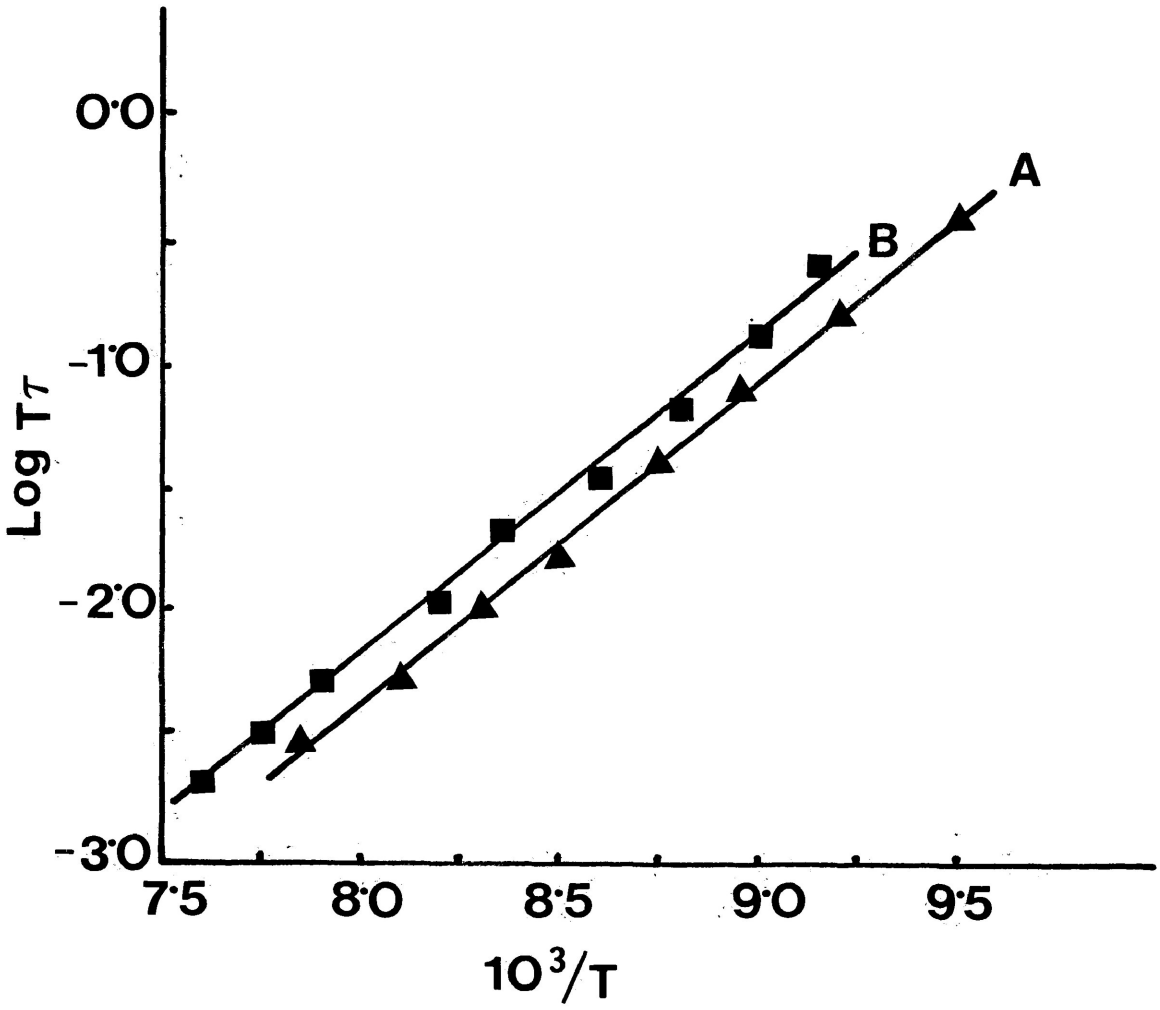

FIGURE V-18d: Eyring plots of logTτ versus 1/T (K^{-1}) for 1,1,1-trichloroethane in carbontetrachloride. A=3.42 M and B=2.05 M.

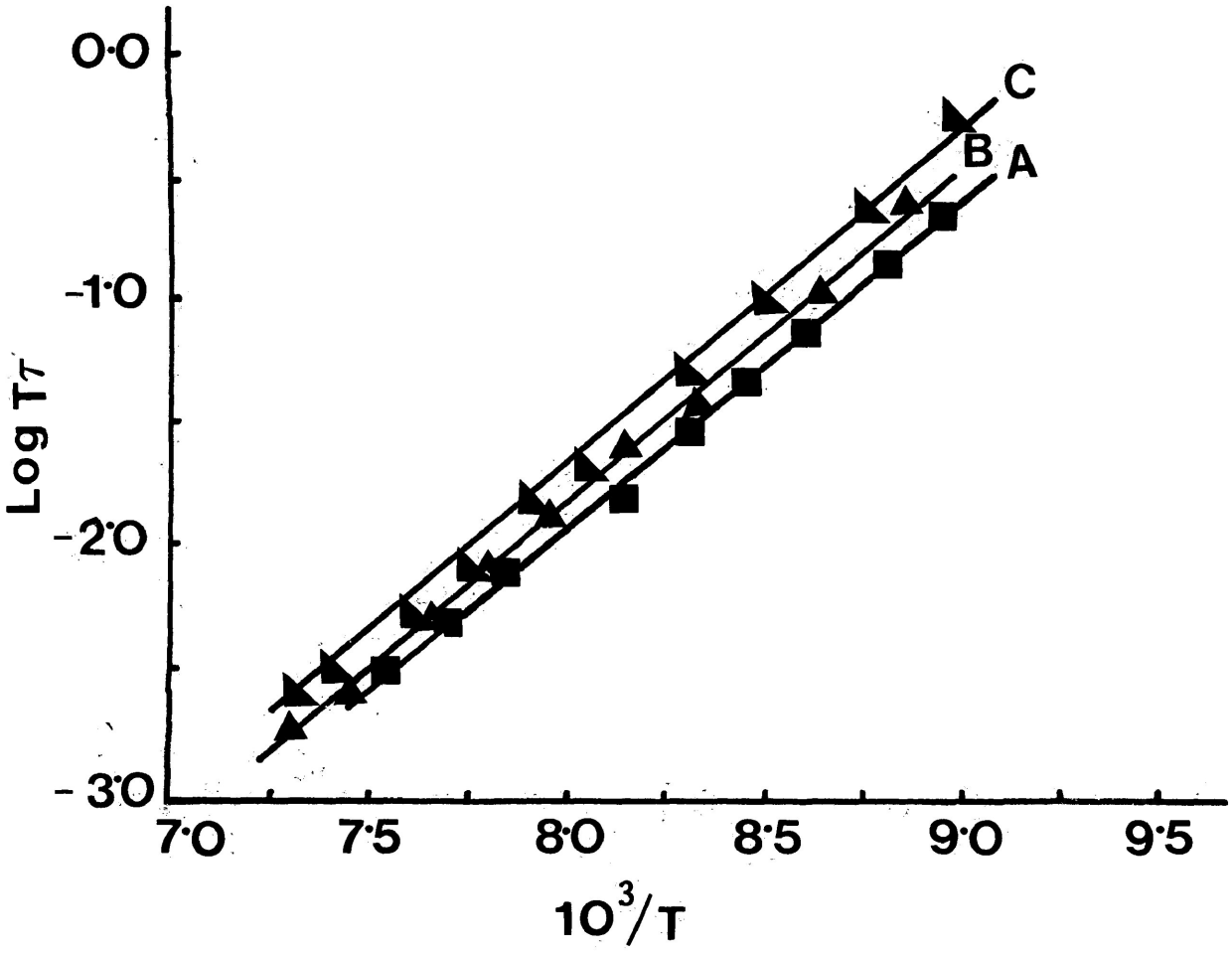

FIGURE V-19d: Eyring plots of logTτ versus 1/T (K^{-1}) for 1,1,1-trichloroethane in carbontetrachloride A=1.07 M; B=0.66 M; and C=0.09 M

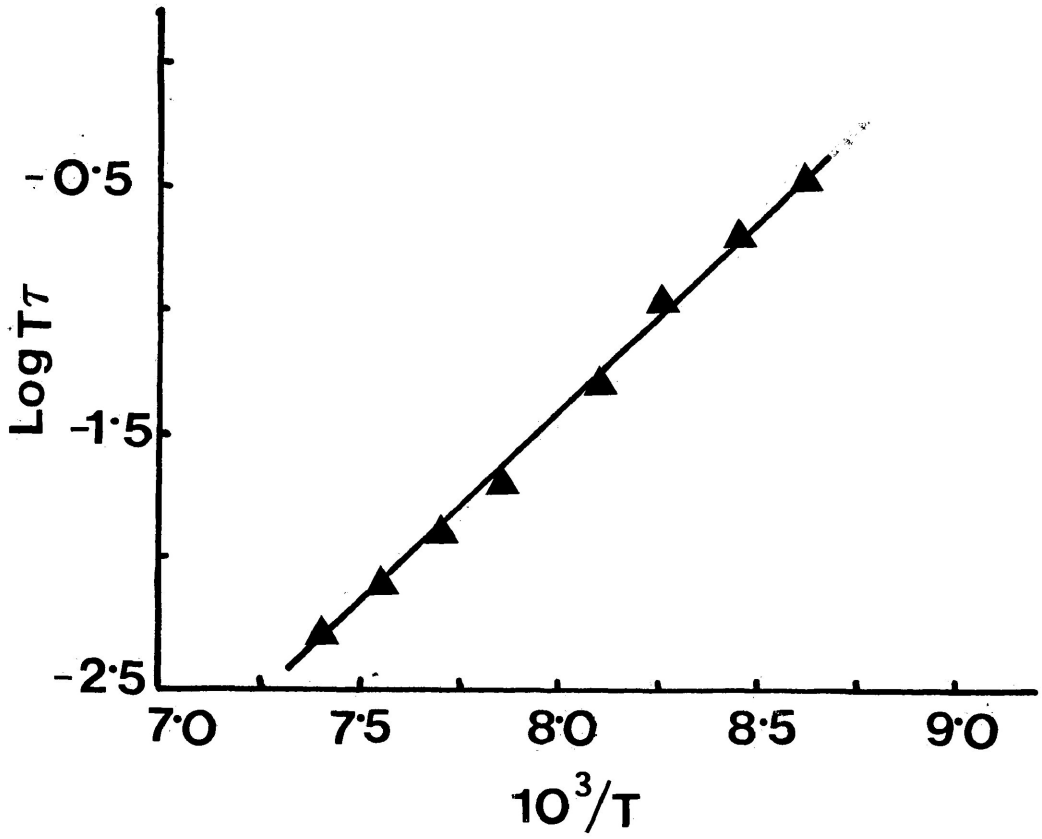

FIGURE V-20d: Eyring plot of logTτ versus 1/T (K^{-1}) for 1,1,1-trichloroethane in silicontetrachloride (5.0 M).

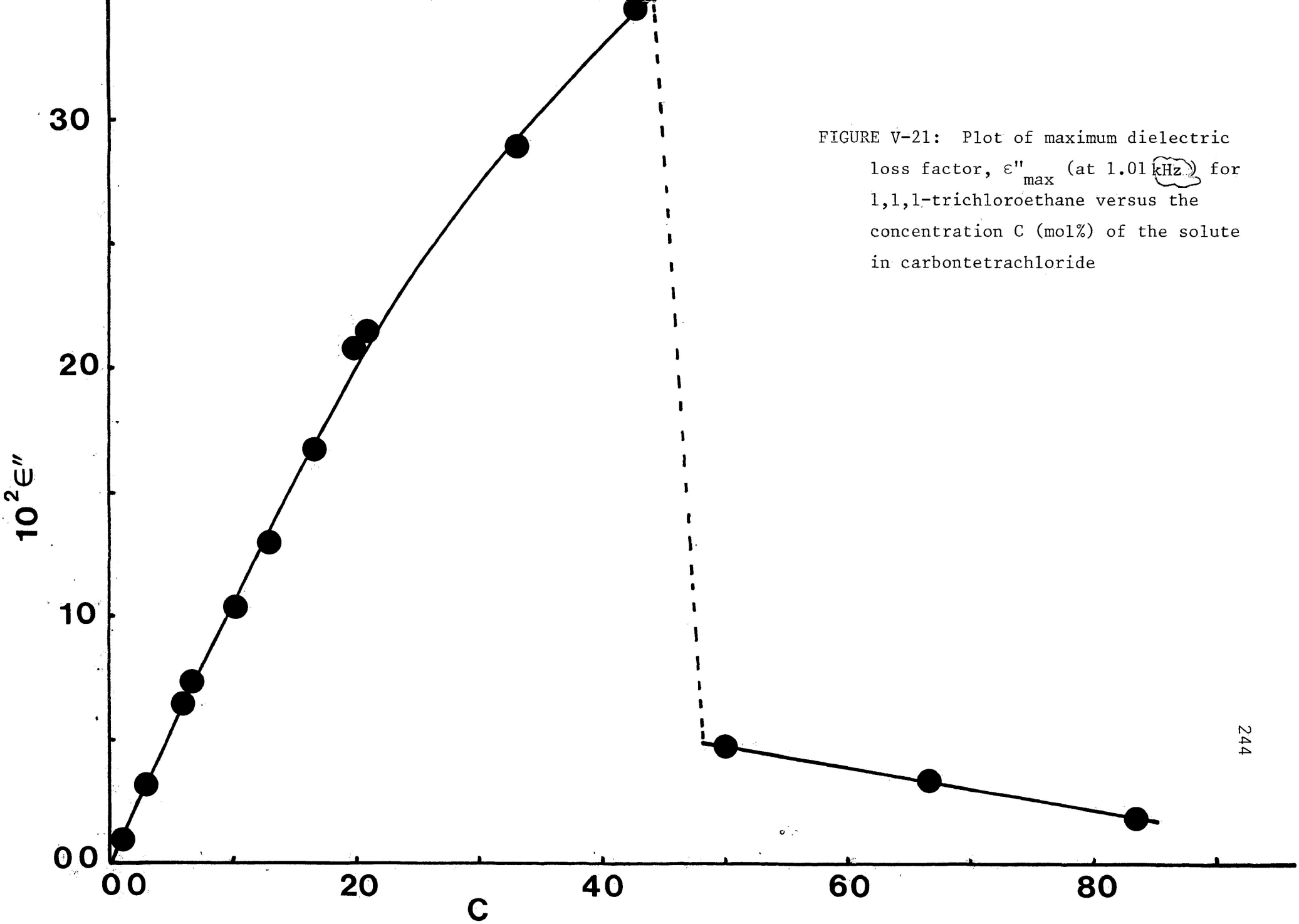

FIGURE V-21: Plot of maximum dielectric loss factor, ϵ''_{max} (at 1.01 kHz) for 1,1,1-trichloroethane versus the concentration C (mol%) of the solute in carbontetrachloride

FIGURE V-22: Plot of maximum dielectric loss factor, $\epsilon''_{max.}$ (at 1.01 kHz) for methyliodide versus the concentration, C (wt %) of the solute in cis-decalin

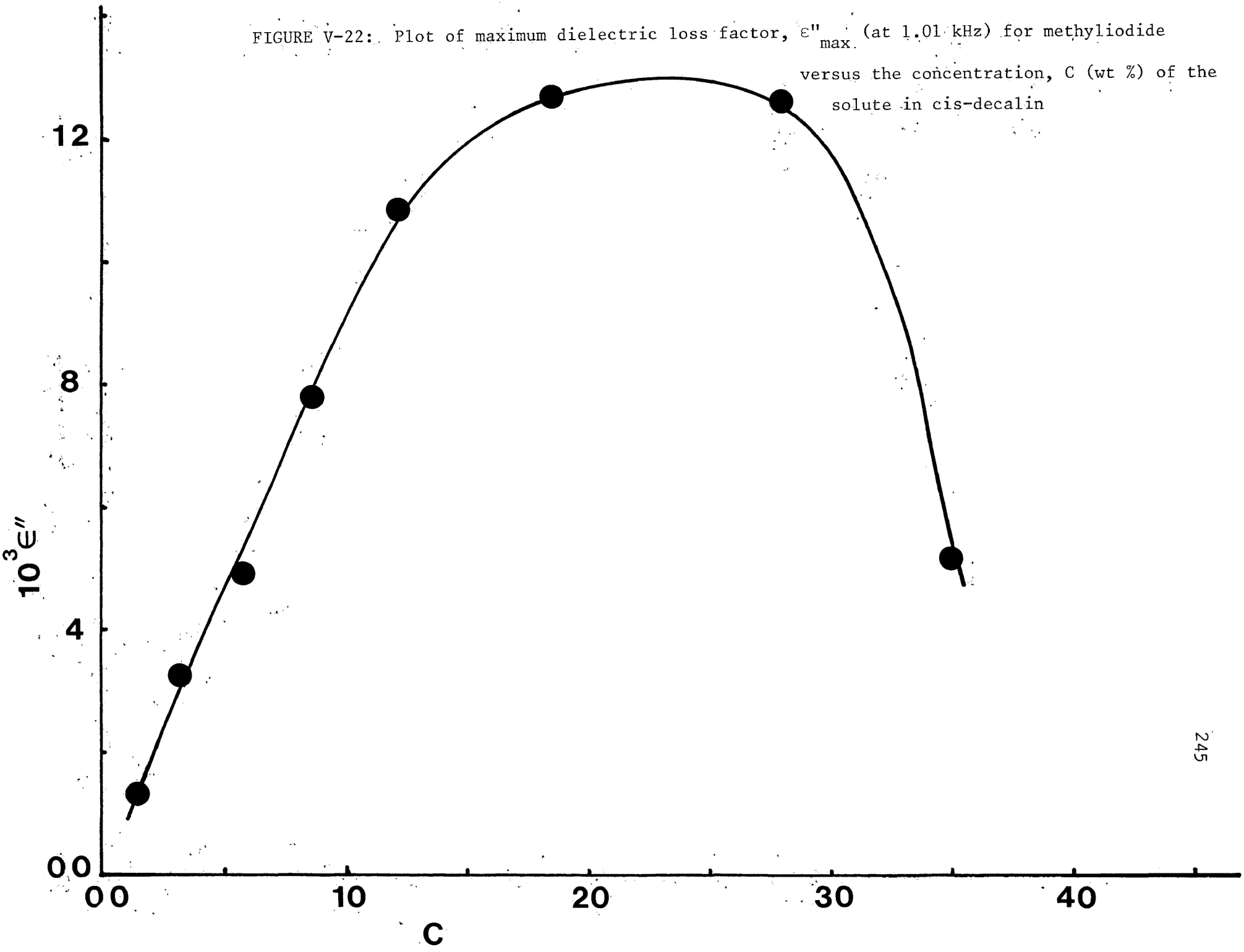

CHAPTER VI

DIELECTRIC RELAXATION OF SOME FAIRLY SPHERICAL SIMPLE ALCOHOLS IN SOME ORGANIC GLASSES

VI-1: INTRODUCTION

Hydrogen bonding is a phenomenon of importance to chemists working in often quite different spheres of chemistry. Broadly speaking there are those concerned with the actual concept and energetics of hydrogen bonds and a majority of others interested in the effects of hydrogen bonding on molecular structure. Infrared absorption and nuclear magnetic resonance spectroscopy have provided very sensitive means of detecting hydrogen bond formation and have been extensively employed in both qualitative and quantitative studies of hydrogen bonded systems. These are not the only tools available and many other techniques have provided important results. Each method has its own particular assets and limitations in its application to hydrogen bonding and these have been well described and discussed elsewhere (1,2). Hydrogen bonding compounds containing hydroxyl groups, especially the aliphatic alcohols and aromatic phenols as well as their solutions have been studied by various dielectric absorption techniques. Studies on primary and secondary alcohols in the pure liquid state (3-7) indicate that the dielectric dispersion may be described by three relaxation times with the dominating low-frequency process of Debye type. Studies (8-13) on alcoholic solutions in non-polar solvents show that the contribution

from the low-frequency process (τ_1) is diminished gradually on dilution and becomes insignificant at high dilution. Despite diverse interpretations (19,15) by different workers, they seem to converge at one point that the absorption process (τ_3) having the shortest relaxation time is due to the reorientation of the OH group in the free monomers around the C-O bond. The other two relaxations become complicated owing to the effect of intermolecular hydrogen bonding.

In general the effect of molecular interaction and specifically intermolecular hydrogen bonding on the dielectric relaxation time of a molecule may be two fold:

(i) Molecules may strongly associate to form a complex which, if polar, will itself reorientate under the influence of the applied field with a relaxation time considerably longer than that of the uncomplexed monomer unit.

(ii) Association into a rigid complex may not occur but the reorientation of the molecules may be slowed down, and thus the relaxation time lengthened by the attractive influence of neighbouring molecules. For these reasons hydrogen bonding has the effect of increasing the barrier to molecular rotation.

Khameshara et al (16) dielectrically studied n-butanol, iso-butanol, sec-butanol and tert-butanol at 35°C and found evidence for the existence of more than one relaxation mechanism in each of the systems. They interpreted their results in terms of simultaneous intramolecular reorientation of OH group with the end-over-end molecular rotation. The higher τ values were accounted for by the formation of dimers by intermolecular association and solute solvent interaction.

From n.m.r. studies on tert-butanol, phenol, and methanol in carbontetrachloride (from 0.01 M - 10 M solution) Saunders and Hyne (17) reported that tert-butanol and phenol form monomer-trimer equilibria whereas methanol forms monomer-tetramer equilibria. Musa et al (18) found monomer-tetramer equilibria in tert-butanol in benzene solution by ultrasonic technique. They obtained the enthalpy of activation for tetramer rotation as 64.4 kJ mol^{-1}.

Errera et al (19) studied a number of simple alcohols in carbontetrachloride by infrared technique and reported that (i) carbontetrachloride has a higher dissociation power owing to the higher dielectric constant compared to that of gas, (ii) alcohol is (in CCl_4) only completely

dissociated at concentrations smaller than 0.1 percent in volume, (iii) in the mechanism of the association of alcohol at least two steps may be distinguished: formation of double molecules and of polymolecular complexes. The latter are very sensitive to the temperature.

Kozodziej and Malarski (20) measured the dielectric permittivity and temperature dependence of infrared absorption of di-tert-butylcarbinol, t-$(But)_2CHOH$, a molecule capable of forming only the dimer in n-heptane and carbontetrachloride and reported that the dimer peak position is around 3530 cm^{-1} and the lower temperature is favourable for cyclic dimers than for the open aggregates.

Dwivedi et al (21) dielectrically studied tert-butanol and tert-amyl alcohol in the pure liquid state in the range 0.1 - 18000 MHz and 30 - 70°C and found only one dielectric dispersion in each case with activation enthalpies 50.3 and 50.8 kJ mol^{-1}, respectively. They interpreted their results in terms of the simultaneous rotation of free monomeric unit and the breaking and reforming of hydrogen bonds in molecular chains of varying length followed by partially free R-OH rotation.

Crossley (10) studied n-, iso-, sec- and tert-butanol in p-xylene solution at concentrations of 2 - 12 mol %

quency range

over the frequency range 1 - 35 GHz at 25°C. For most dilute solution he obtained only one dispersion region which he interpreted as being due to the -OH group rotation. For higher concentration solutions two dispersion regions were found. The new dispersion which depends strongly on the concentrations of alcohol was attributed to the rotation of multimers. Harris et al (22) after measuring the dielectric polarization for 2-octanol, tert-butanol, n-butylchloride and bromide and tert-butylchloride over a temperature range of 14-50°C and pressure of 1 - 200 atms. showed that the average number of molecules per chain of polymerized tert-butanol varies between ∿2-4,

Clemett and Davies (23) dielectrically studied the almost spherical, dipolar molecule isoborneol in the pure solid state and obtained fairly high activation enthalpy and entropy for molecular rotation in comparison to the corresponding rigid molecule bornyl chloride as:

Molecule	ΔH_E (kJ mol^{-1})	ΔS_E (J K^{-1} mol^{-1})
isoborneol	23 ± 0.4	25.5 ± 1.7
bornyl chloride	10.5	7.9

They also found some evidence that the energy barrier

increases with the decrease of temperature and suggested that this could be interpreted by intermolecular interaction. The excess energy is needed to overcome the total interaction of the hydroxyl group with its neighbouring molecules.

It is now well established that the molecular aggregation depends on (a) the concentration of the solute, (b) the nature of the dispersion medium and (c) the temperature of the system. The formation of aggregates in alcohols, especially in the simple spherical alcohols, like tert-butanol and its dielectric dispersion is still controversial. We studied some long-chain aliphatic normal alcohols and thiols in polystyrene matrices (Chapter IV) and found no evidence for hydrogen bonding in our low concentration range (∿5% by wt) which is logical and in line with Meakin's findings (24). It seems worthy to extend this study to some simple spherical alcohols in the pure state and in various glass forming dispersion medium, such as polystyrene, G.O.T.P., carbontetrachloride, etc. in different concentrations. We studied the effect of solute concentration on the relaxation parameters for non-associating, rigid, fairly polar, spherical molecules 1,1,1-trichloroethane and carbontetrachloride system (Chapter V). It will be interesting to extend this study for associating, the non-rigid, fairly polar, spherical molecule

tert-butanol and carbontetrachloride system. This type of study for simple systems may often lead to the solution of a complicated system.

VI-2: EXPERIMENTAL RESULTS

Both tert-butanol and carbontetrachloride were procured from the Aldrich Chemical Co. Although these chemicals were of high grade purity (above 99%) they were further dried and purified through fractional distillation before use. The measured boiling points and refractive indices showed good agreement with the literature values. All other chemicals were used without further purifications but properly dried prior to use. Dielectric measurements were done on a GR 1621 Precision Capacitance Measurement System using a three-terminal parallel plate capacitance and co-axial cell between 10 Hz and 10^5 Hz in the temperature range 77 K to 200 K and in some cases up to 300 K. The empty cell was tested from room temperature to liquid nitrogen temperature (for liquid sample) and it showed no observable dielectric loss at any frequency. Some of the samples were measured twice (both by heating and cooling) and each time the dielectric relaxation was observed almost at the same temperature region suggesting that the absorptions were not the consequence of cracks in the sample.

The apparatus and procedures employed in the dielectric measurements, and the preparation of samples

have been described in a previous chapter (Chapter II). The methods employed for the evaluation of relaxation and activation parameters have also been described previously (Chapter II).

Table VI-1 collects the values of ΔH_E, ΔS_E along with the ΔG_E and τ values at 100 K, 150 K and 200 K for each system where appropriate.

Experimental values of τ, $\log\nu_{max}$, β and ε''_{max} at various temperatures obtained for these systems are listed in Table VI-2.

Figures VI-1a to VI-7a show the sample plots of dielectric loss, ε'' versus T (K) for the dipolar molecules in the medium mentioned. Sample plots of ε'' versus $\log\nu$ are shown in Figures VI-8b to VI-18b while Figures VI-19c to VI-26c present the Cole-Cole plots for these molecules in their respective dispersion region. Sample plots of $\log T\tau$ versus 1/T for different systems are presented in Figures VI-27d to VI-38d. Figure VI-39 represents the variation of ε''_{max} with the concentration of solute at 1.01 kHz in carbontetrachloride.

FIGURE VI-1

1. NORBORNEOL

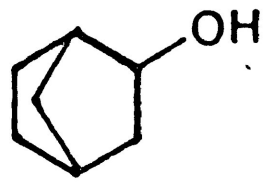

2. ISOBORNEOL

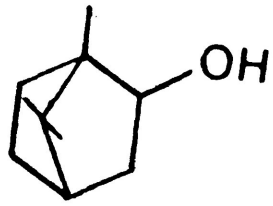

3. FENCHYL ALCOHOL

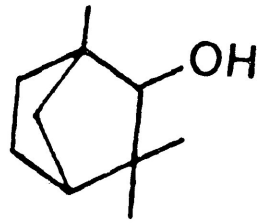

4. 5-NORBORNENE-2-CARBOXALDEHYDE

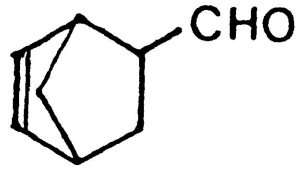

FIGURE VI-1: continued...

5. TERTIARY BUTANOL

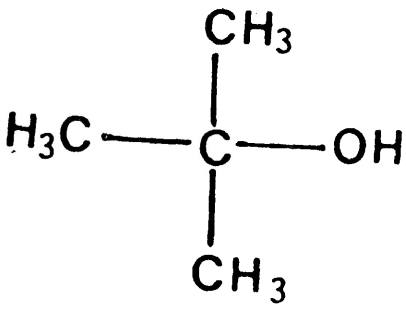

6. METHANOL

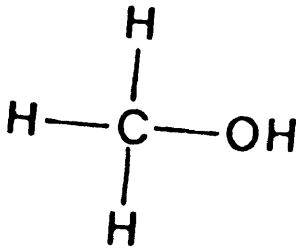

VI-3: DISCUSSION

1. Norborneol

This molecule has been studied in three different media, namely, polystyrene (5.82 % by wt), carbontetrachloride (6.58 % by wt) and G.O.T.P. (8.0 % by wt). In polystyrene and carbontetrachloride only one dispersion is found in the temperature range 80-98 K. The Fuoss-Kirkwood distribution parameter, β, for these dispersions ranges between 0.16-0.19. Such a low value of distribution parameter, β, indicates the wide distribution of relaxation times which is usual for molecular rotation of rigid molecules in various glass forming media (25-28). The relaxation parameters for norborneol in polystyrene matrix and carbontetrachloride are very close to those obtained for molecular rotation in the corresponding rigid molecules norcamphor (Chapter III):

Molecule	Media	τ (s) at 100 K	ΔG_E kJ mol^{-1} at 100 K	ΔH_E kJ mol^{-1}	ΔS_E J K^{-1} mol^{-1}
Norborneol	P.S.	1.7×10^{-5}	15	15	7
	CCl_4	6.8×10^{-6}	14	17	36
Norcamphor	P.S.	1.3×10^{-5}	14	15	12
	CCl_4	6.6×10^{-6}	14	17	29

These results appear to suggest that the dispersions of norborneol in polystyrene and carbontetrachloride are due to the molecular motion of the molecule and there are no intermolecular hydrogen bonding for these systems. This result is consistent with our long chain aliphatic alcohol and thiol results (see Chapter IV).

Two separate dispersion regions were exhibited by relatively higher concentration (8.0 % by wt) norborneol in G.O.T.P., one in the temperature range 85-99 K and the other 144-166 K. The Eyring plot, $\log T\tau$ versus 1/T, which is a clear straight line, yields the relaxation parameters for lower temperature dispersion as: ΔH_E = 13 kJ mol^{-1}, ΔS_E = -22 J K^{-1} mol^{-1} and ΔG_E = 16 kJ mol^{-1} and $\tau = 7.3 \times 10^{-5}$ s at 100 K. The β-value for this dispersion ranges between 0.16-0.18. Within experimental error, these parameters are very close to those for molecular rotation in similar-sized rigid molecule, norcamphor in G.O.T.P.: ΔH_E = 17 kJ mol^{-1}, ΔS_E = 16 J K^{-1} mol^{-1} and ΔG_E = 15.4 kJ mol^{-1} and $\tau = 5.4 \times 10^{-5}$ s at 100 K.(see Chapter III). These results appear to suggest that the lower temperature process obtained for norborneol in G.O.T.P. is due to the molecular rotation of the free monomer unit. The relatively higher enthalpy of activation 13 kJ mol^{-1} cannot be accounted for by OH group rotation. The reported enthalpy of activation for -OH group rotation

in 2,4,6-tri-t-butylphenol in the solid state, where there is significant contribution of conjugation and steric effect is 9.2 kJ mol^{-1} (29). Moreover, the low β-value (0.16-0.18) bears out the nature of molecular rotation for this dispersion.

The higher temperature dispersion for norborneol in G.O.T.P. yields the relaxation parameters: ΔH_E = 30 kJ mol^{-1}, ΔS_E = 31 J K^{-1} mol^{-1} and ΔG_E = 27 kJ mol^{-1} and τ = 9.4×10^{1} s at 100 K. The Fuoss-Kirkwood distribution parameter, β, for this process ranges between 0.12 - 0.23. Such a low β -value indicates the wide distribution of relaxation times which is usual for molecular rotation in various types of rigid molecules in different glassy media (25-28). But the observed activation parameters for this molecule does not appear to correspond to its size as might be expected for simple molecular rotation. The experimental ΔH_E of 30 kJ mol^{-1} for norborneol is significantly higher than the corresponding value of 17 kJ mol^{-1} for the similar-sized rigid molecule norcamphor (see Chapter III). These results appear to indicate that the higher temperature dispersion for norborneol in G.O.T.P. may be due to the breaking of one hydrogen bond followed by molecular rotation of the partially free monomer or owing to the rotation of dimer. This is not unreasonable because in this case slightly higher concentration and different dispersion medium than polystyrene and carbontetra-

chloride was used. These conditions might allow norborneol to form an equilibrium between monomer, dimer and multimer units in lower temperatures (liquid nitrogen).

The ΔH_E obtained for molecular rotation for two similar-sized molecules, 2-naphthol and 2-chloro-naphthalene in polystyrene matrices are 52 and 35 kJ mol^{-1} (30), respectively. The author explained the higher ΔH_E value for 2-naphthol as due to the intermolecular hydrogen bonding. Clemett and Davies (22) interpreted the higher ΔH_E value (23 kJ mol^{-1}) for molecular rotation in isoborneol in comparison to the similar-sized rigid molecule bornyl chloride (10.5 kJ mol^{-1}) in the pure solid state as for the intermolecular hydrogen bonding in isoborneol. We estimated an approximate hydrogen bond strength in alcohol as 13 kJ mol^{-1} (see Chapter IV). If this is taken into account then the 30 kJ mol^{-1} energy barrier for molecular rotation for norborneol in G.O.T.P. is understandable as: 13 kJ mol^{-1} of energy is spent for the breaking of one hydrogen bond and the rest, 17 kJ mol^{-1}, for molecular rotation which is the same for the similar-sized rigid molecule, norcamphor in G.O.T.P. (see Chapter III).

2. Isoborneol

This molecule was previously studied in the pure

solid state by Clemett and Davies (22) and obtained activation enthalpy and entropy as 23 kJ mol^{-1} and 25.5 J K^{-1} mol^{-1}, respectively. They found that the ΔH_E value and the distribution of relaxation time increases with the decrease of temperature. The ΔH_E value is also higher than the corresponding similar-sized rigid molecule, bornyl chloride (10.5 kJ mol^{-1}). These were attributed as to be due to the intermolecular interaction which increases in the solid state as the temperature falls.

Present dielectric investigation of this molecule in a polystyrene matrix shows only one dispersion region in the temperature range 87-109 K. The Eyring plot, $\log T\tau$ versus 1/T, which is a clear straight line (Arrhenius behaviour) yields the relaxation parameters as ΔH_E = 18 kJ mol^{-1}, ΔS_E = 10 J K^{-1} mol^{-1} and ΔG_E = 17 kJ mol^{-1} and $\tau = 2.2 \times 10^{-4}$ s at 100 K, respectively. The β-value for this dispersion ranges between 0.17-0.19. Such a low β-value which indicates the wide distribution of relaxation times in polystyrene matrices is one of the important characteristics of a molecular process (24-17). The relaxation parameters obtained for this molecule are very close to those for molecular rotation in the similar-sized, rigid molecule, camphor in a polystyrene matrix (see Chapter III): ΔH_E = 18 kJ mol^{-1}, ΔS_E = 18 J K^{-1} mol^{-1}

and ΔG_E = 17 kJ mol^{-1} and $\tau = 2.2 \times 10^{-4}$ s at 100 K. These results indicate that there is no intermolecular hydrogen bonding in isoborneol in polystyrene matrix in our concentration range and the dispersion is purely due to a molecular rotation. This finding supports Davies' (23) point that the higher ΔH_E value in isoborneol for molecular rotation in the pure solid state is due to the intermolecular hydrogen bonding. This is also in line with our results for long-chain aliphatic alcohols and thiols in polystyrene matrices (see Chapter IV) and norborneol in different media.

3. Fenchyl alcohol

This molecule exhibits only one dielectric dispersion in a polystyrene matrix in the temperature range 114-127 K. The Fuoss-Kirkwood distribution parameter, β, for this relaxation process varies between 0.14-0.15 which is usual for molecular rotation of rigid molecules in polystyrene matrices. The relaxation parameters obtained for this dispersion are very close to those for molecular rotation of similar-sized rigid molecule 1-fenchone (see Chapter III) as:

Molecule	ΔH_E KJ mol^{-1}	ΔS_E J K^{-1} mol^{-1}	ΔG_E kJ mol^{-1} at 100 K	τ (s) at 100 K
fenchyl alcohol in PS	24	29	21	4.6×10^{-2}
1-fenchone (PS)	23	31	20	1.4×10^{-2}
(G.O.T.P.)	20	-7	21	3.3×10^{-2}

These results appear to indicate that there is no intermolecular hydrogen bonding in fenchyl alcohol in polystyrene matrix and the relaxation process is due to the molecular rotation of the molecule in polystyrene cavity.

4. 5-Norbornene-2-carboxaldehyde

This molecule containing a flexible group (-CHO) exhibits only one relaxation process in a polystyrene matrix in the temperature range 91-106 K. The β-value for this dispersion ranges between 0.17-0.19. The relaxation parameters obtained for this dispersion are: ΔH_E = 18 kJ mol^{-1}, ΔS_E = 20 J K^{-1} mol^{-1} and ΔG_E = 16 kJ mol^{-1} and $\tau = 1.5 \times 10^{-4}$ s at 100 K. The Eyring plot, log$T\tau$ versus 1/T is a clear straight line which dismisses the possibility of overlapping processes. The relaxation parameters for this molecule are very close to those for the molecular rotation of camphor, an almost similar-sized rigid molecule (see Chapter III) and isoborneol in polystyrene matrices. These facts bear out that the relaxation process obtained for this flexible molecule may be due to the whole molecule rotation but not owing to the intramolecular rotation of the -CHO group. This group rotation may then be below the liquid nitrogen temperature for our frequency range. The low β-value (0.17-0.19) for this dispersion is in support of the molecular but not the intramolecular nature of the process in polystyrene matrix.

5. Methanol and tert-butanol

We did not find any indication of intermolecular hydrogen bonding in various types of alcohols and thiols (see Chapter IV) in polystyrene matrices in the usual concentration range of ∿0.5 M (5 %). These two simple alcohols have been studied in polystyrene matrices relatively at higher concentration ranges (above 1.0 M ∿10 %). In each case one dielectric dispersion was obtained in the temperature range 210-263 K with an indication of another process below the liquid nitrogen temperature. The β-value for these dispersions ranges between 0.24-0.33. The relaxation parameters obtained for these two molecules are surprisingly almost similar: ΔH_E = 47 kJ mol^{-1}, ΔS_E = 26 and 21 J K^{-1} mol^{-1}, ΔG_E at 100 K = 45 kJ mol^{-1} and τ at 100 K = 1.0 and 1.1×10^{11} s, respectively. These dispersions have different characteristics from those of an α-process. In fact these dispersions satisfy the characteristics of a β-process, namely, broad symmetric loss curve, less sensitivity of ν_{max} to temperature, linear Eyring plot and relatively small ΔH_E value. These observations cannot be accounted for by the intramolecular OH group rotation. The relaxation parameters obtained for these molecules do not appear to correspond to their size as might be expected for simple

molecular rotation. These dispersions cannot be interpreted simply as owing to the presence of moisture as impurity in the sample. Before making the disk both the samples were properly dried, distilled and middle fraction were collected for experiment. The dielectric loss obtained for these dispersions are of the order $\sim 4 \times 10^{-3}$ .. Desando et al (31) reported dielectric loss peak for moisture impurity, in poly (ethylmethacrylate), Santovac® and G.O.T.P. in the temperature region below 210 K at 1 kHz. Methanol and tert-butanol absorption peak at 1 kHz in polystyrene matrices are around 238 K. The relaxation parameters obtained for moisture impurity are: ΔH_E = 44 kJ mol^{-1}, ΔS_E = 41 J K^{-1} mol^{-1}, $\Delta G_{E(150\ K)}$ = 38 kJ mol^{-1}, $\tau_{(150\ K)} = 7.6 \times 10^{0}$ s, β = 0.38-0.67 (for 0.2 % water in G.O.T.P.); ΔH_E = 43 kJ mol^{-1}, ΔS_E = 38 J K^{-1} mol^{-1}, $\Delta G_{E(150\ K)}$ = 37 kJ mol^{-1}, $\tau_{(150\ K)} = 3.3 \times 10^{0}$ s and β = 0.59-0.86 (for 0.7 % water in Santovac®); ΔH_E = 38 kJ mol^{-1}, ΔS_E = 8 J K^{-1} mol^{-1}, $\Delta G_{E(200\ K)}$ = 36 and $\tau_{(200\ K)} = 6.4 \times 10^{-4}$ s (for moisture in polyethylmethacrylate). All these relaxations exhibited by moisture impurity have a higher β-value (0.38-0.86) and lower relaxation times in comparison to those of methanol and tert-butanol in polystyrene matrices. The ΔH_E and ΔG_E are also lower for moisture impurity. The dielectric loss factor for 0.2% and 0.67% moisture in G.O.T.P. and Santovac® are $\sim 3 \times 10^{-3}$ and $\sim 2 \times 10^{-3}$ which are much lower than those for methanol and tert-butanol ($\sim 4 \times 10^{-3}$) in poly-

styrene matrices. Moreover, it is highly improbable that dried and purified alcohol can contain such a high amount of moisture impurity which lead to dielectric absorption of the order $4x10^{-3}$.

Musa and Eisner (18) reported ΔH_E = 64.4 kJ mol^{-1} for tetramer rotation in pure tert-butanol in the liquid state by an ultrasonic technique. Dwivedi et al (21) dielectrically studied tert-butanol and tert-amyl alcohol in the pure liquid state and found ΔH_E = 50.3 and 50.8 kJ mol^{-1}, respectively. They interpreted their results in terms of breaking the hydrogen bond followed by ROH rotation and the rotation of the free monomer simultaneously. From all of these results it appears to suggest that the dispersions obtained for methanol and tert-butanol in polystyrene matrices at higher concentation may be due to either (a) the rotation of multimer or (b) the breaking of hydrogen bond (more than one) followed by rotation of partially free monomer; or (c) breaking of hydrogen bond (one) followed by rotation of the higher species than monomer; or (d) a combination of (b) and (c).

The results obtained for methanol and tert-butanol in polystyrene matrices are not inconsistent with our previous results for other alcohols. In those cases we used a concen-

tration range of around 5 % (by wt.) but here the concentration was above 10 %. These results support Meakin's (24) view that at around 5 % concentration alcohol molecules will be widely separated from one another by the solvent molecules and there will be no hydrogen bonding but at and above 10 % concentration intermolecular hydrogen bonding will occur which may lead to the formation of multimers.

In the pure solid state tert-butanol exhibits only one dielectric relaxation process in the temperature range 116-146 K. As evident from ε'' versus T plot (Figure VI-6a), the dielectric loss increases rapidly with temperature after this dispersion range and ultimately goes beyond our measurement limit. This may be due to conductivity which is reported for some lower alcohols (32) and, in particular, in cyclopentanol and cyclohexanol (33) in the pure solid state owing to a proton jumping process. The relaxation process obtained for tert-butanol seems not to be completely free from the conductivity influence particularly the higher temperature part which is evident from the non-linear Eyring plot, $\log T\tau$ versus 1/T (Figure VI-35d). The lower temperature slope which is reasonably free from conductivity influences yields the relaxation parameters as: ΔH_E = 18 kJ mol^{-1}, ΔS_E = -41 JK^{-1} mol^{-1} and ΔG_E = 22 kJ mol^{-1} and $\tau = 1.5 \times 10^{-1}$ s at 100 K,

respectively. This dispersion exhibited by tert-butanol in the pure solid state has different characteristics from those of an α-process. In fact it satisfies the criteria which chacterizes a β-process, namely, very broad symmetric loss curves, less sensitivity of ν_{max} to temperature, semi-circular Cole-Cole plot and relatively small ΔH_E values. This process having a ΔH_E value of 18 kJ mol^{-1} cannot be accounted for by the intramolecular OH group rotation. The energy barrier obtained for the OH group rotation in 2,4,6-tri-tert-butylphenol is 9.2 kJ mol^{-1} in the pure solid state (29) and 12.4 kJ mol^{-1} in tri-cyclohexyl carbinol in decalin solution (34). In both of these molecules the OH group is significantly influenced by conjugation and/or steric effect. In tert-butanol, there is no conjugation effect and the effect of steric factor on -OH group rotation is not so significant as in tricyclohexyl carbinol.

tert-Butanol is comparable in size and shape to tert-butyl chloride, tert-butyl bromide and 2-methyl-2-nitropropane. The reported ΔH_E for molecular rotation in the pure solid state for these molecules are 5.4, 6.3, and 6.7 kJ mol^{-1}, respectively (35). The ΔH_E value of 18 kJ mol^{-1} obtained for tert-butanol is significantly higher

for molecular rotation in comparison to those of similar-sized rigid molecules. These results appear to indicate that the relaxation obtained for tert-butanol in the pure solid state may be accounted for by the breaking of hydrogen bond (one) followed by molecular rotation of the partially free monomer. The negative value of activation entropy which indicates the more ordered activated state is in favour of the molecular rotation. The relatively higher β-value (0.28-0.53) may be accounted for by the spherical shape of the molecule for which a very narrow range of environment will be encountered by the molecule at any one temperature during rotation. This type of higher β-value for molecular rotation for fairly spherical molecules in the pure solid state have been reported by Hossain (36) as: 0.34-0.54 for tert-butyl bromide, 0.31-0.47 for methyl bromide and 0.24-0.41 for 2-methyl-2-nitropropane.

A mixture of tert-butanol and carbontetrachloride in various proportions (from 9.03-92.15 mol %) exhibits only one relaxation process for each system within the temperature range 113-146 K (Figure VI-7a). The magnitude of the relaxation peaks depend on the concentration but there is a negligible change in the temperature of the peak with change in concentration. The dielectric relaxation parameters for these dispersions over this wide concentration

range are: ΔH_E = 24-26 kJ mol^{-1}, ΔS_E = 10-39 J K^{-1} mol^{-1} and ΔG_E = 22-24 kJ mol^{-1} and τ = 1.5×10^{-1} - 2.4×10^{0} s at 100 K, respectively. It is remarkable that ΔH_E and ΔG_E stay virtually constant over this wide concentration range. This bears out that we are dealing with the same process over this concentration range. This type of behaviour is found for 1,1,1-trichloroethane and carbontetrachloride mixture (see Chapter V) and reported by Mansingh (37) for chlorobenzene in cis-decalin. These dispersions exhibited by tert-butanol in carbontetrachloride have different characteristics from those of an α-process. In fact they satisfy the criteria which characterize a β-process in glassy media, namely, broad symmetric loss curves, linear Eyring plot, semicircular Cole-Cole plot, less sensitivity of ν_{max} to temperature and relatively small ΔH_E values. These observations, especially, the high activation parameters cannot be accounted for by intramolecular -OH group rotation. Within experimental error, the relaxation parameters for these mixtures are very close to those for the pure tert-butanol in the solid state. The slight variation in the case of the pure compound may be due to higher uncertainty in their estimation from the limiting slope to avoid the conductivity effect. The Fuoss-Kirkwood distribution parameter, β, for all these mixtures ranges between 0.27-0.47. These results appear

to suggest that the same species are responsible for these dispersions both in the pure state and in carbontetrachloride solutions. This means that in carbontetrachloride medium the relaxation may be accounted for by the breaking of the hydrogen bond (one) followed by a partially free monomer rotation. This is reasonable since 24 kJ mol^{-1} of energy is too small to break more than one hydrogen bond. These dispersions cannot be accounted for by dimer rotation. At room temperature we did not find any i.r. peak for dimer at around 3530 cm^{-1} (20) but obtained a very broad band at around 3355 cm^{-1} for multimer (19) for the lowest concentration solution and a very weak peak at around 3670 cm^{-1}. The intensity of the latter peak decreases and the 3355 cm^{-1} peak increases with the increase of concentration. Our equipment temperature was much lower than the room temperature (liquid nitrogen temperature) where the possibility of formation of multimer was even much greater than that of the dimer. The β-value for these relaxations though relatively high (0.27-0.47) is not unreasonable in comparison with those obtained for molecular rotation of the rigid spherical molecule norcamphor (0.28-0.37) and 1,1,1-trichloroethane (0.26-0.80) in carbontetrachloride (see Chapter III and Chapter V). The ΔS_E values of 10-39 J K^{-1} mol^{-1} for all these mixtures are comparable to those for molecular rotation of other spherical rigid molecules (see

Chapter III).

The formation of multimers in carbontetrachloride by tert-butanol is not inconsistent with our previous results for long-chain alcohols, thiols (see Chapter IV), and other spherical alcohols in polystyrene matrices. The lowest concentration we studied here was 0.9 M whereas in polystyrene matrices we studied a concentration of around 0.5 M. 1.0 M solution of methanol and tert-butanol in polystyrene matrices showed evidence of formation of multimers. These results are in agreement with Meakins (24). Moreover, the association of alcohol is highly dependent on the nature of the dispersion medium, e.g., the association constant for monomer-dimer equilibrium for tert-butanol in carbontetrachloride is 0.58 whereas in cyclohexane the association constant for monomer-tetramer equilibrium is 2.49×10^4 at room temperature (2).

The dielectric loss depends upon (a) the dipole moment of the solute (b) the number of dipoles in a certain volume and (c) the ease with which a dipole

can rotate. When a comparison is made of the dielectric data of pure tert-butanol and the solute in carbontetrachloride at various concentrations, an enormous difference is found in the ε''_{max} values (Figure VI-39). In the pure solid it is 1.7×10^{-3} whereas for the solute in carbontetrachloride the value is 19×10^{-3} for certain concentrations. Off hand the loss in the pure solid might have been anticipated to be the greatest since the number of polar molecules in a given volume would be much greater. From the Figure ε''_{max} versus concentration of solute it is observed that only at low concentration is

$$\varepsilon''_{max} \propto \text{concentration}$$

and that at higher concentrations it begins to decrease and thus, as the case of the pure solid is approached the loss factor may be appreciably lower than the value for a 7 mol % concentration, a typical measurement concentration.

It would seem feasible that at the high concentrations where molecular interaction would be the greatest either (a) relatively few molecules are permitted to break the hydrogen bond followed by molecular rotation or (b) the molecules are permitted to turn through a very limited angle after breaking the hydrogen bond or (c) a combination of (a) and (b).

REFERENCES

1. G.C. Pimental and A.L. McClellan, "The Hydrogen Bond", W. H. Freeman and Co., London, 1960.

2. Symposium on Hydrogen Bonding, Ljubljana, Pergamon Press, London, 1957.

3. W. Dannhauser, L. W. Bahe, R. Y. Lin and A. F. Flueckinger, J. Chem. Phys., 43, 257(1965).

4. S. K. Garg and C. P. Smyth, J. Phys. Chem., 69, 1294(1965).

5. S. K. Garg and C. P. Smyth, J. Chem. Phys., 46, 373(1967).

6. W. Dannhauser, J. Chem. Phys., 48, 1918(1968).

7. P. Bordewijk, F. Granschandand and C. J. F. Böttcher, J. Phys. Chem., 73, 3255(1969).

8. G. P. Johari and C.P. Smyth, J. Am. Chem. Soc., 91, 6215(1969).

9. J. Crossley, L. Glasser and C. P. Smyth, J. Chem. Phys., 52, 6203(1970).

10. J. Crossley, Can. J. Chem., 49, 712(1971).

11. J. Crossley, J. Phys. Chem., 75, 1790(1971).

12. L. Glasser, J. Crossley and C. P. Smyth, J. Chem. Phys., 57, 3977(1972).

13. J. Crossley, Can. J. Chem., 56, 352(1978).

14. J. Crossley, Adv. Mol. Relax. Processes, 2, 69(1970).

15. E. Jakusek and L. Sobezyk, Dielectric and Related Molecular Processes (Specialist Periodical Reports), The Chemical Society, 3, 108(1976).

16. S. M. Khameshara, M. S. Kavadia, M. S. Lodha, D. C. Mathur and V. K. Vaidya, J. Mol. Liquids, 26, 77(1983).

17. M. Sanders and J. B. Hyne, J. Chem. Phys., 29, 1319(1958).

18. R. S. Musa and M. Eisner, J. Chem. Phys., 30, 227(1959).

19. J. Errera, R. Gaspart and H. Sack, J. Chem. Phys., 8, 63(1940).

20. H. A. Kozodziej and Z. Malarski, Adv. Mol. Relax. Inter. Processes, 19, 61(1981).

21. D. C. Dwivedi, S. C. Srivastava, P. Kumar and S. L. Srivastava, Indn. J. Pure and Applied. Phys., 19, 650(1981).

22. F. E. Harris, E. W. Haycock and B. J. Alder, J. Chem. Phys., 21, 1943(1953).

23. C. Clemett and M. Davies, Trans. Faraday Soc., 58, 1705(1962).

24. R. J. Meakins, Trans. Faraday Soc., 58, 1953(1962).

25. H. A. Khwaja, M.Sc. Thesis, Lakehead University, Thunder Bay, Ontario, Canada, (1978).

26. M. A. Kashem, M. Sc. Thesis, Lakehead University, Thunder Bay, Ontario, Canada, (1982).

27. S. P. Tay and S. Walker, J. Chem. Phys., 63, 1634(1975).

28. M. A. Mazid, M.Sc. Thesis, Lakehead University, Thunder Bay, Ontario, Canada, (1977).

29. R. J. Meakins, Trans. Faraday Soc., 52, 320(1956).

30. M. A. Enayetullah, M.Sc. Thesis, Lakehead University, Thunder Bay, Ontario, Canada, (1981).

31. M. A. Desando, M. A. Kashem, M. A. Siddiqui and S. Walker, J. Chem. Soc. Faraday Trans. II, (1984).

32. N. E. Hill, W. E. Vaughan, A. H. Price and M. Davies, "Dielectric Properties and Molecular Behaviour", Van Nostrand Reinhold Company, London, (1969), pp. 407.

33. G. Corfield and M. Davies, Faraday Soc. Trans., 60, 10(1964).

34. M. Davies and R. J. Meakins, J. Chem. Phys., 26, 1584(1957).

35. M. Godlewska, M. Massalska-Arodz and S. Urban, Phys. Stat. Sol. (a), 73, 65(1982).

36. M. S. Hossain, M.Sc. Thesis, Lakehead University, Thunder Bay, Ontario, Canada (1982).

37. A. Mansingh, C. B. Agarwal and R. Singh, Indn. J. Pure and Applied Phys., 18, 583(1980).

TABLE VI-1: Eyring Analysis Results for some Simple Alcohols and Related Compounds in different Glassy Media

Molecule	Medium	Temperature Range (K)	Relaxation Time τ(s)			ΔG_E (kJ mol^{-1})			ΔH_E	ΔS_E
			100 K	150 K	200 K	100 K	150 K	200 K	kJ mol^{-1}	J K^{-1} mol^{-1}
Norborneol	PS	80-98	1.7×10^{-5}	2.7×10^{-8}	9.6×10^{-10}	15	14	14	15±1.2	7±13
	CCl_4	80-90	6.8×10^{-6}	4.5×10^{-9}	1.0×10^{-10}	14	12	10	17±1.5	36±18
	GOTP	85-99	7.3×10^{-5}	2.3×10^{-7}	1.2×10^{-8}	16	17	18	13±1.0	-22±10
	GOTP	144-166	9.4×10^{1}	3.2×10^{-4}	5.3×10^{-7}	27	26	24	30±2.7	31±17
Isoborneol	PS	87-109	2.2×10^{-4}	1.3×10^{-7}	2.9×10^{-9}	17	16	16	18±1.1	10±12
Fenchyl alcohol	PS	114-127	4.6×10^{-2}	2.1×10^{-6}	1.3×10^{-8}	21	20	18	24±4.0	29±35
5-Norbornene-2-carboxaldehyde	PS	91-106	1.5×10^{-4}	6.7×10^{-8}	1.3×10^{-9}	16	15	14	18±1.4	20±14
tert-Butanol	PS	215-263	1.0×10^{11}	5.2×10^{2}	3.3×10^{-2}	45	44	43	47±2.2	21±10
Methanol	PS	210-252	1.1×10^{11}	4.3×10^{2}	2.4×10^{-2}	45	43	42	47±3.0	26±13
tert-Butanol in carbontetrachloride	Concentration in mol%									
	Pure	116-128	1.5×10^{-1}	7.7×10^{-5}	1.6×10^{-6}	22	24	26	18±2.8	-41±23
	92.15	113-138	1.5×10^{-1}	3.0×10^{-6}	1.3×10^{-8}	22	20	18	26±0.5	39± 4
	87.30	111-140	1.6×10^{-1}	6.6×10^{-5}	3.8×10^{-7}	22	21	20	24±0.3	22±2
	83.50	121-149	8.0×10^{0}	2.3×10^{-5}	1.2×10^{-7}	23	23	22	25±0.7	17±5
	71.22	119-151	1.2×10^{0}	3.0×10^{-5}	1.4×10^{-8}	24	23	22	25±0.4	16±3
	64.42	118-148	6.2×10^{-1}	1.7×10^{-5}	8.3×10^{-7}	23	22	21	25±0.5	20±4
	50.00	126-153	1.4×10^{0}	3.9×10^{-5}	1.8×10^{-7}	24	23	23	25±0.6	14±5
	33.42	122-156	2.4×10^{0}	4.5×10^{-5}	1.8×10^{-7}	24	23	23	26±1.0	18±7
	24.80	122-156	1.0×10^{0}	3.5×10^{-5}	1.9×10^{-7}	24	23	23	25±1.5	10±11
	9.03	120-146	8.8×10^{-1}	2.8×10^{-5}	1.5×10^{-7}	24	23	22	25±0.4	13±3

TABLE VI-2: Tabulated Summary of Fuoss-Kirkwood Analysis Parameters for some Simple Alcohols and Related Compounds in Different Glassy Media.

T(K)	$10^6\tau$(s)	$\log\nu_{max}$	β	$10^3\epsilon''_{max}$
0.54M Norborneol in a polystyrene matrix				
80.7	1473	2.03	0.18	13.2
83.5	743	2.33	0.17	13.7
85.2	503	2.50	0.17	14.0
87.5	298	2.73	0.17	14.3
89.5	184	2.94	0.16	14.6
94.5	49.5	3.51	0.16	15.2
98.0	23.7	3.83	0.18	15.9
0.80 M Norborneol in GOTP		Lower Temperature Process		
82.2	2105	1.88	0.18	3.9
83.6	1672	1.98	0.18	3.9
85.3	1281	2.09	0.18	4.0
87.1	900	2.25	0.18	4.1
90.0	475	2.53	0.18	4.3
91.8	350	2.66	0.18	4.3
93.2	271	2.77	0.17	4.4
95.0	195	2.91	0.17	4.5
96.8	121	3.12	0.17	4.5
99.5	72.6	3.34	0.16	4.7
0.80 M Norborneol in GOTP		Higher Temperature Process		
145.0	845	2.28	0.12	5.1
150.8	248	2.81	0.15	5.4
153.7	169	2.97	0.17	5.5
157.6	67	3.37	0.17	5.6
160.4	56.3	3.45	0.20	5.7
163.2	40.4	3.60	0.21	5.8
165.1	31.3	3.71	0.21	5.9
166.9	26.6	3.78	0.23	6.0

TABLE VI-2: continued... (page 2 of Table VI-2)

T(K)	$10^6\tau$(s)	$\log \varepsilon''_{max}$	β	$10^3\varepsilon''_{max}$
0.60 M Norborneol in Carbontetrachloride				
79.6	1430	2.05	0.19	1.2
80.6	1205	2.12	0.18	1.2
82.0	883	2.26	0.16	1.2
83.1	542	2.47	0.16	1.2
85.6	263	2.78	0.17	1.3
87.7	133	3.08	0.16	1.3
90.1	78.0	3.31	0.19	1.4
0.47 M Isoborneol in a polystyrene matrix				
87.7	5549	1.46	0.18	17.2
89.2	2768	1.76	0.18	17.6
90.3	1902	1.92	0.19	17.8
92.5	1322	2.08	0.18	18.4
95.0	756	2.32	0.18	18.9
97.6	430	2.57	0.18	19.4
100.8	225	2.85	0.18	20.1
103.8	106	3.17	0.17	20.5
107.0	48.3	3.52	0.18	21.2
109.2	31.4	3.70	0.18	21.6
0.60 M Fenchyl Alcohol in polystyrene				
109.5	2357	1.83	0.14	9.7
112.2	1434	2.05	0.15	10.0
114.7	995	2.20	0.14	10.2
117.4	515	2.49	0.14	10.4
120.1	313	2.71	0.15	10.6
123.7	173	2.96	0.15	10.9
127.4	66.2	3.38	0.15	11.1

TABLE VI-2: continued... (page 3 of Table VI-2)

T(K)	$10^6\tau$(s)	$\log\nu_{max}$	β	$10^3\varepsilon''_{max}$
0.53 M 5-Norbornene-2-carboxaldehyde				
91.6	1118	2.15	0.17	26.0
93.9	753	2.32	0.17	26.4
95.2	472	2.53	0.18	26.9
97.2	304	2.72	0.18	27.5
100.2	160	3.00	0.18	28.2
104.0	60.7	3.42	0.18	29.0
105.8	41.1	3.59	0.19	29.5
1.06 M tert-butyl-alcohol in a polystyrene matrix				
215.4	3847	1.62	0.24	4.0
219.3	2337	1.83	0.25	4.0
223.5	1402	2.06	0.26	4.0
228.7	1023	2.19	0.26	4.0
235.7	420	2.58	0.28	3.9
242.3	203	2.89	0.29	3.8
248.0	115	3.14	0.30	3.7
256.0	51.6	3.49	0.31	3.6
263.5	26.7	3.78	0.33	3.6
Methanol in a polystyrene matrix ($\sim$1.5 M)				
210.5	4124	1.59	0.24	4.2
213.0	3130	1.71	0.25	4.2
216.2	2683	1.77	0.24	4.1
219.7	1523	2.02	0.24	4.1
225.1	807	2.30	0.26	4.0
229.7	505	2.50	0.27	4.0
235.3	285	2.75	0.27	3.9
241.0	163	2.99	0.29	3.9
246.5	88.1	3.26	0.30	3.8
253.0	47.2	3.53	0.33	3.8

TABLE VI-2: continued... (page 4 of Table VI-2)

T(K)	$10^6\tau$(s)	$\log\nu_{max}$	β	$10^3\varepsilon''_{max}$
10.6 M tert-Butanol (pure)				
116.4	6101	1.42	0.53	1.7
119.4	4075	1.59	0.49	1.7
121.9	2365	1.83	0.50	1.7
125.5	1470	2.03	0.46	1.7
128.5	1016	2.19	0.45	1.7
133.5	608	2.42	0.44	1.7
140.8	377	2.63	0.34	1.7
145.7	287	2.74	0.28	1.7
9.75 M tert-Butanol in Carbontetrachloride (92.15 mol%)				
113.2	3367	1.67	0.42	10.0
115.4	1919	1.92	0.41	10.2
118.3	1062	2.18	0.39	10.3
120.2	674	2.37	0.38	10.3
123.7	320	2.70	0.37	10.4
126.8	161	3.00	0.35	10.4
129.4	99.4	3.20	0.36	10.5
132.0	60.2	3.42	0.34	10.5
134.8	35.4	3.65	0.33	10.7
137.5	21.0	3.88	0.31	10.7
9.23 M tert-Butanol in carbontetrachloride (87.3 mol%)				
111.2	6460	1.39	0.43	10.6
114.2	3685	1.64	0.40	10.7
117.0	2160	1.87	0.40	10.8
120.8	1010	2.20	0.34	10.9
124.3	468	2.53	0.33	11.0
127.0	286	2.75	0.30	11.0
129.7	161	3.00	0.28	11.0
132.6	97.0	3.22	0.30	11.2
136.5	45.6	3.54	0.28	11.4
140.1	24.7	3.81	0.27	11.5

TABLE VI-2: continued... (page 5 of Table VI-2)

T(K)	$10^6\tau$(s)	$\log \nu_{max}$	β	$10^3\varepsilon''_{max}$
8.82 M tert-Butanol in Carbontetrachloride (83.5 mol %)				
120.8	3581	1.65	0.32	13.7
123.6	2030	1.89	0.31	14.0
126.5	1147	2.14	0.30	14.1
129.9	602	2.42	0.29	14.3
133.0	356	2.65	0.28	14.5
137.9	168	2.98	0.27	14.6
139.9	100	3.20	0.28	14.9
143.2	60.1	3.42	0.28	15.1
146.3	38.8	3.61	0.28	15.4
148.8	27.4	3.76	0.29	15.5
7.50 M tert-Butanol in Carbontetrachloride (71.22 mol %)				
118.8	7121	1.35	0.38	16.6
121.0	4994	1.50	0.35	16.7
123.7	2773	1.76	0.34	17.0
125.8	1840	1.94	0.33	17.2
129.8	853	2.27	0.32	17.5
133.7	410	2.59	0.31	17.9
137.5	213	2.87	0.31	18.1
140.3	127	3.10	0.30	18.2
145.3	57.8	3.44	0.31	18.7
147.9	39.0	3.61	0.33	19.0
151.3	25.8	3.79	0.34	19.2
6.78 M tert-Butanol in Carbontetrachloride (64.42 mol %)				
118.0	5096	1.49	0.35	13.1
122.0	2099	1.88	0.33	13.5
124.0	1498	2.03	0.32	13.5
126.0	975	2.21	0.32	13.6
129.0	537	2.47	0.31	13.9
131.5	342	2.67	0.30	14.0
134.2	206	2.89	0.29	14.1
137.3	116	3.14	0.30	14.3
141.7	55.8	3.45	0.30	14.6
145.3	32.8	3.69	0.31	14.8
148.4	23.4	3.83	0.33	15.0

TABLE VI-2: continued... (page 6 of Table VI-2)

T(K)	$10^6\tau$(s)	$\log\nu_{max}$	β	$10^3\varepsilon''_{max}$
5.24 M tert-Butanol in Carbontetrachloride (50 mol %)				
126.1	2167	1.87	0.31	8.4
128.0	1459	2.04	0.31	8.5
130.1	1001	2.20	0.31	8.6
133.2	562	2.45	0.31	8.8
135.0	408	2.59	0.30	8.8
139.0	204	2.89	0.31	9.1
142.8	106	3.18	0.32	9.3
147.4	51.6	3.49	0.32	9.5
150.1	40.2	3.60	0.35	9.7
153.4	25.6	3.79	0.35	9.9
3.49 M tert-Butanol in Carbontetrachloride (33.42 mol %)				
122.0	7609	1.32	0.32	4.2
126.2	2673	1.77	0.35	4.3
128.9	1607	2.00	0.35	4.4
132.2	862	2.27	0.36	4.5
136.0	422	2.58	0.36	4.6
140.0	203	2.89	0.38	4.7
146.0	78.5	3.31	0.38	4.9
149.7	44.5	3.55	0.38	5.0
153.6	25.0	3.80	0.37	5.1
156.4	22.5	3.85	0.41	5.2
2.58 M tert-Butanol in Carbontetrachloride (24.8 mol %)				
122.7	4145	1.58	0.34	3.4
125.0	2217	1.86	0.36	3.4
128.5	1112	2.16	0.37	3.5
131.2	628	2.40	0.38	3.6
135.7	286	2.75	0.39	3.7
139.3	153	3.02	0.40	3.7
143.2	83.3	3.28	0.41	3.8
146.8	47.2	3.53	0.41	3.9
150.7	38.8	3.61	0.47	4.0
155.6	19.5	3.91	0.45	4.0

TABLE VI-2: continued... (page 7 of Table VI-2)

T(K)	$10^6\tau$(s)	$\log \nu_{max}$	β	$10^3\varepsilon''_{max}$
0.94 M tert-Butanol in Carbontetrachloride (9.03 mol %)				
120.4	5862	1.43	0.26	0.80
122.9	2734	1.77	0.29	0.80
124.8	1729	1.96	0.30	0.80
127.2	1102	2.16	0.31	0.80
129.8	658	2.38	0.33	0.90
134.0	327	2.69	0.35	0.90
137.2	192	2.92	0.35	0.90
141.6	93.3	3.23	0.36	0.90
146.4	56.1	3.45	0.41	1.00

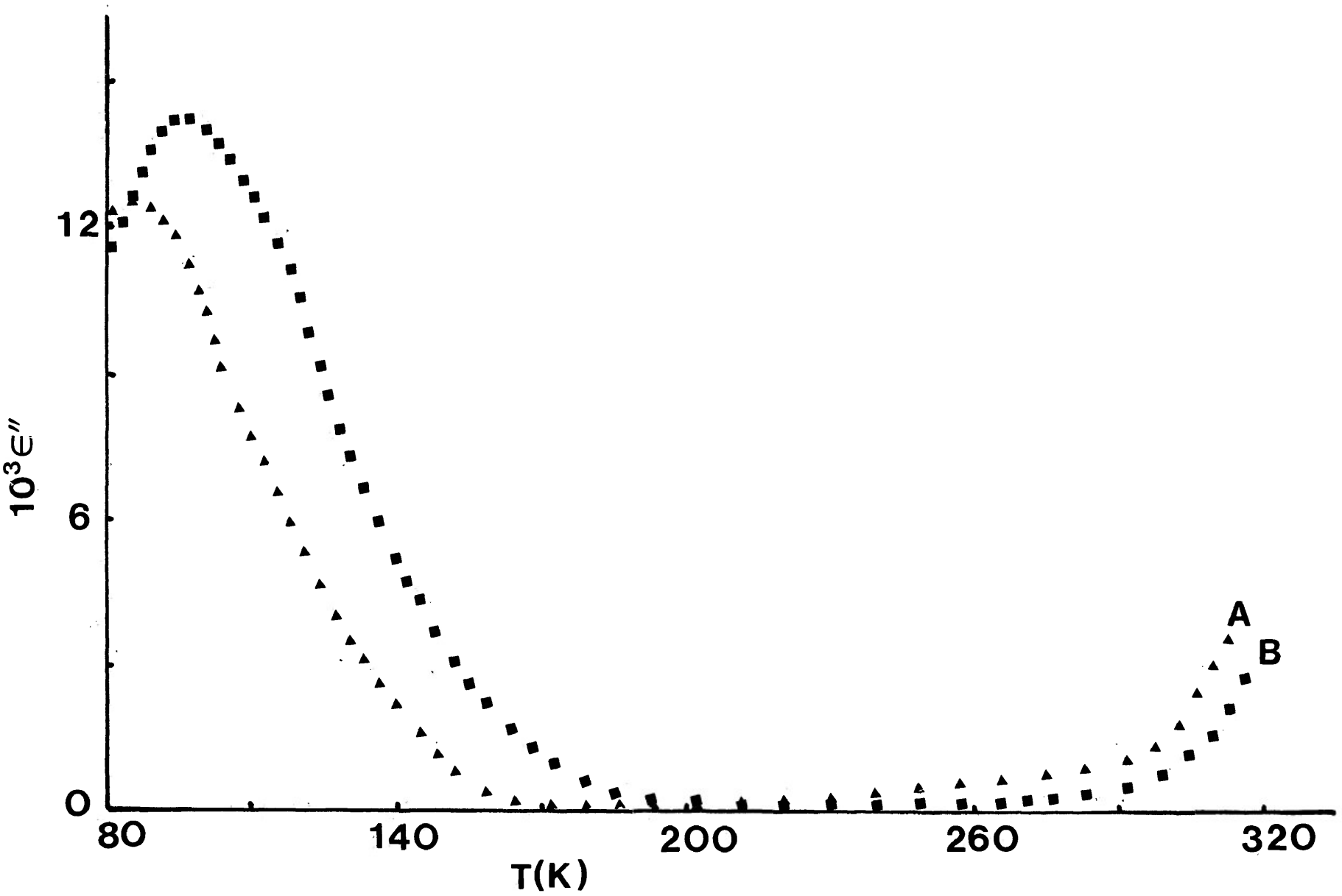

FIGURE VI-1a: Plots of dielectric loss factor, ϵ'' versus temperature (K) for norborneol in a polystyrene matrix. A=50.2 Hz, B=1.01 kHz.

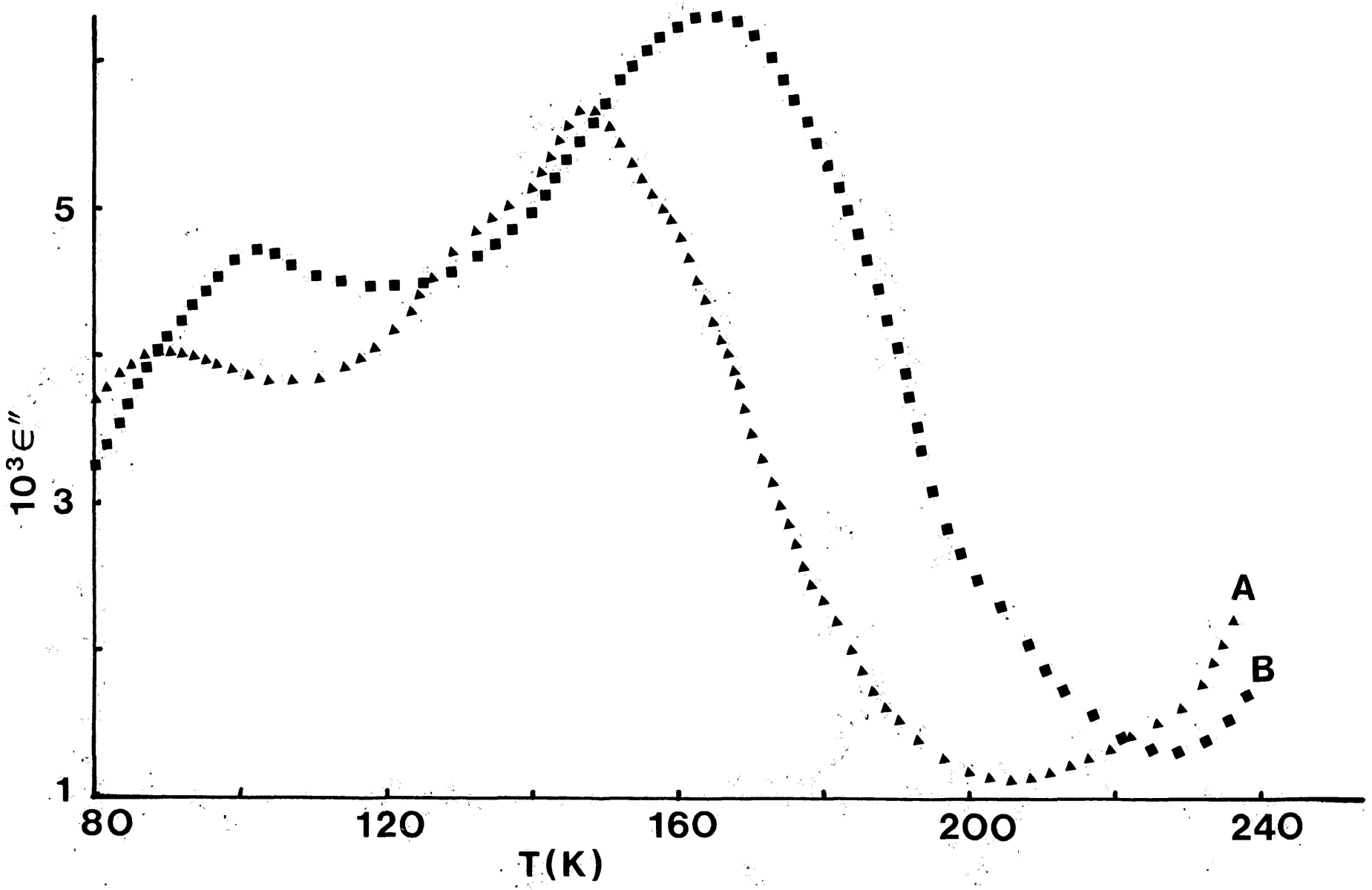

FIGURE VI-1a': Plots of dielectric loss factor, ε'' versus temperature (K) for norborneol in G.O.T.P. A=50.2 Hz, B=1.01 kHz.

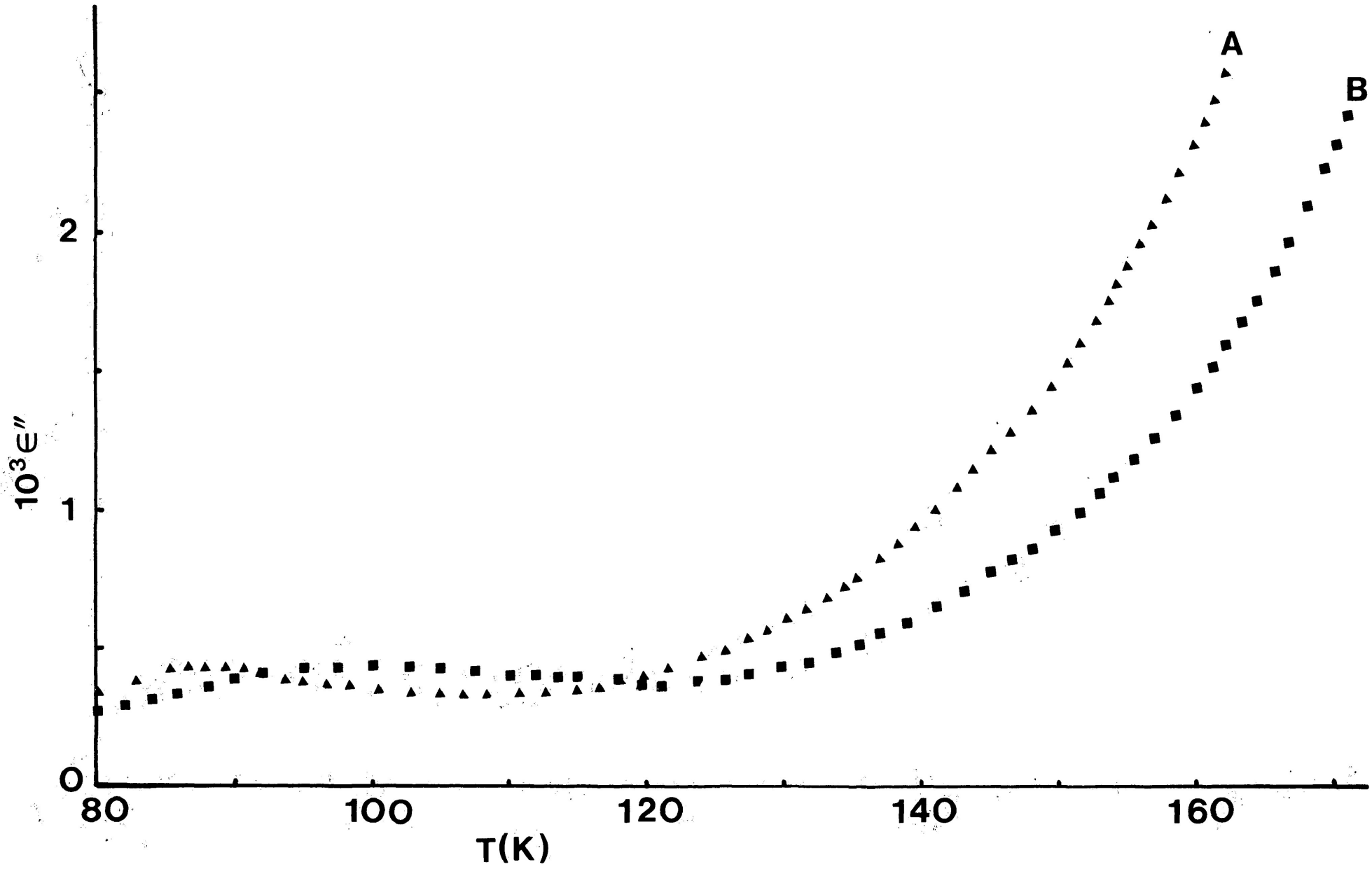

FIGURE VI-1a": Plots of dielectric loss factor, ε" versus temperature (K) for norborneol in carbontetrachloride. A=50.2 Hz, B=1.01 kHz.

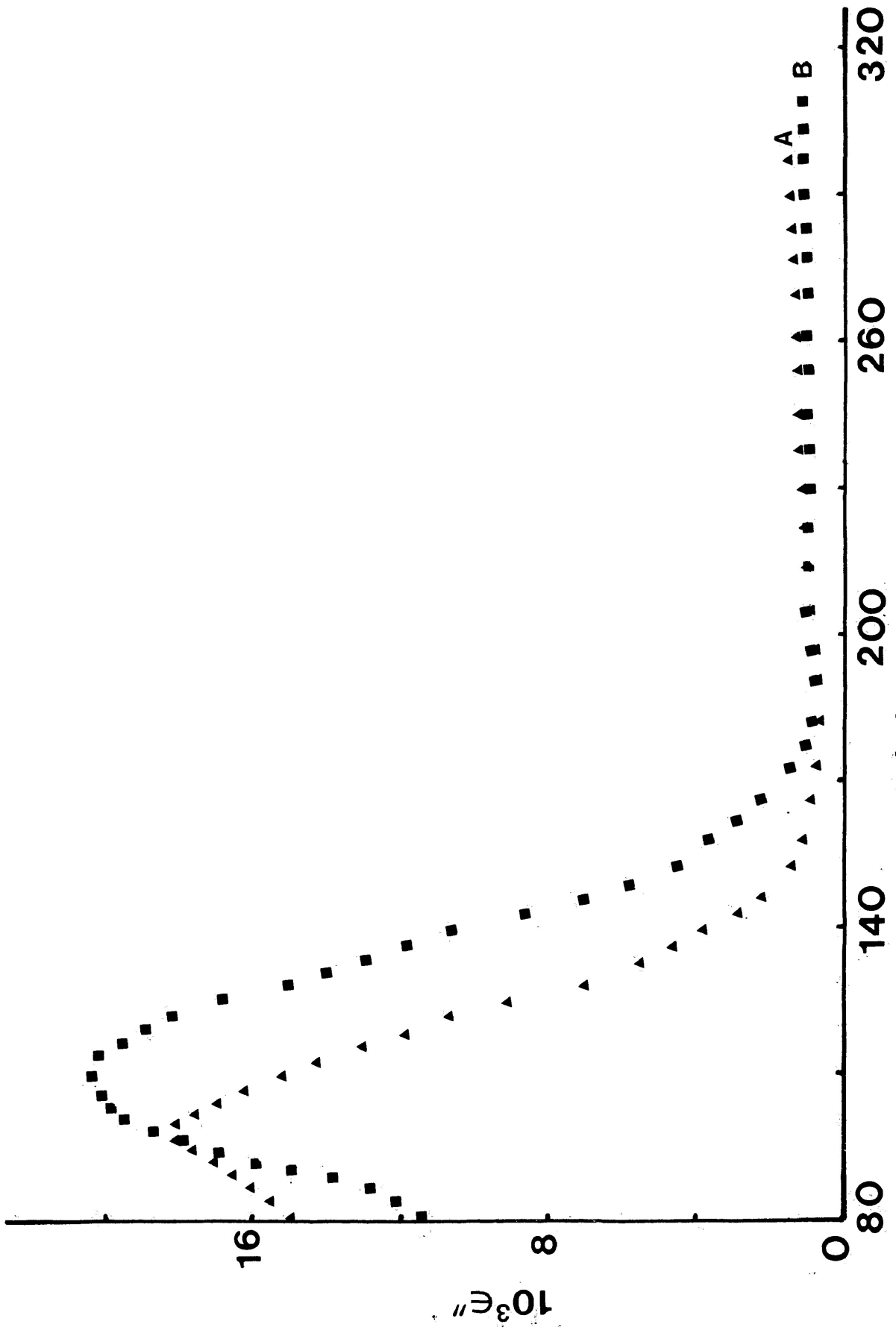

FIGURE VI-2a: Plots of dielectric loss factor, ε'' versus temperature (K) for isoborneol in a polystyrene matrix. A=50.2 Hz, B=1.01 kHz

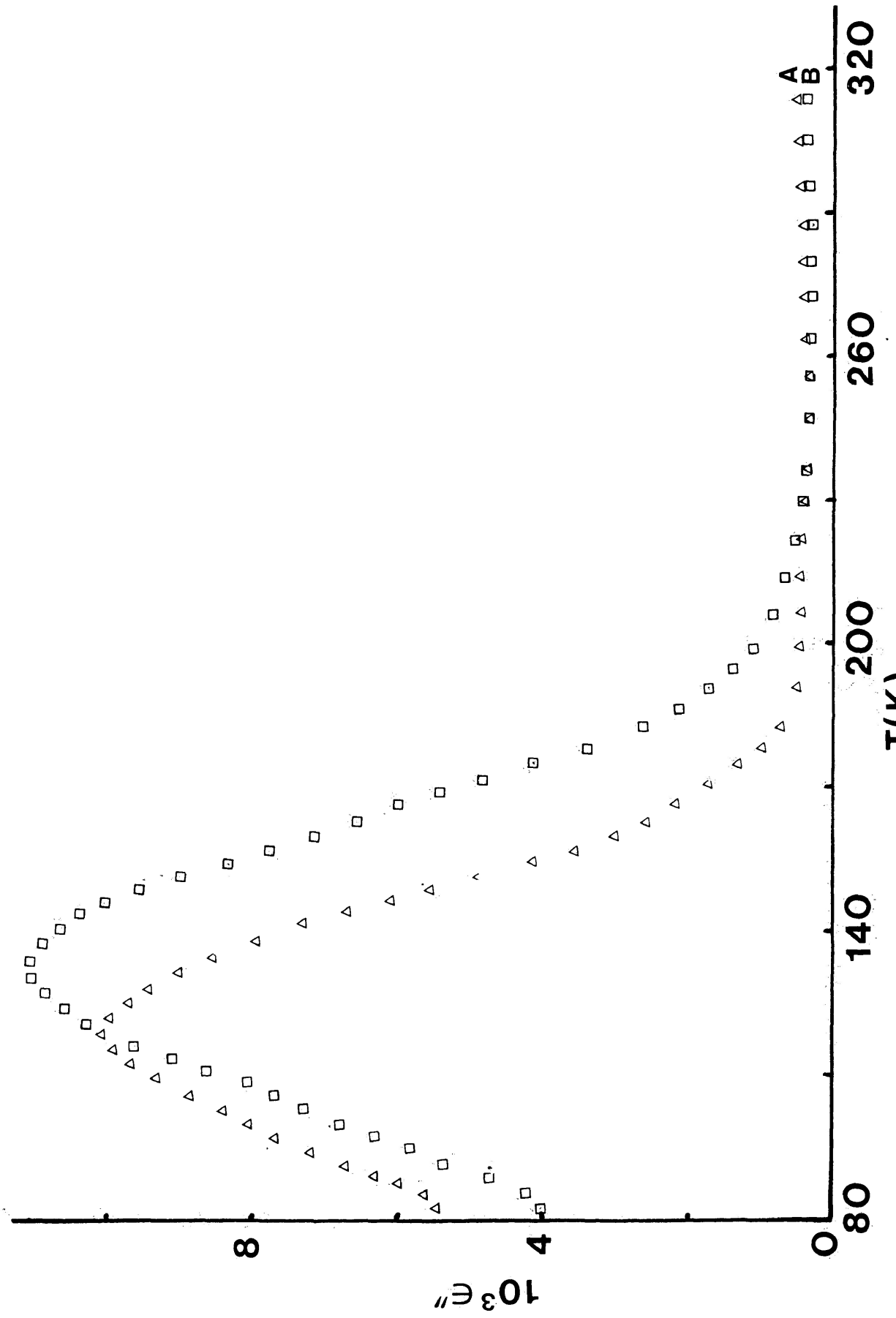

FIGURE VI-3a: Plots of dielectric loss factor, ε'' versus temperature (K) for fenchyl alcohol in a polystyrene matrix. A=50.2 Hz, B=1.01 kHz.

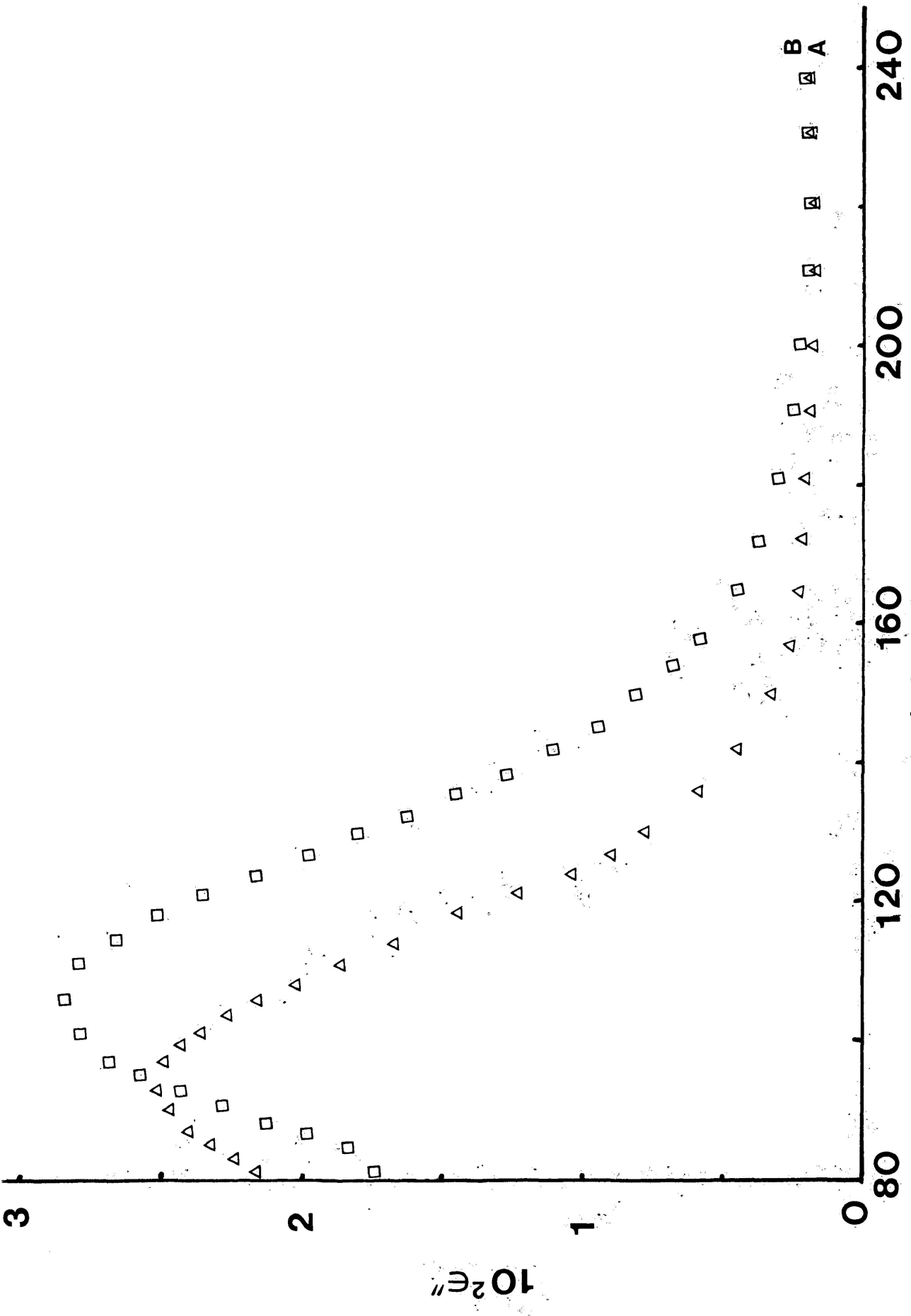

FIGURE VI-4a: Plots of dielectric loss factor, ε'' versus temperature (K) for 5-norbornene-2-carboxaldehyde in a polystyrene matrix. A=50.2 Hz, B=1.01 kHz.

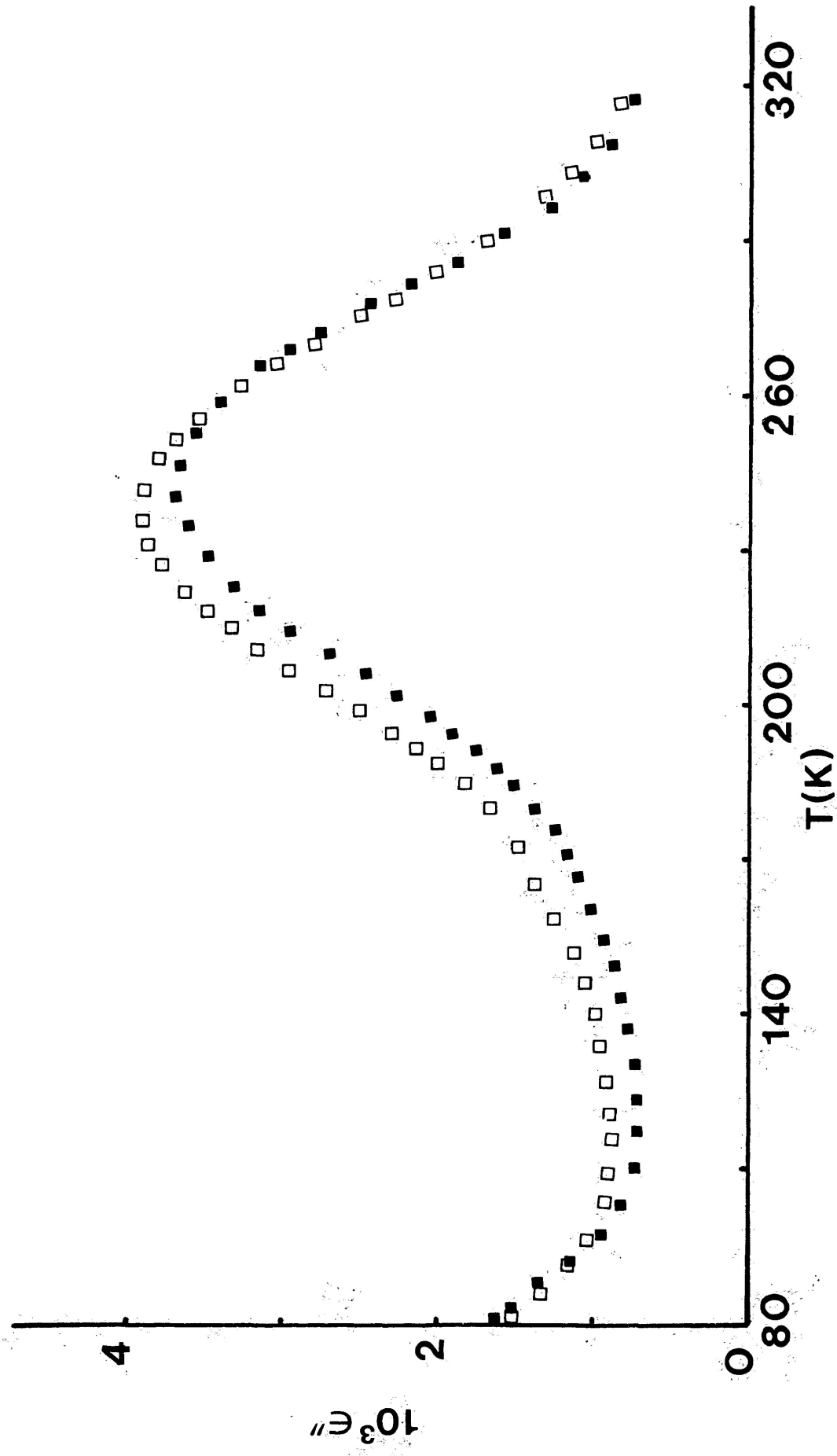

FIGURE VI-5a: Plots of dielectric loss factor, ε'' versus temperature (K) for tert-butanol (■) and methanol (□) in a polystyrene matrix at 1.01 kHz

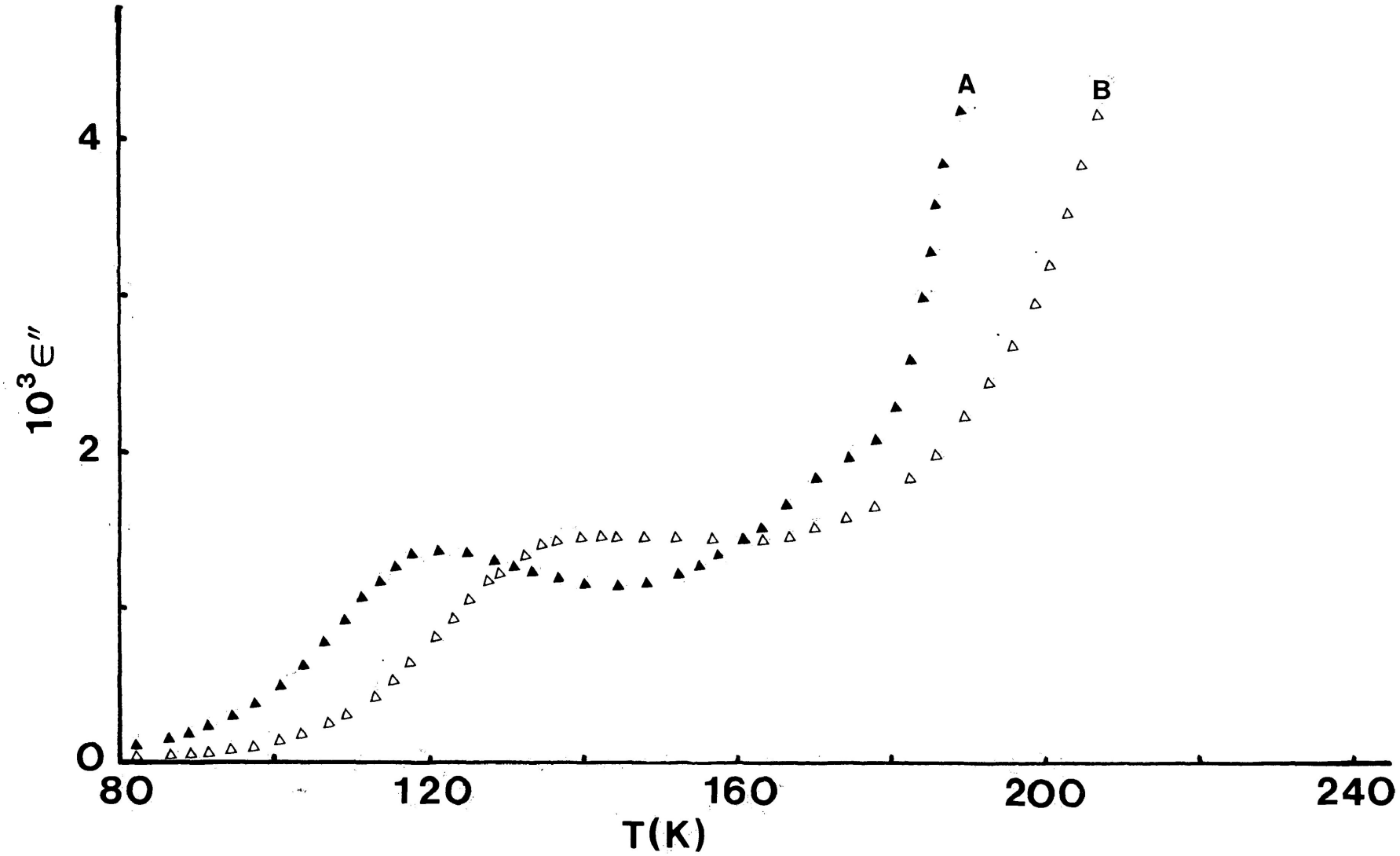

FIGURE VI-6a: Plots of dielectric loss factor, ε" versus temperature (K) for tert-butanol in the pure solid state. A=50.2 Hz, B=1.01 kHz

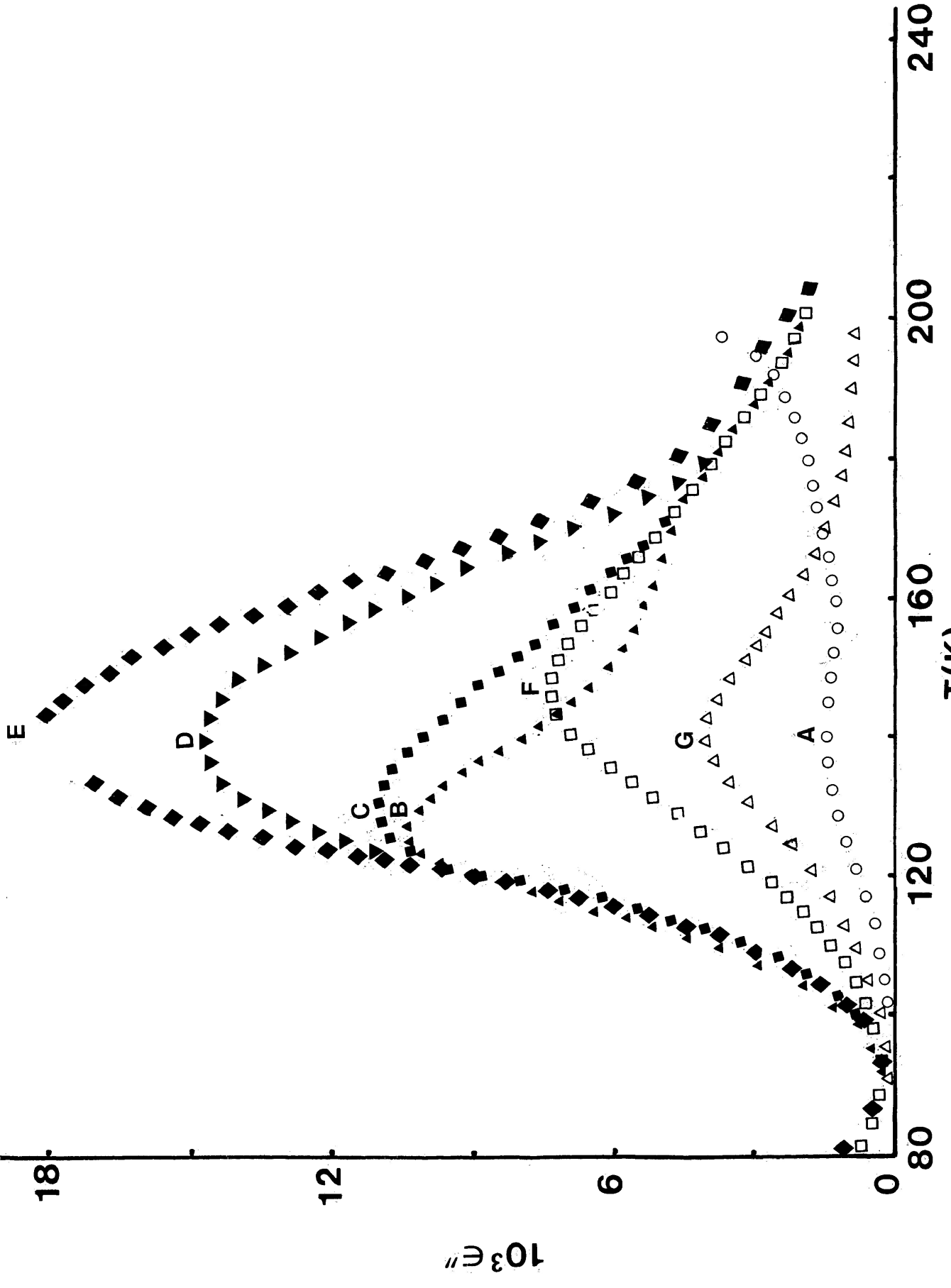

FIGURE VI-7a: Plots of dielectric loss factor, ε'' versus temperature (K) for tert-butanol in carbontetrachloride at 1.01 kHz (for several mixtures). A=100 mol% (10.6 M); B=92.15 mol % (9.75 M); C=87.3 mol % (9.23 M); D=83.5 mol % (8.82 M); E=71.22 mol % (7.50 M); F=50 mol % (5.24 M); and G=24.8 mol % (2.58 M).

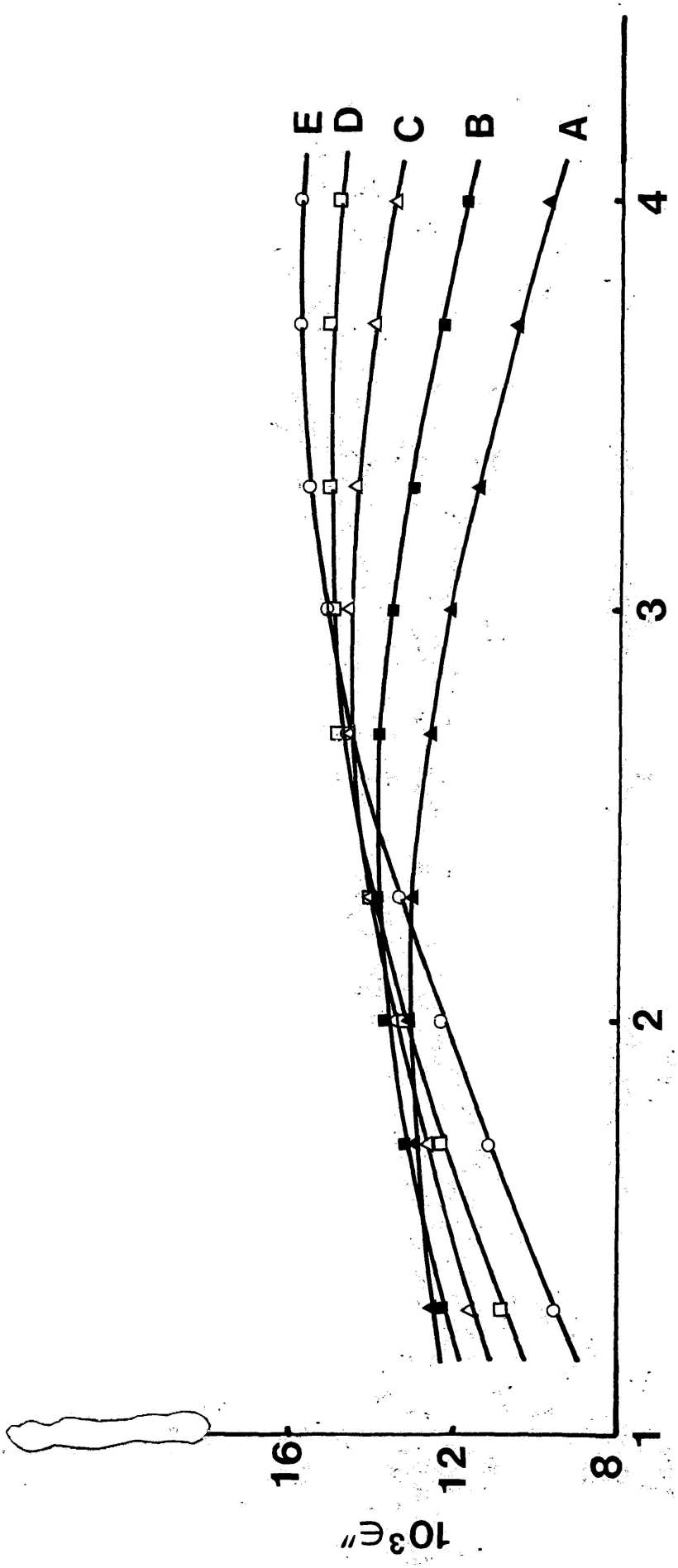

FIGURES VI-8b: Plots of dielectric loss factor, ε'' versus $\log\nu$ (Hz) for norborneol in a polystyrene matrix. A=80.7 K; B=85.2 K; C=89.5 K; D=94.5 K; and E = 98.0 K.

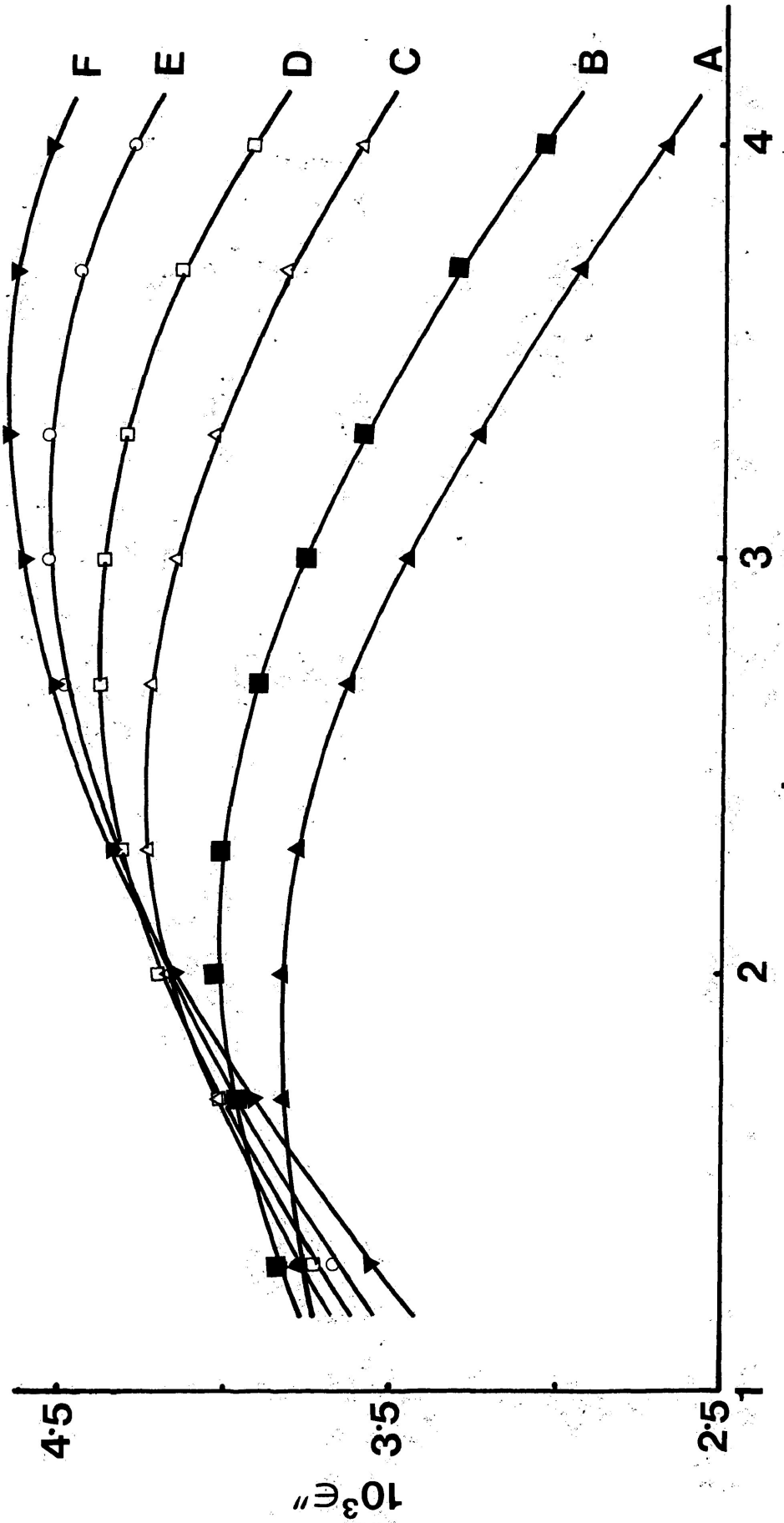

FIGURE 8b': Plots of dielectric loss factor, ε'' versus logν (Hz) for norborneol in G.C.T.P. A=82.2 K; B=85.3 K; C=90.0 K; D=93.2 K; E=96.8 K; and F=99.5 K.

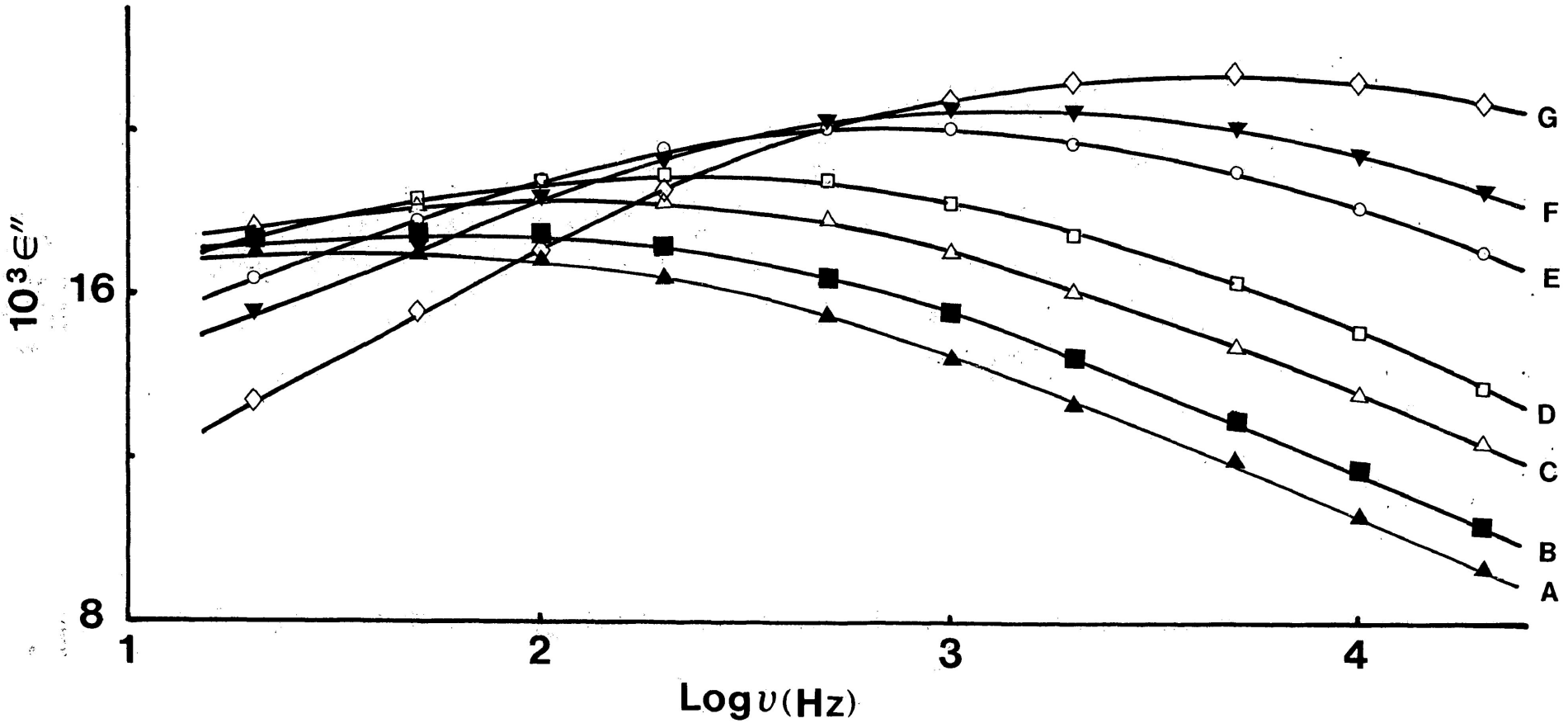

FIGURE 9b: Plots of dielectric loss factor, ε'' versus logν (Hz) for isoborneol in a polystyrene matrix. A=87.7 K; B=89.2 K; C=92.5 K; D=95.0 K; E=100.8 K; F=103.8 K; and G=109.2 K.

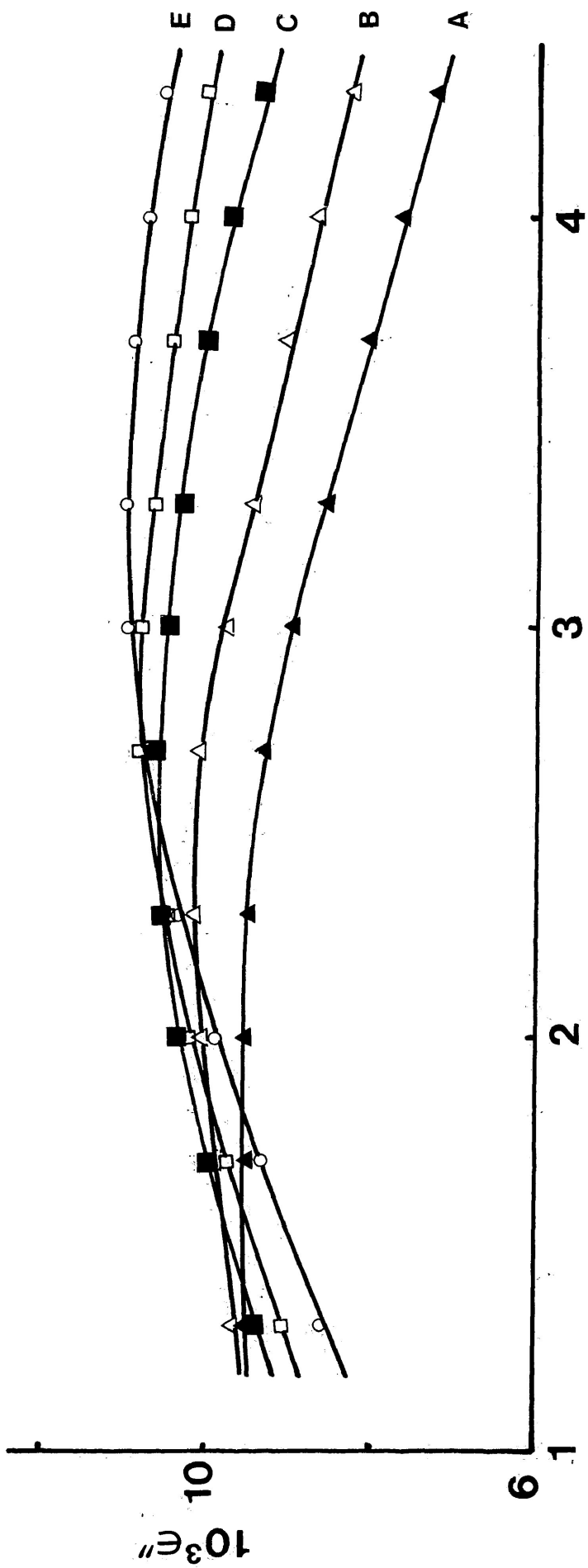

FIGURE V-10b: Plots of dielectric loss factor, ε'' versus $\log\nu$ (Hz) for fenchyl alcohol in a polystyrene matrix. A=109.5 K; B=114.7 K; C=120.1 K; D=123.7 K and E=127.4 K.

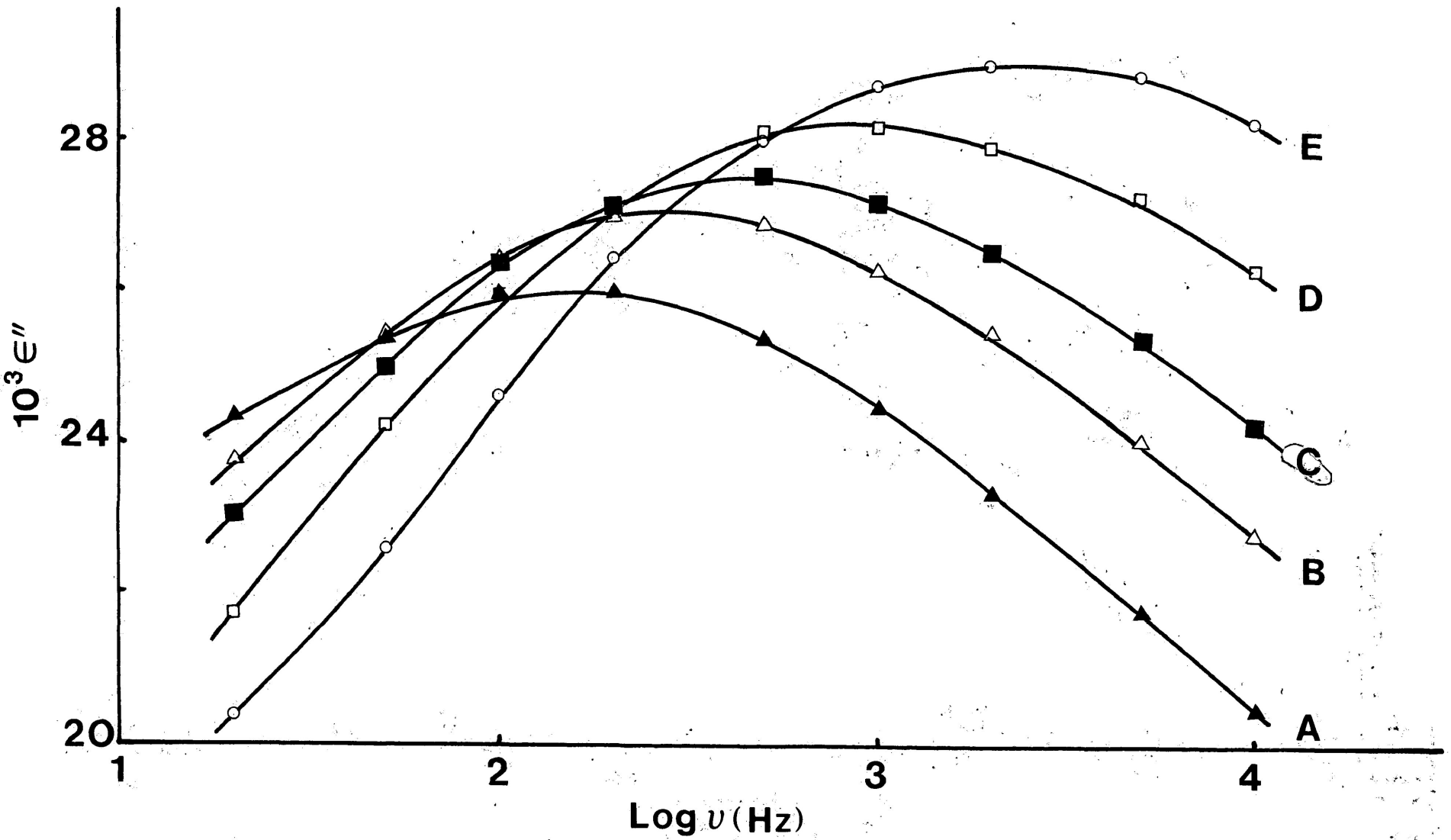

FIGURE VI-11b: Plots of dielectric loss factor, ε" versus logν (Hz) for 5-norbornene-2-carboxaldehyde in a polystyrene matrix. A=91.6 K; B=95.2 K; C=97.2 K; D=100.2 K; and E=104.0 K.

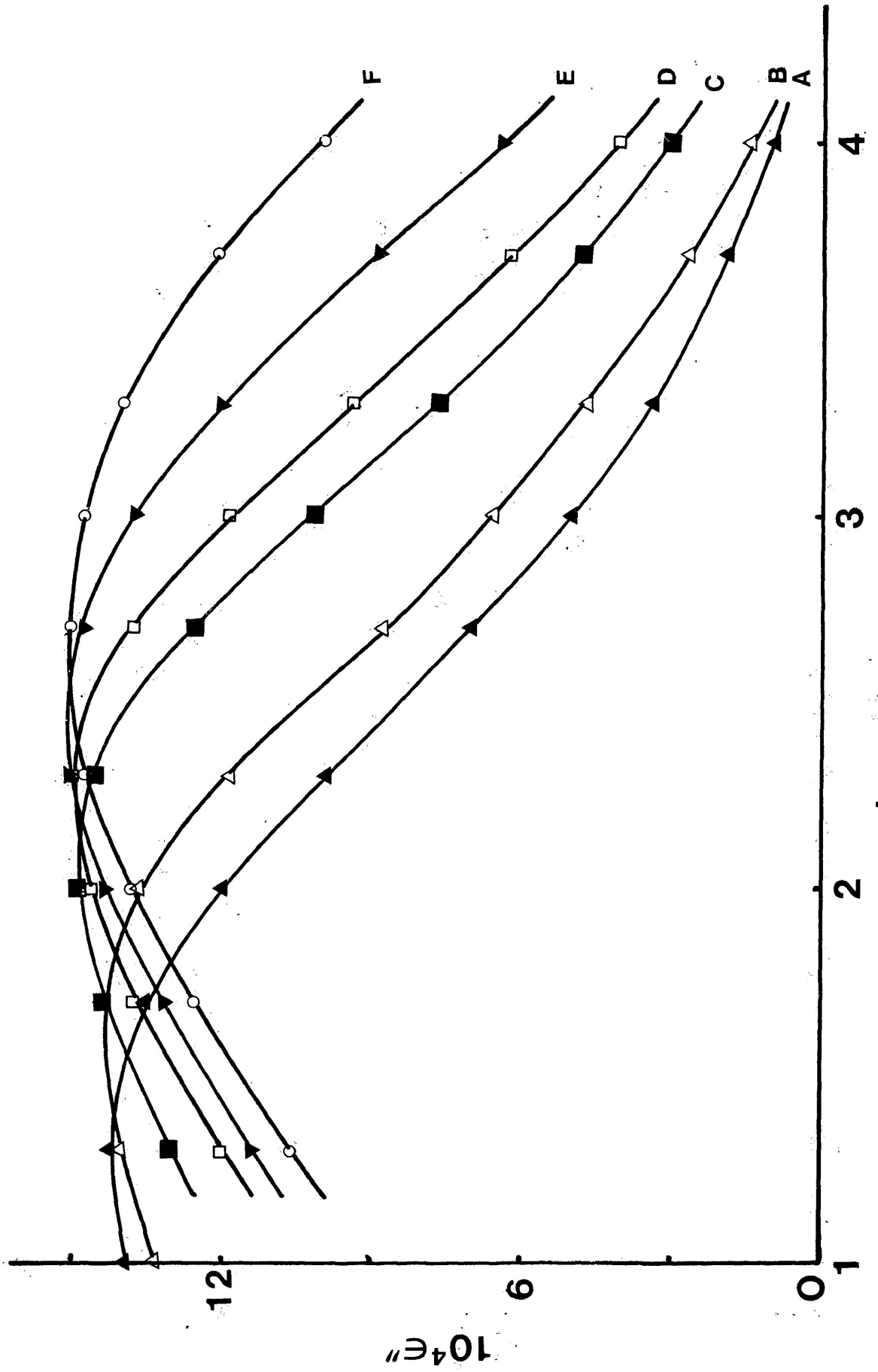

FIGURE VI-13b: Plots of dielectric loss factor, ε'' versus logυ (Hz) for tert-butanol in the pure solid state. A=116.4K; B=119.4 K; C=125.5 K; D=128.5 K; E=133.5 K; and F=140.8 K.

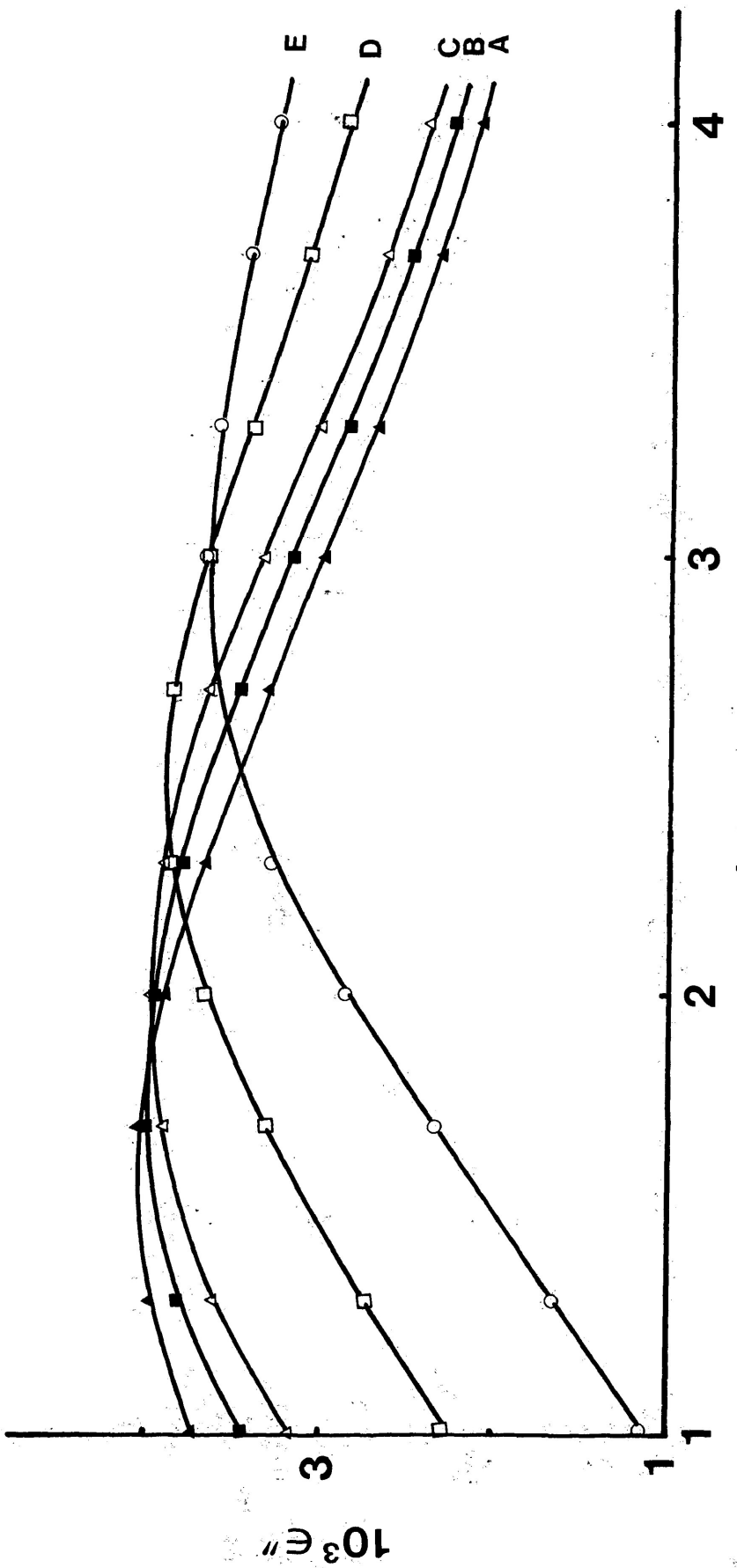

FIGURE VI-12b: Plots of dielectric loss factor, ε'' versus logν (Hz) for tert-butanol in a polystyrene matrix. A=215.4 K; B=219.3 K; C=223.5 K; D=235.7 K; E=248.0 K.

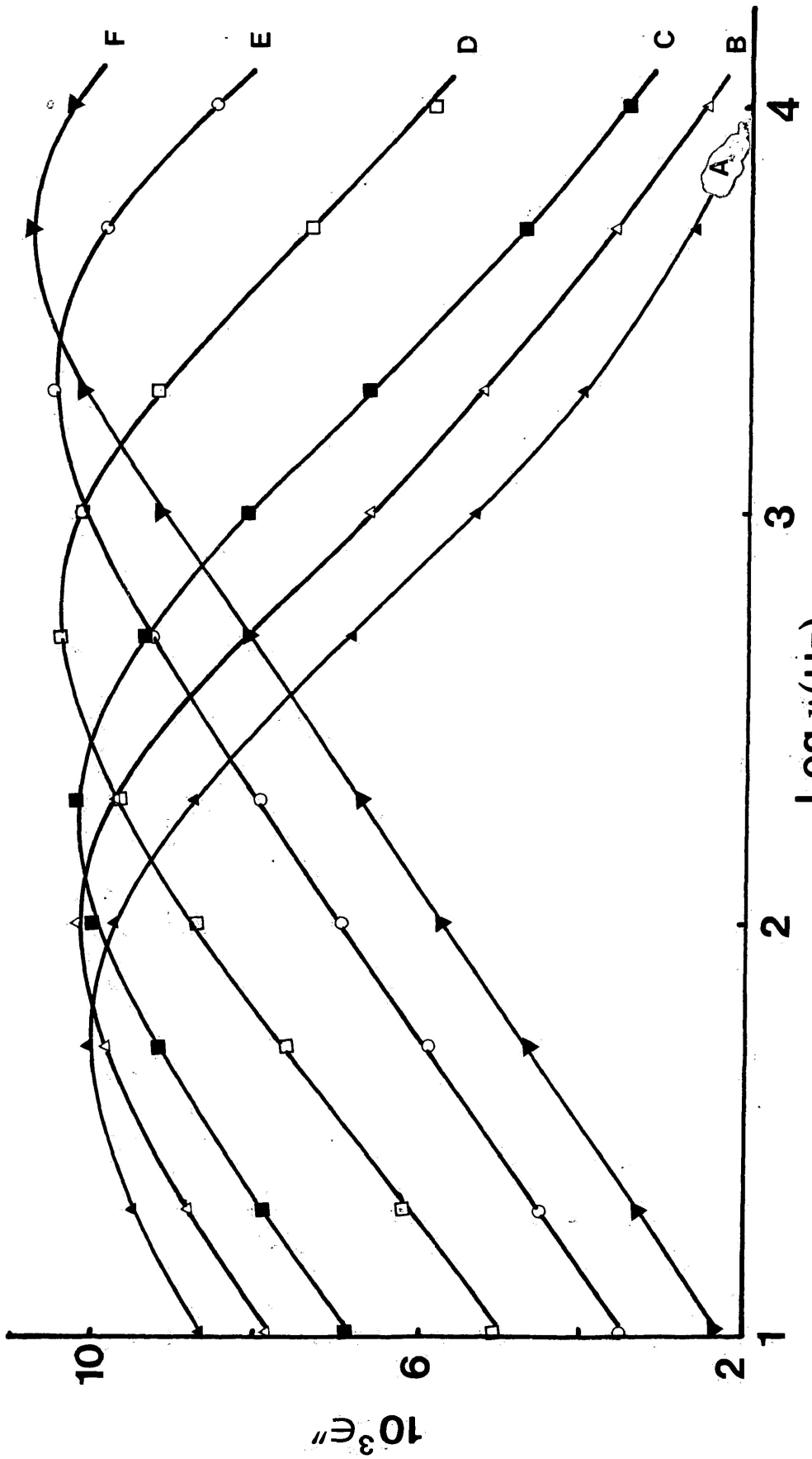

FIGURE VI-14b: Plots of dielectric loss factor, ε'' versus logν (Hz) for tert-butanol in carbon-tetrachloride (92.15 mol %). A=113.2 K; B=115.4 K; C=118.3 K; D=123.7 K; E=129.4 K; and F=134.8 K.

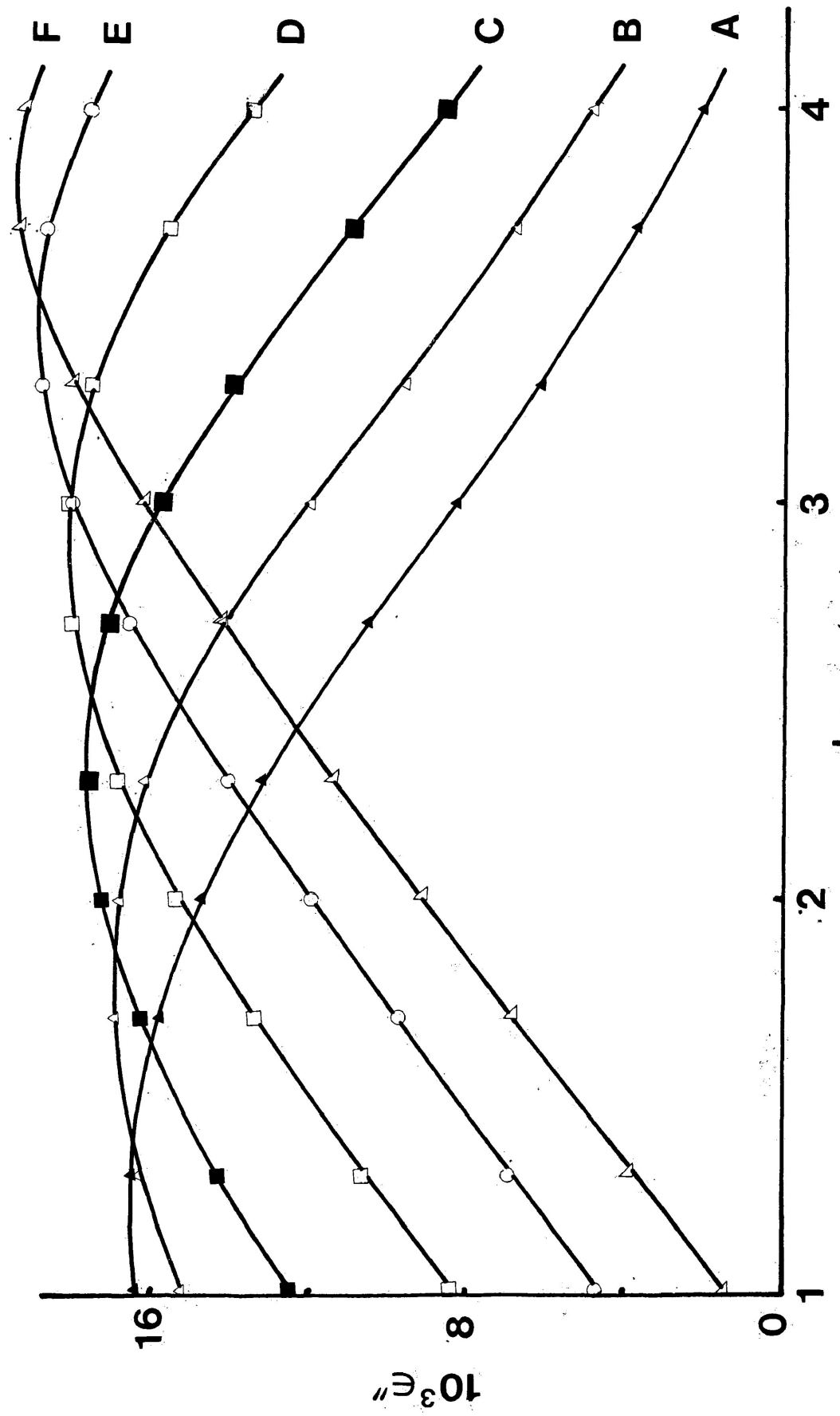

FIGURE VI-15b: Plots of dielectric loss factor, ε'' versus $\log\nu$ (Hz) for tert-butanol in carbontetrachloride (71.22 mol %). A=118.8 K; B=123.7 K; C=129.8 K; D=137.5 K; E=145.3 K; and F=151.3 K.

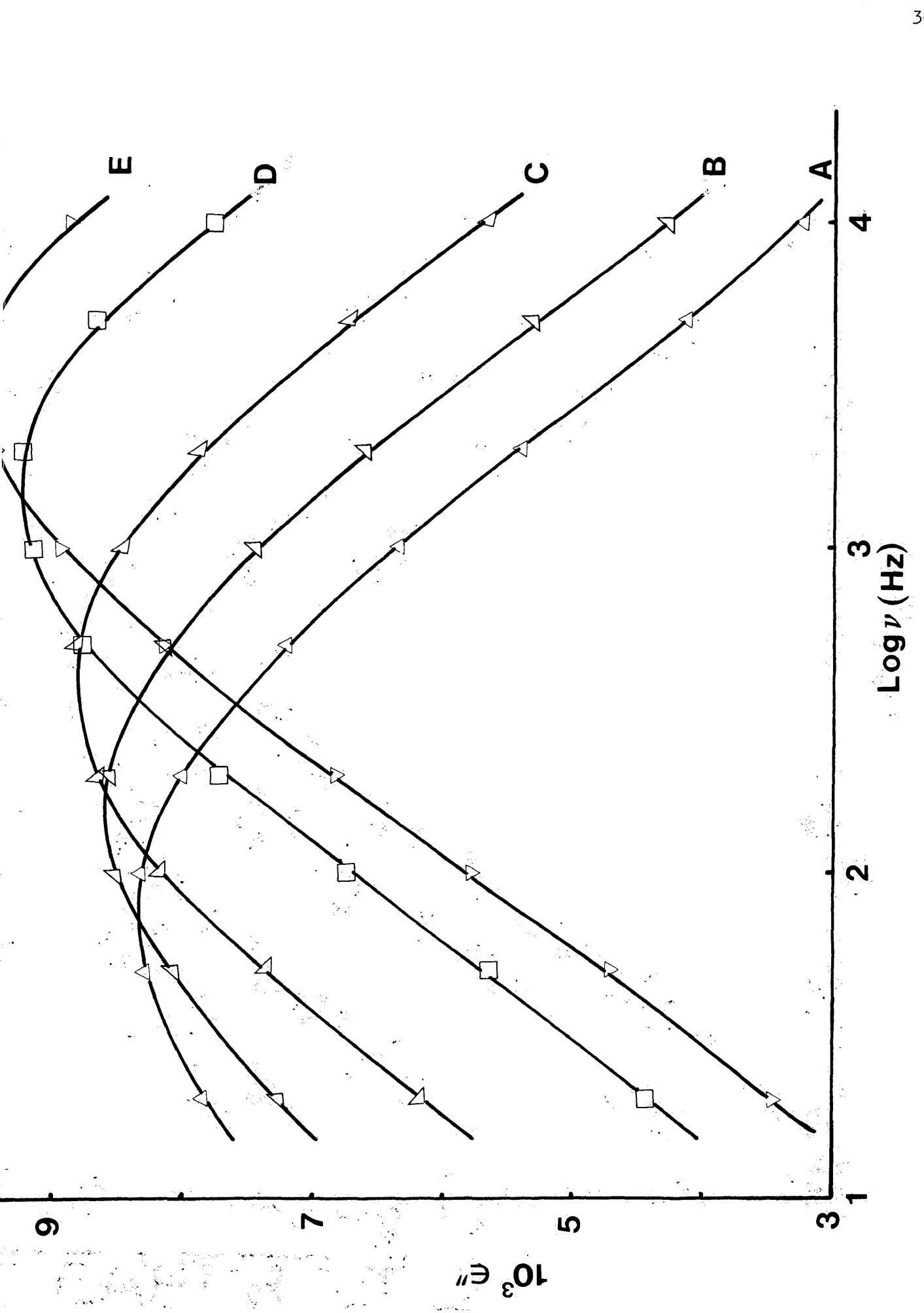

FIGURE VI-16b: Plots of dielectric loss factor, ε" versus logν (Hz) for tert-butanol in carbontetrachloride (50 mol %). A=126.1 K; B=130.1 K; C=135.0 K; D=142.8 K; and E=147.4 K.

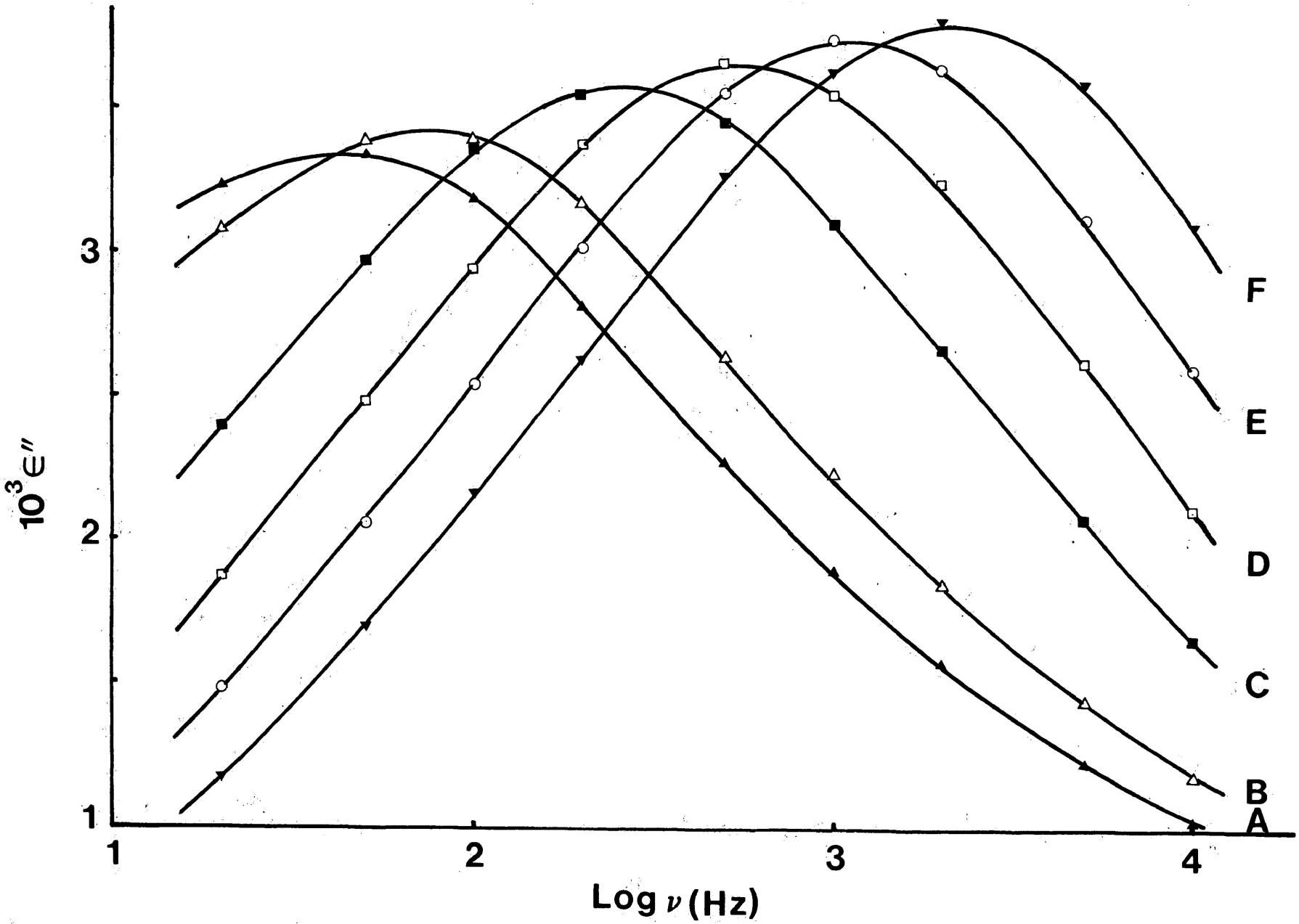

FIGURE VI-17b: Plots of dielectric loss factor, ε'' versus logν (Hz) for tert-butanol in carbontetrachloride (24.80 mol %). A=122.7 K; B=125.0 K; C=131.2 K; D=135.7 K; E=139.3 K; and F=143.2 K.

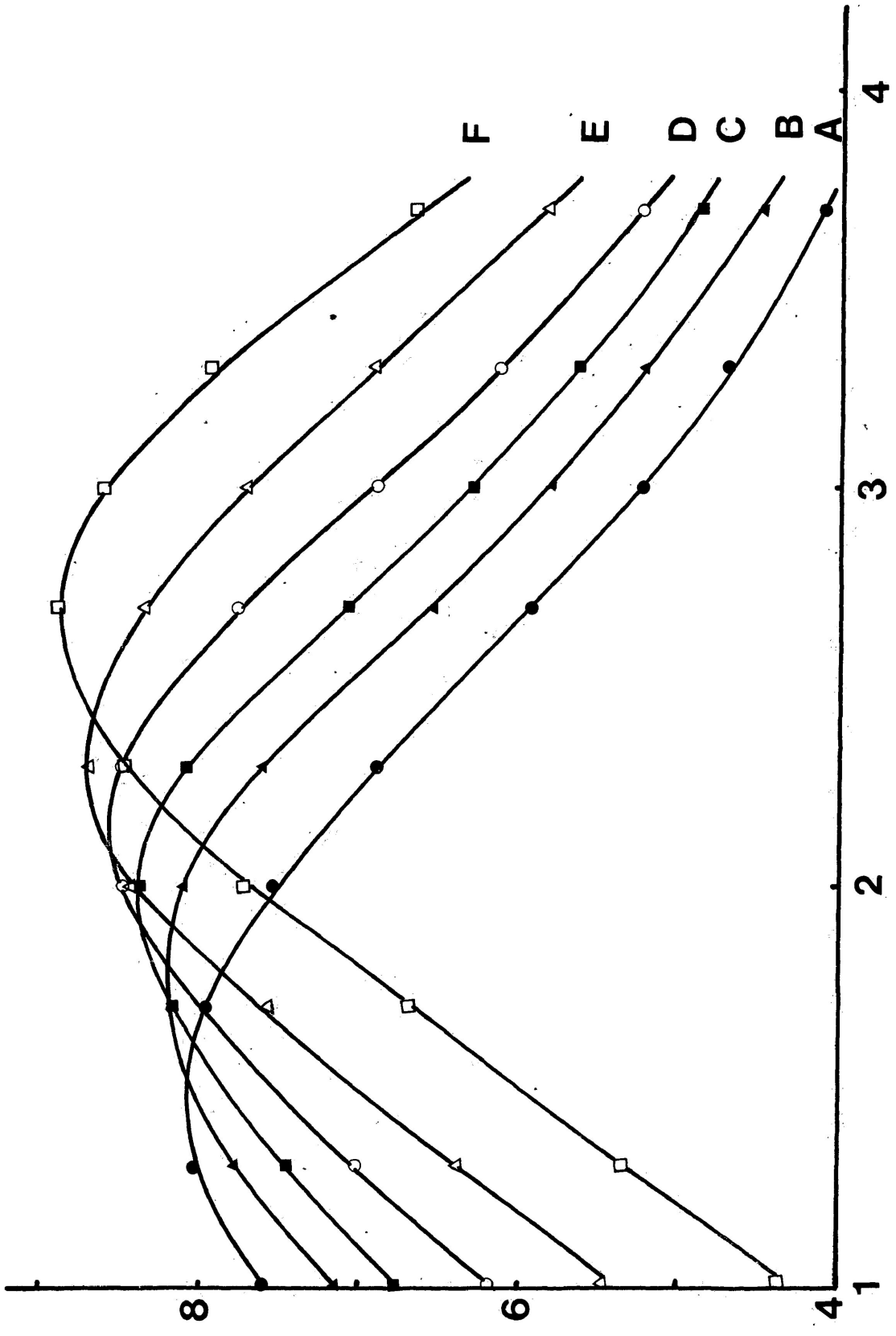

FIGURE VI-18b. Plots of dielectric loss factor, ε'' versus logν (Hz) for tert-butanol in carbon-tetrachloride (9.03 mol %). A=120.4 K; B=122.9 K; C=124.8 K; D=127.2 K; E=129.8 K; and F=134.0 K.

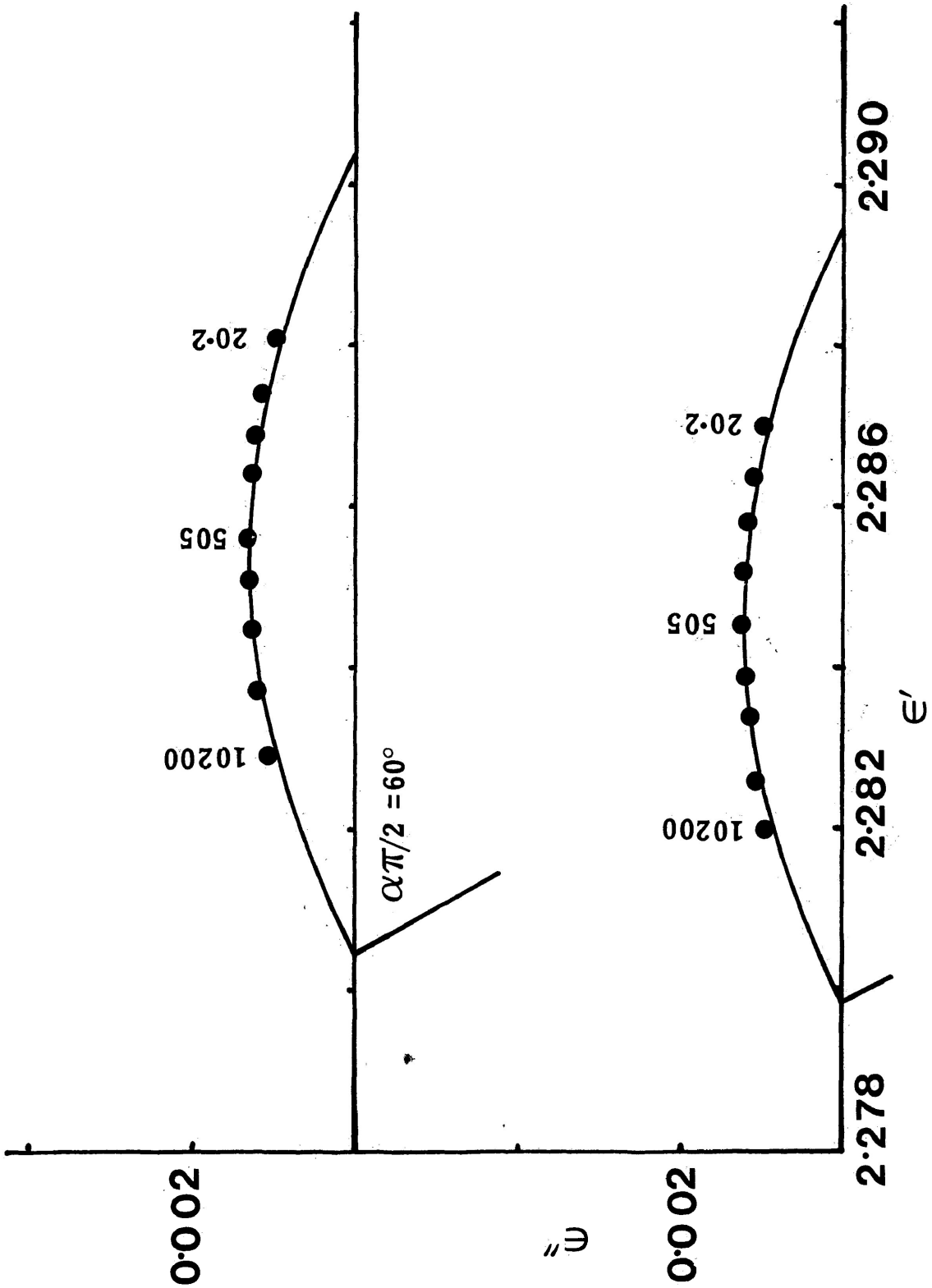

FIGURE VI-19c: Cole-Cole plots for norborneol in carbontetrachloride at 83.1 K (lower) and 85.6 K (Upper). Numbers beside points are frequencies in Hz.

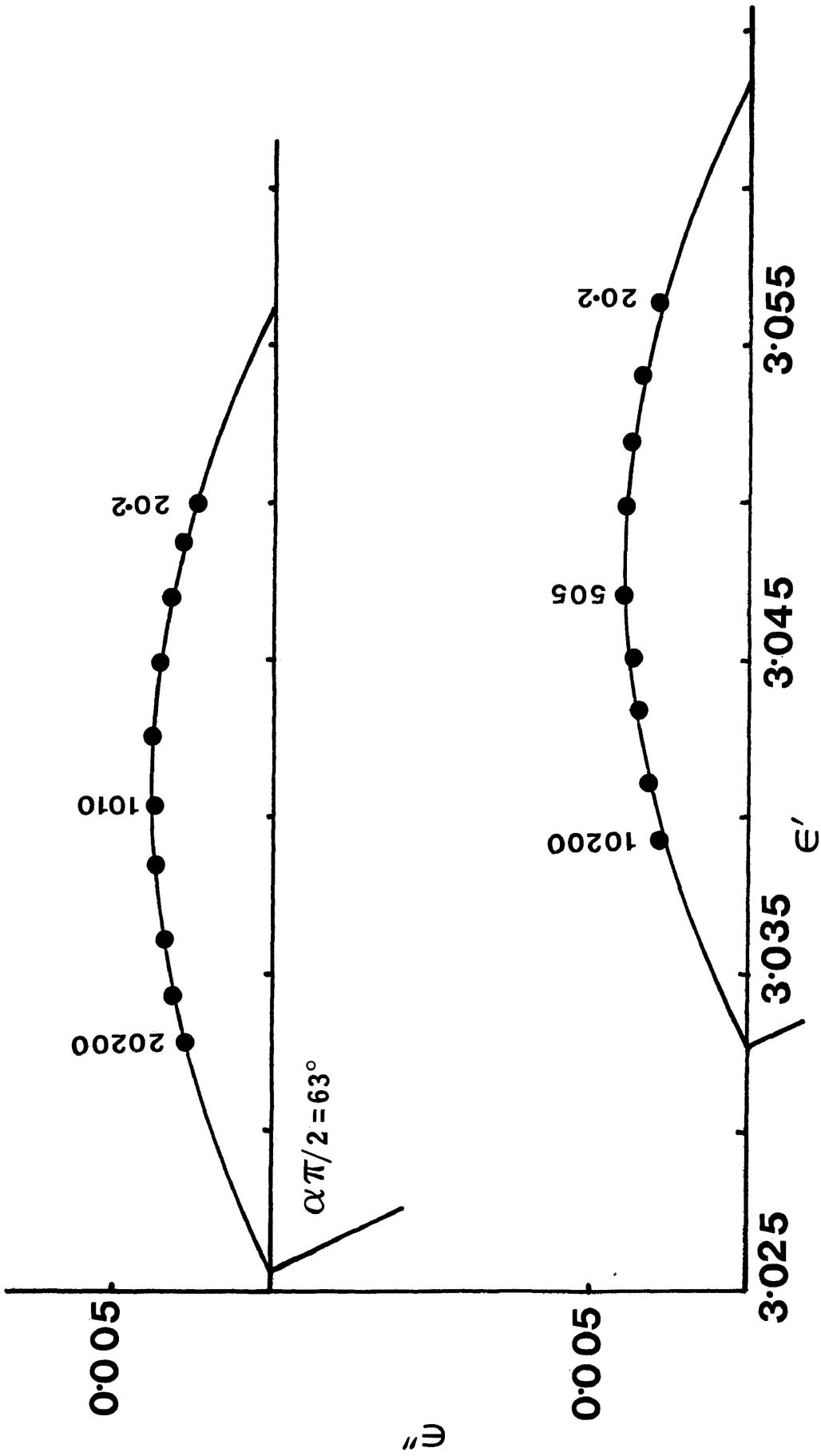

FIGURE VI:20c: Cole–Cole plots for tert-butanol in a polystyrene matrix at 235.7 K (lower) and 242.3 K (upper). Numbers beside points are frequencies in Hz.

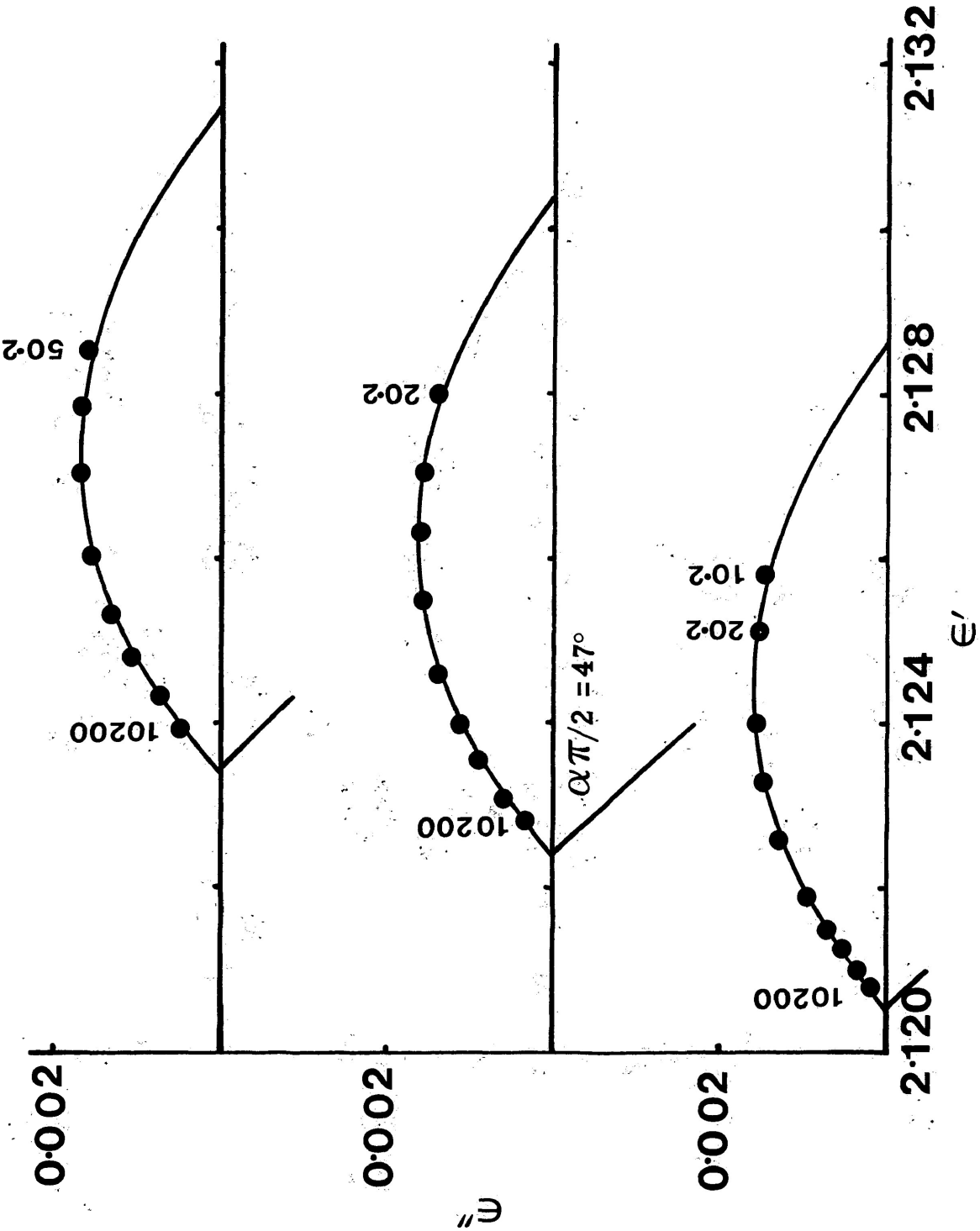

FIGURE VI-21c: Cole-Cole plots for tert-butanol in the pure solid state at 119.4 K (lower), 125.5 K (middle) and 128.5 K (upper). Numbers beside points are frequencies in Hz.

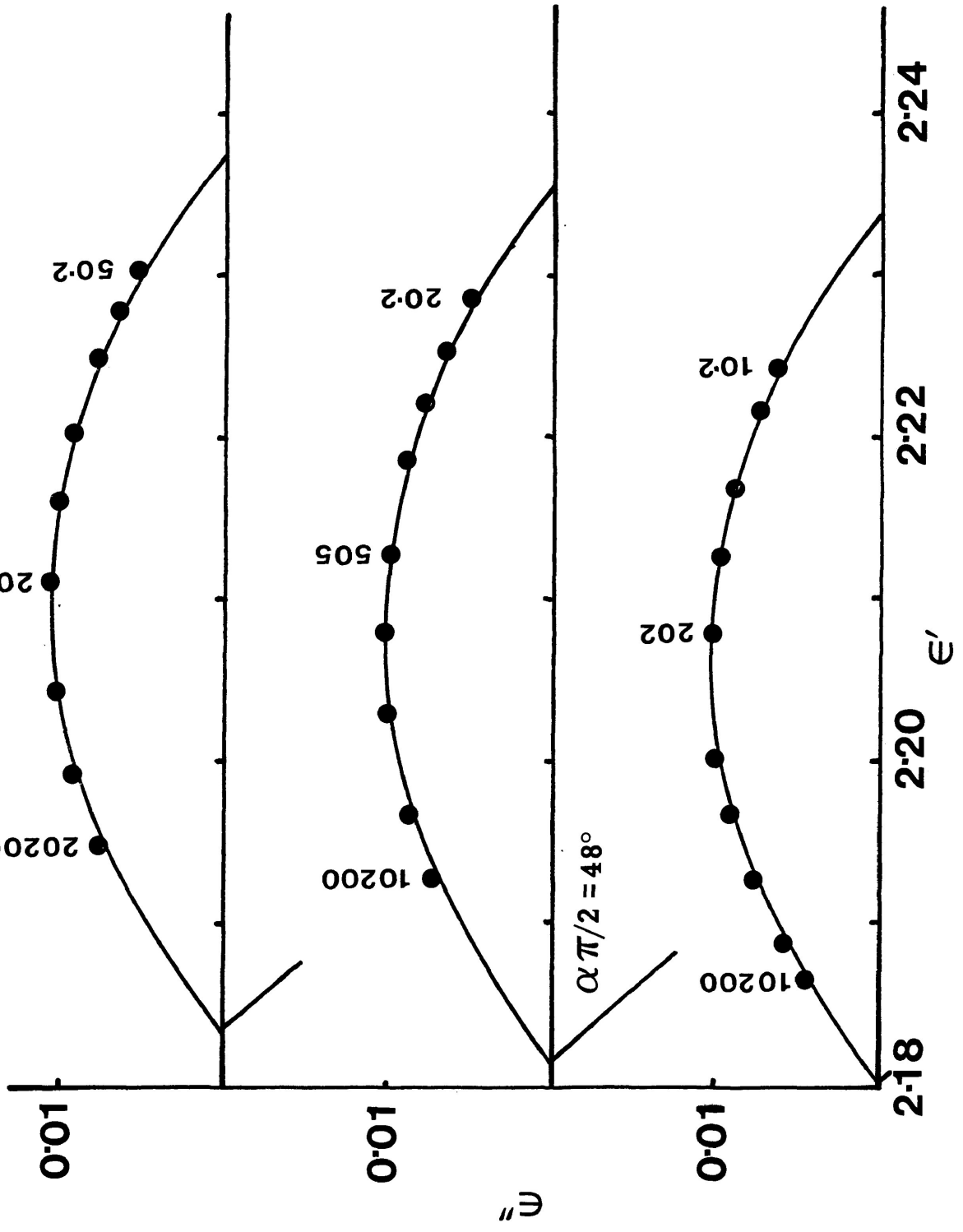

FIGURE VI-22c: Cole-Cole plots for tert-butanol in carbontetrachloride (92.15 mol %) at 120.2 K (lower), 126.8 K (middle) and 132.0 K (upper). Numbers beside points are frequencies in Hz.

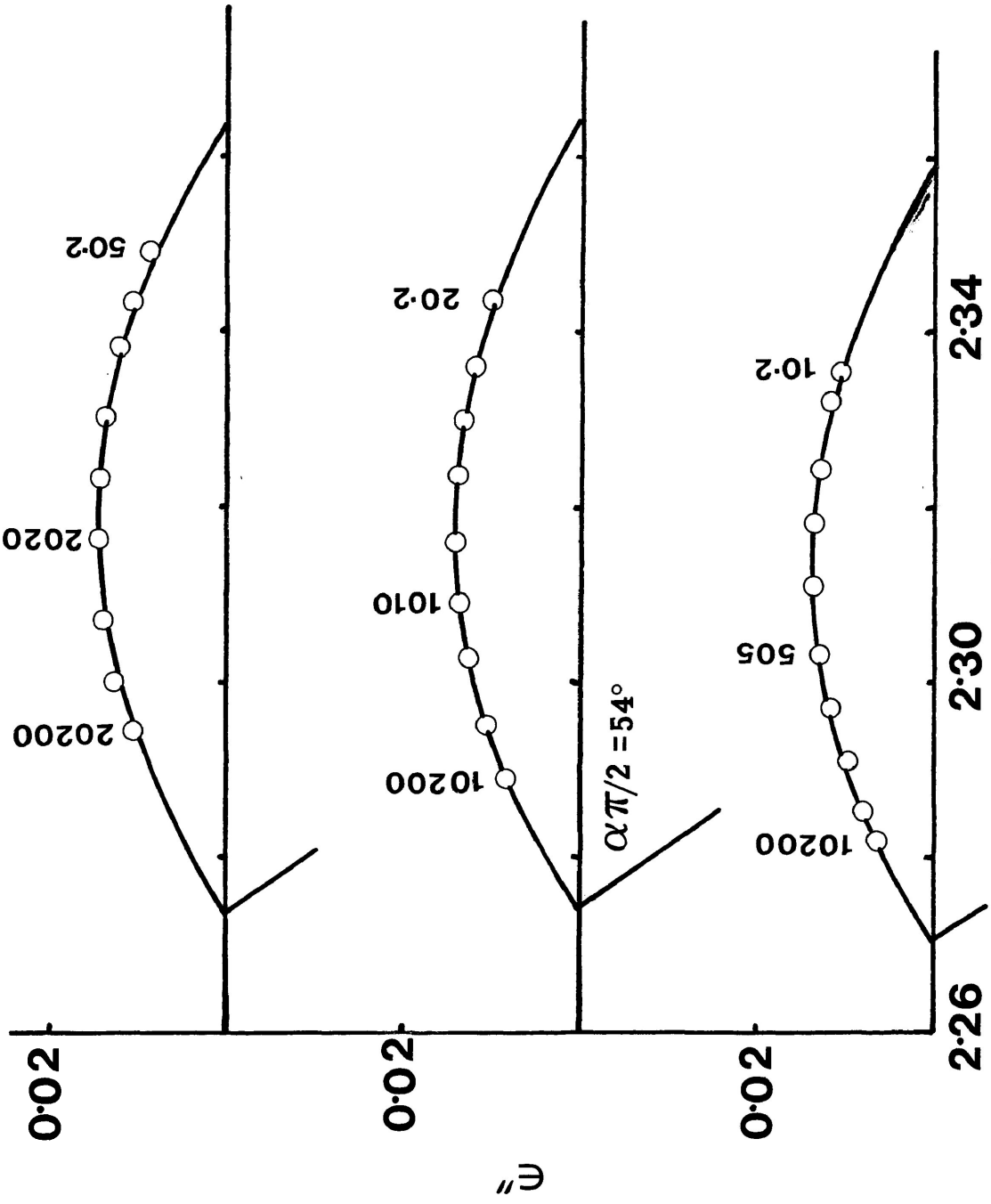

FIGURE VI-23c: Cole-Cole plots for tert-butanol in carbon tetrachloride (83.5 mol %) at 126.5 K (lower), 133.0 K (middle) and 139.9 K (upper). Numbers beside points are frequencies in Hz.

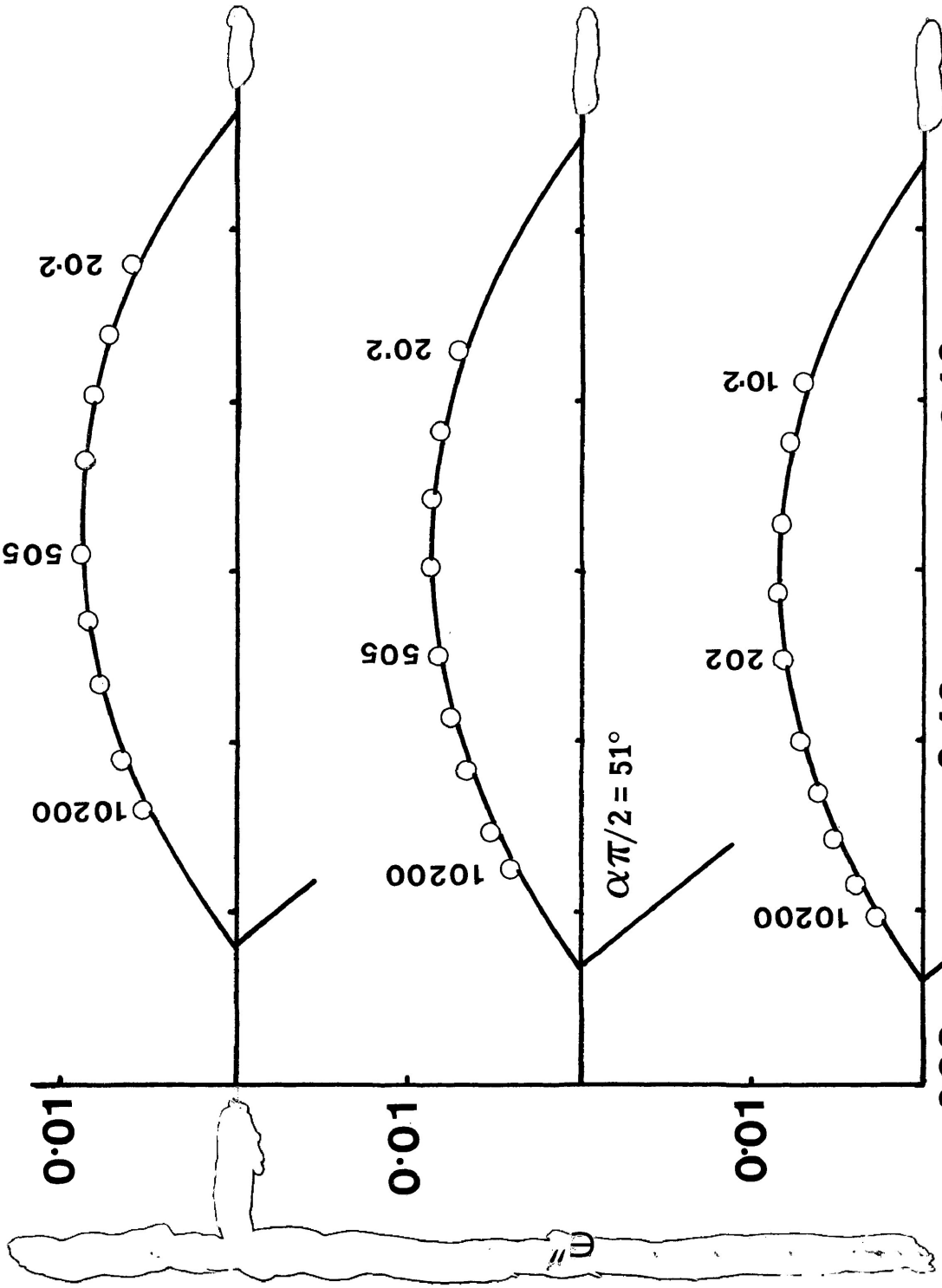

FIGURE VI-24c: Cole-Cole plots for tert-butanol in carbontetrachloride (50 mol %) at 126.1 K (lower), 130.1 K (middle) and 135.0 K (upper). Numbers beside points are frequencies in Hz.

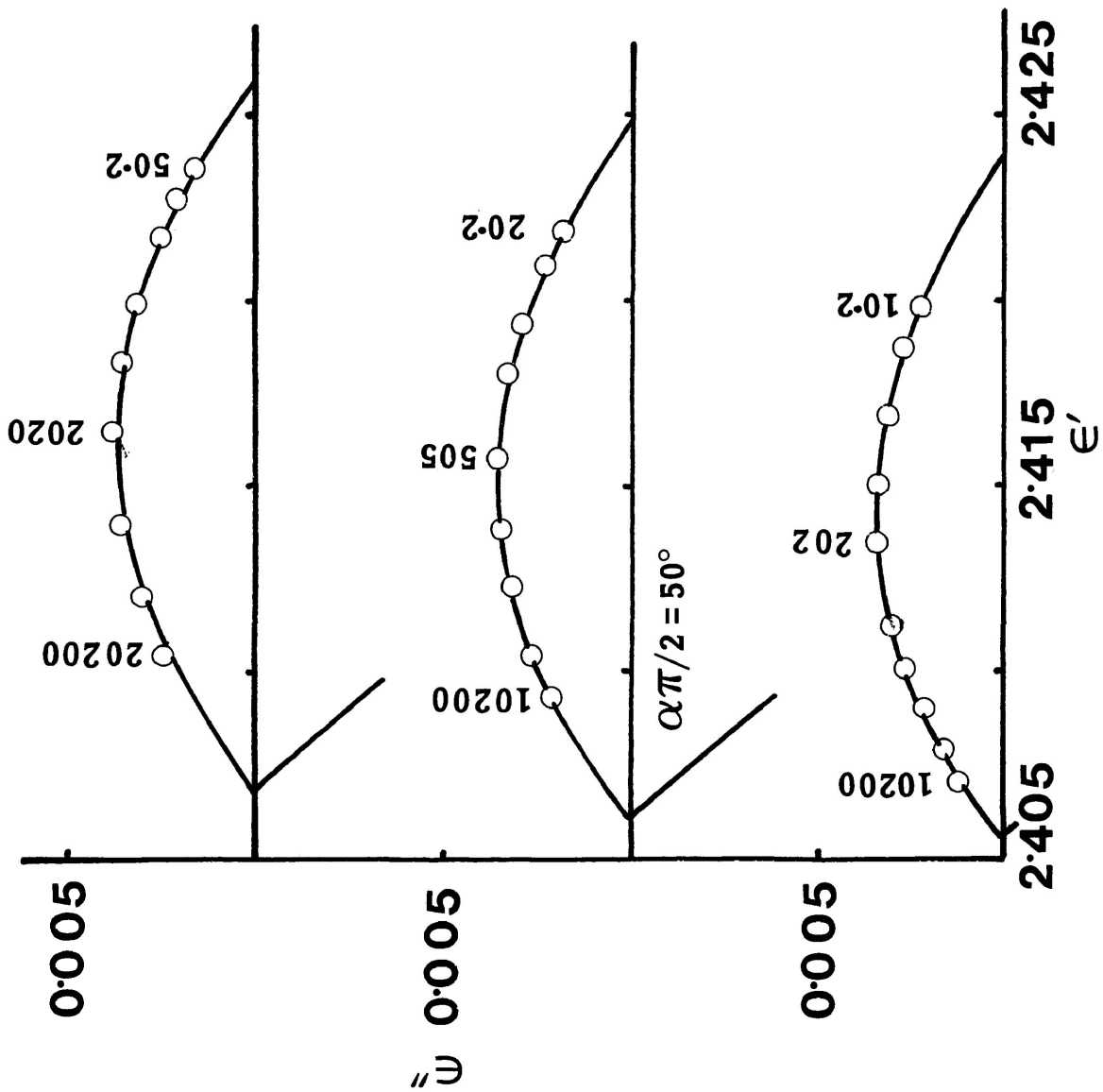

FIGURE VI-25c: Cole-Cole plots for tert-butanol in carbontetrachloride (24.8 mol %) at 128.5 K (lower), 135.7 K (middle) and 143.5 K (upper). Numbers beside points are frequencies in Hz.

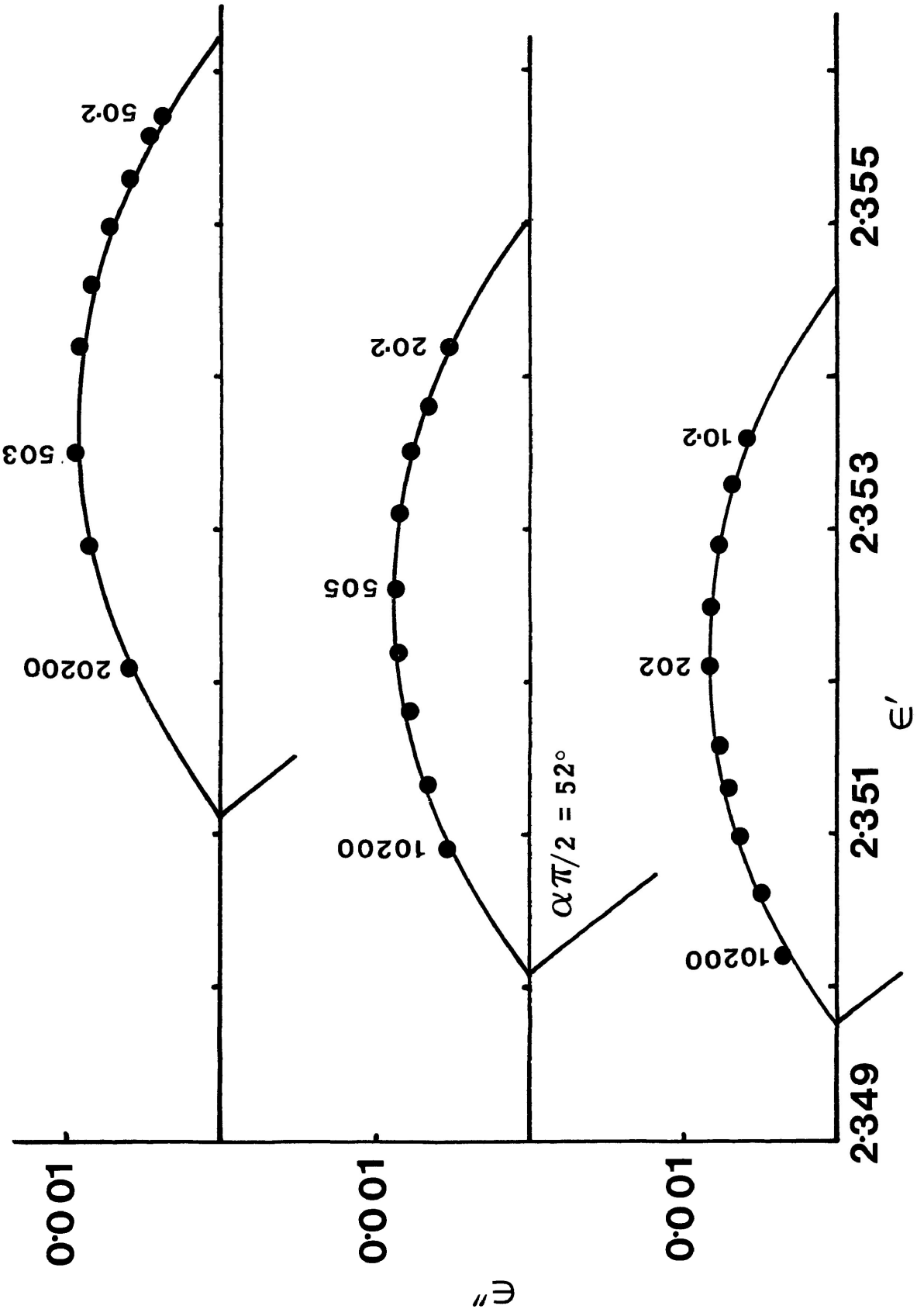

FIGURE VI-26c: Cole-Cole plots for tert-butanol in carbontetrachloride (9.02 mol %) at 127.2 K (lower), 134.0 K (middle) and 146.4 K (upper). Numbers beside points are frequencies in Hz.

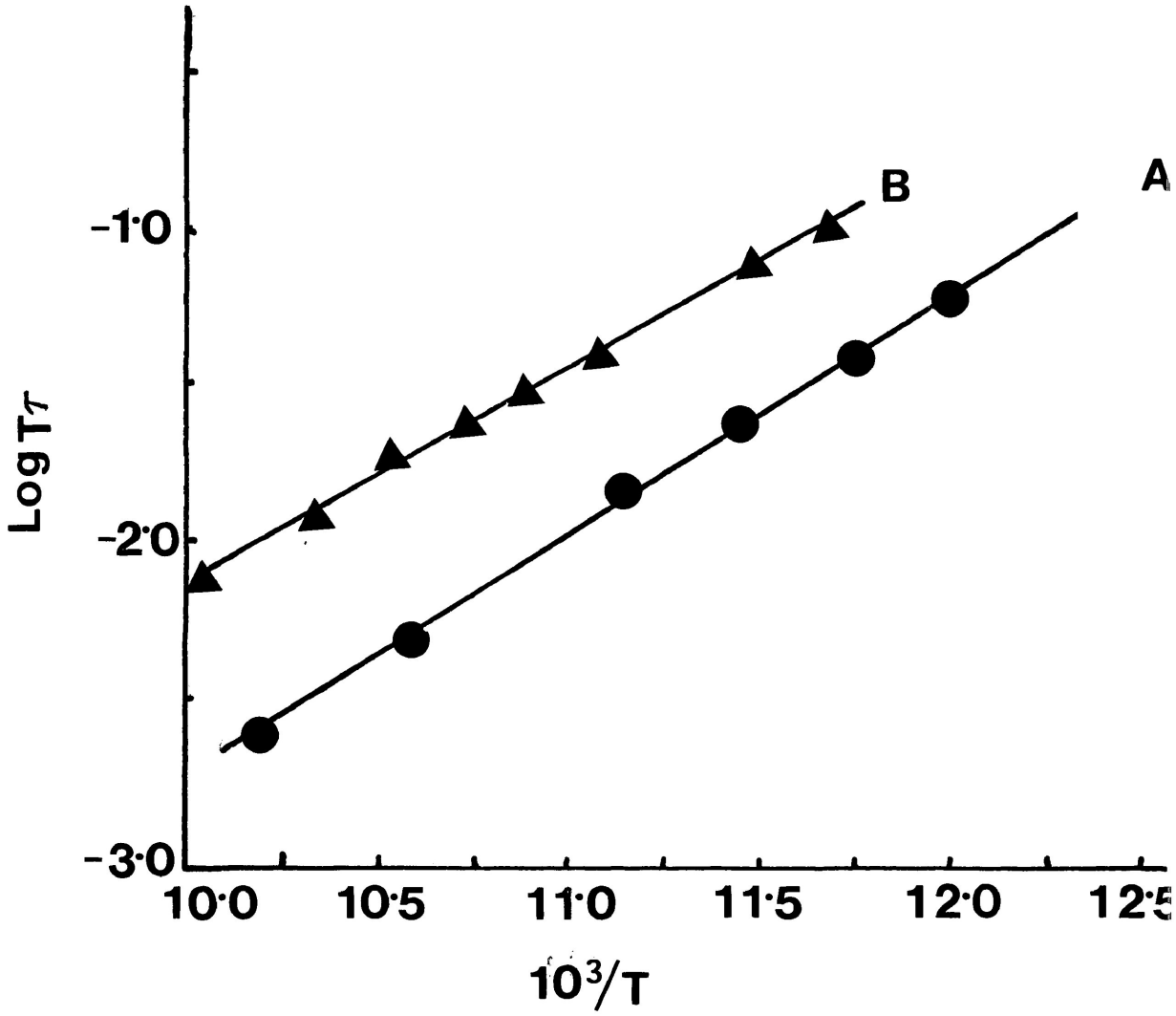

FIGURE VI-27d: Eyring plots of logTτ versus 1/T (K^{-1}) for norborneol in polystyrene (A) and G.O.T.P. (B) (lower temperature process).

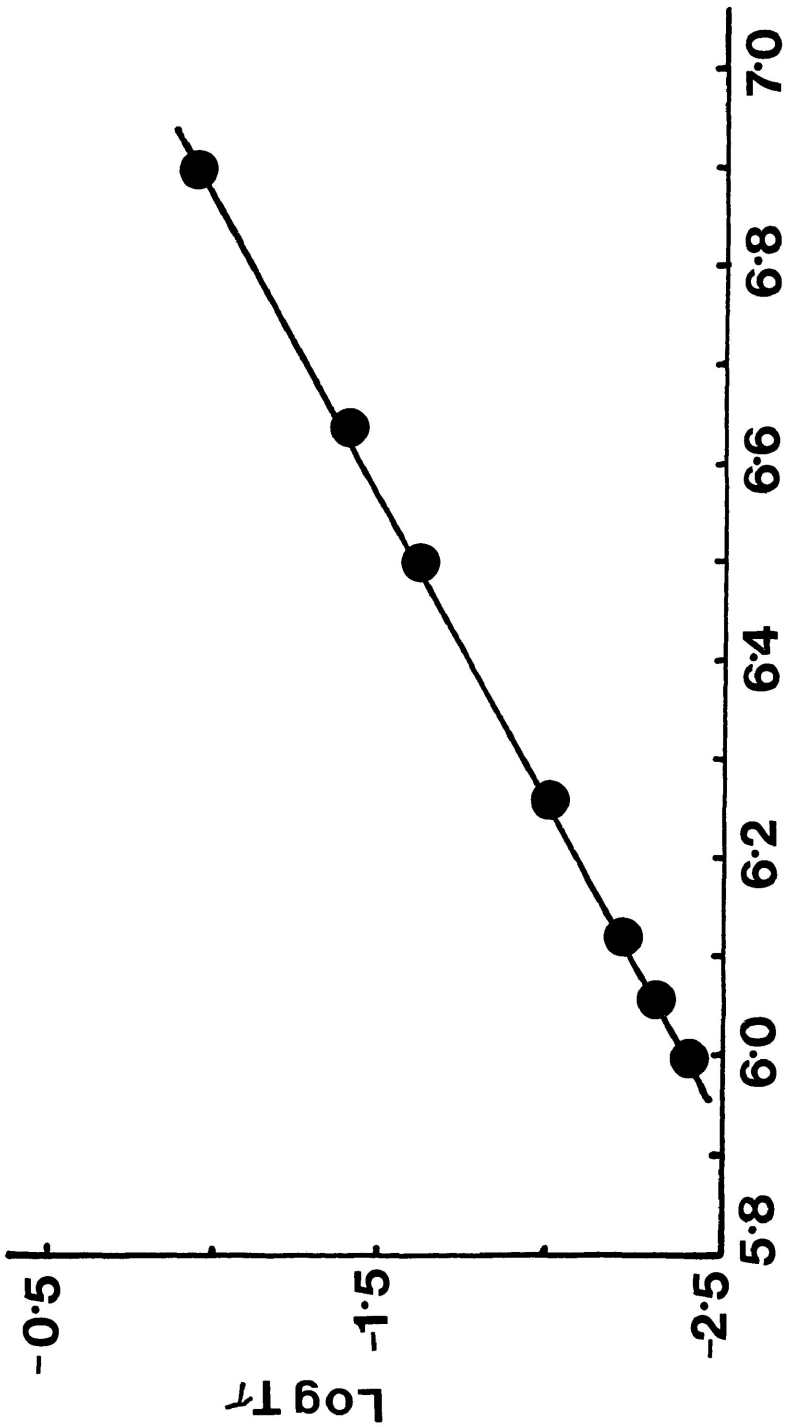

FIGURE 28d: Eyring plot of $\log T_T$ versus $1/T$ (K^{-1}) for norborneol in G.O.T.P. (higher temperature process).

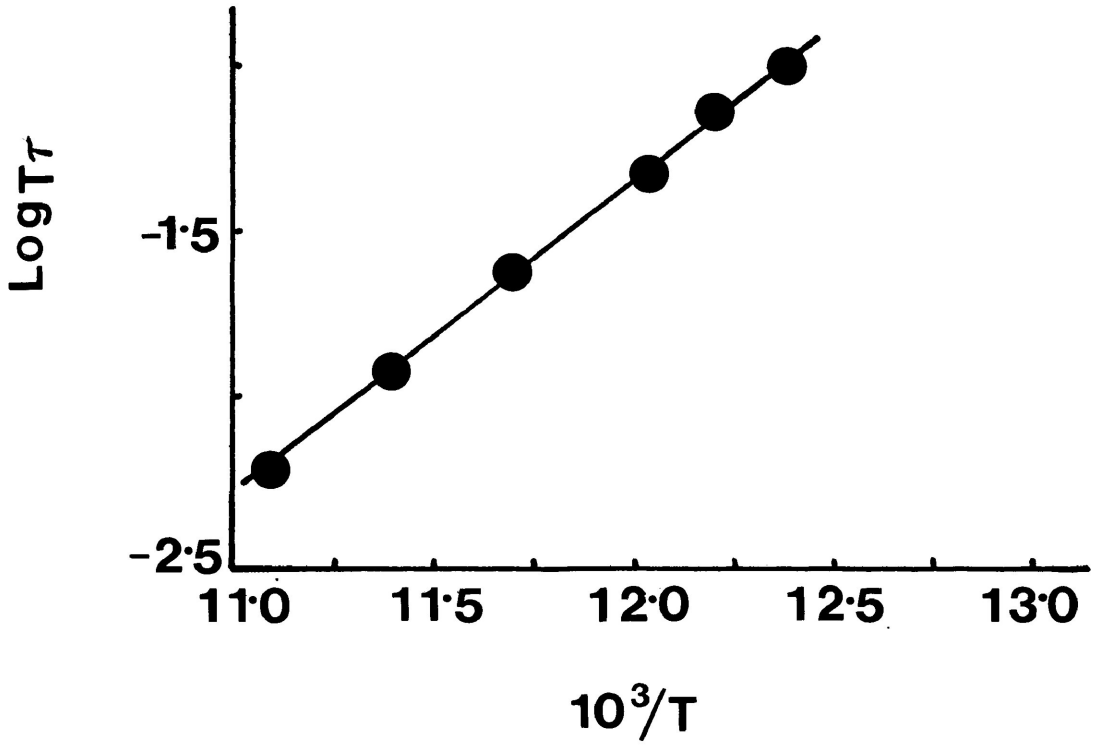

FIGURE VI-29d: Eyring plot of logTτ versus 1/T (K^{-1}) for norborneol in carbontetrachloride

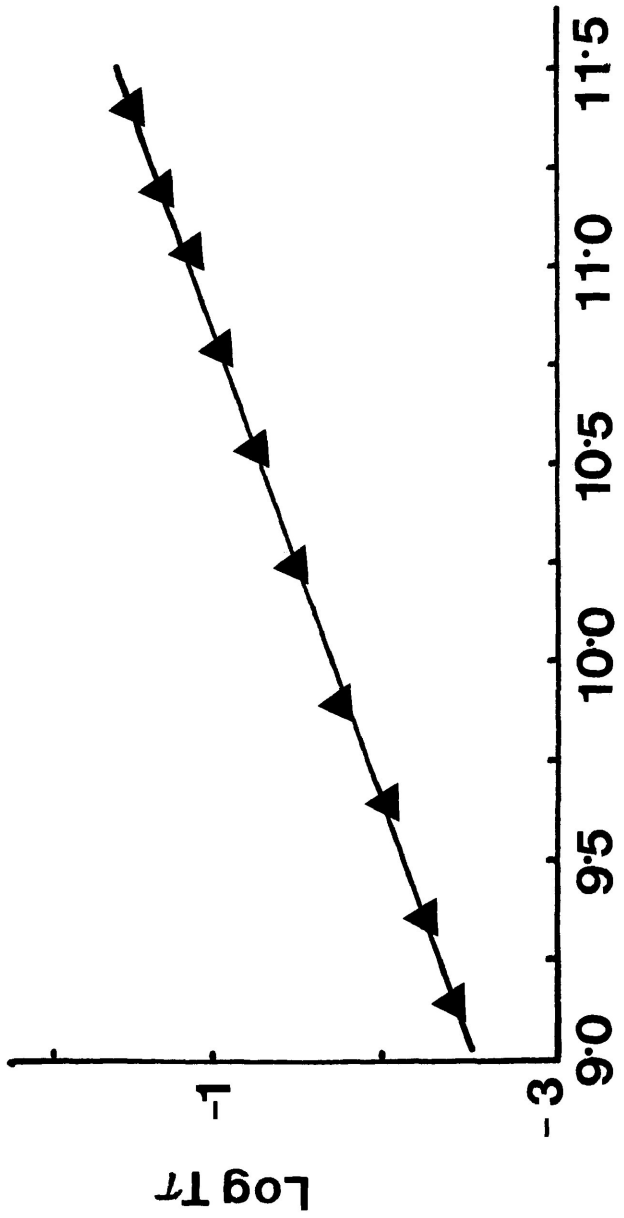

FIGURE VI-30d: Eyring plot of logTτ versus 1/T (K^{-1}) for isoborneol in a polystyrene matrix.

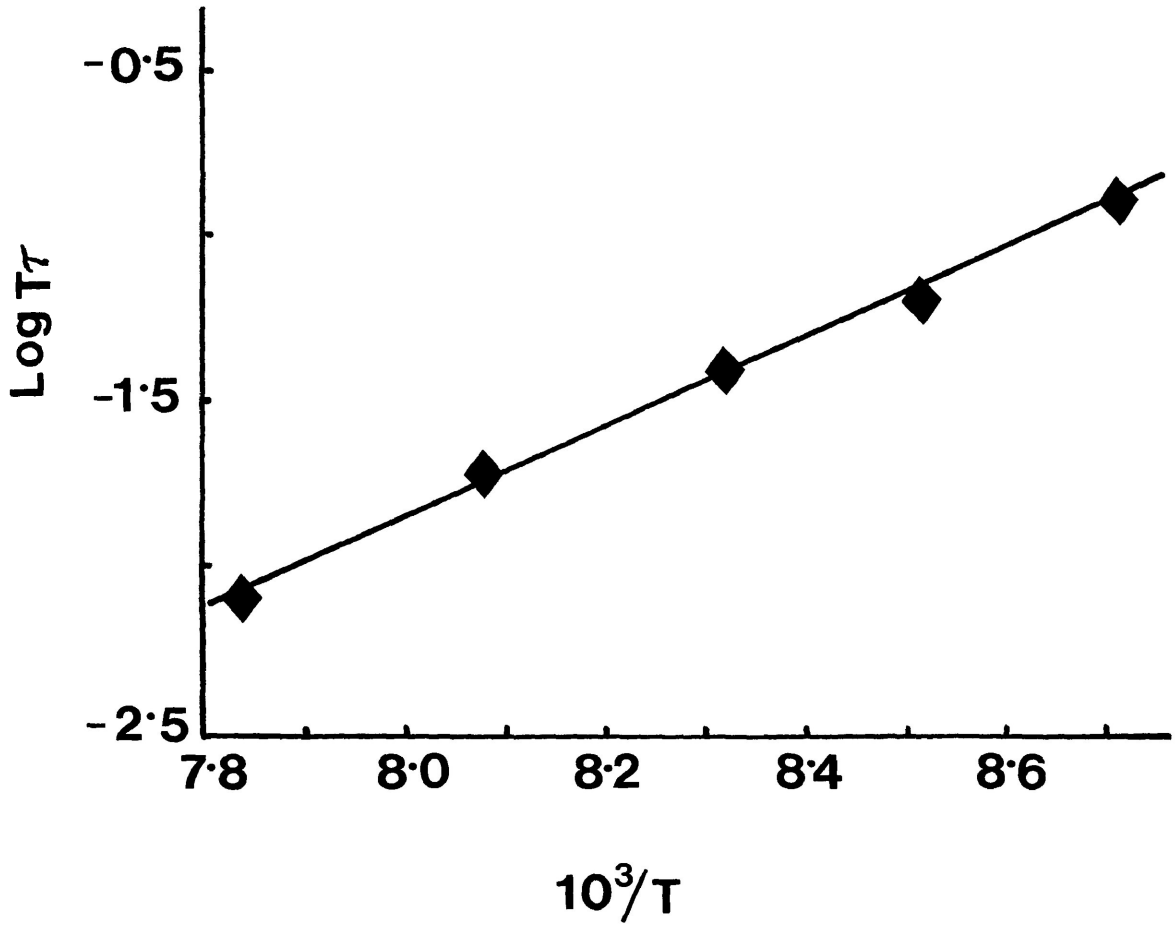

FIGURE VI-31d: Eyring plot of logTτ versus 1/T (K^{-1}) for fenchyl alcohol in a polystyrene matrix.

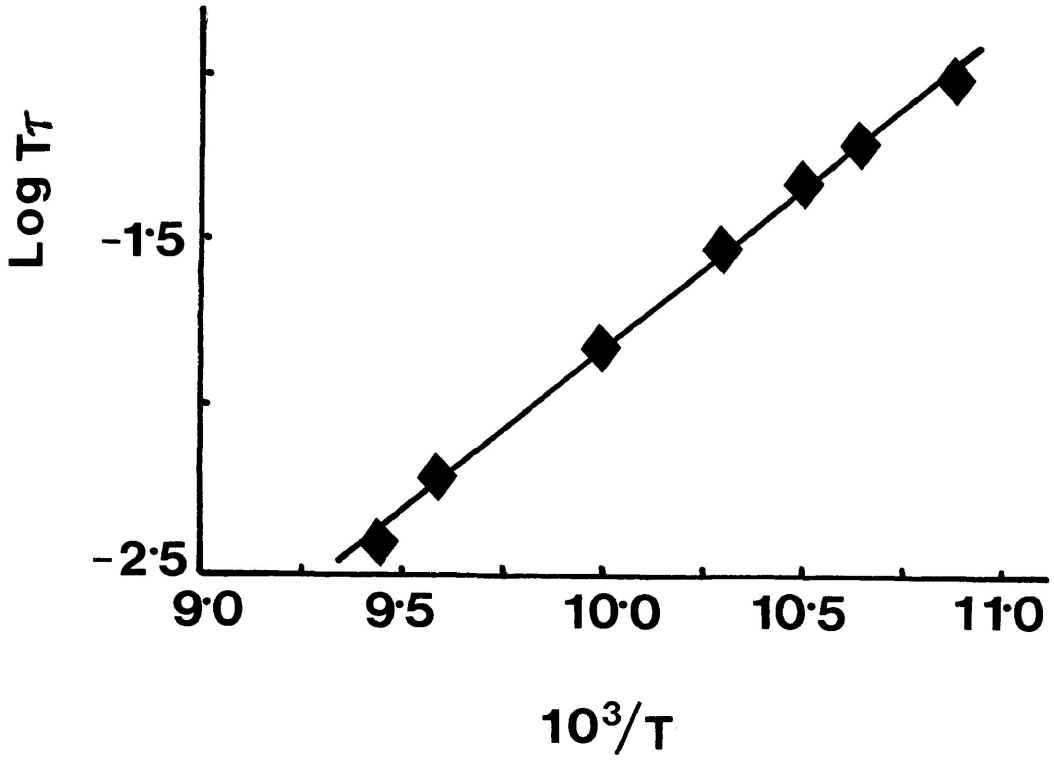

FIGURE VI-32d: Eyring plot of logTτ versus 1/T (K^{-1}) for 5-norbornene-2-carboxaldehyde in a polystyrene matrix.

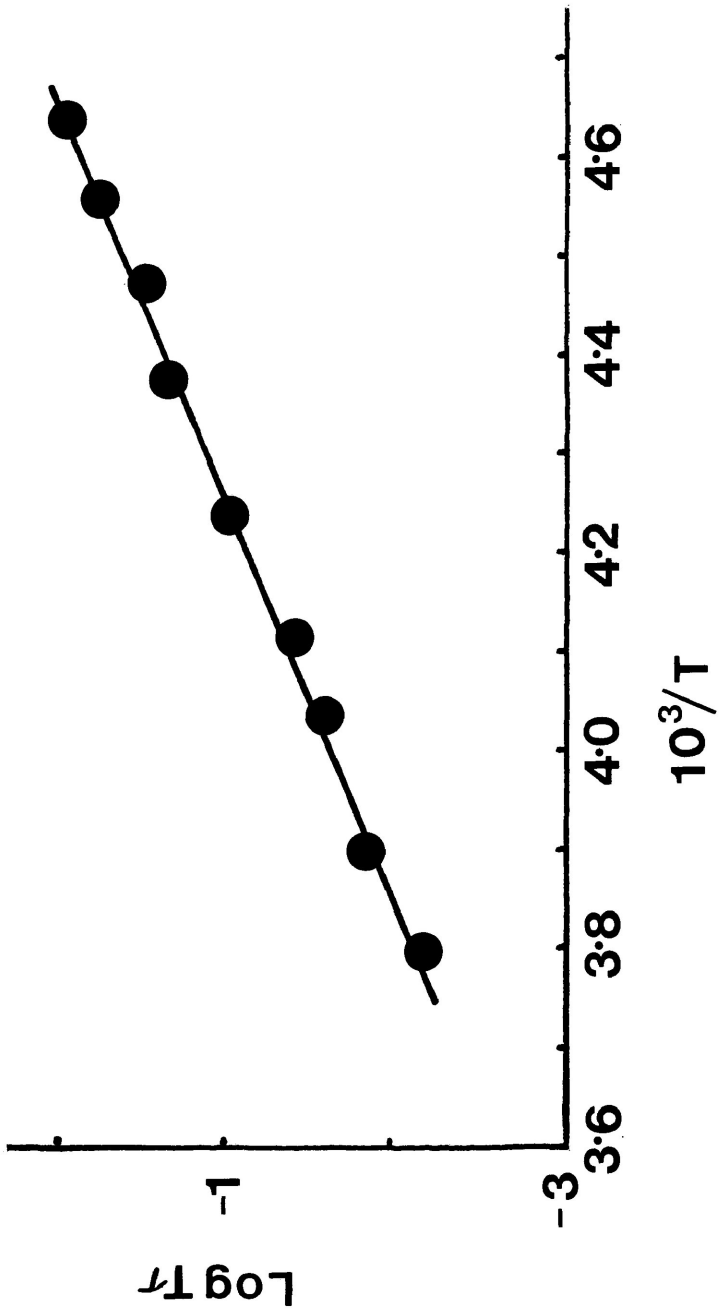

FIGURE VI-33d: Eyring plot of $\log T_\tau$ versus $1/T$ (K^{-1}) for tert-butanol in a polystyrene matrix.

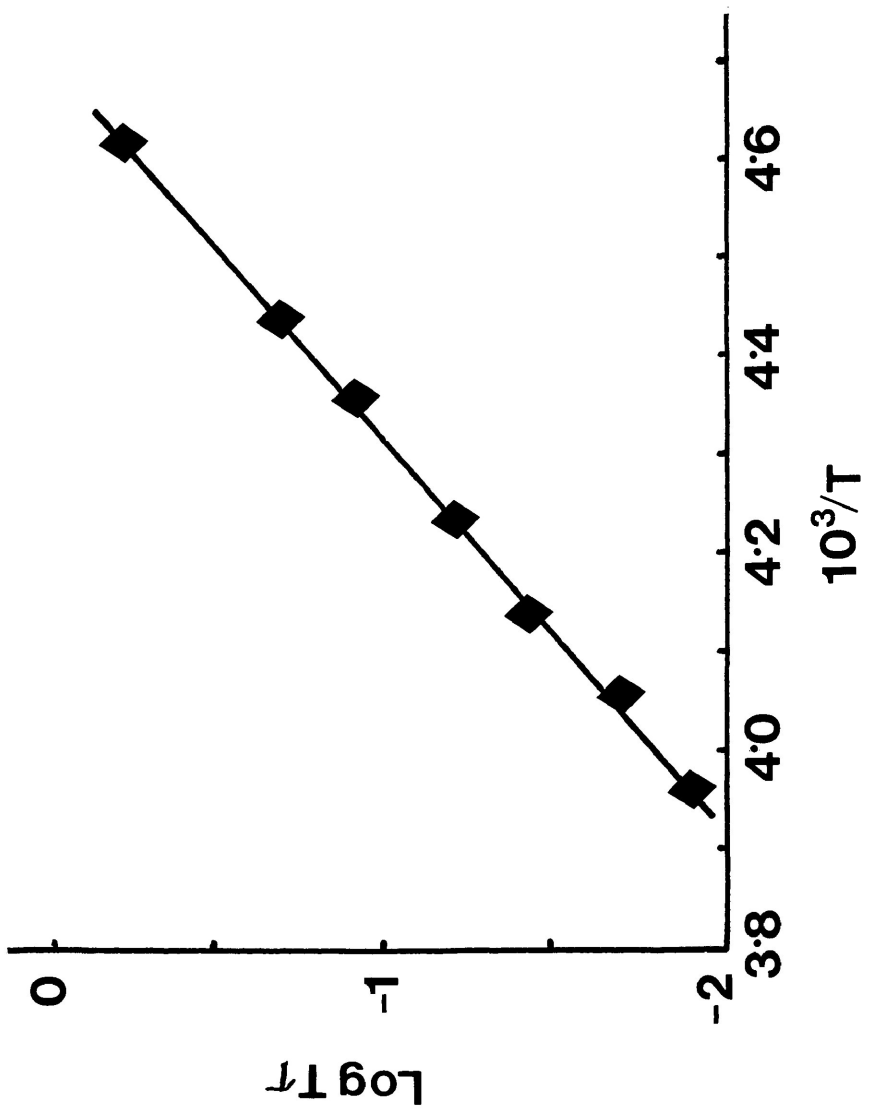

FIGURE VI-34d: Eyring plot of logTτ versus 1/T (K^{-1}) for methanol in a polystyrene matrix.

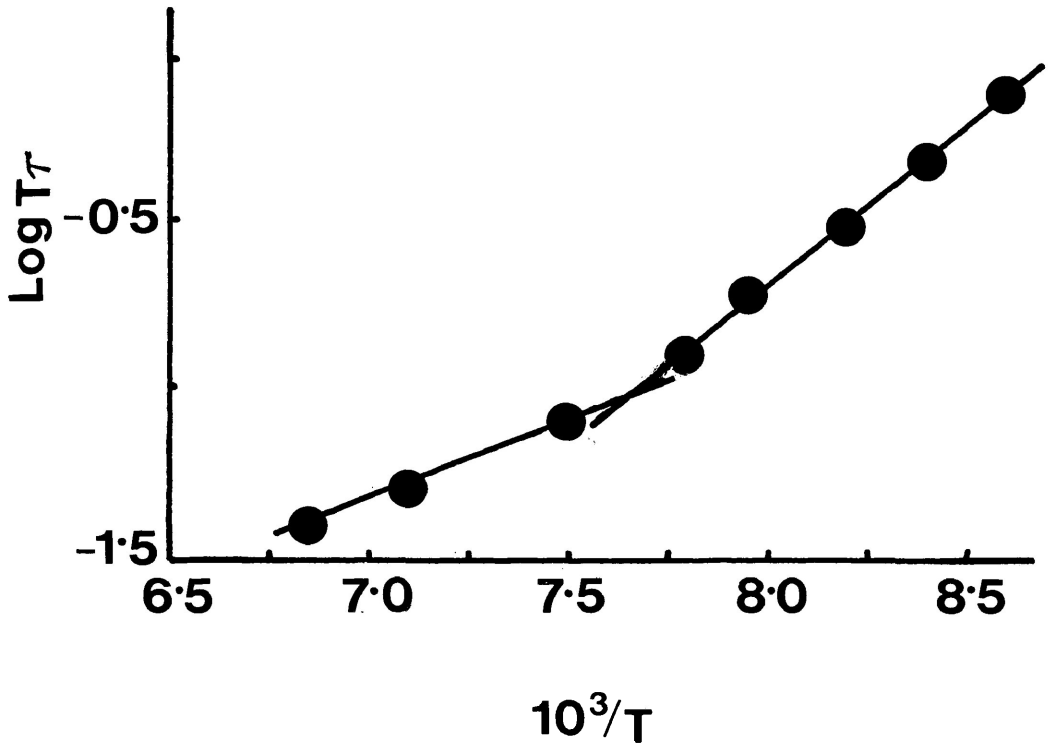

FIGURE VI-35d: Eyring plot of logTτ versus 1/T (K^{-1}) for tert-butanol in the pure solid state

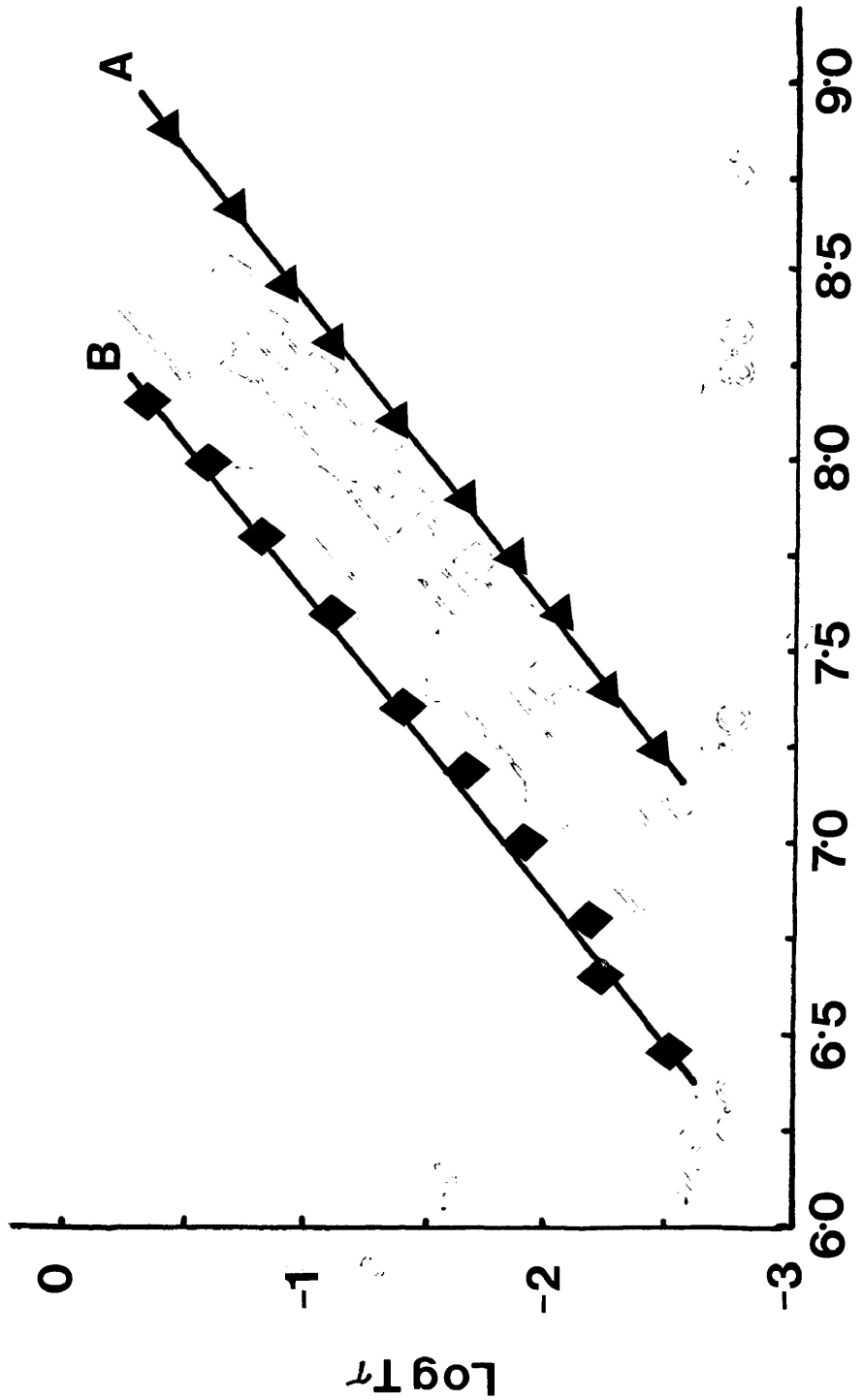

FIGURE VI-36d: Eyring plots of $\log T_T$ versus $1/T$ (K^{-1}) for tert-butanol in carbontetrachloride. A=92.15 mol%, B=24.8 mol %.

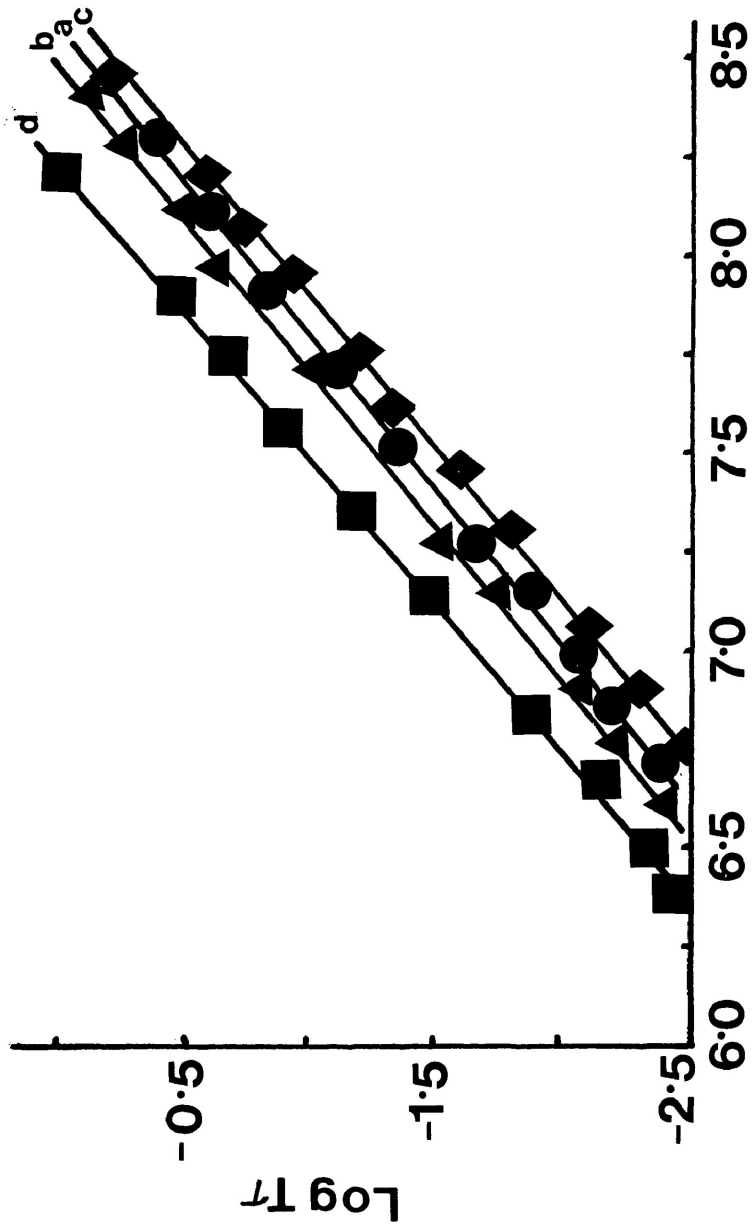

FIGURE VI-37d: Eyring plots of logTτ versus 1/T (K^{-1}) for tert-butanol in carbontetrachloride {a=83.5 mol %, {b=71.22 mol %, {c=64.42 mol %, and {d=33.42 mol %.

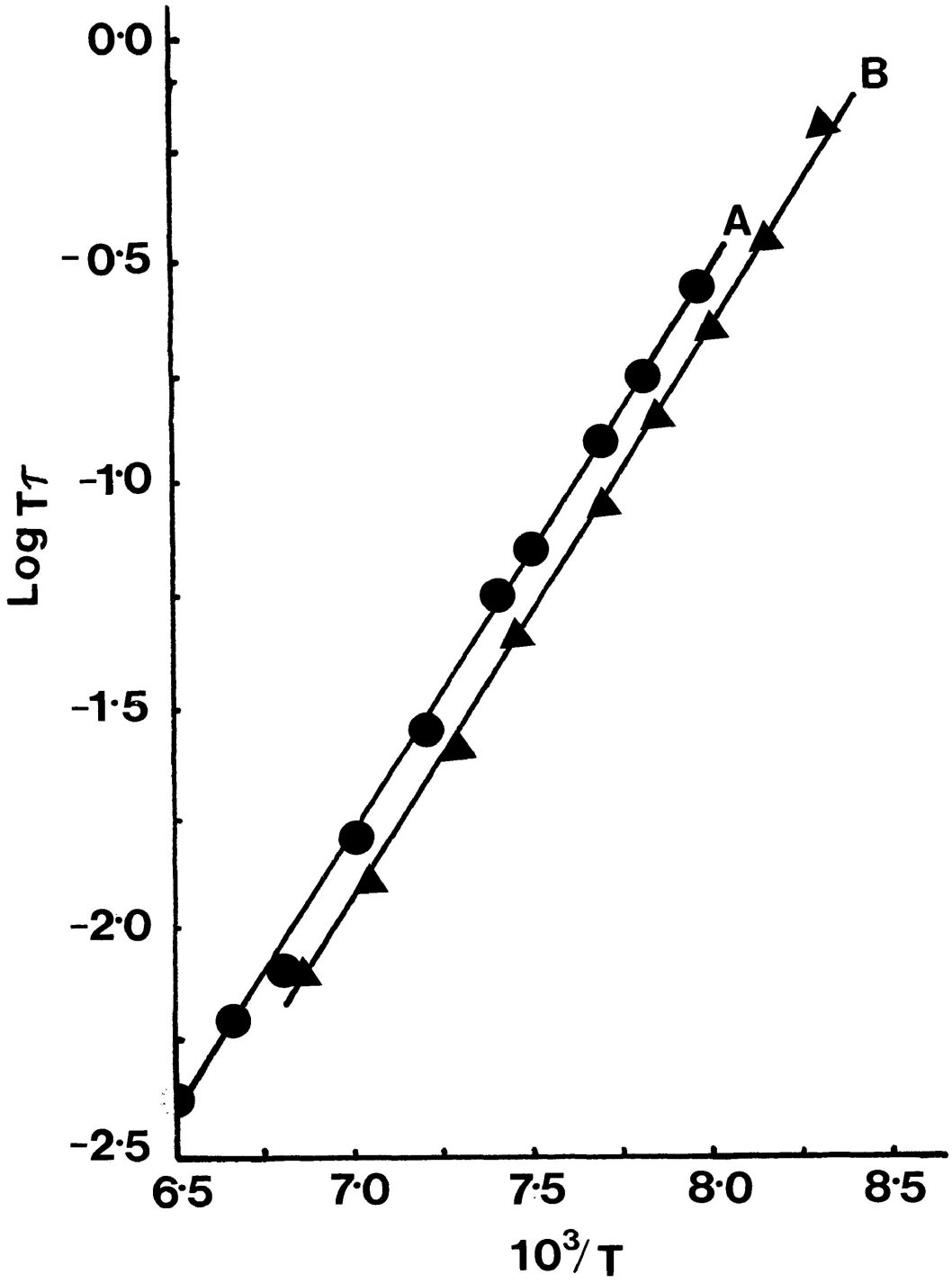

FIGURE VI-38d: Eyring plots of logTτ versus 1/T (K^{-1}) for tert-butanol in carbontetrachloride. A=50 mol %, B=9.03 mol %.

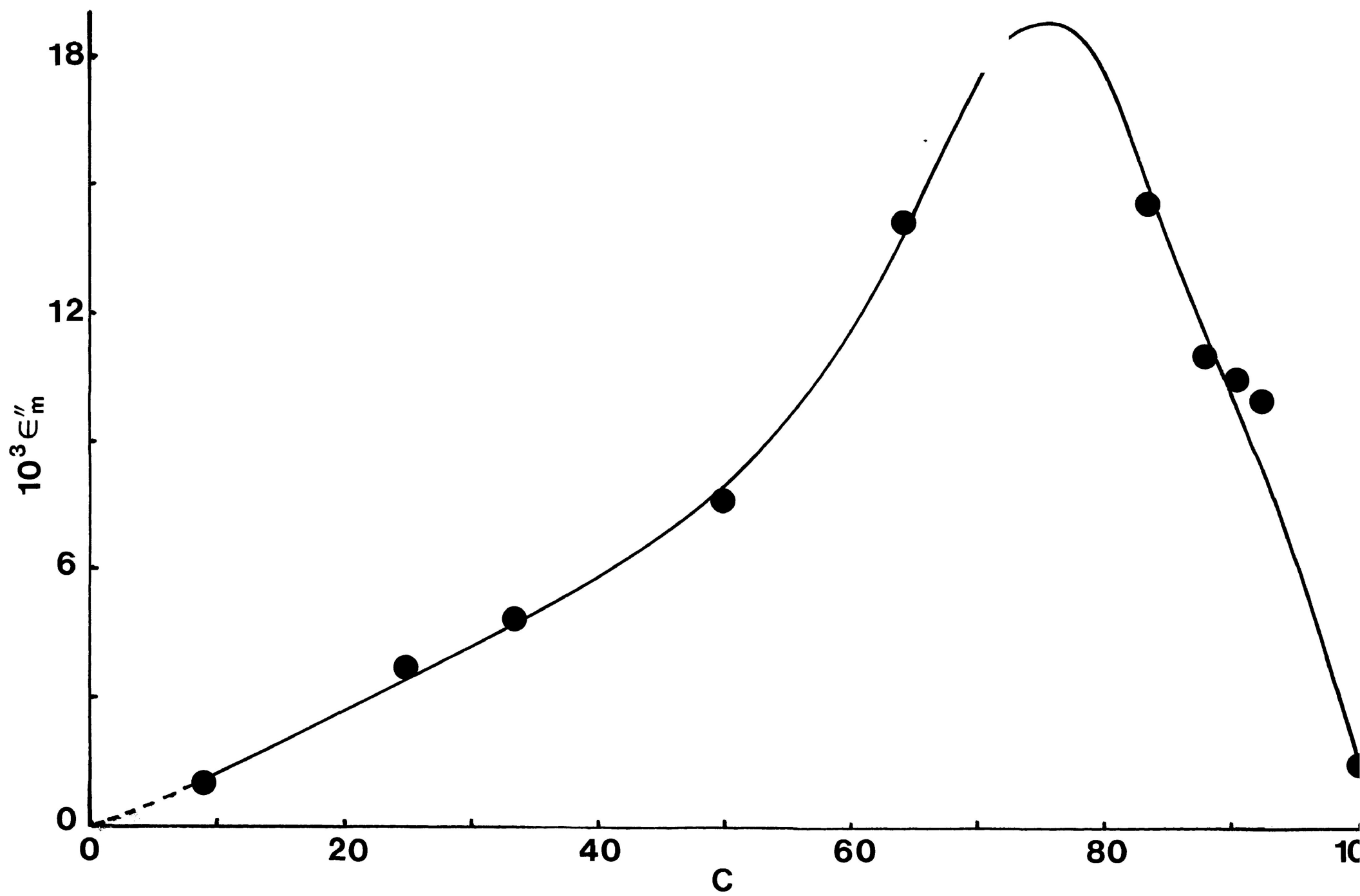

FIGURE VI-39: Plot of maximum dielectric loss factor, ε''_m versus concentration C (mol %) for tert-butanol in carbontetrachloride at 1.01 kHz.

CHAPTER VII

DIELECTRIC RELAXATION OF SOME 2,6-DI- AND 2,4,6-TRI-SUBSTITUTED PHENOLS AND RELATED MOLECULES IN SOME ORGANIC GLASSES

VII-1: INTRODUCTION

Hydroxyl group containing compounds, especially the aliphatic alcohols and their solutions, have been studied extensively by various dielectric absorption techniques, but the precise nature and concentration of the various hydrogen-bonded species including monomers and a variety of linear and cyclic multimers are still controversial (Chapter IV and VI). Aromatic phenols have also been studied by dielectric techniques in the pure solid state and in non-polar solvents, and the relaxation data have often been analyzed in terms of two relaxation times with respect to molecular and intra-molecular relaxation processes. In dielectric absorption studies the latter process having a very short relaxation time ($\sim$3 p.s.) has been invariably interpreted as hydroxyl group relaxation, as for example, by Fong and Smyth (1) in the study of 1-naphthol, 4-hydroxybiphenyl, and 2,6-dimethylphenol. In a later and more detailed study using dielectric relaxation, proton magnetic resonance, and infrared spectroscopy, Fong et al. (2) confirmed that the substitution of alkyl groups, particularly the bulky tert-butyl groups at the ortho positions of phenol, provides effective screening of the OH group from interaction but does not prevent rotation of the hydroxyl group. Similar conclusions were also drawn by Gough and Price (3) from

their dielectric absorption study over a wide frequency range on a number of cryptophenols (2,4,6-tri-tert-butylphenol, deuteroxy 2,4,6-tri-tert-butylphenol, 2,6-di-tert-butylphenol, 2,4,6-tri-tert-pentylphenol and 2,6-di-tert-butyl 4-formylphenol) both in the pure state and in decalin solution. With the exception of the 4-formyl derivative, all these molecules show two dielectric dispersion regions of which the higher frequency one is attributed as to the motion of the phenolic OH group. This relaxation process of tert-butylphenols in decalin involved an activation energy of 9.2 - 11.7 kJ mol^{-1}. In the solid state the corresponding value was found to be significantly lowered (4.6 kJ mol^{-1}) which was interpreted as due to the greater experimental uncertainty in the measurement of solid samples.

Meakins (4) and Davies et al (5) measured the dielectric dispersion of 2,4,6-tri-tert-butylphenol and tricyclohexylcarbinol in pure solids and in decalin solutions. In both the cases two distinct relaxation processes were observed for each molecule at frequencies up to 2.4×10^{10} Hz, the higher frequency one being due to the hydroxyl group relaxation. The activation energy obtained for the hydroxyl group relaxation in 2,4,6-tri-tert-butylphenol and tricyclohexylcarbinol (4,5) are 11.7 and 12.4 kJ mol^{-1}

in decalin solution and 9.2 and 18 kJ mol^{-1} in the pure solid state. The higher energy barrier for tricyclohexylcarbinol in the solid state was accounted for by the more highly hindered rotation about the C-O bond than in 2,4,6-tri-tert-butylphenol.

Phenol itself has a planar structure which is stabilized by delocalization of the p-type lone pair electrons of the oxygen atom to the π-electrons of the ring, resulting in some double bond character of the C-O bond which causes the hydrogen atom to lie in the plane of the ring. Various spectroscopic studies (6-9) indicate a potential energy barrier (V_2) of 14 - 15 kJ mol^{-1} for the rotation of the OH group in phenols.

Davies and Edwards (10) studied dielectric absorption of β-naphthol in a polystyrene matrix and obtained a ΔH_E value of 2.1 kJ mol^{-1} for the hydroxyl group relaxation which did not reflect any appreciable double bond character in the C-O linkage. The hydroxyl rotational barrier can be appreciably increased for some appropriately o-substituted phenols due to intramolecular hydrogen bonding. Thus, much higher activation (∿35 kJ mol^{-1}) enthalpies have been obtained by Tay et al (11) for the OH group relaxation in 2,6-dinitrophenol and 2,6-dinitro-4-methylphenol

in polystyrene matrices. Mazid et al (12) studied a series of 2,4,6-tri- and penta-substituted phenols in polystyrene matrices, and in all halogenophenols the lower temperature processes were identified as hydroxyl group relaxation. The enthalpy of activation for this intramolecular process was found to depend on the strength of the intramolecular hydrogen-bonds formed with o-substituents. Thus, the intramolecular ΔH_E value increased from 15 kJ mol^{-1} for 2,4,6-trichlorophenol to 26 kJ mol^{-1} for pentachlorophenol. The relatively lower ΔH_E value for pentachlorobenzenethiol in comparison to pentachlorophenol was accounted for by the weaker intramolecular hydrogen bond formed by the SH relative to the OH group.

Very recently Enayetullah (13) studied a number of alkylphenols and other related hydroxy compounds in polystyrene matrices. In alkylphenols the author obtained only one relaxation process which was accounted for by molecular rotation, but he could not detect OH group relaxation in any case in his frequency range 10^2-10^5 Hz. For 2,6-dichlorophenol he obtained an overlapping process due to contribution of whole molecule rotation and OH group rotation whereas Mazid et al (12) obtained two separate absorption processes for the fairly similar type of molecule 2,4,6-trichlorophenol in a polystyrene matrix.

The enthalpy of activation for OH group rotation in 4-phenyl phenol, triphenylmethanol and 1-naphthol in the pure solid state has been reported (13) as: 13, 17 and 35 kJ mol^{-1} respectively. The higher energy barrier was accounted for by the hydrogen bond breaking followed by OH group rotation. The OH group rotation in 2-naphthol involved an energy barrier of 12 kJ mol^{-1} (13) in polystyrene matrices.

From the above discussion it would appear that the barrier to hydroxyl group relaxation in substituted phenols depends upon the steric and probably on the inductive effects of the substituents as well as on the strength of the intramolecular hydrogen bond. Intermolecular hydrogen bonding may similarly influence the barriers of molecular rotation of such systems. It seemed desirable to investigate the energy barrier to hydroxyl group relaxation in such systems as 2,6-disubsituted phenols and in related compounds bearing additional substituents, such as 2,4,6-tri-substitued phenols, so that the effect of various factors might be deduced. The work was particularly aimed at a study of the effect of dispersion media on the intramolecular hydrogen bond as well as the relaxation parameters of hydroxyl group rotation.

One particular aspect of the intramolecular process

which, in general, has rearely been considered by dielectric-absorption workers is to examine whether the intramolecular process in phenols and other hydroxy compounds may be attributed to proton tunneling as opposed to hydroxyl group relaxation. Energy barriers for hydroxyl and methoxy group relaxation in non-intramolecularly hydrogen-bonded phenols (4,14) and aromatic $-OCH_3$ systems are of the same order (15,16). The ΔH_E of 9.6 kJ mol^{-1} for methoxy group rotation (15) in 3,5-dimethyl anisole was virtually the same as the ΔH_E value (9.2 kJ mol^{-1}) which Meakins (4) found for hydroxyl group relaxation in pure solid 2,4,6-tri-tert-butylphenol. These results appear to negate the possibility of proton tunneling in non-intramolecularly hydrogen bonded phenols. Mazid et al (12) did not find any evidence of proton tunneling in the intramolecular processes of 2,4,6-tri- and penta-halogenophenols in polystyrene matrices. Gough and Price (3) also did not find any indication of proton tunneling in 2,6-di and 2,4,6-tri-tert-butylphenol in the pure solid state and in decalin solution in the temperature range−70 to 20°C.

Recent spectroscopic study (infrared and microwave) has demonstrated proton tunneling in the intramolecularly hydrogen bonded system of tropolone (17) in the gaseous phase, but Enayetullah (13) has not found any evidence of such

effect in tropolone and in related compounds by dielectric technique in polystyrene matrices. Thus, the experimental evidence for proton tunneling in a non-aqueous solution is extremely sparce, and, as yet, there does not appear to be any convincing case obtained from dielectric studies. It seems worthwhile to apply the dielectric absorption technique to some of these molecules already studied in polystyrene matrices to other glass forming media, such as, G.O.T.P. to investigate the possibility of proton tunneling as an intramolecular process in these systems.

VII-2: EXPERIMENTAL RESULTS

The dielectric measurements of a variety of substituted phenols and related hydroxy compounds (listed in Figure VII-1) have been made over suitable ranges of temperature and frequency (usually 10 Hz to 10^5 Hz) by the use of a General Radio 1621 Precision Capacitance Measurement system and three-terminal co-axial cell, the procedure being described in Chapter II. The methods employed for the evaluation of relaxation and activation parameters have also been described previously (Chapter II). All the chemicals were commercially available with sufficient purity and were used without further purification but properly dried prior to use.

Tables VII-1 and VII-2 collect the values of ΔH_E and ΔS_E evaluated from dielectric data as well as ΔG_E and τ values at 100 K, 150 K and 200 K for each system where appropriate. A tabulated summary of Fuoss-Kirkwood analysis parameters, τ, $\log\nu_{max}$, β and ε''_{max}, at various experimental temperatures is presented in Table VII-3.

Sample plots of dielectric loss factor, ε'' versus T(K) for the dipolar molecules in the mentioned medium are shown

in Figures VII-1a to VII-8a, while Figures VII-9b to VII-17b present the sample plots of dielectric loss factor versus logarithm of frequency (ε'' versus $\log\nu$). Figures VII-18c to VII-21c present the Cole-Cole plots for the mentioned molecules in their respective dispersion region as sample while Figures VII-22d to VII-32d present the sample plots of $\log T\tau$ versus $1/T$.

FIGURE VII-1

1. 2,6-DICHLOROPHENOL

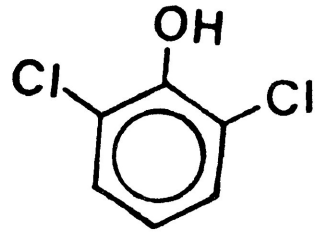

2. 2,4,6-TRICHLOROPHENOL

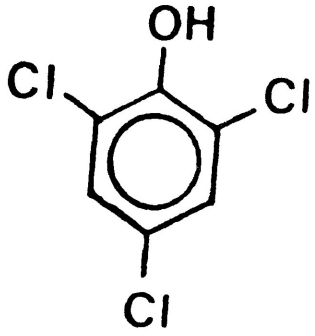

3. 2,4,6-TRIBROMOPHENOL

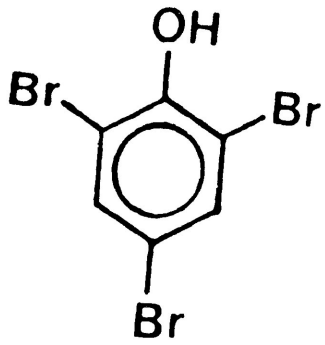

4. 2,4,6-TRIIODOPHENOL

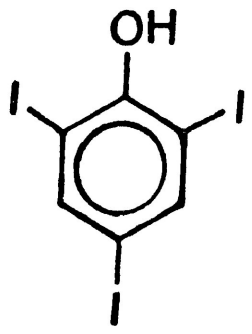

FIGURE VII-1: continued...

5. 2,6-DICHLORO-4-NITROPHENOL

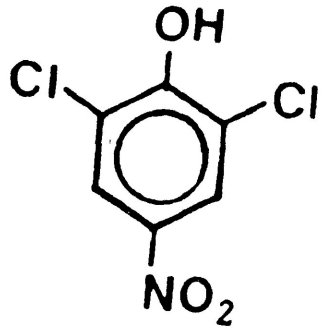

6. 2,6-DIBROMO-4-NITROPHENOL

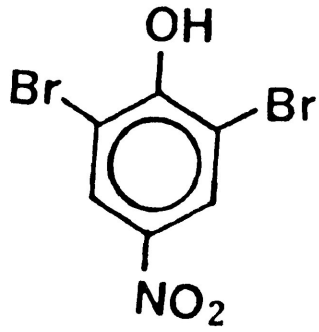

7. 2,6-DINITRO-4-METHYLPHENOL

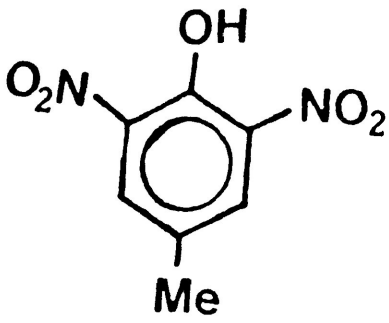

8. 2,6-DI-TERTIARY-BUTYLPHENOL

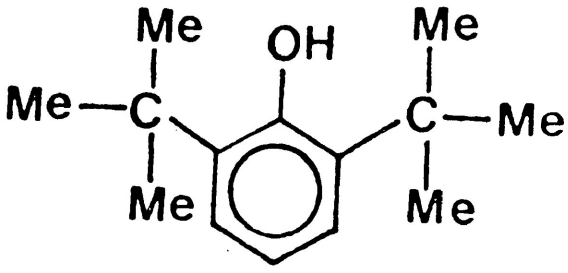

FIGURE VII-1: continued...

9. 2,4,6-TRI-TERTIARY-BUTYLPHENOL

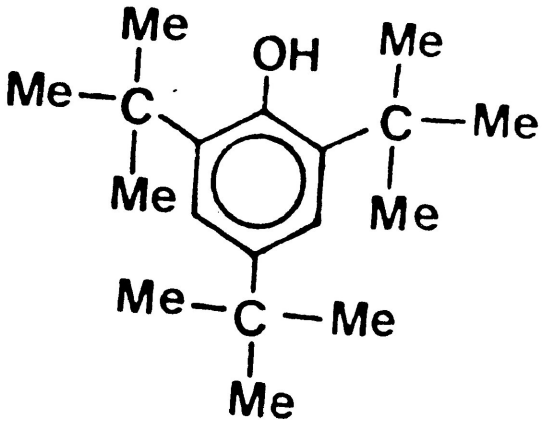

10. 2,3,4,5,6-PENTACHLORO-BENZENETHIOL

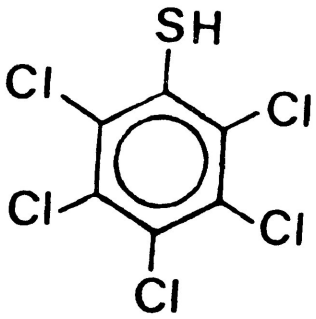

11. TROPOLONE

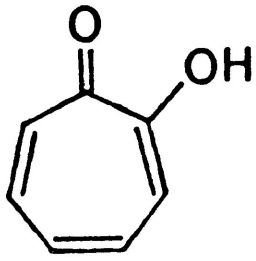

VII-3: DISCUSSION

The molecule, 2,6-dichlorophenol, exhibits only one dielectric relaxation process in cis-decalin in the temperature range 84-109 K. The relaxation parameters obtained for this dispersion are: ΔH_E = 10 kJ mol^{-1}, ΔS_E = -64 J K^{-1} mol^{-1} and ΔG_E = 17 kJ mol^{-1} and $\tau = 2.0 \times 10^{-4}$ s at 100 K, respectively. The β-value for this process ranges between 0.41 - 0.74. From earlier works (1-5) on phenols and related hydroxy compounds, two relaxation processes need to be considered, one, due to the rotation of -OH group and the other due to the whole molecule relaxation. m-Dichlorobenzene, a fairly polar rigid molecule, is almost similar in size to 2,6-dichlorophenol. The relaxation parameters obtained for this molecule in a polystyrene matrix are (18): ΔH_E = 16 kJ mol^{-1}, ΔS_E = -30 J K^{-1} mol^{-1} and ΔG_E = 19 kJ mol^{-1} and $\tau = 4.7 \times 10^{-3}$ s at 100 K. The enthalpies of activation for molecular rotation of other similar-sized rigid molecules are: 16 kJ mol^{-1} for o-dichlorobenzene in a polystyrene matrix (19), 13 kJ mol^{-1} in cis-dcalin (20) and 16 kJ mol^{-1} for o-xylene in the pure solid state (21). Enayetullah (13) reported the relaxation parameters for 2,6-dichlorophenol in polystyrene matrices as: ΔH_E = 16 kJ mol^{-1}, ΔS_E = -29 J K^{-1} mol^{-1} and ΔG_E = 18 kJ mol^{-1} and $\tau = 2.0 \times 10^{-3}$ s at 100 K, respectively. The

author interpreted these relaxation parameters as being due to the overlapping processes of OH group and whole molecule rotation. The enthalpy of activation for hydroxyl group rotation in 2,4,6-tri-tert-butylphenol was found to be 9.2 kJ mol^{-1} (4) in the solid state and 11.7 kJ mol^{-1} in decalin solution. Within experimental error, these values are very close to the observed value (10 kJ mol^{-1}) for 2,6-dichlorophenol in cis-decalin. Moreover, the relaxation parameters for 2,6-dichlorophenol are in excellent agreement with those obtained for methoxy group rotation in para-chloroanisole in cis-decalin (see Table VII-2). All these results strongly indicate that the hydroxyl group relaxation is the potential candidate for the observed dielectric absorption in 2,6-dichlorophenol. The observed high β-value (0.41-0.74) strongly favours the intramolecular nature of the process.

The molecule 2,4,6-trichlorophenol like 2,6-dichlorophenol exhibits only one dielectric dispersion in the temperature range 84-103 K. The Fuoss-Kirkwood distribution parameter, β, which measures the distribution of relaxation time varies between 0.49 - 0.63. The linear Eyring plot, log$T\tau$ versus 1/T, yields the relaxation parameters for this molecule as: ΔH = 12 kJ mol^{-1}, ΔS_E = -37 J K^{-1} mol^{-1} and ΔG_E = 16 kJ mol^{-1} and τ = 6.7×10^{-5} s at 100 K, respectively. The relaxation parameters

for almost similar-sized, rigid molecules in polystyrene matrices are (18):

Molecules	ΔH_E kJ mol^{-1}	ΔS_E J K^{-1} mol^{-1}	$\Delta G_{E100\ K}$ kJ mol^{-1}	τ(s) at 100 K
2,4,6-tri-chloro-pyridine	38	35	34	2.8×10^{5}
2,4,6-trimethyl benzonitrile	29	6	29	4.2×10^{2}
2,4,6-trichloro nitrobenzene	29	1	29	8.3×10^{2}

All these results demonstrate that the relatively lower energy barrier (12 kJ mol^{-1}) and shorter relaxation time (6.7×10^{-5} s at 100 K) for 2,4,6-trichlorophenol cannot be accounted for by molecular relaxation. Mazid et al (12) studied this compound in a polystyrene matrix and reported the relaxation parameters for OH group rotation as: ΔH_E = 15 kJ mol^{-1}, ΔS_E = -5 J K^{-1} mol^{-1} and ΔG_E = 16 kJ mol^{-1} and $\tau = 6.7\times10^{-5}$ s at 100 K. They interpreted the relatively higher activation parameters for OH group rotation as being due to the intermolecular hydrogen bonding. The observed enthalpy of activation for 2,4,6-trichlorophenol in cis-decalin is very close to the value obtained for OH group rotation (4) in 2,4,6-tri-tert-butylphenol (11.7 kJ mol^{-1}) and methoxy group rotation in para-chloroanisole in cis-decalin (see Table VII-2). Thus, it will not be unreasonable to interpret the

observed dispersion for 2,4,6-trichlorophenol in cis-decalin as due to the hydroxyl group rotation. The relatively higher β-value and lower activation entropy are consistent with the intramolecular nature of the relaxation process. The acidity of the chlorophenols depends upon the number of chlorine atoms in the ring (22), e.g., the pKa of pentachlorophenol is 4.8 whereas it is 6.5 for 2,4,6-trichlorophenol. This indicates that the double bond nature of the bond from the phenolic oxygen to the ring carbon may be greater in 2,4,6-trichlorophenol than that in 2,6-dichlorophenol. Though the variation is within experimental error, the slightly higher ΔH_E (12 kJ mol^{-1}) for 2,4,6-trichlorophenol than those of 2,6-dichlorophenol (10 kJ mol^{-1}) in cis-decalin could be accounted for by an additional resonance contribution.

The enthalpy of activation, ΔH_E for hydroxyl group rotation is lowered (8 kJ mol^{-1}) for dilute solution of 2,4,6-trichlorophenol in cis-decalin. This indicates that there may be some weak intermolecular hydrogen bonding in the usual concentration range of 2,6-dichloro- and 2,4,6-trichlorophenol in cis-decalin. When the solution is diluted, the intermolecular interaction decreases causing thereby the energy barrier for -OH group relaxation to be lowered. The very low entropy of activation for the dilute solution (-81 J K^{-1}

mol^{-1}) supports this view. The stronger the intramolecular hydrogen bond, the more energy will be required to achieve -OH group relaxation and, possibly, greater disorder in the system leading to a higher ΔS_E value. The high β-value (0.38-0.94) for this relaxation for dilute solution also suggests negligible interaction of the hydroxyl group with its surrounding at the time of rotation at a particular temperature.

For each of the two molecules, 2,4,6-tribromophenol and 2,4,6-triiodophenol, one relaxation process was observed in G.O.T.P. The relaxation parameters obtained for these molecules are: ΔH_E = 9 and 6 kJ mol^{-1}, ΔS_E = -62 and -83 J K^{-1} mol^{-1}, ΔG_E at 100 K = 15 and 14 kJ mol^{-1} and τ at 100 k = 2.3×10^{-5} and 1.2×10^{-3} s, respectively. The activation enthalpies and free energies at 100 K for these molecules are comparable to those for 2,4,6-trichlorophenol in decalin except that the activation enthalpy in the case of 2,4,6-triiodophenol appears to be slightly lower than those of the other two cases. These values are also very close to those obtained for methoxy group rotation in para-bromoanisole and para-iodoanisole in G.O.T.P. (see Table VII-2). Similar low activation energies of 2.1 (10), 5.0 (3), 9.2 (4) and 11.7 (5) kJ mol^{-1} for the hydroxyl group relaxation have been obtained for 2-naphthol in a polystyrene matrix, 2,4,6-tri-tert-butylphenol in the

solid state and in decalin solution, respectively. On the other hand, Tay et al (11) reported much higher ΔH_E of $\sim$35 kJ mol^{-1} for -OH group relaxation in 2,6-dinitro- and 2,6-dinitro 4-methylphenols in polystyrene matrices, suggesting that "the intramolecular hydrogen bond in 2,6-dinitro phenol is much closer to being a strong hydrogen bond than a weak one." It was also proposed that the transition of the hydroxyl group from one planar hydrogen bonded position to the other takes place over an energy barrier which is strongly dependent on the energy required to break the intramolecular hydrogen bond. Thus, the low energy barriers obtained for the trihalogenophenols would appear to suggest that the intramolecular hydrogen bonding of the hydroxyl groups with the various halogens is of the weak type. The generally accepted order of the intramolecular halogen-hydroxyl interaction is Cl>Br>I (23). This bears out that the hydroxyl group relaxation barrier depends on the energy required to break the hydrogen-bond. With the increase of the size of the halogen atom the barriers may have been compensated to some extent by an adverse steric effect which is evident from the longer relaxation time for 2,4,6-triiodo-phenol.

In terms of the acidity of the substituted halo-phenols, the potential energy barrier (V) for the -OH group

relaxation correlates well with the OH torsional frequencies obtained by Fateley and his co-workers (14). They have clearly demonstrated that the phenolic -OH torsional frequency is a direct measure of the double bond character of the phenolic C-O bond. Thus, the sequence of activation enthalpy of 12, 9 and 6 kJ mol^{-1} for 2,4,6-trichloro-, tribromo- and triiodo-phenol, respectively, compares well with the sequence of the corresponding OH-torsional frequency of 393, 393 and 382 cm^{-1} observed in cyclohexane solutions. 2,4,6-trichloro and 2,4,6-tribromophenol show a similar double bond character of the C-O bond as evidenced from the same OH torsional frequency.. A slightly higher ΔH_E value (12 kJ mol^{-1}) in 2,4,6-trichlorophenol from those in 2,4,6-tribromo-phenol may be due to some weak intermolecular hydrogen bonding in the former.

The acidic properties of halogenophenols can be increased by substituting a strong electron withdrawing group in the appropriate position, such as, a nitro group in the 4-positin of the ring. Two such compounds, namely, 2,6-dichloro-4-nitrophenol and 2,6-dibromo 4-nitrophenol, have been studied in glassy o-terphenyl. One dispersion region was obtained for each molecule in the temperature range 90-133 K. The relaxation parameters obtained for these molecules are: ΔH_E = 10 and 12 kJ mol^{-1}, ΔS_E = -84 and -58 J K^{-1} mol^{-1},

ΔG_E = 18 kJ mol^{-1} at 100 K and τ 2.0×10^{-3} and 6.8×10^{-4} s at 100 K, respectively. The relatively lower values of enthalpy of activation for these molecules cannot be accounted for by molecular rotation. Moreover, the activation enthalpies and free energies obtained for the almost similar-sized rigid molecules, 2,4,6-trichloronitrobenzene and 2,4,6-trimethyl benzonitrile in polystyrene matrices, are 29 kJ mol^{-1} and 29 kJ mol^{-1} at 100 K, respectively (18). These results appear to suggest that the relaxations obtained for 2,6-dichloro 4-nitrophenol and 2,6-dibromo 4-nitrophenol may be attributed to the rotation of the hydroxyl group. The ΔH_E and ΔG_E at 100 K for these molecules are virtually the same as 2,6-dichlorophenol in cis-decalin. This indicates that the same mechanism is responsible for the relaxation in 2,6-dichlorophenol and in 2,6-dihalo-4-nitrophenol. The electron-withdrawing group (nitro group) at the para-position virtually has no effect on these relaxations. A slightly higher ΔH_E value (12 kJ mol^{-1}) for hydroxyl group rotation in 2,6-dibromo-4-nitrophenol is not beyond the experimental error. Moreover, a slightly higher energy barrier for 2,6-dibromo-4-nitrophenol may be appreciated for the steric effect of the larger sized bromine atom at the ortho-position of the molecule.

The molecule, 2,6-dinitro-4-methylphenol, exhibits

only one relaxation process in the temperature range 157-194 K in G.O.T.P. and Santovac®. The relaxation parameters obtained for this relaxation are: ΔH_E = 29 and 28 kJ mol^{-1}, ΔS_E = -13 and -19 J K^{-1} mol^{-1}, ΔG_E = 30 kJ mol^{-1} and $\tau = 2.8 \times 10^3$ and 1.8×10^3 s at 100 K, respectively. Within experimental error, these parameters are virtually the same in both the dispersion media. This indicates that the relaxation is almost independent of the dispersion medium. The relaxation parameters for the almost similar-sized rigid molecule,(18) 2,4-dinitrochlorobenzene in a polystyrene matrix, are: ΔH_E = 39 kJ mol^{-1}, ΔS_E = 25 J K^{-1} mol^{-1} and ΔG_E = 37 kJ mol^{-1} and $\tau = 8.5 \times 10^6$ s at 100 K. The activation free energy and relaxation time at 100 K for another similar-sized rigid molecule, 3,5-dinitrobenzonitrile, are 33 kJ mol^{-1} and 7.0×10^4 s, respectively. The relaxation parameters obtained for 2,6-dinitro-4-methylphenol are appreciably lower than the corresponding parameters for rigid molecules in polystyrene matrices. We did not obtain any suitable rigid molecule data in G.O.T.P. and Santovac® for comparison. However, the activation parameters for molecular relaxation are very sensitive to the length of the molecule on the long principal axis. The free energies of activation and relaxation times at 200 K for p-chlorotoluene in G.O.T.P. and Santovac® are 38 and 37 kJ mol^{-1} and 2.0×10^{-3} and 9.1×10^{-4} s, respectively.(24). 2,6-dinitro-4-methylphenol is comparable to p-chlorotoluene

in length along the long prinicpal axis. The activation parameters for the former are considerably lower than those for the latter. All this evidence appears to indicate that the relaxation observed for 2,6-dinitro-4-methylphenol in G.O.T.P. and Santovac® is not a molecular relaxation process. The relaxation may then be best accounted for by intramolecular relaxation due to the rotation of the (intramolecularly hydrogen bonded) -OH group. The virtually identical parameters in both the G.O.T.P. and Santovac® supports this view.

Tay et al (11) studied 2,6-dinitro-4-methylphenol in polystyrene and polyethylene matrices. In both the cases they obtained only one process in the temperature range 186-206 K. The activation enthalpies and free energies for these processes are 35 and 36 kJ mol^{-1} and 31 kJ mol^{-1} at 100 K, respectively. They interpreted their results in terms of the intramolecular -OH group relaxation. Meakins (25) reported the enthalpy of activation for hydroxyl group relaxation in picric acid in the pure solid state as 25 kJ mol^{-1}. Within experimental error, the relaxation parameters obtained for 2,6-dinitro-4-methylphenol in G.O.T.P. and Santovac® are comparable to those obtained in polystyrene and polyethylene matrices and also to the picric acid parameters in the pure solid state. From

all the evidence it would seem likely that for 2,6-dinitro-4-methylphenol in G.O.T.P. and Santovac® the hydroxyl group relaxation occurs from one planar hydrogen-bonded position to the other and that the intramolecular hydrogen bond in 2,6-dinitro-4-methylphenol is much closer to being a strong hydrogen bond than a weak one.

Only one family of absorption curves has been observed for each of the two substituted phenols, 2,6-di-tert-butylphenol and 2,4,6-tri-tert-butylphenol, in cis-decalin in the temperature range 129-144 K. The relaxation parameters obtained for these relaxations are: ΔH_E = 38 and 48 kJ mol^{-1}, ΔS_E = 103 and 177 J K^{-1} mol^{-1}, ΔG_E = 28 and 31 kJ mol^{-1} at 100 K and $\tau = 2.3 \times 10^2$ and 5.4×10^3 s at 100 K, respectively. From the single OH stretching vibration peak at 3684 cm^{-1} Davies and Meakins (5) reported that the bulky alkyl groups at the ortho-positions prevent the hydroxyl group of phenol from hydrogen bonding. They reported that the enthalpy of activation for OH group rotation in 2,4,6-tri-tert-butylphenol is 9.2 kJ mol^{-1} in the pure solid state (5) and 11.7 kJ mol^{-1} in decalin solution (3,5). The enthalpy of activation for -OH group rotation in other substituted phenols in cis-decalin and G.O.T.P. is relatively lower, around 10 kJ mol^{-1} (see Table VII-1). Fong and Smyth (1), Gough and Price (3), Meakins (4) and Davies and Meakins (5)

observed the OH group relaxation in 2,4,6-tri-tert-butylphenol at frequencies around 10^{10} Hz. Mazid et al (12) could only detect the tail-end of the absorption due to the OH group relaxation at the highest frequencies (around 10^{7} Hz) of their measurement for 2,4,6-tri-tert-butylphenol both in the pure solid state and in a polystyrene matrix. It is thus highly improbable that the relaxation involving relatively higher enthalpy of activation (38 and 48 kJ mol^{-1}) for 2,6-di-tert-butylphenol and 2,4,6-tri-tert-butylphenol could be due to the OH group relaxation. The observed absorption in each of these molecules under consideration should then be assigned to their respective molecular relaxation process.

The relaxation time for molecular rotation of 2,6-di-tert-butylphenol in cis-decalin at 300 K (3.3×10^{-12} s) is comparable to the value 6.6×10^{-12} s obtained by Gough and Price (3). Mazid et al (12) reported fairly high values of activation enthalpy and entropy for molecular rotation of 2,4,6-tri-tert-butylphenol in polystyrene matrices (78 kJ mol^{-1} and 91 J K^{-1} mol^{-1}). These values are very high compared to those for the molecular process observed by Davies and Meakins (5). The higher enthalpy of activation (48 kJ mol^{-1}) in 2,4,6-tri-tert-butylphenol than those in 2,6-di-tert-butylphenol (38 kJ mol^{-1}) is reasonable in

terms of the larger effective volume for molecular rotation in the former molecule. The higher entropy of activation for these dispersions indicates the greater disorder in the system due to larger swept volume. The relatively lower β-value (0.18-0.23) for these relaxations also bears out the molecular nature of the relaxation process.

The molecule, pentachlorobenzenethiol in G.O.T.P., exhibits only one relaxation process in the temperature range 85-115 K. The relaxation parameters obtained for this dispersion are: ΔH_E = 14 kJ mol^{-1}, ΔS_E = -26 J K^{-1} mol^{-1} and ΔG_E = 19 kJ mol^{-1} and τ = 2.9×10^{-8} s at 100 K, respectively. Within experimental error, these parameters are comparable to those obtained for OH group rotation in 2,4,6-trichlorophenol in cis-decalin (see Table VII-1). The energy barrier obtained for this molecule is relatively lower and cannot be accounted for by molecular relaxation. The enthalpy and free energy of activation for molecular rotation for an almost similar-sized rigid molecule, pentachlorotoluene, are 47 kJ mol^{-1} and 40 kJ mol^{-1} at 200 K, respectively in a polystyrene matrix (18). Mazid et al (12) studied pentachlorobenzenethiol in a polystyrene matrix and observed the relaxation parameters for SH group rotation as: ΔH_E = 14 kJ mol^{-1}, ΔS_E = -26 J K^{-1} mol^{-1} and ΔG_E = 16 kJ mol^{-1} and τ = 1.6×10^{-4} s at 100 K,

respectively. The relaxation parameters for pentachlorobenzenethiol obtained in G.O.T.P. are in excellent agreement with those in a polystyrene matrix. The ΔH_E value for SH group rotation in G.O.T.P. and polystyrene matrices (12) are much lower than the corresponding value for OH group rotation in pentachlorophenol (26 kJ mol^{-1})(12). The lower barrier to SH group relaxation in comparison to pentachlorophenol may be due to the strength of the intramolecular hydrogen bond. As the S-H bond is much less ionic than the O-H bond it would be expected to form weaker hydrogen bonds with the chlorine atoms at the ortho positions. There is evidence that thiols form only weak hydrogen bonds (26) and "relative weakness of the SH as a proton donor accounts for the absence of hydrogen bonds in some systems".

The molecule tropolone was studied previously by Enayetullah (13) in a polystyrene matrix. He reported the relaxation parameters as: ΔH_E = 13 kJ mol^{-1}, ΔS_E = -19 J K^{-1} mol^{-1} and ΔG_E = 15 kJ mol^{-1} and $\tau = 1.9 \times 10^{-5}$ s at 100 K, respectively. Comparing these parameters with the similar-sized rigid molecule o-fluorochlorobenzene, the author suggested that the relaxation is due to the whole molecule rotation in the polystyrene cavity.

Present investigation of tropolone in G.O.T.P. reveals only one relaxation process in the temperature range 79-107 K. The Fuoss-Kirkwood distribution parameter, β, for this dispersion ranges between 0.13-0.18. Such a low β-value indicates the wide distribution of relaxation times for this dispersion. The linear Eyring plot, $\log T\tau$ versus 1/T, yields the relaxation parameters as: ΔH_E = 13 kJ mol^{-1}, ΔS_E = -23 J K^{-1} mol^{-1} and ΔG_E = 15 kJ mol^{-1} and $\tau = 3.7 \times 10^{-5}$ s at 100 K, respectively. These parameters are very close to those obtained by Enayetullah (13) in a polystyrene matrix.

Tropolone is comparable in size and shape to norcamphor and norborneol. Both molecules exhibit molecular relaxation in G.O.T.P. involving the relaxation parameters as (Chapters III and VI):

Molecule	ΔH_E kJ mol^{-1}	ΔS_E J K^{-1} mol^{-1}	ΔG_E kJ mol^{-1} at 100 K	τ(s) at 100 K
norchamphor	17	16	15	5.4×10^{-5}
norborneol	13	-22	16	7.3×10^{-5}

Within experimental error, these values are in excellent

agreement with those observed for tropolone in G.O.T.P. All these results appear to suggest that the relaxation for tropolone may be accounted for by the whole molecule rotation but not the hydroxyl group relaxation. The lower β-value is also consistent with this suggestion.

The effects of tunneling are generally shown by the reaction rate constant and the presence of appreciable tunneling can be identified by one or more of the following criteria (27):

(a) tunneling usually leads to greatly enhanced isotope effects;
(b) the Arrhenius plots (plots of log k versus 1/T) are generally curved at lower temperatures and at very low temperatures, if the tunneling rate is large enough, the rate constant is essentially temperature independent;
(c) tunneling usually lowers the energy barriers for equilibrium processes, and unexpectedly large differences in effective activation energies are observed for hydrogen and deuterium species.

The intramolecular processes for substituted anisoles (28) and halogenophenols occur almost in the same low-temperature region, 80-119 (see Tables VII-1 and 2).

Within experimental error, the enthalpy of activation for both the anisoles and phenols is virtually the same and sometimes in the latter molecules slightly larger than that for methoxy group relaxation. This is precisely what would be expected for hydroxyl group relaxation with weak intramolecular hydrogen bonding. Previous work has established that the OH group relaxation barriers for non-intramolecularly hydrogen bonded phenols and anisoles are very similar (4,14-16). Thus, there is no sign that the intramolecular energy barrier has been lowered by a tunneling mechanism. The Eyring plots, $\log T\tau$ versus $1/T$, for all the halogenophenols and tropolone are linear (Figures VII-22d-32d) and by no means parallel to the abscissa. All the evidence appears to suggest that there is no justification to invoke proton tunneling in 2,6-di- and 2,4,-6-tri-halogeno-phenols and in tropolone.

The differences in energy barrier for 2,4,6-trichloro-, 2,4,6,-tribromo- and 2,4,6-triiodophenol are due to the difference in strength of the intramolecular hydrogen bond between the OH and halogen atoms in the 2,6-position. The results of 2,6-dichloro-4-nitro- and 2,6-dibromo-4-nitrophenol clearly indicate that the barrier to OH group relaxation is insensitive to para-substituents and virtually remains the same. This behaviour

is consistent with those found for methoxy group relaxation in various para-substituted anisoles in different dispersion media (28). The most striking point is that the energy barrier for OH group relaxation is significantly higher when the nitro-group is substituted at the 2,6-position of the phenol. This is due to the strong intramolecular hydrogen bond between the OH and nitro-groups. Thus, the energy barrier for -OH group relaxation is highly dependent upon the strength of the intramolecular hydrogen bond and almost independent of the dispersion medium.

REFERENCES

1. F. K. Fong and C. P. Smyth, J. Am. Chem. Soc., 85, 1565(1963).

2. F. K. Fong, J. P. McTague, S. K. Garg and C. P. Smyth, J. Phys. Chem., 70, 3567(1966).

3. S. R. Gough and A. H. Price, Faraday Soc. Trans., 61, 2435(1965).

4. R. J. Meakins, Trans. Faraday Soc., 52, 320(1956).

5. M. Davies and R. J. Meakins, J. Chem. Phys., 26, 1584(1957).

6. H. Forest and B. P. Dailey, J. Chem. Phys., 45, 1736(1966).

7. T. Pedersen, L. W. Larsen and L. Nygaard, J. Mol. Structure, 4, 59(1969).

8. H. D. Bist and D. R. Williams, Bull. Am. Phys. Soc., 11, 826(1966).

9. L. Radom, W. J. Hehre, J. A. Pople, G. L. Carlson and W. G. Fately, J. Chem. Soc. Chem. Comm., 308(1972).

10. M. Davies and A. Edwards, Trans. Faraday Soc., 63, 2163(1967).

11. S. P. Tay, J. Kraft and S. Walker, J. Phys. Chem., 80, 303(1976).

12. M. A. Mazid, M. A. Enayetullah and S. Walker, J. Chem. Soc. Faraday Trans. 2, 77, 1143(1981).

13. M. A. Enayetullah, M.Sc. Thesis, Lakehead University, (1981).

14. W. G. Fateley, G. H. L. Carlson and F. F. Bently, J. Phys. Chem., 79, 199(1975).

15. M. A. Mazid, J. P. Shukla and S. Walker, Can. J. Chem., 56, 1800(1978).

16. T. B. Grindley, A. R. Katritzky and R. D. Topsom, J. Chem. Soc. Perk. Trans. 2, 289(1974).

17. R. L. Redington and T. E. Redington, J. Mol. Spectrosc., 78, 229(1979).

18. M. A. Mazid, M.Sc. Thesis, Lakehead University, (1978).

19. M. Davies and J. Swain, Trans. Faraday Soc., 67, 1637(1971).

20. M. S. Ahmed, Private Communication.

21. M. S. Hossain, M.Sc. Thesis, Lakehead University, (1982).

22. M. M. Davies, "Acid-Base Behaviour in Aprotic Organic Solvents". N.B.S. Monograph 105, U.S. Department of Commerce (1968).

23. A. W. Baker and A. T. Shulgin, Can. J. Chem. 43, 650(1965).

24. M. A. Kashem, M.Sc. Thesis, Lakehead University, (1982).

25. R. J. Meakins, Trans. Faraday Soc., 51, 371(1955).

26. G. C. Pimental and A. L. McClellan, "The Hydrogen Bond". W. H. Freeman, San Fransisco, California (1960).

27. M. D. Harmony, Quart. Rev. Chem. Soc., 211(1972).

28. M. S. Ahmed, M. A. Kashem and S. Walker, J. Phys. Chem., (In press).

TABLE VII-1: Eyring Analysis Results for some Substituted Phenols and Related Compounds in Organic Glasses

Molecule	Medium	Temperature Range (K)	Relaxation Time τ(s)			ΔG_E (kJ mol^{-1})			ΔH_E	ΔS_E
			100 K	150 K	200K	100 K	150 K	200 K	kJ mol^{-1}	J K^{-1} mol^{-1}
2,6-dichloro-phenol	cis-decalin	84-109	2.0×10^{-4}	2.3×10^{-6}	2.3×10^{-7}	17	20	23	10±0.6	-64±6.4
2,4,6-trichloro-phenol (8.2 mol %)	cis-decalin	84-103	6.7×10^{-5}	3.8×10^{-7}	2.6×10^{-8}	16	17	19	12±0.6	-37±7
2,4,6-trichloro-phenol (2.0 mol %)	cis-decalin	82-98	9.2×10^{-5}	2.8×10^{-6}	4.4×10^{-7}	16	20	24	8±1.8	-81±20
2,4,6-tribromo-phenol	G.O.T.P.	79-103	2.3×10^{-5}	5.0×10^{-7}	6.8×10^{-8}	15	18	21	9±0.7	-62±8.1
2,4,6-triiodo-phenol	G.O.T.P.	81-97	1.2×10^{-3}	8.0×10^{-7}	1.9×10^{-7}	14	18	23	6±0.4	-83±4.4
2,6-dichloro-4-nitrophenol	G.O.T.P.	100-133	2.0×10^{-3}	2.4×10^{-5}	2.4×10^{-6}	18	23	27	10±0.8	-84±7
2,6-dibromo-4-nitrophenol	G.O.T.P.	90-119	6.8×10^{-4}	4.1×10^{-6}	2.9×10^{-7}	18	20	23	12±0.5	-58±4.5
2,6-dinitro-4-methyl phenol	G.O.T.P.	159-194	2.8×10^{3}	1.8×10^{-2}	4.0×10^{-5}	30	31	32	29±3.2	-13±18
2,6-dinitro-4-methyl phenol	Santovac®	157-191	1.8×10^{3}	1.6×10^{-2}	4.5×10^{-5}	30	31	32	28±2.2	-19±12.8

continued...

TABLE VII-1: continued...

Molecule	Medium	Temperature Range (K)	Relaxation Time τ(s)			ΔG_E (kJ mol^{-1})			ΔH_E	ΔS_E
			100 K	150 K	200K	100 K	150 K	200 K	kJ mol^{-1}	J K^{-1} mol^{-1}
2,6-di-tert-butyl phenol	cis-decalin	129-139	2.3×10^{2}	3.2×10^{-5}	1.1×10^{-8}	28	23	18	38±5.5	103±41
2,4,6-tri-tert-butylphenol	cis-decalin	131-144	5.4×10^{3}	1.3×10^{-5}	6.0×10^{-10}	31	22	13	48±5.2	177±38
pentachloro-benzenethiol	G.O.T.P.	85-115	2.9×10^{-4}	6.6×10^{-7}	2.9×10^{-8}	17	18	19	14±0.8	-26±7.9
tropolone	G.O.T.P.	79-107	3.7×10^{-5}	1.4×10^{-7}	8.2×10^{-9}	15	16	17	13±0.7	-23±7.9

TABLE VII-2: Eyring Analysis Results for some Anisoles in Organic Glasses

MOLECULE	MEDIUM	ΔT (K)	Relaxation Times τ (s)		ΔG_E (kJ mol^{-1})		ΔH_E	ΔS_E
			100 K	200 K	100 K	200 K	kJ mol^{-1}	J K^{-1} mol^{-1}
anisole	G.O.T.P.	82-120	4.9×10^{-5}	3.3×10^{-8}	15	20	11.0±0.5	-43±6
para-methyl anisole	P.S.	79-111	1.7×10^{-5}	6.1×10^{-7}	14	22	7.2±0.5	-73±5
	G.O.T.P.	80-110	9.9×10^{-6}	3.4×10^{-8}	14	20	8.3±0.4	-57±5
	S.V.	80-107	1.0×10^{-5}	3.3×10^{-8}	14	20	8.4±0.6	-56±8
	cis-decalin	83-98	2.8×10^{-6}	6.4×10^{-9}	13	17	8.9±3.1	-40±34
para-chloro-anisole	G.O.T.P.	80-110	2.6×10^{-5}	1.5×10^{-7}	15	22	7.5±0.6	-74±7
	cis-decalin	80-107	2.8×10^{-4}	2.7×10^{-7}	17	23	10.4±1.6	-64±17
para-bromo-anisole	G.O.T.P.	87-118	3.9×10^{-5}	1.3×10^{-7}	15	22	8.3±0.3	-68±3
	cis-decalin	85-109	6.9 ± 10^{-4}	8.4×10^{-7}	18	25	10±3.1	-75±14
para-iodo-anisole	G.O.T.P.	79-111	4.1×10^{-5}	2.3×10^{-7}	15	23	7.5±0.4	-77±5
	cis-decalin	83-101	5.9×10^{-5}	8.4×10^{-8}	15	21	9.7±2.2	-57±25
3,5-dimethyl-anisole	cis-decalin	84-106	2.3×10^{-4}	4.7×10^{-8}	17	20	12.9±2.6	-37±28

NOTE: Data provided through the courtesy of M. S. Ahmed et al (Ref. 28)

TABLE VII-3: Tabulated Summary of Fuoss-Kirkwood Analysis Parameters for some substituted phenols and related compounds in organic glasses

T(K)	$10^6\tau$(s)	$\log \nu_{max}$	β	$10^3\varepsilon''_{max}$
8.9 mol % 2,6-dichlorophenol in cis-decalin				
83.6	2510	1.80	0.56	0.1
86.8	1522	2.02	0.56	0.1
89.7	980	2.21	0.52	0.1
91.7	570	2.45	0.74	0.2
92.8	529	2.48	0.73	0.2
94.6	439	2.56	0.59	0.2
97.4	302	2.72	0.52	0.2
101.8	156	3.01	0.47	0.2
109.0	66.2	3.38	0.41	0.2
8.2 mol % 2,4,6-trichlorophenol in cis-decalin				
84.4	1207	2.12	0.49	0.4
86.5	656	2.38	0.54	0.4
88.6	487	2.51	0.56	0.5
92.2	244	2.81	0.60	0.4
95.8	132	3.08	0.59	0.4
98.9	78.2	3.31	0.62	0.4
102.5	46.8	3.53	0.63	0.4
2.0 mol % 2,4,6-trichlorophenol in cis-decalin				
82.1	891	2.25	0.39	0.1
85.7	550	2.46	0.38	0.1
88.1	294	2.73	0.42	0.1
90.4	276	2.76	0.48	0.1
92.9	211	2.88	0.41	0.1
98.2	114	3.14	0.94	0.2

TABLE VII-3: continued...

T(K)	$10^6\tau$(s)	$\log\nu_{max}$	β	$10^3\varepsilon''_{max}$
7.3 mol % 2,4,6-tribromophenol in G.O.T.P.				
79.5	434	2.56	0.21	1.8
82.0	286	2.74	0.22	1.8
83.7	215	2.87	0.22	1.8
85.8	124	3.11	0.23	1.9
88.2	96.2	3.22	0.24	1.9
90.7	65.1	3.39	0.25	1.9
92.0	54.3	3.47	0.25	1.9
95.3	39.2	3.61	0.28	2.0
97.8	30.3	3.72	0.29	2.0
102.9	18.9	3.93	0.31	2.0
5.3 mol % 2,4,6-triiodophenol in G.O.T.P.				
81.0	84.8	3.27	0.23	2.2
81.6	70.5	3.35	0.24	2.2
82.7	63.1	3.40	0.25	2.3
84.1	55.4	3.46	0.26	2.3
85.1	47.4	3.53	0.26	2.3
86.4	41.7	3.58	0.27	2.3
87.1	39.2	3.61	0.27	2.3
89.3	31.2	3.71	0.29	2.3
92.3	24.0	3.82	0.31	2.3
96.8	16.5	3.98	0.34	2.3
4.2 mol % 2,6-dichloro-4-nitrophenol in G.O.T.P.				
99.5	2013	1.90	0.22	0.9
101.1	1712	1.97	0.21	0.9
104.8	1068	2.17	0.20	1.0
109.5	619	2.41	0.22	1.1
115.0	420	2.58	0.20	1.1
118.5	278	2.76	0.19	1.1
125.4	121	3.12	0.21	1.2
133.3	71.5	3.35	0.18	1.3

TABLE VII-3: continued...

T(K)	$10^6\tau$(s)	$\log\nu_{max}$	β	$10^3\varepsilon''_{max}$
3.2 mol % 2,6-dibromo-4-nitrophenol in G.O.T.P.				
89.6	4043	1.60	0.23	0.9
92.9	1991	1.90	0.24	0.9
96.5	1143	2.14	0.23	0.9
98.9	849	2.27	0.23	1.0
103.6	406	2.59	0.24	1.0
108.5	233	2.84	0.26	1.1
112.2	130	3.09	0.25	1.1
115.2	92.2	3.24	0.26	1.1
119.3	54.0	3.47	0.27	1.1
3.7 mol % 2,6-dinitro-4-methylphenol in G.O.T.P.				
158.7	3896	1.61	0.30	4.2
161.3	2607	1.79	0.31	4.3
164.9	1852	1.93	0.29	4.4
167.9	1266	2.10	0.29	4.5
175.8	533	2.47	0.27	4.9
180.9	325	2.69	0.25	5.0
186.8	146	3.04	0.24	5.2
193.8	64.9	3.39	0.23	5.5
3.8 Percent (by wt.) 2,6-dinitro-4-methylphenol in Santovac®				
157.4	5345	1.47	0.28	6.4
161.3	2914	1.74	0.28	6.5
166.5	1641	1.99	0.28	6.8
173.5	715	2.35	0.26	7.2
181.4	310	2.71	0.23	7.6
191.4	90.3	3.25	0.19	8.1
200.8	24.5	3.81	0.16	8.7
210.3	10.0	4.20	0.14	9.4

TABLE VII-3: continued...

T(K)	$10^6\tau$(s)	$\log\nu_{max}$	β	$10^3\epsilon''_{max}$
8.2 mol % 2,6-di-tert-butylphenol in cis-decalin				
129.4	4792	1.52	0.21	1.1
130.6	4095	1.59	0.20	1.1
132.4	2024	1.90	0.21	1.1
133.8	1332	2.08	0.21	1.1
136.4	710	2.35	0.22	1.1
139.2	403	2.60	0.22	1.2
8.2 mol % 2,4,6-tri-tert-butylphenol in cis-decalin				
131.8	3787	1.62	0.18	1.1
133.2	1862	1.93	0.19	1.1
135.0	992	2.21	0.20	1.1
137.7	418	2.58	0.21	1.2
140.9	183	2.94	0.23	1.2
143.5	83.7	3.28	0.22	1.3
7.0 mol % 2,3,4,5,6-pentachlorobenzenethiol in G.O.T.P.				
85.2	6536	1.39	0.20	1.4
87.2	4508	1.55	0.20	1.5
88.8	2101	1.88	0.23	1.5
91.5	1349	2.07	0.22	1.5
93.4	974	2.21	0.22	1.6
95.2	682	2.37	0.22	1.6
97.9	426	2.57	0.23	1.6
100.5	278	2.76	0.22	1.7
103.4	168	2.98	0.21	1.7
108.3	90.5	3.25	0.25	1.7
110.9	60.8	3.42	0.25	1.8
114.8	42.3	3.58	0.26	1.8

TABLE VII-3: continued....

T(K)	$10^6\tau$(s)	$\log\nu_{max}$	β	$10^3\varepsilon''_{max}$
7.5 mol % tropolone in G.O.T.P.				
79.2	2273	1.85	0.13	6.6
81.7	1390	2.06	0.13	6.9
83.9	958	2.22	0.13	7.1
86.8	473	2.53	0.14	7.2
90.4	253	2.80	0.14	7.5
93.9	104	3.19	0.14	7.8
96.9	56.0	3.45	0.15	8.1
99.4	37.8	3.62	0.16	8.3
102.9	20.6	3.89	0.17	8.6
107.0	13.9	4.06	0.18	9.0

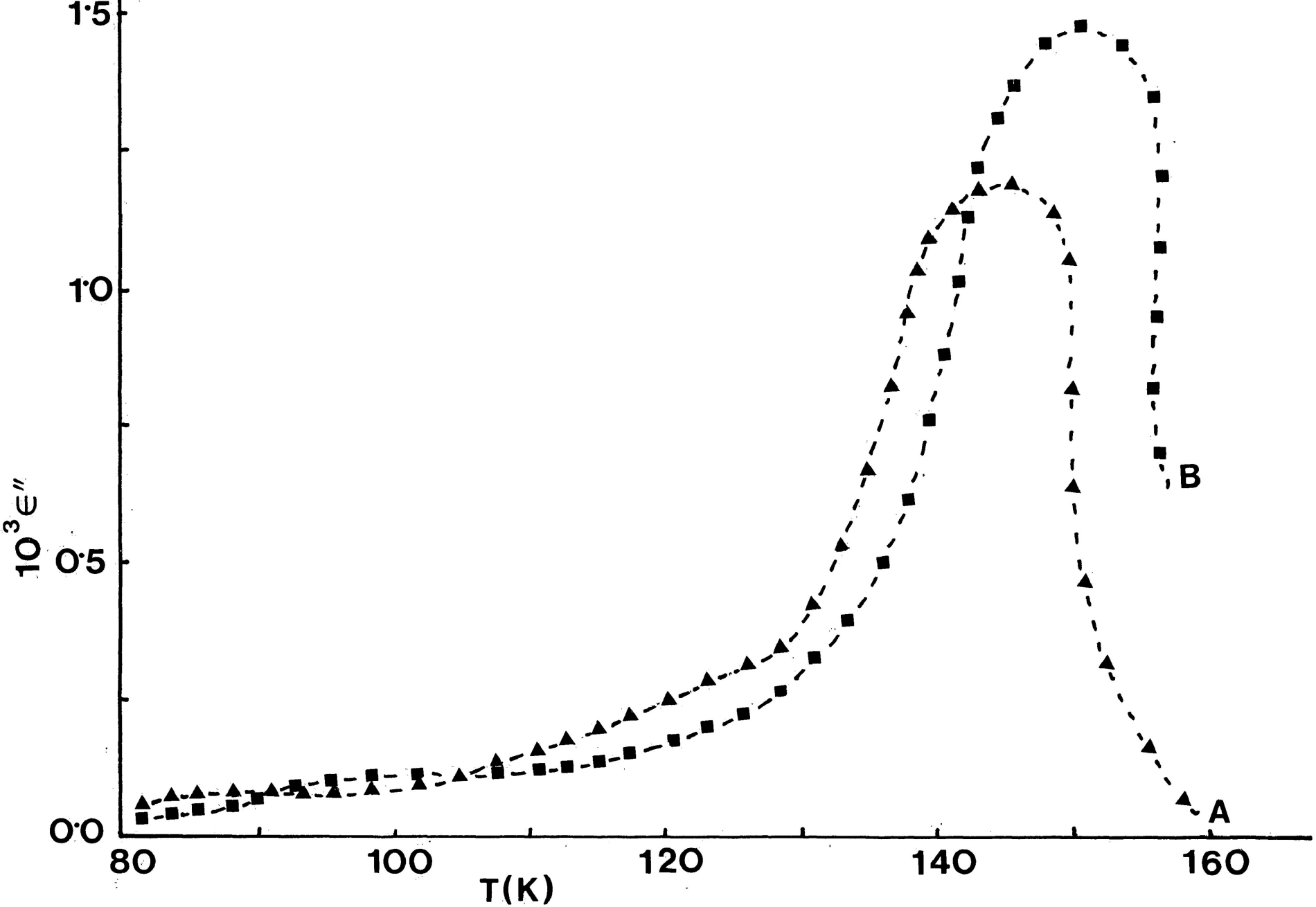

FIGURE VII-1a: Plots of dielectric loss factor, ε" versus temperature (K) for 2,6-dichlorophenol in cis-decalin. A=10.2 Hz and B=1.01 kHz

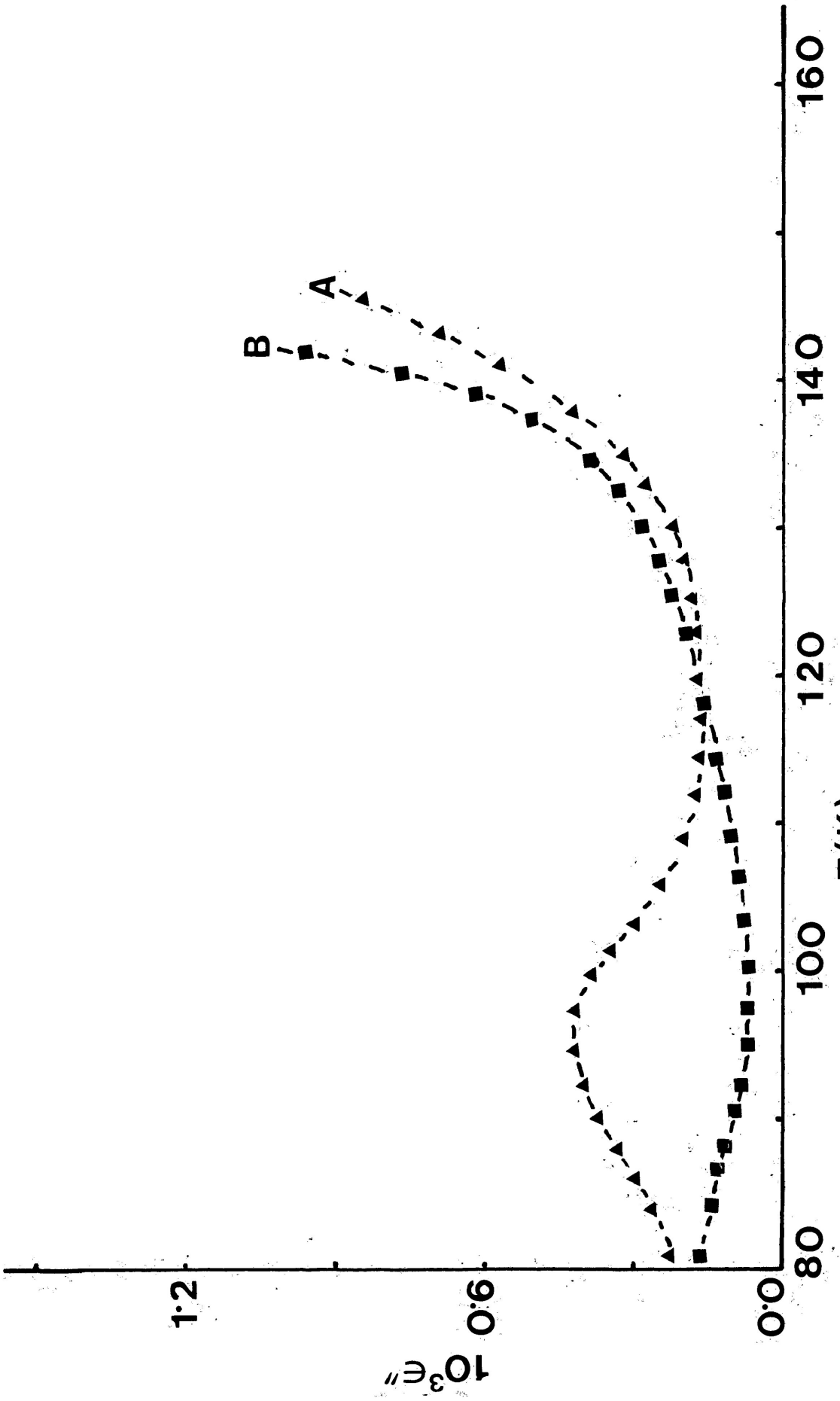

FIGURE VII-2a: Plots of dielectric loss factor, ε'' versus temperature (K) vor 2,4,6-trichlorophenol in cis-decalin. A=10.2 Hz, B=1.01 kHz.

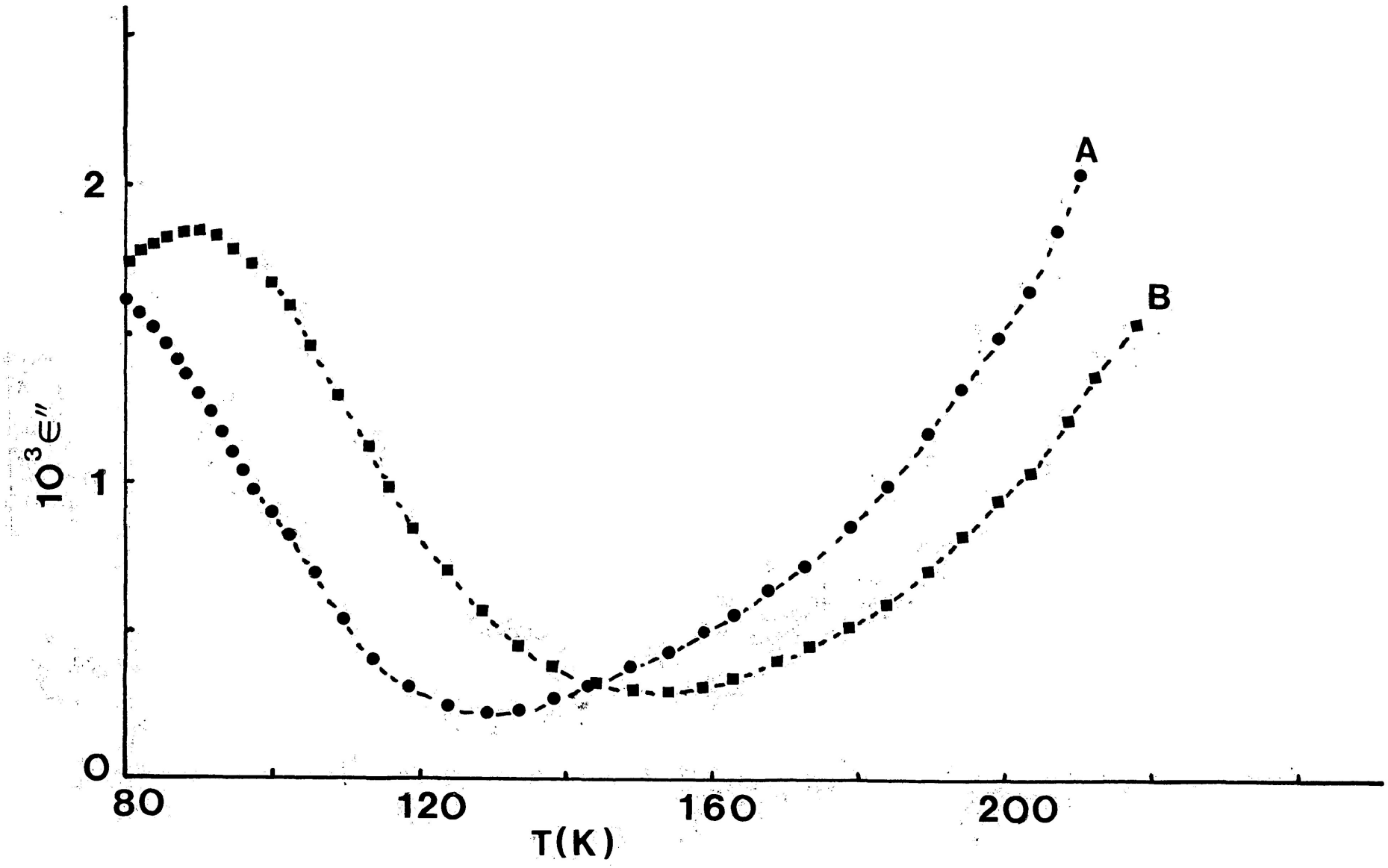

FIGURE VII-3a: Plots of dielectric loss factor, ε'' versus temperature (K) for 2,4,6-tribromophenol in G.O.T.P. A=50.2 Hz, B=1.01 kHz

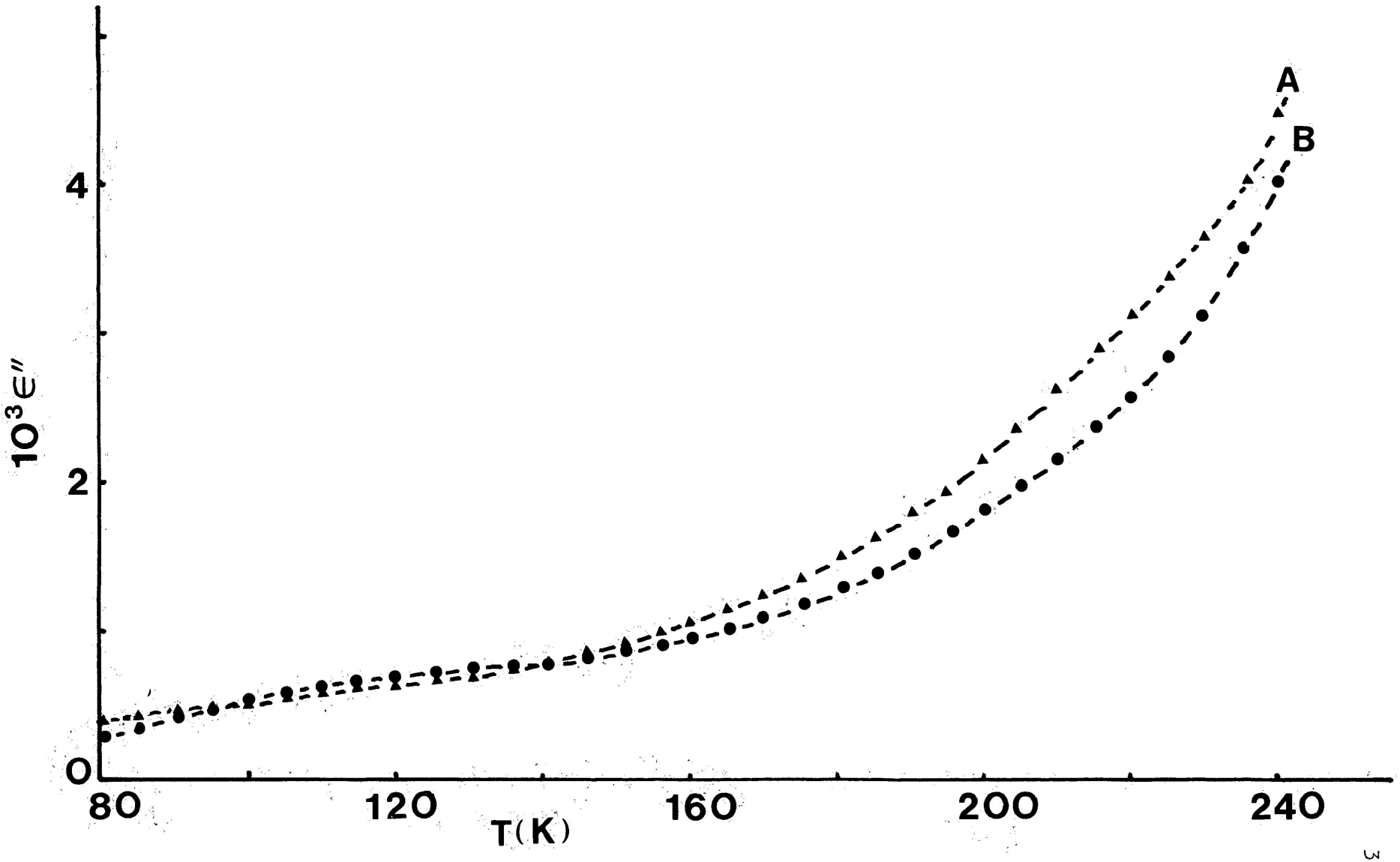

FIGURE VII-4a: Plots of dielectric loss factor, ε" versus temperature (K) for 2,6-dichloro-4-nitrophenol in G.O.T.P. A=50.2 Hz, B=1.01 kHz.

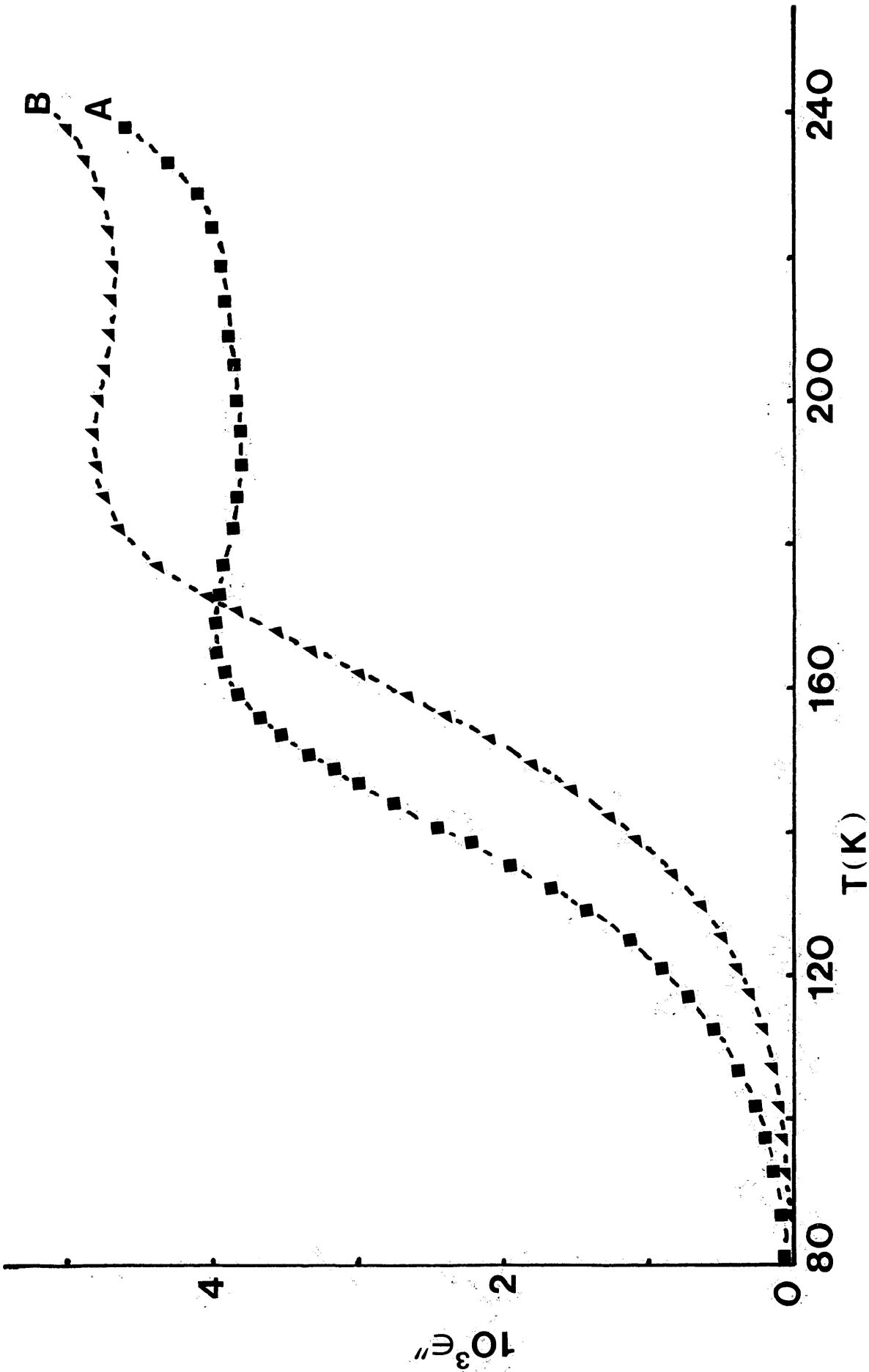

FIGURE VII-5a: Plots of dielectric loss factor, ε'' versus Temperature (K) for 2,6-dinitro-4-methylphenol in G.O.T.P. A=50.2 Hz, B=1.01 kHz

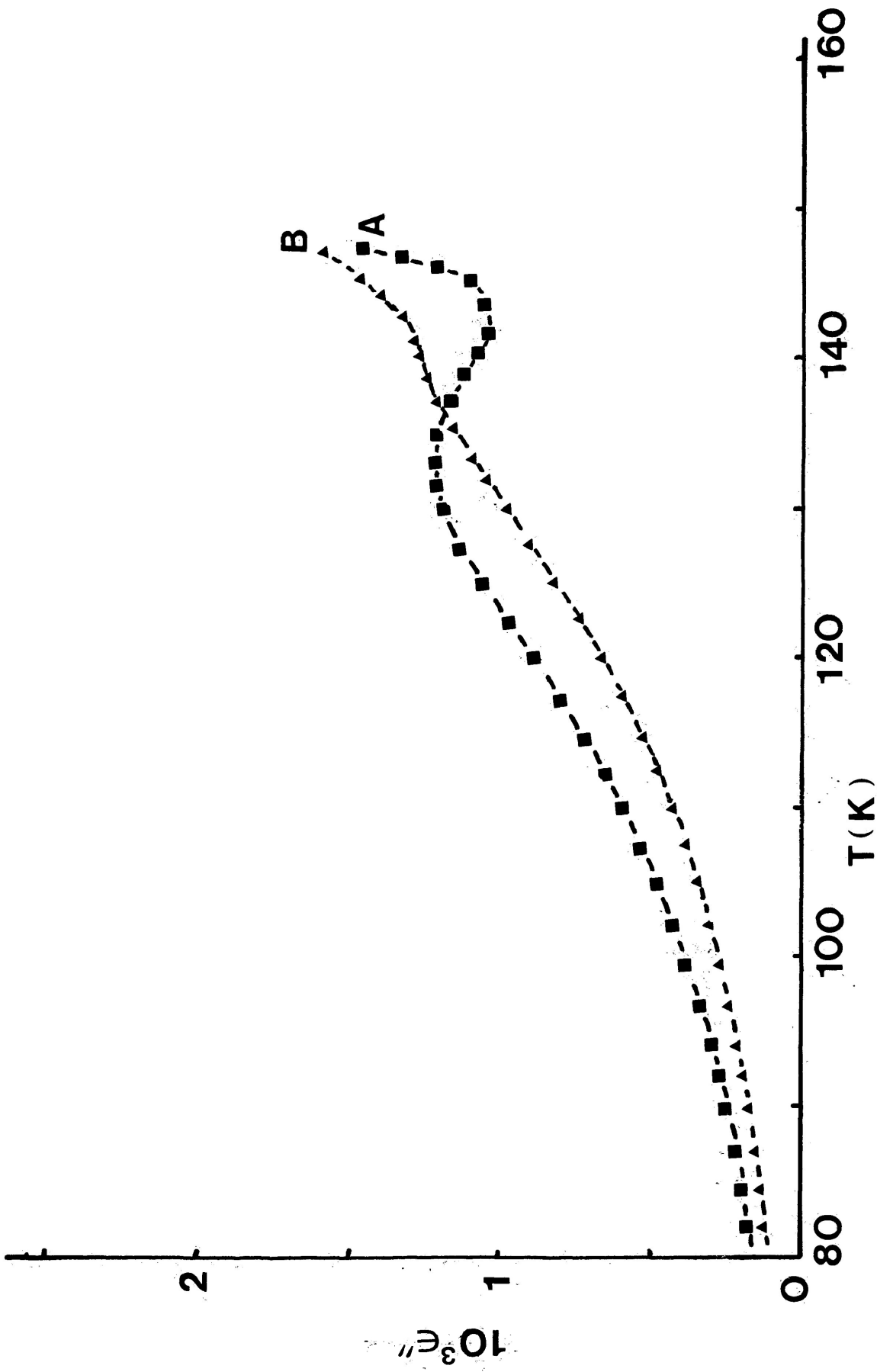

FIGURE VII-6a: Plots of dielectric loss factor, ε'' versus temperature (K) for 2,4,6-tri-tert-butylphenol in cis-decalin. A=50.2 Hz, B=1.01 kHz

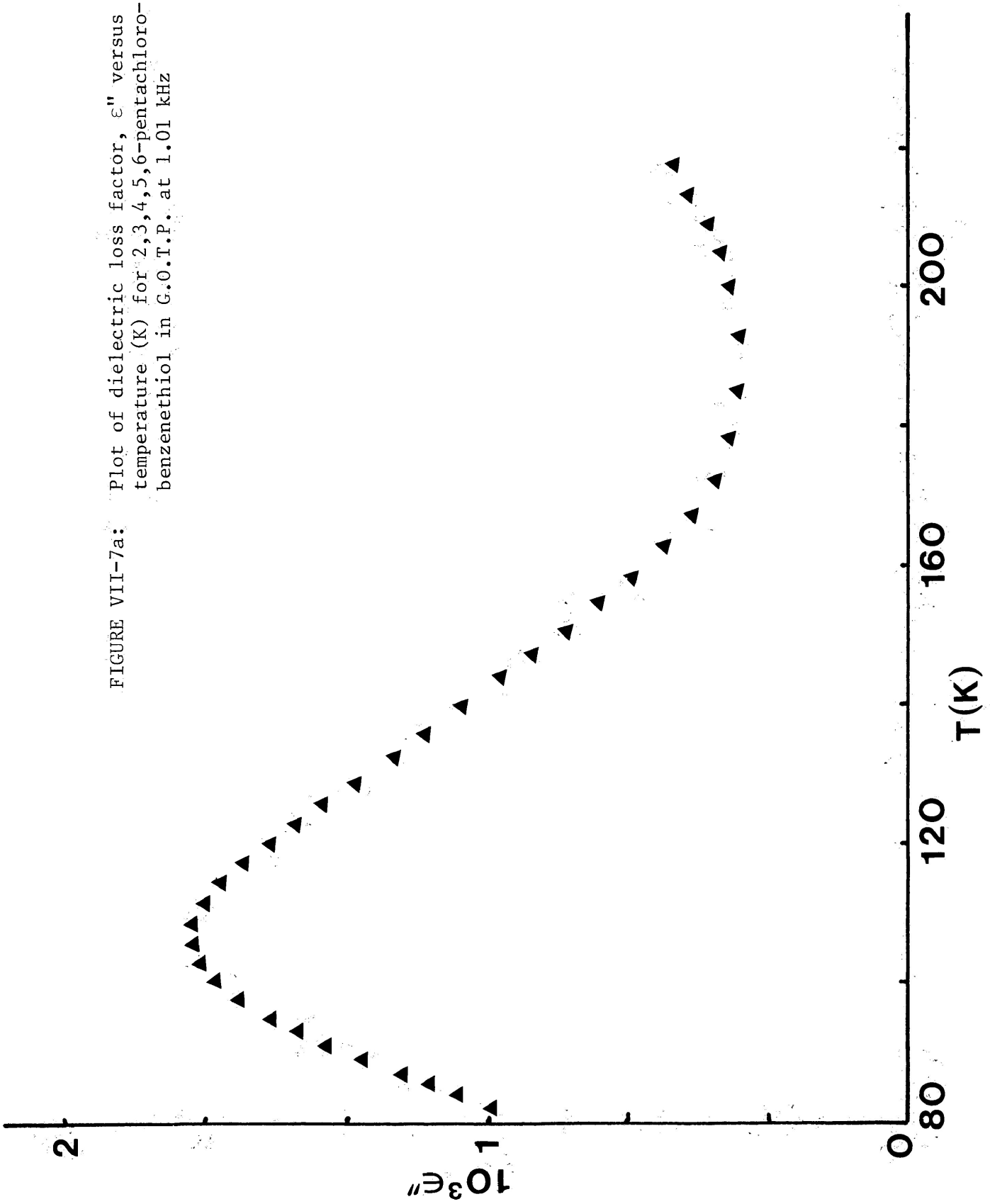

FIGURE VII-7a: Plot of dielectric loss factor, ε'' versus temperature (K) for 2,3,4,5,6-pentachloro-benzenethiol in G.O.T.P. at 1.01 kHz

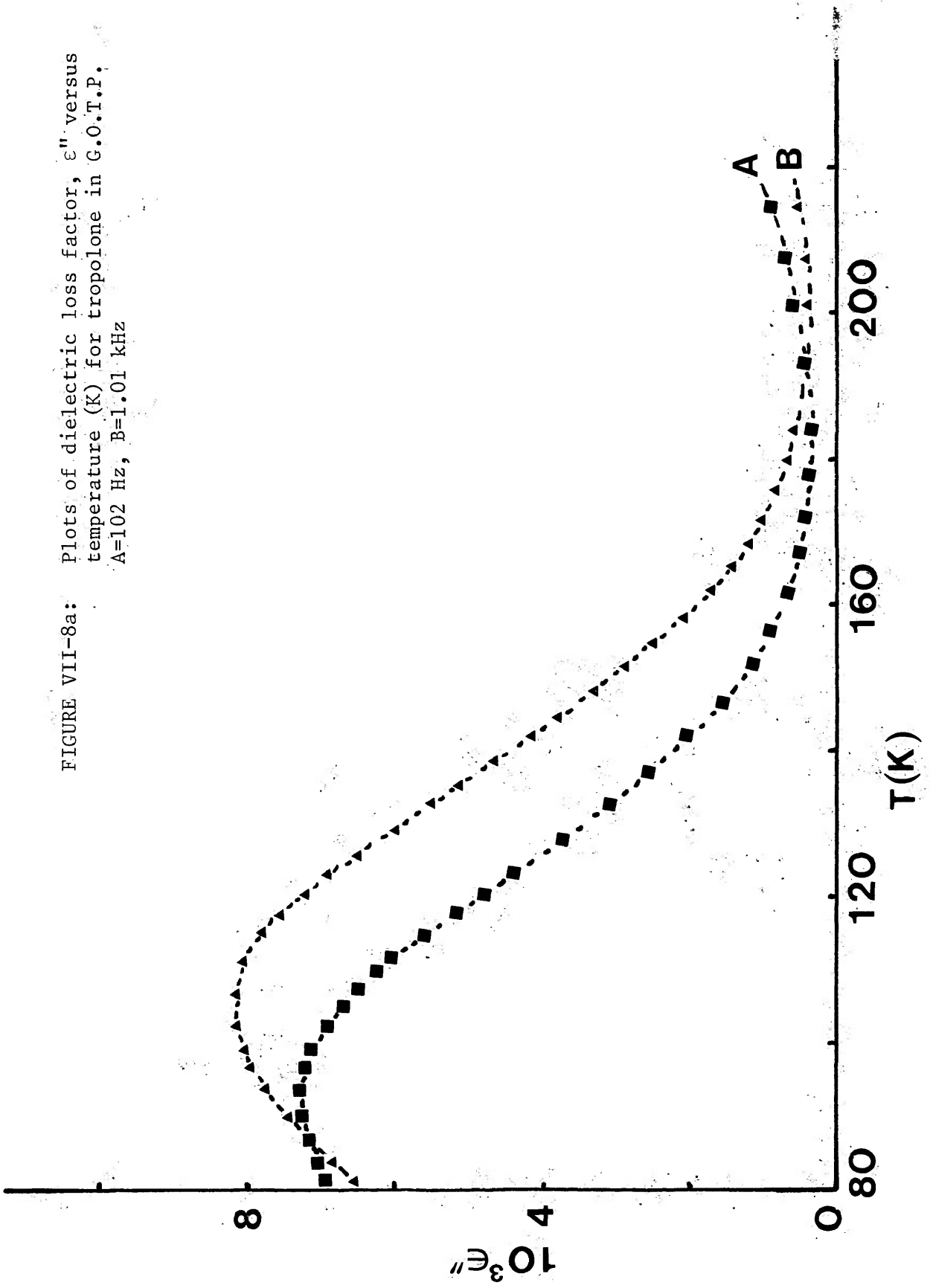

FIGURE VII-8a: Plots of dielectric loss factor, ε'' versus temperature (K) for tropolone in G.O.T.P. A=102 Hz, B=1.01 kHz

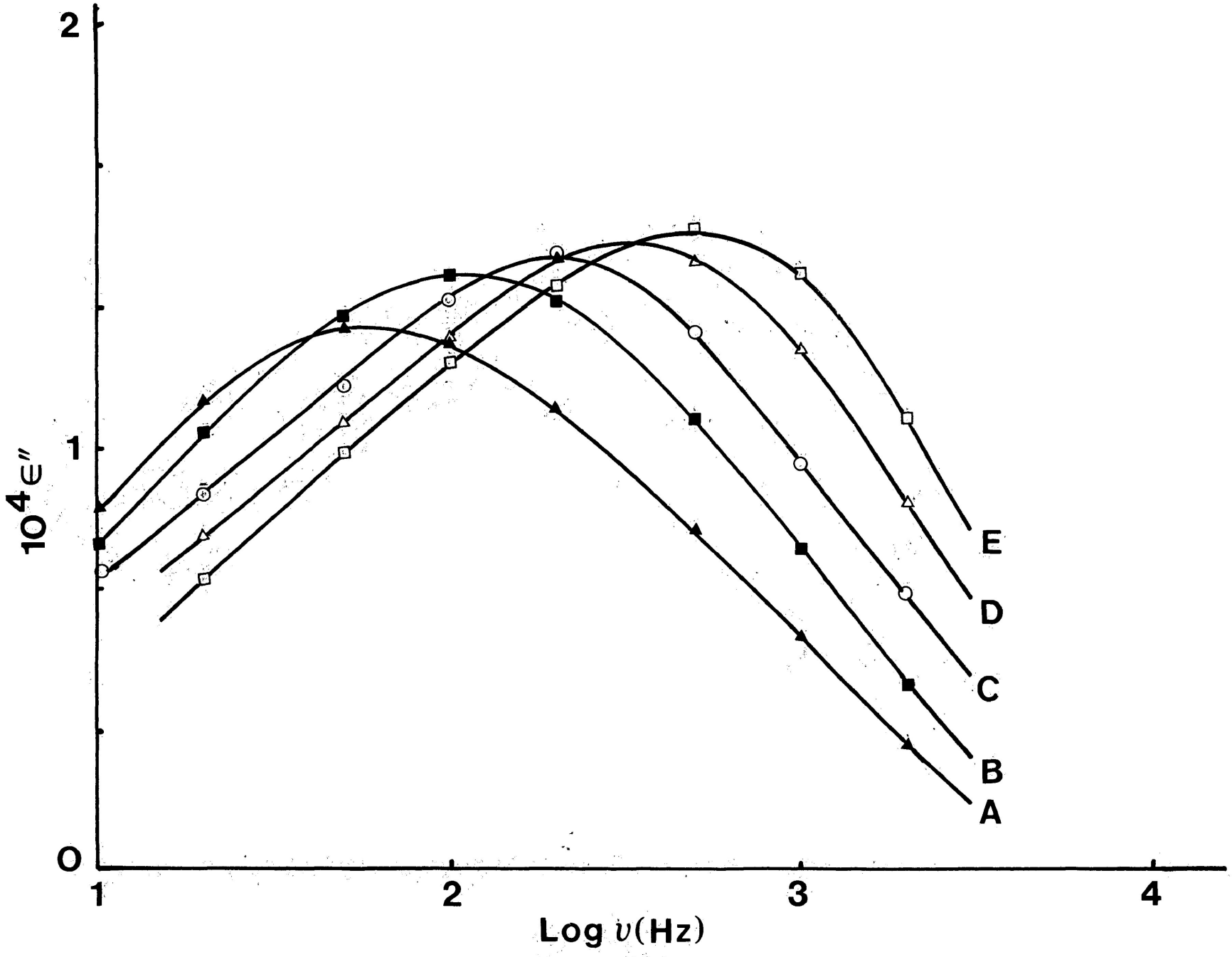

FIGURE VII-9b: Plots of dielectric loss factor, ε" versus log frequency (Hz) for 2,6-dichlorophenol in cis-decalin. A=83.6 K, B=86.8 K; C=89.7 K, D=91.7 K, and E=94.6 K.

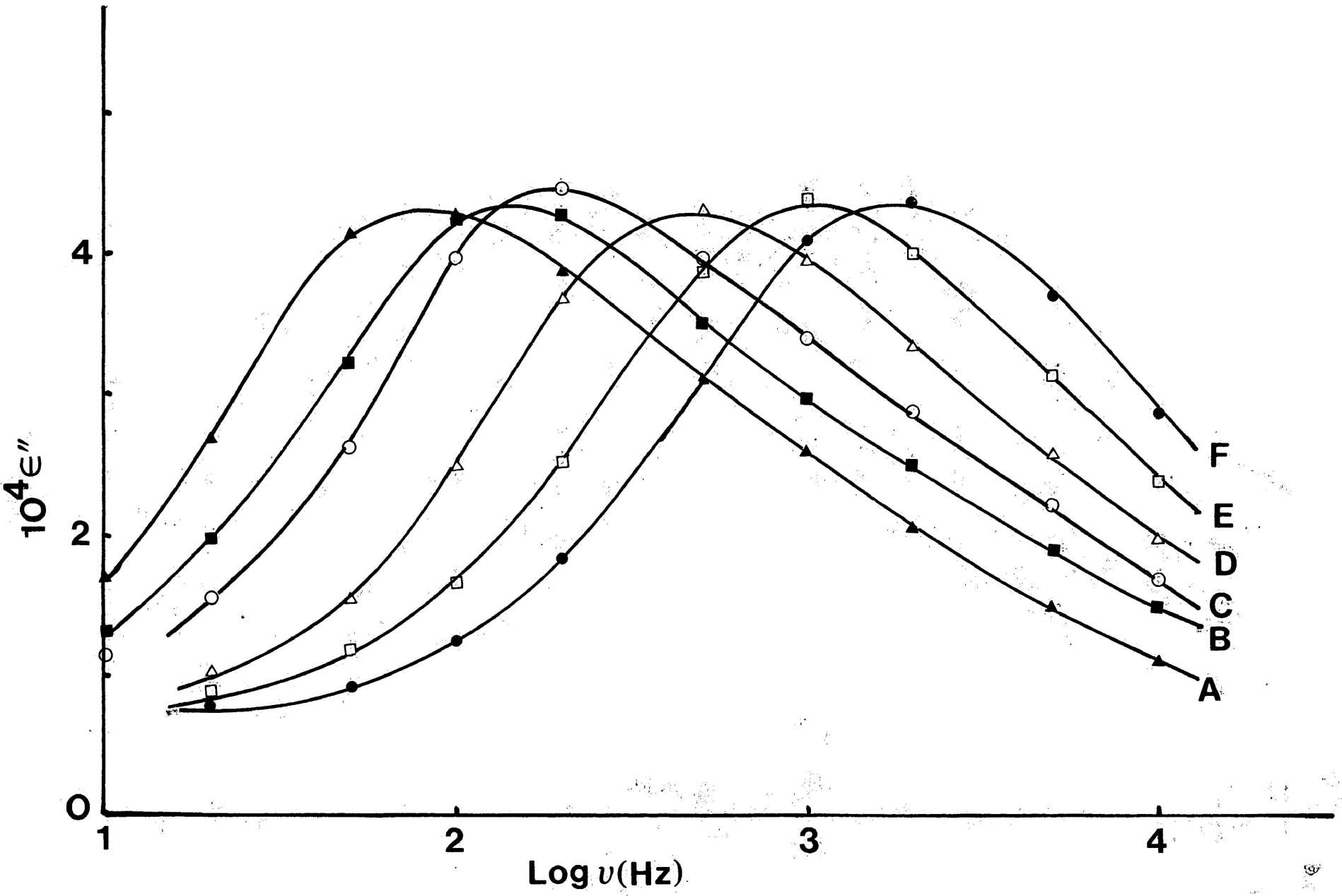

FIGURE VII-10b: Plots of dielectric loss factor, ε" versus log frequency (Hz) for 2,4,6-trichlorophenol in cis-decalin. A=84.4 K; B=86.5K; C=88.6 K; D=92.2 K; E=95.8 K; and F=98.9 K.

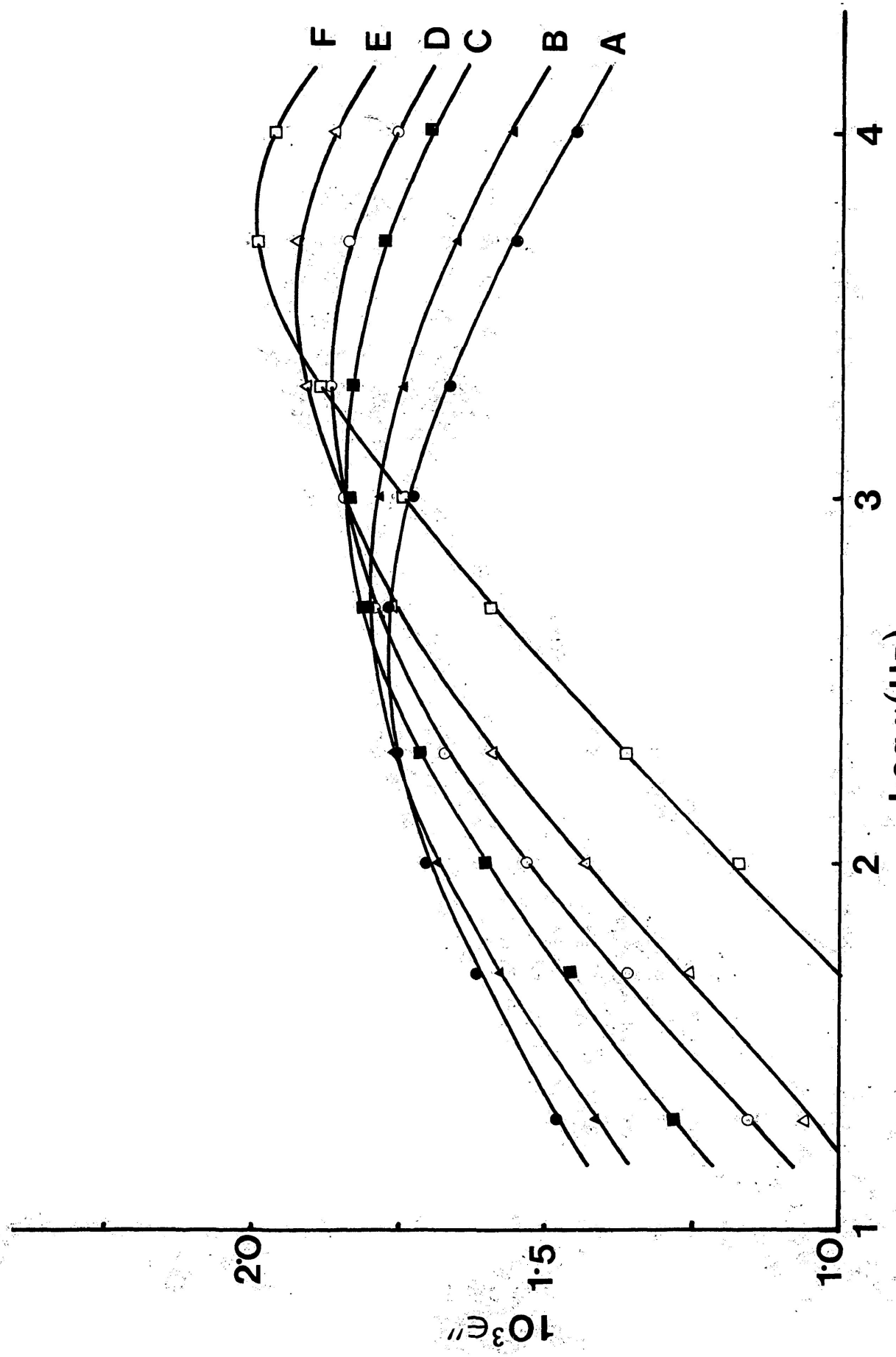

FIGURE VII-11b: Plots of dielectric loss factor, ε'' versus log frequency (Hz) for 2,4,6-tribromophenol in G.O.T.P. A=79.5 K; B=82.0 K; C=85.8 K; D=88.2 K; E=92.0 K, and F=97.8 K.

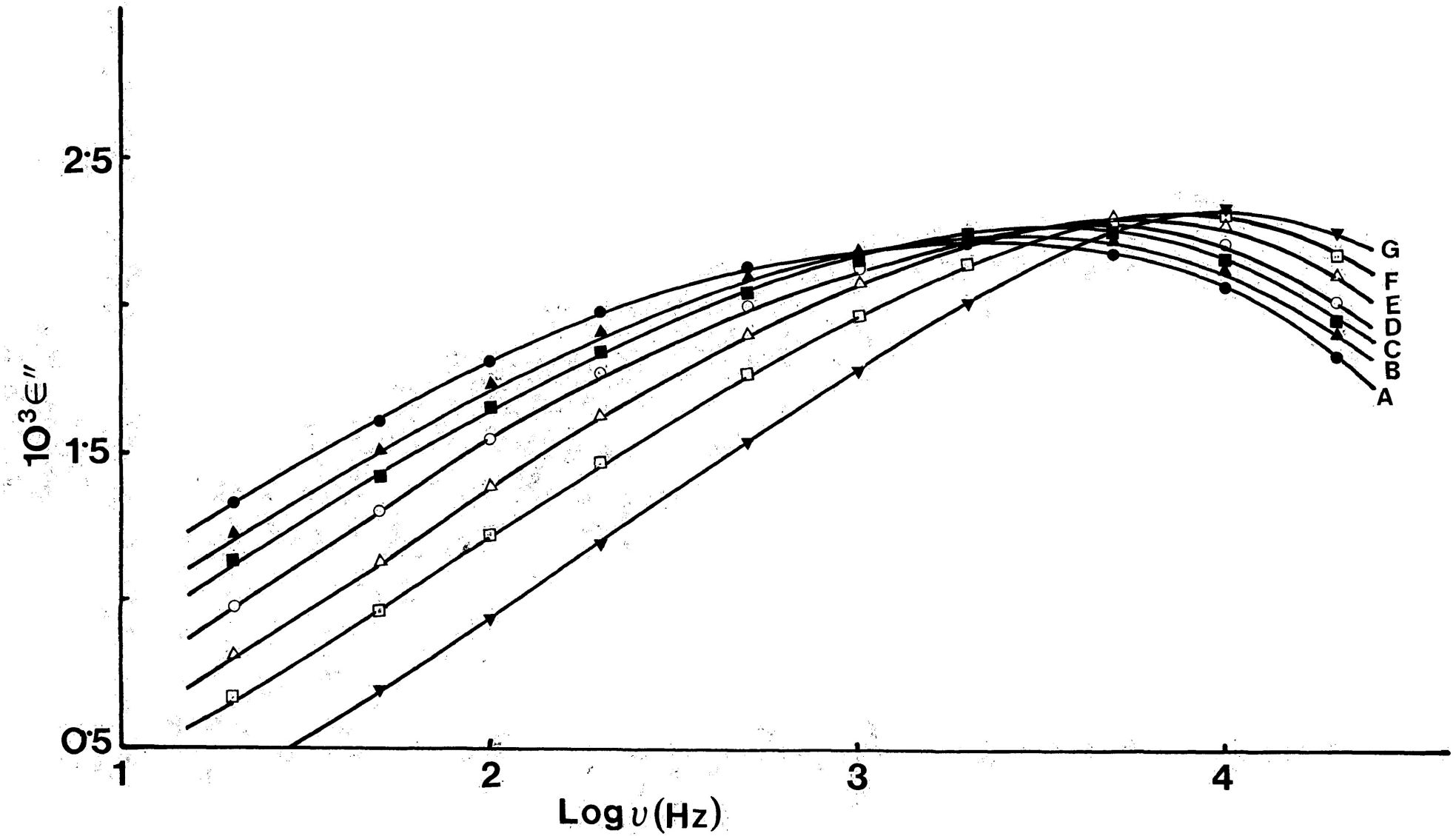

FIGURE VII-12b: Plots of dielectric loss factor, ε" versus log frequency (Hz) for 2,4,6-triiodophenol in G.O.T.P. A=81.0 K; B=82.7 K; C=84.1 K; D=86.4 K; E=89.3 K; F=92.3 K; and G=96.8 K.

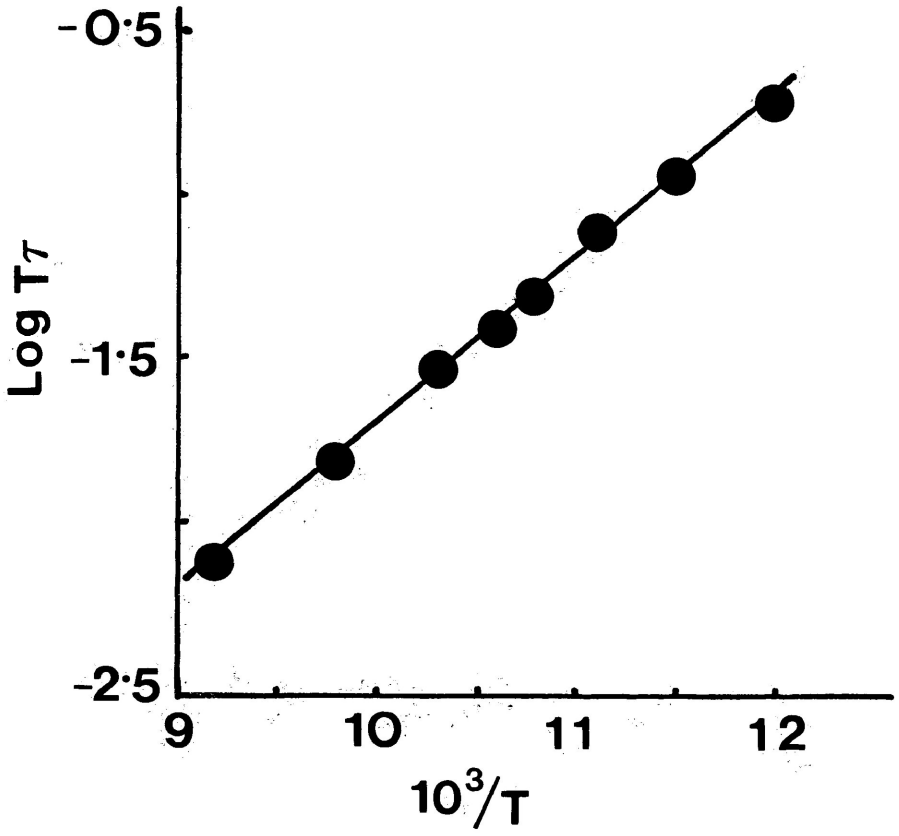

FIGURE VII-22d: Eyring plot of logTτ versus 1/T (K^{-1}) for 2,6-dichlorophenol in cis-decalin

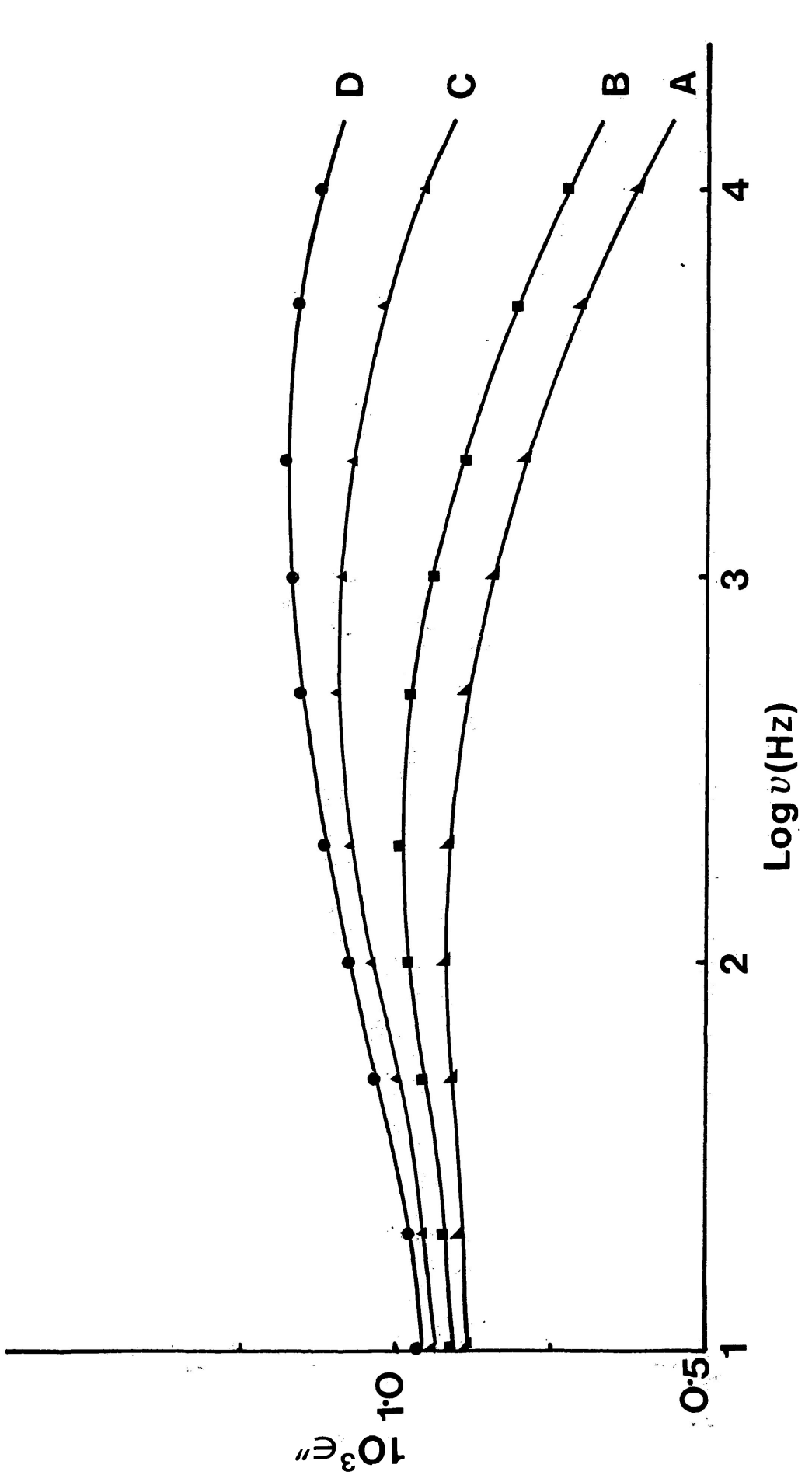

FIGURE VII-13b: Plots of dielectric loss factor, ε'' versus log frequency (Hz) for 2,6-dichloro-4-nitrophenol in G.O.T.P. A=99.5 K; B=104.8 K; C=115.0 K and D=125.4 K.

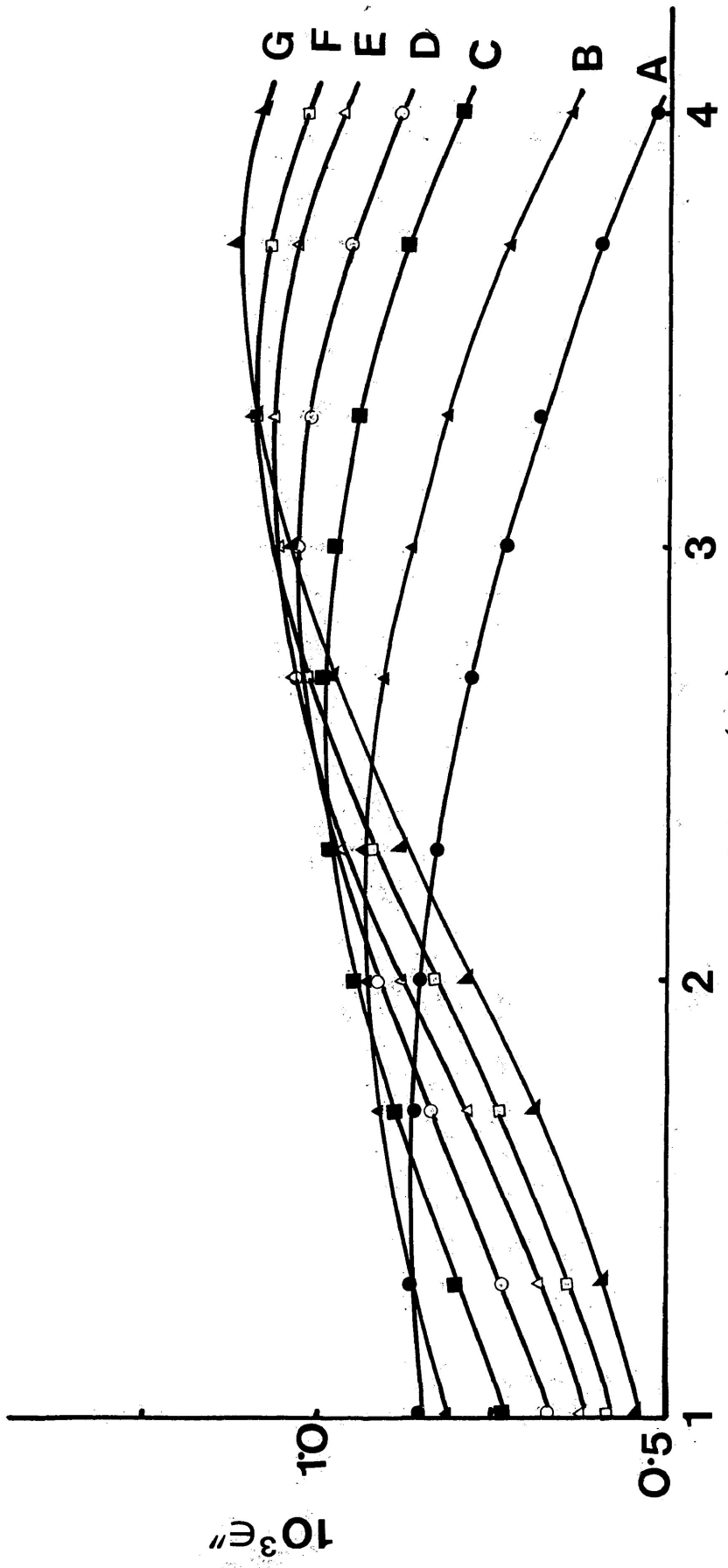

FIGURE VII:14b: Plots of dielectric loss factor, ε'' versus log frequency (Hz) for 2,6-dibromo-4-nitrophenol in G.O.T.P. A=89.6 K; B=96.9 K; C=103.6 K; D=108.5 K; E=112.2 K; F=115.2 K; and G=119.3 K.

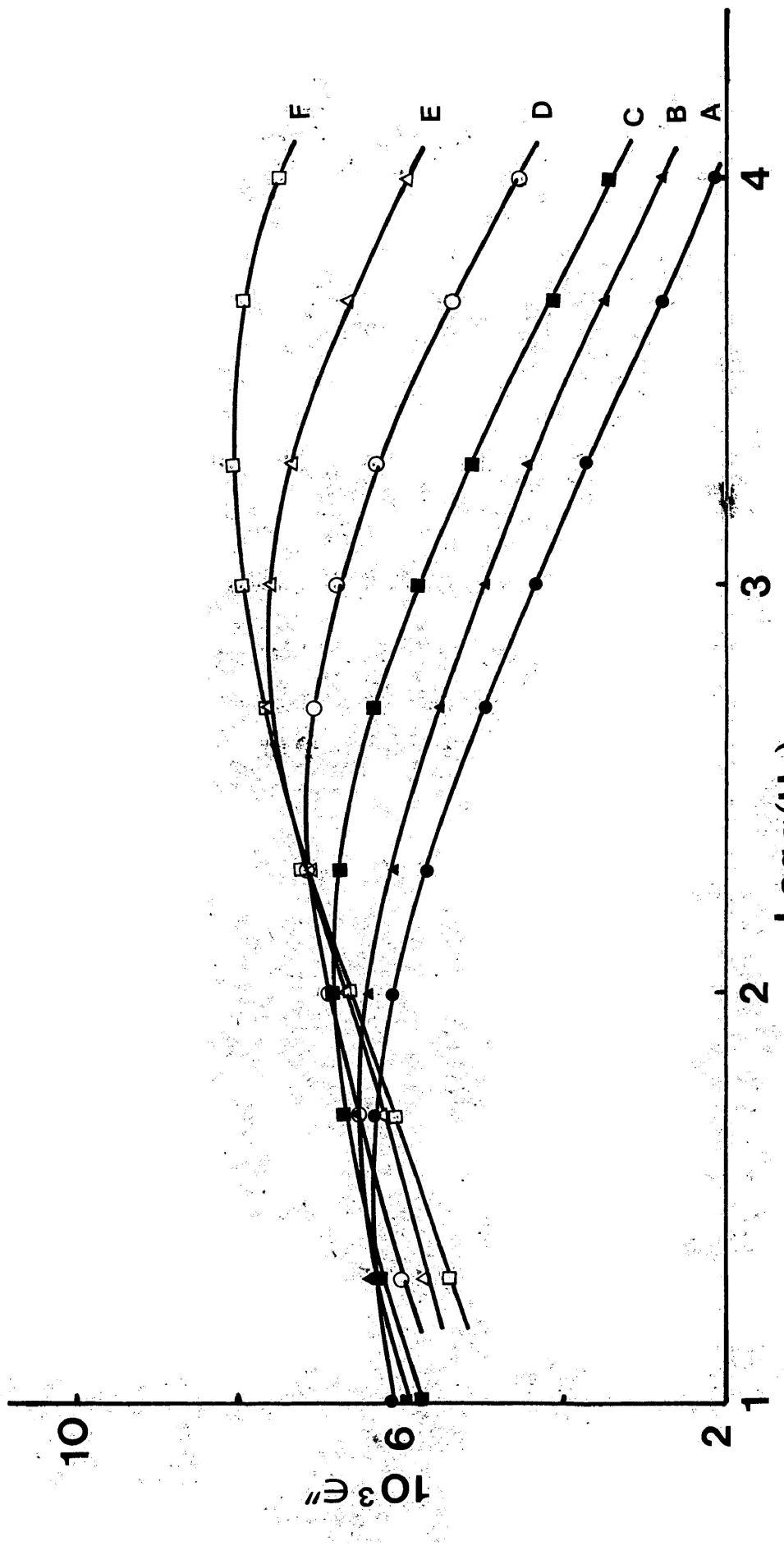

FIGURE VII-15b: Plots of dielectric loss factor, ε'' versus log frequency (Hz) for 2,6-dinitro-4-methylphenol in Santovac®. A=157.4 K; B=161.3 K; C=166.5 K; D=173.5 K; E=181.4 K and F=191.4 K.

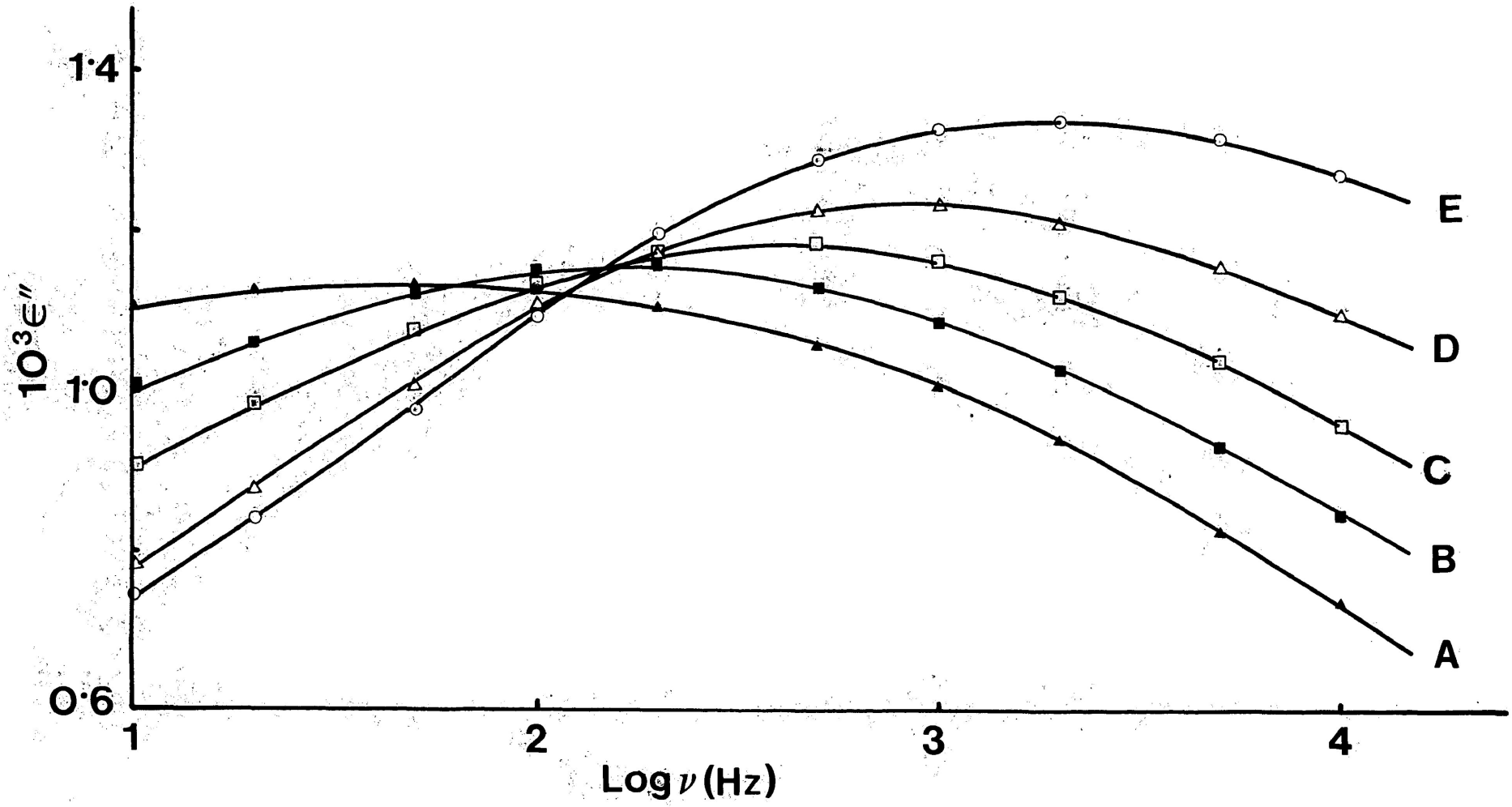

FIGURE VII-16b: Plots of dielectric loss factor, ε" versus log frequency (Hz) for 2,4,6-tri-tert-butylphenol in cis-decalin. A=131.8 K; B=135.0 K; C=137.7 K; D=140.9 K; and E=143.5 K.

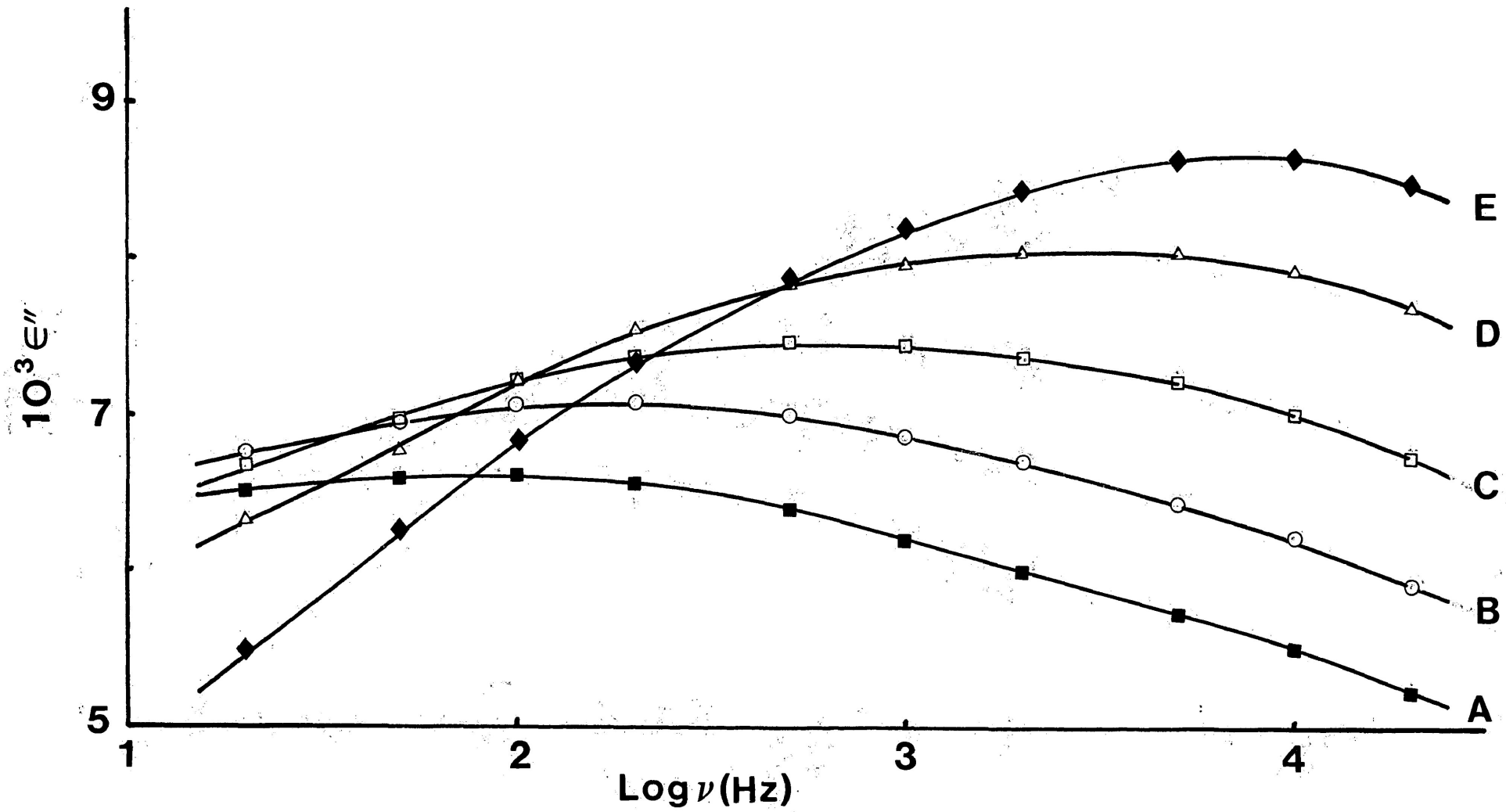

FIGURE VII-17b: Plots of dielectric loss factor, ε" versus log frequency (Hz) for tropolone in G.O.T.P. A=79.2 K; B=83.9 K; C=90.4 K; D=96.9 K and E=102.9 K.

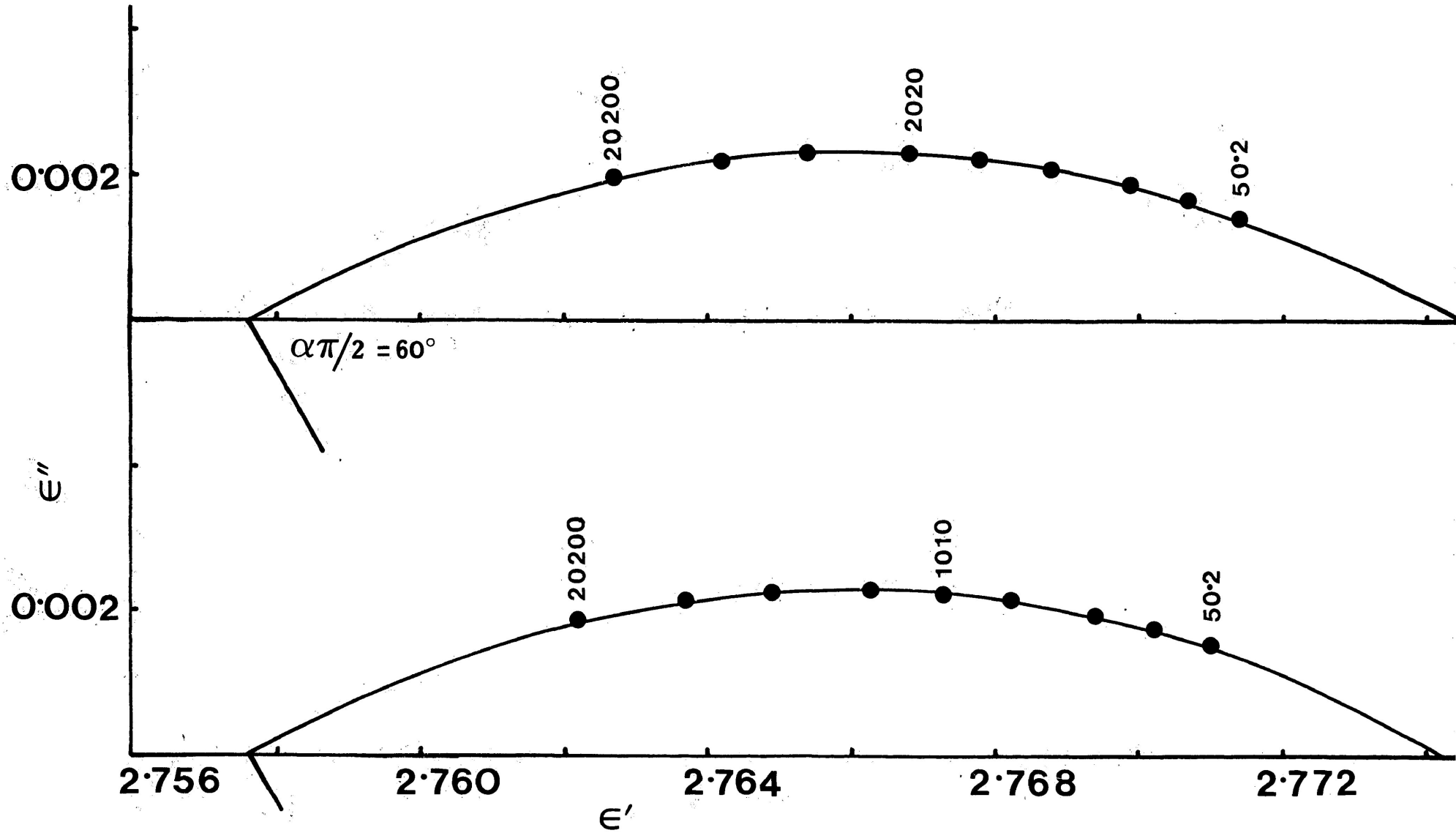

FIGURE VII-18c: Cole-Cole plots for 2,4,6-triiodophenol in G.O.T.P. at 82.7 K (lower) and 85.1 K (upper). Numbers beside points are frequencies in Hz.

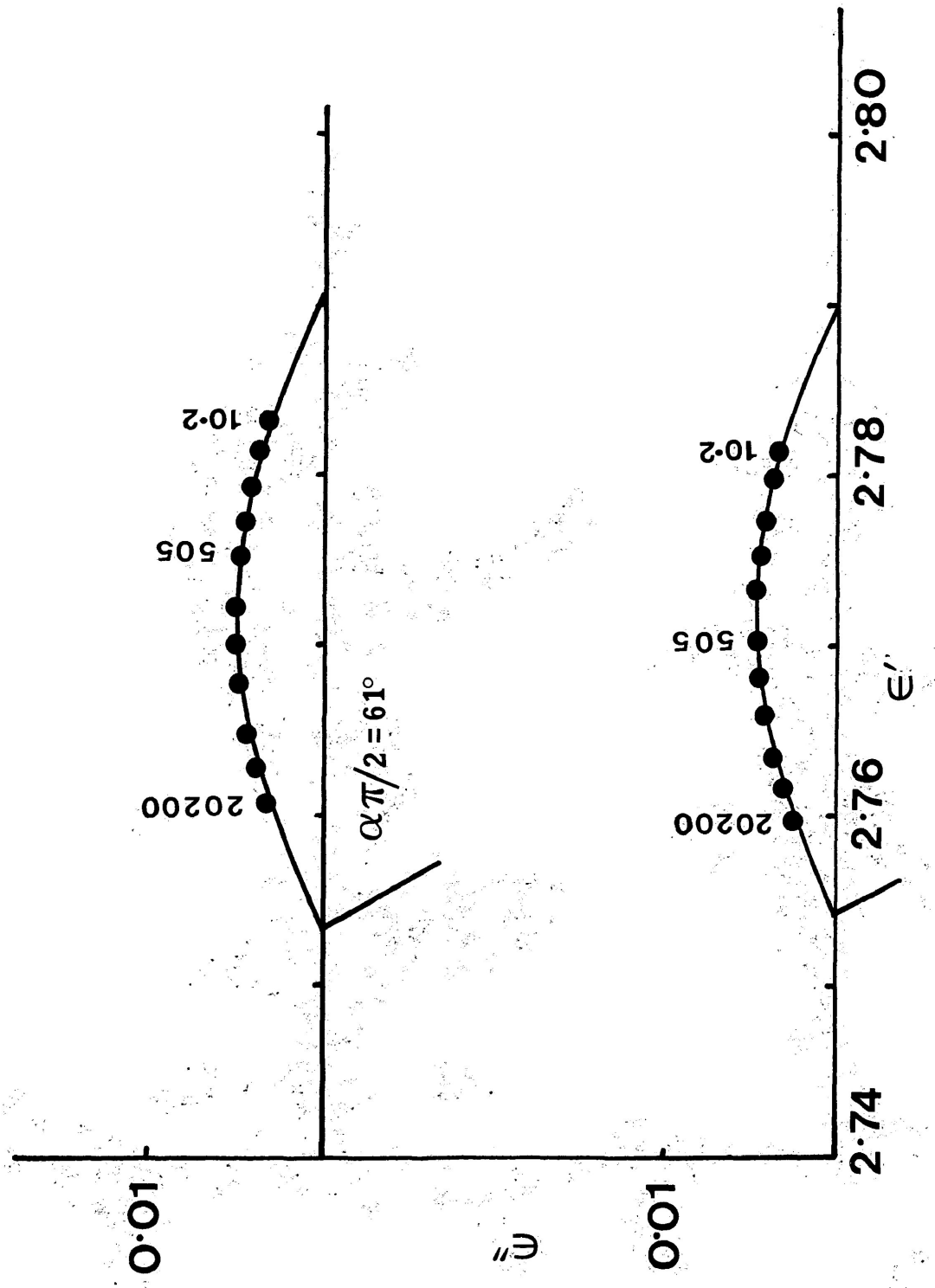

FIGURE VII-19c: Cole-Cole plots for 2,6-dinitro-4-methylphenol in G.O.T.P. at 175.8 K (lower) and 180.9 K (upper). Numbers beside points are frequencies in Hz.

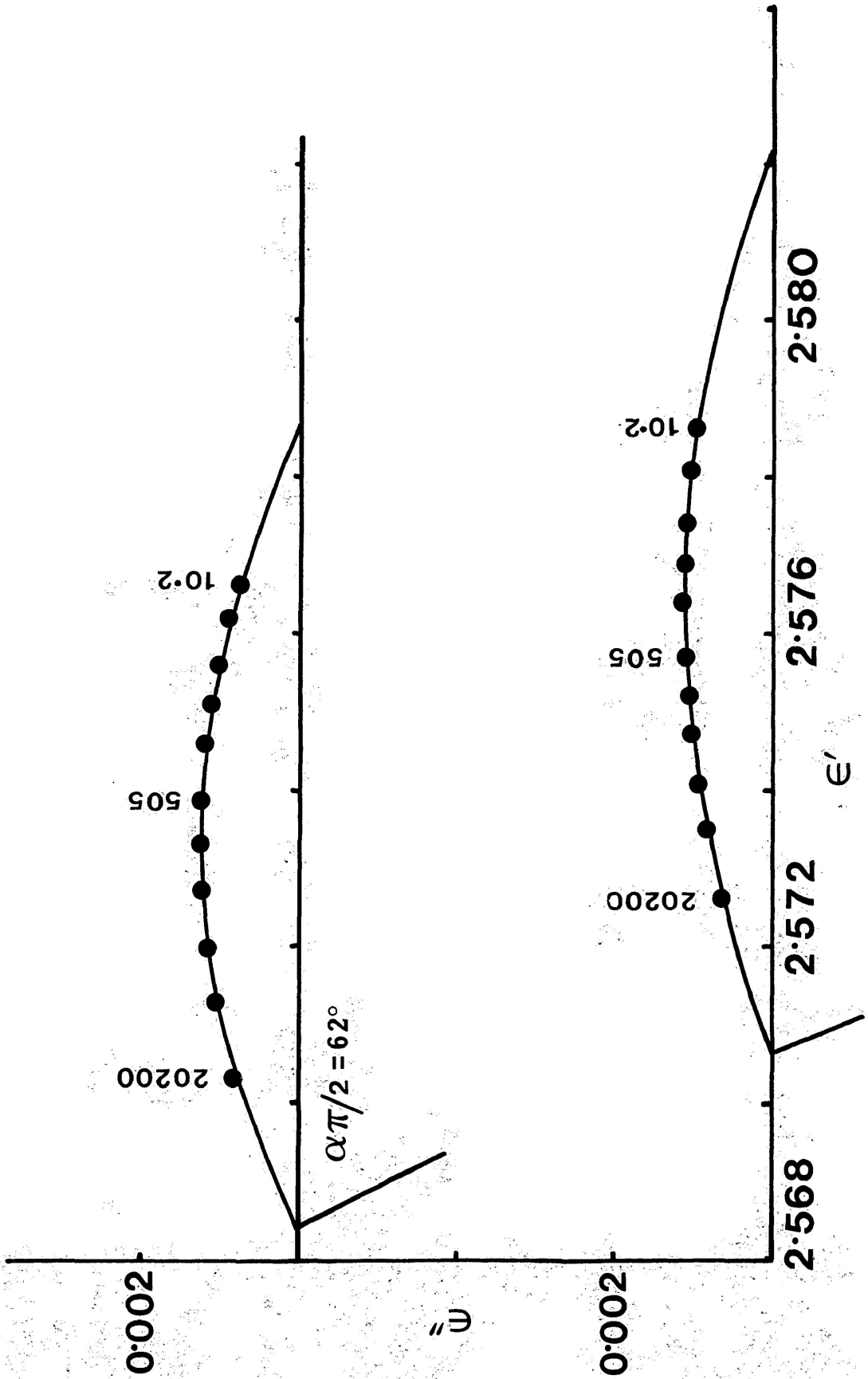

FIGURE VII-20c: Cole-Cole plots for 2,4,6-tri-tert-butylphenol in cis-decalin at 135 K (lower) and 140.9 K (upper). Numbers beside points are frequencies in Hz.

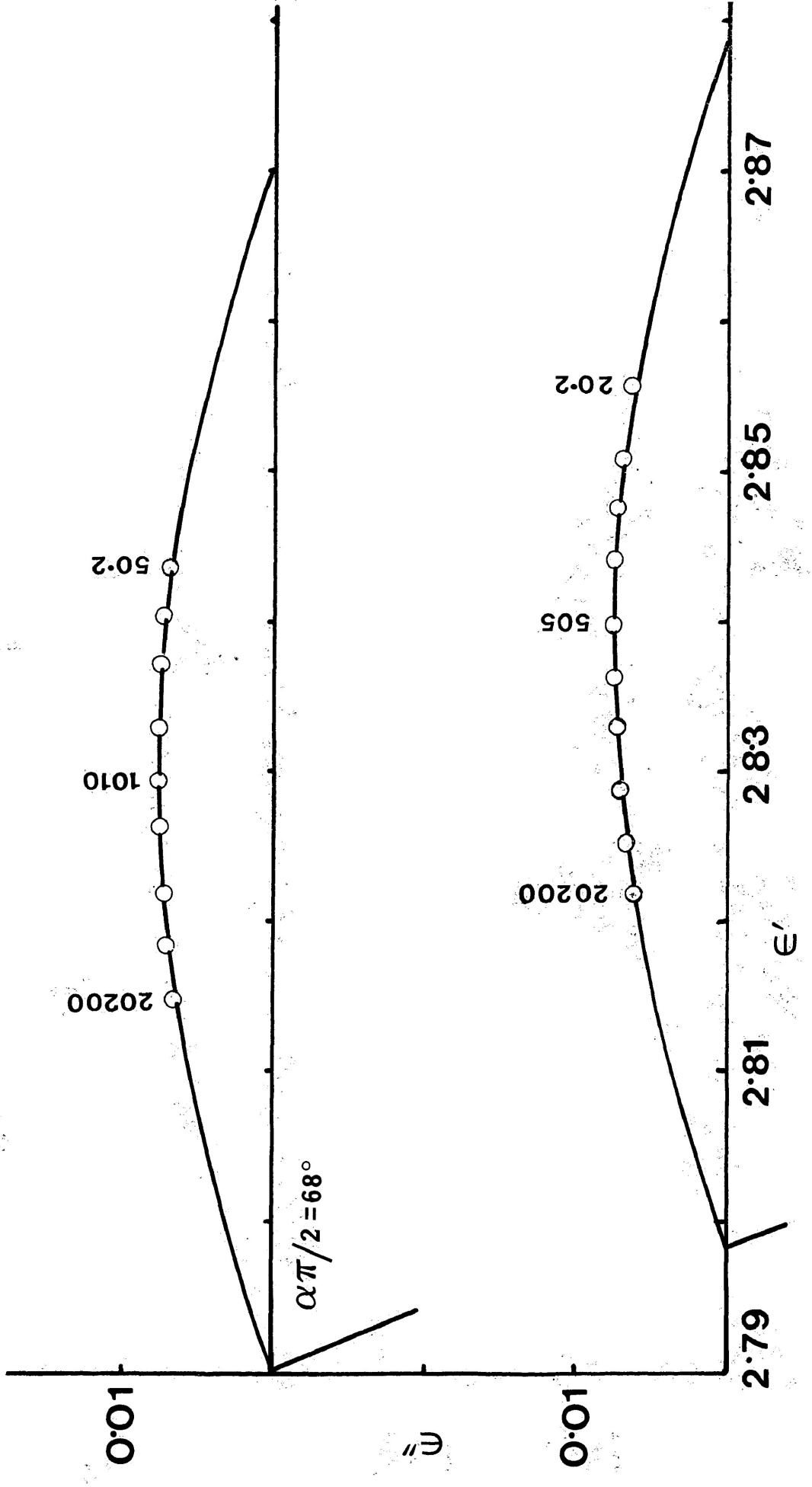

FIGURE VII-21c: Cole-Cole plots for tropolone in G.O.T.P. at 86.8 K (lower) and 90.4 (upper). Numbers beside points are frequencies in Hz.

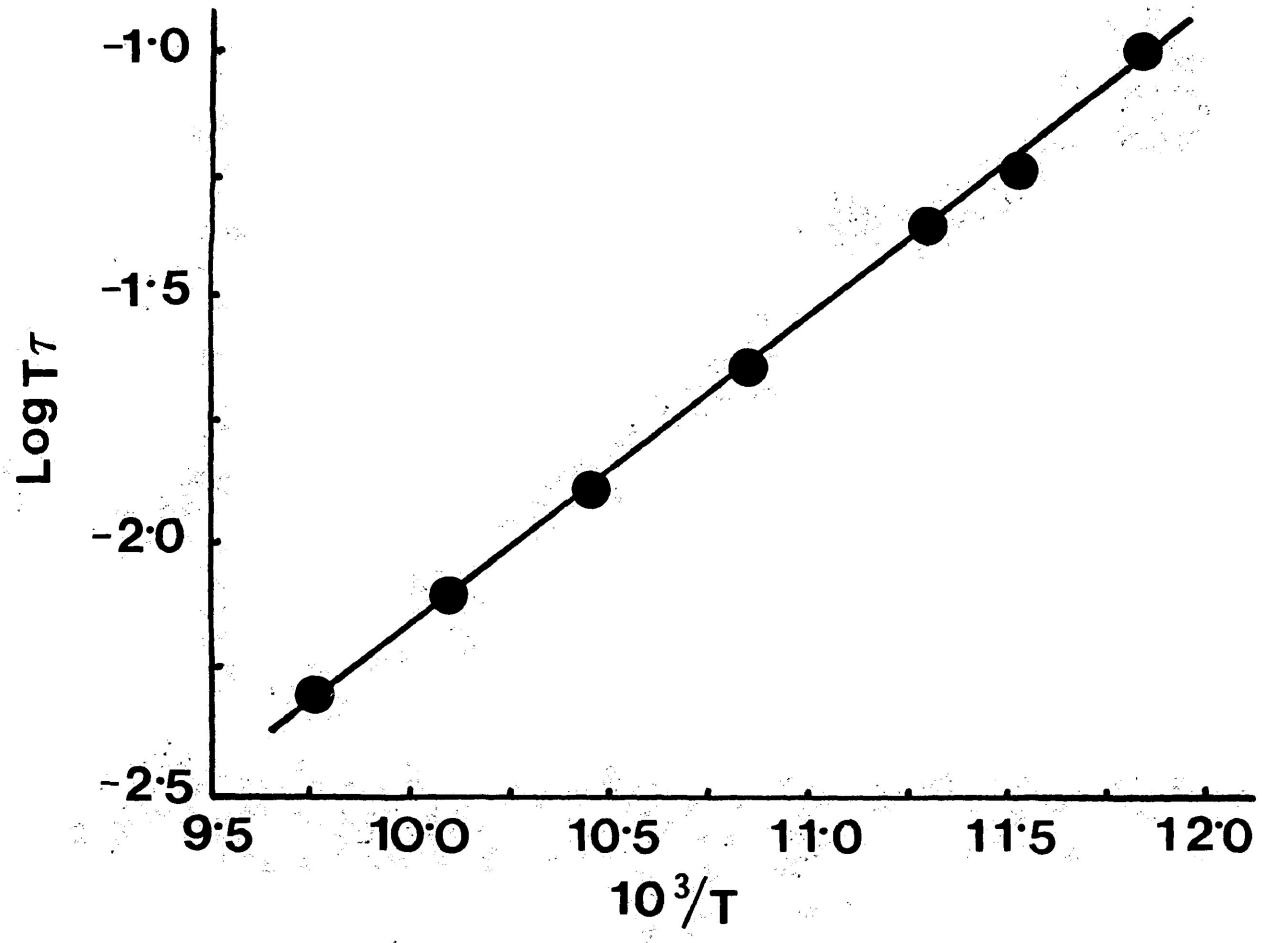

FIGURE VII-23d: Eyring plot of logTτ versus 1/T (K^{-1}) for 2,4,6-trichlorophenol in cis-decalin (8.2 mol %).

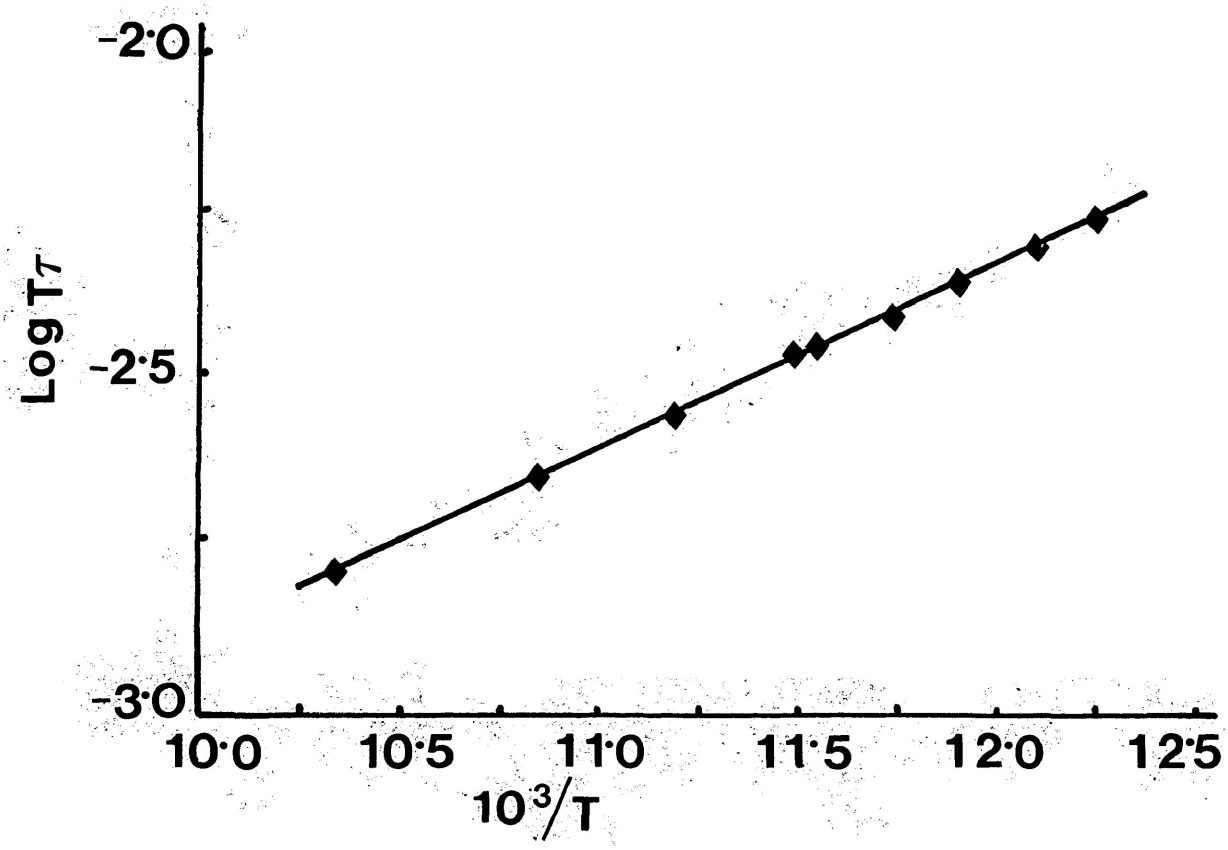

FIGURE VII-24d: Eyring plot of logTτ versus 1/T (K^{-1}) for 2,4,6-triiodophenol in G.O.T.P.

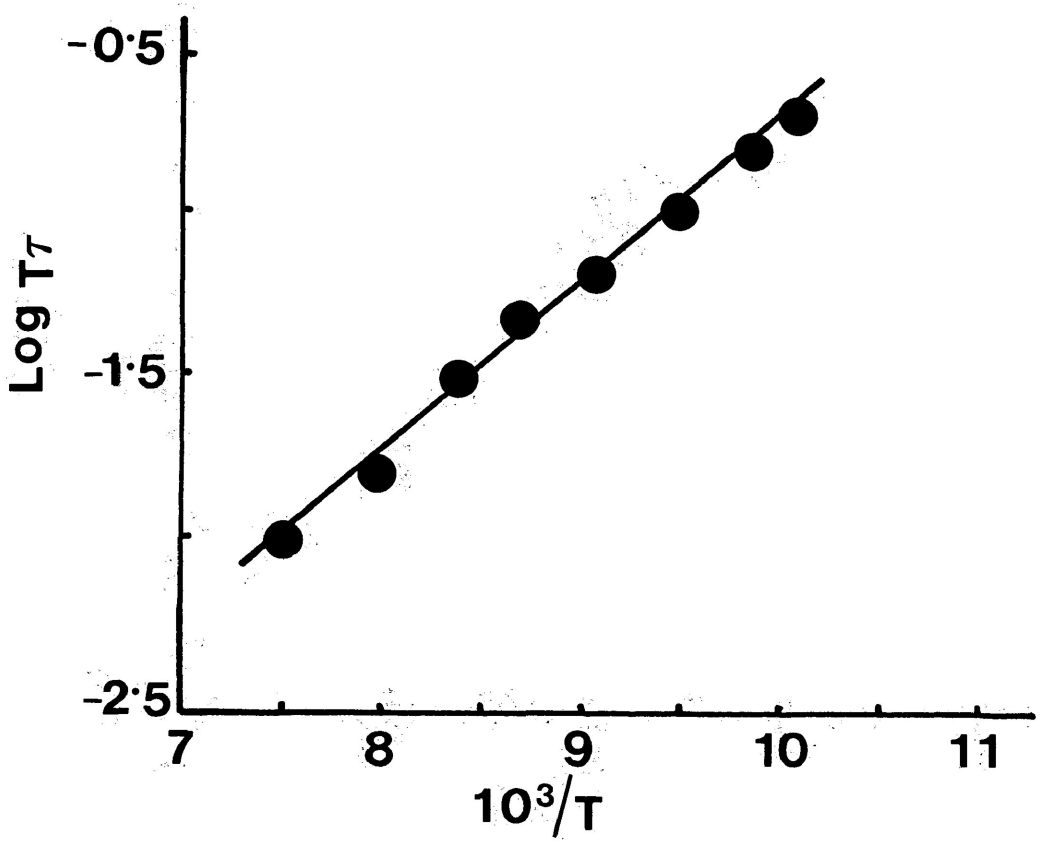

FIGURE VII-25d: Eyring plot of logTτ versus 1/T (K^{-1}) for 2,6-dichloro-4-nitrophenol in G.O.T.P.

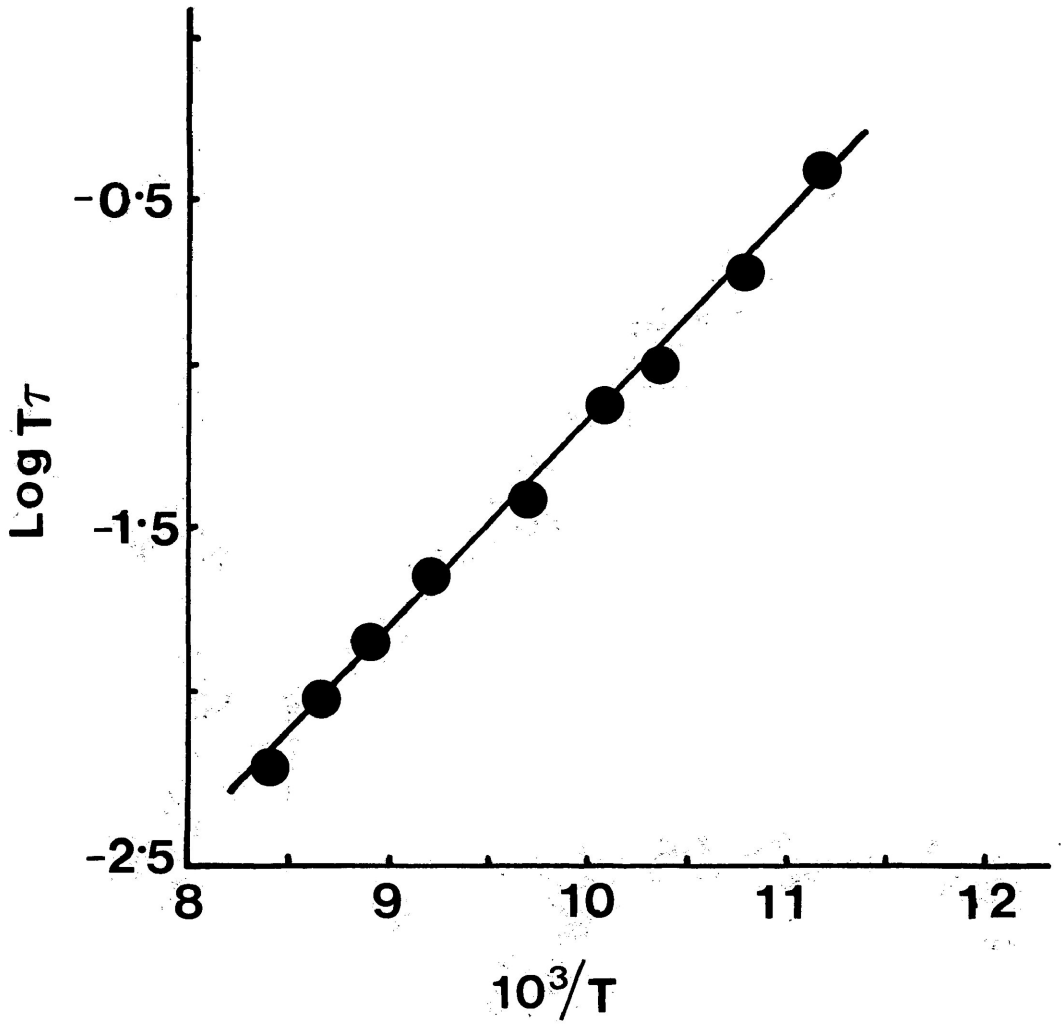

FIGURE VII-26d: Eyring plot of logTτ versus 1/T (K^{-1}) for 2,6-dibromo-4-nitrophenol in G.O.T.P.

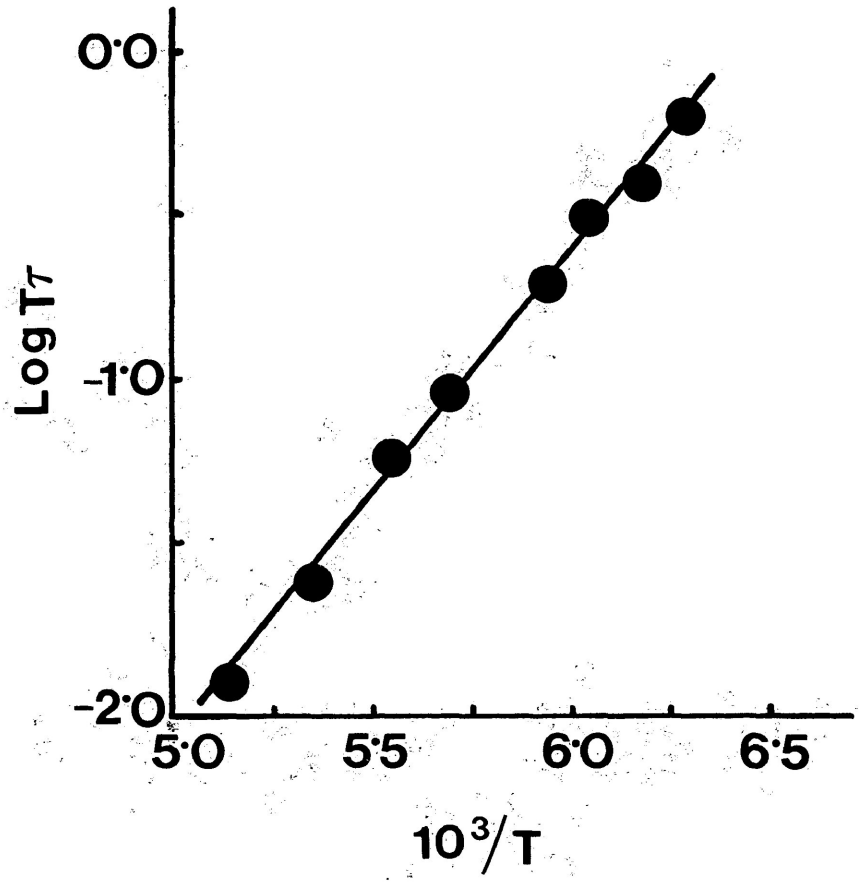

FIGURE VII-27d: Eyring plot of logTτ versus 1/T (K^{-1}) for 2,6-dinitro-4-methylphenol in G.O.T.P.

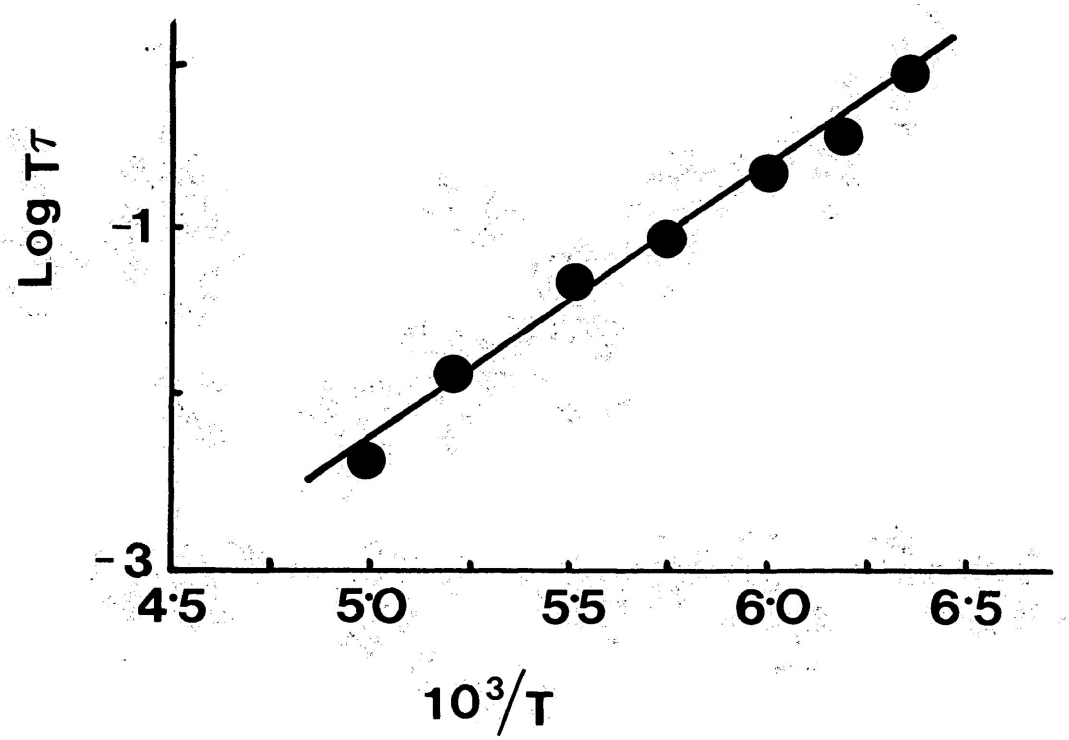

FIGURE VII-28d: Eyring plot of logTτ versus 1/T (K^{-1}) for 2,6-dinitro-4-methylphenol in Santovac®.

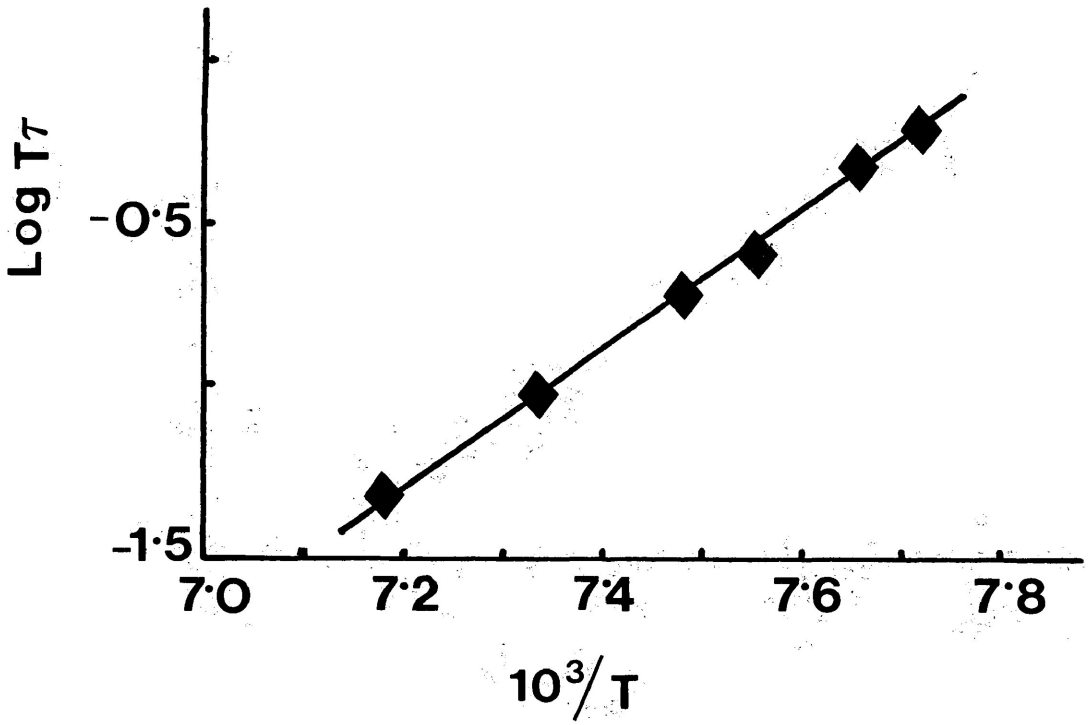

FIGURE VII-29d: Eyring plot of logTτ versus 1/T (K^{-1}) for 2,6-di-tert-butylphenol in cis-decalin

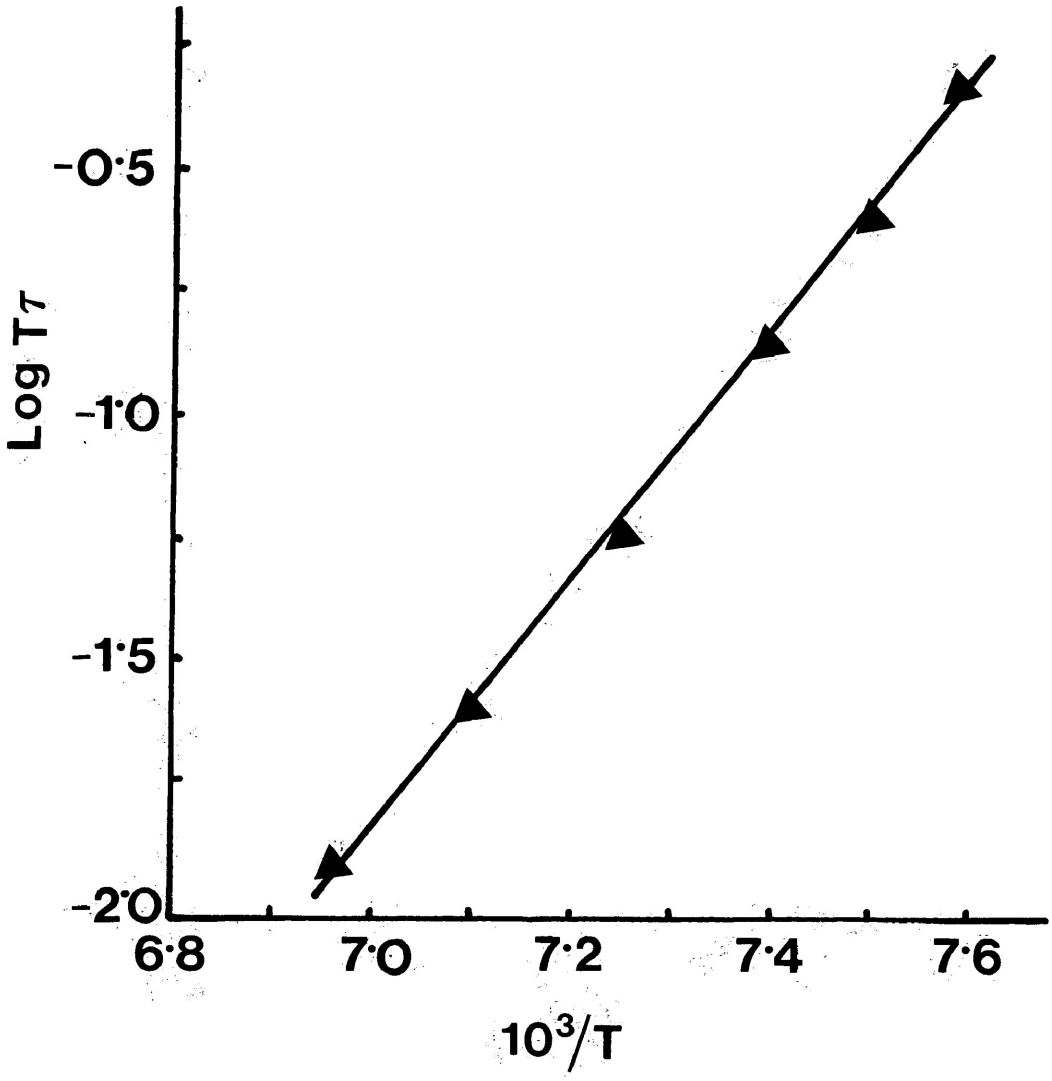

FIGURE VII-30d: Eyring plot of logTτ versus 1/T (K^{-1}) for 2,4,6-tri-tert-butylphenol in cis-decalin.

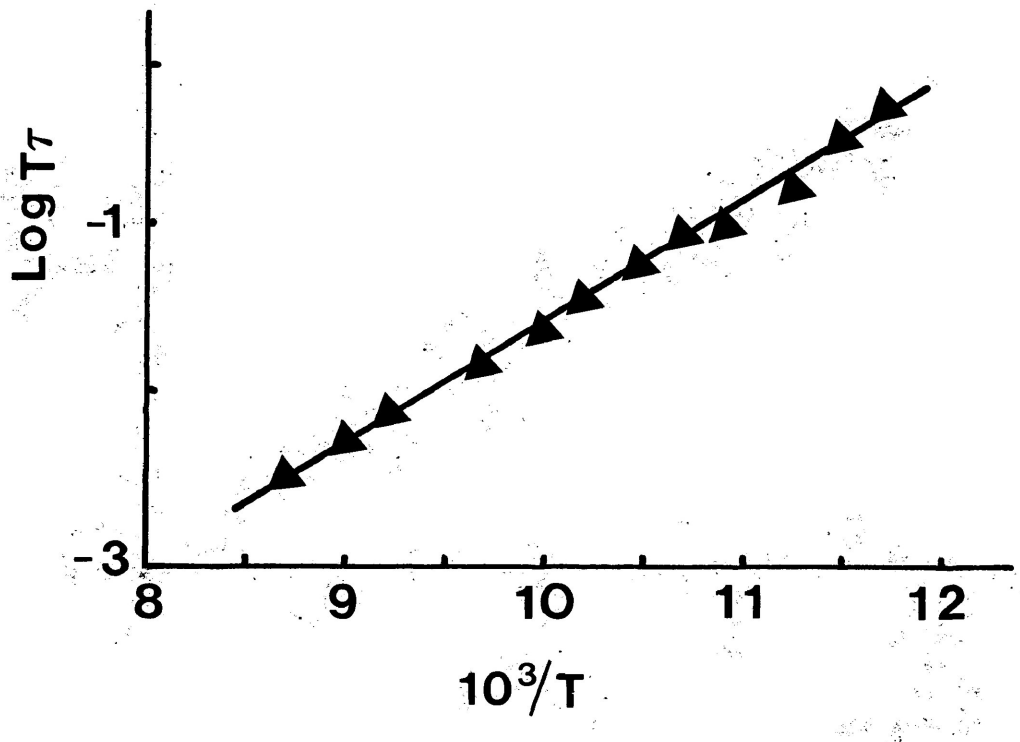

FIGURE VII-31d: Eyring plot of logTτ versus 1/T (K^{-1}) for 2,3,4,5,6-pentachlorobenzenethiol in G.O.T.P.

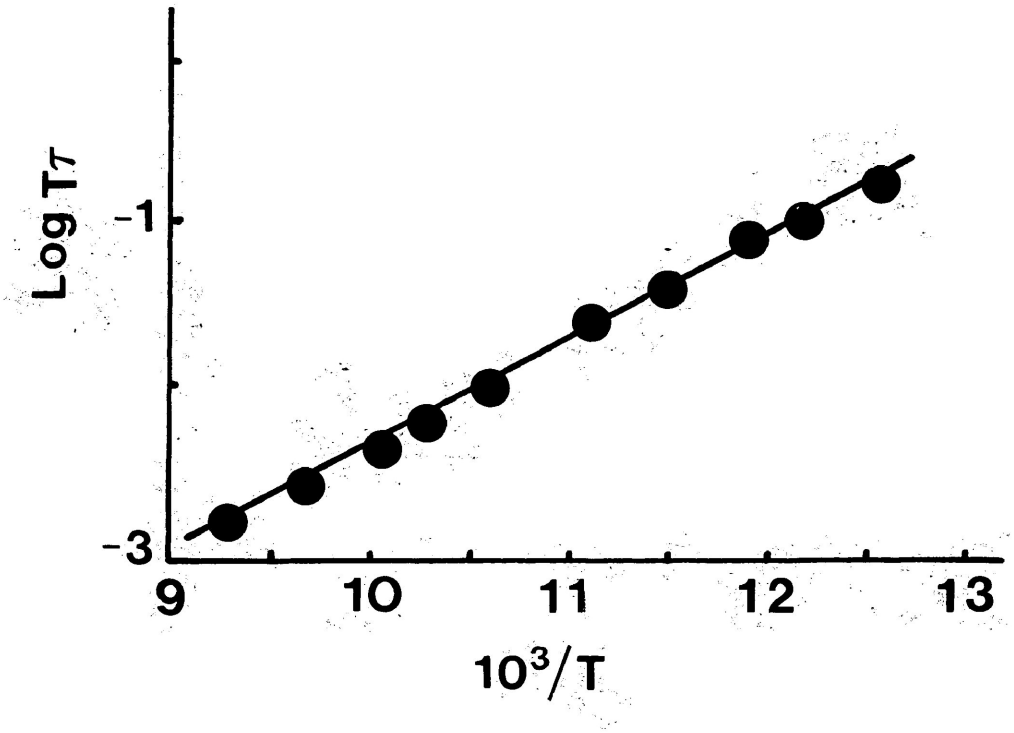

FIGURE VII-32d: Eyring plot of logTτ versus 1/T (K^{-1}) for tropolone in G.O.T.P.